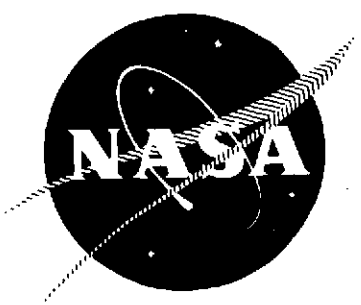


P
2 May

CR 134242

R-9167



SPACE SHUTTLE APS
PROPELLANT THERMAL CONDITIONER STUDY
FINAL REPORT

May 1973

(NASA-CR-134242) SPACE SHUTTLE APS
PROPELLANT THERMAL CONDITIONER STUDY
Final Report (Rocketdyne) ~~418~~ p HC
\$24.00

400

CSSL 21I

N74-22401

Unclas
G3/27 37874

ROCKETDYNE DIVISION
ROCKWELL INTERNATIONAL

prepared for

National Aeronautics and Space Administration
Manned Spacecraft Center
Houston, Texas 77058
Auxiliary Propulsion and Pyrotechnics Branch

SPACE SHUTTLE APS
PROPELLANT THERMAL CONDITIONER STUDY

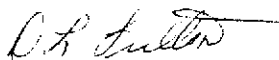
FINAL REPORT

NAS9-12046

May 1973

Prepared for
National Aeronautics and Space Administration
Manned Spacecraft Center
Houston, Texas 77058
Auxiliary Propulsion and Pyrotechnics Branch
Technical Monitor J. W. Akkerman

Prepared by



D. L. Fulton
Project Development Engineer

Approved by



R. W. Helsel
Program Manager
SS/APS Program



Rocketdyne Division
Rockwell International
6633 Canoga Avenue
Canoga Park, California 91304

FOREWORD

This report summarizes the work accomplished under Contract NAS9-12046 for the Auxiliary Propulsion and Pyrotechnics Branch of the Manned Spacecraft Center, National Aeronautics and Space Administration. Work was performed by the Rocketdyne Division of Rockwell International.

The NASA Technical Monitor was Mr. James Akkerman. The Program Manager was Mr. Ronald Helsel and the Project Engineer was Mr. Donald Fulton. Principal contributors were:

J. Gerstley
J. Federer
N. Bergstresser
R. McKown
L. Tignac
S. Fischler
D. Levack
E. Pucker

This report completes DRL Item 11 of NASA Form 1106A.

PRECEDING PAGE BLANK NOT FILMED

ABSTRACT

An analytical and experimental effort was completed to evaluate a baffle type thermal conditioner for superheating O_2 and H_2 at supercritical pressures. The thermal conditioner consisted of a heat exchanger and an integral reactor (gas generator) operating on O_2/H_2 propellants.

In compliance with the long life, fail safe requirements, the reactor mixture ratio was set at 1.0 with cold gaseous propellant and hot gas exhaust temperature was 750 R. Nominal operating conditions for the two conditioners were:

	<u>H_2</u>	<u>O_2</u>
Flowrate, lb/sec.	4.5	15.6
Inlet Conditions		
Temperature, R	55	180
Pressure, psia	1600	1600
Outlet Conditions		
Temperature, R	225	400
Pressure, psia	1500	1500
Heating Rate, Btu/sec.	2800	1800

Primary emphasis was placed on the hydrogen conditioner with some effort on the oxygen conditioner and a study completed of alternate concepts for use in conditioning oxygen.

A hydrogen conditioner was hot fire tested under a range of conditions to establish ignition, heat exchange and response parameters. A parallel technology task was completed to further evaluate the integral reactor and heat exchanger with the side mounted electrical spark igniter.

CONTENTS

<u>Introduction</u>	1
<u>Summary</u>	5
<u>Discussion</u>	21
Selected Design Concept	24
Configuration Analysis	27
Summary of Operating Parameter Selection	27
Selection of Operating Parameters	29
Configuration Analysis	43
Structural and Cyclic Life Analysis	95
System Balance Analysis	102
Design and Fabrication	104
Baffle Material Selection	104
Sample Baffle Assembly	107
Final Evaluation of Candidate Materials for the Baffle Assembly	115
Conditioner Detail Design and Fabrication	115
Reactor (Injector) Configuration	144
Reactor Propellant Flow Control Valves	161
Hydrogen Conditioner Assembly Configuration	161
Conditioner Test Effort	167
Facility	167
Test Plan	182
Test Program	186
Posttest Thermal Analysis	198
Posttest Hardware Evaluation	264
Technology Development	275
Injector Thermal Analysis	275
Test Results	282
Solid Wall Baffle Data Analysis	284
Experimental Combustor Heat Flux	295
Injector Thermal Response	299
Conclusions	306

Conclusions and Recommendations 309
References 311
Appendix A
System Balance Analysis A-1
Appendix B
Evaluation of Alternate Oxygen Conditioner Concepts B-1
Appendix C
DEAP Computer Program C-1
Appendix D
Heat Transfer D-1

ILLUSTRATIONS

1. Hydrogen Conditioner (Development Configuration)	7
2. Baffle Assembly, Hydrogen Conditioner	8
3. Conditioning System Total Weight vs Hot-Gas Exhaust Temperature	10
4. Partially Formed Baffle	12
5. Completed Baffle and Details	12
6. Conditioner Subassemblies and Details	13
7. Completed Conditioner	13
8. Trislot Injector	13
9. Conditioner Assembly	13
10. Test 213-Nominal 5-Second Test	15
11. Test 219 - "Worst Case" Cycling With LH ₂ Flowing Continuously	16
12. Test 227 - Cycle Test Data, 3 Seconds On/2 Seconds Off	16
13. Conditioner Response, Extreme Cases	18
14. Thermal Conditioner Control System	25
15. O ₂ /H ₂ Combustion Temperature vs Mixture Ratio and Injection Temperature	31
16. Hot-Gas Water Condensation, MR = 1	33
17. Effect of GH ₂ Injection Temperature on Hot-Gas Flow Requirements - H ₂ Conditioner	34
18. Effect of LH ₂ Inlet and Outlet Temperature Range on Hot-Gas Flow Requirements	36
19. H ₂ Conditioner Propellant Weight vs Exhaust Temperature and Mixture Ratio	37
20. H ₂ Conditioner Surface Area	39
21. H ₂ Conditioner, Total Weight Versus Outlet Temperature	40
22. H ₂ Conditioner, Total Weight Optimization	41
23. H ₂ Conditioner, Total Weight Versus Outlet Temperature	42
24. Effect of Injector End Hot Gas Mass Velocity on Heat Flux and Wall Temperature Distribution	45
25. Minimum H ₂ Temperature vs Heat Flux Life Requirements for Haynes-188 Baffles	46
26. Temperature Gradients Near Baffle Leading Edge, No H ₂ Bypass	48

27.	Temperature Gradients Near Baffle Leading Edge	49
28.	Leading Edge Wall Temperature vs H ₂ Bulk Temperature	51
29.	Exit End Wall Temperature	52
30.	Techniques for Varying Channel Flow Area	54
31.	Effect of Coolant Bypass on Outlet Temperature	55
32.	Conditioned Hydrogen Drop vs Mass Velocity and Bypass	57
33.	Channel Geometry and Hot-Gas Gap as a Function of Station	58
34.	Channel Geometry and Hot-Gas Gap as a Function of Station	61
35.	Heat Flux and Gas Temperature as a Function of Station	62
36.	Wall and Hydrogen Temperatures as a Function of Station	63
37.	Hot Gas and Conditioned Propellant Pressure Profiles	65
38.	Baffle Edge Temperatures	68
39.	Reactor H ₂ Pressure Drop in Shell	70
40.	Shell Cooling, Reactor Hydrogen Channel Geometry	71
41.	Baffle and Top/Bottom Wall Geometry	73
42.	Baffle and Top/Bottom Wall Geometry	74
43.	Hydrogen Conditioner Hot Gas Flow vs Mixture Ratio	77
44.	Hydrogen Conditioner Thermal Characteristics vs Mixture Ratio	79
45.	H ₂ Conditioner Thermal Transients	81
46.	H ₂ Conditioner Thermal Transients	82
47.	H ₂ Conditioner Thermal Transient W _{H₂} Thermal Transient = 4.5 lb/sec, 40-Percent Bypass, MR = 1, P _c ~ 240 psia	84
48.	Oxygen Conditioner Heat Input	86
49.	High Mixture Ratio Gas Requirements for O ₂ Conditioner	87
50.	Oxygen Conditioner Total Weight Versus Hot-Gas Exhaust Temperature	89
51.	Oxygen Conditioned in H ₂ Conditioner Baffles	90
52.	Predicted Stability at Nominal Conditions	91
53.	Oxygen Conditioner Temperatures Versus Hot Gas Flowrate, MR = 3	93
54.	Oxidizer Conditioner Hot Gas Flow Requirements Versus Mixture Ratio	94
55.	Oxygen Conditioner Thermal Transients	96
56.	Estimated Allowable Temperatures for Haynes 188 Baffles	101
57.	Sample Baffle Assembly	108
58.	Manufacturing Sequence for Panel Assembly	109
59.	Furnace Arrangement for Test Panel	111

60.	Baffle Sample Formed to 0.375 Radius	112
61.	Baffle Sample Formed to 0.25 Radius Showing Resulting Surface Cracks	114
62.	Prototype Baffle Fabrication	116
63.	Baffle Assembly Hydrogen Conditioner	118
64.	Baffle Detail	119
65.	Baffle Detailing	121
66.	Baffle Assembly	123
67.	EDM Setup	125
68.	Partially Formed Baffle	127
69.	Baffle in Forming Fixture	128
70.	Completed Baffle and Details	129
71.	Completed Instrumented Baffle Assembly	134
72.	Instrumented Baffle Assembly	135
73.	Baffle Thermocouple Installation	136
74.	Side-Wall Assembly	137
75.	Conditioner Side Wall Details	139
76.	Bottom Wall Assembly	141
77.	Conditioner Bottom Wall Detail	143
78.	Miscellaneous Details for Hydrogen Conditioner	145
79.	Hydrogen Conditioner Assembly	146
80.	Hydrogen Conditioner Details and Partial Assemblies	147
81.	Hydrogen Conditioner Partially Assembled	148
82.	Hydrogen Conditioner Partially Assembled	149
83.	Hydrogen Conditioner Assembly	150
84.	Hydrogen Conditioner Assembly	151
85.	Instrumentation-Conditioned Hydrogen Outlet	152
86.	Injector Element Arrangement	154
87.	Trislot Injector	155
88.	Trislot Element Injector	157
89.	EDM of Injector Elements	159
90.	Air Gap Igniter	1609
91.	Hydrogen Conditioner Assembly	163
92.	Completed Hydrogen Conditioner Assembly	165

93.	Conditioner Flow Circuits	168
94.	Thermal Conditioner Installed in Test Facility	169
95.	Propellant Schematic - Facility Setup	170
96.	Sequencing Schematic	174
97.	Heat Input to Conditioner Hydrogen Versus Hot Gas Flowrate, Tests 201-236, O ₂ /H ₂ Ambient Propellants	200
98.	APS Thermal Conditioner Heat Input Parameter Versus Test Number, Q Based on LH ₂ Flowrate and Mixer Outlet Temperature Propellants Injected at Ambient Temperature	201
99.	Experimental Combustion Efficiency Versus Mixture Ratio O ₂ /H ₂ , Injector Number 2	203
100.	Fraction of Available Energy Versus Combustion Efficiency O ₂ /H ₂ , 600 R Injection Temperature	204
101.	Liquid Hydrogen Outlet Temperature Versus Heat Input, LH ₂ Flowrate and Inlet Temperature, P _{OUT} = 1500 psia	206
102.	Predicted Total Hot Gas Pressure Ratio Versus Hot Gas Exhaust Temperature and Mixture Ratio with a Sonic Exit O ₂ /H ₂ Propellants	208
103.	Relative Hot Gas Flow Area Versus Ratio Hot Gas Flow to LH ₂ Flow	209
104.	APS Thermal Conditioner Effective Hot Gas Flow Area Versus Test Number	210
105.	Test 164 Thermal Response	212
106.	Test 213 Thermal Transients	214
107.	Test 221 Thermal Response	215
108.	Test 222 Thermal Response	216
109.	Test 235 Transient Response	218
110.	Test 219 LH ₂ Exit Temperature and Flowrate Response	219
111.	Test 229 LH ₂ Outlet Temperature and Flowrate Response	220
112.	Water Calibration of APS Thermal Conditioner Baffles	225
113.	O ₂ /H ₂ Enthalpy Versus Temperature	232
114.	Baffle No. 3 Temperature Profiles, Test 213	247
115.	Experimental Temperature Profiles, Test 201, Baffle No. 3	248
116.	Experimental Temperature Profiles, Test 236, Baffle No. 3	250

117.	Experimental Side Plate Temperature Profiles, Test 201	251
118.	Experimental Side Plate Temperature Distribution, Test 213	252
119.	Predicted Baffle Temperature Profiles, Test 213	254
120.	Predicted Baffle Hot Wall and LH ₂ Temperature Profiles, Test 222	255
121.	Predicted Baffle Hot-Wall Temperature Profiles, Test 236	256
122.	Predicted Effect of Differential Heat Flux on Both Sides of the Baffle on the Differential Hot-Wall Temperature	257
123.	Hydrogen Conditioner, Unit No. 1, Baffle Deflection	265
124.	Hot-Gas Gap Dimensions	266
125.	Sketch of Honeycomb Cutout	267
126.	Sections of Instrumented Baffle	268
127.	Baffle-Buckling Test Specimen	270
128.	As Fabricated -003 Sample Baffle	271
129.	As Fabricated -005 Sample Baffle	272
130.	-003 Sample Baffle After Collapse at 1450 psig	273
131.	-005 Sample Baffle After Collapse at 1250 psig	274
132.	Solid Wall Chamber	276
133.	Uncooled Dummy Baffle Thermocouple Locations	277
134.	Solid Wall Conditioner	278
135.	H ₂ Conditioner - Injector Face Temperature	280
136.	H ₂ Conditioner Injector Face Temperature	281
137.	Uncooled Workhorse Dummy Baffle Hot Wall Thermal Response	286
138.	Uncooled Workhorse Dummy Baffle Hot Wall Thermal Response	287
139.	Experimental Baffle Stagnation Point Heat Flux Versus Flowrate	288
140.	Experimental Dummy Baffle Heat Flux in Gap vs Flowrate	290
141.	Experimental Dummy Baffle Heat Flux vs Mixture Ratio	291
142.	Baffle Heat Flux Values	293
143.	Baffle Heat Flux Values	294
144.	Uncooled Workhorse Combustor Thermal Transients 0.5-Inch Thick, 347 CRES	296
145.	Combustor Wall Thermocouple, Tests 002 Through 014, Theoretical Combustion Temperature	297

146.	Combustor Wall Thermocouple, Tests 015 Through 025, Theoretical Combustion Temperature	298
147.	Injector Center Thermocouple Transients, Tests 567 Through 572	300
148.	Injector Center Thermocouple Transients, Tests 006 Through 011, Igniter Off During Mainstage	301
149.	Injector Center Thermocouple Transients, Tests 015 Through 025	302
150.	Injector Center Face Temperatures, Steady-State Mainstage, Tests 015 Through 024	303
151.	Typical Heat Flux Distribution on the Baffles	305

TABLES

1. Contioner Operational Parameters	9
2. Nominal Design Point (Hydrogen Conditioner)	12
3. LH ₂ Conditioner Test Summary	14
4. LH ₂ Conditioner Test Matrix	15
5. Posttest Thermal Analysis	19
6. Program Assessment	20
7. Thermal Conditioner Design Requirements and Goals	22
8. Thermal Conditioner Operating Requirements	22
9. Thermal Conditioner Operating Parameters	23
10. H ₂ Baffle Operating Characteristics, Steady State	66
11. Top Wall/Baffle Interface Temperatures	75
12. Evaluation of Candidate Material Combinations	100
13. Hot Wall Thermal Cycle Capability--Hydrogen Conditioner	102
14. Nominal Design Point--H ₂ Conditioner	105
15. Material Properties - Candidate Conditioner Materials	106
16. Baffle Fabrication, RS 00 5578X	130
17. APS Thermal Conditioner Instrumentation	175
18. Test Matrix - LH ₂ Conditioner	184
19. LH ₂ Conditioner Test Summary	187
20. LH ₂ Conditioner Test Matrix	188
21. Conditioner Test Results	189
22. LH ₂ Thermal Conditioner Test Conditioner	196
23. Instrumentation Used to Determine Flow Distribution	223
24. Typical Heat Input Distributions	227
25. Proportional Heat Input Distribution to Baffles	228
26. Test 213 Flow Distribution Analysis	233
27. Test 222 Analysis	234
28. Hot-Gas Outlet Temperature Distribution	237
29. Correlation Between Gas Flow Area and LH ₂ Enthalpy Rise, Test 219	240
30. Comparison of Predicted and Experimental Parameters - Test 213	243

31.	Comparison of Predicted and Experimental Parameters - Test 222	244
32.	Comparison of Predicted and Experimental Parameters - Test 236	245
33.	Preliminary Baffle ΔP Analysis	259
34.	Test Results	283

INTRODUCTION

The National Aeronautics and Space Administration is currently engaged in the development of a recoverable and reusable space transportation system, commonly referred to as the space shuttle vehicle. As originally conceived, the vehicle consisted of two separate manned elements, a booster stage and an orbiter stage, each of which was individually recoverable. The space shuttle vehicle was launched vertically on rocket thrust alone, with the booster staging-off and flying back to the recovery site. The orbiter stage proceeded to orbit under main rocket propulsion and, in orbit, maneuvered as a true spacecraft. At the conclusion of its mission, the orbiter stage reentered and flew back like a conventional aircraft.

The hydrogen-oxygen propellant combination was chosen for use in the main propulsion systems of both the booster and orbiter stages because of its high performance, relatively low cost, and nontoxic, noncorrosive nature. These propellants were also selected for the auxiliary propulsion system (APS) for the same reasons plus additional benefits derived from commonality between the main and auxiliary propulsion storage and feed systems. These benefits include possible use of main engine boost residuals for auxiliary propulsion requirements and potential flexibility in distribution of orbital maneuvering propellant between the main engine and the APS to provide capability for a wide range of missions.

All of the requirements for auxiliary propulsion on the two stages were not fully determined. The booster stage required auxiliary propulsion principally for attitude control after staging and during the descent phase until the aerodynamic control surfaces take over. The auxiliary propulsion requirements for the orbiter stage were less clearly defined but included attitude control during all phases of the mission from staging until returning to lower altitudes and a variety of possible translation maneuvers. The space shuttle vehicle is to provide low cost transportation to earth orbit to support a variety of missions, including logistic resupply of a space station.

In order to achieve maximum cost effectiveness the space transportation system will be designed for up to 100 flights (reuses) over a 10-year operational lifetime and will be capable of relaunch within 2 weeks after landing. The system will be designed to minimize required postflight refurbishment, maintenance, and checkout. As a result the APS must provide long life, high reliability, high performance, reusability, minimum complexity, and minimal and easy system maintenance and refurbishment.

A variety of propellant feed systems were studied for the auxiliary propulsion system. These systems differed greatly in configuration and operating characteristics. One common characteristic, however, was the delivery of gaseous hydrogen and gaseous oxygen to the thrusters.

Thermal conditioners were required in the auxiliary propulsion system to convert (at a maximum required flowrate) cryogenically stored propellants to the gaseous state at a temperature high enough to minimize the possibility of a phase change during use in the rocket engines. These conditioners used hydrogen-oxygen as reactants to generate the hot gas required to heat and vaporize the propellants. Conditioners consisted of a reactor and a heat exchanger combined. The input cryogenic fluid was supplied by a pump, located just downstream of the cryogenic storage tank. The output gas flowed into an accumulator of sufficient size to store enough gas to operate the system between the times that the propellant conditioner (pump and thermal conditioner) are operating. A tradeoff is involved between accumulator size and cycles of operation of the conditioning system. Also, conditioning system response is a factor in the accumulator sizing.

The timing of the system sequence is a primary consideration because it affects the size of the accumulator. The accumulator required to hold enough gas to operate the system weighs nearly 1000 pounds per second of system operation. (Assuming four thrusters operating). Typical time delay between the instant the accumulator reaches its low pressure limit (about 500 psia) and the time that the pump is supplying fluid to the thermal conditioner is on the order of 1/2 to 1.5 seconds.

The thermal conditioning unit (hot gas generator and heat exchanger assembly) used the same "on-off" signal as the pump (i.e., the low or high pressure signal from the accumulator). This means that the thermal conditioning unit can anticipate the flow of cold fluid by only 1/2 to 1.5 seconds. Likewise, shutdown signal will provide warning of termination of the flow of cold fluid by no more than 1/2 to 1.5 seconds.

On occasion, the filling of the accumulator will occur with all engines "off", meaning that the conditioning systems will only operate for 2 to 3 seconds. Then, just as the accumulator fills and the conditioning system shuts down, four thrusters can come on steady (for a translation maneuver) emptying the accumulator within about 2 to 4 seconds at which time another run period of the conditioner system is required. Therefore, the demand intervals may be separated by as little as 2 seconds or as much as 24 hours.

Operation of the type described above is expected to be very demanding upon the hardware in terms of reliability. It is easy to visualize hundreds of cycles of operation in each mission. Failure of the control systems to initiate the hot gas flow should not cause damage to the conditioner unit. Likewise, failure of the control system to initiate cold fluid flow should not cause damage to the conditioner unit.

The environmental requirements for the propellant conditioner unit are those to be encountered in assembly, checkout, launch, space flight, reentry and landing of the shuttle orbiter stage. During all these situations, the outer surface of the propellant thermal conditioner unit must not exceed 600 F as required by other equipments installed nearby. This limit must be maintained even though the interior of the compartment in which the unit is installed may reach as much as 500 F. Essentially, this requires that the thermal conditioner unit outer surface operate at 600 F or below even though it is thermally isolated.

Cognizant of these very stringent requirements, NASA-MSC awarded Rocketdyne a contract to analytically and experimentally evaluate a baffle-type thermal conditioner designed to accomplish these requirements and to document the results. This effort was to establish a technology base for this type of thermal conditioner, eventually leading to a development and production program.

The results of this program are presented in this report.

SUMMARY

The objective of this program was to establish a technology base for a highly efficient, compact baffle type thermal conditioner with an integral reactor and heat exchanger. This was accomplished through the analysis, design, fabrication and test of a heavily instrumental development type conditioner.

Criteria for the thermal conditioner were:

- Minimum weight - hardware plus reactants
- Long life - 100 missions over 10 years
- Standard materials and manufacturing processes where possible
- Simultaneous or individual operation
- Unlimited duty cycle
- 1/2 to 1-1/2 seconds precondition time
- Provide conditional fluid within 1/2 second after flow initiated
- Cease to produce conditional fluid within 1/2 second after flow terminated
- Hot gas flow only - unit could be safely shut down and could complete mission
- Cold propellant flow only - no damage or degradation
- Outer surface temperature 600 F maximum - even with double failure

Nominal operating parameters as specified in the work statement were:

<u>Cold Propellant Side</u>	LH ₂	LO ₂
Flowrate, lb/sec	4.5	15.6
Inlet Temperature, R	55	180
Outlet Temperature, R	225	400
Inlet Pressure, psia	1600	1600
<u>Hot-Gas Side</u>		
Flowrate, lb/sec	As Required	
Mixture Ratio	As Required	
Inlet Temperature, R		
H ₂	275 to 600	
O ₂	375 to 600	
Inlet Pressure, psia	375	

The conditioner concept selected by NASA-MSFC to be evaluated on this program consists of the integral reactor and baffle-type heat exchanger shown in Fig. 1. Hot gases are generated at the forward end of the conditioner and then ducted through relatively small passages between the slotted and formed baffles through which the propellant to be conditioned flows. A baffle is

shown in more detail in Fig. 2. The heat exchanger and reactor shell used channel wall construction and standard material and fabrication techniques (Haynes-188 and stainless steel, electrical discharge machining, furnace brazing and electron beam welding). The injector incorporated a trislot injection pattern (where two fuel streams impinge on a central oxidizer stream). Ignition was accomplished using a NASA-LeRC developed torch igniter; valves are existing ball valves. Nominal operating parameters are listed in Table 1.

Initial analysis on the conditioners consisted of establishing heat input requirements to condition the hydrogen and oxygen to the specified value.

Results showed the hydrogen conditioner had a required heat input range of 1500 to 5000 Btu/sec with a nominal requirement of 2800 Btu/sec. Nominal requirement for the oxygen conditioner was 1800 Btu/sec.

The next step in the analysis was to establish nominal reactor mixture ratios such that, under all conditions and failure modes discussed previously, the conditioner would not be damaged should the reactor be on without flow of conditioned fluid (i.e., hardware run uncooled).

A study of hydrogen/oxygen combustion temperature as a function of mixture ratio and hydrogen inlet temperature (combustion temperature is virtually independent of oxygen inlet temperature) resulted in a selected of a mixture ratio of 1.0 o/f for the nominal case of 275 R as shown in the table below.

Mixture Ratio	0.9	1.0	1.1
<u>H₂ Injection</u>			
T = 275 R (nominal)	1890	2040	2200
T = 600 R (maximum)	2200	2360	2520

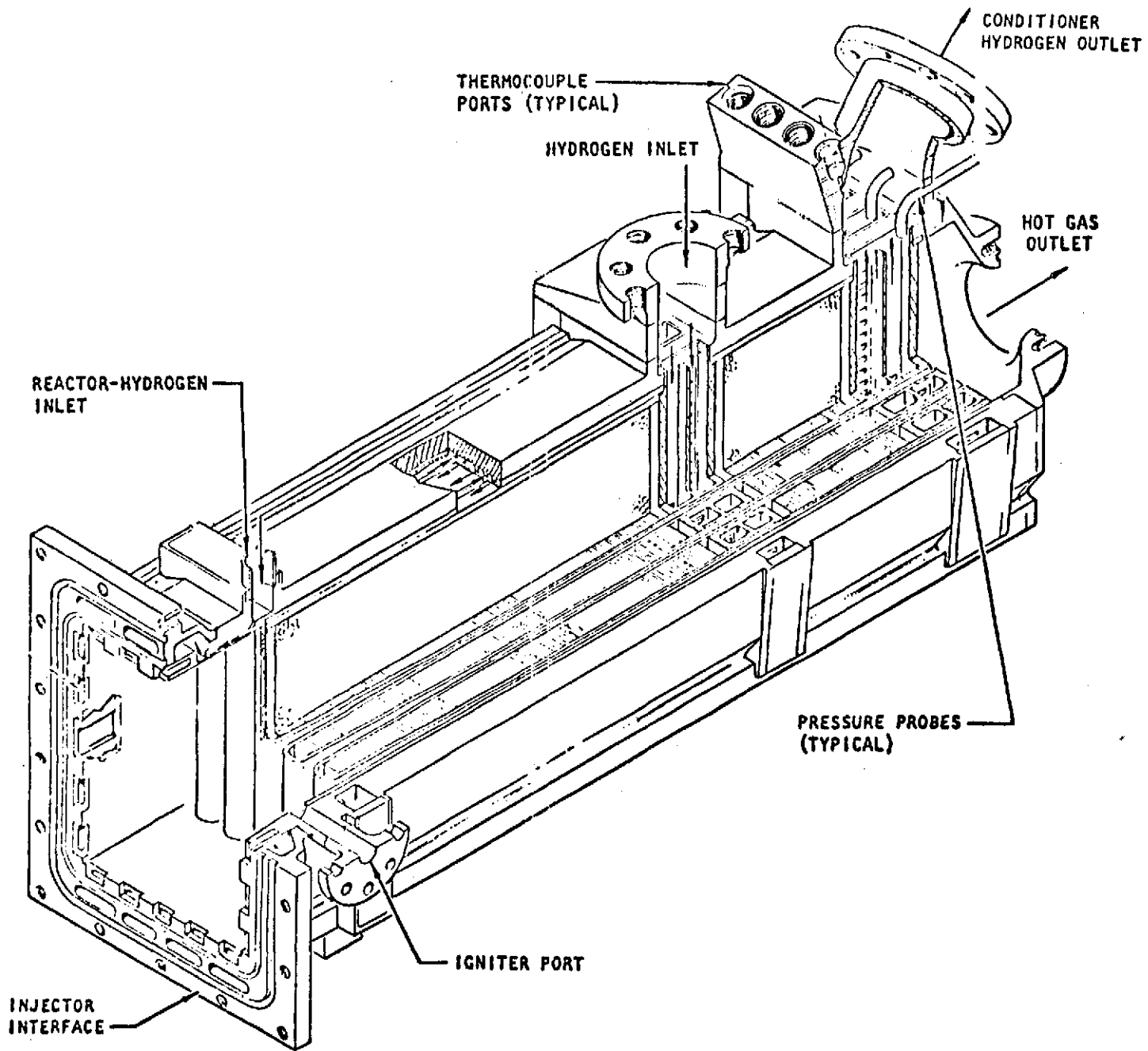


Figure 1. Hydrogen Conditioner (Development Configuration)

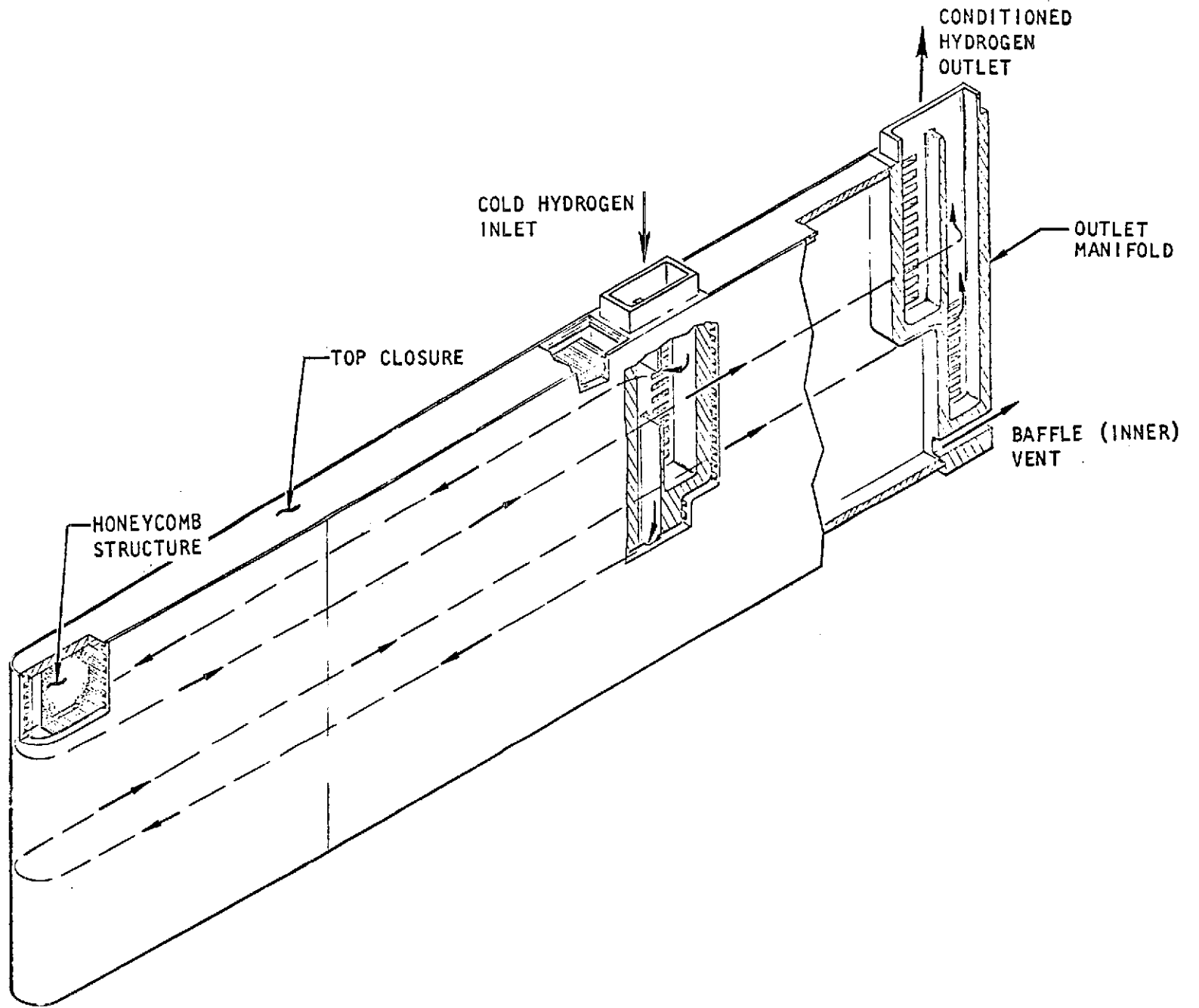


Figure 2. Baffle Assembly, Hydrogen Conditioner

TABLE 1. CONDITIONER OPERATIONAL PARAMETERS

	HYDROGEN CONDITIONER	OXYGEN CONDITIONER
COLD SIDE		
\dot{W} , LB / SEC	4.5	15.6
P_{IN} , PSIA	1600	1600
T_{IN} , R	55	180
T_{OUT} , R	225	400
ΔQ , BTU / SEC	2800	1800
BYPASS, PERCENT	40	0
HOT GAS SIDE		
MIXTURE RATIO	1.0	1.0
\dot{W} , LB / SEC	1.2	0.75
P_C , PSIA	240	150
T_{H2} , R	275	275
T_{O2} , R	375	375

A trade study was completed to determine what reactant exhaust gas temperature resulted in a minimum weight system. This was done for a system which conditions 5000 pounds of propellant at an MR of 3.5 to the values specified previously. Both reactor propellant flow and heat exchanger surface area were determined for the hydrogen and oxygen conditioners as a function of hot gas exhaust temperatures. These were then combined to determine a minimum weight system assuming three conditioners each for hydrogen and oxygen are used in the vehicle (as specified for the Space Shuttle). These data, presented in Fig. 3, show that the minimum weight system occurs at an exhaust temperature of 650 to 750 R. To minimize icing potential at the baffle exit plane and downstream of the conditioners, the exhaust temperature was set at 750 R.

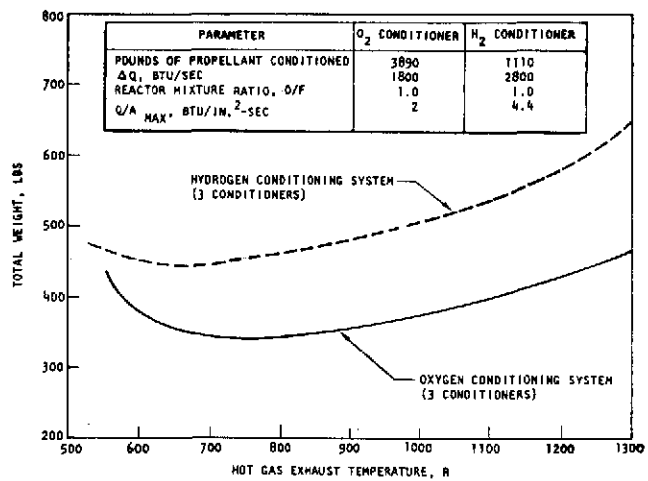


Figure 3. Conditioning System Total Weight vs Hot-Gas Exhaust Temperature

One additional parametric study conducted was to evaluate the use of bypass on the conditioners. The advantages of using bypass are:

1. Higher wall temperature at exit end, minimizing potential icing problems.
2. Allow for flow control to compensate for hardware fabrication tolerances.
3. Smaller, lower ΔP manifolds and reduced cross-section channels to reduce conditioner weight.

An additional and very significant potential advantage is that by proper selection of bypass ratio it may be possible to use the same size conditioner for the hydrogen and oxygen conditioners with the attendant advantages in any application. After considerable analysis, a 40 percent bypass was selected for the hydrogen conditioner. This same conditioner can then be used to condition oxygen with a bypass of ~5 percent.

The effect of bypass on the total weight of the conditioner, and thus on the hot-gas exhaust temperature selection, must be considered in terms of reactant weight and conditioner hardware weight. For a parallel flow conditioner as selected, the exhaust gas temperature must be at least sufficiently high to prevent ice formation on the walls. In addition, the reactant exhaust temperature must be higher than the conditioned propellant exhaust temperature, and the latter increases as the amount of bypass increases. Up to a point, then, the amount of bypass has no effect on the reactant weight, but when the bypass increases to the point where it results in an increase in reactant outlet temperature, then the reactant weight must increase. Once this happens, increased bypass will shift the total weight curve upward and to the right, resulting in higher weight at a higher optimum reactant exhaust temperature. The second effect is that increased bypass results in smaller channels, and thus lighter weight, of the conditioner. This would result in slightly reducing the total weight and causing a somewhat lower optimum exhaust reactant temperature. However, since the weight represented by the lands between coolant passages is a small part of the overall weight, and this is the only weight affected by bypassing flow, the overall effect will be essentially negligible.

At this point, a detailed thermal analysis was completed on the hydrogen conditioner. Resulting nominal design point conditions for the hydrogen conditioner are given in Table 2 as typical.

The conditioner baffles were fabricated by electrical discharge machining the hydrogen flow passages into the Haynes-188 panels; furnace brazing the stainless steel closure in place; forming to shape; and furnace brazing the internal structure, closeouts, and manifolds in place (Fig. 4 and 5).

TABLE 2. NOMINAL DESIGN POINT (HYDROGEN CONDITIONER)

HYDROGEN SIDE	
W, LB/SEC	4.5
P _{IN} , PSIA	1600
P _{OUT} , PSIA	1500
T _{IN} , R	55
T _{OUT} , R	225
ΔQ, BTU/SEC	2800
HOT GAS SIDE	
MIXTURE RATIO, O/F	1.0
H ₂ INJECTION TEMPERATURE, R	275
O ₂ INJECTION TEMPERATURE, R	375
CHAMBER PRESSURE, PSIA	240
COMBUSTION TEMPERATURE, R	2060
EXHAUST TEMPERATURE, R	750
HOT GAS FLOWRATE, LB/SEC	1.2

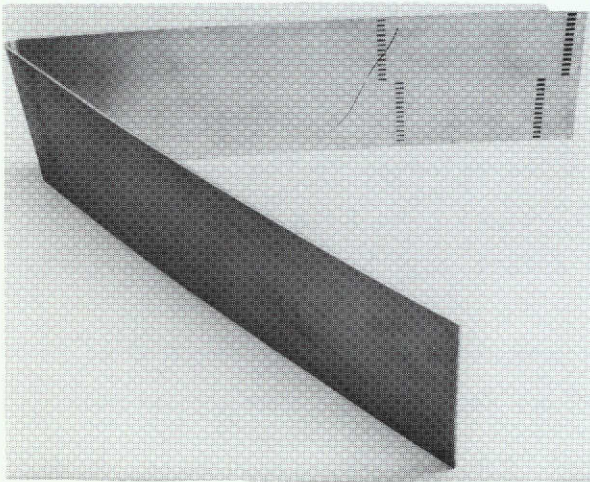


Figure 4. Partially Formed Baffle

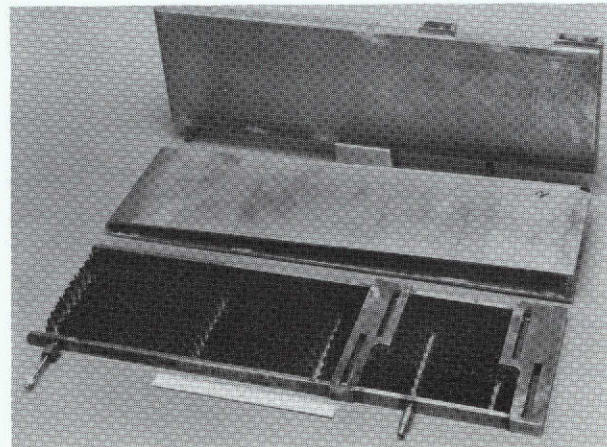


Figure 5. Completed Baffle and Details

The other components were fabricated in a comparable manner (Fig. 6) and then welded together (electron beam or TIG) to form the conditioner (Fig. 7). The trislot injector (two fuel streams injected into a central oxidizer stream) was also fabricated. A completed injector is shown in Fig. 8. The injector, conditioner subassembly, valves, igniter, and associated plumbing were then assembled to complete the conditioner (Fig. 9).

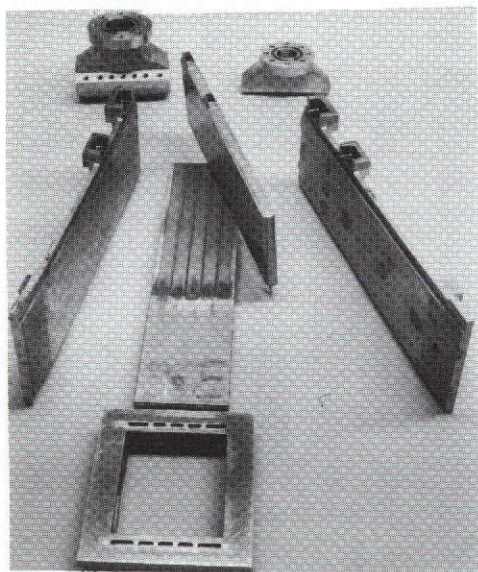


Figure 6. Conditioner Subassemblies and Details

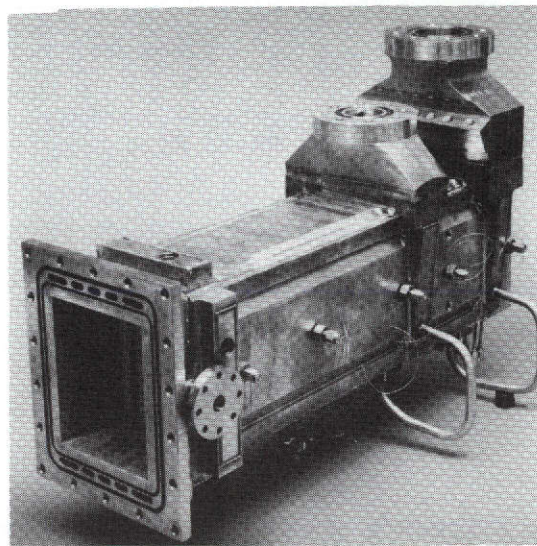


Figure 7. Completed Conditioner

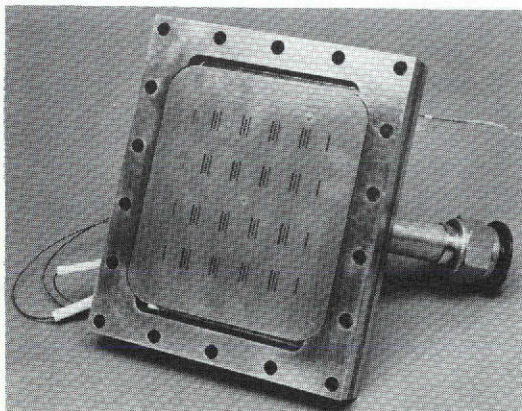


Figure 8. Trislot Injector

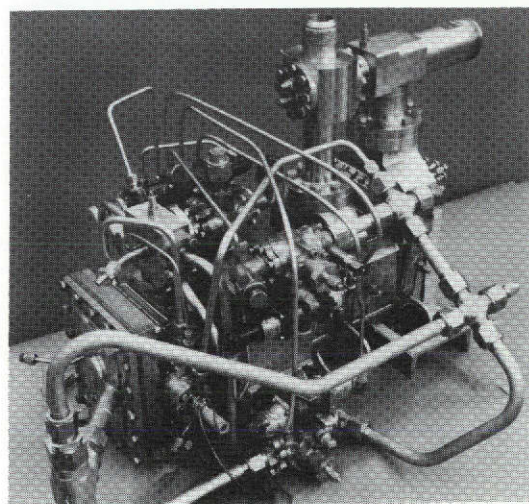


Figure 9. Conditioner Assembly

One complete hydrogen conditioner was fabricated along with details and subassemblies for two additional units.

The conditioner was heavily instrumented to allow for a detailed assessment of hot-gas distribution, heat exchange to each baffle, and baffle wall temperature and injector face temperatures.

After fabrication, the completed unit was pressure tested to verify structural integrity and hot-fire tested at Rocketdyne's Santa Susana Test Facility.

A total of 85 hot-firing tests were completed on this unit including 23 ignition only tests and 62 heat exchange, response, and cycling tests (duration of 0.5 to 30.0 seconds). In addition, a number of no-ignitions were experienced in which the torch igniter did not light the reactor propellants. Investigation showed this to occur at reactor mixture ratios below 0.70. It is noted that during the solid-wall conditioner test effort, the No. 1 injector ignited successfully on every test, even with reactor mixture ratios as low as 0.50. The primary difference between the two test series was the injector. The unit No. 2 injector used on the conditioner tests was a modified version of the unit No. 1 injector used in the solid-wall conditioner tests. This modification consisted of eliminating the injection elements adjacent to the side wall and replacing them with fuel film coolant slots. This change was apparently sufficient to preclude the igniter effluent from reaching an ignitable mixture on the lower mixture ratio tests.

The test program is summarized in Table 3 and the test matrix is shown in Table 4. Traces of typical tests are shown in Fig. 10 through 12.

TABLE 3. LH₂ CONDITIONER TEST SUMMARY

● Total Number of Hot-Firing Tests	85
Ignition Only	23
Heat Exchange/Response Tests	62
● Accumulated Duration (reactor burn time), seconds	197
● Range of Test Conditions	
Reactor Mixture Ratio	0.70 to 0.95
Reactor Flowrate, lb/sec	0.73 to 1.07
LH ₂ Flowrate, lb/sec	2.32 to 4.08
Test Duration, seconds	0.6 to 30.0

TABLE 4. LH₂ CONDITIONER TEST MATRIX

● IGNITION/RESPONSE DATA	13 TESTS
DURATION	0.5 sec
MIXTURE RATIO RANGE	0.70 to 0.93 o/f
LH ₂ FLOWRATE	2.36 to 2.82 lb/sec
● BASIC HEAT EXCHANGE DATA	9 TESTS
DURATION	2.0 to 5.0 sec
MIXTURE RATIO RANGE	0.90 to 0.94 o/f
LH ₂ FLOWRATE	2.32 to 3.11 lb/sec
● "WORST CASE" PULSE DATA	9 TESTS
DURATION	3 sec on/ 2 sec off
MIXTURE RATIO RANGE	0.70 to 0.92 o/f
LH ₂ FLOWRATE	2.61 to 3.23 lb/sec (continuous)
● NOMINAL PULSE DATA	19 TESTS
DURATION	3 sec on/ 2 sec off
MIXTURE RATIO RANGE	0.93 to 0.95 o/f
LH ₂ FLOWRATE	2.92 to 3.79 lb/sec
● SIMULATED MISSION DUTY CYCLE	11 TESTS
DURATION	3-5 sec on/ 5 sec-5 min off
MIXTURE RATIO	0.90 to 0.95 o/f
LH ₂ FLOWRATE	3.19 to 4.08 lb/sec
● DURATION CAPABILITY DEMONSTRATION	1 TEST
DURATION	30 sec
MIXTURE RATIO	0.87 o/f
LH ₂ FLOWRATE	3.40 lb/sec
62 TOTAL TESTS	

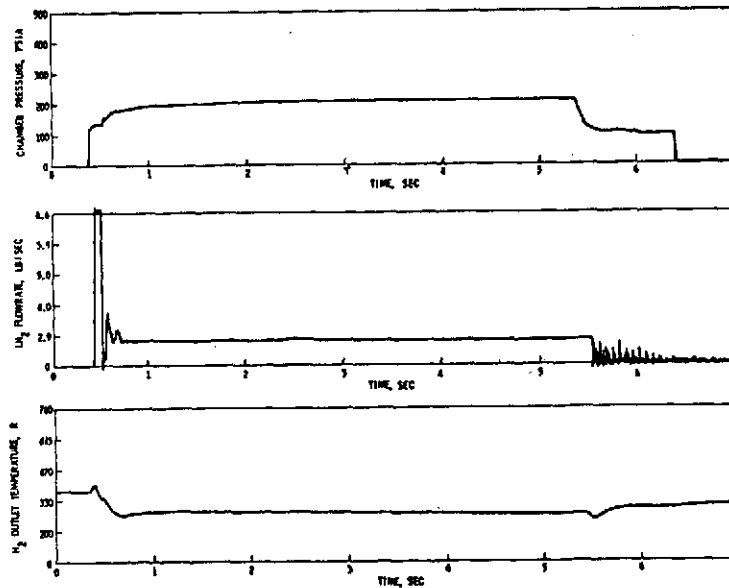


Figure 10. Test 213-Nominal 5-Second Test

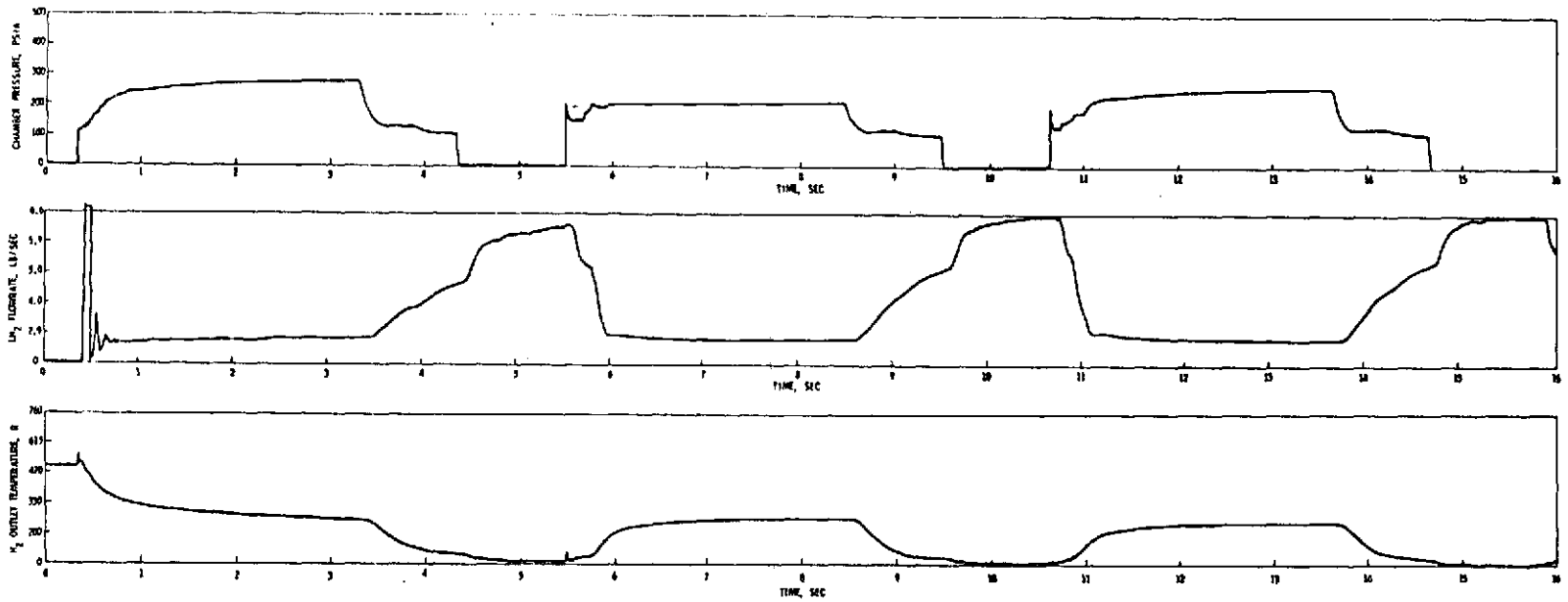


Figure 11. Test 219 - "Worst Case" Cycling With LH₂ Flowing Continuously

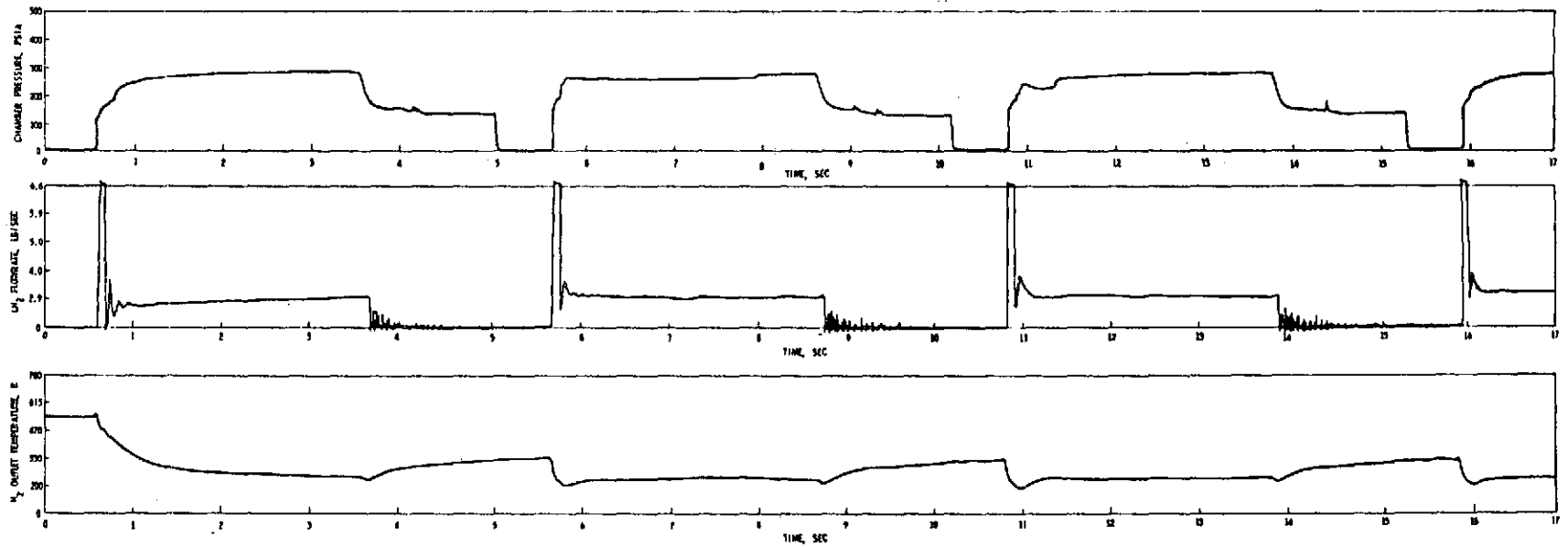


Figure 12. Test 227 - Cycle Test Data, 3 Seconds On/2 Seconds Off (LH₂ Flow Off Between Cycles)

Posttest evaluation of the hardware showed no signs of overheating; however, there was evidence of some baffle distortion.

Disassembly of the hardware showed the center baffle, which had been instrumented for the wall temperature measurement, had collapsed somewhat. The collapse occurred in the region where the internal honeycomb structure had been cut away to allow installation of the thermocouples. Review of the test data showed this collapse occurred during the worst-case cycling tests and has been attributed to a combination of pressure and nonsymmetrical thermal loads.

Posttest data analysis has shown the response of the conditioner to be quite good, as shown in Fig. 13. The experimental data verified the heat exchanger design values within 10 percent. This could be improved even more with a more efficient injector. A typical case illustrating these results is shown in Table 5.

The pressure drop of the LH_2 through the baffles was higher than calculated (due to lower-than-design channel cross-section dimensions and higher-than-design surface roughness in the channels). However, this had no apparent effect on determining the heat transfer rates. In addition, due to manufacturing tolerance buildup, the hot-gas passages were somewhat smaller than design, reducing the hot-gas flowrate at the design chamber pressure. The heat exchange results of the program were very satisfactory; however, experimental results did show the sensitivity of the concept to reactor mixture ratio and hot-gas flowrate.

An assessment of program accomplishment versus requirements is given in Table 6, showing that a strong technology base was established for the baffle type conditioner.

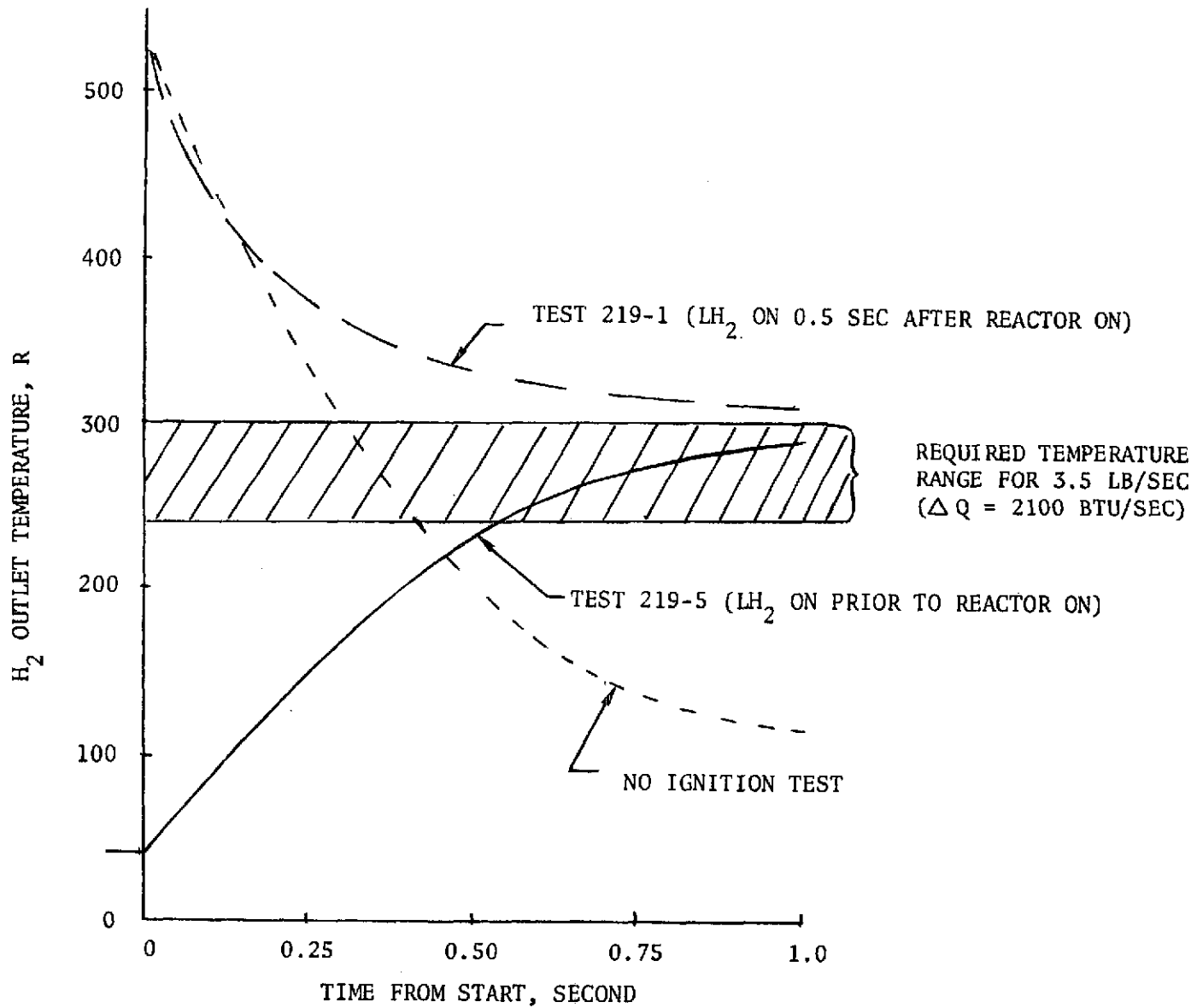


Figure 13. Conditioner Response, Extreme Cases

TABLE 5. POSTTEST THERMAL ANALYSIS

TYPICAL HEAT EXCHANGE RESULTS (TEST NO. 213)

OPERATING CONDITIONS

DURATION = 5.0 SECONDS

\dot{W}_{LH_2} = 2.767 LB/SEC

\dot{W}_{HG} = 0.973 LB/SEC

$T_{IN_{H_2}}$ = 52 R

MR = 0.910 o/f

$T_{OUT_{MIXER}}$ = 230 R

HEAT INPUT

ΔQ_{DESIGN} = 2360 BTU/SEC (η_{c^*} = 100 PERCENT)

= 2130 BTU/SEC (η_{c^*} = 97 PERCENT)

$\Delta Q_{MEASURED}$ = 2107 BTU/SEC (SUM OF HEAT INPUT TO EACH BAFFLE)

HEAT EXCHANGE RESULTS

$\frac{\Delta Q_{MEASURED}}{\Delta Q_{DESIGN}}$ = 89.3 PERCENT (η_{c^*} = 100 PERCENT)

= 99.0 PERCENT (η_{c^*} = 97 PERCENT)

TABLE 6. PROGRAM ASSESSMENT

REQUIREMENT	RESULT
ANALYTICALLY ESTABLISH GRAPH OF TOTAL WEIGHT VERSUS REACTANT EXHAUST TEMPERATURE	ANALYSIS COMPLETED AND 750 R EXHAUST TEMPERATURE SELECTED FOR REACTOR MIXTURE RATIO EQUAL TO 1.0
PROVIDE CONDITIONED FLUID WITHIN 1/2 SECOND AFTER FLOW IS STARTED	DEMONSTRATED ON HOT-FIRING TESTS. RESPONSE <0.5 SECOND
CONDITIONER MUST BE CAPABLE OF STEADY- STATE OPERATION AND SHORT INTERMITTENT RUNS (2 SECONDS) WITH OFF TIMES OF 2 SECONDS TO 24 HOURS	TEST DURATIONS OF 0.5 TO 30 SECONDS ACCOMPLISHED. HARDWARE ALSO CYCLED: 3 SECONDS ON/2 SECONDS OFF 3 SECONDS ON/5 SECONDS OFF 3 SECONDS ON/10 SECONDS OFF 5 SECONDS ON/10 SECONDS-2 MINUTES, 5 MINUTES OFF (MDC)
<u>COLD FLUID (LH₂ SIDE)</u> P _{IN} , PSIA 1100 TO 2100, 1600 (NOMINAL) P _{OUT} , PSIA RANGE NOT SPECIFIED, 1500 (NOMINAL) T _{IN} , R 40 TO 70	P _{IN} , PSIA 1350 TO 1880 P _{OUT} , PSIA 1308 TO 1638 T _{IN} , R 52 TO 65 ALL TEST OF DURATION >2 SECONDS EXCEPT TEST 235 61 TO 106 TEST 235 (30 SECONDS DURATION) DUE TO LOW LEVEL OF LH ₂ IN RUN TANK
T _{OUT} , R 200 TO 250	T _{OUT} , R 155 TO 206* LOWER THAN REQUIREMENT DUE TO REDUCED η _{inj} OF INJECTOR (94 TO 95 PERCENT VERSUS PREDICTED 98 PERCENT) *ADJUSTED TO W = 4.5 LB/SEC
ΔP, PSI 100 (NOMINAL)	ΔP, PSI 140 ΔP HIGHER THAN DESIGN DUE TO REDUCED CHANNEL CROSS-SECTION DIMENSION AND INCREASED ROUGHNESS IN CHANNEL
W _{LH₂} , LB/SEC THROUGH CONDITIONER 1.8 TO 3.57 2.7 (NOMINAL) OVERALL 3.0 TO 5.95 4.5 (NOMINAL)	W _{LH₂} , LB/SEC THROUGH CONDITIONER 2.3 TO 4.2 LB/SEC OVERALL 2.32 TO 4.2 LB/SEC (NO BYPASS USED)
<u>REACTOR</u> INLET PRESSURE, PSIA 375	INLET PRESSURE, PSIA 520 (TYP) EXISTING VALVE ΔP MUCH GREATER THAN EVENTUAL FLIGHT VALVE. ALSO INCREASED ΔP DUE TO FLOW CIRCUITRY USED TO PROVIDE FLOW MEASUREMENT
INLET TEMPERATURE, R H ₂ = 275 TO 600 O ₂ = 375 TO 600 530 NOMINAL MIXTURE RATIO AS REQUIRED-0.85 AT 530 R (NOMINAL) W, LB/SEC AS REQUIRED-1.05 LB/SEC AT 530 R (NOMINAL)	INLET TEMPERATURE, R 560 (TYP) AMBIENT TEMPERATURE AT SITE MIXTURE RATIO - - - 0.70 TO 0.95 (TESTS ≥ 2 SECONDS DURATION) W, LB/SEC - - - 0.73 TO 1.07 (TESTS > 2 SECONDS DURATION)
<u>TECHNOLOGY</u> DETERMINE SERIOUS PROBLEM AREAS	SOLID WALL CONDITIONER TESTED 54 TIMES TO VERIFY CONCEPT
<u>LIFE</u> MUST BE CAPABLE OF 100 FLIGHTS OVER 10-YEAR PERIOD. NO DEGRADATION DUE TO FAILURE OF REACTOR OR COLD FLUIDS TO FLOW	LOW MIXTURE RATIO OPERATION (<1.0) ALLOWS CONDITIONER TO RUN UNCOOLED IGNITION PHASE OPERATION PRECLUDES REACHING FULL COMBUSTION IN REACTOR WITHOUT COLD FLUID FLOW (DEMONSTRATED ON SOLID WALL CONDITIONER)

DISCUSSION

The space shuttle vehicle as originally configured used oxygen/hydrogen propellants for the auxiliary propulsion system (APS). These propellants were to be stored as low pressure liquids in the main propellant tanks and then pumped to high pressure, gasified and stored in accumulators until used by the APS. This was accomplished by a propellant conditioning assembly (PCA) which consisted of a turbopump, a propellant thermal conditioner (gas generator and heat exchanger) and the associated valves and controls. As the quantity of gaseous propellants in these accumulators diminished the PCA was to be cycled on again to replenish the supply.

The PCA was required to operate many times during any one mission and as such demanded high efficiency to minimize system weight and volume.

Cognizant of this NASA-MSC awarded Rocketdyne a technology program to evaluate a compact highly efficient baffle type thermal conditioner for this application. Conditioner design and operating criteria are set forth in Tables 7 through 9.

TABLE 7. THERMAL CONDITIONER DESIGN REQUIREMENTS AND GOALS

- MINIMUM WEIGHT - HARDWARE + REACTANT
- LONG LIFE - 100 MISSIONS OVER 10 YEARS
- STANDARD MATERIALS & MANUFACTURING PROCESSES WHERE POSSIBLE
- REALISTIC DESIGN SPECIFICATIONS
- SPECIAL OPERATING PROCEDURES &/OR SUPPORT HARDWARE DEFINED

TABLE 8. THERMAL CONDITIONER OPERATING REQUIRMENTS

- SIMULTANEOUS OR INDIVIDUAL OPERATION
- UNLIMITED DUTY CYCLE
- 1/2 TO 1-1/2 SECONDS PRECONDITION TIME
- PROVIDE CONDITIONED FLUID WITHIN 1/2 SECOND AFTER FLOW STARTED
- CEASE TO PRODUCE CONDITIONED FLUID WITHIN 1/2 SECOND AFTER FLOW TERMINATED
- HOT GAS FLOW ONLY - NO DAMAGE OR LIFE DEGRADATION
- COLD PROPELLANT FLOW ONLY - NO DAMAGE OR LIFE DEGRADATION
- OUTER SURFACE TEMPERATURE 600°F MAXIMUM (even with double failure)

TABLE 9. THERMAL CONDITIONER OPERATING PARAMETERS

	Hydrogen	Oxygen
<u>Cold Fluid Side</u>		
Flowrate, lb/sec	4.5 Nominal 3.0 Minimum 5.95 Maximum	15.6 Nominal 11.5 Minimum 21.0 Maximum
Inlet Temperature, R	40 to 70	160 to 200
Outlet Temperature, R	200 to 250	375 to 425
Inlet Pressure, psia	1600 (nominal) (at 4.5 lb/sec) 1100 (minimum) (at 5.95 lb/sec) 2100 (maximum) (at 3.0 lb/sec)	1600 (nominal) (at 15.6 lb/sec) 1100 (minimum) (at 21.0 lb/sec) 2100 (maximum) (at 11.5 lb/sec)
Outlet Pressure, psia	1500 (nominal)	1500 (nominal)
<u>Hot-Gas Side</u>		
Inlet Pressure, psia		
Steady State	375 ±10 percent	375 ±10 percent
Start-Up	375 ±20 percent	375 ±20 percent
Inlet Temperature, R	275 to 600	375 to 600
Mixture Ratio, o/f	As required	
Flowrate, lb/sec	As required	as required

SELECTED DESIGN CONCEPT

The thermal conditioner concept selected to meet these requirements consisted of the integral heat exchanger and reactor shown previously in Fig. 1.

Hot gases are generated at the forward end of the conditioner and then ducted through relatively small passages between the slotted and formed baffles through which the propellant to be conditioned flows. The heat exchanger and reactor shell uses channel wall construction and standard material and fabrication techniques (Haynes-188 and stainless steel, electrical discharge machining, furnace brazing and electron beam welding). The injector incorporates a tri-slot injection pattern (where two fuel streams impinge on a central oxidizer stream). Ignition is accomplished using a side mounted NASA-LeRC developed spark igniter, and the valves are existing ball valves.

The selected thermal conditioner design utilized a reactor supplying hot gas ($MR = 1$) to a baffle type heat exchanger fabricated of a high temperature alloy, Haynes 188, precluding hot gas leakage into the vehicle. An envelope temperature of less than 600 F is maintained by actively cooling the hot gas portions of the conditioner with the reactor hydrogen flow. With this design the thermal conditioner is not duty cycle restricted.

Propellant flow is sequenced by a flow ladder sequence (similar in concept to a pressure ladder sequence which ensures the capability of coping with the propellant (for conditioning) "no-flow" situation (Fig. 14)). A venturi is placed in the propellant flow circuit and the pressure difference between the venturi inlet and throat is used to actuate a valve to supply to the reactor injector. With this valve closed, oxygen is supplied to the igniter and reduced flowrate to the reactor giving a low mixture ratio. A latch on the valve, actuated by igniter chamber pressure, precludes main oxidizer flow without igniter operation. Thus, the heat exchanger cannot be heated to a high temperature during a "no flow" condition, precluding a condition which will degrade life. Also, cold propellants are not normally introduced into a hot

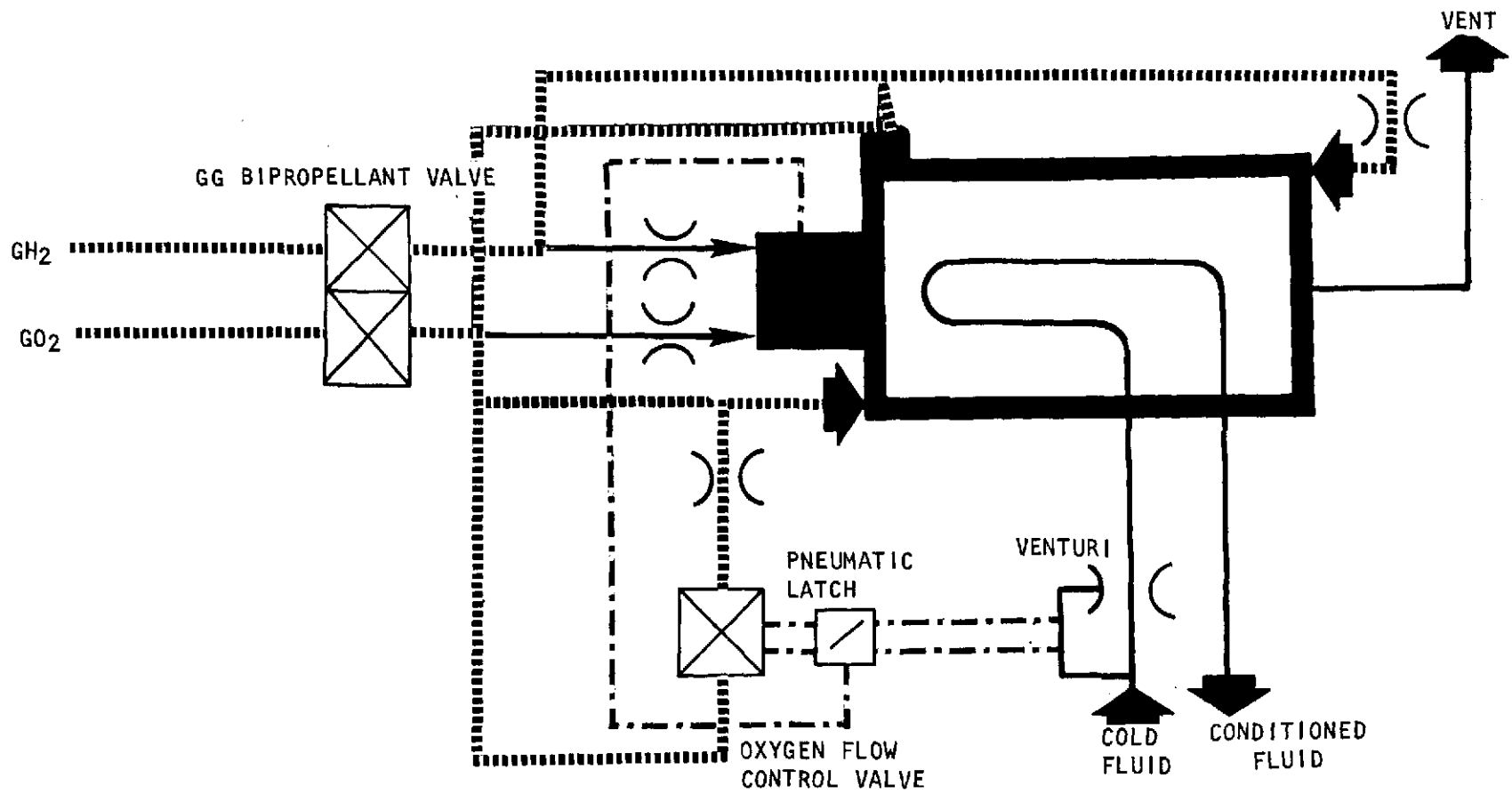


Figure 14. Thermal Conditioner Control System

heat exchanger, thus minimizing the severity of thermal shock and cycling. The cold propellant-flow-only-condition was also analyzed and it was established that no life degradation will result.

The baffle type heat exchanger design allows a controlled heat transfer profile and a more efficient heat exchange. Also, local temperatures can be controlled to avoid icing. A square heat exchanger cross-section was selected over a round cross-section (cylindrical package), since it allows more efficient integration of the heat exchange surfaces into the pressure vessel and results in better heat transfer control. The plate (or baffle) is quite stiff, thus avoiding vortex generated flutter induced by the high velocity hot gas flow around and by the heat transfer surface. The baffle construction is based on standard techniques of high temperature brazing and forming. The baffles are restrained only at one end and free to expand over most of their length. Life analysis showed achievement of the specified life goals with a significant margin.

The reactor is close coupled to the heat exchanger to provide a compact package, simplifying the design by eliminating hot gas interconnects. A tri-slot injector design was selected for this low mixture ratio gas generator application. This injector type promotes recirculation, a desirable attribute for a low mixture ratio gas generator, and characteristically produces uniform mixing. The spark igniter is similar to the air gap igniter developed during the NASA-LeRC-sponsored ignition systems programs. The igniter is mounted on the side of the reactor, and its effluent is impinged and mixed with a row of elements to provide the proper mass flow and mixture ratio. Existing values were used for propellant flow control.

CONFIGURATION ANALYSIS

SUMMARY OF OPERATING PARAMETER SELECTION

Of all the operating requirements set forth for the thermal conditioner, the one which had the greatest single influence on the design was the requirement that no damage or life degradation would result with hot gas flow only. A brief summary of the individual requirements and their effect on the design is summarized below.

No Damage or Degradation of Life with Hot Gas Flow Only

Normally a design which minimized propellant consumption by operating at mixture ratios in the range of 3-8 would be considered for this application. As a result of this requirement Haynes 188, a high temperature conventional material was selected; in addition, the mixture ratio was limited so that the wall temperature would not exceed about 1800 F under this failure mode, with a 10 percent variation in mixture ratio. This resulted in a mixture ratio selection of 1.0 at the nominal hydrogen injection temperature of 275 R. In addition, the first 4 inches of the side walls were cooled with injector GH_2 , so these walls would be cooled with or without the conditioned propellant flow.

Life Requirements - 100 Flights over 10 Year Period

For a given material and design, the life requirements indicated the maximum temperature gradient and thus the maximum heat flux level. This had a strong effect on the conditioner size (surface area requirements). This constraint in conjunction with the desire for low weight and fast response led to tapering the hot gas passage for the first 5 inches from the leading edge.

Avoid Icing on the Hot Gas Side

Requires the minimum hot wall temperature and gas exit temperature be above 32 F. This in conjunction with the selected low mixture ratio for a failsafe design limits the thermal effectiveness of the conditioner. Since icing is most likely to occur at the exit end, the hydrogen outlet manifold was located at this point so as to have the warmest possible hydrogen at this location. In addition, 40 percent of the hydrogen was bypassed to further increase the hydrogen temperature in order to avoid icing, with little sacrifice in pressure drop or surface area requirements. This, in conjunction with a required minimum total weight, resulted in a selected hot gas outlet temperature of 750 R at mixture ratio = 1; this temperature can be increased at higher mixture ratio.

Outer Shell Not to Exceed 600 F

All outer surfaces are cooled. The first 4 inches are cooled by injector GH_2 ; the rest by the conditioned propellant.

Separate Operation of the Hydrogen and Oxygen Conditioners

This requirement led to a selection of two separate conditioners, each with its own reactor.

Fluid Response Within 1/2 Second After Initiation of Flow

This led to use of thin wall construction on all heated surfaces, with the wall thickness determined by stress and manufacturing capability consistent with reliability. This also led to use of the maximum heat fluxes consistent with life requirements and available hot gas pressure.

Duty Cycle With Minimum 2 Seconds On, and 2 Seconds - 24 Hours Off

This along with a simultaneous start signal to the pump and conditioner negated use of a thermal bed in which hot gas is used to heat the bed, and conditioned fluid is run some time later. Without an advance signal, the bed may not be heated sufficiently by the time conditioned propellant is introduced; if on the other hand the bed is always maintained at temperature, this results in more propellant consumption with long off periods (or more insulation requirements).

The above gives a brief summary as to how the operational requirements affect the conditioner design. These are covered in greater detail in other sections of the report.

SELECTION OF OPERATING PARAMETERS

A number of parametric studies were conducted prior to the design of the hardware. The purpose of these studies was to aid in selecting the operating point of the conditioner and to determine the sensitivity of the design to various operational parameters.

The following section discusses in detail the selection of mixture ratio and hot gas outlet temperature.

Mixture Ratio Selection

Selection of the hot gas mixture ratio is based on the requirement that no damage or life degradation result if either hot gas or cold flow is not initiated.⁽¹⁾ Superimposed on this is the requirement that the conditioner be capable of accommodating a situation where full hot gas flow is experienced

⁽¹⁾ It is noted that with the unique flow ladder sequence used in the design concept, this can only occur after a double failure (i.e., oxidizer flow control valve must fail open and pump system must fail to deliver cold propellant).

tion temperature cannot exceed the maximum allowable uncooled steady-state wall temperature of the heat exchanger baffles. This maximum temperature for Haynes 188 (the selected heat exchanger material) is about 2100 F. A discussion of the rationale used to select Haynes 188 for the heat exchanger baffles is presented in a subsequent section. Combustion temperature as a function of mixture ratio and hydrogen injection temperature is shown in Fig. 15 . At the low mixture ratios under investigation, the oxygen injection temperature has negligible effect on the combustion temperature. Another restraint initially placed on the mixture ratio selection is that the maximum combustion temperature should not be exceeded with a ± 10 percent control tolerance on mixture ratio. Subsequent analysis also explored the system benefits of a tighter control on mixture ratio. For the analysis, a nominal mixture ratio of 1.0 was selected, giving the combustion temperature range shown below:

Mixture Ratio	0.9	1.0	1.1
H ₂ injection T = 275 R (nom.)	1430 F	1580 F	1740 F
T = 600 R (max.)	1740 F	1900 F	2060 F

Selection of a nominal mixture ratio of 1.0 resulted in a nominal combustion temperature of 1580 F and a maximum combustion temperature with maximum hydrogen inlet temperature of 2060 F. This was considered an acceptable design point.

The development conditioners to be tested on this program were to be tested with ambient temperature propellants. As is shown in Fig. 15, testing with hydrogen at 530 R results in a combustion temperature approximately 250 degrees higher than that experienced with 275 R hydrogen when operating at the same mixture ratio and chamber pressure.

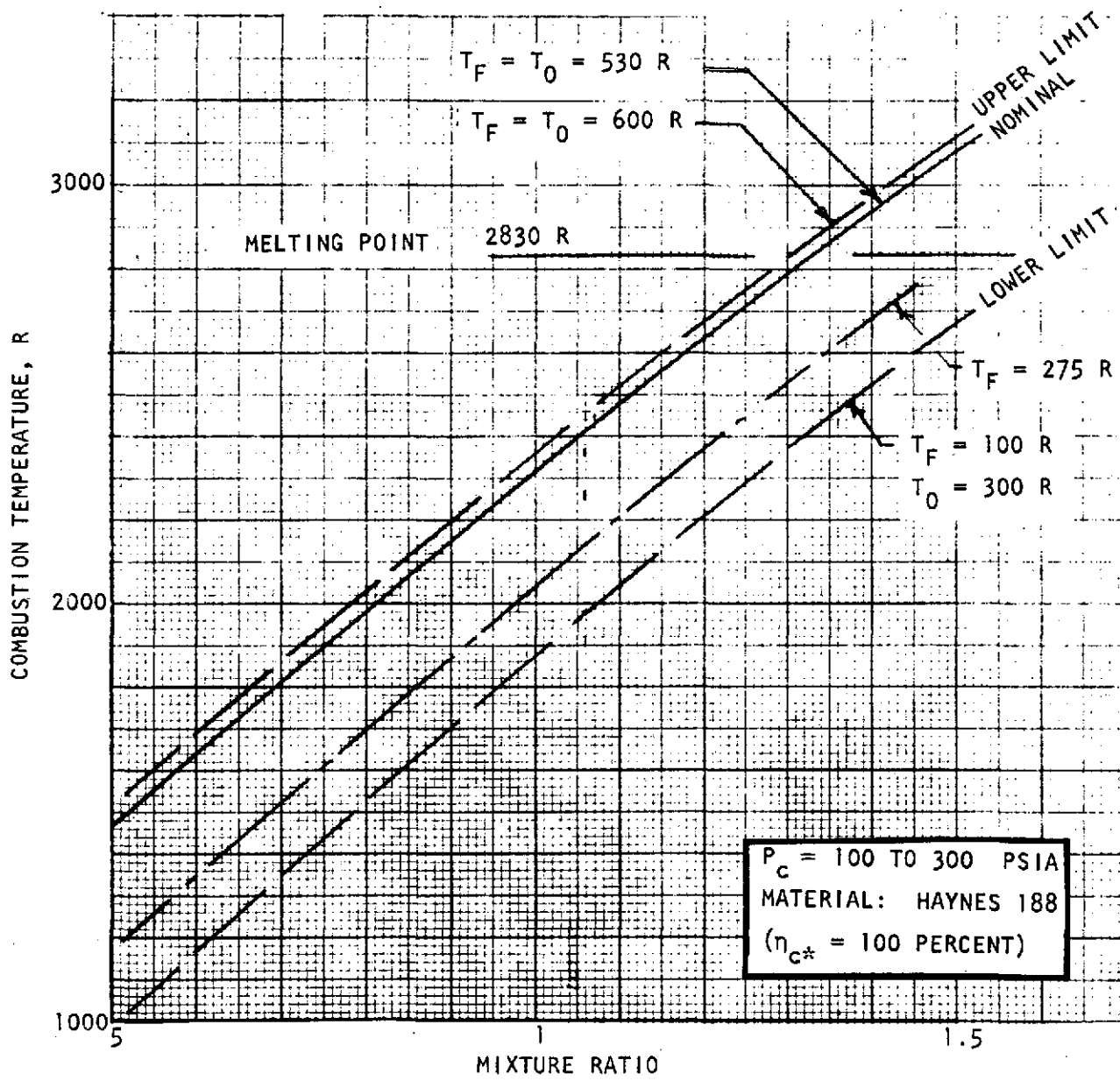


Figure 15. O_2/H_2 Combustion Temperature vs Mixture Ratio and Injection Temperature

Therefore, two possibilities existed for selecting the mixture ratio for the development conditioners - the same mixture ratio or the same nominal combustion temperature can be maintained. If the same nominal temperature is maintained, the resulting mixture ratio and combustion temperatures are:

Mixture Ratio	0.75	0.83	0.91
H ₂ Injection temperature = 275 R	1150 F	1290 F	1420 F
= 530 R	1440 F	1530 F	1700 F
= 600 R	1490 F	1620 F	1750 F

The above numbers are based on a combustion efficiency of 100 percent. Lower combustion efficiencies will result in higher allowable mixture ratios. For example with a 96 percent efficiency and ambient hydrogen, the mixture ratio can be raised from 0.83 to 0.93 while maintaining the same combustion temperature. To be conservative, total combustion was assumed, resulting in the selection of MR = 1.0 for 275 R H₂ and MR = 0.83 with 530 R H₂. In order to minimize propellant consumption, it is desirable to operate at the highest combustion temperature which will satisfy the failsafe criteria; this indicates the desirability of reactor flow regulators which can compensate for the injection temperature of the reactants.

Hot Gas Flow Requirements

The hot gas flow requirements were determined by the conditioned propellant flowrate and enthalpy rise as well as by the hot gas injection temperature, mixture ratio, and outlet temperature. The hot gas enthalpy change as a function of temperature and mixture ratio is shown in Fig. 16 over the range of interest. Below 700 R, water condensation occurs, resulting in a steeper slope to the enthalpy curve. The effect of the hydrogen injection temperature on the hot gas flow requirements is shown in Fig. 17. For example, a hydrogen injection temperature of 100 R requires about 50 percent more flow than with 600 R hydrogen, whereas 275 R hydrogen only requires about 30 percent more

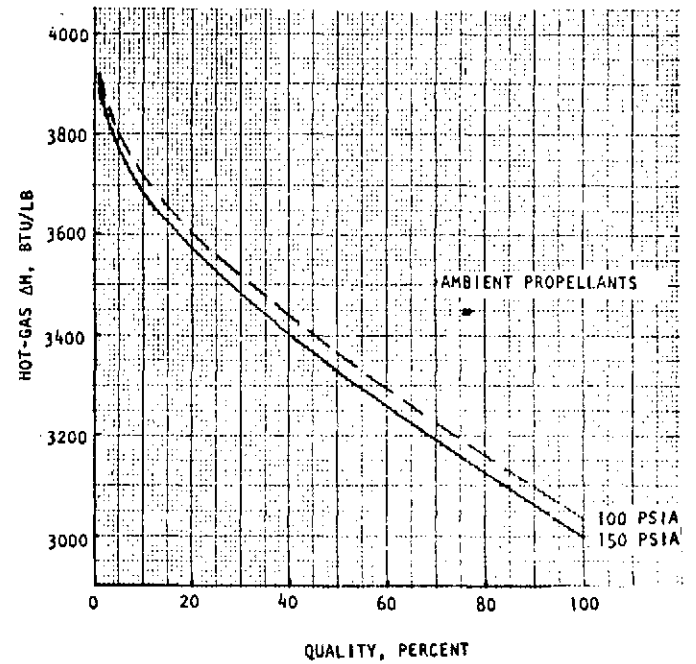
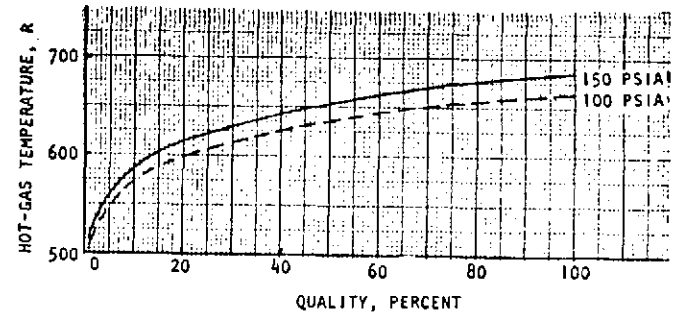
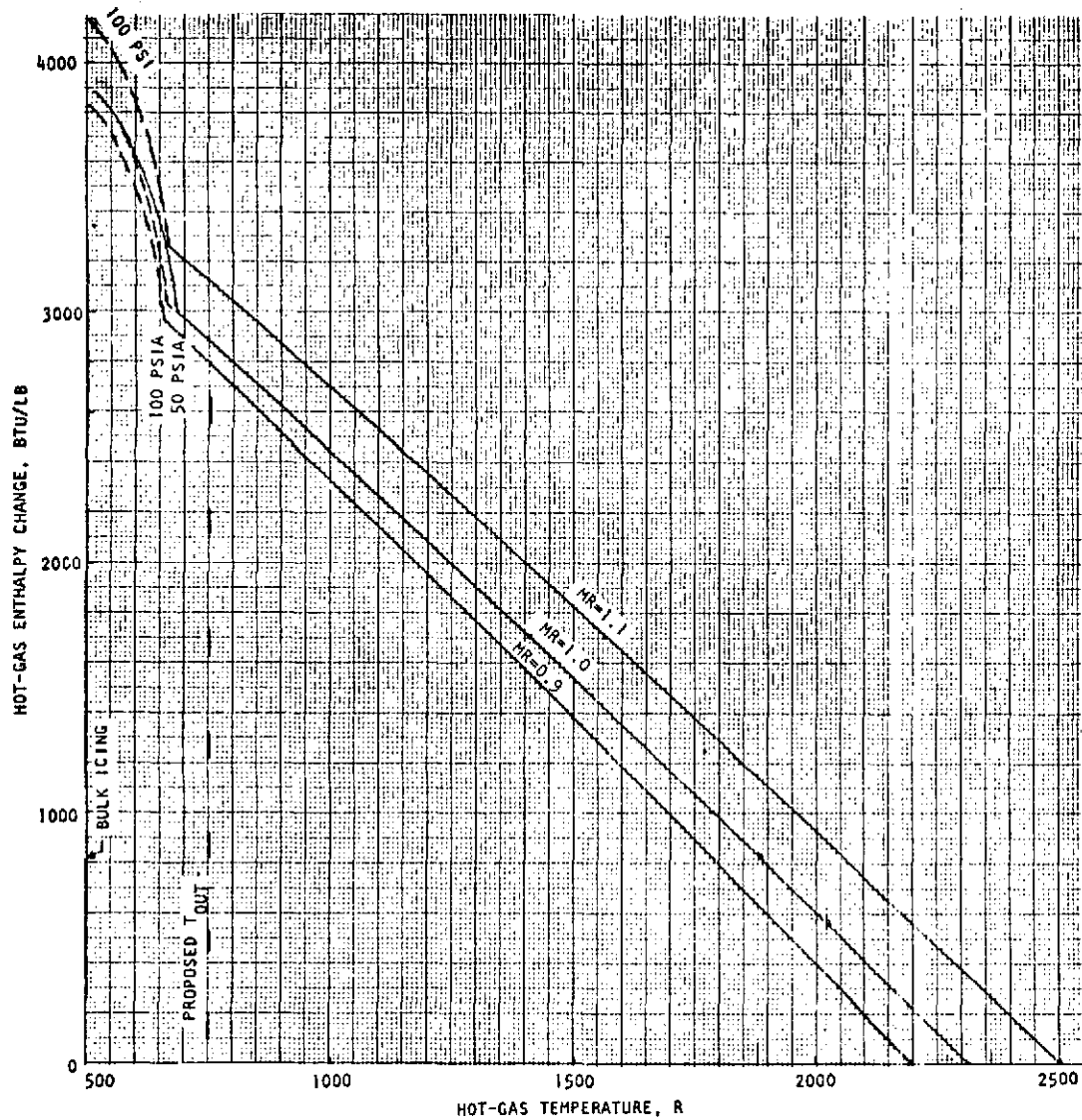


Figure 16. Hot-Gas Water Condensation, MR = 1

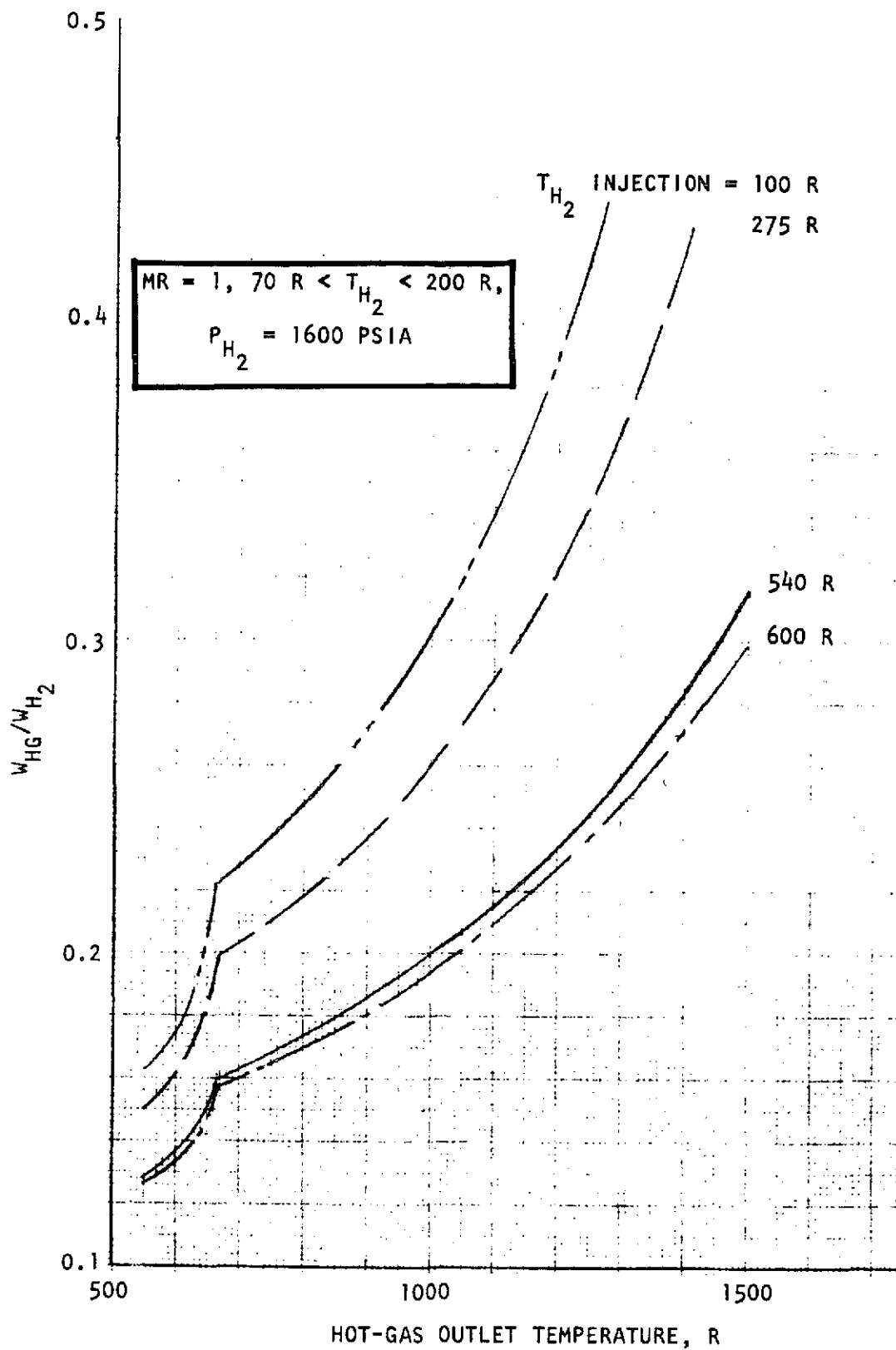


Figure 17. Effect of GH_2 Injection Temperature on Hot-Gas Flow Requirements - H_2 Conditioner

hot gas flow. For a 750 R outlet temperature and a 275 R hydrogen injection temperature, the required hot gas flow is about 21 percent of the hydrogen flow, again assuming perfect combustion.

The effect of the hydrogen enthalpy band specified (40 R-70 R inlet, 200 R-250 R outlet) is shown in Fig. 18. The effect of hydrogen pressure is small; however, the difference between the minimum and maximum hydrogen temperature rise specified in Table 9 is about an additional 50 percent in hot gas flowrate. Due to the large differences involved, the heat input requirements were based on the nominal hydrogen flowrate of 4.5 lb/sec and the average enthalpy change of the hydrogen; the result is a required heating rate of 2800 Btu/sec. The total heat input for 1110 lb of hydrogen is 690,700 Btu. The resulting required total reactor propellant requirements are shown in Fig. 19 as a function of reactor discharge temperature, mixture ratio, and hydrogen injection temperature. The biggest gain in reactor propellant savings occurs around 700 R when condensation occurs. Around 700 R discharge temperature, an increase in mixture ratio of 0.1 results in a propellant savings of 30 pounds with 275 R hydrogen and 15 pounds with 600 R hydrogen. This is equivalent to dropping the discharge temperature from 800 R to 700 R. These weight savings are offset by the increase in conditioner weight as the discharge temperature decreases.

It is noted that for the oxygen conditioner the propellant weight is only about 62 percent of that for the hydrogen conditioner.

Surface Area Determination

The weight of the conditioner is a function of the conditioner surface area. For an initial surface area determination, a maximum heat flux of 4.4 Btu/in.²-sec was used to meet life requirements. A maximum hot gas mass velocity of 0.88 lb/in.²-sec was assumed, based on a chamber pressure of 240 psia, a 750 R discharge temperature, and a mixture ratio of 1. In addition, a minimum wall gas side surface temperature of 525 R was assumed. The resultant surface area is based on the nominal heat input of 2800 Btu/sec. A typical curve of surface

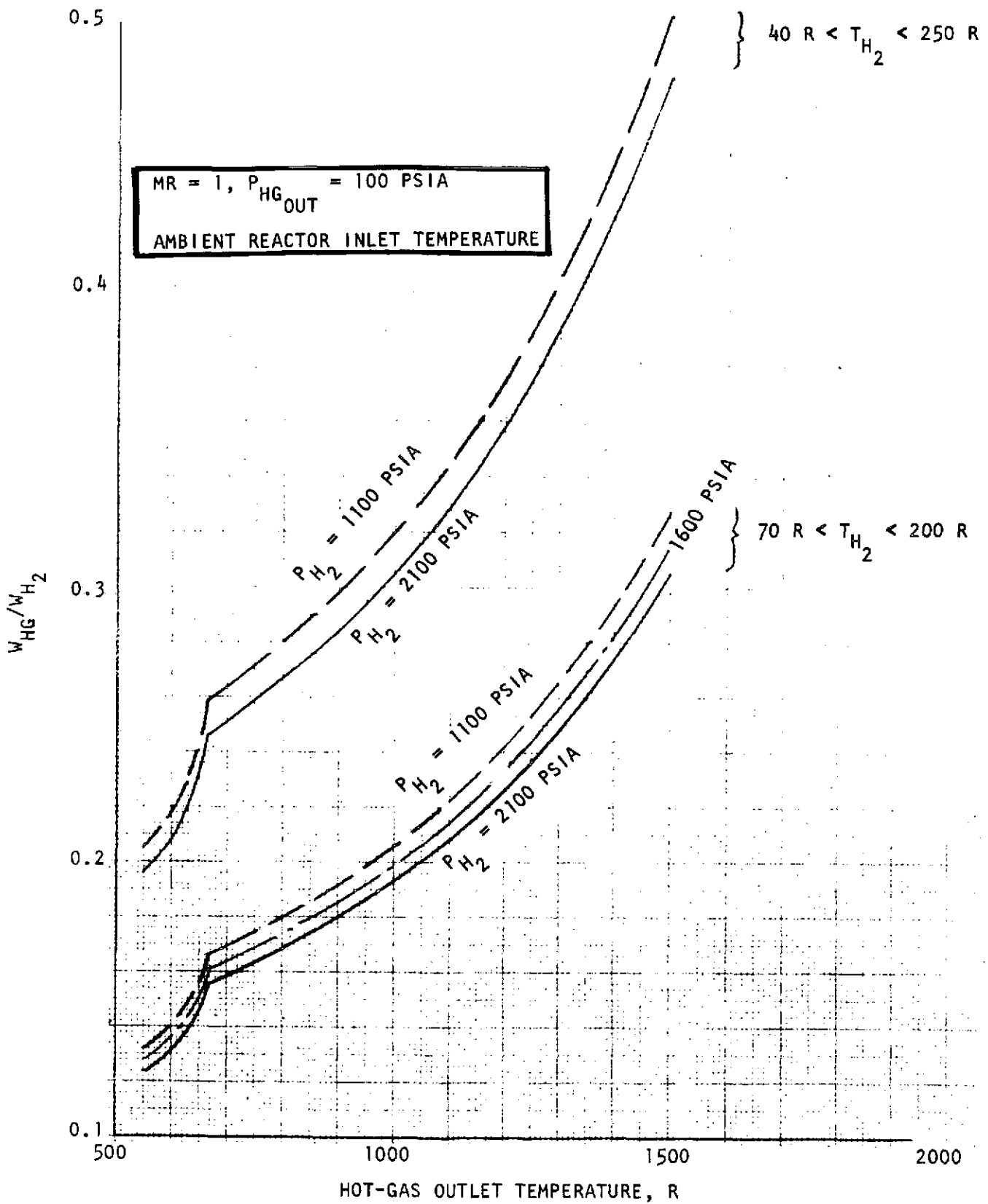


Figure 18. Effect of LH_2 Inlet and Outlet Temperature Range on Hot-Gas Flow Requirements

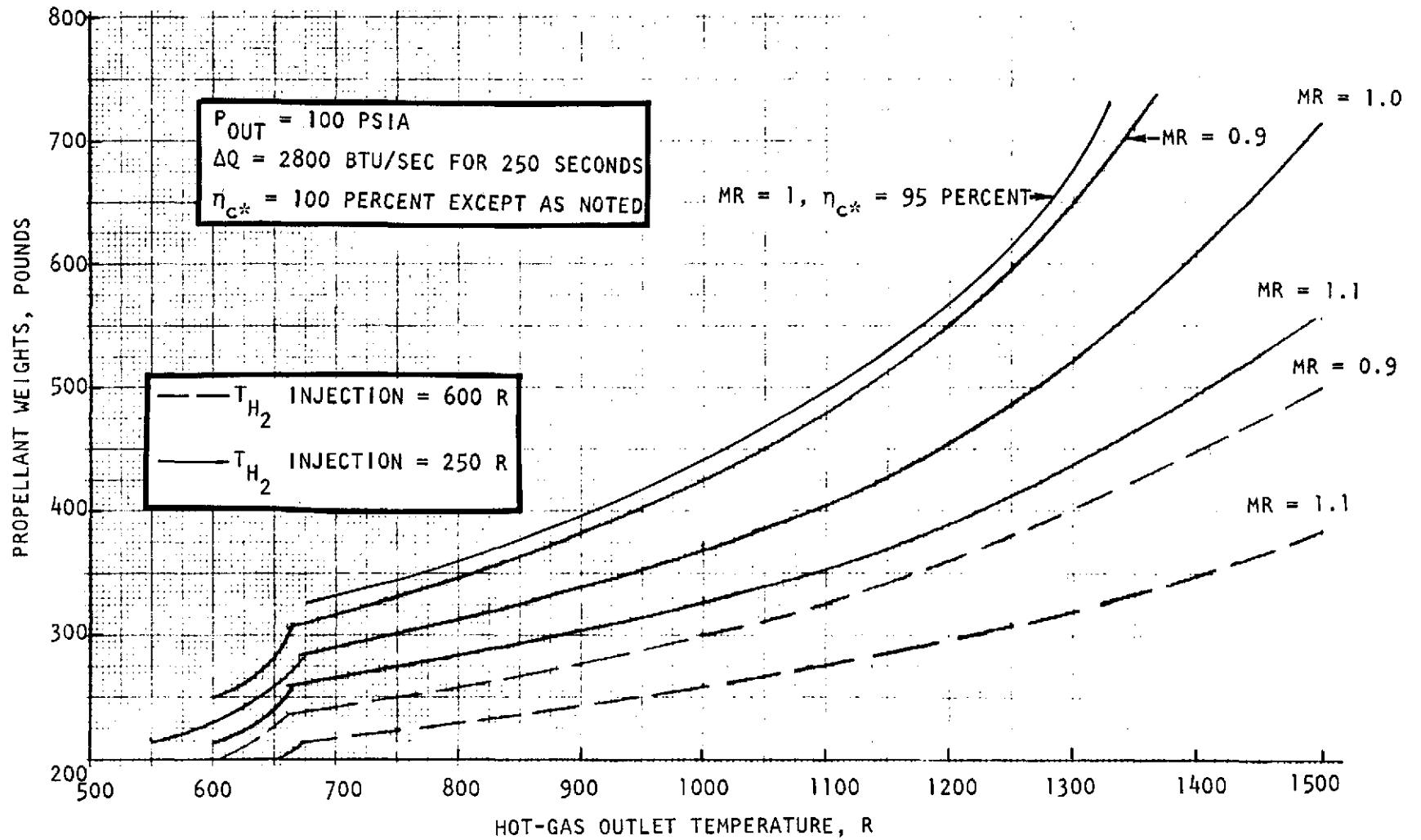


Figure 19. H_2 Conditioner Propellant Weight vs Exhaust Temperature and Mixture Ratio

area vs hot gas exhaust temperature is shown in Fig. 20. This curve is applicable for mixture ratios of 0.9 to 1.1. For hot gas exhaust temperatures in excess of 1500 R, the surface area is essentially independent of exhaust temperature since the heat flux can be maintained at a constant value by tapering the hot gas passage appropriately. For exhaust temperatures below 700 R, the hot gas temperature approaches the minimum wall temperature (525 R assumed) with the result that the conditioner size is increasing very rapidly. For example, if the exhaust temperature is dropped from 700 R to 650 R, the size of the conditioner must be increased about 30 percent. This increase in size shows up principally as an increase in conditioner length.

Hot Gas Outlet Temperature Determination

The hot gas (reactor) outlet temperature was based on minimizing total conditioner weight (sum of hardware and propellant weights). Results of this investigation are shown in Fig. 21 to 23 for mixture ratios of 0.9, 1.0 and 1.1, respectively. The analysis indicates that the minimum weight with one conditioner and 275 R hydrogen injection temperature occurs at a hot gas exhaust temperature of about 600 R. However, if the weight is optimized based on three conditioners, the minimum weight occurs at hot gas exhaust temperatures of 650 R to 750 R. This is the case with or without a reactor tank weight factor of 0.3 lb/lb of reactant included. In order to keep the conditioner size as small as possible, 750 R was selected for the nominal hot gas exhaust temperature. This also has the added benefits of minimizing potential freezing problems and faster response times.

The oxygen conditioner is required to transfer only 1800 Btu/sec compared to the 2800 Btu/sec for the hydrogen conditioner. Since both the surface area (and baffle weight) and the reactant flow requirements are proportional to the heating requirements, it would be expected that the oxygen weight versus outlet temperature curves would be proportionally lower than those for the hydrogen conditioner. The only consideration which might change the shape of the curves at the lower reactant exhaust temperature is that oxygen has poorer heat transfer characteristics and its outlet temperature is nominally higher than

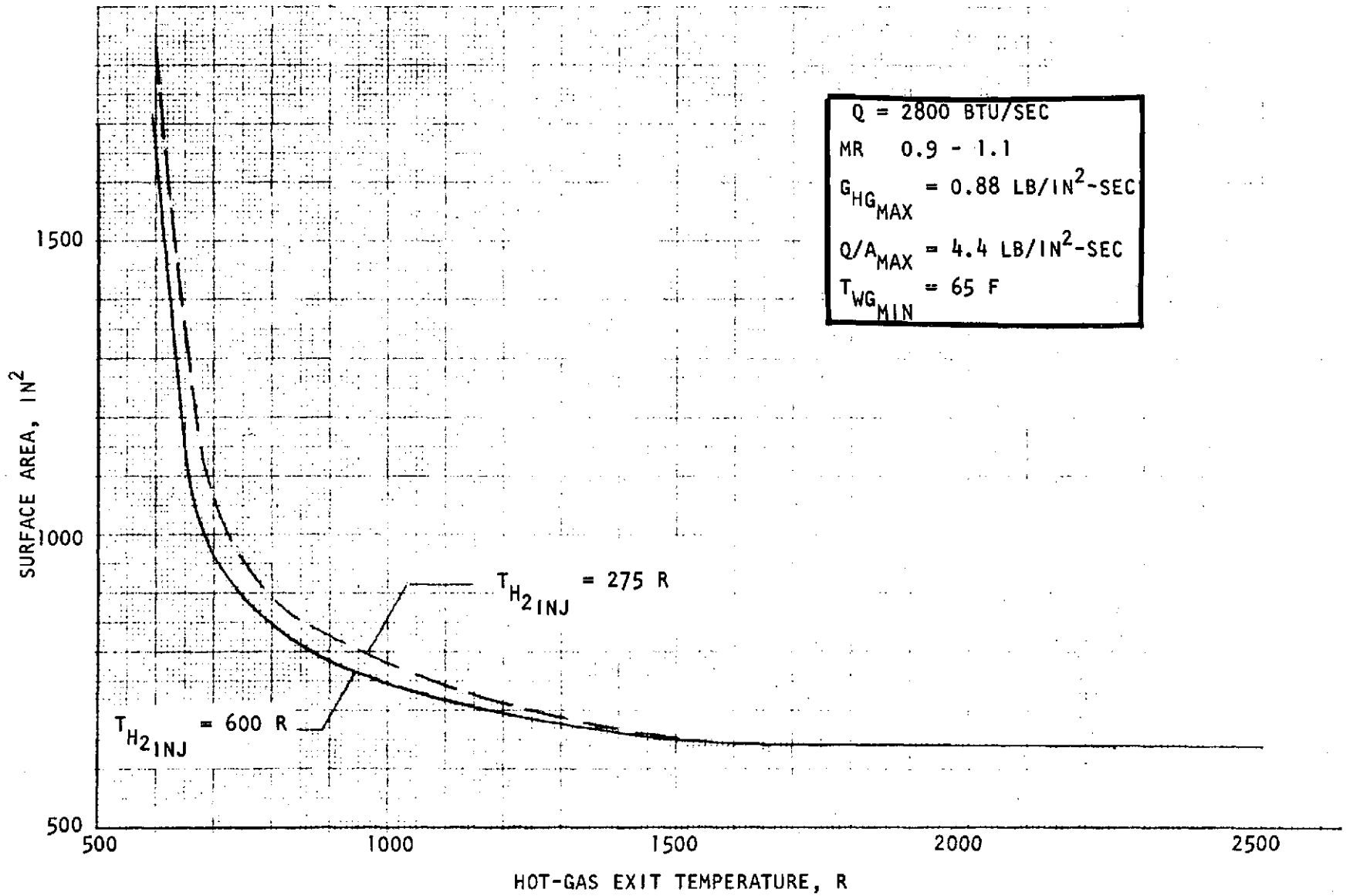


Figure 20. H_2 Conditioner Surface Area

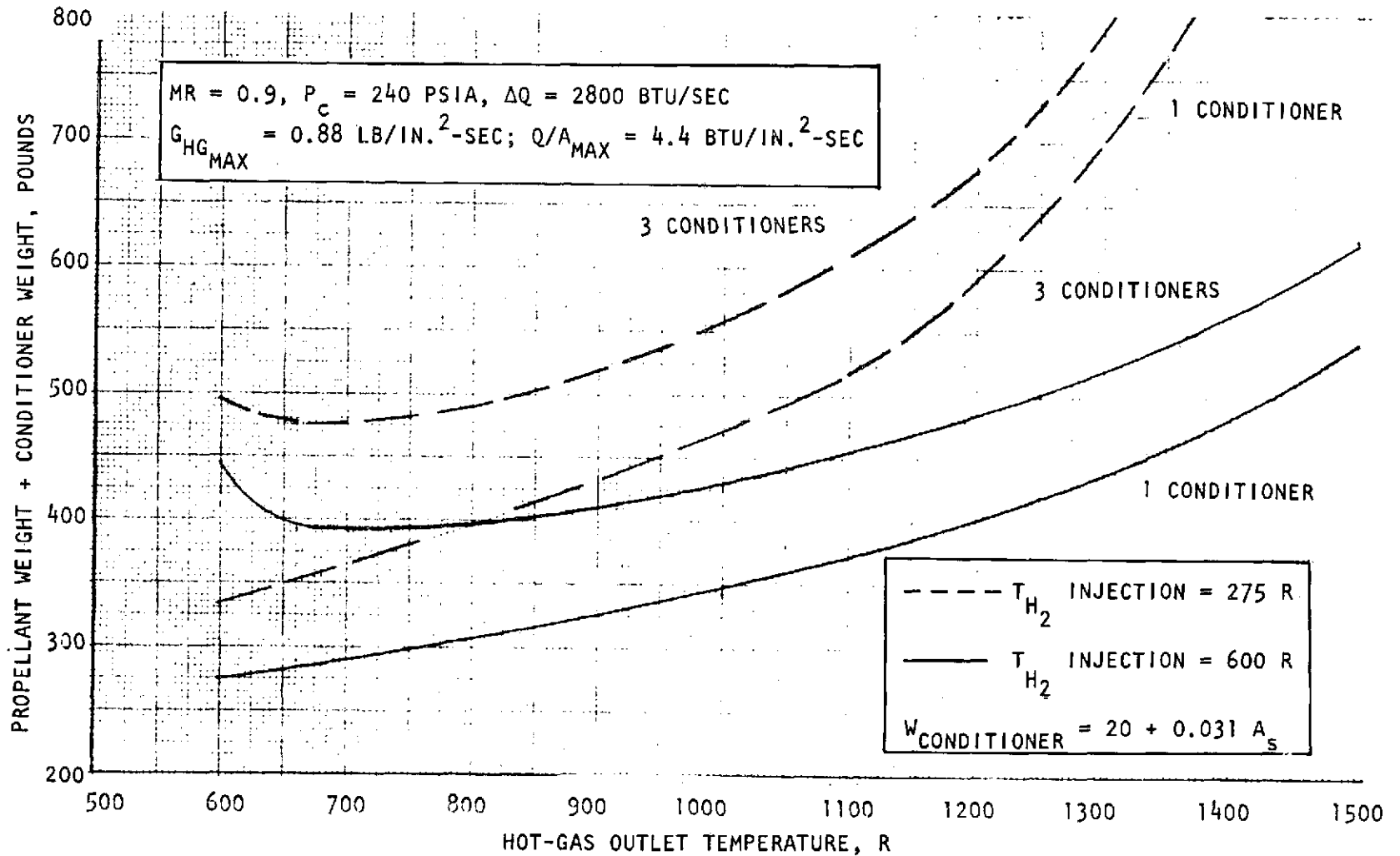


Figure 21. H_2 Conditioner, Total Weight Versus Outlet Temperature

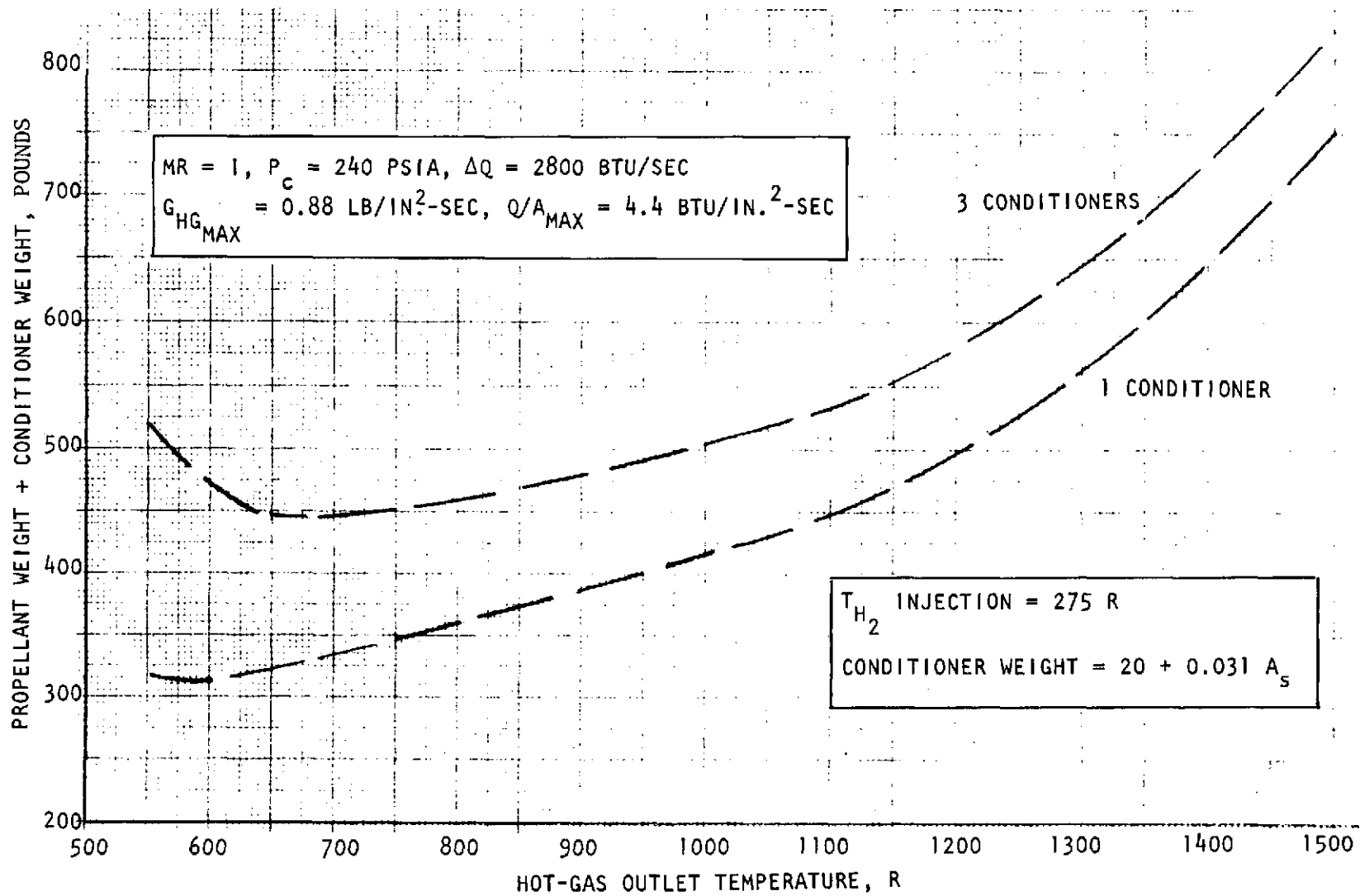


Figure 22. H_2 Conditioner, Total Weight Optimization

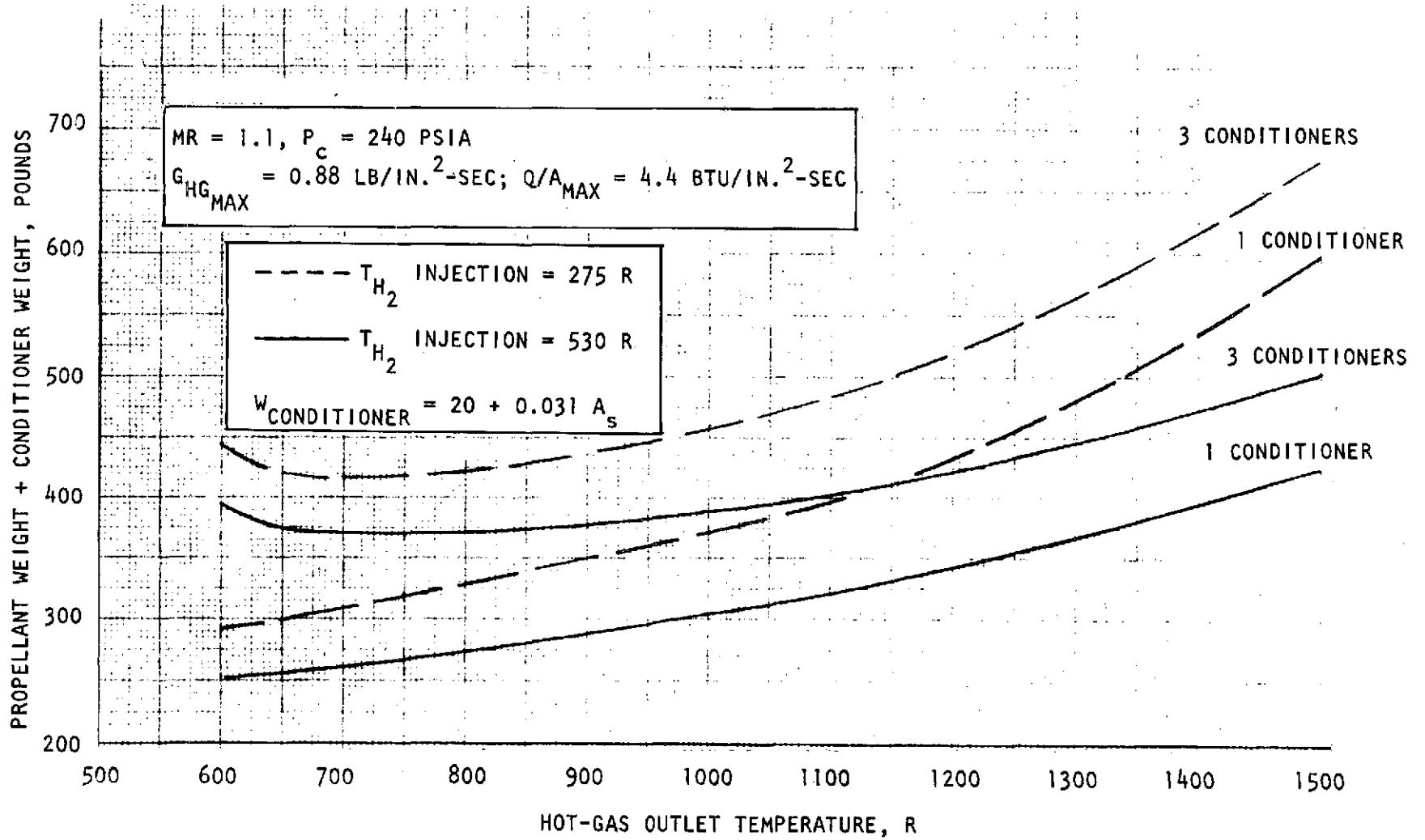


Figure 23. H_2 Conditioner, Total Weight Versus Outlet Temperature

for the hydrogen; this would indicate that the oxygen conditioner may optimize at somewhat higher reactant exhaust temperatures. In addition, because of the higher nominal oxygen outlet temperature, the weight optimization will be more sensitive to bypass on the oxygen conditioner.

A similar conclusion would be expected from the oxidizer conditioner at the same mixture ratios since both the conditioner size and the reactor propellant requirements are proportional to the amount of heat transferred.

CONFIGURATION ANALYSIS

This section covers the selection of the heat flux level, methods to prevent icing including bypassing some of the conditioned propellant, selection of the coolant circuit and channel geometry, and finally the design complete with the operating conditions.

Many parameters affect the design of the hydrogen conditioner. On the gas side, these include mixture ratio, combustion temperature, outlet temperature and chamber pressure. On the conditioned propellant side, this includes flowrate, inlet and outlet temperature, inlet pressure, and allowable pressure drop. In addition, of major importance is the selection of material and the limitations imposed by the failsafe requirement, the life requirement, and the requirement that the gas side be ice free. The finished conditioner must also meet the thermal response requirement. A further consideration in the design is both the manufacturing and the mixture ratio control tolerances.

The total heating rate is important since the required surface area of the conditioner is directly proportional to this parameter. A nominal value of 2800 Btu/sec was selected based on a nominal hydrogen flowrate of 4.5 lb/sec, a nominal inlet temperature of 55 R, and a nominal outlet temperature of 225 R.

The next most important parameters are the selection of the mixture ratio and combustion temperature. In the previous section a mixture ratio of 1.0 was selected based on the fail-safe requirement, using Haynes 188 baffles and assuming a ± 10 percent tolerance on mixture ratio control. The nominal combustion temperature used in the design is 2060 R (1600 F), based on a hydrogen injection temperature of 275 R and an oxygen injection temperature of 375 R. It is noted that at this mixture ratio, the oxygen injection temperature has a very small effect on combustion temperature.

The hot gas outlet temperature of 750 R (290 F) was also selected based on a minimum weight (reactor plus hardware weight for three conditioners). Using the selected hot gas outlet temperature, a hot gas flowrate of 1.2 lb/sec was determined.

Maximum Heat Flux

The maximum heat flux to which the baffles are designed is potentially a function of three variables: chamber pressure affect the maximum heat flux obtainable (not limiting); coolant pressure drop affects the maximum mass velocity and determines the wall temperature for a given wall material as a function of heat flux (not limiting); and the life requirement determines the maximum thermal gradients for a given constraint and a given material (limiting). Using the heat transfer correlations presented in subsequent sections, wall temperature gradients were analyzed for a Haynes 188 baffle with a 0.015 in. gas wall thickness, an assumed hydrogen temperature of -300 F (typical of the baffle leading edge), and using a hydrogen mass velocity of 3 lb/in²-sec (near the upper limit for a 100 psi pressure drop if no bypass is utilized). The resulting temperature gradients are shown in Fig. 24; the closeout temperatures (not shown) are within 5 F of the hydrogen bulk temperature. This figure also shows the heat flux as a function of the hot gas mass velocity under various mixture ratio and hydrogen injection temperatures. Results show that the injection temperature shift has a greater effect on heat

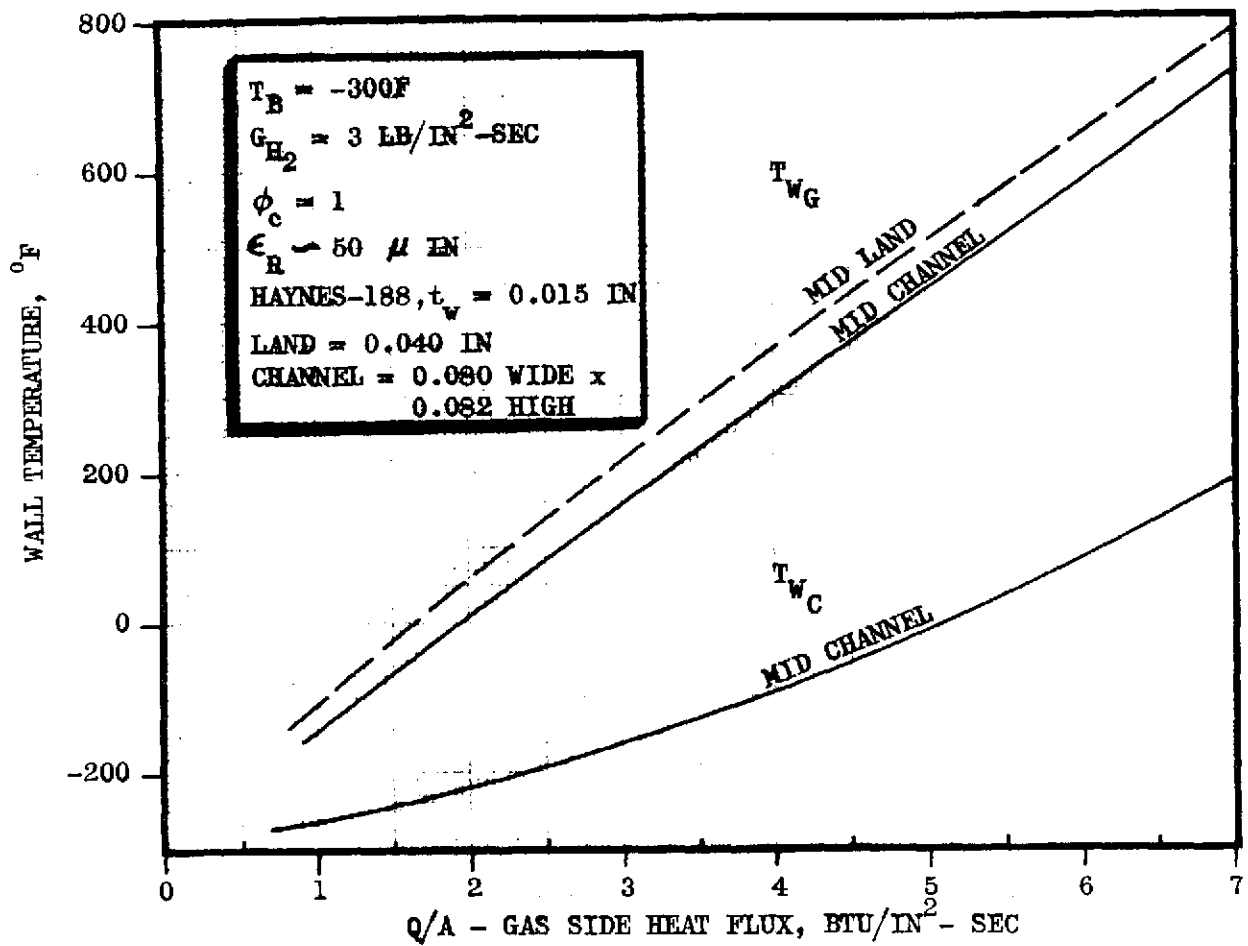
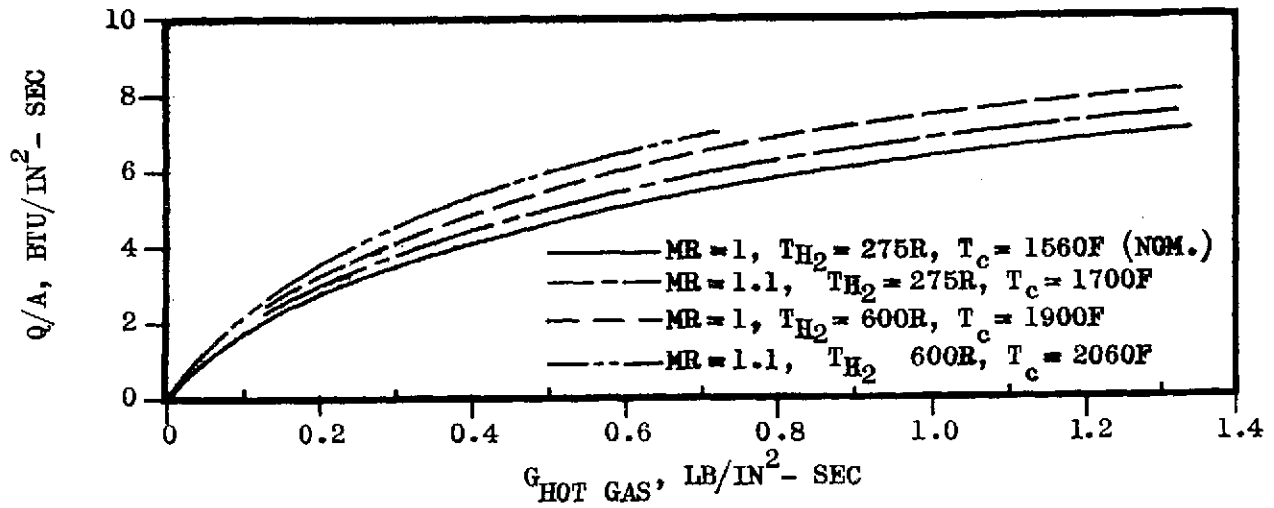


Figure 24. Effect of Injector End Hot Gas Mass Velocity on Heat Flux and Wall Temperature Distribution (H_2 Conditioner)

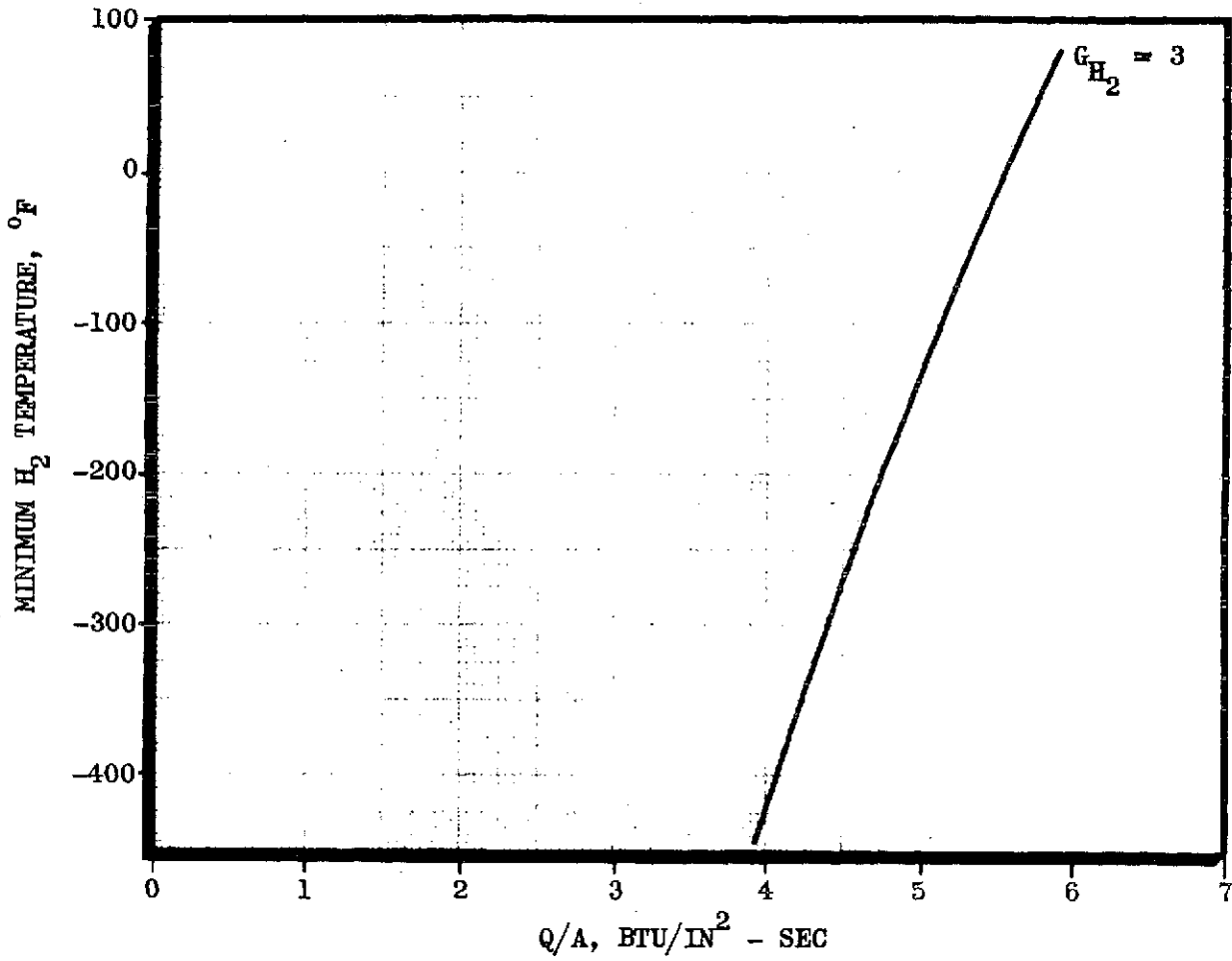


Figure 25. Minimum H₂ Temperature vs Heat Flux Life Requirements for Haynes-188 Baffles (H₂ Conditioner)

flux than the selected mixture ratio shift. These heat fluxes vs hot gas mass velocity were determined using the Bartz equation, as discussed in Appendix D. The wall temperatures as a function of heat flux were determined using the DEAP program (Appendix C) with thermal conductivity varying with temperature and with hydrogen heat transfer coefficients as a function of coolant wall temperature. As will be shown later, these wall temperatures are insensitive to the hydrogen bulk temperature and to the channel geometry, mainly because of the low thermal conductivity of Haynes 188.

Using the data generated in Fig. 24 and the specified life requirements, a resultant curve of minimum hydrogen temperature (back wall temperature) as a function of heat flux was generated (Fig. 25). For hydrogen temperatures typical of those found in the leading edge region for bypass ratios up to 50 percent (-300 F to -250 F) the maximum heat flux is 4.5 Btu/in²-sec. This was reduced slightly to a value of 4.2 Btu/in²-sec in the design. The design value is predicated on the control system being able to maintain the constant heat flux as injection conditions change. If this is not possible, then the peak heat flux at nominal conditions must be reduced to about 3.5 Btu/in²-sec (Fig. 24) so that the peak heat flux (predicated by the life requirements) is not exceeded under the most adverse injection temperature and mixture ratio conditions. The effect of decreasing the peak heat flux from about 4.2 to 3.5 Btu/in²-sec is to increase the surface area requirement approximately 6 percent.

Coolant Bypass

One of the next tasks was to select the amount of hydrogen to run through the conditioner, and how much to bypass around it. First, two-dimensional wall temperatures were determined using the DEAP program for both the case of no bypass and also 50 percent bypass, using a heat flux of about 4 Btu/in²-sec. The resulting temperatures are shown as a function of hydrogen mass velocity in Fig. 26 and 27, respectively. It is seen by comparing these two figures that the effect of bypass on wall temperature is negligible. In

$MR = 1, T_c = 1560F, h_g = 0.0035 B/IN^2 - SEC - F$
 HAYNES-188 GAS WALL THICKNESS = 0.015 INCH
 CHANNEL WIDTH = 0.07-0.08 INCH, LAND WIDTH = 1/2 CHANNEL WIDTH
 $H_2 T_B = -299F, NO CURVATURE$

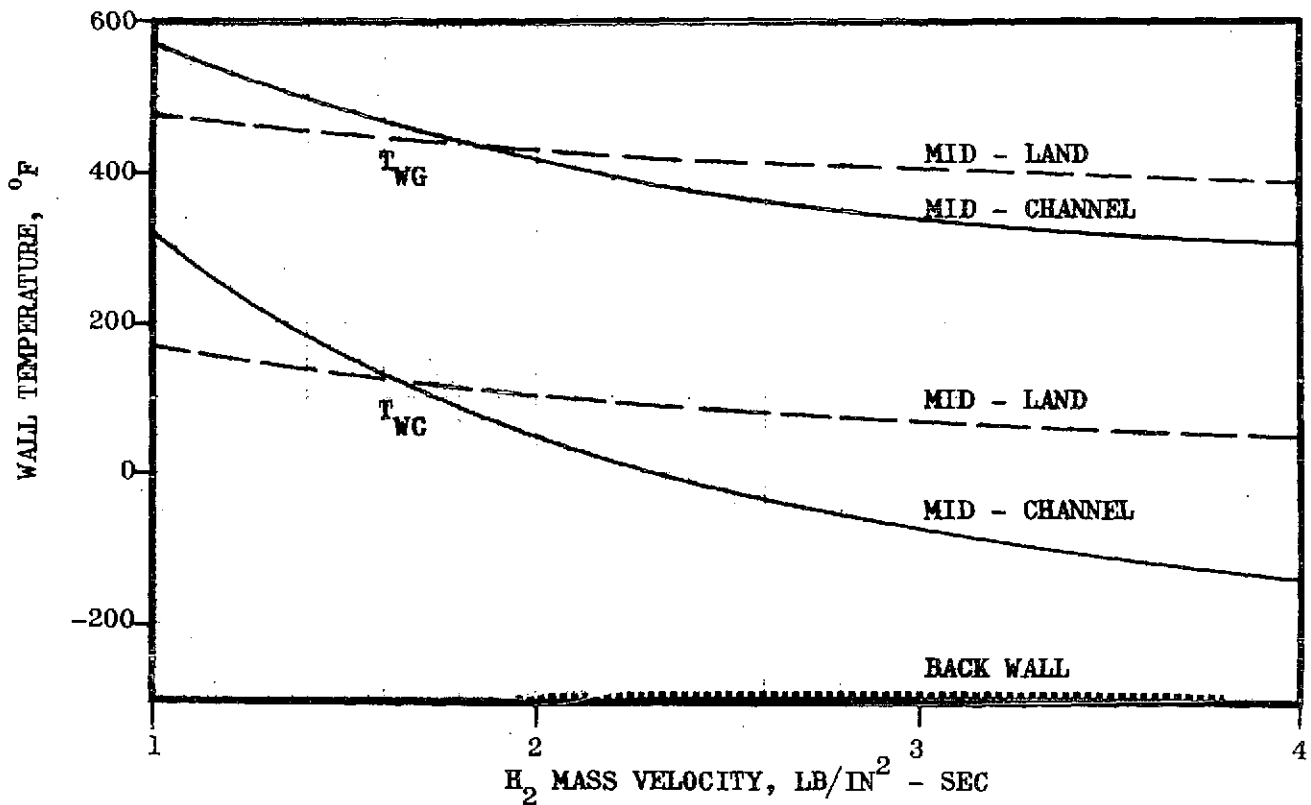
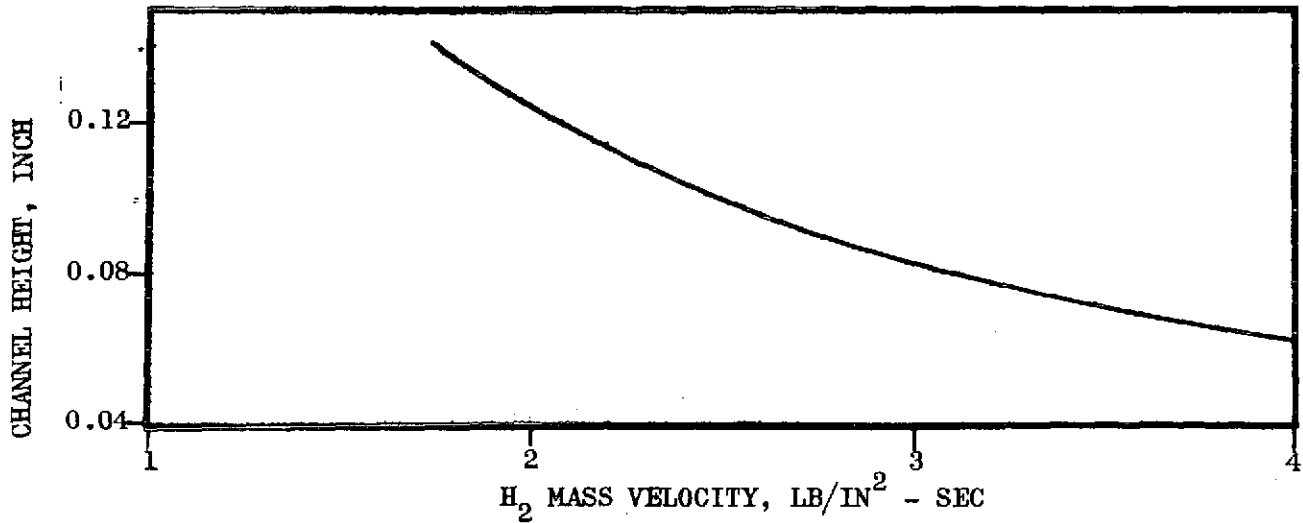


Figure 26. Temperature Gradients Near Baffle Leading Edge, No H_2 Bypass

H_2 OUTLET AT BAFFLE EXIT, H_2 INLET AT 2/3 FROM LEADING EDGE
 MR = 1
 $T_c < 1560$ °F
 $h_g = 0.0035$ BTU/IN²-SEC-°F
 HAYNES-188 GAS WALL THICKNESS = 0.015 IN
 LAND WIDTH = 0.040 IN
 50 PERCENT BYPASS

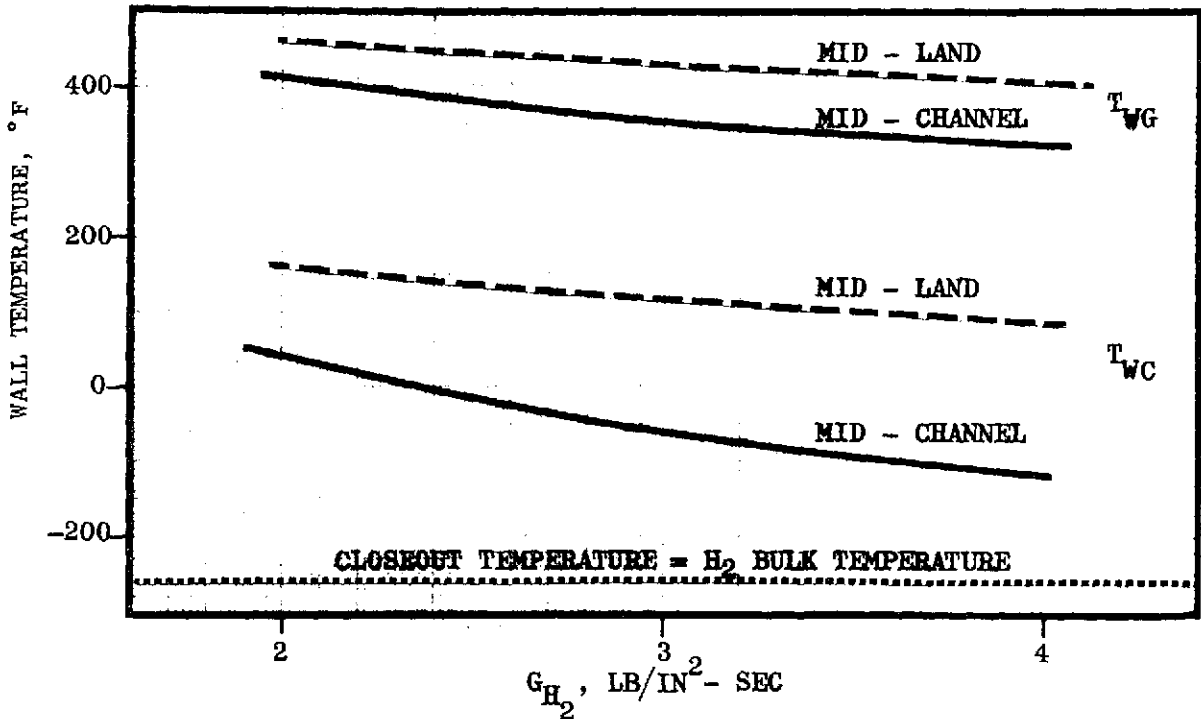
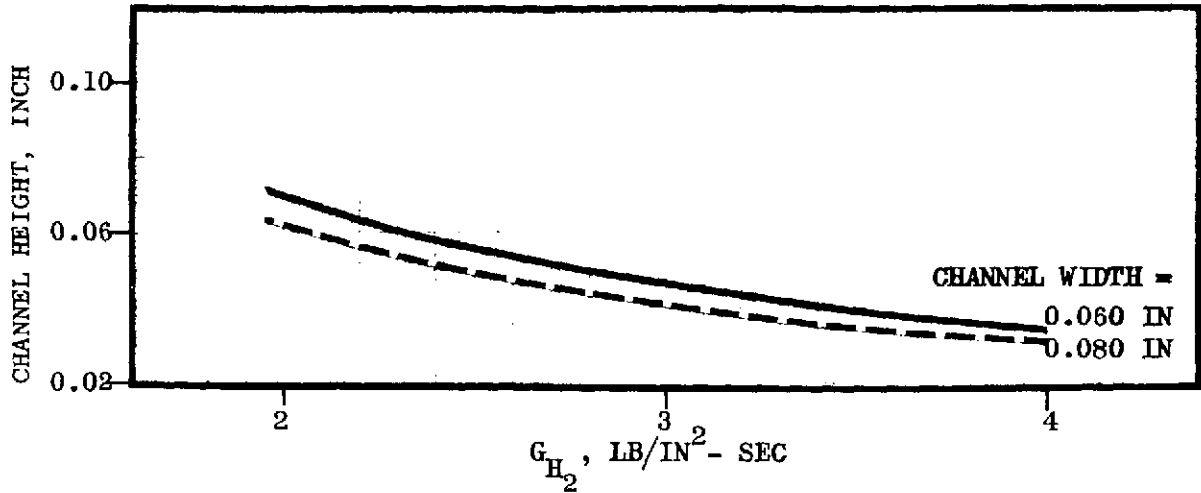


Figure 27. Temperature Gradients Near Baffle Leading Edge (H_2 Conditioner)

addition, the effect of the hydrogen mass velocity is not particularly strong; the effect of decreasing the hydrogen mass velocity from 3 to 2 lb/in²-sec is to increase the mid-channel wall temperature about 70 F, while the mid-land temperature only changes about 20 F. Consequently the hydrogen mass velocity selected will have little bearing on the maximum allowable heat flux nor on the overall conditioner size. It does, however, have a strong effect on channel size (primarily channel height), as does the amount of coolant bypass, as shown in Fig. 26 and 27. This will affect conditioner weight and thermal response. It is noted that a further advantage of the insensitivity of wall temperature to hydrogen mass velocity is that the wall temperature, and thus the life, will be insensitive to variations in the hydrogen flowrate. Thus the lowest flowrate case of 3 lb/sec will have nearly the same life and the same heat input as the highest flowrate case of 5.95 lb/sec.

Next, the effect of hydrogen temperature on the wall temperature at both the maximum and minimum heat flux locations was studied. Using the nominal peak heat flux and a hydrogen mass velocity of 3 lb/in²-sec, the appropriate two-dimensional wall temperatures were determined; these are shown in Fig. 28. The wall temperatures are not very sensitive to the hydrogen temperature, with a 100 F change in the hydrogen temperature resulting in about a 30 F change in wall temperature. Consequently the amount of hydrogen bypass will have little effect on the life or wall temperature in the peak heat flux range of the baffle.

In the low heat flux region at the baffle exit, the wall temperature is not highly sensitive either to hydrogen mass velocity or hydrogen bulk temperature, as seen in Fig. 29. The difficulty arises, however, in maintaining a wall temperature above 32 F--the freezing point of water. If no bypass is used, the hydrogen mass velocity would have to be less than 1 lb/in²-sec to meet this condition. With a mass velocity of 0.5 lb/in²-sec, the wall temperature would be about 70 F whether the hydrogen inlet or exit manifold were located at this point (due to the relatively poor cooling capability of hydrogen at low temperatures).

$T_c = 1560F$, $h_g = 0.0035 \text{ B/IN}^2 - \text{SEC} - F$
 HAYNES 188 $t_w = 0.015 \text{ IN}$, LAND = 0.040, CHANNEL = 0.080W x 0.082H
 $G_{H_2} = 3 \text{ LB/IN}^2 - \text{SEC}$

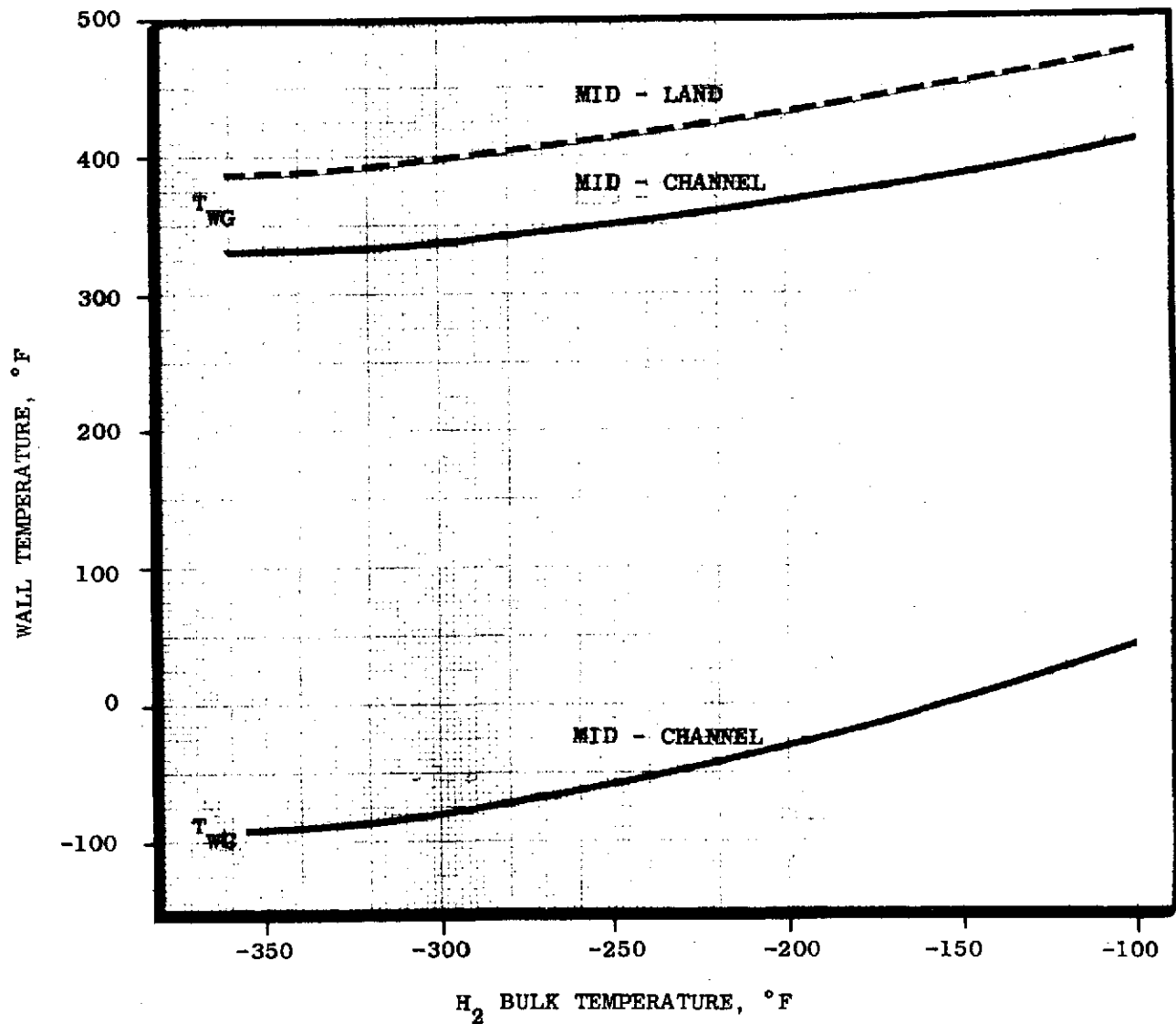


Figure 28. Leading Edge Wall Temperature vs H₂ Bulk Temperature (H₂ Conditioner)

50 percent Bypass, $T_{H_2} = 290^\circ\text{F}$, $h_g = 0.0049 \text{ B/IN}^2 - \text{SEC} - \text{F}$
 $T_{H_2} = 70^\circ\text{R}$

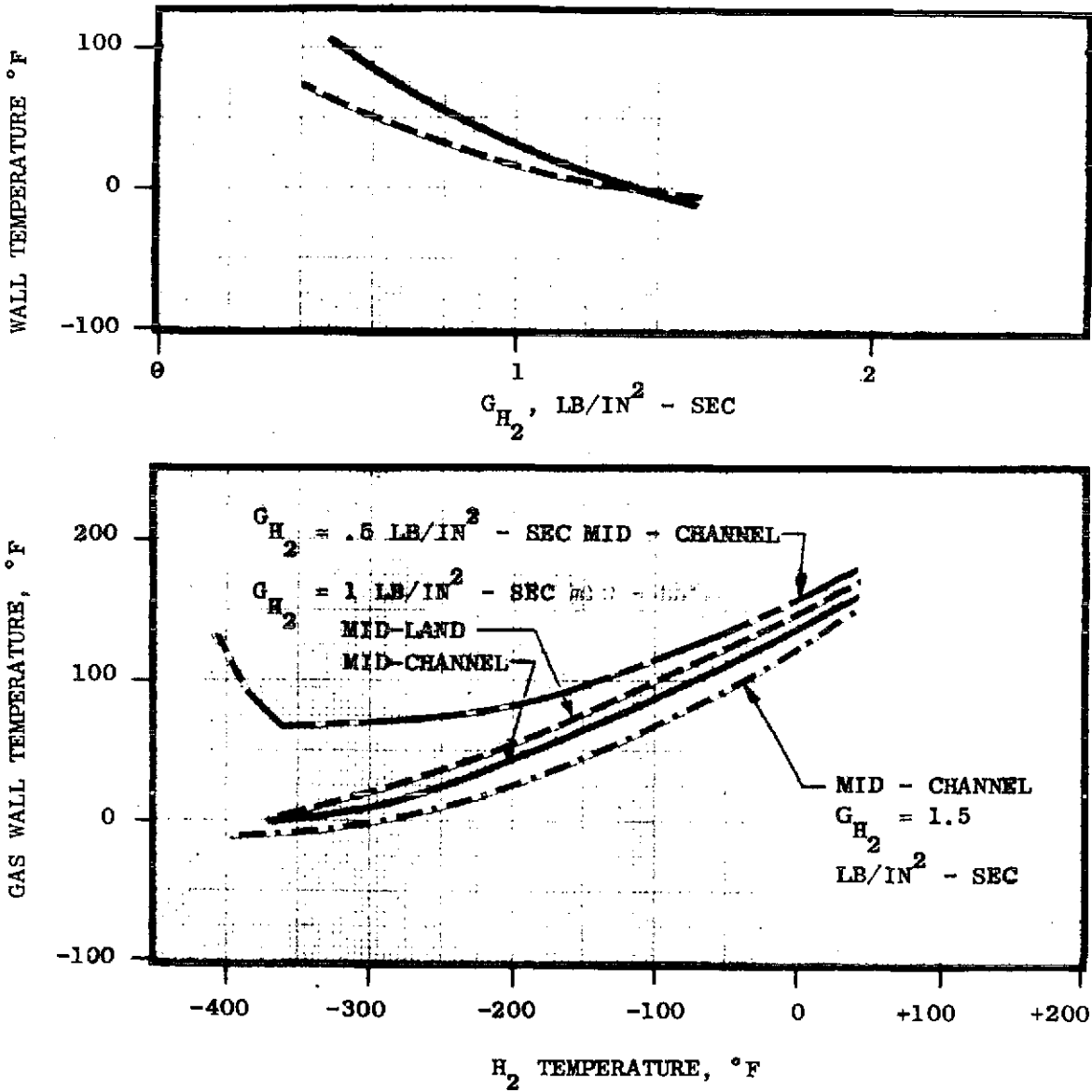


Figure 29. Exit End Wall Temperature (H₂ Conditioner)

Although a hydrogen mass velocity of $0.5 \text{ lb/in}^2\text{-sec}$ would provide a theoretically satisfactory design, a manufacturing requirement was introduced at this point. This requirement specified that the combined gas wall thickness and channel height should be held constant over the full length of the baffle. This meant that the only way in which the hydrogen mass velocity could be reduced was by either widening the channel or by branching the number of channels (illustrated in Fig. 30). The latter is possible between the inlet and outlet manifolds since normally only half the number of total channels exist in this region. This would make possible a 2/1 decrease in mass velocity. This latter method is more complex in manufacturing than changing the channel width, and consequently was discarded in favor of the former (channel widening) technique. At this point a stress restriction was introduced, requiring that the ratio of channel width to hot wall thickness not exceed approximately 6; this meant that the maximum allowable channel width for a 0.015 wall was about 0.090 in. An additional manufacturing requirement indicated that the land widths should not be less than 0.040 in. for ease in making the EDM tooling. The channel width and land width could be split 50-50 to a value of 0.045 in. each upstream of the hydrogen inlet manifold. However, the channel width was increased to 0.050 in., holding the land to 0.040 in order to minimize channel height.

As a result, the hydrogen mass velocity change is held by geometry restrictions to approximately 2:1. Thus selecting an injector-end hydrogen baffle mass velocity of about $2 \text{ lb/in}^2\text{-sec}$ would result in a minimum mass velocity of about $1 \text{ lb/in}^2\text{-sec}$. Returning to Fig. 29, it is seen that for a minimum mid-channel temperature of about 70 F, a hydrogen bulk temperature of approximately -140 F (320 R) is required. Referring to Fig. 31, where hydrogen

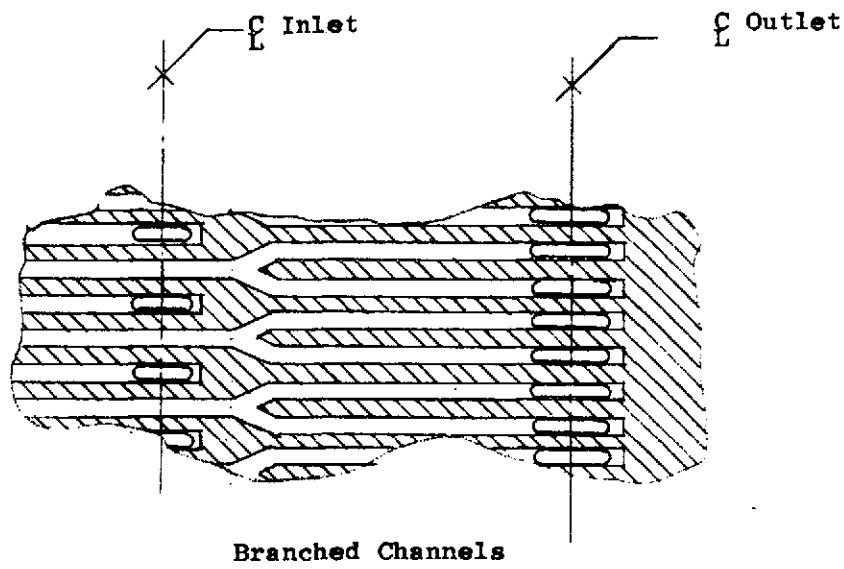
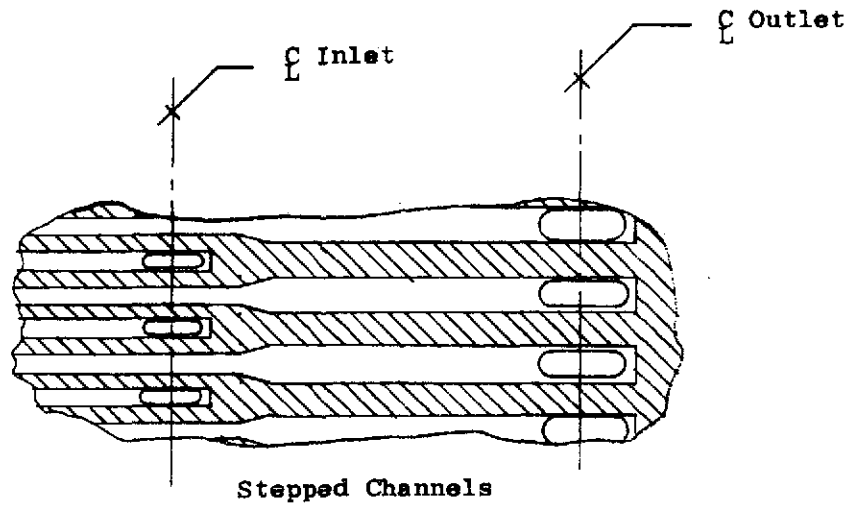


Figure 30. Techniques for Varying Channel Flow Area

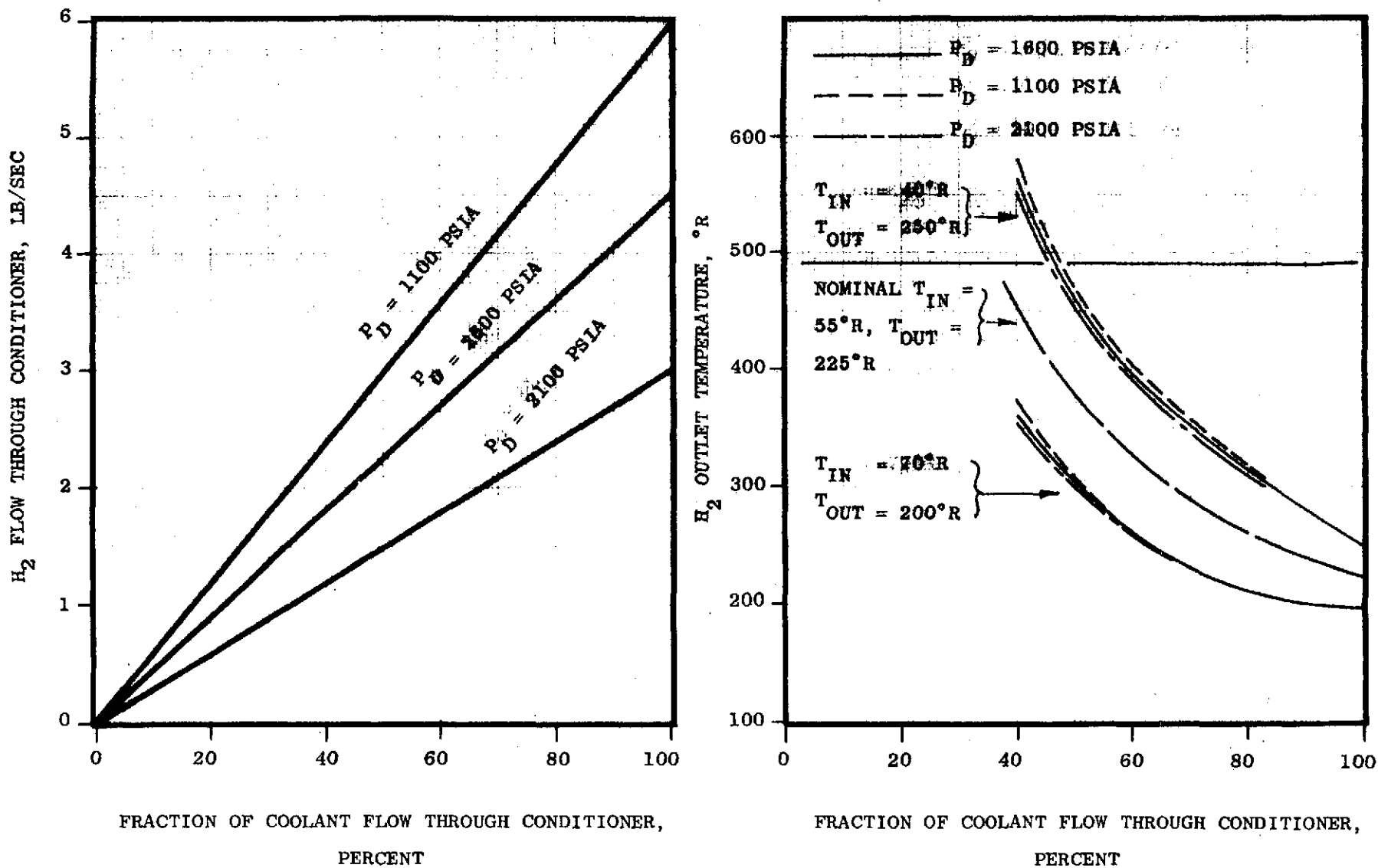


Figure 31. Effect of Coolant Bypass on Outlet Temperature (H₂ Conditioner)

outlet temperature is shown as a function of the hydrogen flow through the conditioner and as a function of the hydrogen temperature range, an outlet temperature of 320 R would correspond to 40 percent bypass (60 percent of the flow passing through the conditioner heat exchange baffles at the nominal design point).

Theoretically, from a freezing point, the higher the bypass the better. However, the higher the bypass, the higher the wall temperature and the lower the heat flux at the exit. Since the lowest heat flux is at the exit, reduction of the heat flux has a larger adverse effect on the surface area than a proportional reduction at the injector end, where the heat flux is about 4 times as high. Consequently to minimize surface area and weight, it is desirable to maintain the maximum heat flux and the lowest wall temperature while maintaining an acceptable margin of safety above the freezing point of water. In addition, as the amount of bypass goes up, the coolant pressure drop increases due to the decreased hydraulic diameter of the coolant passages. This is shown in Fig. 32, where pressure drop is shown as a function of the hydrogen mass velocity and the amount of hydrogen bypass. To stay within the hydrogen pressure drop limit of 100 psi at the 4.5 lb/sec flow condition, the maximum mass velocity for 50 percent bypass is $2.3 \text{ lb/in}^2\text{-sec}$ (Fig. 33). By comparison, a mass velocity of about 2.6 is possible with 40 percent bypass, resulting in less critical tolerance control of the coolant passage in order to meet the pressure drop limitation. In the other extreme, reducing the percentage of bypass reduced the exit wall temperature and increased channel height (Fig. 33), resulting in a weight penalty with no immediate advantage. As a result, a coolant bypass of 40 percent was selected for the hydrogen conditioner. At the same time, the hydrogen outlet manifold was located at the baffle exit, in order to take full advantage of the bypass design.

Channel Dimension Selection

To keep the channel height down below 0.085 in. with 40 percent bypass, a minimum mass velocity of $2.1 \text{ lb/in}^2\text{-sec}$ was required, with a land width of 0.040 in. and a channel width of 0.05 in. While the channel height could be

$\dot{W}_{H_2} = 4.5 \text{ LB/SEC}$, $T_{in} = 55^\circ\text{R}$, $T_{out} = 225^\circ\text{R}$, $P_{in} = 1600 \text{ psia}$

57

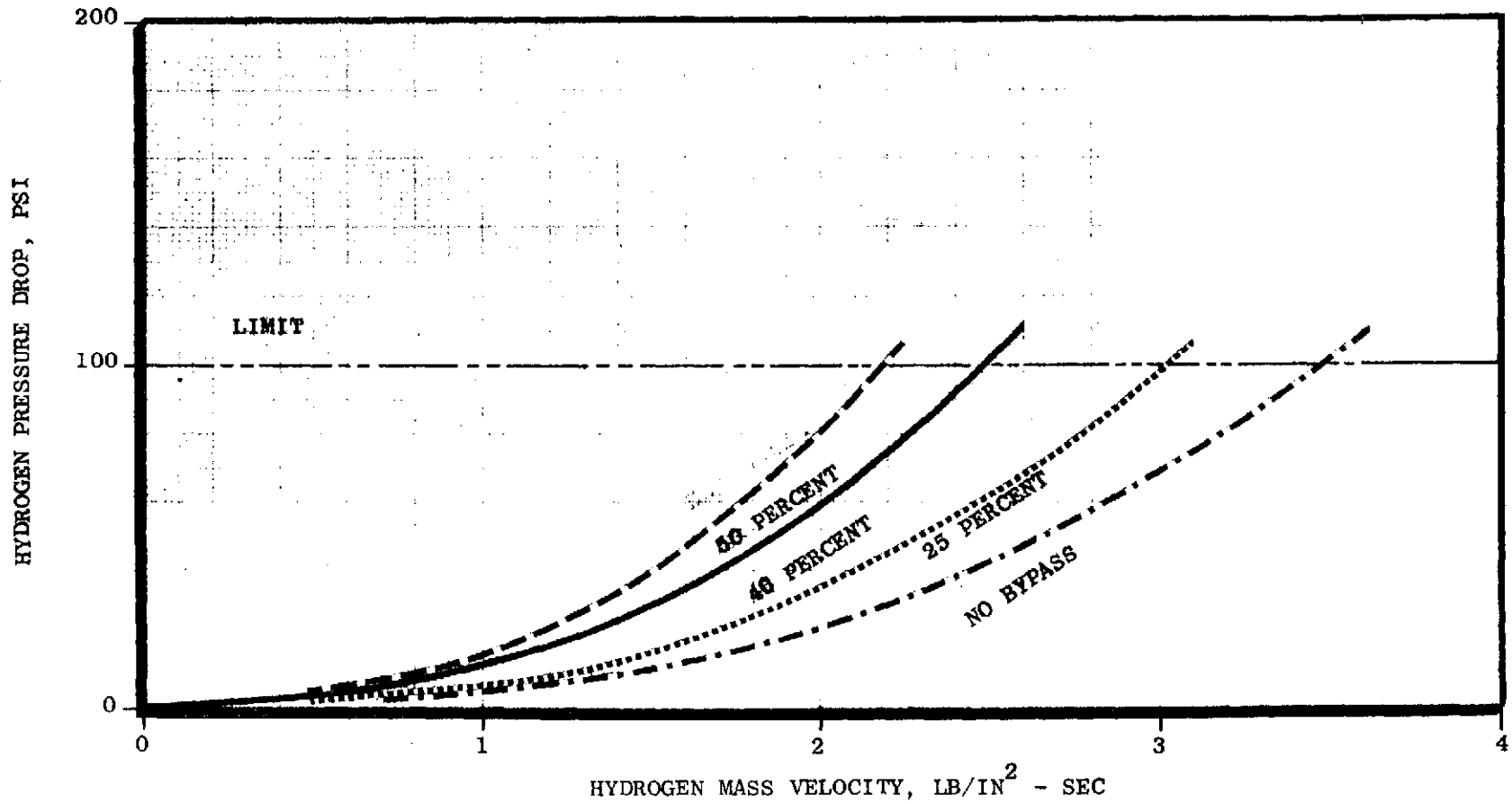


Figure 32. Conditioned Hydrogen Drop vs Mass Velocity and Bypass

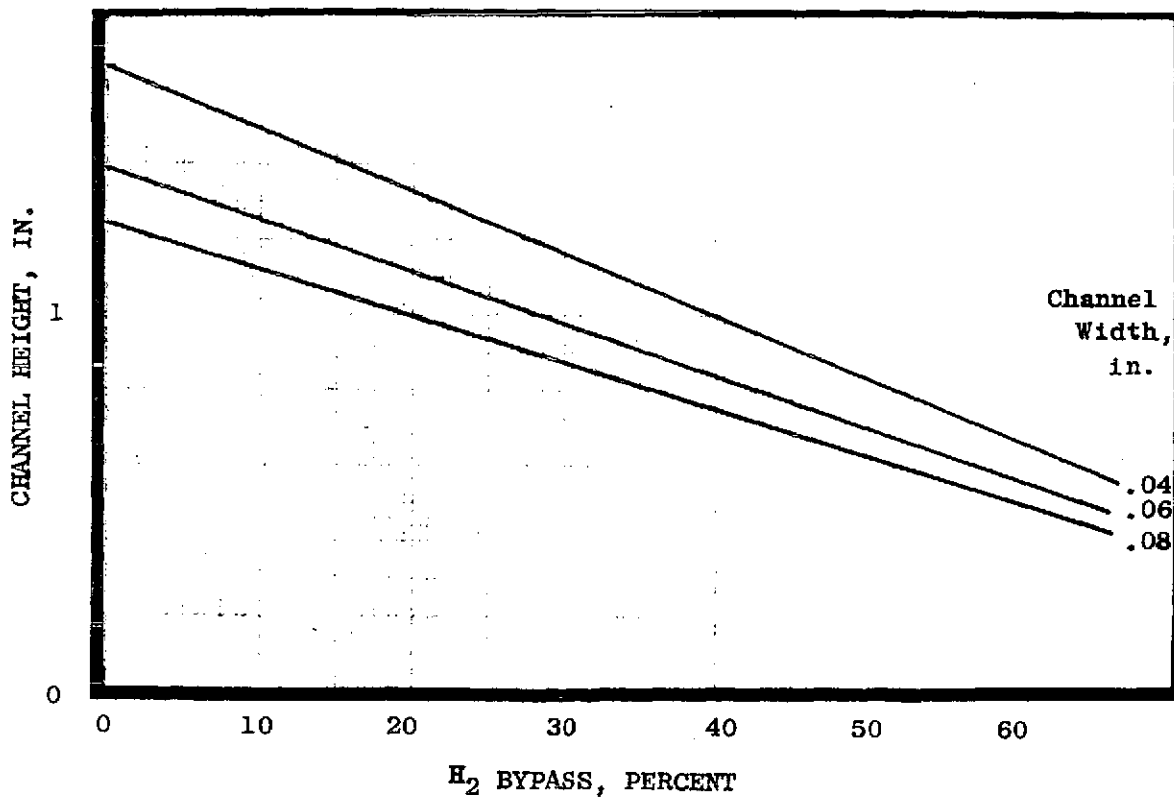
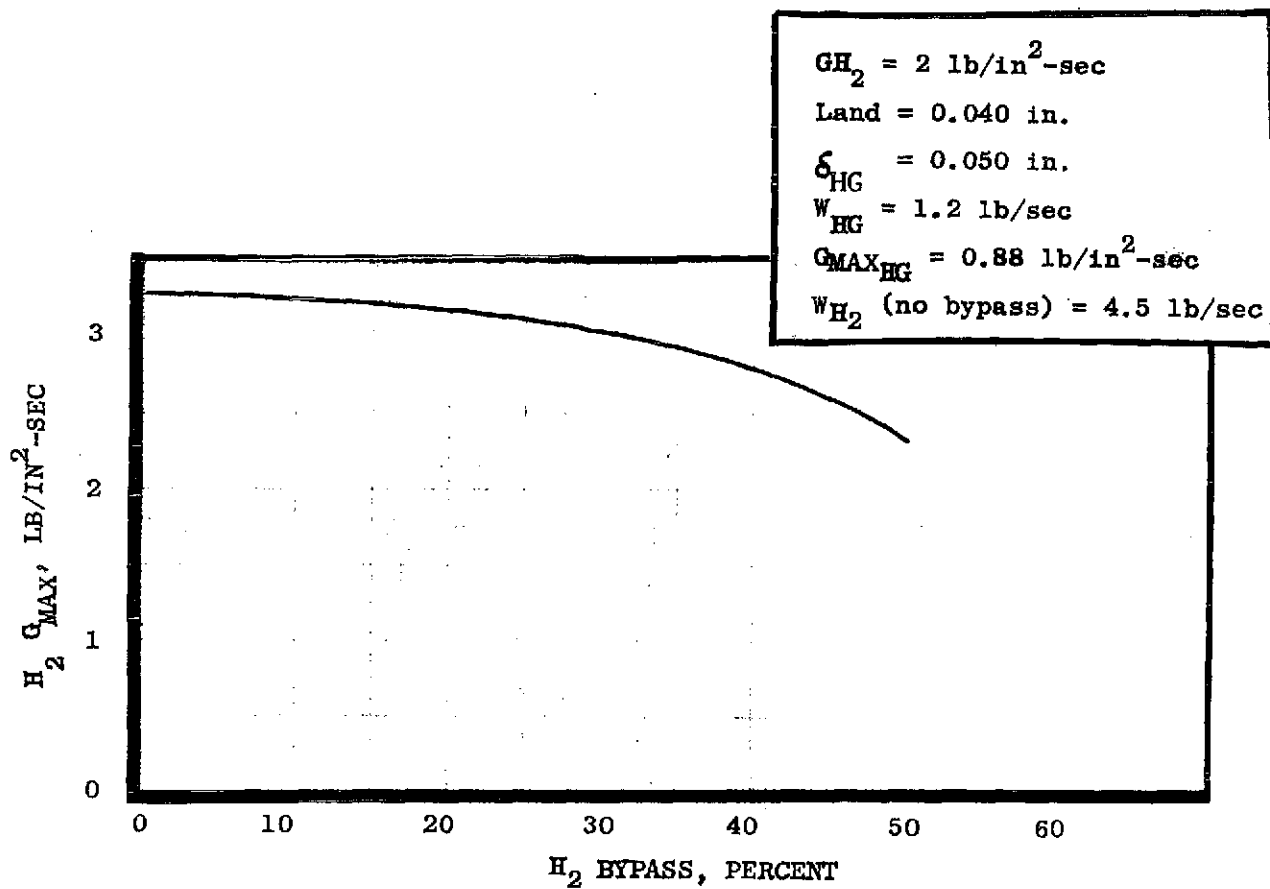


Figure 33. Channel Geometry and Hot-Gas Gap as a Function of Station

reduced further by increasing the channel width, this was not desirable since this made the low velocity region between the inlet and outlet manifolds difficult to design (to obtain a 2:1 change in areas the wall thickness would have to be increased in order to safely handle a wider channel). While this is possible, it seemed preferable to avoid doing so. The final selected mass velocity was 2.2 lb/in.²-sec at the forward end, and a value of 1.25 at the exit end, with a 0.090-inch-wide channel resulting in acceptable wall temperatures along the baffle.

The selected design required a surface area of 1010 in.² (ignoring possible heat transfer enhancement from condensation along the wall) and a baffle length of 17.2 inches, identical to that previously tested on the company-funded program. Selecting a maximum hot-gas mass velocity of about 0.88 lb/in.²-sec commensurate with a design chamber pressure of 240 psia, the hot-gas passage width was 0.046 inch (neglecting the baffle guide rails). For a baffle height of about 5 inches and with two center guide rails 0.060 inch high and two edge guide rails 0.040 inch high, this was modified to a 0.048-inch gap in order to maintain the hot-gas cross-sectional area. This results in a hydrogen passage channel height of 0.076 inch, and a combined channel height and hot-wall thickness of 0.091 inch.

The hot-gas gap was maintained at a constant value from the aft end of the baffle forward to where the heat flux reached the maximum design value of 4.2 Btu/in.²-sec. From this point forward, the hot-gas width was increased to maintain this heat flux at a constant value. As a result, the hot-gas passage width at the forward end of the baffle is 0.096 inch--twice the downstream value.

The effect of the tolerance on the hot-gas gap must be considered in terms of the effect on a particular gap and, also, the effect of variations between the hot-gas gaps in a given conditioner. Assuming first that all of the gaps in a given conditioner are identical, a smaller gap at the leading edge will result in an increased heat flux and somewhat reduced life; this is not a particular problem as the baffles readily meet the life requirement. An increase in the leading edge gap results in somewhat reduced heat fluxes but, again, the leading edge heat flux has a small effect on total heat input, as discussed previously. At the exit end of the baffle, a smaller gap will result in higher chamber pressure, whereas a larger gap will result in reduced heat fluxes, with reduced wall temperatures and

somewhat reduced heat inputs. If insufficient margin is left in the design, icing may occur on the wall with a larger gap.

The effect of the gap-to-gap tolerance is more complex. In this case, a smaller than nominal gap (compared to the others) will carry less gas flow, with a resultant reduced heat flux to the wall, a reduced exit temperature (both due to a reduced flowrate capability and both of which can lead to icing in that passage), and an increased conditioned propellant flow through that baffle due to the higher average density (unless compensated for by an adjacent gap--one of the advantages of the U-baffle configuration). Consequently, it is highly desirable to minimize the gap-to-gap variations within a conditioner assembly.

The location of the inlet manifold is not critical. A point about 5 inches upstream of the outlet manifold was selected in order to keep the thermal stresses and hydrogen pressure drops down. In general, the closer together the inlet and outlet manifolds, the higher the hydrogen temperature at the baffle leading edge, which helps reduce thermal strain. However, the same condition also increases pressure drop, particularly where the hydrogen is warm and thus at low density. If the manifold is too far forward, the hydrogen at the leading edge is too cold and thus not as good or as predictable a coolant; in addition, the baffle thermal strains will be higher.

Operating Characteristics

The hot gas and coolant geometry are shown in Fig. 34. The design point operating characteristics are shown in Fig. 35 and 36. Figure 35 depicts the hot-gas heat flux and temperature profiles along the baffle. The heat flux is seen to be nearly constant for the first 4.6 inches from the leading edge, in which range the hot-gas gap tapers 2:1 (as was shown in Fig. 34). From this point aft, the heat flux decreases steadily until the hydrogen inlet manifold, at which point the heat flux drops due to the presence of fewer coolant passages and larger lands between channels, resulting in a higher average wall temperature (Fig. 36).

The hydrogen bulk temperature and the wall temperature profiles are shown in Fig. 37. Assuming the hydrogen enters at its mean temperature of 55 R (-405 F), the predicted hydrogen temperature at the baffle leading edge is about 180 R (-280 F), and the

H₂ Conditioner
40 percent Bypass

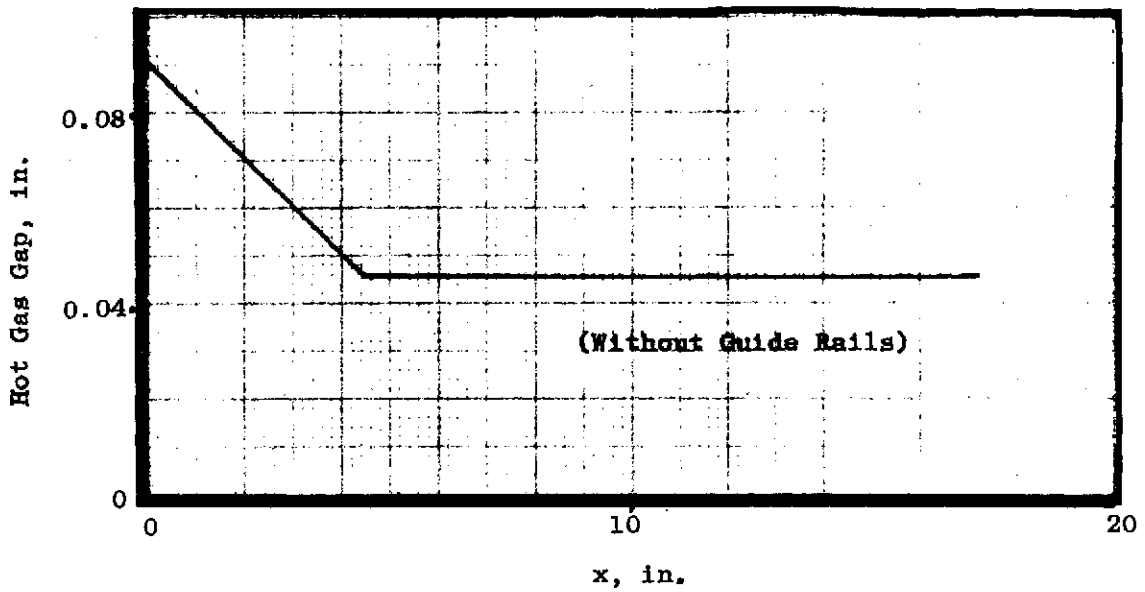
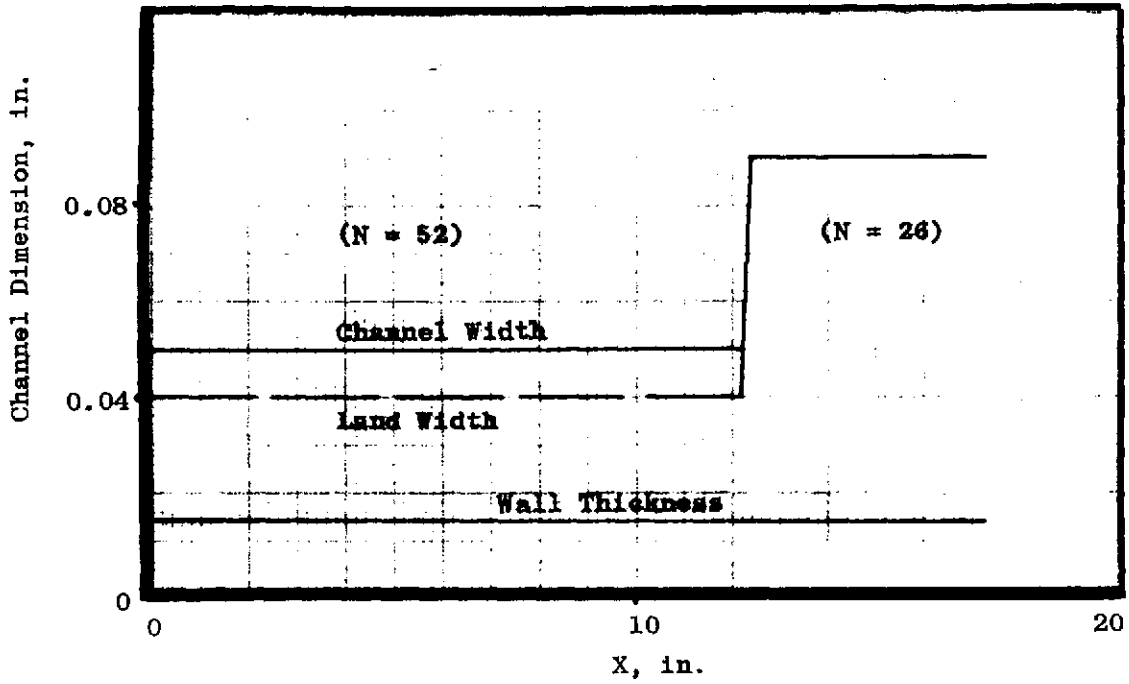


Figure 34. Channel Geometry and Hot-Gas Gap as a Function of Station

H₂ CONDITIONER
 40 PERCENT BYPASS
 MR = 1.0
 T_{H2} = 275R
 A_S = 1010 IN²

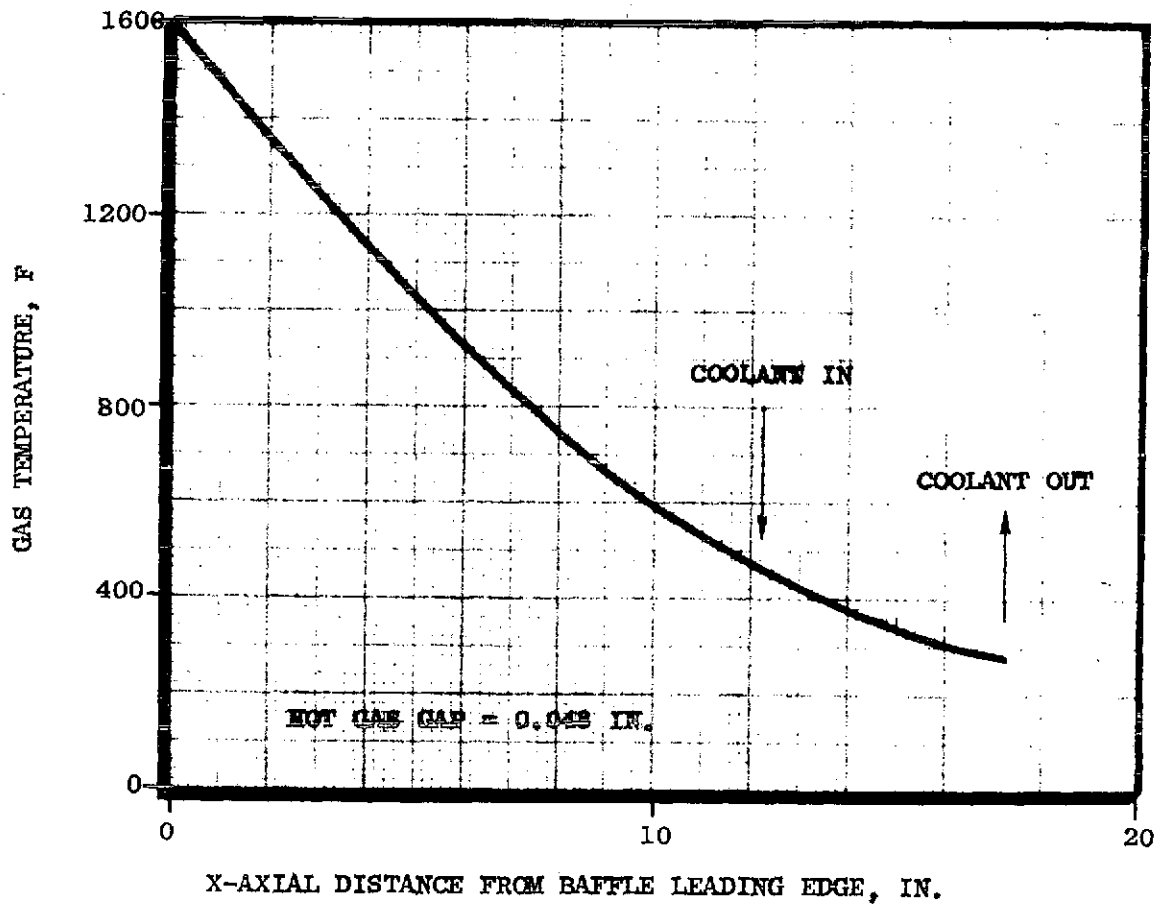
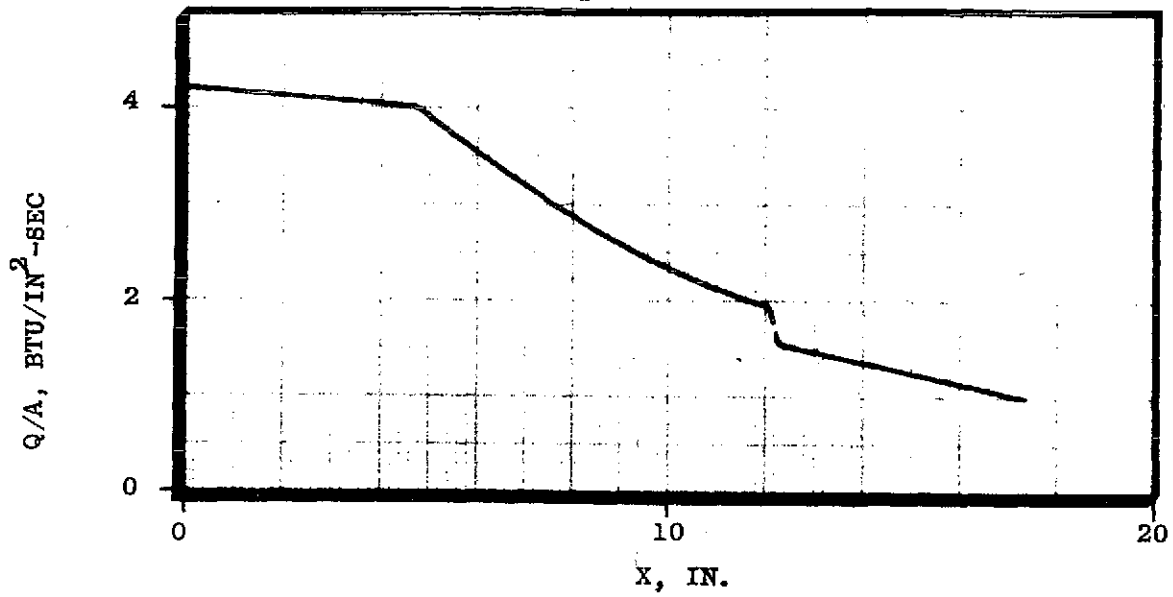


Figure 35. Heat Flux and Gas Temperature as a Function of Station

H₂ Conditioner
40 percent Bypass
Nominal Design Point

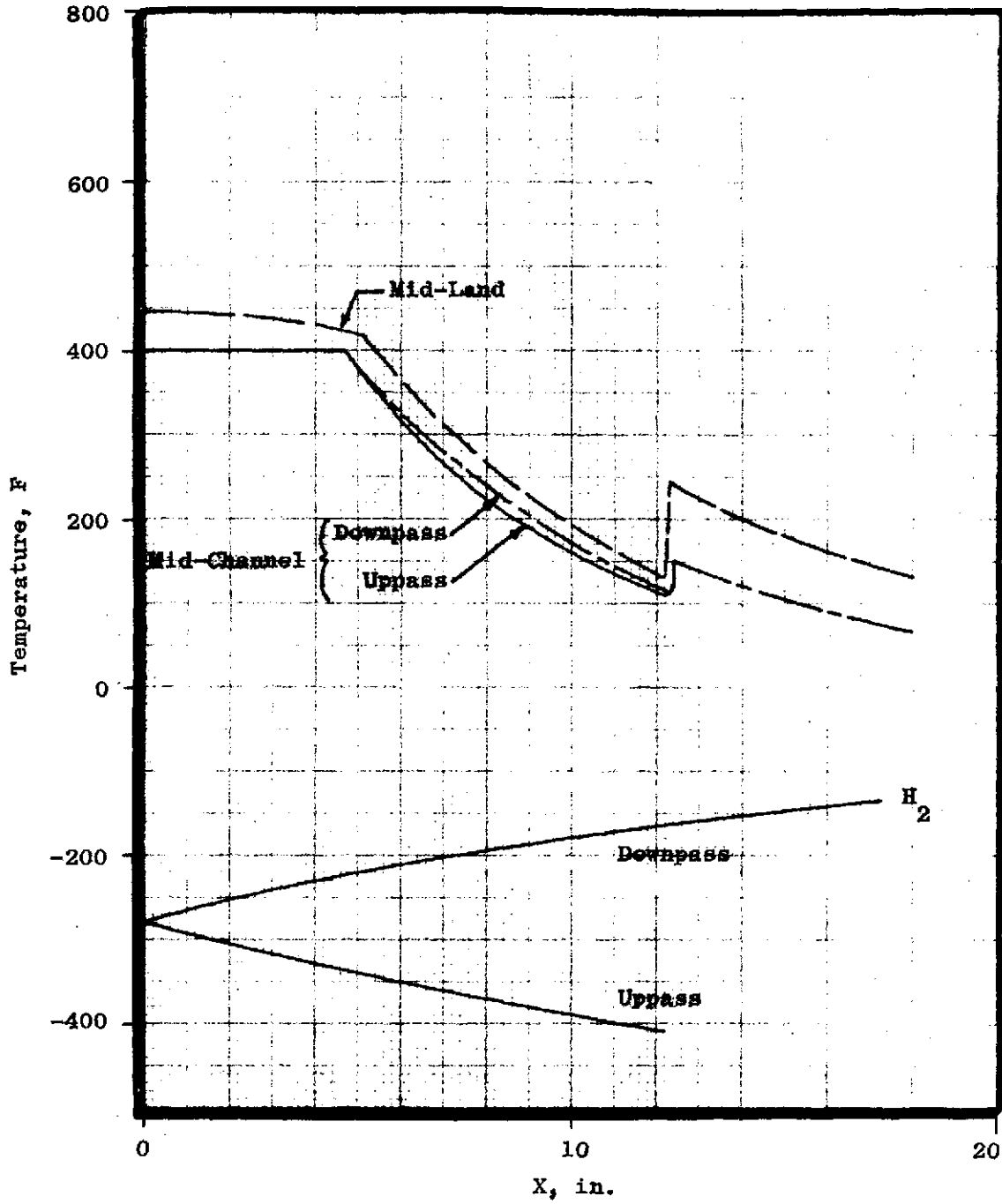


Figure 36. Wall and Hydrogen Temperatures as a Function of Station

exhaust temperature is 330 R (-130 F), with 2.7 lb/sec of hydrogen flowing through the conditioner. Predicted maximum wall temperature at the forward end is 400 F above the center of the channel and about 440 F midway between channels. This drops to about 110 and 130 F, respectively, at the hydrogen inlet manifold. Downstream of the manifold, where half the number of channels exist and where the channel width has been increased to 0.090 inch, the temperature rises to about 150 and 240 F at mid-channel and mid-land, respectively. This drops to 65 and 130 F, respectively, at the hydrogen exit manifold. It is concluded that the wall temperature is sufficiently high at all points to prevent ice formation.

The pressure drop and Mach number profiles on both the hot-gas side and the conditioned propellant side are shown in Fig. 37. On the hot-gas side, the exit is choked at nominal conditions, and the chamber pressure is running approximately twice as high as the exit total pressure (220 psia). While this chamber pressure is about 10 percent lower than the design value of 240 psia, this gives some margin in terms of tolerance control of the hot-gas gap as well as in control of the hot-gas flowrate. It is noted that the allowable design chamber pressure (for a given mixture ratio and outlet temperature) determines the maximum achievable hot-gas mass velocity, and thus the maximum exit heat flux attainable. This exit heat flux value has the greatest effect on the conditioner size.

The hydrogen pressure drop at nominal conditions is seen to be 75 psi (25 psi less than the 100-psi limit). This gives some margin for tolerance during manufacturing. It also leaves some extra pressure drop for mixing the conditioned hydrogen and the bypass hydrogen downstream of the conditioner.

Flowrate Variation--Conditioned Propellant

Three steady state analyses were conducted over the specified range of hydrogen flowrates (3.0 to 5.95 lb/sec), while maintaining a constant bypass of 40 percent. The hot gas was held at the nominal mixture ratio and flowrate for each case. The resultant numbers given below are conservative, for although the computer program, as currently structured, predicts the correct local heat flux, it appears to underestimate the average heat flux. The result is that the heat input appears to be slightly low. The results are summarized in Table 10.

H₂ CONDITIONER
 40 PERCENT BYPASS
 NOMINAL DESIGN POINT

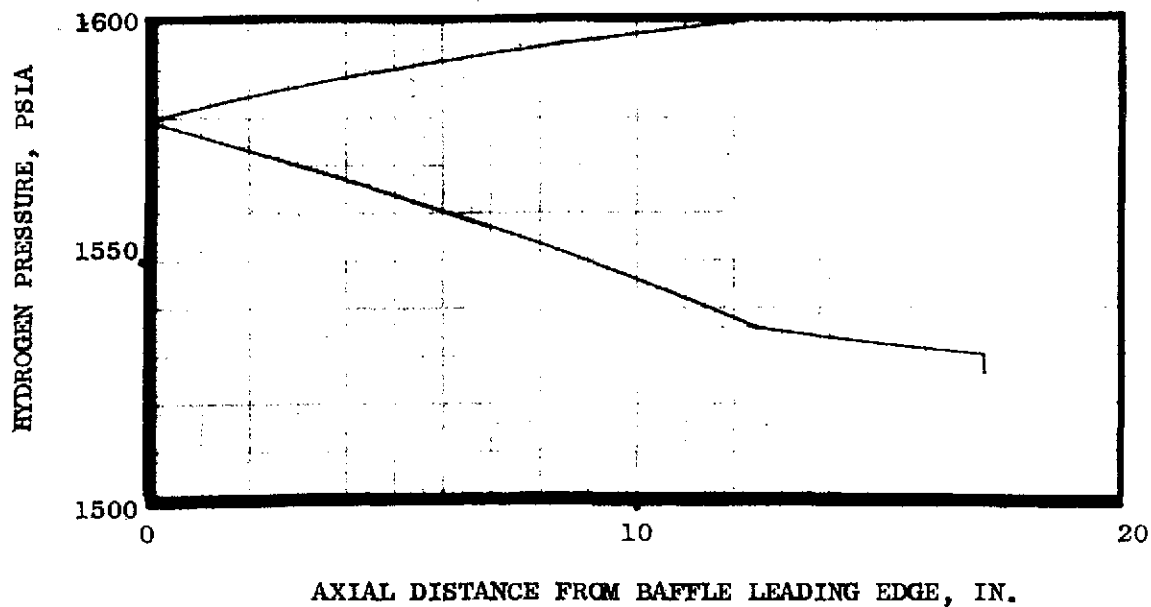
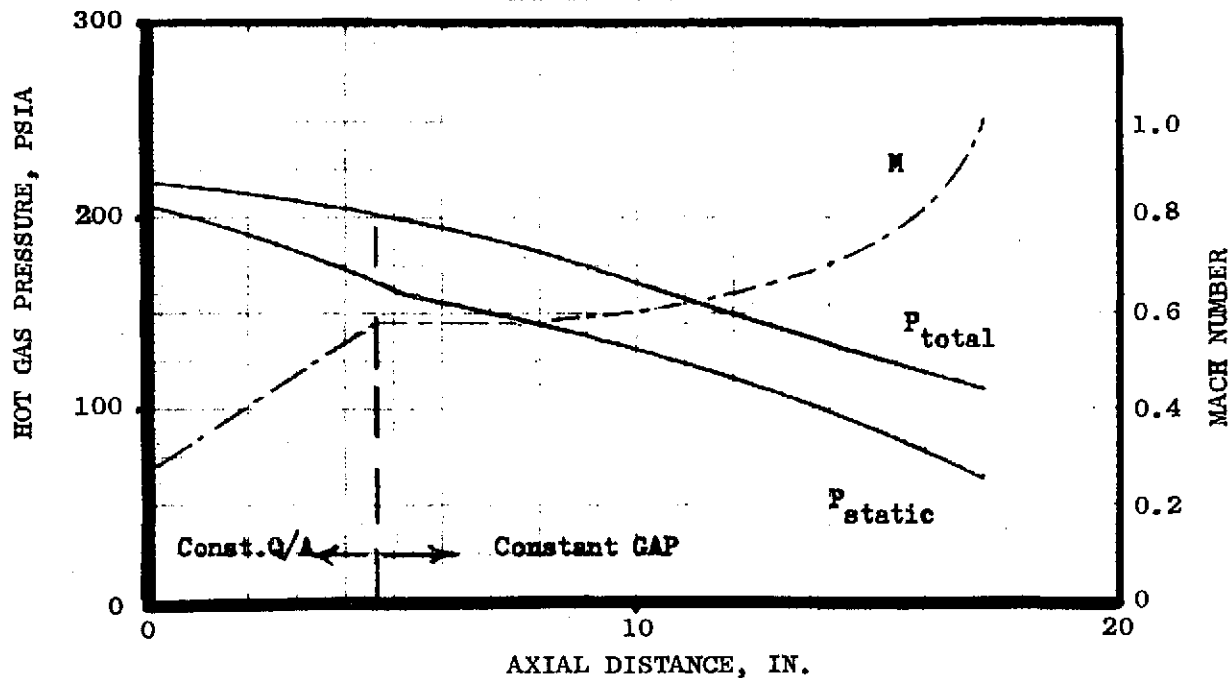


Figure 37. Hot Gas and Conditioned Propellant Pressure Profiles

TABLE 10. H₂ BAFFLE OPERATING CHARACTERISTICS, STEADY STATE

Parameter	Reduced η_{c*}	Nominal Design	Maximum Flow	Minimum Flow
Hot Gas Side				
MR	1.0	1.0	1.0	1.0
\dot{w} , lb/sec	1.2	1.2	1.2	1.2
η_{c*}	98	100	100	100
T _c , R	1980	2060	2060	2060
T _{exit} , R	770	797	757	871
ΔQ , Btu/sec	2590	2710	2800	2540
Cold Side				
W _{H₂} (total), lb/sec	4.5	4.5	5.95	3.0
T _{inlet} , R	55	55	55	55
T _{out} , R	308	319	261	427
Mixed T, R	207	213	179	278
Maximum Wall Temp, F	390	420	380	490
Minimum Wall Temp, F	75	90	40	190

The range of hydrogen flowrates has some effect on wall temperature. These range from a minimum of 380 F to a maximum of 490 F (420 F nominal) at the forward end of the baffle. At the baffle exit, these temperatures range from an average value of 40 F at the high flow to 190 F at the low flow (90 F nominal). While the wall temperature at the highest flowrate condition is approaching the freezing point of water, it still remains about 8 F above it. The lower flowrate case may have a slight reduction in life, though this should be minor since the higher wall temperature is nearly offset by the higher hydrogen bulk temperature. While hydrogen pressure drops will exceed 100 psi at the highest flowrate case, this has not been considered limiting from a design or operational standpoint since this is the condition of minimum pump discharge pressure. The important conclusion is that the wall temperature and the total heat transferred is not very sensitive to the hydrogen flowrate and that all temperatures appear acceptable. In addition, there is additional freedom with the bypass design, where the amount of hydrogen bypassed around the conditioner could be varied as a function of the hydrogen flowrate, or even from the unit to unit to account for tolerance differences.

The preceding analysis assumed a combustion efficiency of 100 percent which should be attainable with the trislot injector and the high contraction ratio (~ 7.3) used on the hydrogen conditioner. However, a nominal design point was evaluated to determine the effect on conditioned hydrogen outlet temperature for a reduced combustion efficiency. Results shown in Table 10 indicate that for a 98-percent combustion efficiency, the outlet temperature of the conditioned hydrogen is reduced approximately 4 percent, well within the specified range.

Baffle Edge Heat Transfer

A two-dimensional steady-state heat transfer analysis of the top and bottom edge of the baffle was conducted to determine the effect of the larger land between the edge channel and the top/bottom of the baffle. Neglecting possible edge effects, and neglecting the top/bottom baffle guide rail, which does not exist in the highest heat flux region of the baffle, maximum baffle wall temperatures were determined as a function of the spacing between the channel and the baffle edge at nominal operating conditions. The results are shown in Fig. 38. It is noted that the lowest distance shown, 0.02 inch, is essentially the same as that between the other channels, since it represents half a land width. While the mid-channel temperature is not particularly sensitive to the distance from the channel to the edge, the maximum temperature at the edge is quite sensitive (assuming that the baffle does not have thermal contact with the outer walls of the conditioner). Maintaining a minimum edge distance at the downstream end of the baffle of 0.040 inch for reliable brazing, and accounting for the 0.020-inch change in this dimension as a result of the channel narrowing from 0.090 inch to 0.050 inch, the resultant distance from the channel edge to the edge of the baffle is 0.060 inch. The corresponding maximum predicted wall temperature is seen to be 720 F. As shown in Fig. 38, these maximum temperatures decay toward the downstream end of the baffle due to reduced heat fluxes. In actual practice they may decay even faster due to the presence of the guide rails.

Reactor Shell Cooling

The 2-1/2 inches between the injector face and the upstream end of the baffles is cooled by the reactor hydrogen. The inlet manifold is located just upstream of the baffles, and the hydrogen flows in a single pass toward the

H₂ CONDITIONER
 40 PERCENT BYPASS
 NOMINAL DESIGN POINT

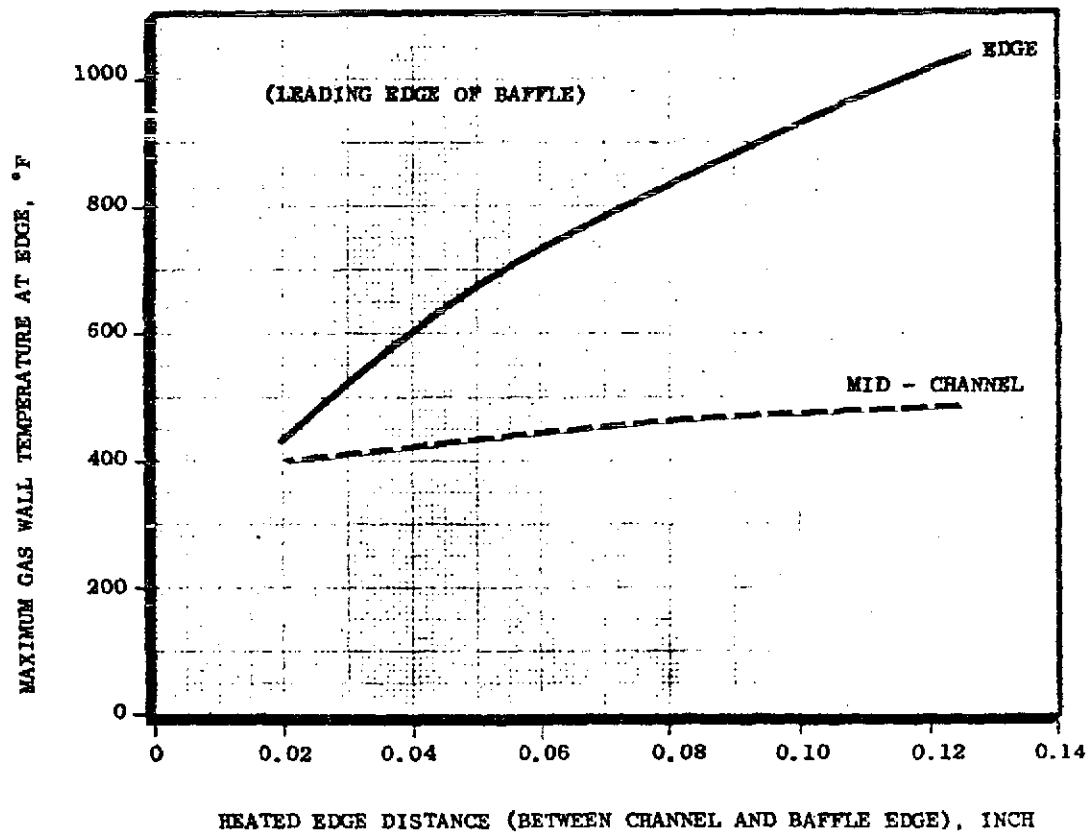
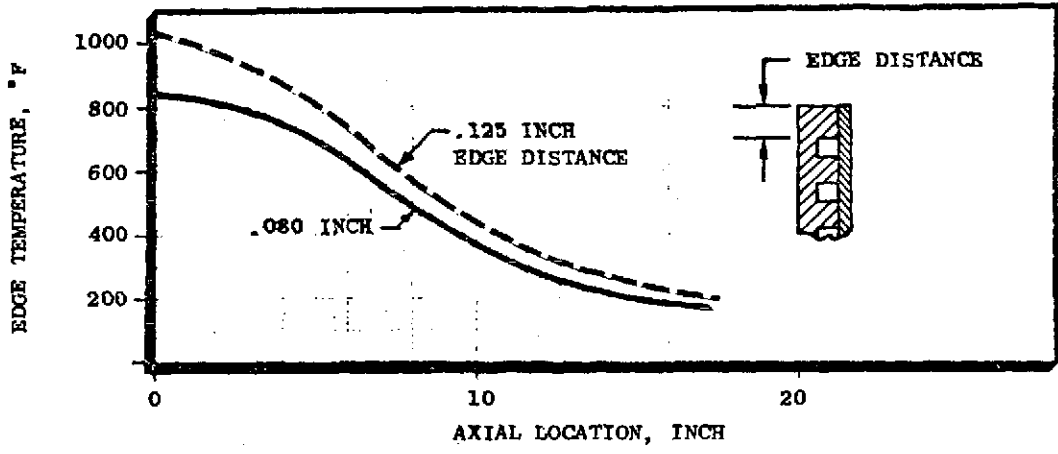


Figure 38. Baffle Edge Temperatures

injector face. Since all of the injector hydrogen is used to cool the four walls in this area, the hydrogen injection temperature should be uniform across the injector face. At a mixture ratio of 1.0 and nominal operating flowrates, the predicted hydrogen temperature rise is 12 R. The cooling passages are designed for a hydrogen mass velocity of $0.5 \text{ lb/in}^2\text{-sec}$ with a resulting pressure drop in the cooling jacket of about 5.5 psi (Fig. 39).

There are 19 channels in each side wall and 14 channels in each of the other two walls, for a total of 66 channels. A channel width of 0.156 inch ($5/32$ inch) results in a channel height of 0.117 inch (Fig. 40).

Between the baffle leading and trailing edges, the side walls of the reactor are cooled in exactly the same manner as the U-baffles, while the top and bottom walls are cooled by hydrogen flowing from the inlet manifold to the leading edge through channels located above each baffle, while the hydrogen flowing toward the exit manifold passes through channels located directly over the hot-gas gap between baffles. This region is cooled entirely by conditioned hydrogen flowing in parallel to the baffles. This coolant flow is in addition to the 2.7 lb/sec utilized by the U-baffles and side walls (at the nominal 4.5 lb/sec flowrate).

Baffle Closeout - Reactor Shell Interface

Several configurations for the top and bottom cooling passages were studied in an attempt to keep temperatures within reasonable operating limits and also prevent ice formation on both the baffle and the top/bottom surfaces, which could in time result in deforming the hardware. Two heating conditions were analyzed for each geometry and location. The first assumed no hot gas between the baffle and the top/bottom surface (insulated case); the second assumed the same heating conditions here as on the adjacent baffle side (heated case). Four locations were analyzed as being representative of the most critical regions: (1) just upstream of the exit manifold, (2) just upstream of the hydrogen inlet manifold, (3) baffle leading edge at the

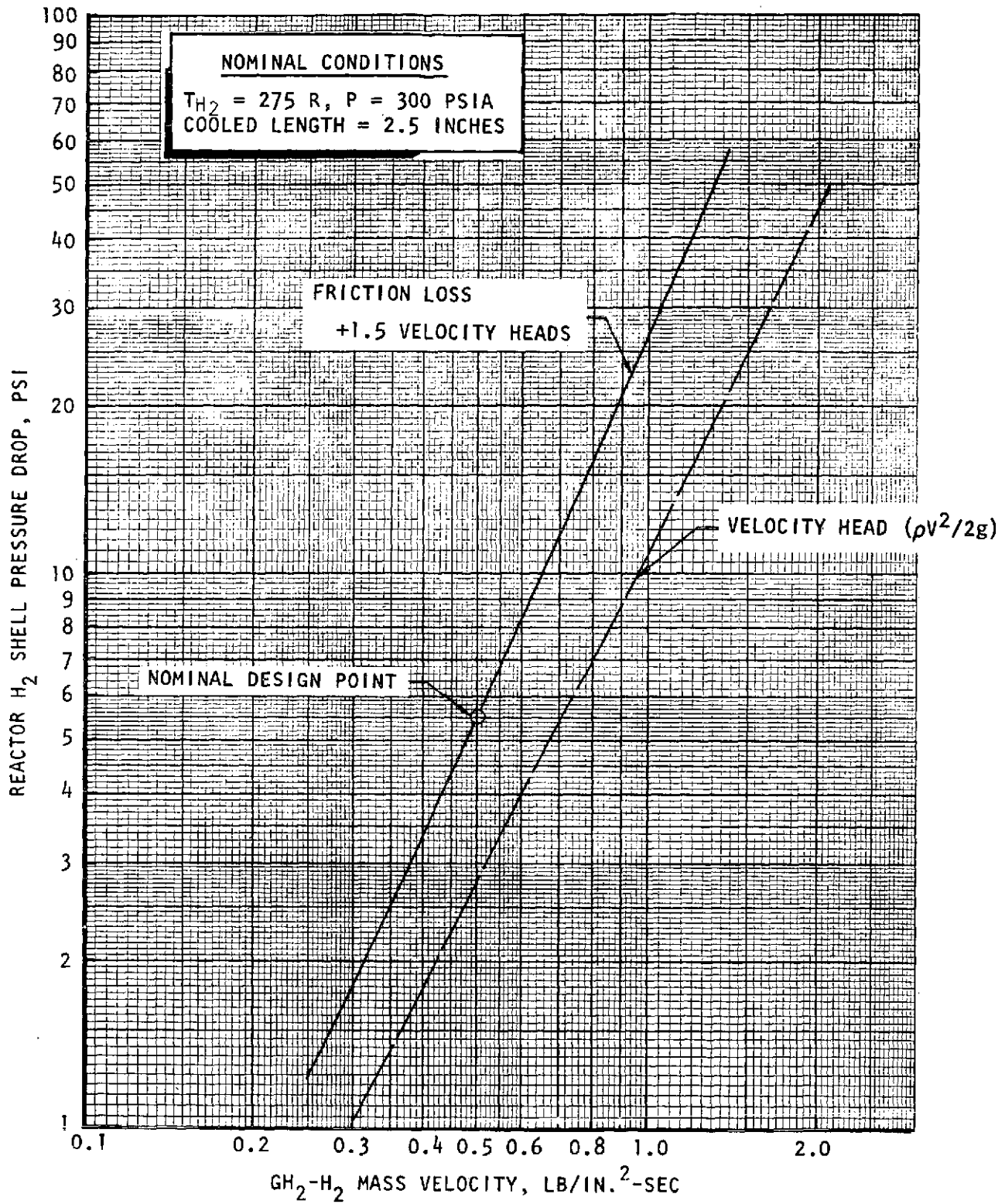
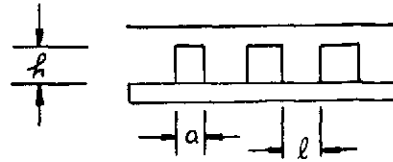


Figure 39. Reactor H_2 Pressure Drop in Shell



$w_{H_2} = 0.6$ LB/SEC, INSIDE HEATED CIRCUMFERENCE = 18 INCHES

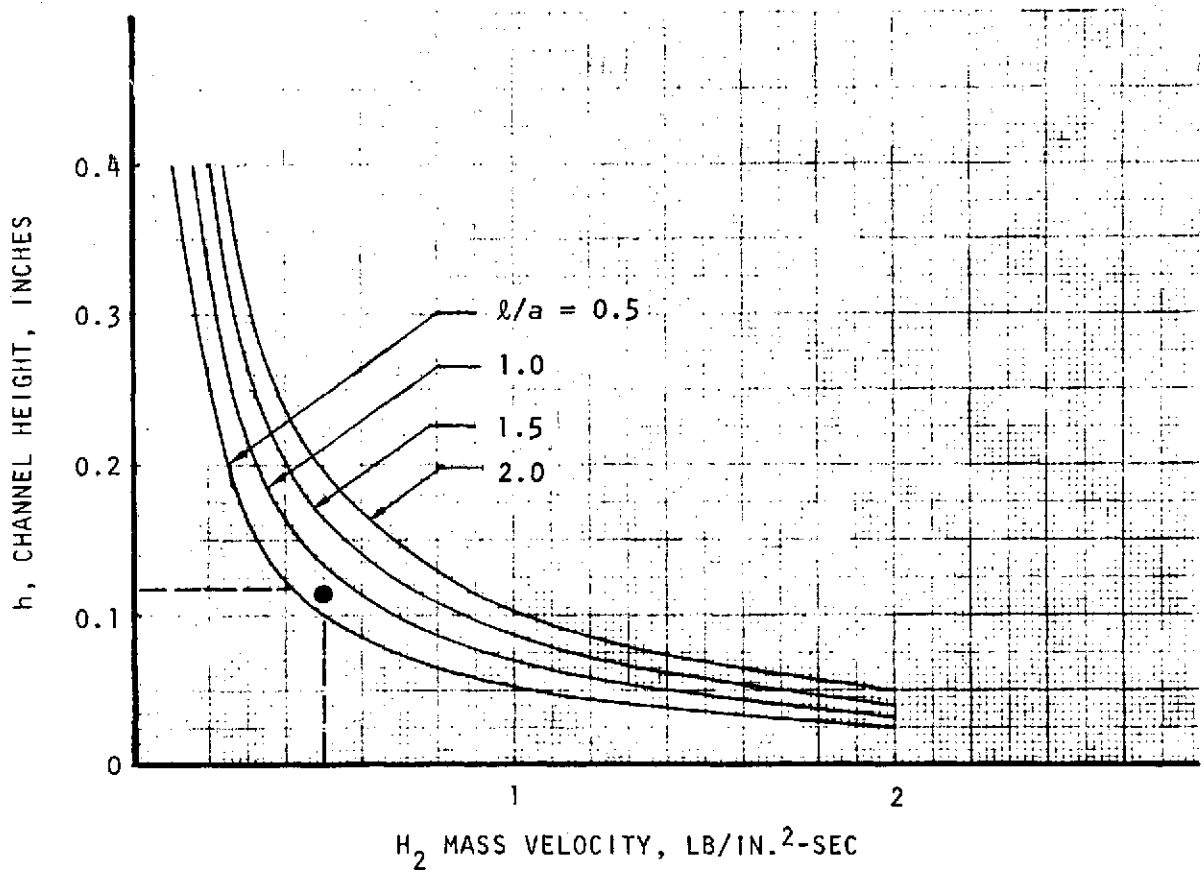


Figure 40. Shell Cooling, Reactor Hydrogen Channel Geometry

tangent point of the hot-gas ramp and, (4) the downstream end of the hot gas ramp (about 5 inches from the baffle leading edge--also referred to as the D/S taper point).

The four geometries are shown in Fig. 41 and 42, and the results of the analysis are shown in Table 11. Since the results were analyzed using the HEATING program, they are only approximate, as this program is not capable of handling variable thermal conductivity versus wall temperature or variable hydrogen heat transfer coefficients versus wall temperature. In addition, the hydrogen temperatures in the top/bottom walls are only approximate, and require a hand integration along the length. The hot gas and the baffle coolant boundary conditions are based on the more exact baffle analysis. In spite of the approximations involved, the analysis is useful for determining problem areas and for selecting a design configuration.

By studying the comparative results for the four configurations in Table 11, it is seen that configuration 1 has the least icing problems of any; however, it has high maximum baffle surface temperatures (at the heated corner farthest from the hydrogen coolant passages) because of the 0.180 inch distance to the closest coolant passage. Configuration 2 has no advantage since its minimum temperatures are lower (more icing) and the maximum temperatures are higher.

Configurations 3 and 4 are nearly identical except for the location of the uppass H₂ coolant passage in the top/bottom wall. As a result, the temperature limits are almost the same for each. The principal difference between the first two configurations and the last two are (1) in 1 and 2, the baffle is in thermal contact with the top plate at the baffle center, while in 3 and 4, the baffle is only in contact with the baffle spacer lip from the D/S taper point to the baffle exit; and (2) the maximum edge distance from the nearest coolant passage to the heated corner is 0.180 inch for configuration 1, 0.210 inch for configuration 2, and 0.070 inch for configurations 3 and 4.

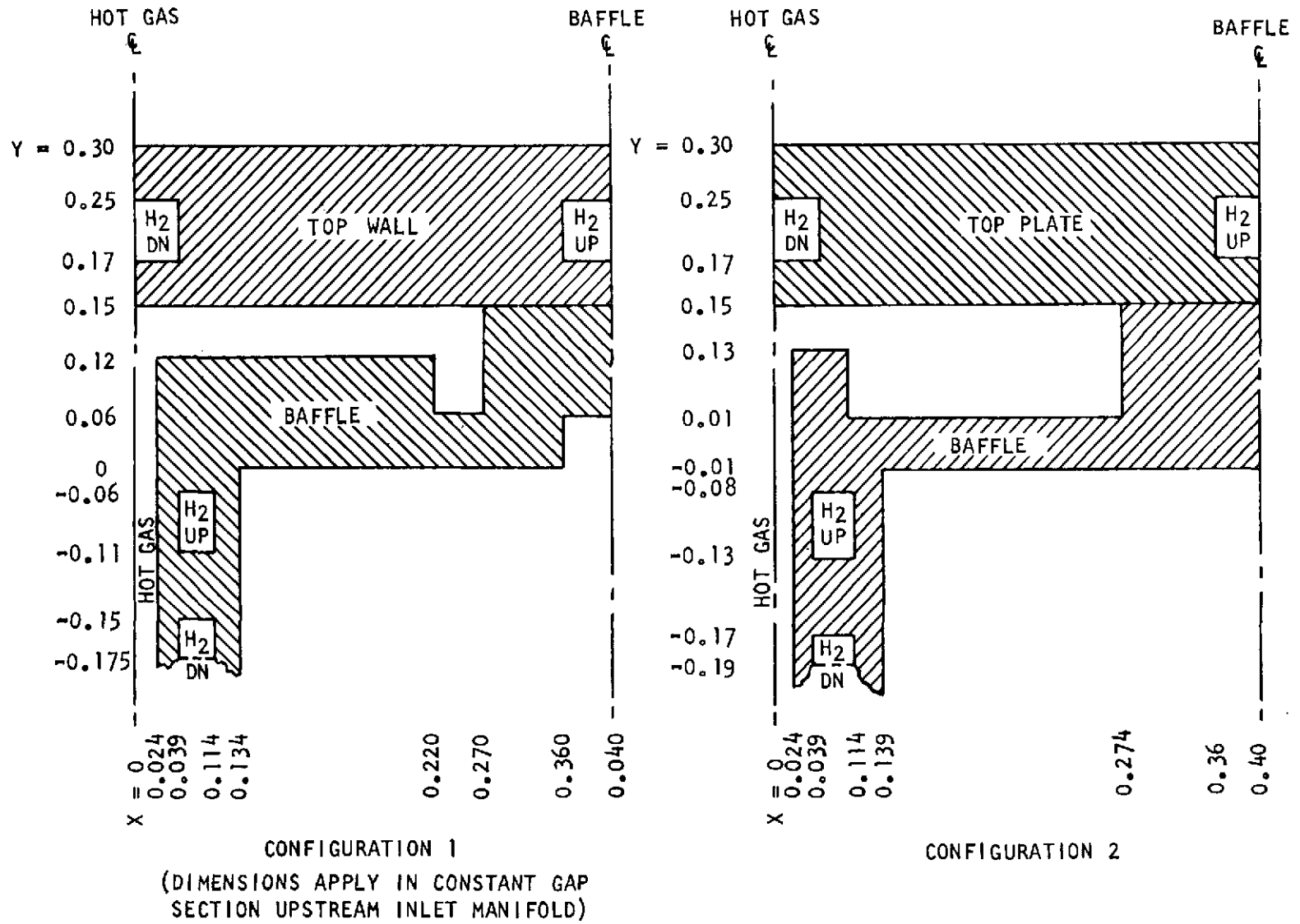


Figure 41. Baffle and Top/Bottom Wall Geometry
(Cross-Section Through Baffle and Wall)

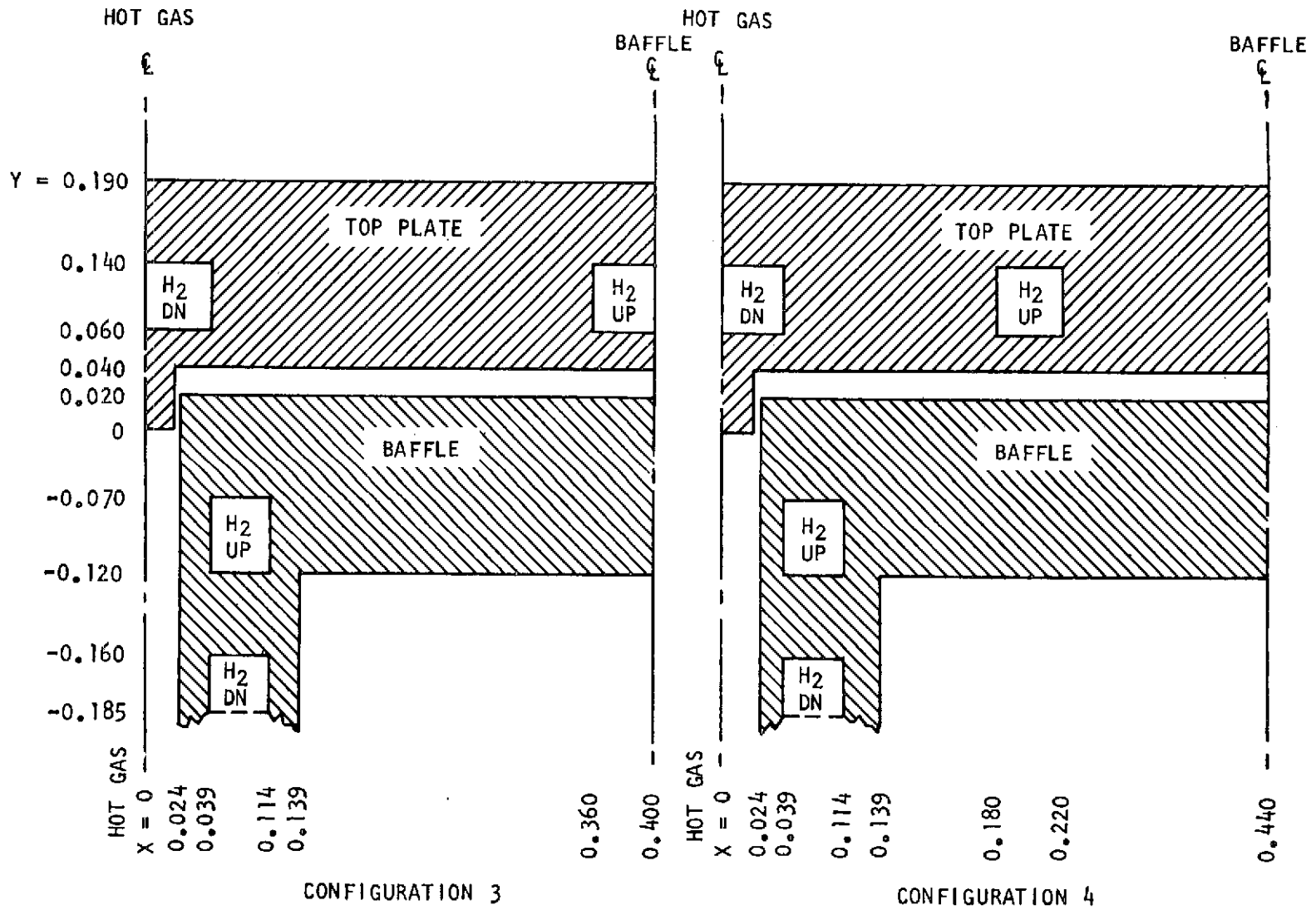


Figure 42. Baffle and Top/Bottom Wall Geometry (cross section through baffle and wall)

TABLE 11. TOP WALL/BAFFLE INTERFACE TEMPERATURES*

Configuration Location	1		2		3		4	
	Insulated	Heated	Insulated	Heated	Insulated	Heated	Insulated	Heated
H ₂ Exit Manifold								
Baffle Interface	22/220	260/280	-78/16	190/290	-113	200/260	-110	200/260
Top Interface	-100/-60	70/220	-115	75/260	-129	90/280	-130	90/280
Top Exterior	-65	227	-115	230	-133	238	-130	250
Baffle Surface Maximum	230	275	275	290	101	194	101	194
H ₂ Inlet Manifold								
Baffle Interface	7/370	460	-230/30	340/478	-250	360/450	-250	360/450
Top Interface	-290/-110	140/360	-300/11	140/340	-390	75/170	-390	100/380
Top Exterior	-180	85	-180	85	-180	102	-200	116
Baffle Surface Maximum	370	460	459	478	190	350	190	350
D/S Taper Point								
Baffle Interface	260/830	970/1015	-140/315	830/1010	-160	860/1000	-160	830/1000
Top Interface	-300/120	420/850	-350/-250	430/830	-390	430/870	-390	470/890
Top Exterior	-320	335	-330	340	-340	374	-345	460
Baffle Surface Maximum	880	1015	1010	1030	590	840	590	840
Leading Edge								
Baffle Interface	420/1210	1410/1490	-230/800	1240/1490	-87	1130/1460	-87	1120/1460
Top Interface	-270/-100	400/1180	-320/-80	500/1140	-390	470/1210	-390	480/1220
Top Exterior	-280	560	-305	560	-310	600	-310	600
Baffle Surface Maximum	1210	1490	1480	1560	880	1300	880	1300

*Minimum for insulated case, maximum for heated case; all temperatures in degrees Fahrenheit

As a result, the maximum surface temperatures of the baffle are considerably less for the last two configurations, which was the reason for their selection. However, the insulated temperatures at all locations along the baffle will result in ice formation. To avoid this, the baffle is designed to permit the hot-gas to freely pass between the baffle and the top/bottom wall in the region between the inlet and outlet manifolds. Upstream of the inlet manifold, transverse ribs will be used to limit the gas flow and thus the heat flux to the wall, thereby maintaining a reasonable balance between avoiding ice formation and avoiding overheating. It is noted that even if the full hot gas heat flux is assumed to exist in the interface region, that the exterior temperature of the shell meets the design requirements of 600 F or less, and even then the average exterior temperature is lower. The fourth and final configuration consisted of a 3/16 inch nickel closeout. This closeout design is theoretically capable of operating satisfactorily at a MR=3.

High Mixture Ratio Operation--Hydrogen Conditioner

Hot gas flowrates were determined as a function of mixture ratio and hot gas outlet temperature, using ambient propellants and based on a fixed heat rejection rate of 2800 Btu/sec (constant conditioned hydrogen discharge temperature). The results are shown in Fig. 43, along with the combustion temperature as a function of mixture ratio. It is noted that with ambient propellants, the required hot gas flow at a MR=3 is about 60 percent of that required at the design mixture ratio of 1.0. An additional savings of ~10 percent can be realized by going to a mixture ratio of 8.0. It is noted that the hot gas discharge temperature becomes sensitive to the hot gas flowrate; this not only determines the gas temperature in the overboard dump system but also determines whether ice formation will occur at the exit of the conditioner.

In terms of control requirements, this means that higher mixture ratio operation requires good control of the overall flowrate; the exact mixture

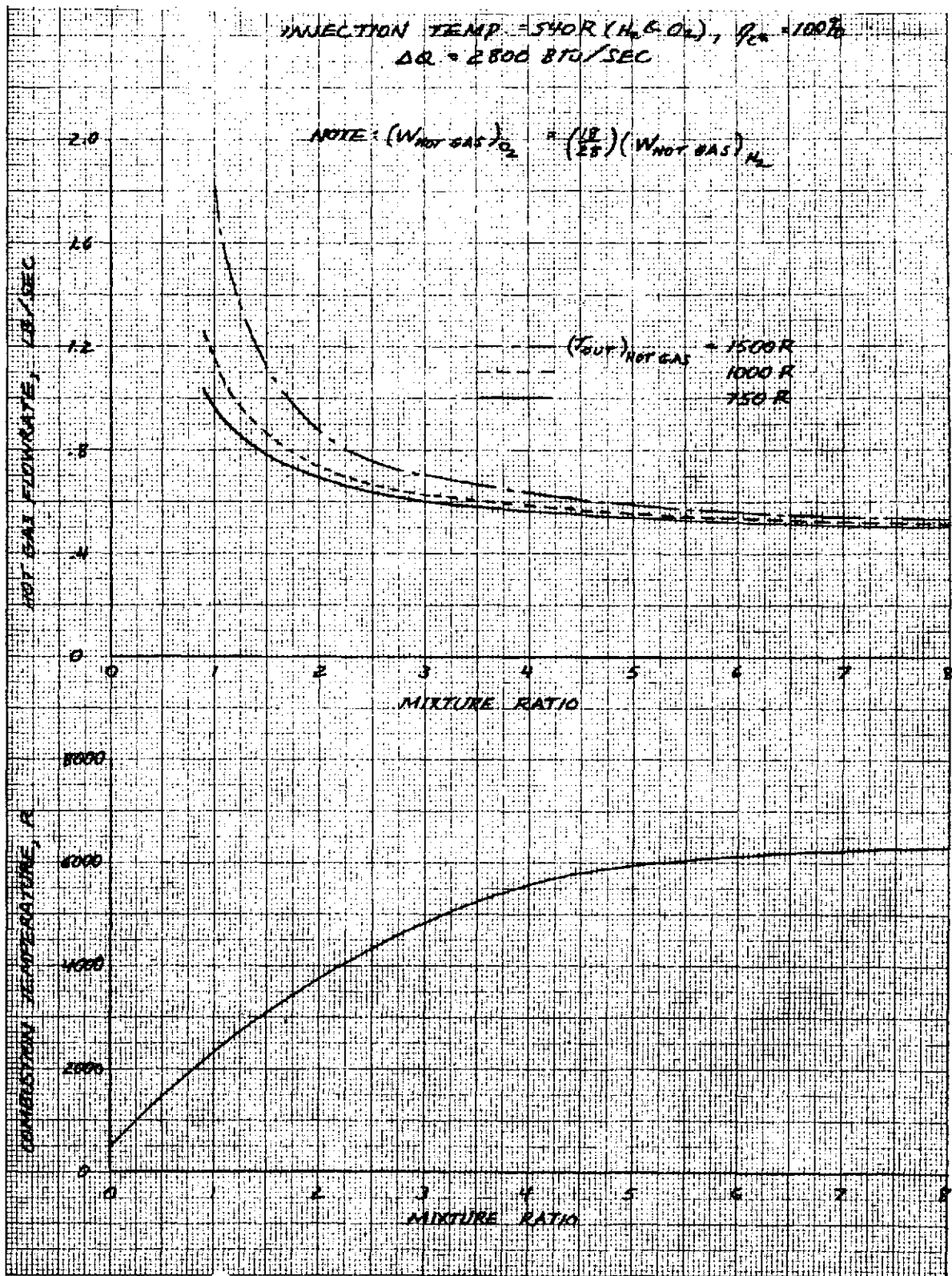


Figure 43. Hydrogen Conditioner Hot Gas Flow vs Mixture Ratio

ratio and propellant injection temperature are not critical since neither has a strong effect on heat rejection, maximum gas temperature, or wall temperature at mixture ratios of 3-8. On the other hand, the overall hot gas flowrate affects not only the exit conditions but also the local heat flux, and thus the wall temperatures and life as well as hydrogen exit temperature.

Using the required hot gas flowrates as a function of mixture ratio as shown in Fig. 43, the maximum baffle heat flux as well as minimum and maximum hot wall temperatures and conditioned fluid exit temperatures are shown in Fig. 44. The peak heat flux is seen to increase from 4.1 to 6.5 Btu/in²-sec going from a mixture ratio of 1.0 to 3.0. Very little increase in heat flux occurs as the mixture ratio increases, since the higher combustion temperature is offset by both the hot gas specific heat reduction and the reduced hot gas flow requirements at higher mixture ratio. This is reflected in the maximum gas wall temperature, which increases from 880 R at a mixture ratio of 1.0 to about 1220 R at a mixture ratio of 3. This range of temperatures is well within the operating capability of the baffle. The minimum wall temperature at the baffle exit decreases with increasing mixture ratio, for an approximately constant hot gas exit temperature, due to the reduced exit heat flux resulting from both reduced flowrates and specific heats. This would indicate that a thin layer of ice may start forming on the baffles at mixture ratios in excess of 2; this can easily be remedied by an increase in hot gas flowrate, which would increase both the exit hot gas temperature and the exit heat transfer coefficient.

Transient Response - Failure Mode

A transient start analysis was performed at mixture ratios of 1, 3, and 5. This analysis assumed that the hot gas flow was initiated at time 0, and the hydrogen flow was uniformly ramped starting 1 sec later and reaching full flow in the next half second (1-1/2 sec after hot gas initiation). This is a double failure mode operation, since the system as presently conceived cannot operate

$W_{H_2} = 2.7 \text{ LB/SEC}$ THROUGH CONDITIONER; $\Delta Q \sim 2800 \text{ BTU/SEC}$

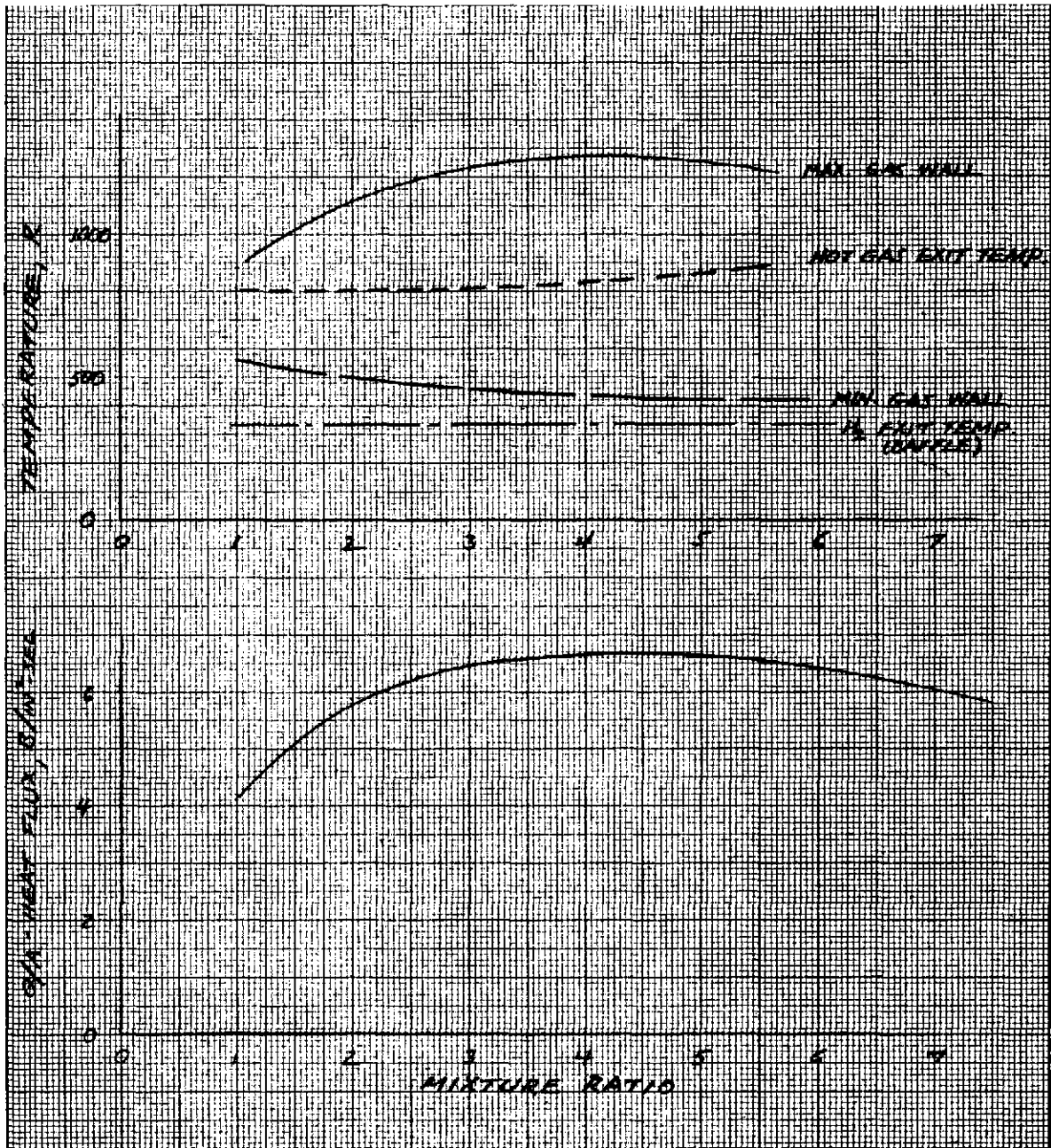
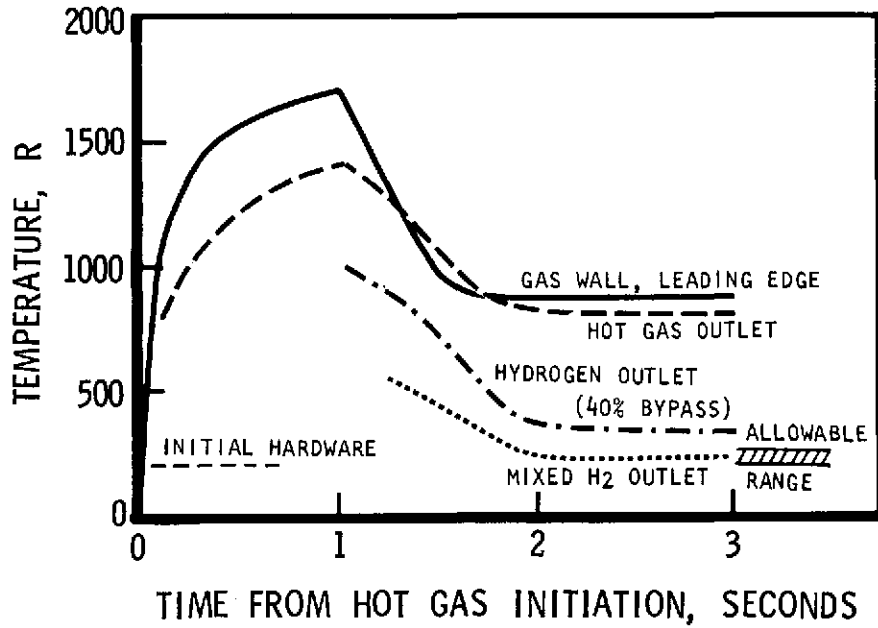
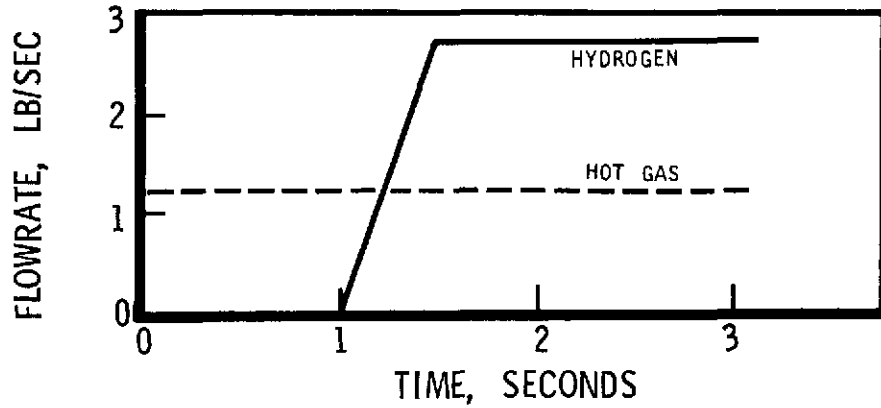


Figure 44. Hydrogen Conditioner Thermal Characteristics vs Mixture Ratio

at high mixture ratio with no coolant flow unless the flow control valve fails open. The results for mixture ratios of 1 and 3 are shown in Fig. 45 and 46 respectively. The transients for a mixture ratio of 5 are nearly identical to those at a mixture ratio of 3, as is to be expected from the similarity in the steady state results. At a mixture ratio of 1, there is no problem in this failure mode, since the maximum wall temperature is 1700 R at the leading edge after 1 sec of uncooled operation. The hot gas temperature at the exit is only 1400 R, so that there is no problem in terms of the exit end of the conditioner nor in the overboard dump system. In addition, it is seen that the conditioned hydrogen exit temperature reaches its design value half a second after the flow reaches its nominal value, so that the thermal transient requirements are easily met, even in a failure mode situation. At a mixture ratio of 3, the Haynes would start to melt in approximately 3/4 seconds of uncooled operation. Again, the flow control valve would prevent this situation from ever happening. It is noted that even after 1 second of uncooled operation, the hot gas exit temperature is only 1500 R, which is still compatible with the heat exchanger exit and probably also with the dump system. In this case because of the resultant higher hardware temperatures, it takes the hydrogen slightly longer to reach equilibrium exit temperature once the hydrogen flow has been established--about 0.7 sec; this would be faster with a 'normal' start. It is noted that if the baffle were to be designed to withstand this type of transient at high mixture ratio, several design changes could be made. These could include the use of a higher thermal conductivity material to prevent the hot wall from heating at such a fast rate, and/or reducing the peak heat flux, which will slow the wall temperature transient. In addition, it is noted that this analysis was performed with the assumption that there was no hydrogen in the coolant passages at the start; under most conditions there would be hydrogen at about 200 R in the channels at the start, and this would absorb some of the heat, resulting again in a slower hot wall temperature response.

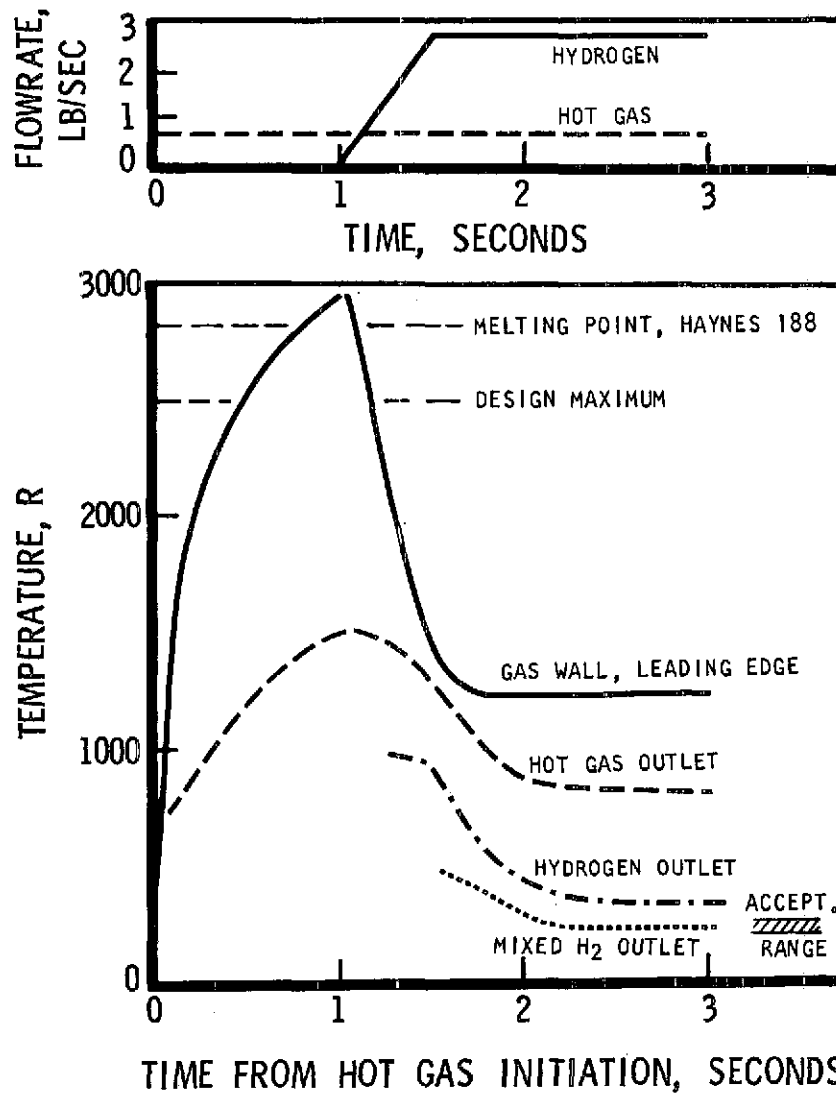


H₂ CONDITIONER THERMAL TRANSIENTS

MR = 1, T_c = 2060R, FAILURE MODE

DRY START

Figure 45. H₂ Conditioner Thermal Transients



H₂ CONDITIONER THERMAL TRANSIENTS

MR=3, T_c=4810R, FAILURE MODE
DRY START

Figure 46. H₂ Conditioner Thermal Transients

Thermal Start Transients

Study of the start transients of the hydrogen conditioner was conducted to determine baffle maximum wall temperatures and conditioned propellant temperatures as a function of time. Four cases were run using the nominal mixture ratio (1.0) at a combustion temperature of 1600 F in addition to the nominal conditioned propellant flowrate of 4.5 lb/sec H₂, with 40 percent bypass. The study assumed that the hardware initial temperature was equal to the average conditioned propellant temperature of 200 R, and that the hot-gas flow was initiated at the nominal value at time $\tau=0$. The conditioned propellant flow was assumed to increase at a linear rate from 0 at time $\tau=0$ until the full value was reached. The coolant transient times were assumed to be 0, 0.5, 1.0, and 1.5 seconds. The resulting transients are shown in Fig. 47.

For a simultaneous hot-gas and coolant start on the H₂ conditioner, the conditioned propellant reaches an acceptable temperature in 0.4 second (200 R mixed temperature), whereas the maximum wall temperature reaches the steady-state value in about 0.1 second. For the other start transients, the conditioned propellant temperature exceeds the nominal target value during the transient, reaching a maximum mixed temperature for the 1.5 second start of about 370 R (580 R out of the conditioner, 370 R out of the mixer), with an associated maximum wall temperature of 1210 R (750 F).

Oxygen Conditioner

The analysis for the oxygen conditioner consisted of determining the heat input requirements, the hot gas outlet temperature, nominal operating characteristics using the hydrogen conditioner, high mixture ratio operation, and transient operation. The same analytical techniques were used for both the hydrogen and oxygen conditioner. No analysis was performed on a separate optimum oxygen conditioner. It is noted that one of the advantages of having designed the hydrogen conditioner to bypass some of the flow around

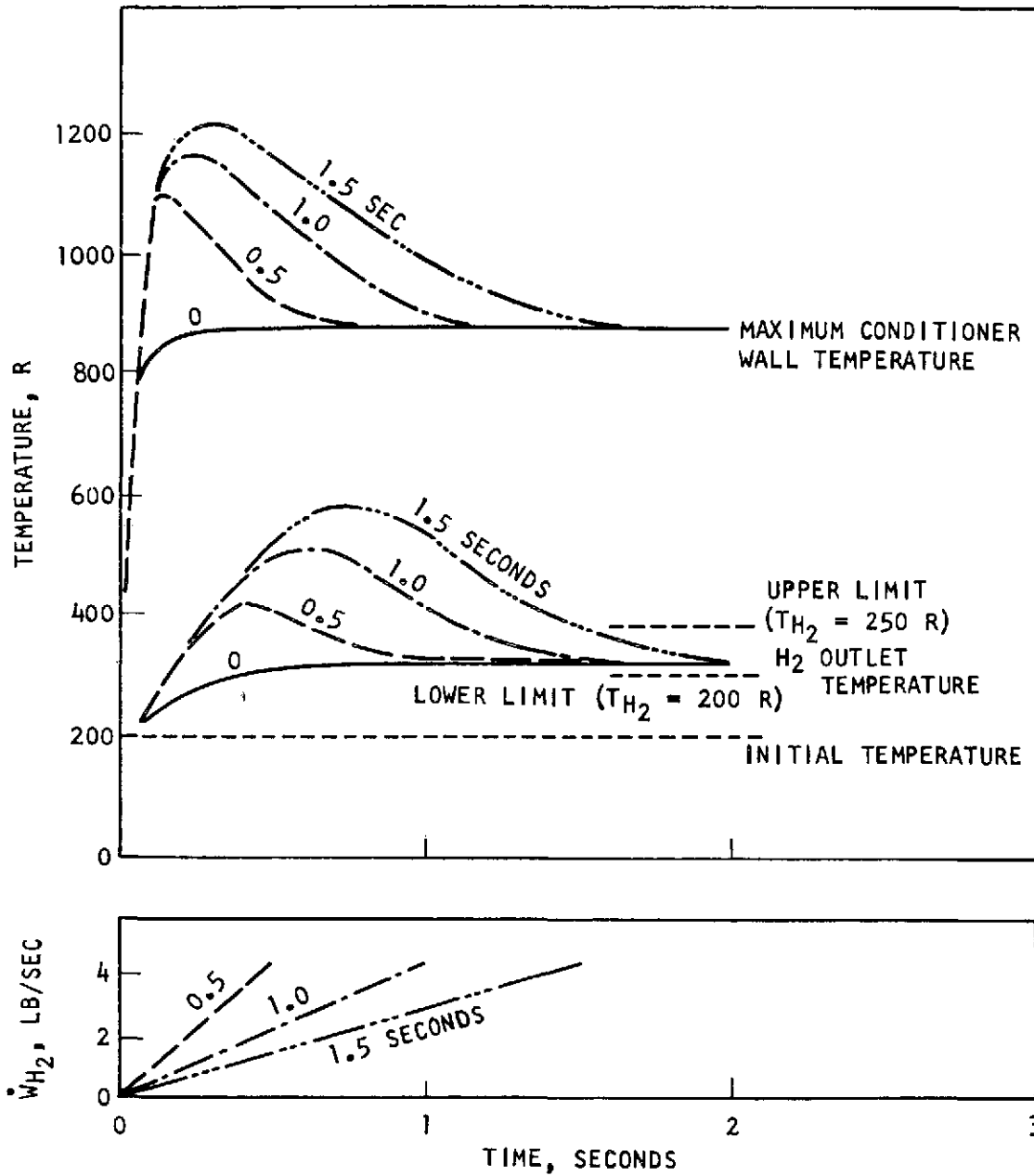


Figure 47. H₂ Conditioner Thermal Transient \dot{W}_{H_2} Thermal Transient = 4.5 lb/sec, 40 Percent Bypass, MR = 1, $P_c \sim 240$ psia

C-2

the conditioner is that the design is better suited for use as a common oxygen or hydrogen conditioner, with no bypass used with the oxygen. This is possible since (1) freezing is not as severe a problem with oxygen since the average exit temperature is 400 R and oxygen has poorer heat transfer characteristics; and (2) the oxygen pressure drop can be held to approximately the nominal 100 psi level. The main effect of using a common conditioner is that the oxygen is not capable of handling as high a heat flux as the hydrogen, resulting in higher wall temperatures when the hydrogen design is operated with oxygen. A study of alternate oxygen conditioner concepts was also performed. Results are presented in Appendix B.

Selection of Operating Conditions. The specified operating range of the oxygen flowrate and inlet and outlet temperatures is given in Table 9. As shown in Fig. 48, this covers a range in the required heat input from 1000 to 2900 Btu/sec, with a nominal value of about 1750 Btu/sec. The nominal value was used as the design point. Also, as in the case of the hydrogen conditioner, the nominal pressure drop was assumed to exist at the nominal operating point, with the result that lower pressure drops would result at higher inlet pressure and lower pressure, while the reverse would also be true.

A mixture ratio of 1.0 was selected as the nominal operating point, for the same safety oriented reasons as for the hydrogen conditioner. A high mixture ratio may have been safer with oxygen, since no combustion could occur in the event of a leak; however, a high mixture ratio of the same combustion temperature results in much higher hot gas flowrates. Furthermore this would require an injector redesign due to the tremendous difference in oxidizer and fuel flowrates at a mixture ratio of about 110, as shown in Fig. 49.

An analysis of the minimum weight requirements (exclusive of tankage) indicates that the minimum weight with one conditioner occurs with an outlet hot gas temperature of 600-650 R. With three conditioners, the optimum outlet

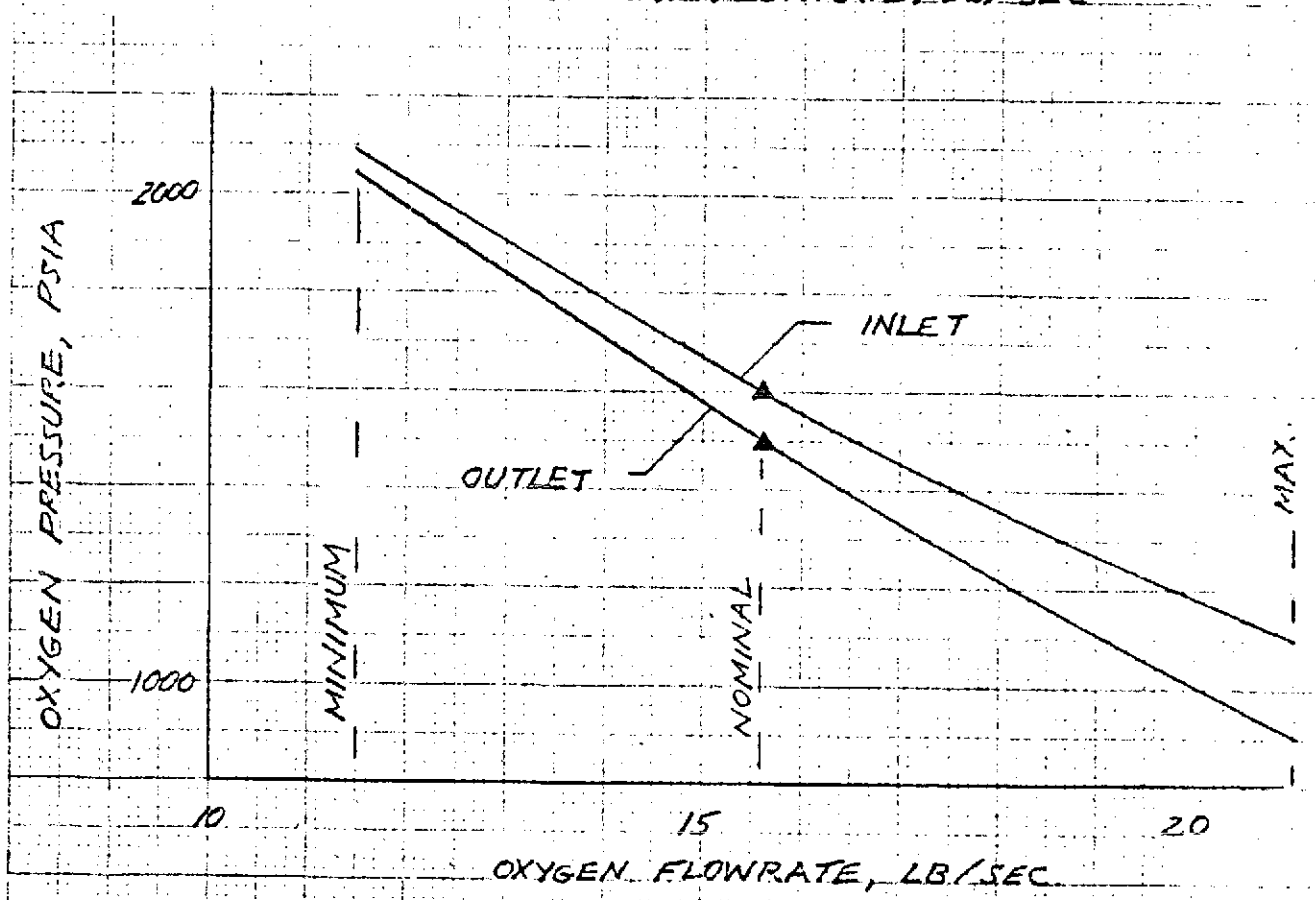
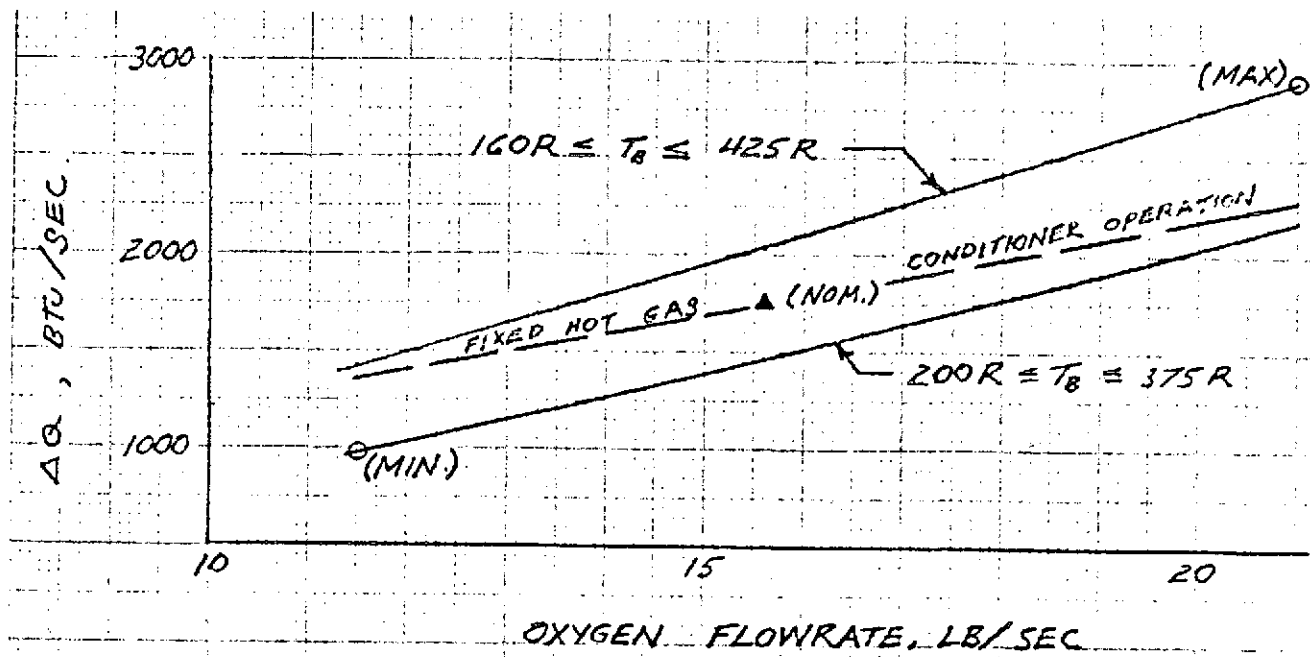


Figure 48. Oxygen Conditioner Heat Input

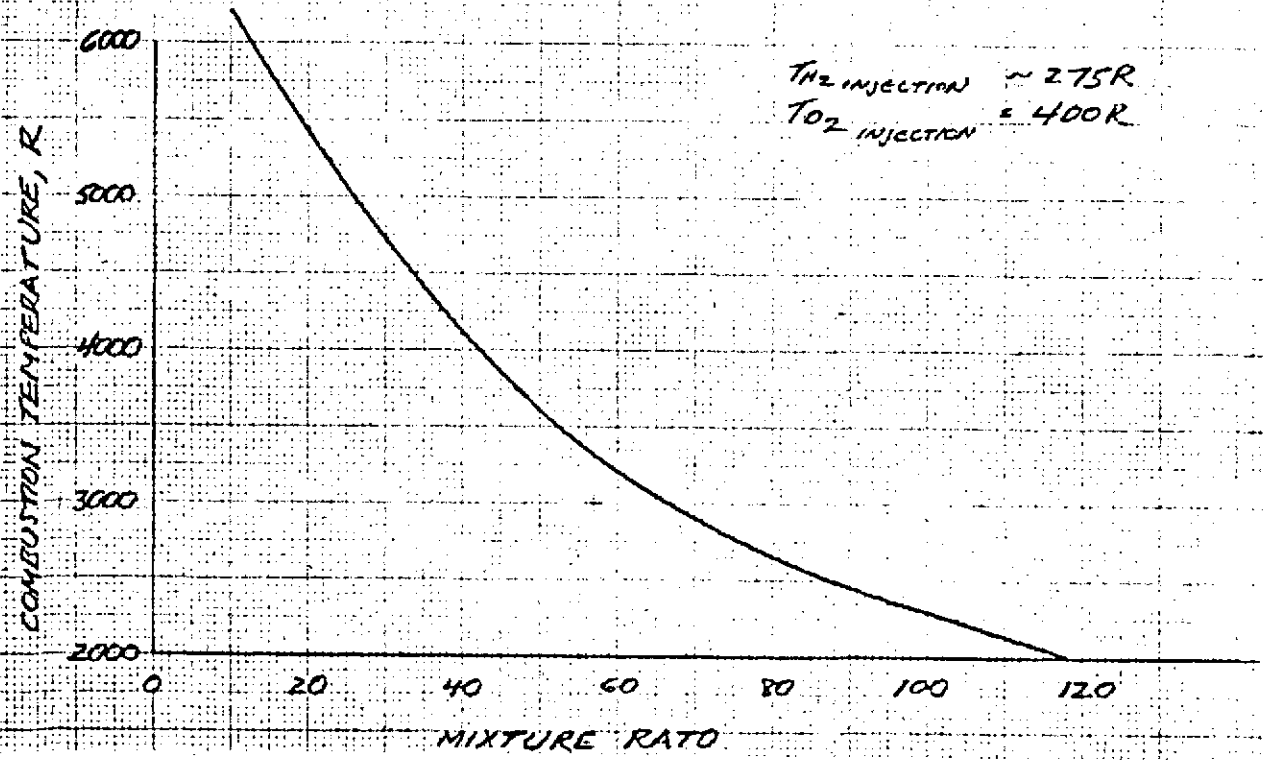
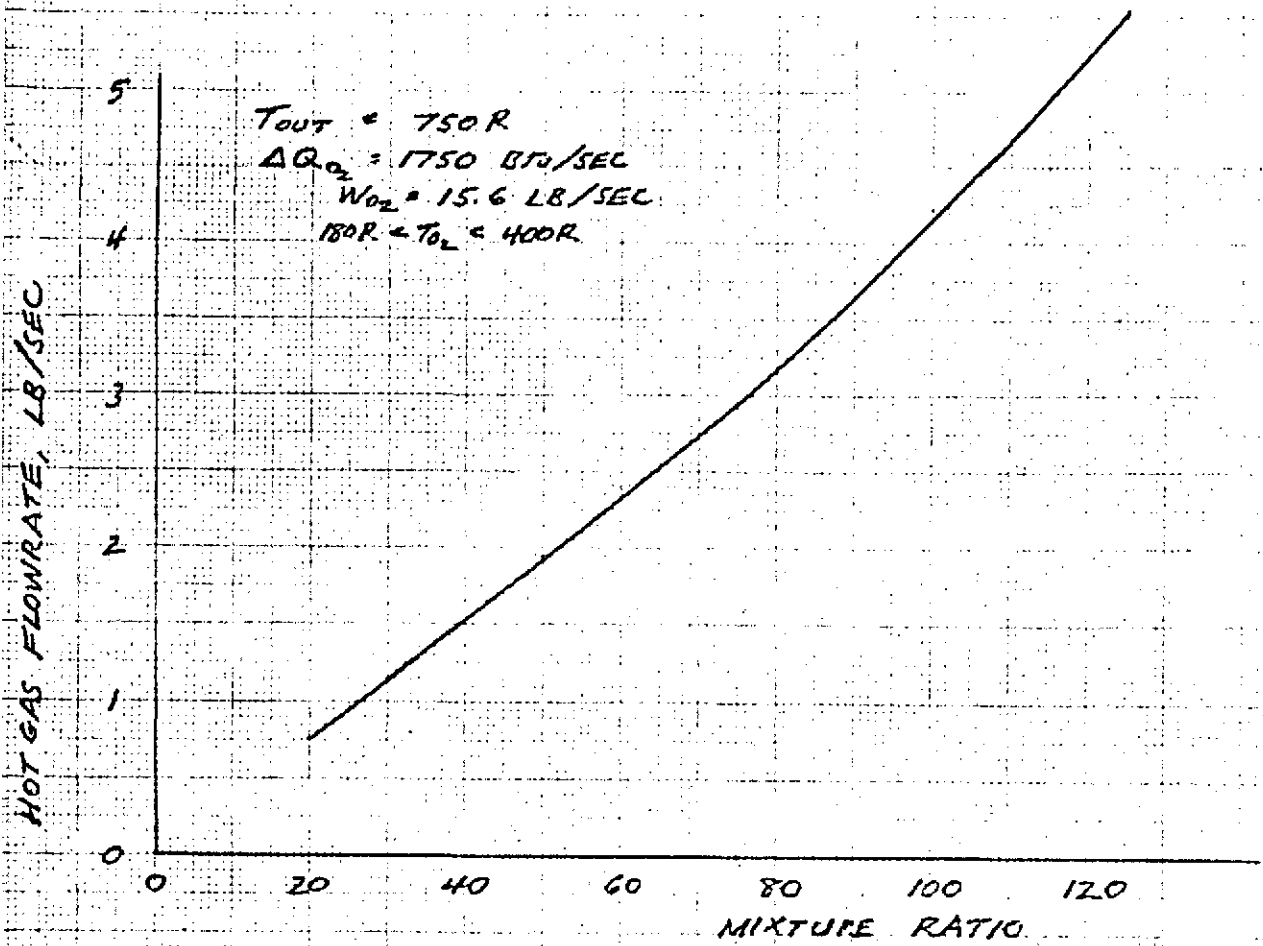


Figure 49. High Mixture Ratio Gas Requirements for O₂ Conditioner

temperature is 700-800 R, as shown in Fig. 50. As in the case of the hydrogen conditioner, 750 R was selected for the nominal operating point.

Thermal Analysis - Common Conditioner. Results with a mixture ratio of 1.0 indicate that the conditioner should work satisfactorily and still be able to condition the oxygen to the desired 400 R outlet temperature. The resulting fluid and hot wall temperature profiles are shown in Fig. 51, along with the heat flux. The maximum predicted wall temperature is 995 R, corresponding to a heat flux of about 2.5 Btu/in²-sec (about 20 percent higher than would have been designed for if a separate design had been generated). Exit wall temperatures are about 600 R--well above the freezing point.

Stability Analysis. A stability analysis of the conditioned fluid was performed for both the hydrogen conditioner and for the oxygen conditioner. The analysis was performed at the nominal flow and temperature conditions, using Friedly's criteria (Ref. 1). The results of the analysis indicate that both designs should be stable (Fig. 52).

The pressure drop ratio (ψ) in Fig. 52 represents the ratio of stabilizing to destabilizing pressure drops. The abscissa represents the Nyquist loop size parameter (σ).

The requirement for stability is that $\psi > \sigma$. It is noted that this stability criteria has been successfully applied to heat exchangers on the J-2 and other heat exchangers with considerable success (Ref. 2).

High Mixture Ratio Operation. Due to the interest in exploring the possibilities of higher mixture ratio operation with its higher performance potential, an analysis was conducted using a reactor mixture ratio of 3.0, maintaining a fixed oxygen flowrate at the 15.6 lb/sec nominal value and varying the hot gas flowrate to determine what operating point, if any,

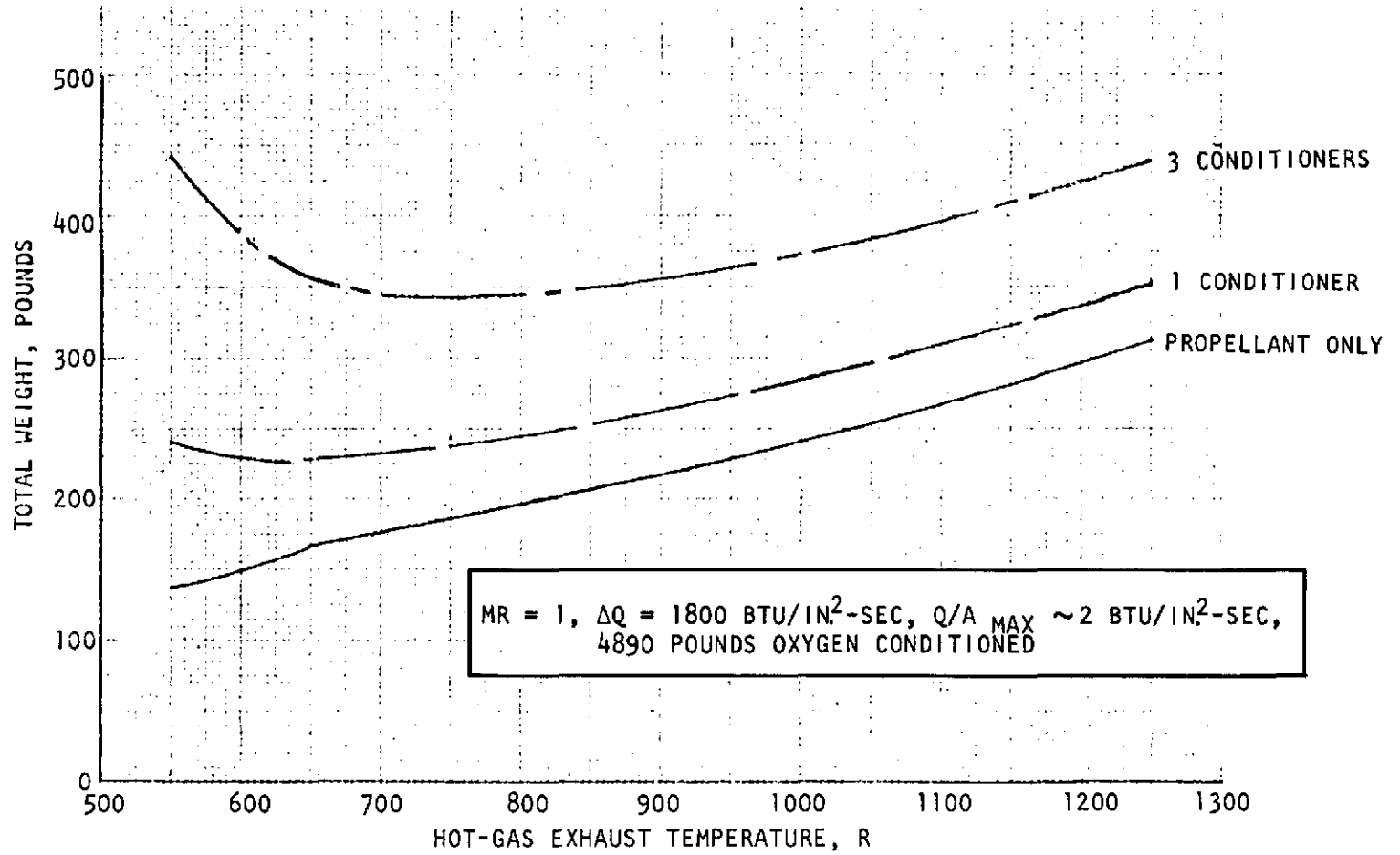


Figure 50. Oxygen Conditioner Total Weight Versus Hot-Gas Exhaust Temperature

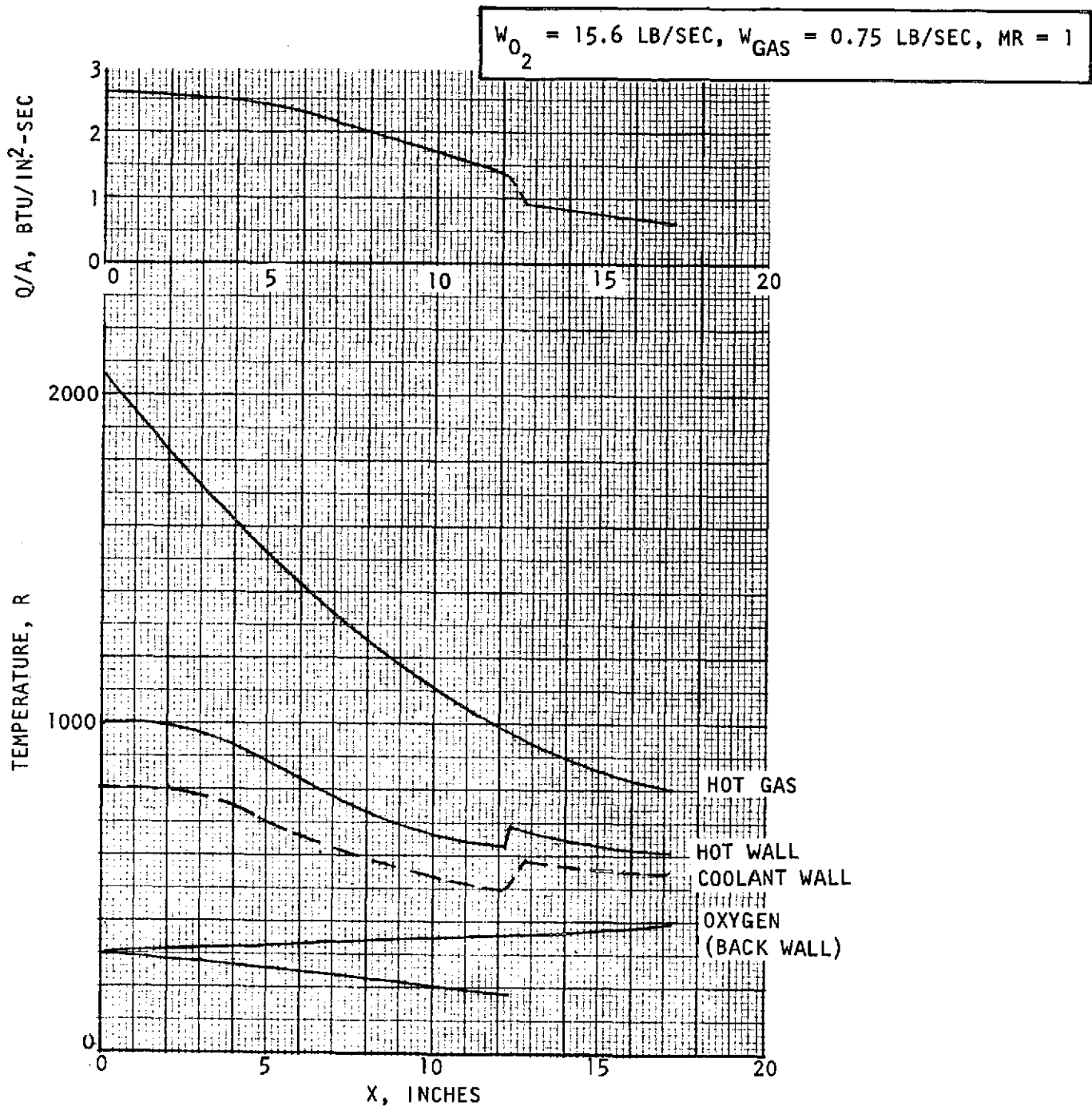


Figure 51. Oxygen Conditioned in H₂ Conditioner Baffles

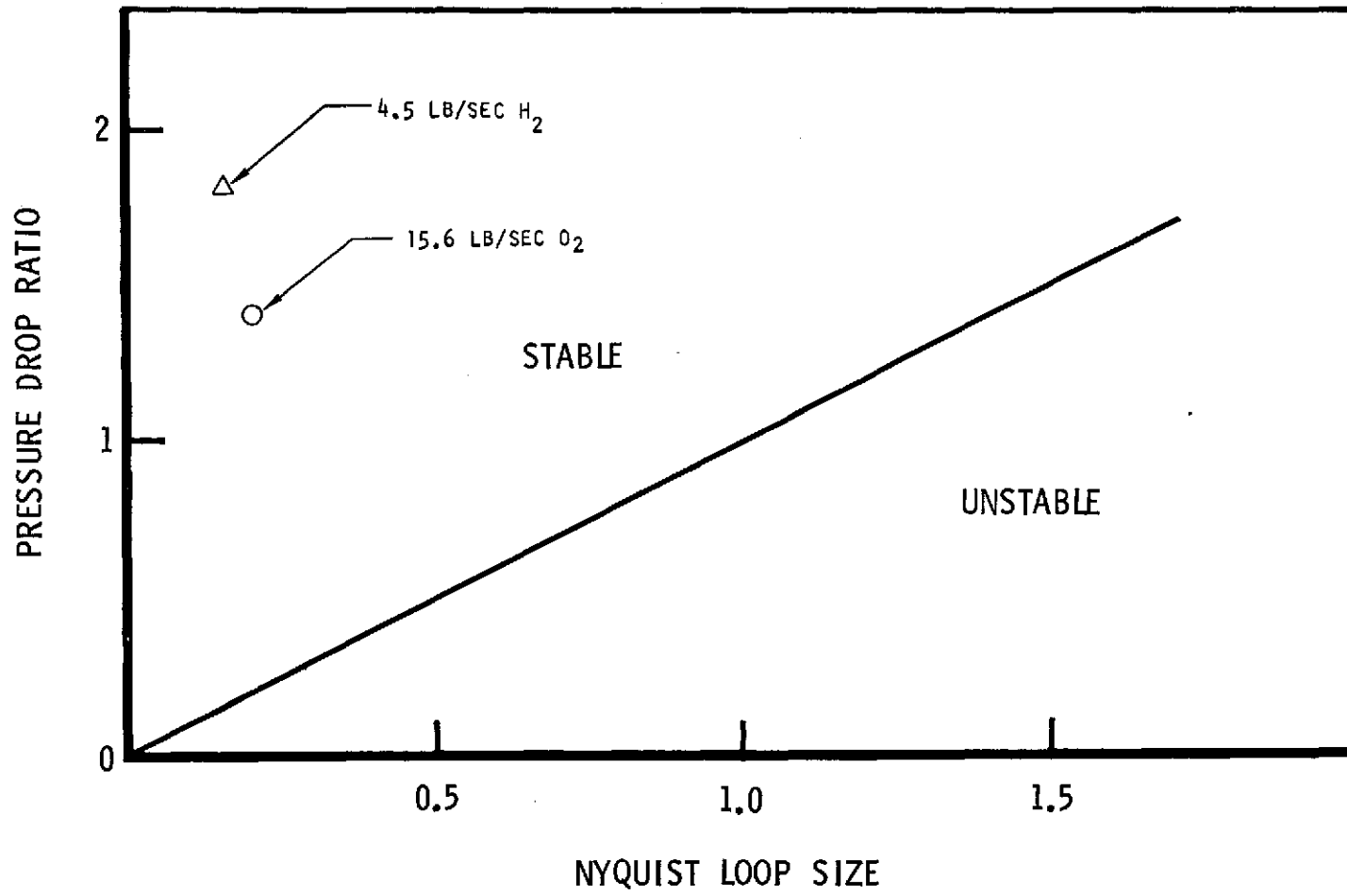


Figure 52. Predicted Stability at Nominal Conditions (Friedly Method)

appears attractive. The effect of reducing the hot gas flowrate is principally to reduce the leading edge heat transfer, and thus reduce the maximum wall temperature. Additional effects include reducing the conditioned oxygen outlet temperature and reducing the wall temperature at the conditioner exit. These are shown in Fig. 53.

From the standpoint of keeping the maximum hot wall temperature as low as possible, it would be desirable to test with a hot gas flowrate of about 0.25 lb/sec (at MR=3.0) resulting in maximum wall temperatures of approximately 700 F. At this point the conditioned oxygen outlet temperature would be 320 R and the hot gas outlet temperature would be 620 R. However, the minimum wall temperature predicted at the trailing edge of the baffle would be about 380 R, indicating that ice formation on the rear part of the baffle could be expected. A better compromise at a mixture ratio of 3.0 is a hot gas flowrate in the range of 0.32 to 0.35 lb/sec, resulting in a maximum wall temperature at the leading edge of 900 - 1000 F, and a minimum exit wall temperature of about 440 - 475 R--probably close enough to the freezing point that any layer of ice formed would be thin enough to have little effect on the overall operation of the conditioner. The resultant conditioned oxygen outlet temperature is 360-380 R--in the range of the lower specified oxygen discharge temperature of 375 R.

It is noted that when operating at higher mixture ratio, it is necessary to reduce the hot gas flowrate; otherwise the conditioned propellant will be heated more than is desirable, and furthermore it causes an unnecessarily high heat flux at the forward end of the conditioner, resulting in higher temperatures and reduced life. The required flowrates for the required heat rejection rate of 1800 Btu/sec are shown in Fig. 54 for ambient hydrogen and oxygen injection conditions. It is seen that the hot gas requirements at a mixture ratio of 2 is about 2/3 that at a mixture ratio of 1, for an outlet temperature of 750 R.

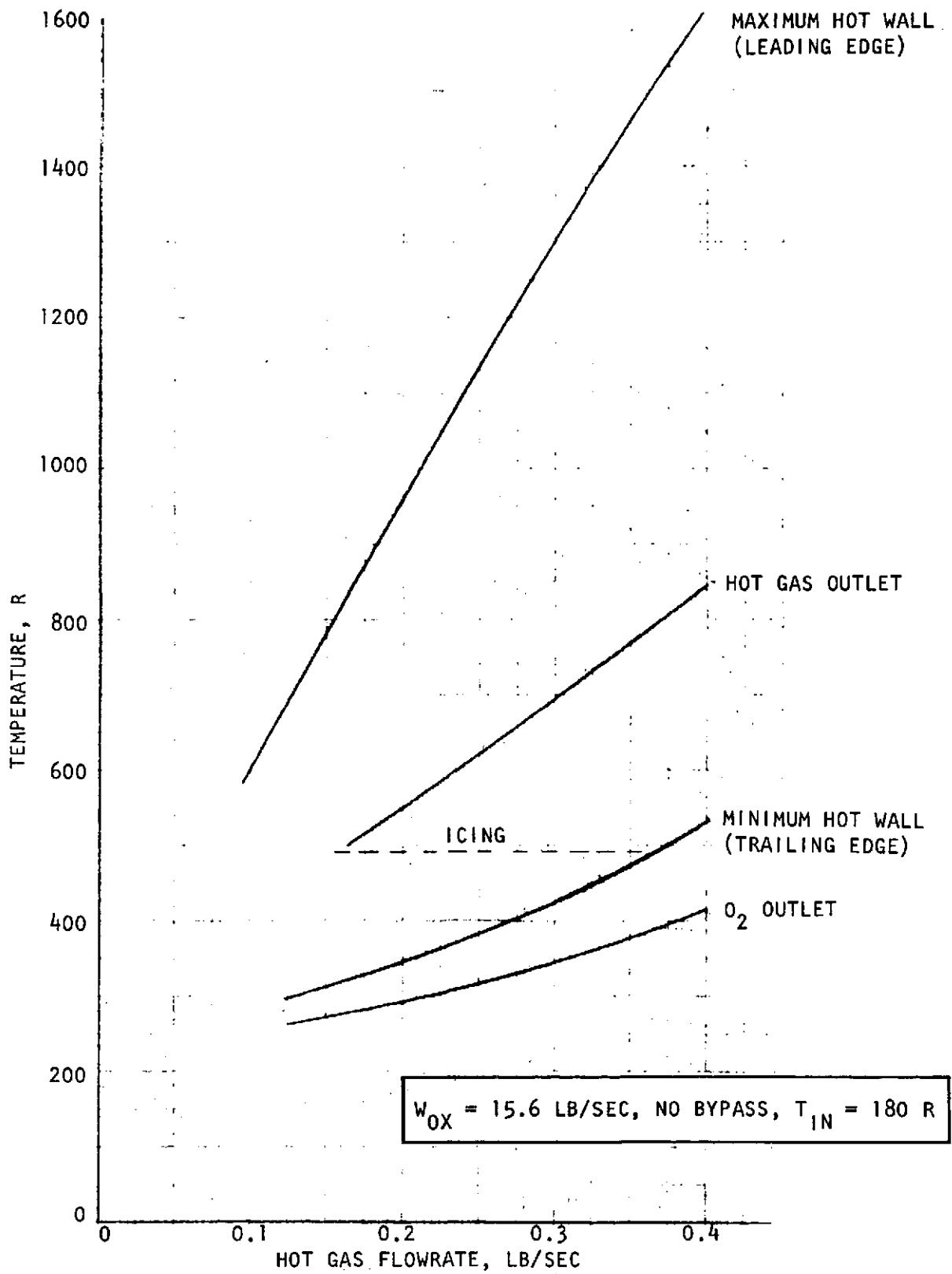


Figure 53. Oxygen Conditioner Temperatures Versus Hot Gas Flowrate, MR = 3

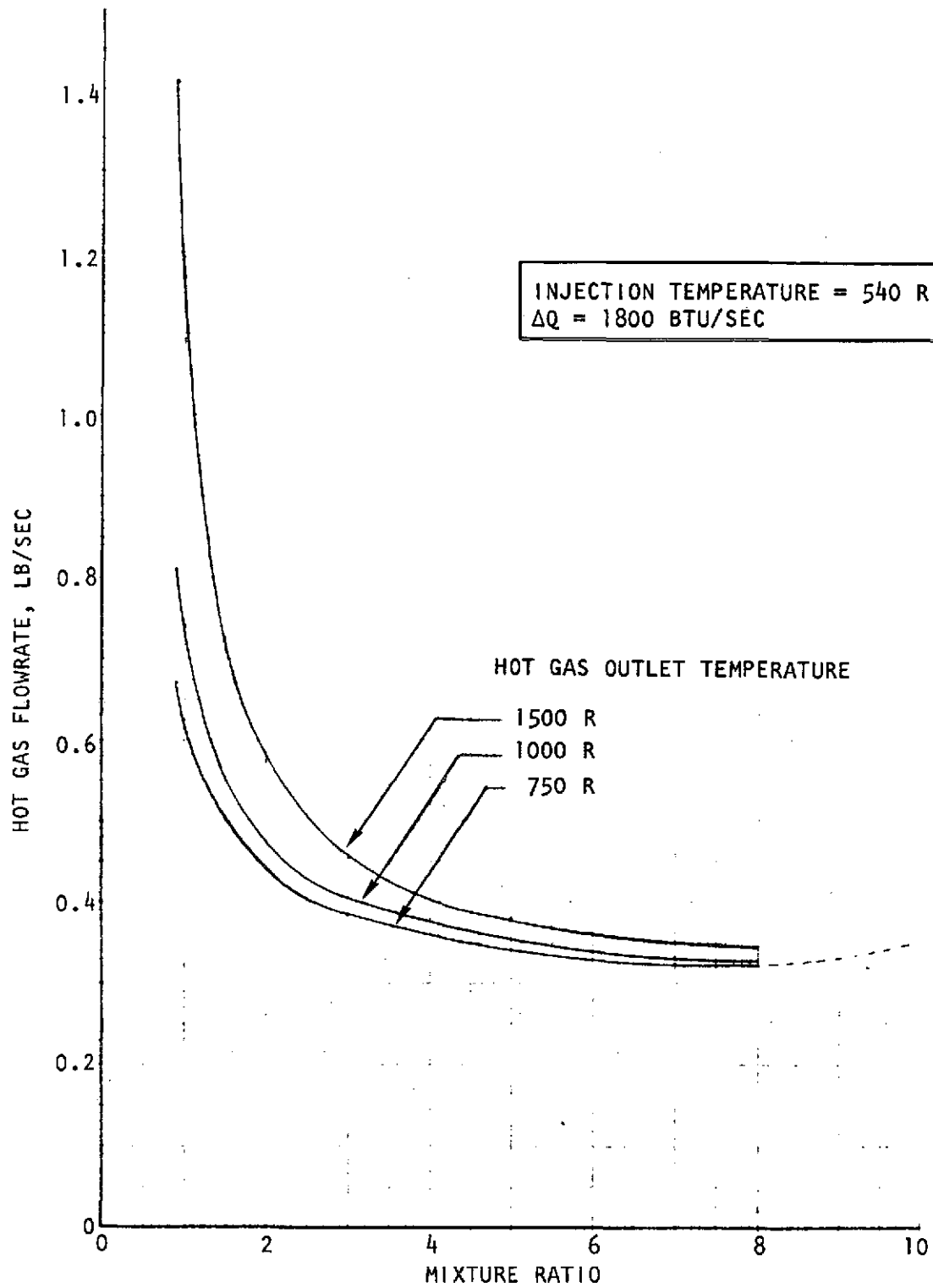


Figure 54. Oxidizer Conditioner Hot Gas Flow Requirements Versus Mixture Ratio

Thermal Start Transients. To determine the effect of a delayed oxygen flowrate on the transient baffle hot wall temperatures, a series of transient solutions were generated assuming that the oxygen flow ramped up in a linear manner over a 0, 1/4, 1/2, and 3/4 second period. The resulting oxygen outlet temperature and baffle hot wall maximum predicted temperature is shown in Fig. 55 at the nominal MR=1 design point. The initial hardware temperature was assumed equal to the average conditioned oxygen temperature of 290 R.

Results of the analysis indicate (1) that conditioned oxygen at the required operating temperature can be supplied with the required 1/2 second; and (2) that the hardware can easily sustain a condition where the oxygen ramps over 3/4 second period with the hot gas running at nominal mixture ratio.

The oxygen conditioner attains an acceptable conditioned outlet temperature in 0.2 to 0.4 second, depending on the start transient. The instant LO₂ flow response results in the longest time to reach the minimum outlet temperature of 375 R. The maximum overshoot at the 0.75 second transient is only 490 R, and the value for the 0.5 second start is only just above the upper limit (450 R versus the limit of 425 R).

STRUCTURAL AND CYCLIC LIFE ANALYSIS

Effort on this task was concerned with:

- (1) Establishing design criteria,
- (2) Evaluating candidate materials,
- (3) Generating parametric cyclic life data for use in the thermal analysis,
- (4) Structurally analyzing the design, and
- (5) Predicting the cyclic life capability of the selected design.

INITIAL HARDWARE TEMPERATURE = 290R = AV O₂ TEMPERATURE
 $\dot{W}_{O_2} = 15.6$ LB/SEC, MR = 1, P_c 240 PSIA
 HOT GAS STARTS AT $\tau = 0$

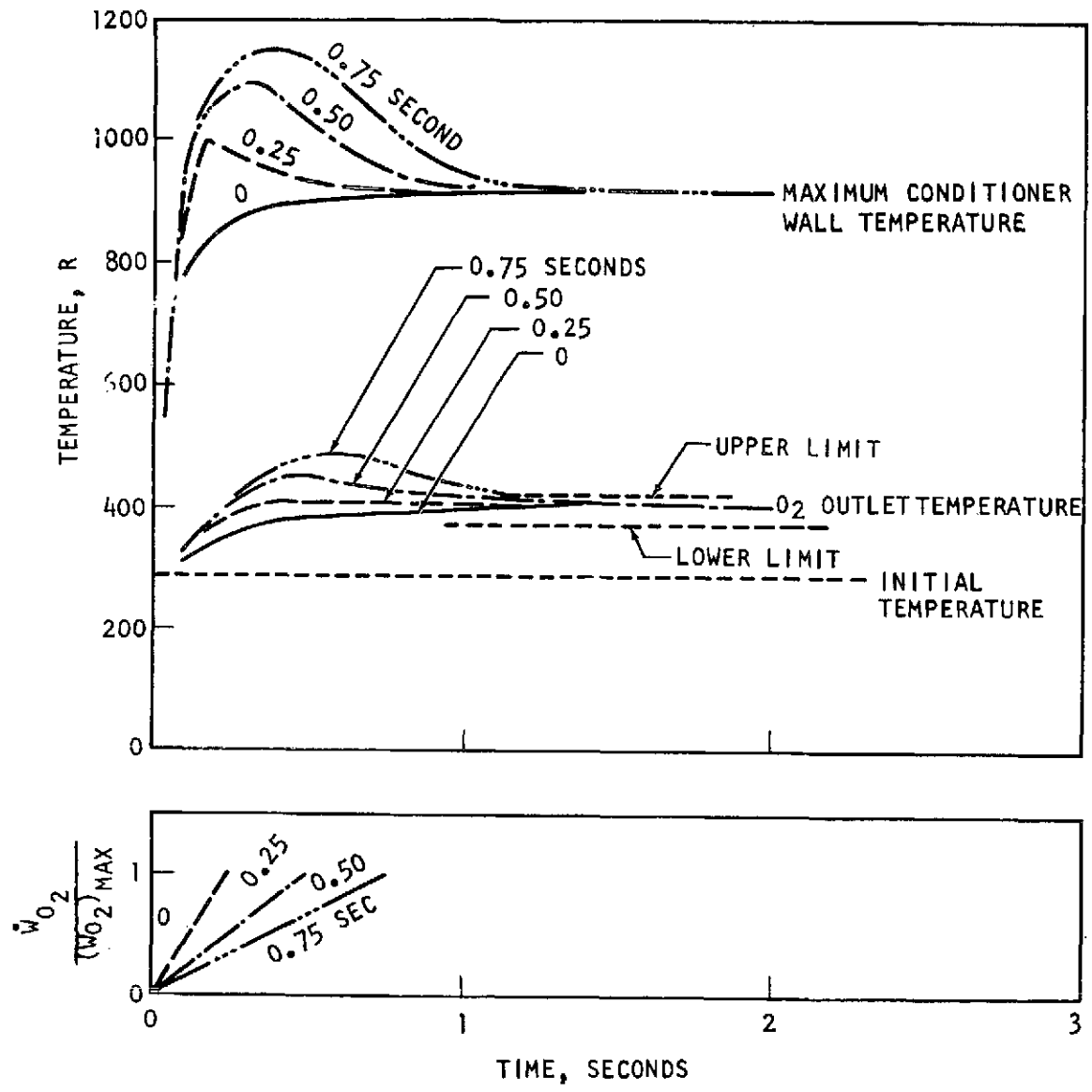


Figure 55. Oxygen Conditioner Thermal Transients

Design Criteria

The structural criteria set forth for each component included a yield safety factor of 1.1 and an ultimate safety factor of 1.4, using minimum guaranteed material properties.

Rocketdyne's approach to evaluating the cyclic life capability of long life components is predicted on the fundamental theory that failure depends on the accumulation of creep damage and fatigue damage.

The life analysis is based on a definition of the stress-strain-time-temperature history during each operating cycle. Creep damage is evaluated from the stress-time-temperature cycle and fatigue damage from the strain-time-temperature cycle.

The increment of creep damage, $\Delta\phi_c$, is determined by the ratio of time spent at a particular stress level, t , to the time-to-rupture at that stress level, t_r

$$\Delta\phi_c = \Sigma \left(\frac{t}{t_r} \right) \sigma$$

$\Delta\phi_c$ = creep rupture damage

t = time at stress, σ

t_r = time to rupture at the stress, σ

The total creep damage, ϕ_c , is given by:

$$\phi_c = \Sigma \Delta\phi_c$$

Fatigue damage, ϕ_f , is determined by the ratio of the actual number of cycles (starts and stops) applied at a particular strain range to the number of cycles which would cause failure at that strain range.

$$\phi_f = \Sigma \frac{n}{N_f}$$

In the absence of experimental fatigue data on the material of interest, the Method of Universal Slopes is used to obtain isothermal fatigue design values for cycles to failure.

The method is given by:

$$\epsilon_t = e.t \left(\frac{F_{tu}}{E} \right) N_f^{-.12} + D \cdot 6 N_f^{-.6}$$

where

ϵ_t = total calculated strain range

F_{tu} = material ultimate strength

E = Young's Modulus

D = Fracture Ductility, $\ln \left[\frac{100}{100-RA} \right]$

RA = percent reduction-in-area

The basic properties are used at the temperature of interest while the straining process with varying temperature is considered incrementally. Cyclic life for the strain range is based on values for F_{tu}/E and RA obtained over the temperature range of the strain cycle.

Ultimately this is replaced by isothermal fatigue data generated on the material(s) of construction over the predicted temperature and strain range. A plot of fatigue life vs. temperature for the specific strain range of interest is the key element in the incremental technique. The number of allowable cycles, N_f , for the strain range, ϵ_t , is determined by graphically averaging the value of N_f over the operating temperature range.

A generalized life equation is used to consider the total damage caused by the interaction of low and high cycle fatigue and creep rupture.

The equation takes the following form:

$$4\phi_{fL} + 4\phi_c + 10\phi_{fH} = 1.0$$

where

ϕ_{fL} = low cycle fatigue damage

ϕ_c = creep rupture damage

ϕ_{fH} = high cycle fatigue damage

Safety Factor = 4 on low cycle fatigue and creep rupture
= 10 (on high cycle fatigue)

Evaluation of Candidate Materials

To maximize cyclic life capability of the conditioner heat exchanger baffles, it was desirable to evenly distribute the thermal strains in the hot gas wall and the closure. Since the hot gas wall will operate at a temperature level of several hundred degrees while the closure operates at a temperature nearly equivalent to the propellant bulk temperature, it is appropriate to use dissimilar materials on the two surfaces with the weaker material used as the closure. Analysis showed that use of Haynes 188 or the Armco alloys 21-6-9 or 22-13-5 on the hot gas wall in conjunction with 304L or 347 stainless steel on the closure offers a good combination from a cyclic life standpoint (Table 12). The allowable strains are relatively close and can be made nearly equal by selective variation of the appropriate wall thickness as operating temperatures become finalized. Evaluation of these material combinations from a fabrication and processing standpoint (discussed in a later section) led to the selection of Haynes 188 for the hot gas wall and 304L stainless steel for the closure. Additional discussion is included in the DESIGN AND FABRICATION section.

Parametric Cyclic Life Data

With the selection of the Haynes 188 stainless steel material combination, an analysis was completed to determine allowable temperatures for use in the thermal analysis. This data, shown in Fig. 56 for a life capability of 42,000 cycles, is predicted on the cyclic life ground rules and procedures summarized earlier.

TABLE 12. EVALUATION OF CANDIDATE MATERIAL COMBINATIONS

HOT GAS WALL MATERIAL	CLOSURE MATERIAL	TEMP F	ULTIMATE STRENGTH KSI ^①	YIELD STRENGTH KSI ^①	REDUCTION OF AREA PERCENT ^①	ALLOWABLE STRAIN RANGE IN/IN ^②
Haynes 188	-	400	123	53	57	.0054
	-	600	117	48	55	
Armco 21-6-9	-	400	90	42	65	.0048
	-	600	86	38	60	
Armco 22-13-5	-	400	101	49	64	.0053
	-	600	98	46	63	
-	304L SS	-300	180	45	53	.0069
		-200	154	44	56	
-	347 SS	-300	190	51	65	.0075
		-200	160	49	67	

① Typical material properties.

② Based on Universal Slopes equation, a required cyclic capability of 42,000 cycles, and a thickness of 0.015 inches

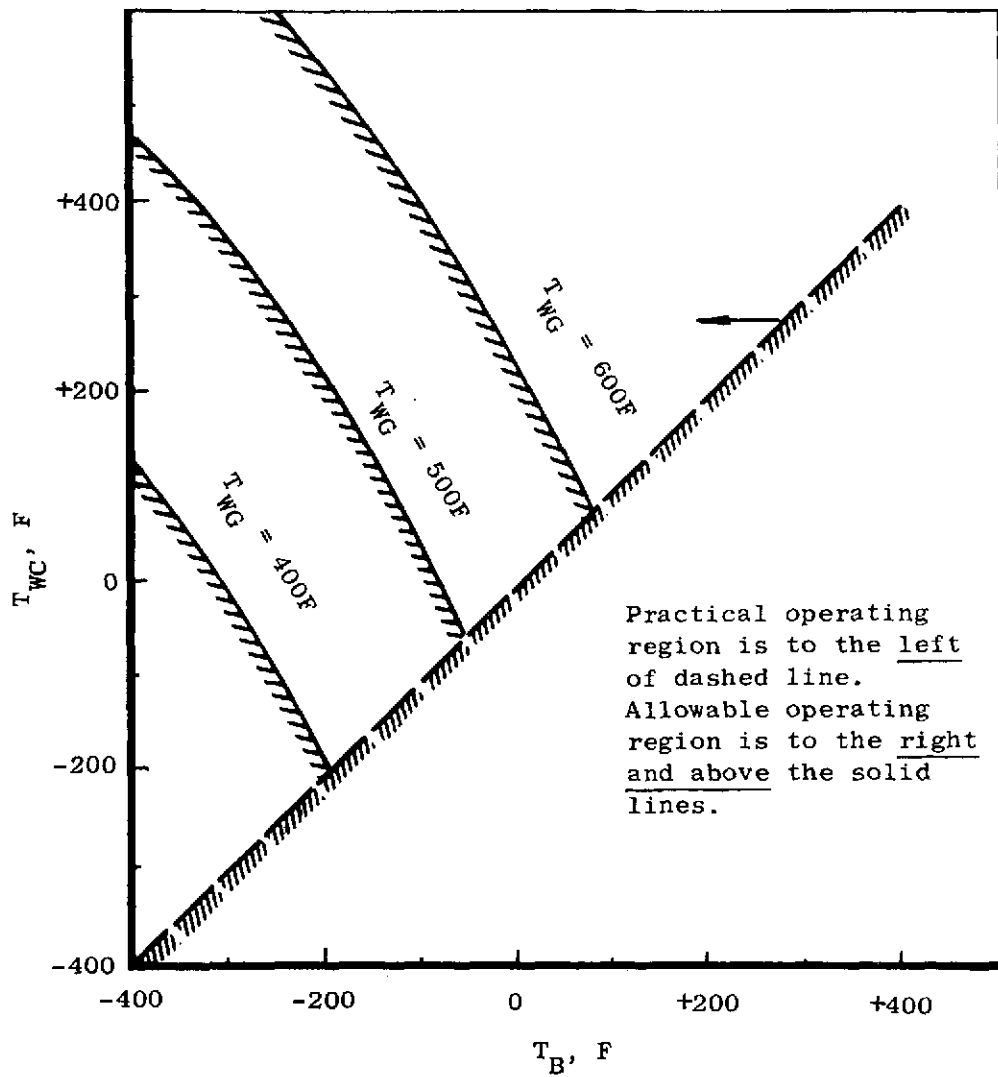
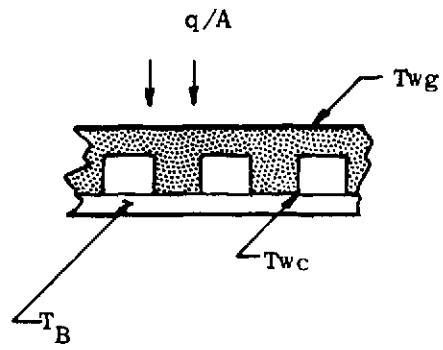


Figure 56. Estimated Allowable Temperatures for Haynes 188 Baffles

Cyclic Life Capability of Selected Design

Thermal cycle capability of the hot face of conditioned hydrogen channels was evaluated and is presented in Table 13 below. Creep damage is negligible since hydraulic stresses are very low for nominal operating conditions.

TABLE 13. HOT WALL THERMAL CYCLE CAPABILITY--HYDROGEN CONDITIONER

Location	Station*	N_f Cycles**
Baffle	0.0***	35,000
	5.0***	35,000
	12.0****	58,000
Side Wall	0.0****	7,400
	5.0****	7,500
	12.0****	58,000

*Inches from baffle leading edge

**Cycles to initiation of cracking

***50-percent thermal restraint

****100-percent thermal restraint

SYSTEM BALANCE ANALYSIS

A system balance analysis was undertaken to establish regulator requirements for controlling reactor propellants flowate over the specified range of inlet temperatures.

Results, presented in detail in Appendix A, showed that regulating gaseous hydrogen inlet pressure on the basis of inlet temperature provided acceptable control with a regulation accuracy of ± 3 percent. However, the oxygen should be regulated on the basis of hydrogen and oxygen inlet temperatures to assure satisfactory reactor operation.

To eliminate the need for this complex oxygen regulator, study was also done on a system which incorporated thermal equalizer upstream of the regulator such that the gaseous hydrogen and gaseous oxygen propellant are supplied at the same temperature. The results showed that regulating inlet pressure on the basis of inlet temperature and assuming a ± 3 percent regulator accuracy produced satisfactory reactor conditions. Nominal values (add 2800 Btu/sec to LH₂) for reactor operation as a function of reactor propellant inlet temperatures are tabulated below.

Inlet Temp. R	Inlet Pressure, psia		psia	Flowrate Lb/sec	MR (o/F)
	GO ₂	GH ₂			
275	306	292	245	1.25	1.16
450	325	306	236	1.17	1.13
600	324	310	222	1.09	1.00

DESIGN AND FABRICATION

The basic conditioner design approach and some of the major design features and operating conditions were based on the overall goal of obtaining long life, high reliability with high performance, and minimum weight. These goals, with the exception of minimum weight, which was compromised for ease of manufacture and reduction of cost, were maintained throughout the program.

The requirements and operational parameters for the hydrogen propellant conditioner as set forth in the Work Statement were presented previously in Tables 7 through 9. Nominal design parameters are shown in Table 14.

BAFFLE MATERIAL SELECTION

The early heat transfer analysis and the requirement that no damage or life degradation would result if either hot gas or cold flow is not initiated dictated a need for a material which could:

1. Afford high resistance to oxidation and hydrogen embrittlement at variable temperatures.
2. Have high strength and ductility at elevated temperatures.
3. Meet the NASA requirement of standard materials.
4. Be readily fabricated, brazed and welded.

Some of the materials evaluated to meet the above requirements included:

Haynes 188	Armco 22-13-5
Haynes 25	A-286
Hastelloy X	304L stainless
Armco 21-6-9	OFHC copper

A comparison of some material properties is shown in Table 15. As can be noted from Table 15, several of the materials, such as copper and the stainless steels are not recommended for high temperature service and therefore

TABLE 14. NOMINAL DESIGN POINT--H₂ CONDITIONER

H ₂ SIDE	
\dot{w}	= 4.5 LB/SEC
P_{in}	= 1600 PSIA
P_{out}	= 1500 PSIA
T_{in}	= 55 R
T_{out}	= 225 R
ΔQ	= 2800 BTU/SEC
40 PERCENT BYPASS	
HOT GAS SIDE	
MIXTURE RATIO	= 1.0
H ₂ INJECTION TEMPERATURE	= 275 R
CHAMBER PRESSURE	= 240 PSIA
COMBUSTION TEMPERATURE	= 2060 R
EXHAUST TEMPERATURE	= 750 R
COMBUSTION EFFICIENCY	= 100 PERCENT
HOT GAS FLOWRATE	= 1.2 LB/SEC
DESIGN MIXTURE RATIO TOLERANCE	= ±10 PERCENT
MAXIMUM HEAT FLUX	~ 4 BTU/IN. ² -SEC
MIN. GAS SIDE WALL SURFACE TEMP.	~ 530 R
MIN. HOT GAS PASSAGE WIDTH	= 0.050 IN.
WALL MATERIAL	
HAYNES 188 - HOT GAS WALL AND LANDS	
STAINLESS STEEL - CLOSEOUT	
MIN. LAND WIDTH 0.035 - 0.040 IN.	
CONSTANT PLATE THICKNESS (GAS WALL + LAND)	
CONSTANT CHANNEL WIDTH (WITH STEP CHANGES)	

TABLE 15. MATERIAL PROPERTIES - CANDIDATE CONDITIONER MATERIALS

MATERIAL	TEMPERATURE F	ULTIMATE STRENGTH ksi	YIELD STRENGTH ksi	ELONGATION %	MELTING TEMP F	RECOMMENDED MAX. SERVICE F
Haynes 188	R.T.	135	65	60	2375	2000
	600	120	45	75		
	1700	35	30	80		
Haynes 25	R.T.	140	70	50	2350	2000
	600	130	65	45		
	1700	25	25	100		
Hasteloy X	R.T.	110	50	40	2350	2000
	600	100	40	40		
	1700	25	20	50		
Aimco 21-6-9	R.T.	110	65	40		
	600					
	1700					
ARMCO 22-13-5	R.T.	120	65	45		
	600					
	1700					
A-286	R.T.	145	100	25		
	600					
	1700					
304L Stainless	R.T.	85	30	40	2650	1600
	600	55	25	40		
	1700	10	--	45		
347 Stainless	R.T.	90	35	40	2650	1600
	600	60	30	35		
	1700	10	--	45		
OFHC Copper	R.T.	30	10	45	1980	1200
	600	20	5	50		
	1700	5	--	90		

eliminated for consideration. Of the remaining materials evaluated, Haynes 188 and A-286 showed the greatest promise as a candidate material. The A-286 material has very good resistance to hydrogen embrittlement and shows good strength properties; however, it has some undesirable features which eliminated it from consideration for this application. These features are:

Plating is required in a brazed structure.

The alloy is difficult to weld without cracking.

Being a precipitation hardened alloy, optimum natural properties cannot be obtained when processed through a braze cycle.

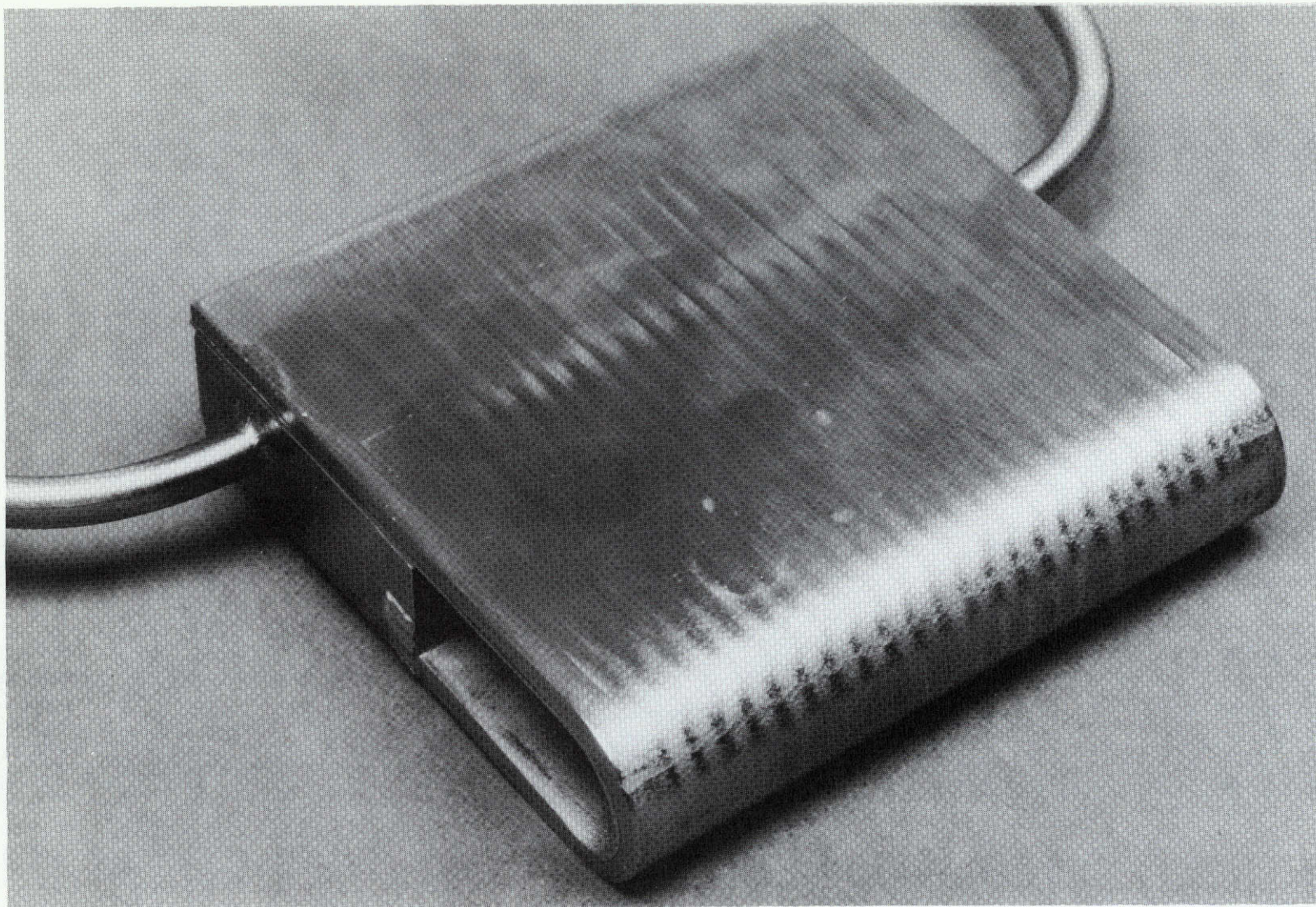
The alloy is not stable at elevated temperatures.

Haynes 188 is a non-hardenable cobalt base alloy which exhibits a metallurgically stable structure over a wide temperature range and for prolonged exposure time at temperature. The material was evaluated for propellant compatibility, welding and brazing characteristics, fabricability, and has established guaranteed tensile property design values. Haynes 188 is compatible with both hydrogen and oxygen within the temperature range of the conditioner. The material has exhibited a high degree of resistance to high-pressure hydrogen embrittlement in both notch bar testing and low cycle fatigue testing. Haynes 188 is weldable and brazeable to itself and to other alloys. To assure the feasibility of manufacture and guarantee the laboratory properties, several sample baffle assemblies were designed and manufactured.

SAMPLE BAFFLE ASSEMBLY

Several sample baffle assemblies as shown in Fig. 57 were fabricated and laboratory tested. The manufacturing sequence as shown in Fig. 58 and the techniques used in the manufacture of this panel assembly were identical to those eventually used in the manufacture of the full scale baffle assembly.

The Haynes 188 material as received from the supplier was solution annealed plate, 0.125 inches thick. Several techniques for machining the slots in the



1ST42-10/8/71-C1

Figure 57. Sample Baffle Assembly

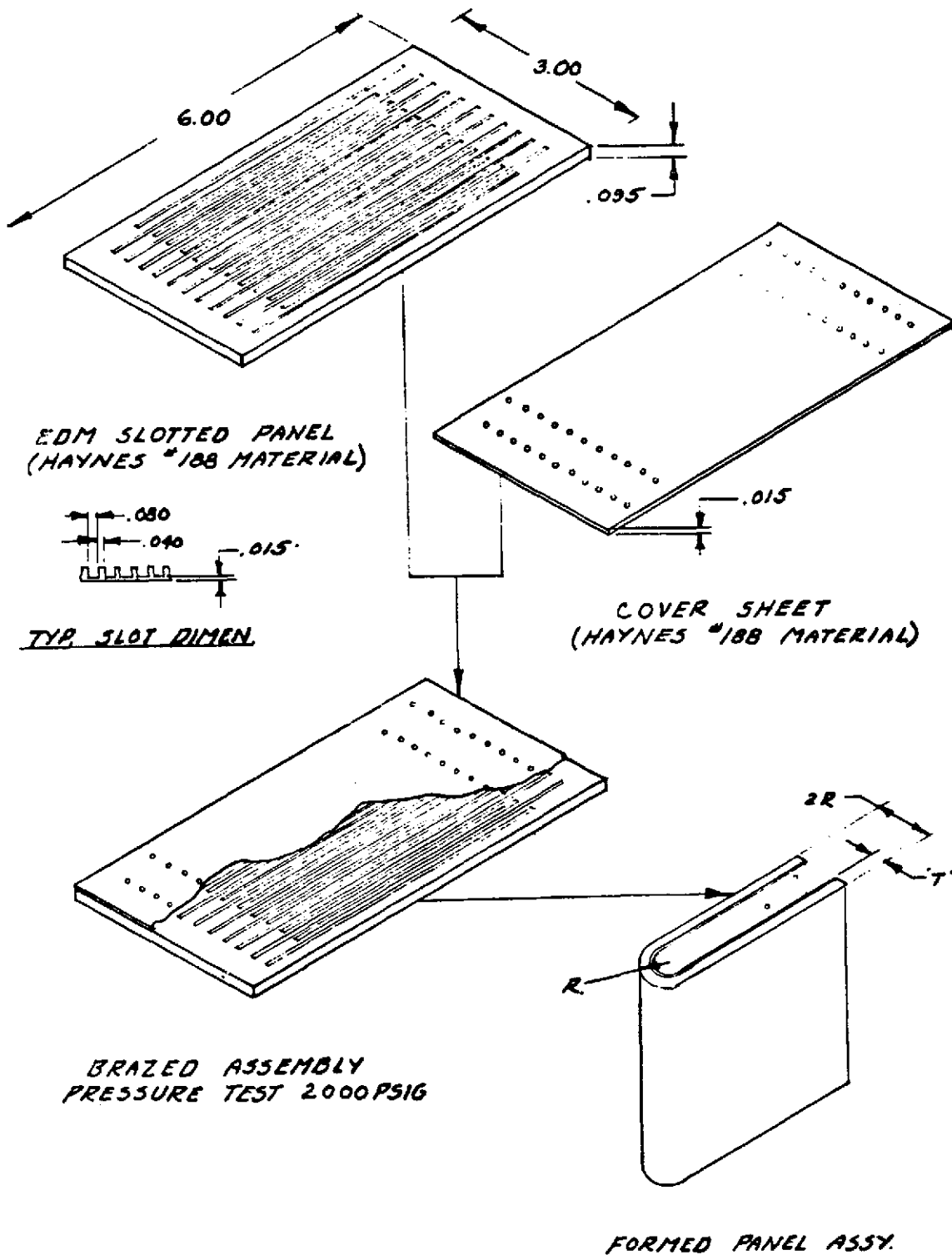


Figure 58. Manufacturing Sequence for Panel Assembly

Haynes 188 were evaluated and the following results obtained:

The material is very difficult to mill.

The material tends to distort during normal machining, such as milling or grinding.

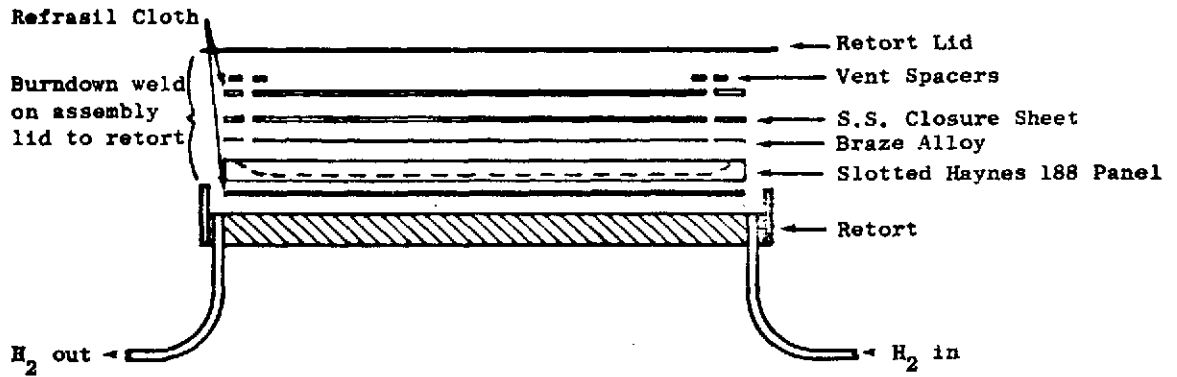
Haynes 188 is readily EDM (electrically discharge machined), and will not distort during this process.

Double disc grinding Haynes 188 is a good technique for machining this material to a desired thickness.

In the manufacture of the sample panel assembly, the 0.125 thickness Haynes material was double-disc ground to the desired 0.095 thickness, then EDM machined to the desired 3.0 x 6.0 inch shape, followed by machining of the 0.080 x 0.080 slots using the EDM process. Alternate slots were machined at the same time using a small carbon electrode. Subsequent to the machining of the slots, the panel was cleaned, degreased, cleaned with acetone, and soaked in a hydrogen atmosphere furnace at 1800 F. The slotted panel and the Haynes 188 cover sheet were then brazed using 0.002 thick Palniro #1 braze foil at 2100 F. To assure a good braze joint, a differential pressure technique developed at Rocketdyne was used. With this technique, high and uniform loads can be applied to the part during the brazing process. A sketch of this technique and the arrangement in the furnace are shown in Fig. 59.

In addition to several samples brazed with 0.002 thick braze foil, several sample panels were brazed with 0.001 thick Palniro braze foil. These samples exhibited strength properties equal to those of the 0.002 thick foil and minimizes the possibility of channel blocking by excess braze alloy, and it was decided to use the 0.001 thick foil for all other panel assemblies.

Subsequent to the brazing operation, panel assemblies were successfully pressure and leak tested at 2000 psig and then formed to the desired 0.25 and 0.375 radii. Forming of a panel to the 0.375 radius showed no evidence of material cracking or braze joint damage in the formed region as shown in Fig. 60. Conversely, the sample formed to the smaller 0.25 inch radius showed



Braze Assembly - Test Panel

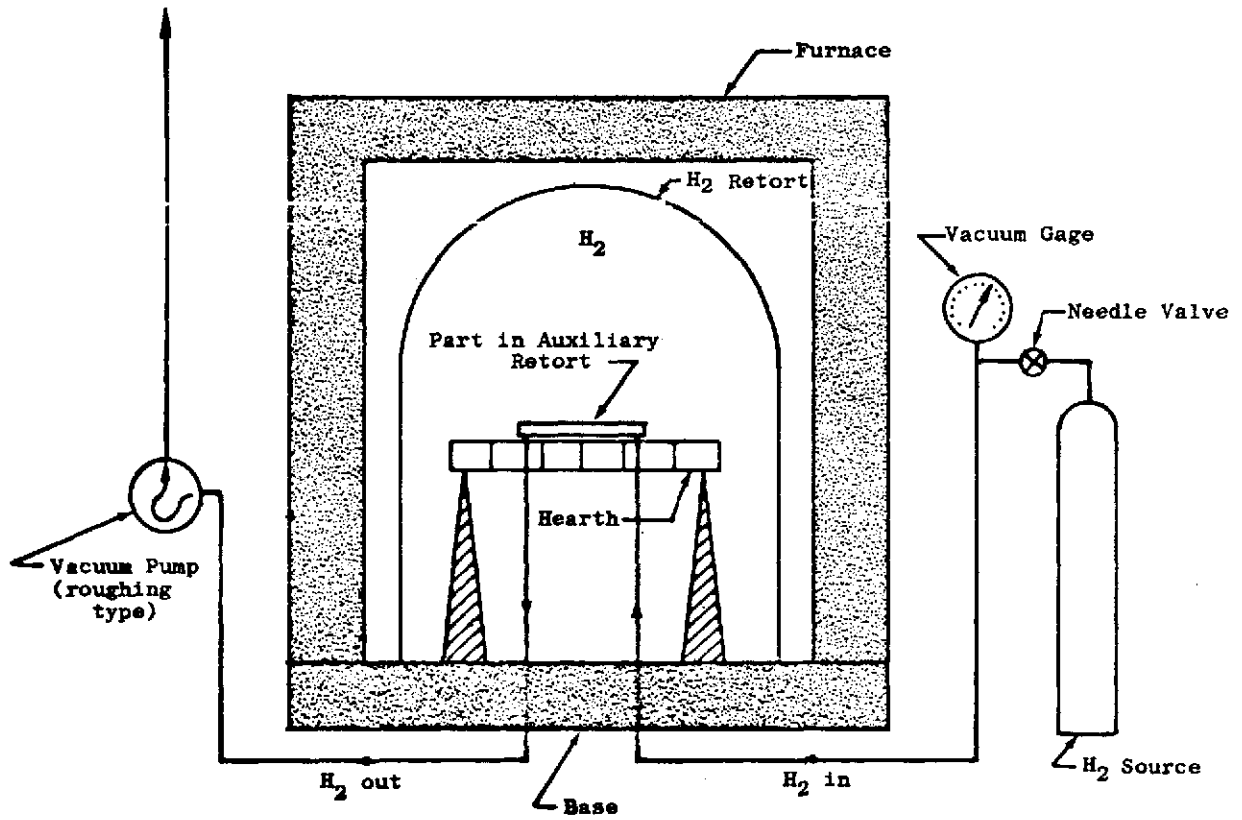
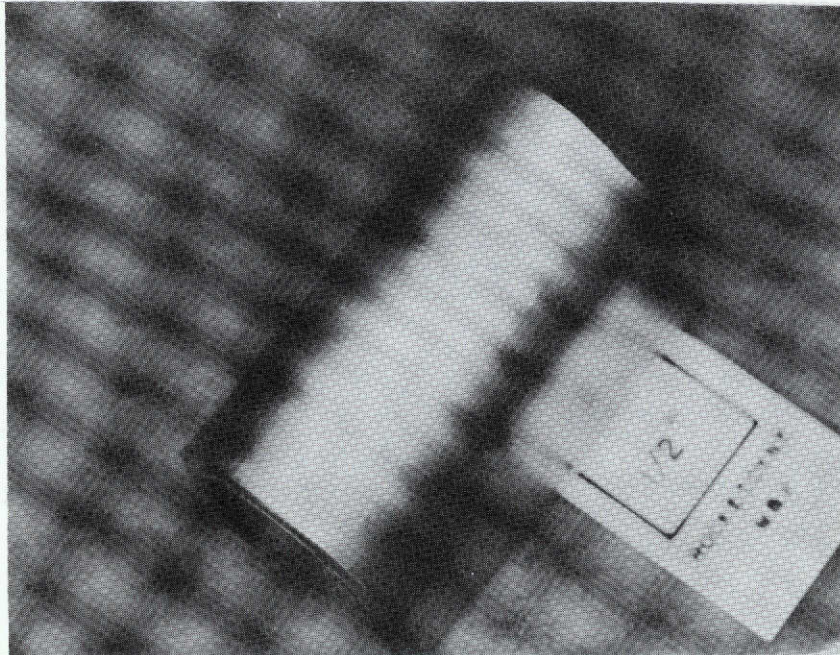
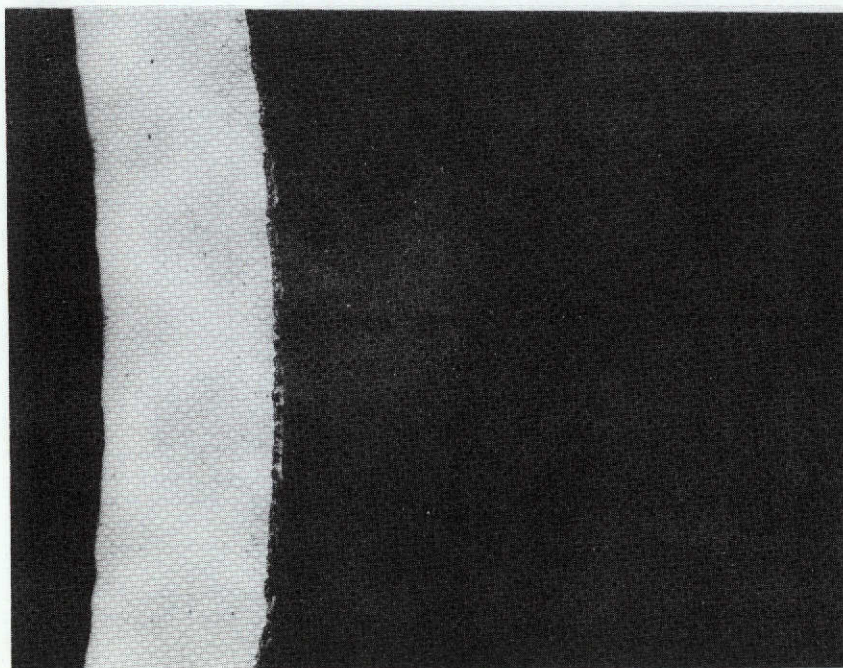


Figure 59. Furnace Arrangement for Test Panel



(A) Leading Edge of Baffle Sample With
0.375 Forming Radius



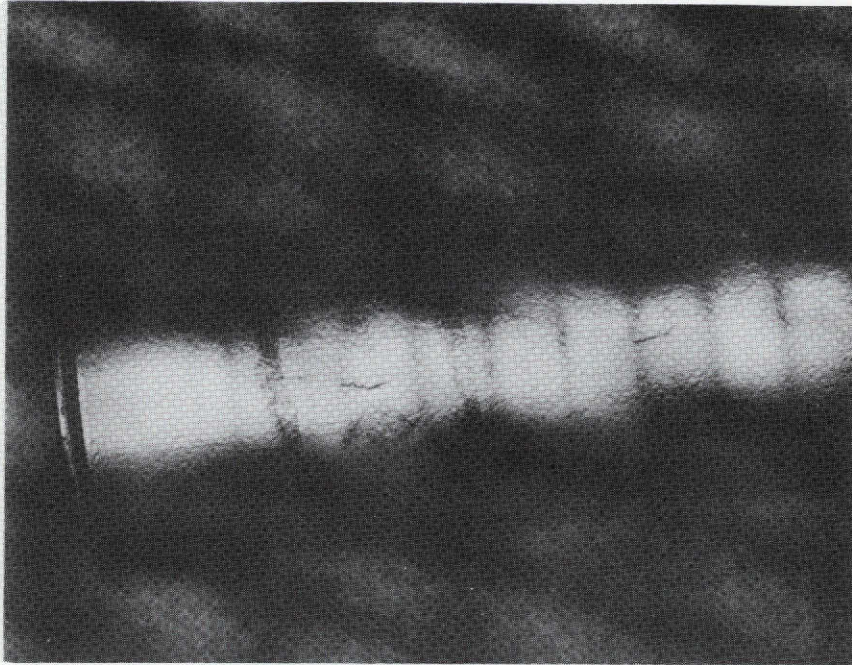
(B) Section Through Baffle Leading Edge
Figure 60. Baffle Sample Formed to 0.375 Radius

visible evidence of cracking on the outer surface, Fig. 61, indicating severe straining of the Haynes 188 alloy during the forming operation. Calculated strains in the material for the 0.25 radius bend were approximately 35% and approximately 15% for the 0.375 radius bend. An instrumented panel assembly recorded a strain level of 16.5 % during the 0.375 radius bend operation. This value is well within the recommended 25% strain value for Haynes 188. As a result of this test, it was decided that the baffle width would be 0.75 inches at the nose.

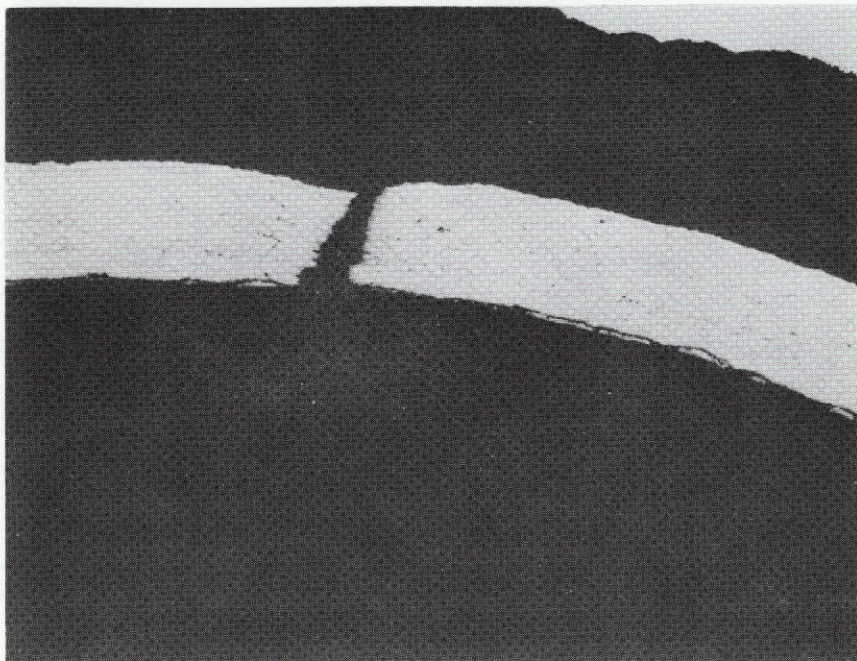
A trade study was performed to determine the effect on conditioner cross section and weight of varying baffle width the total number of baffles. These results (shown below) combined with the sample fabrication effort discussed earlier, led to the decision to use five baffles in the conditioner. The surface area of these five baffles combined with the reactor wall heat exchanger area met the required 950 square inches of surface area.

No. of Baffles	Baffle Length, In.	Conditioner Width In.	Baffle Width In.	Baffle Height In.	Weight Change Lbs.
3	17.3	4.25	1.30	6.60	+2
4	17.3	4.25	.95	5.34	+1
5	17.3	4.25	.74	4.47	0
6	17.3	4.25	.60	3.84	-1
7	17.3	4.25	.50	3.37	-2

Several panel assemblies which were formed to the 0.375 radius were subsequently brazed to a manifold assembly as shown in Fig. 57 using 0.001 inch thickness of Palnro #7 foil at 1950 F and with the same differential pressure technique as discussed previously. The assembly was then pressure tested first to 10,000 psi at ambient temperature and then burst pressure tested at 1500 F. Rupturing occurred at 4500 psi and was the result of a braze joint separation between the sample baffle panel and the manifold (second



(A) Leading Edge of Baffle Sample With 0.25
Forming Radius



(B) Section Through Baffle Leading Edge Showing
Forming Crack

Figure 61. Baffle Sample Formed to 0.25 Radius Showing
Resulting Surface Cracks

braze cycle), Fig. 62. In addition, four other specimens were tested to failure at a temperature of 1700 F. Results of these four tests were as follows:

Specimen	Temp. F	Burst Pressure psig	Joint Stress psi
1	1720	6,900	23,000
2	1700	10,400	34,600
3	1695	7,300	24,300
4	1700	8,800	29,300

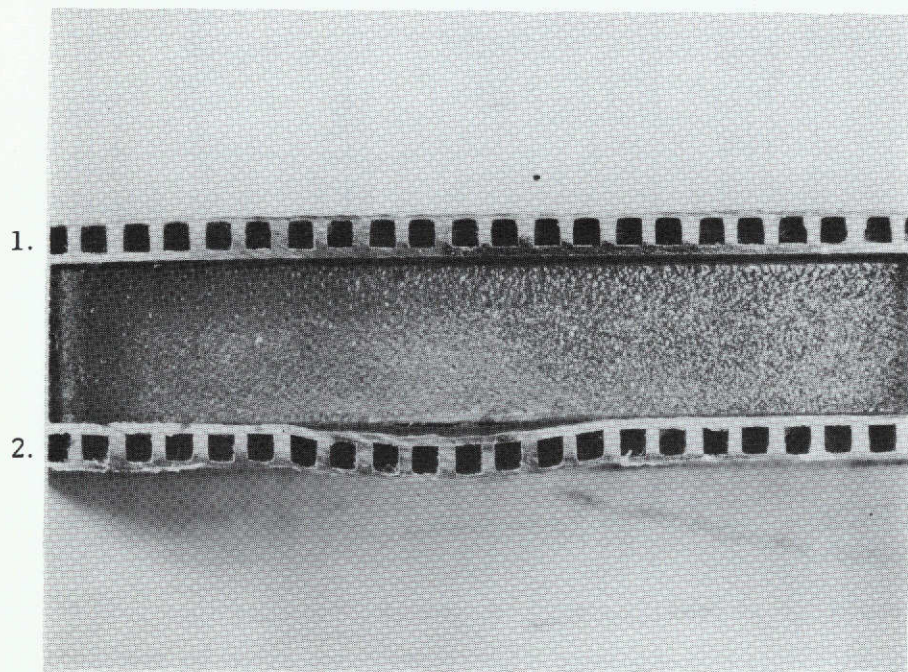
These results showed exceptional strength in the braze joint and the technique of brazing and braze alloy selection was fixed.

FINAL EVALUATION OF CANDIDATE MATERIALS FOR THE BAFFLE ASSEMBLY

To maximize cyclic life capability of the conditioner heat exchanger baffles, it was desirable to evenly distribute the thermal strains in the hot gas wall and the closure. Since the hot gas wall operates at a temperature level of several hundred degrees while the closure operates at a temperature nearly equivalent to the propellant bulk temperature, it is appropriate to use dissimilar materials on the two surfaces with the weaker material used as the closure. Analysis showed that the use of Haynes 188 on the hot gas wall and 304L stainless steel on the closure offered a good combination from a cyclic life standpoint.

CONDITIONER DETAIL DESIGN AND FABRICATION

As a result of the sample fabrication and studies discussed previously the detail design and fabrication effort on the hydrogen conditioner components and assembly was initiated.



1. Tested to 10,000 psi at ambient temperature - No Failure
2. Tested to 4,500 psi at 1500 F - Failed as Shown

Figure 62. Prototype Baffle Fabrication

Final Baffle Design

A baffle assembly consisted of a slotted wall for passage of the coolant, a close-out, manifolds to feed and return the coolant, top and bottom closures, and honeycomb within the baffle for structural support.

Four of the five baffles (as shown isometrically in Fig. 63) were identical while the center baffle was different in that all of the needed baffle thermocouples were located in this assembly. The baffle details are shown in Fig. 64 and 65 while the baffle assembly is shown in Fig. 66.

The slotted wall portion of the baffle assembly is made of Haynes 188 and manufactured in the same method as the small 3.0 x 6.0 sample panel assemblies. The slots were EDMed simultaneously using a Speer carbon electrode (shown mounted in the EDM machine in Fig. 67). As shown, the electrode was mounted on the upper platen and the work mounted on the work table portion of the EDM machine. This technique permitted easy flushing of the electrode and the physical part, and was instrumental in obtaining a good surface finish. Like other good machining processes, the part was rough machined to within a few thousands of the final dimensions, then the electrode was redressed for the final machining.

The holes or slots in the 304L stainless closure sheet were also EDM machined in a manner similar to the Haynes material. EDM machining caused no distortion in the material, eliminated the need for any deburring after machining, and once the electrode was machined produced identical parts.

Subsequent to the machining of the slotted Haynes 188 panel and the 304L stainless closure sheet, these parts were cleaned and brazed in a similar manner to that perfected on the small samples.

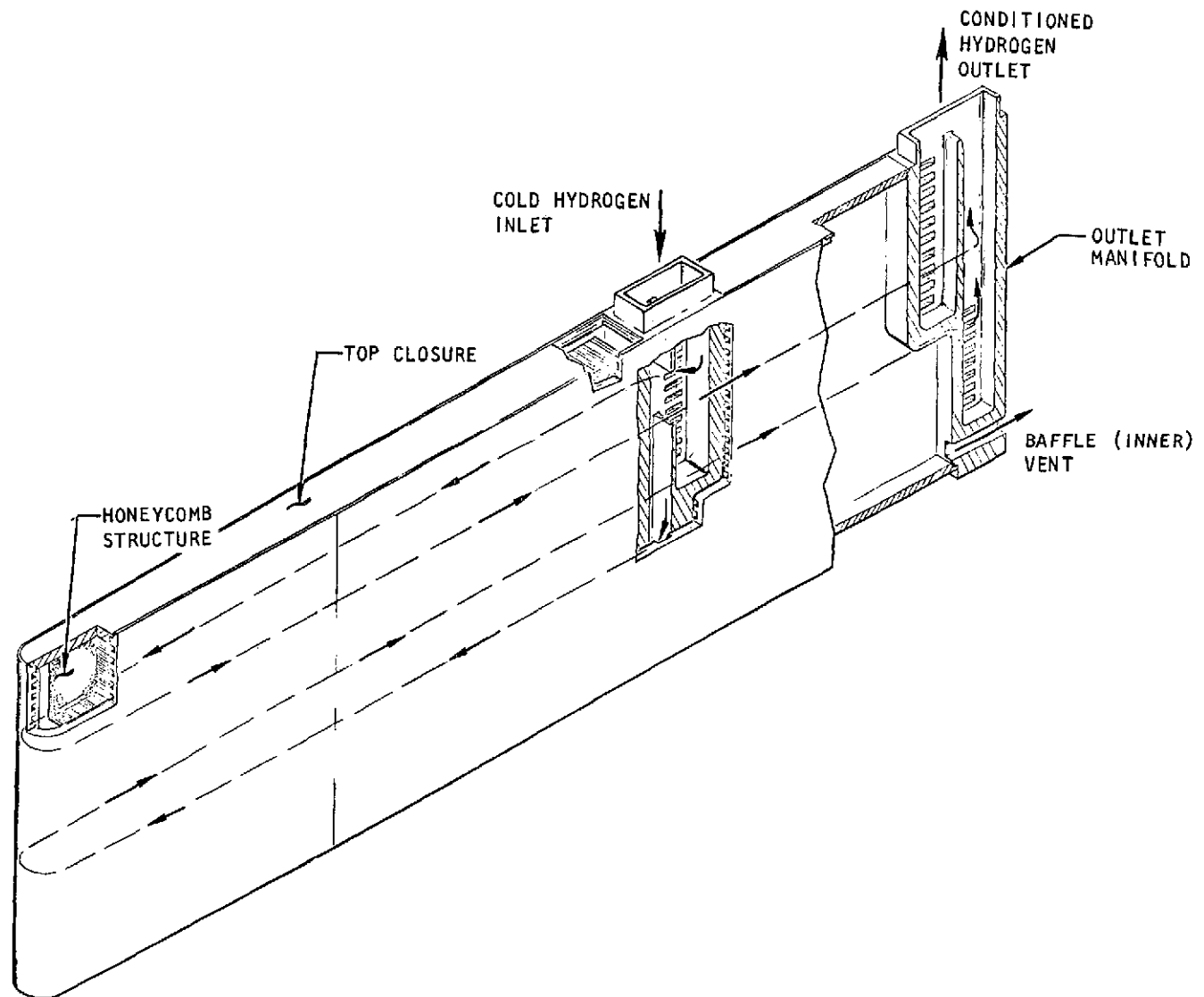


Figure 63. Baffle Assembly Hydrogen Conditioner

Page intentionally left blank

Page intentionally left blank

121/122

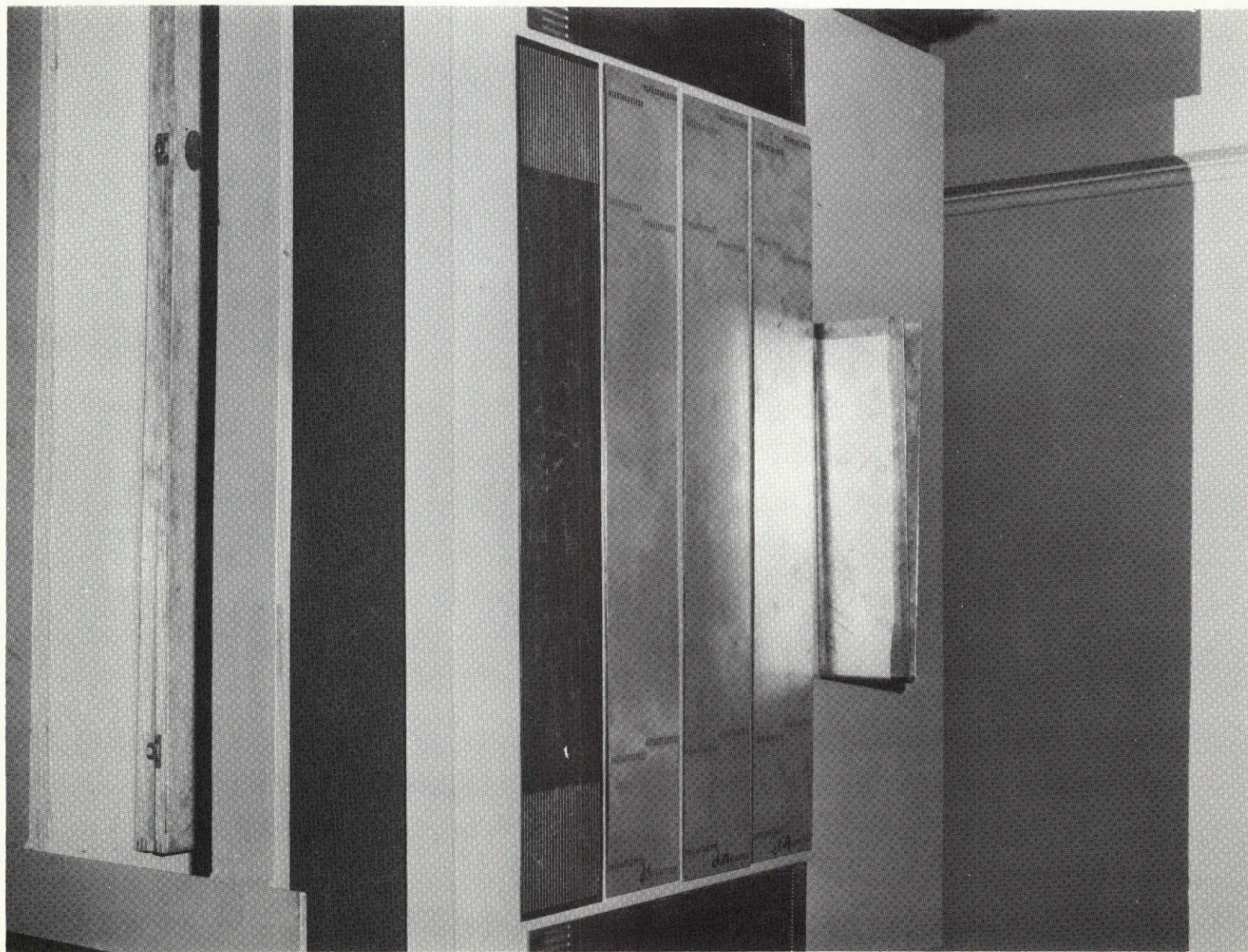


Figure 65. Baffle Detailing

Page intentionally left blank

Page intentionally left blank

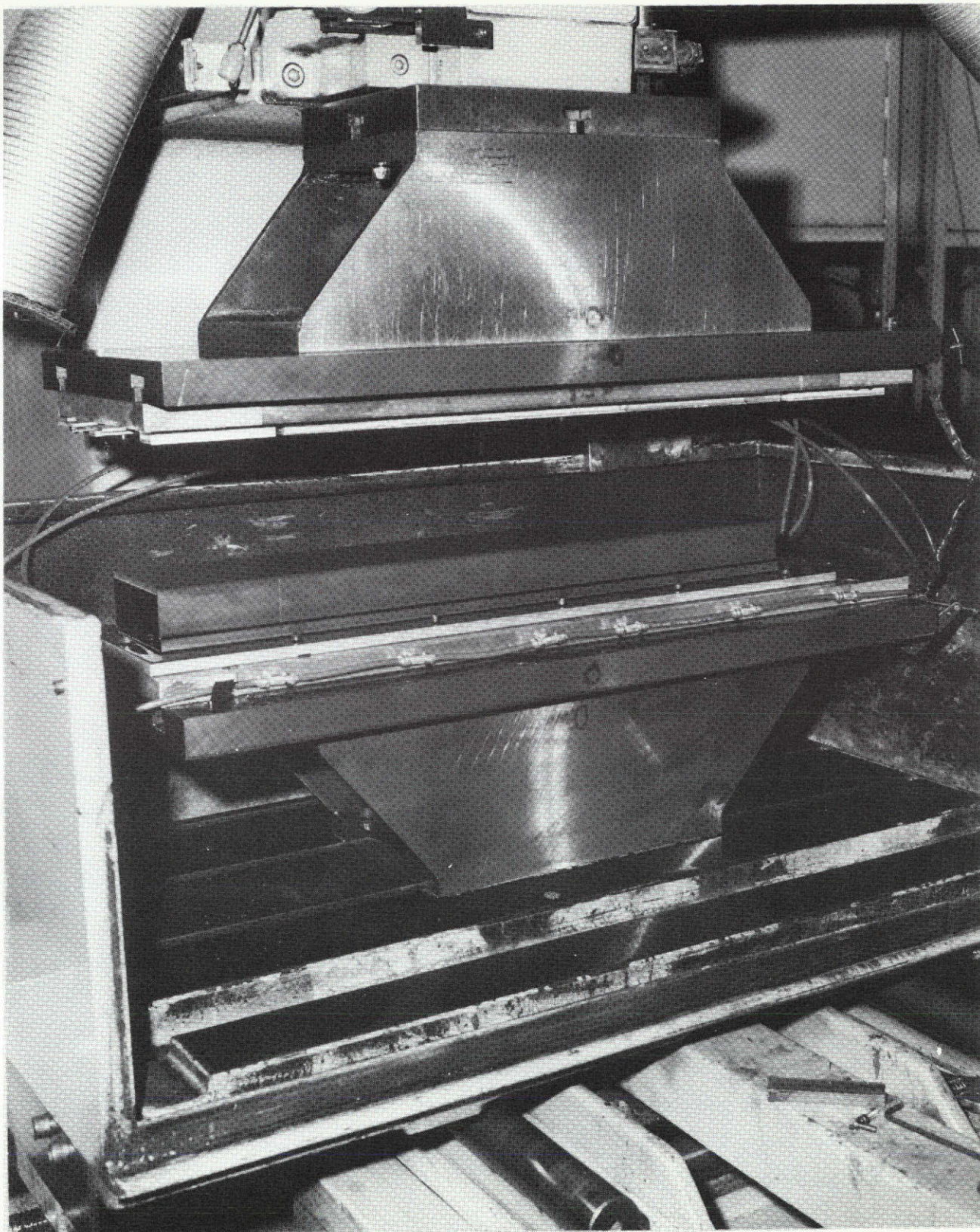


Figure 67. EDM Setup

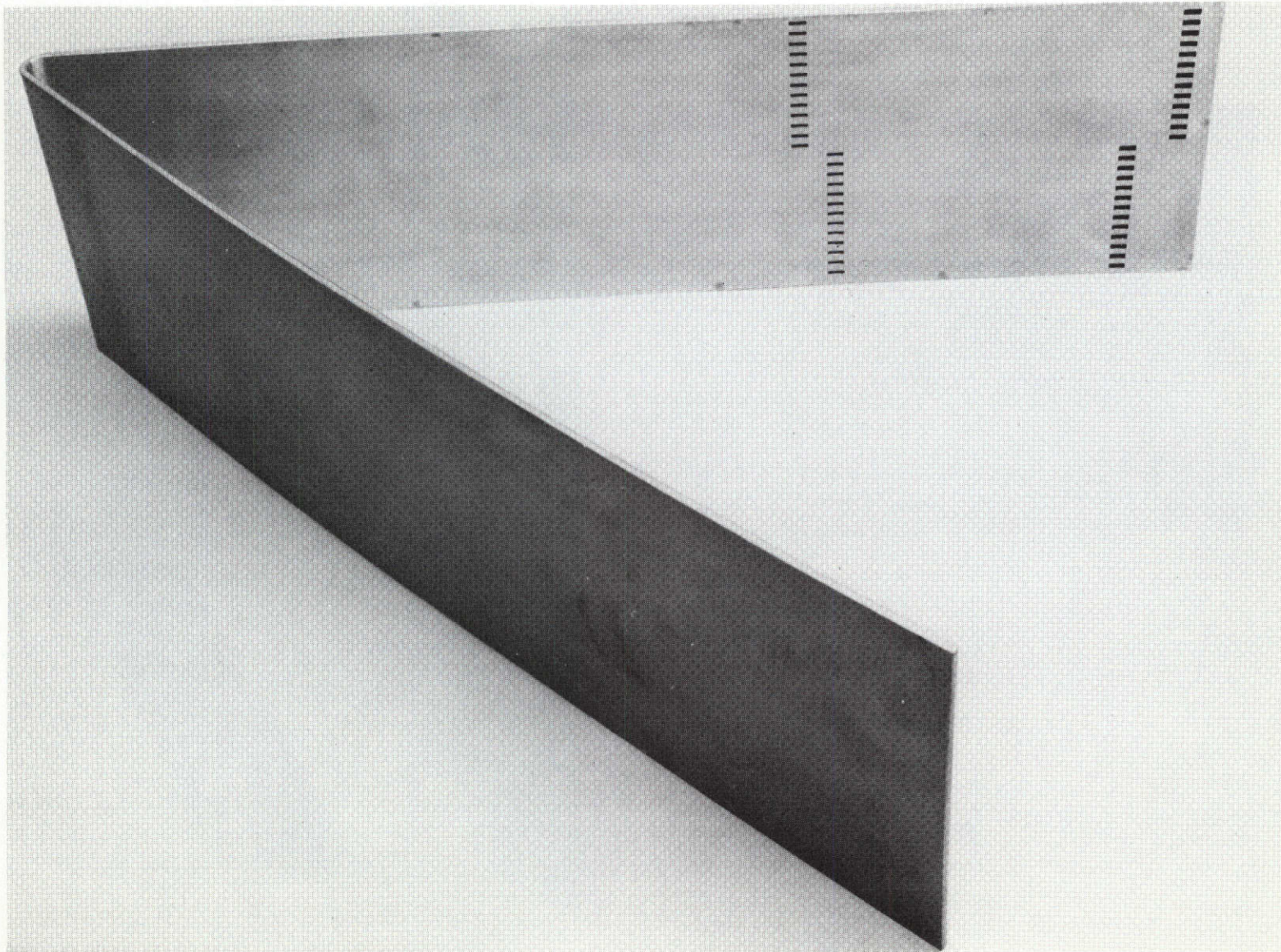
Figure 68 depicts the brazed assembly after the initial or partial forming operation, and Fig. 69 shows the partially formed panel assembly in the bending fixture. Following this operation, the panel assembly was solution-annealed in a hydrogen atmosphere furnace to relieve any strains induced during the initial form operation.

The manifolds, top and bottom closures, and the honeycomb support structure together with a fully formed panel assembly and a completed baffle assembly are shown in Fig. 66 and 70. The 304L stainless steel manifolds and the nickel 200 closures were welded together before the second braze cycle. The stainless steel honeycomb pieces as shown were used in the instrumented baffle assembly; the cutouts shown are grooves for routing the thermocouple wires. Each cell of the honeycomb structure was notched to eliminate any dead pockets and assure a good hydrogen purge to all areas during the brazing cycle. The small bellows shown in the lower nickel closure served as the outlet for the sixteen thermocouple wires and the fitting shown was used for purging during the brazing operation. This fitting was subsequently removed and the hole welded shut. The baffle assembly after the second braze cycle was pressure and leak checked to 2000 psig in the coolant passages and to 50 psi in the internal structure region.

The top and bottom of the baffles were closed out with a brazed-in-place Nickel 200 plate, as shown in Fig. 66, to prevent reactor gases from getting in behind the baffles.

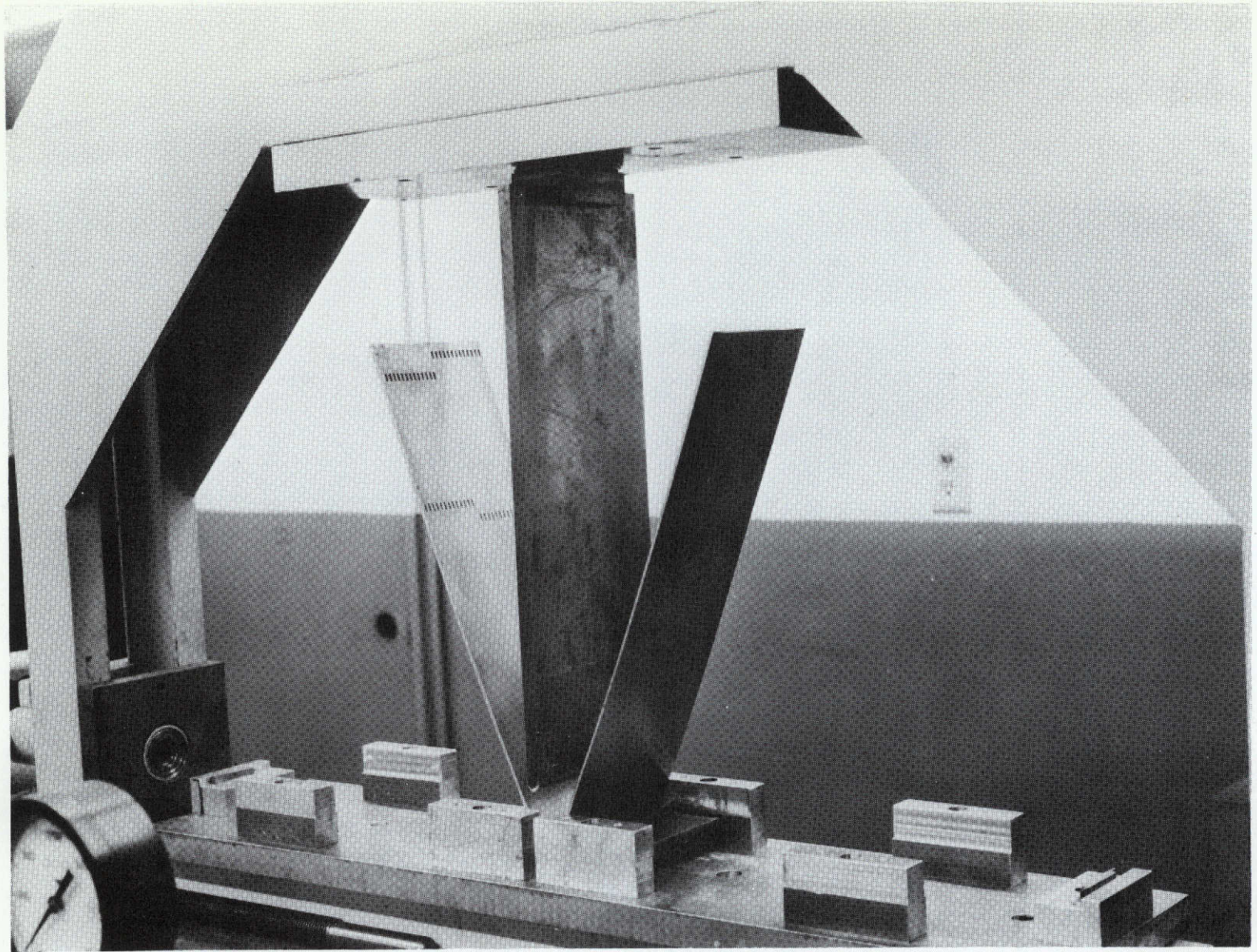
Verification of the integrity of these closures in preventing hot-gas leakage to the back side of the baffles was made by monitoring baffle cavity pressures. This was done using the baffle vent ports (needed during the braze operation) shown in Fig. 66.

The above procedure for manufacturing a baffle assembly is summarized in Table 16.



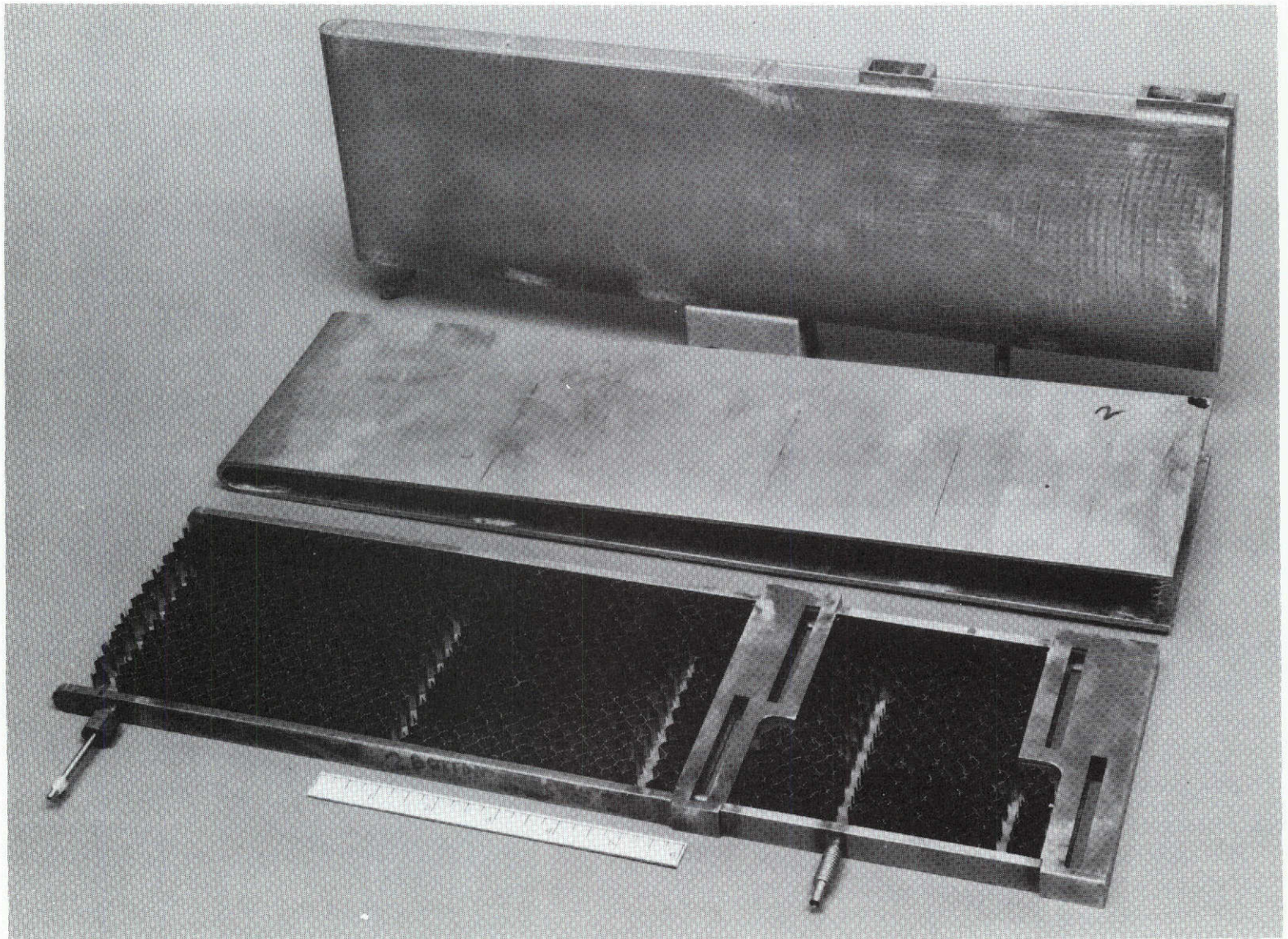
1ST62-3/16/72-C1F

Figure 69. Partially Formed Baffle



1ST62-3/16/72-C1

Figure 69. Baffle in Forming Fixture



1XZ62-2/14/72-C2

Figure 70. Completed Baffle and Details

TABLE 16. BAFFLE FABRICATION, RS 00 5578X

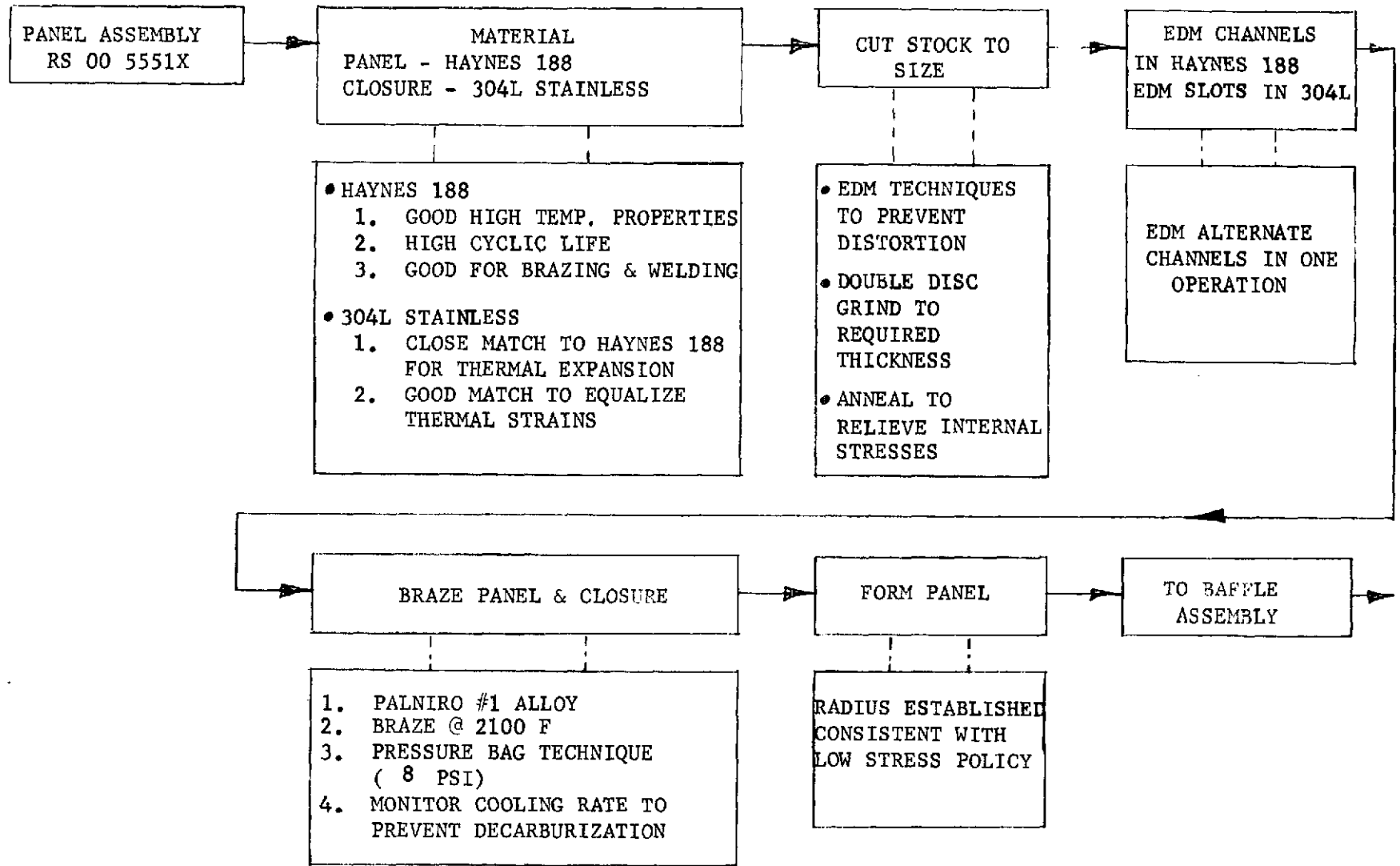


TABLE 16 (Continued)

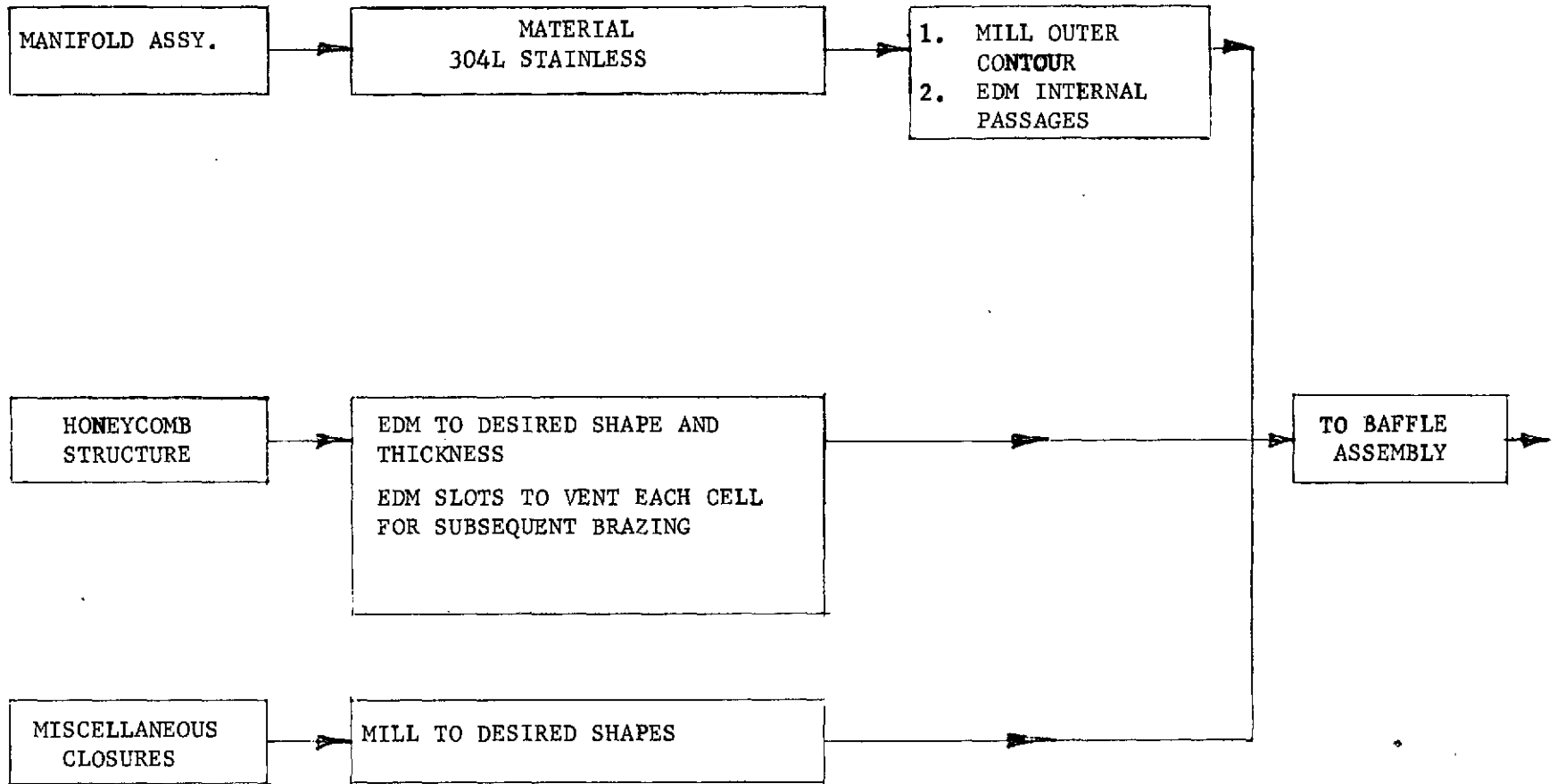
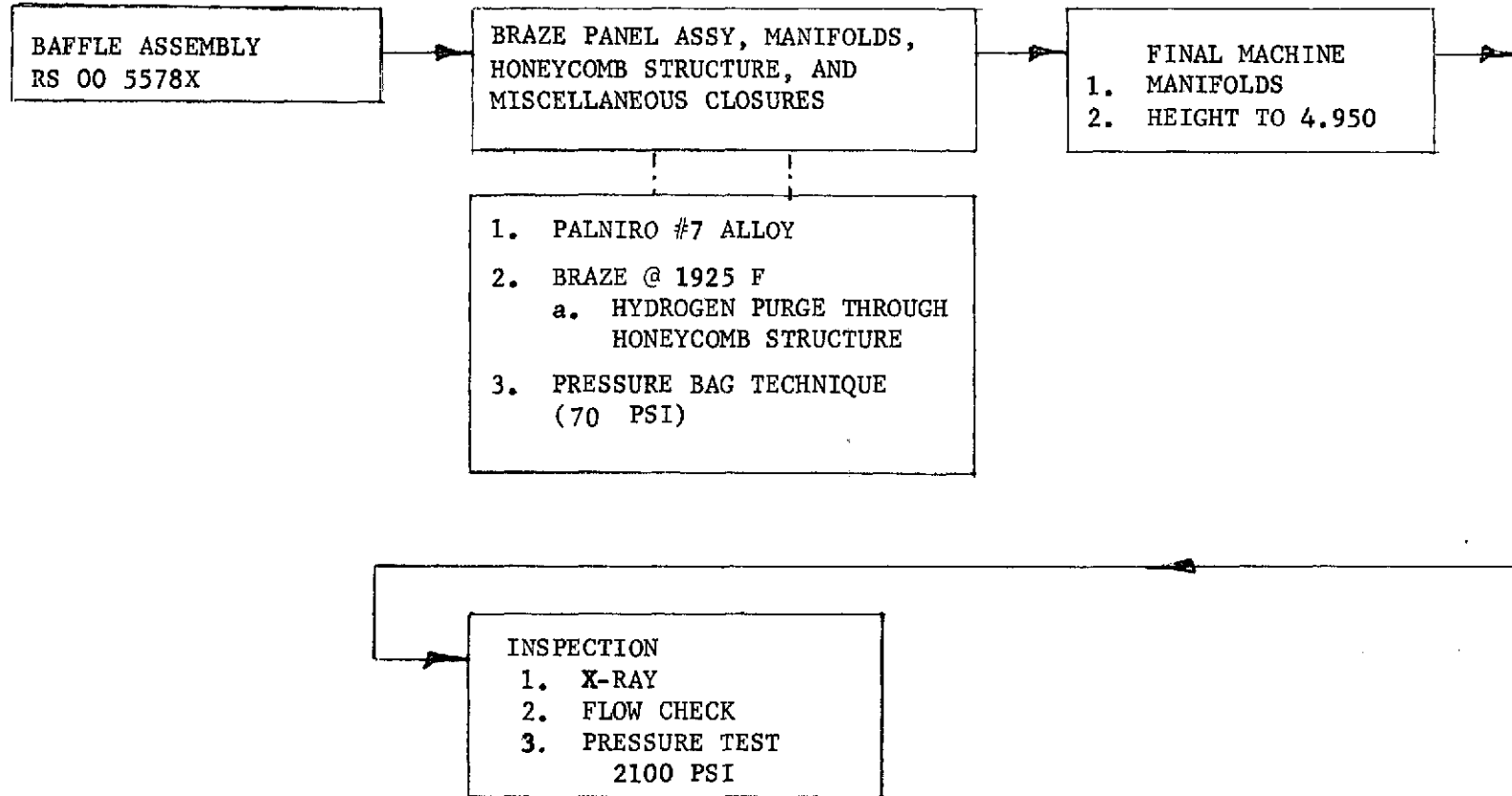


TABLE 16. (Concluded)

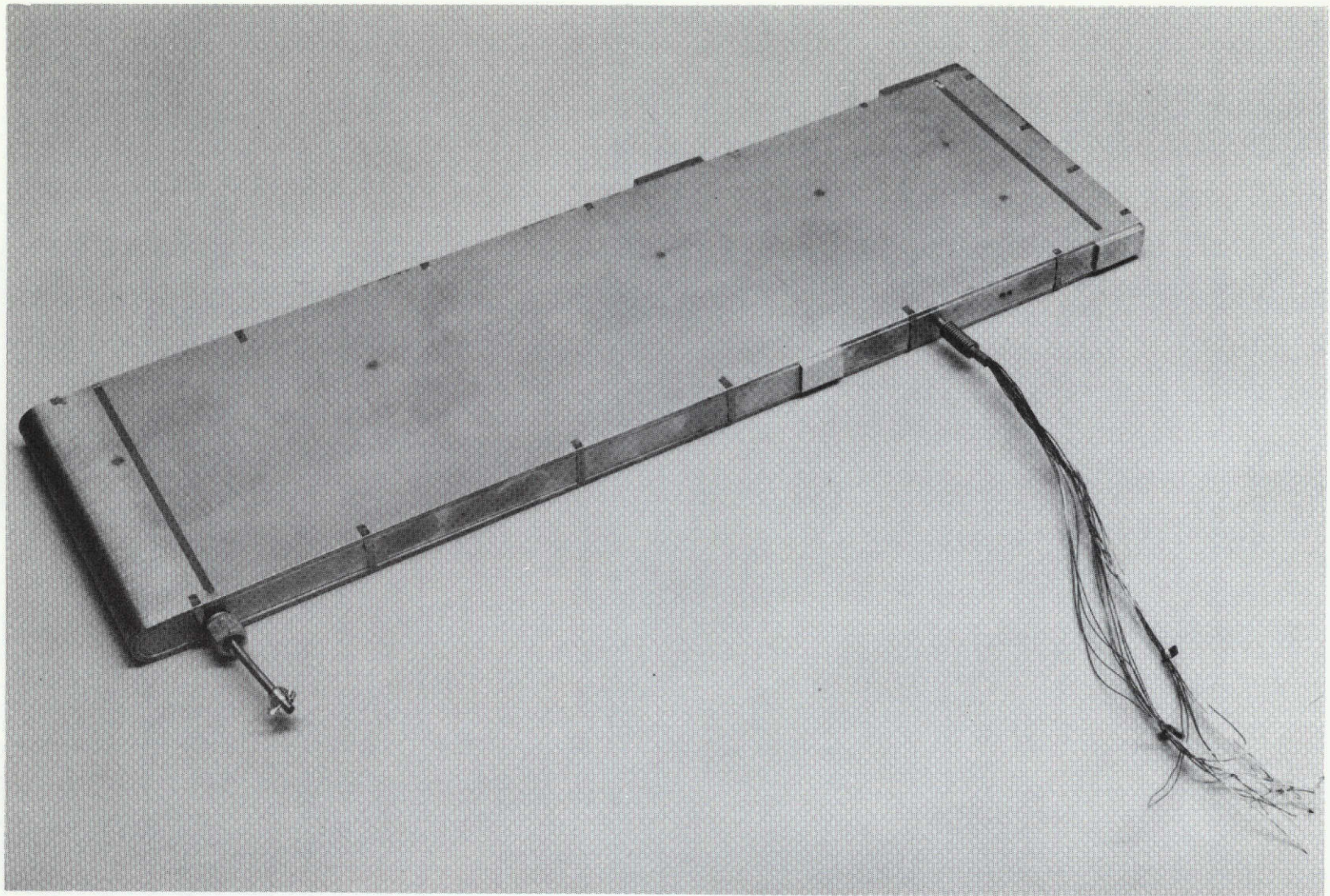


The instrumented baffle assembly is identical to the other baffles, with the exception of the thermocouples. This completed baffle assembly is shown in Fig. 71 and 72. The small dark spots on the face of the baffle in Fig. 71 indicate the location of some of the hot-gas wall thermocouples; a total of sixteen thermocouples were installed. A typical thermocouple installation is shown in Fig. 73.

As shown, the inlet and outlet manifolds are located near the aft end of the baffle assembly because in this area the hot-gas temperature, the baffle wall, and the conditioner walls' temperature more closely approach each other, thereby reducing the amount of differential growth between components. In the frontal areas and high differential temperatures, the baffle assembly is free to grow axially, thereby eliminating any strain caused by differential temperatures between the baffle and the outer walls.

Conditioner Walls

As in the case of the baffle assembly, the material exposed to the hot reactor combustion gases was Haynes 188, and the backup or structural material was 304L stainless steel. As mentioned before, 304L stainless and Haynes 188 are closely matched in thermal growth, are readily brazed, and 304L stainless is one of the most easily electron beam welded materials. A completed side wall assembly and its individual details of the slotted Haynes wall and the 304L stainless wall structure are shown in Fig. 74, and 75. The slotted Haynes 188 wall was EDM machined in a manner similar to the baffle assembly. Most of the 304L stainless wall material was removed by milling, but the final rectangular shaped manifolds were EDM machined. Brazing was accomplished in a manner similar to the baffle assembly. The top and bottom walls (bottom wall shown in Fig. 76 and 77) are very similar in design and in their method of construction as the conditioner wide walls. Of significance are the guide rails, which were EDM machined into the Haynes 188 material to form tracks for locating the baffles in their proper location and maintaining a predetermined hot gas gap.



1ST62-3/16/72-C1A

Figure 71. Completed Instrumented Baffle Assembly

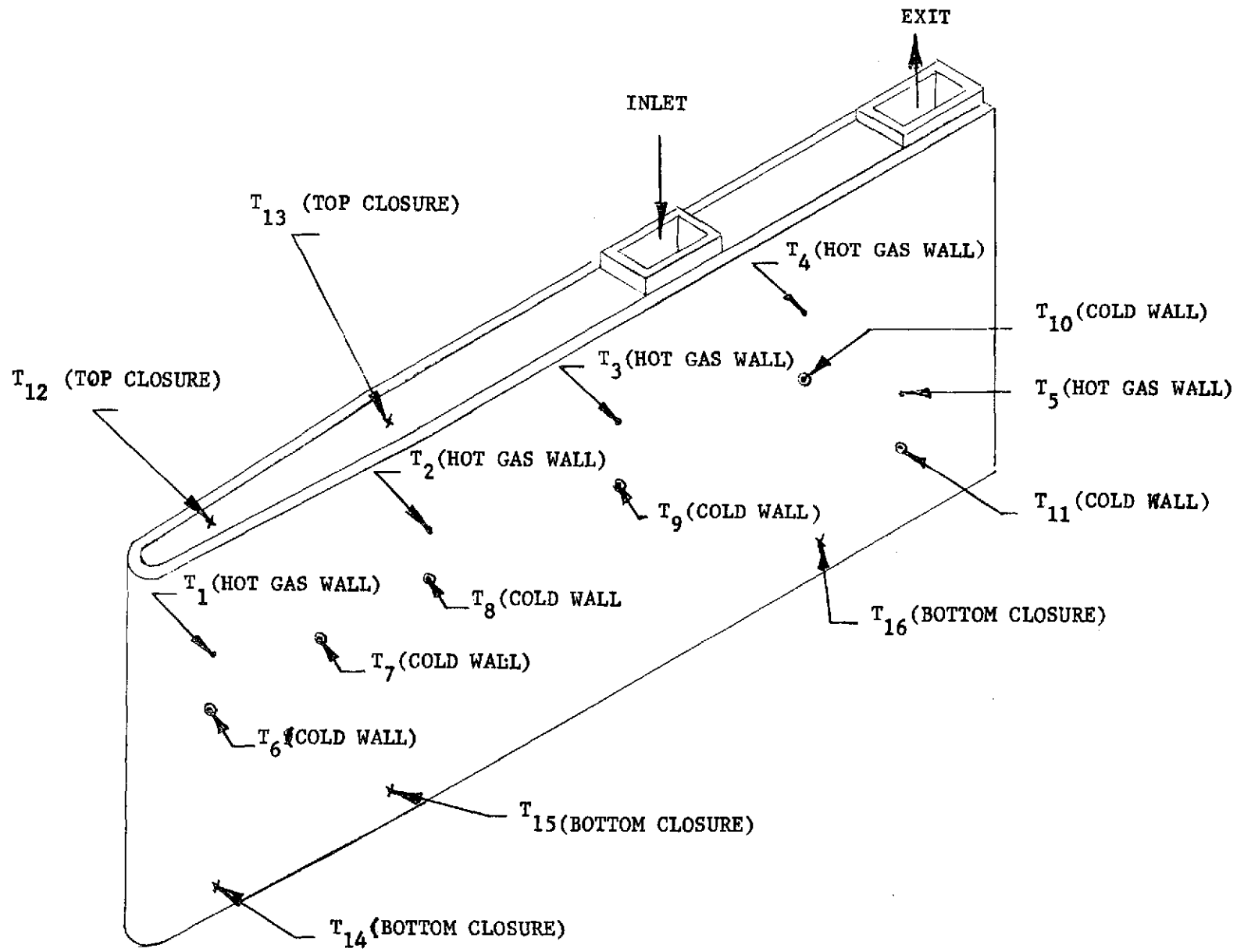


Figure 72. Instrumented Baffle Assembly (RS 00 5591X)

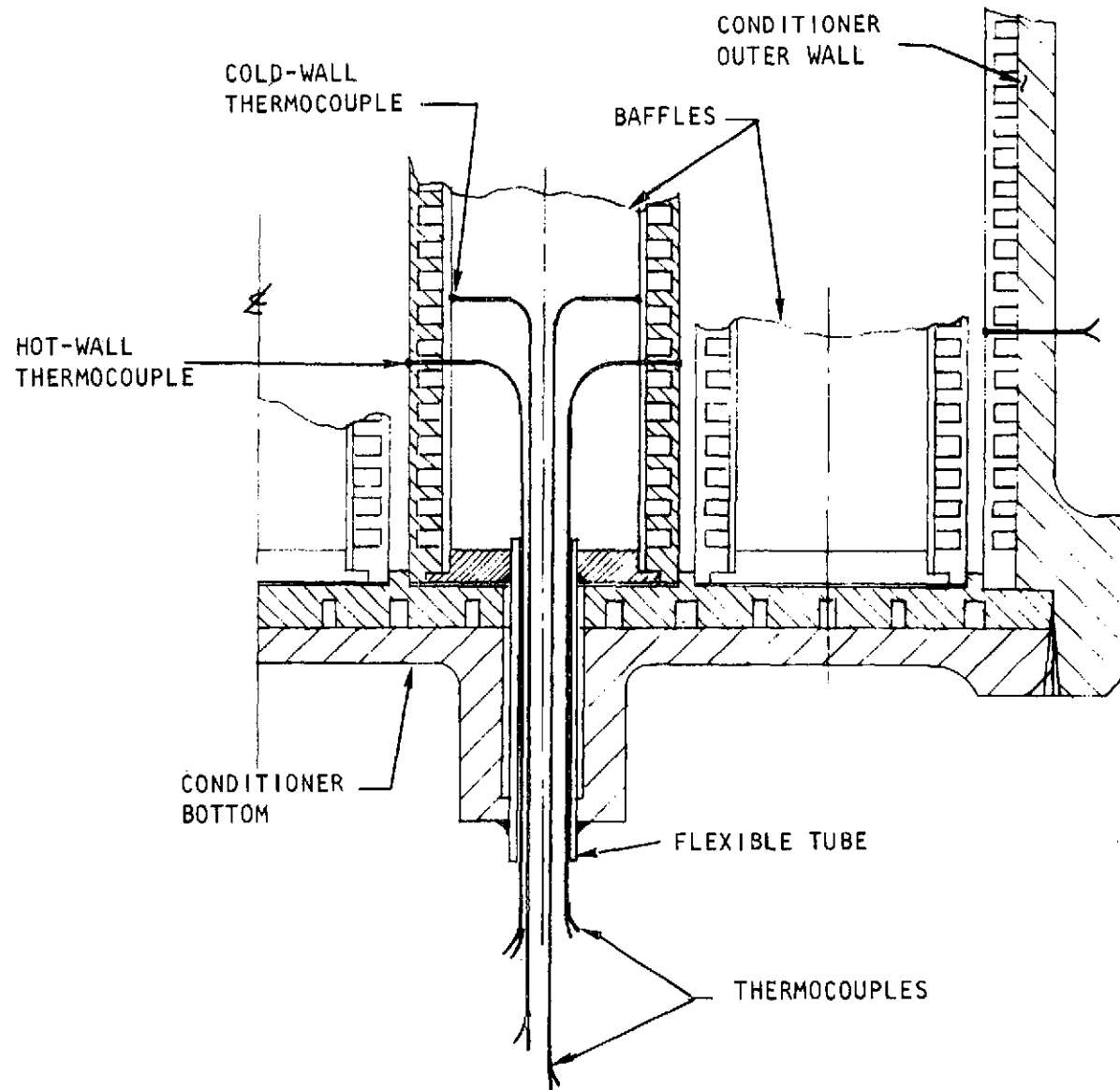
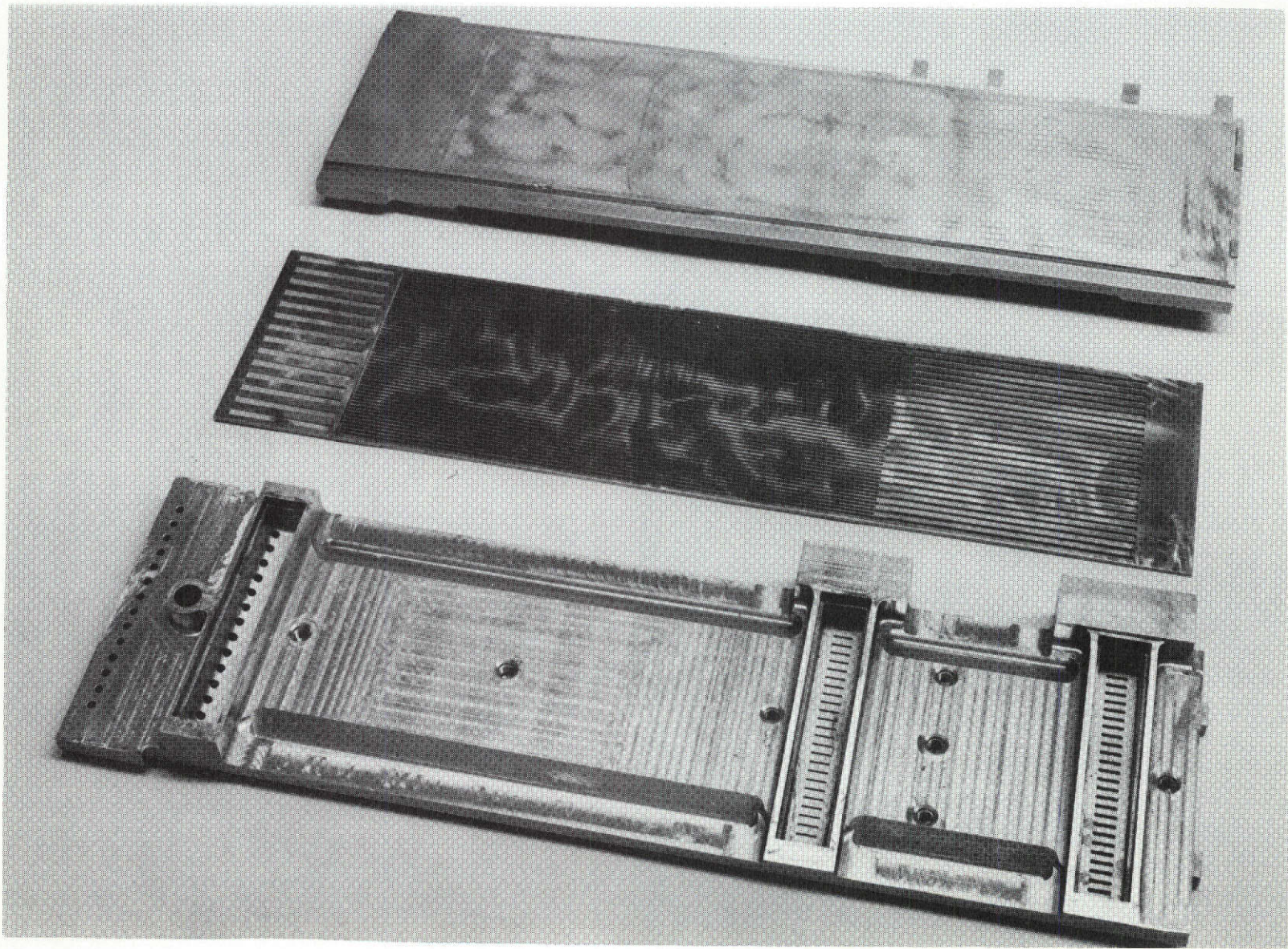


Figure 73. Baffle Thermocouple Installation

Page intentionally left blank

Page intentionally left blank

139/140

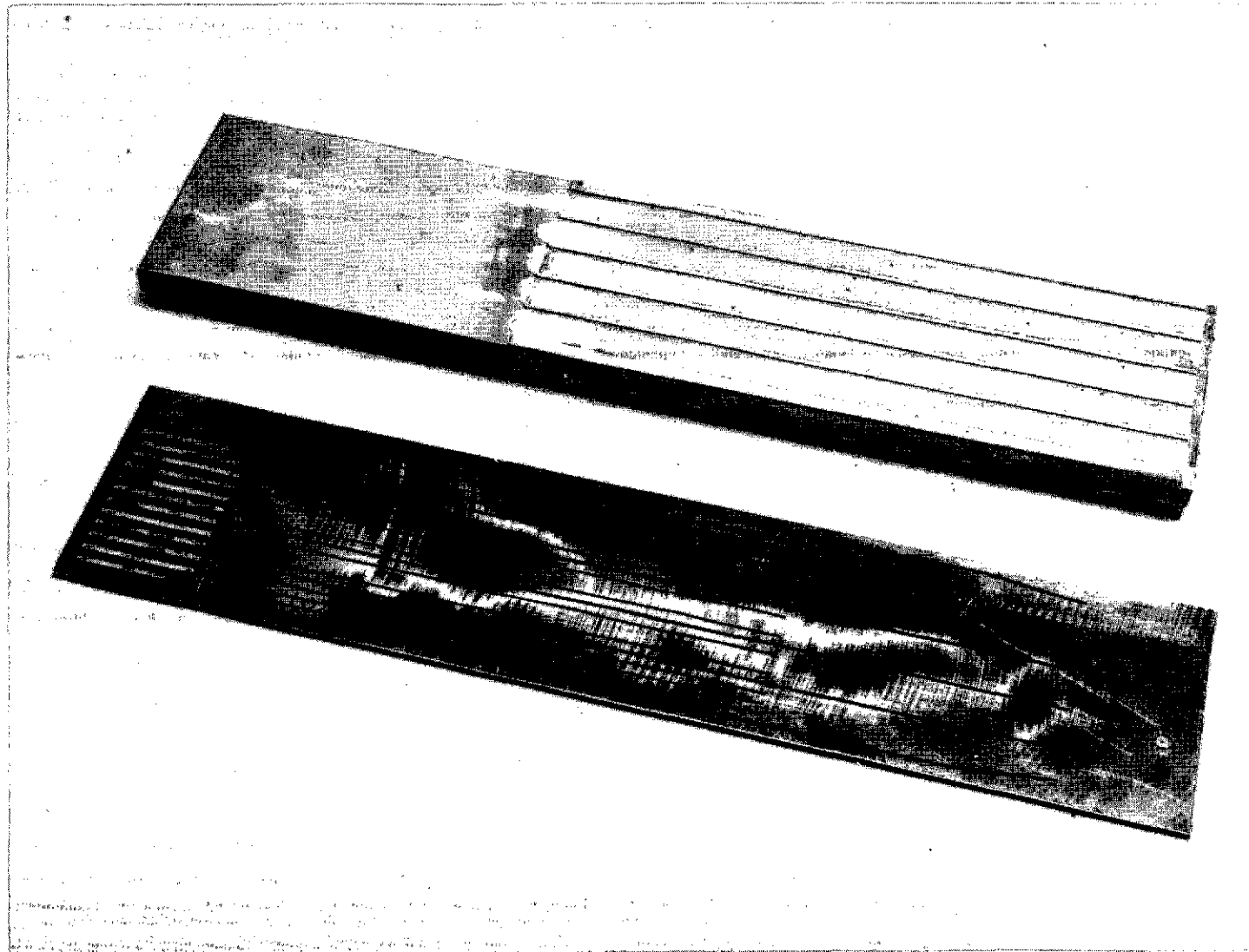


1ST62-3/16/72-C1H

Figure 75. Conditioner Side Wall Details

Page intentionally left blank

Page intentionally left blank



1ST62-3/16/72-C1G

Figure 77. Conditioner Bottom Wall Detail

Miscellaneous Components

Miscellaneous pieces of hardware such as the inlet and outlet manifolds for the coolant, reactor interface flange, and associated cover plates were all machined from 304L stainless steel and are shown in Fig. 78.

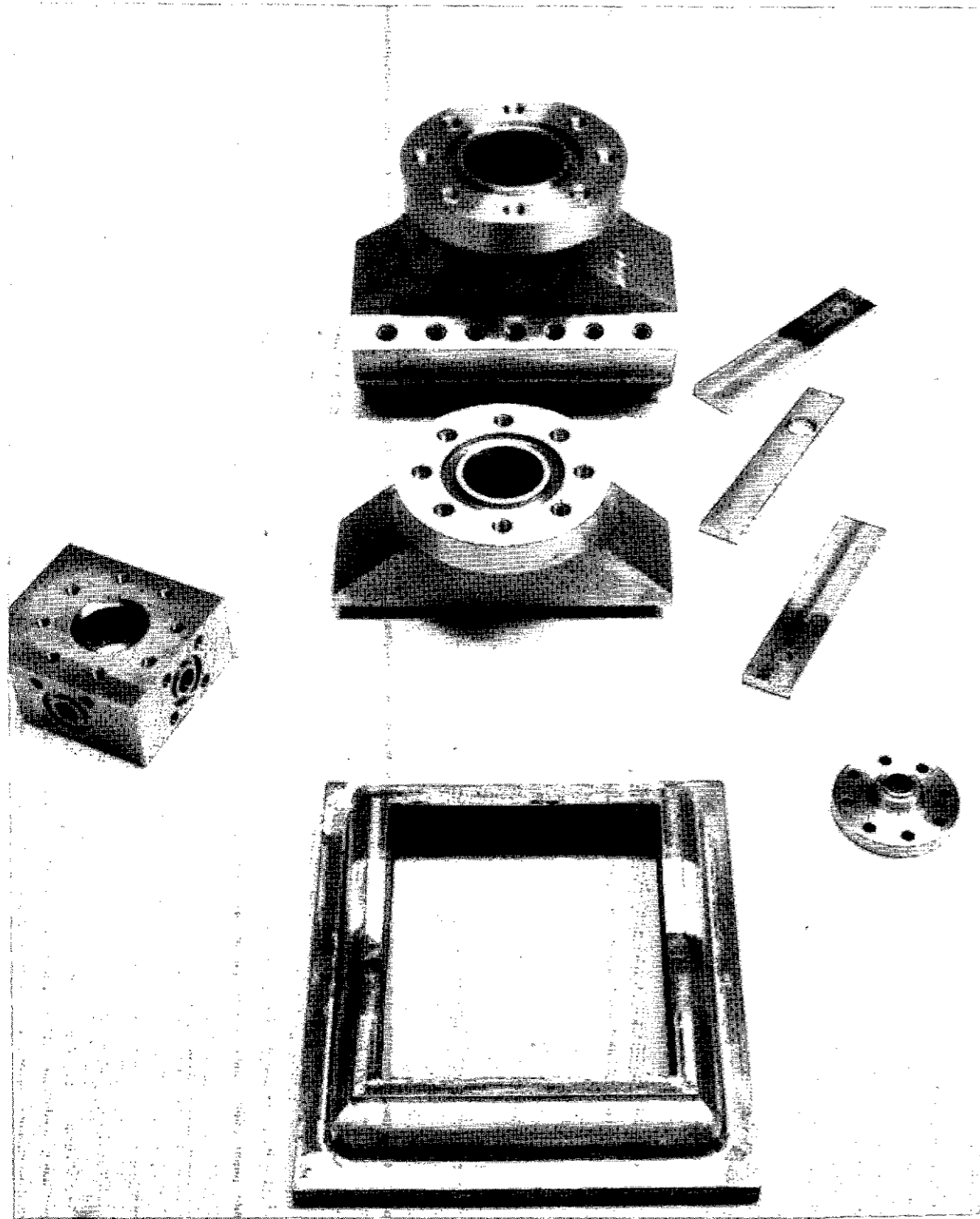
Hydrogen Conditioner Assembly

A drawing of the conditioner assembly is shown in Fig. 79, an exploded view of some of the major components for the conditioners is shown in Fig. 80 and a subassembly of the five baffle assemblies electron beam welded into the top wall assembly is shown in Fig. 81. As shown, the bottom wall assembly with guide rails was used as a locating fixture during the weld operation; and it also can be noted that the baffle thermocouple wires protrude from the bottom of the assembly. This is better shown in Fig. 82, which is a view of the bottom of the conditioner. Fig. 83 shows the assembly of the side walls to the conditioner just prior to the weld operation, and shows the side wall thermocouples installed.

A complete assembly of the conditioner is shown in Fig. 84. The slotted passages in the reactor interface flange provide the path for the reactor hydrogen flow into the reactor injector. The flange on the right front is used for attaching the reactor igniter. The small ports on the side of the coolant outlet are used to measure the outlet temperature of each baffle. A physical drawing of the thermocouple installation is shown in Fig. 85. Also shown in this drawing are static and pressure ports, which protrude into each baffle assembly outlet.

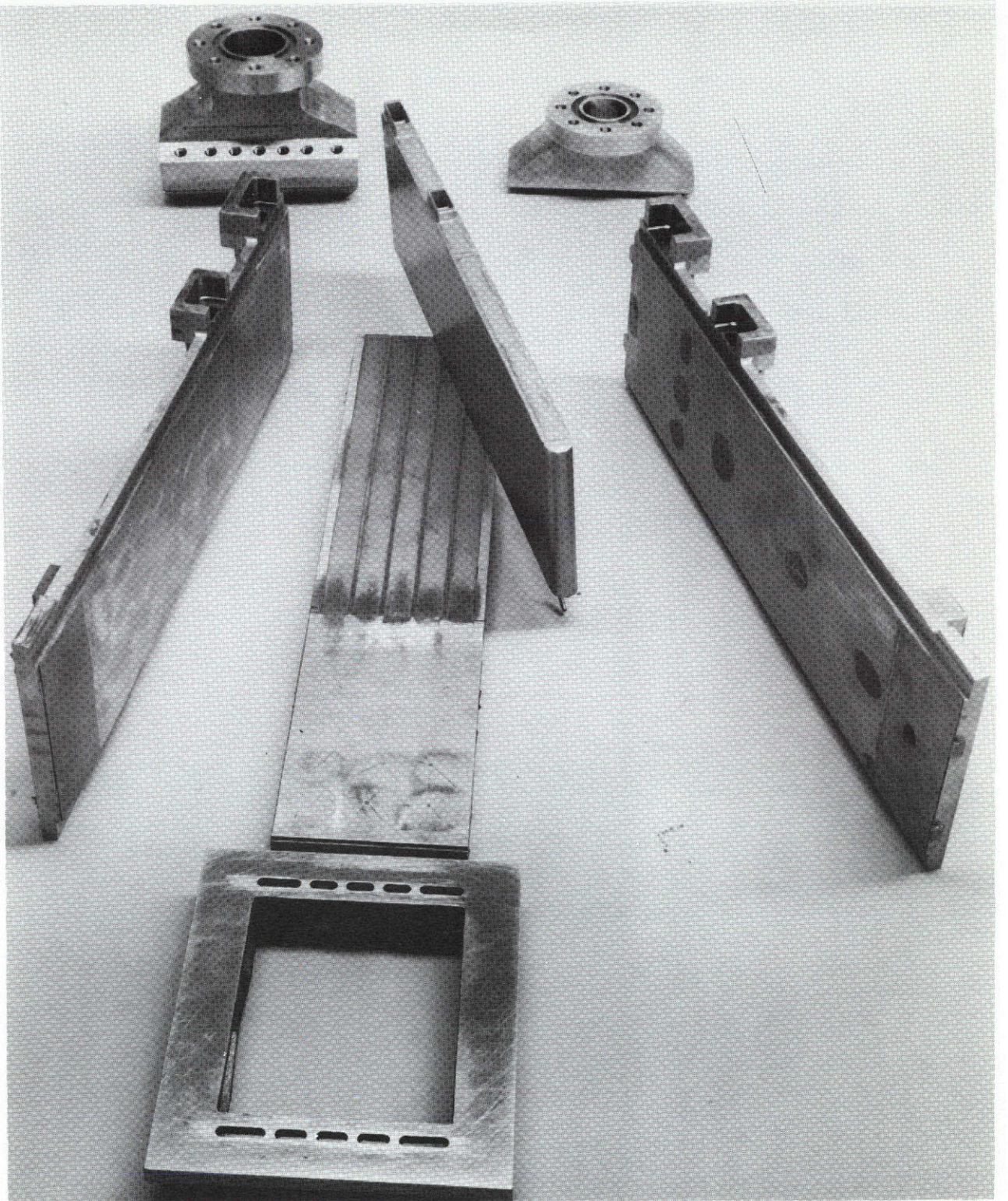
REACTOR (INJECTOR) CONFIGURATION

Based on company funded studies completed prior to the start of this program the injector selected for this effort incorporated trislot injection elements (where two hydrogen streams impinge on a centrally located oxygen stream). The elements were arranged in a rectangular pattern and oriented in such a manner that they are aligned with the hot gas passages between the heat exchanger baffles.



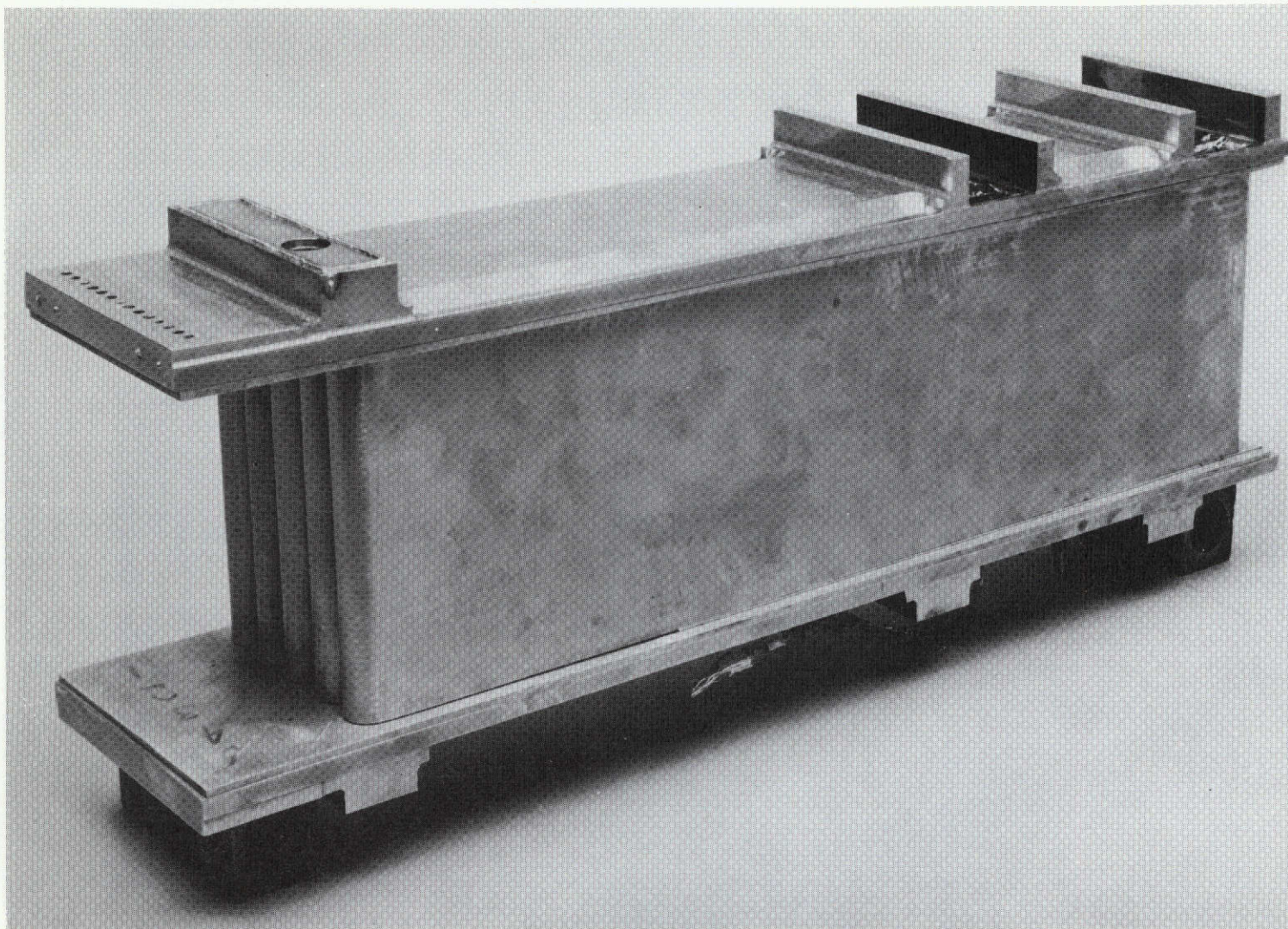
1ST62-3/16/72-C10

Figure 78. Miscellaneous Details for Hydrogen Conditioner



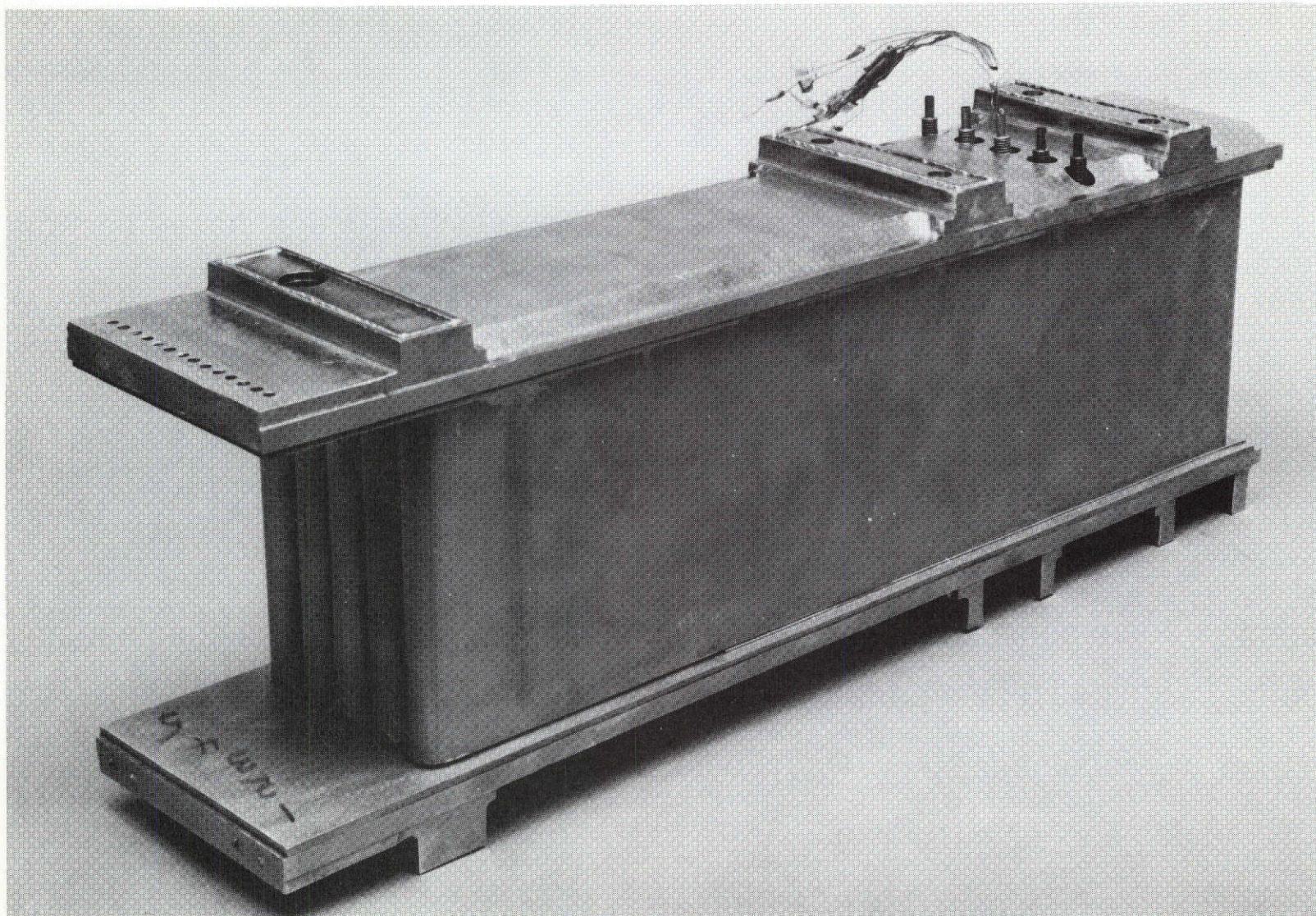
1ST62-3/16/72-C1N

Figure 80. Hydrogen Conditioner Details and Partial Assemblies



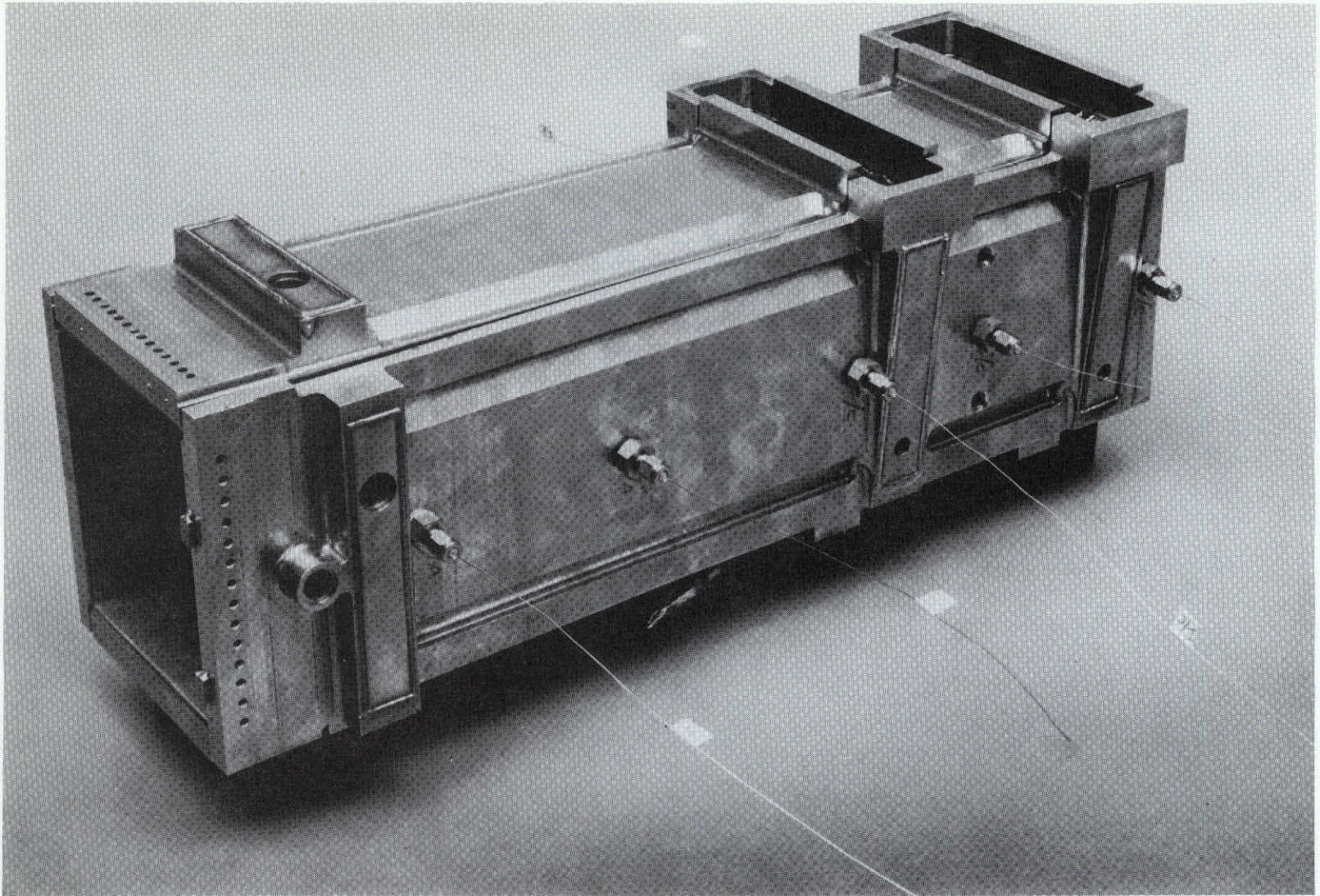
1XZ62-4/5/72-C1D

Figure 81. Hydrogen Conditioner Partially Assembled
(Top wall shown)



1XZ62-4/5/72-C1A

Figure 82. Hydrogen Conditioner Partially Assembled
(Bottom wall shown)



1XZ62-4/5/72-C1C

Figure 83. Hydrogen Conditioner Assembly

151

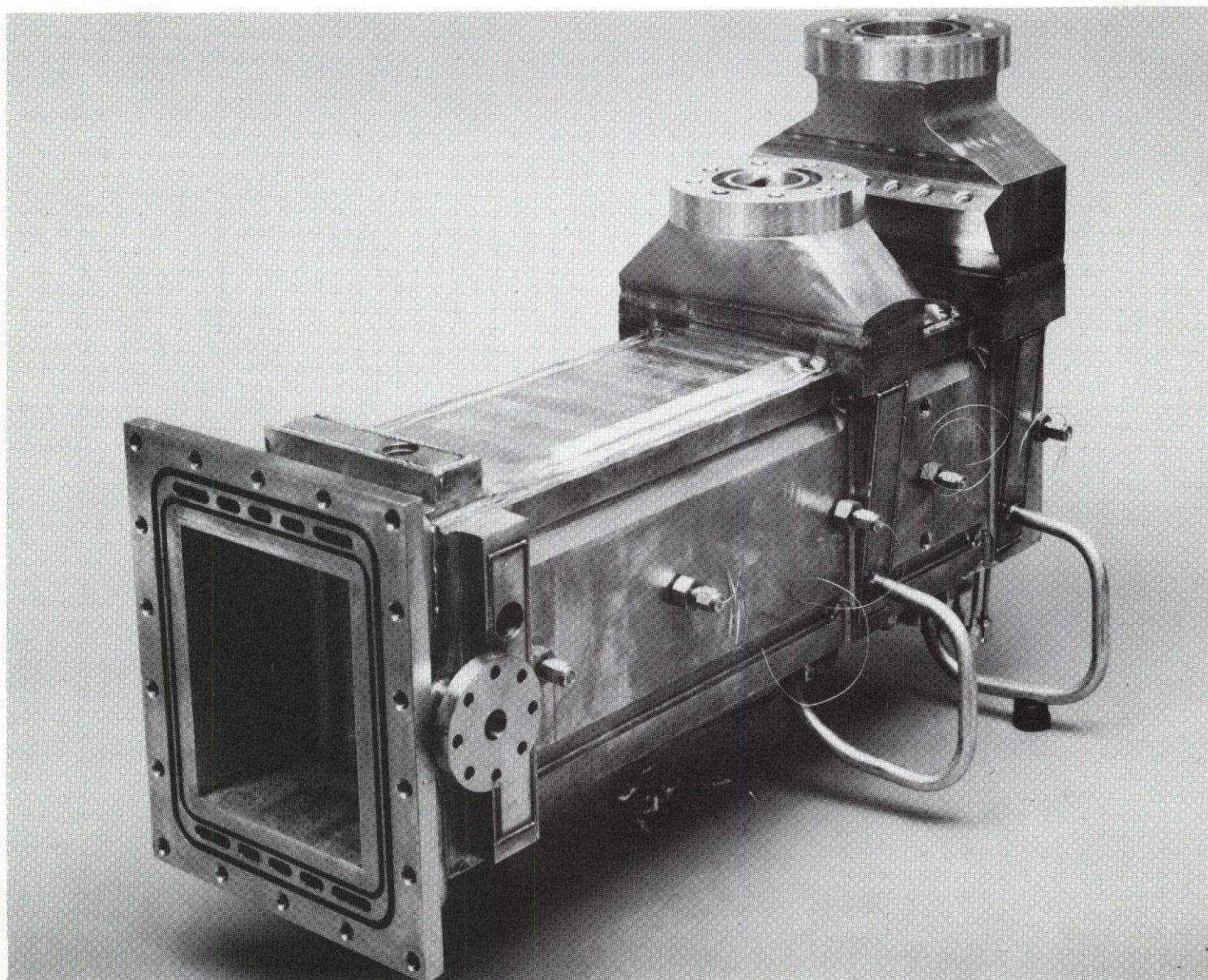


Figure 84. Hydrogen Conditioner Assembly

1ST62-5/1/72-C1B

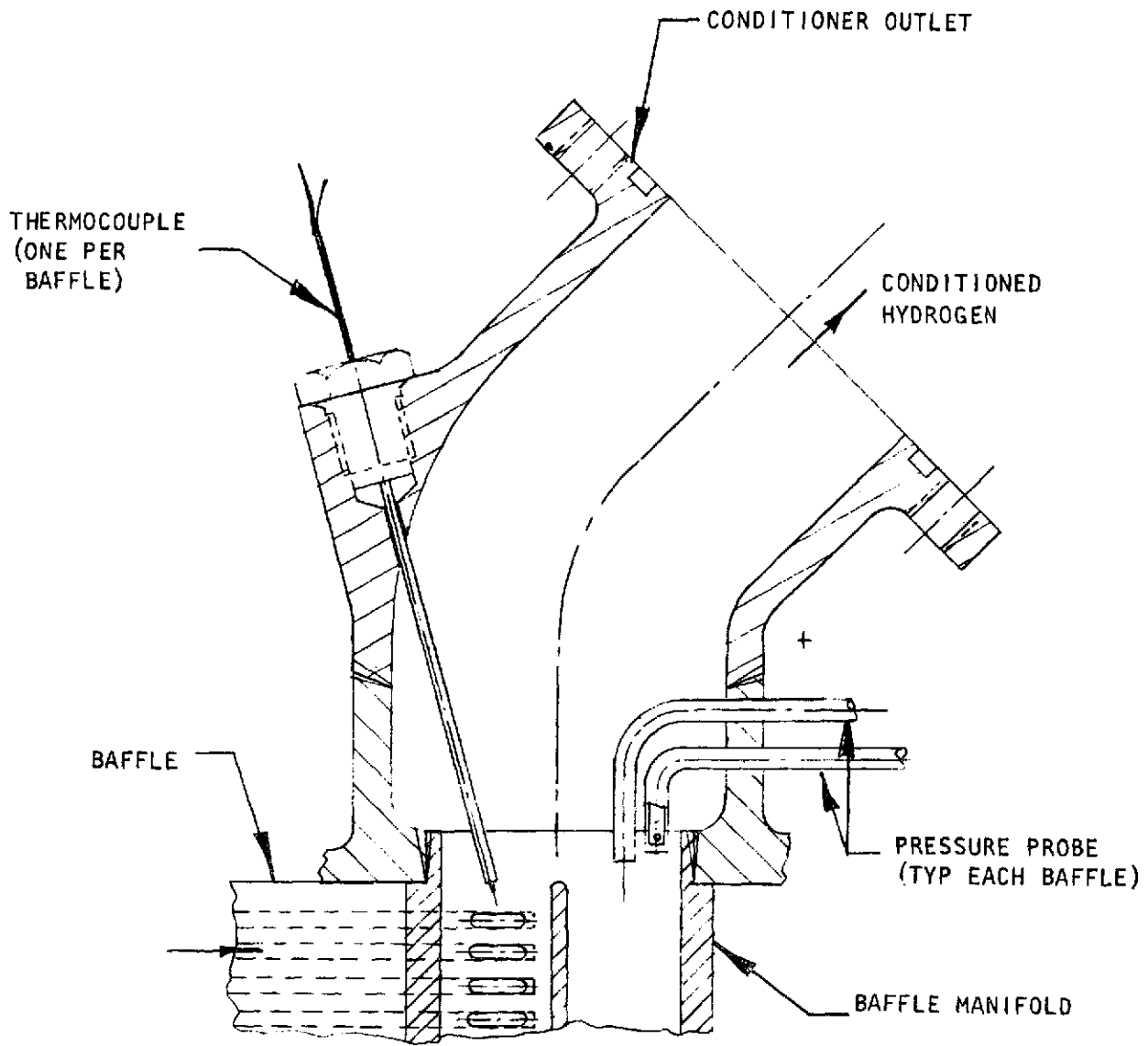


Figure 85. Instrumentation-Conditioned Hydrogen Outlet

The original configuration incorporated 24 elements arranged in a 4 by 6 pattern as shown in Fig. 86 and 87. This injector was hot-fire tested on the solid wall conditioner as a part of the related technology effort (discussed later). Test results showed a tendency for localized hot spots on the conditioner side walls, attributed to the close proximity of the elements with the wall. As a result, the injector was redesigned into a 4 by 4 pattern, eliminating the outer row of elements on the side walls as shown in Fig. 86. Fuel film coolant slots were added along these side walls to further reduce side-wall heat flux.

The detail design of the injector is shown in Fig. 88. Hydrogen enters the injector through manifolds or passages from a collection manifold located on the solid wall chamber or heat exchanger assembly. Oxygen enters the injector through the back side of the injector.

The injector was designed as a furnace brazed assembly with an OFHC copper face and stainless steel manifolds and backup structure. In this design, there are no weld or braze joints between the propellants and the copper face is free floating in any direction as a result of thermal growth. The trislot elements were EDM machined, as shown in Fig. 89.

IGNITER CONFIGURATION

Based upon previous NASA funded and Rocketdyne IR&D studies of various types of igniters including the electric spark, resonance, and catalytic the air-gap electric spark igniter configuration was selected for use in the conditioner program. This igniter is shown in Fig. 90. It operates with a flowrate of 0.06 lbs/sec, an overall mixture ratio of 0.85:1, and a core mixture ratio of 40:1. Oxidizer flows past an annular gap between the spark electrode and combustor wall. A spark discharge occurs across the gap and oxidizer flow. Fuel is injected immediately downstream of the gap in a 40:1 mixture ratio. Ignition occurs and produces a high-temperature (about 4200 R) core. The core body is dump cooled by additional hydrogen flow which brings the overall mixture ratio to 0.85:1. All of the component head end parts are machined from Nickel 200, and the combustion chamber was made from OFHC copper.

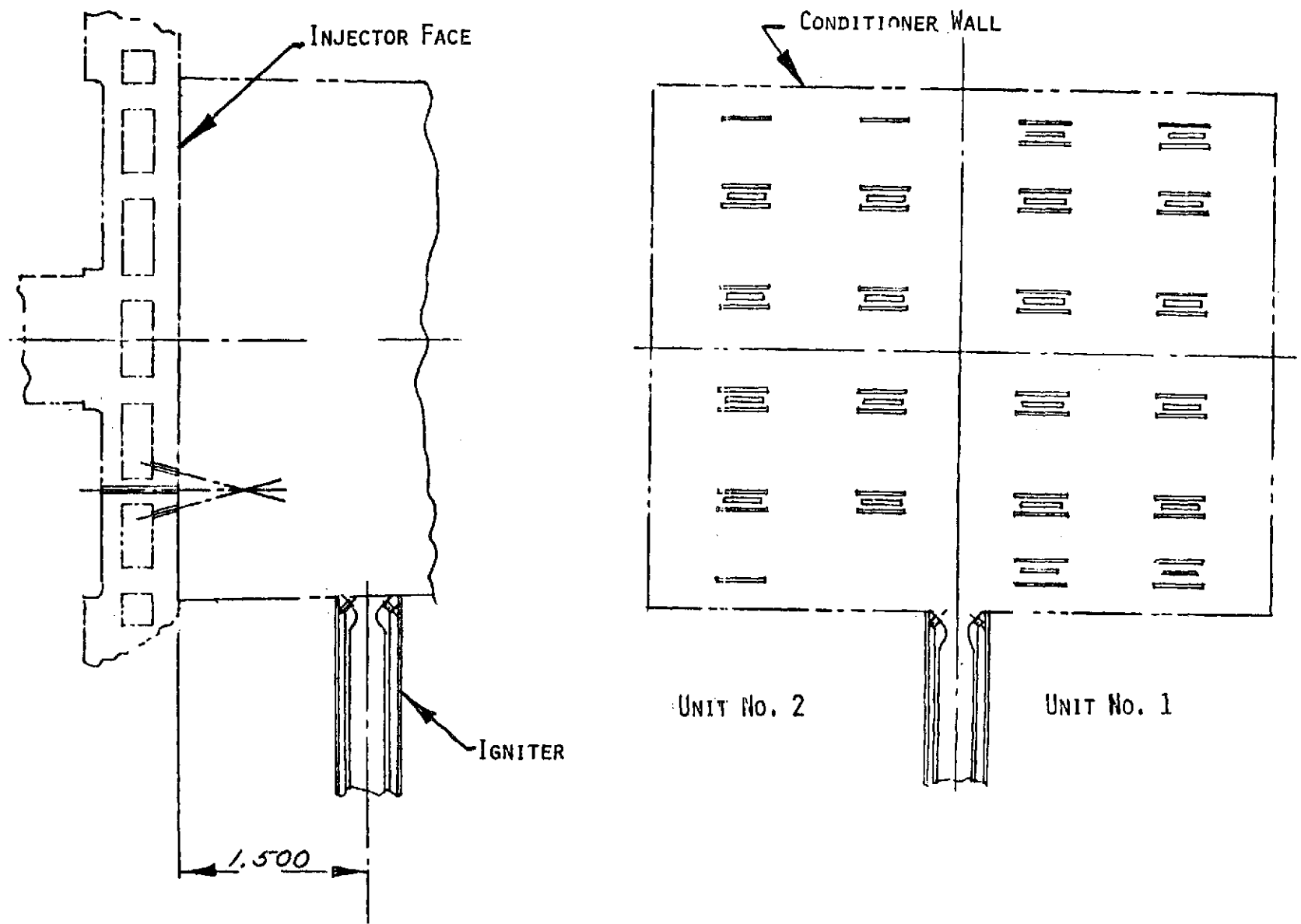


Figure 86. Injector Element Arrangement

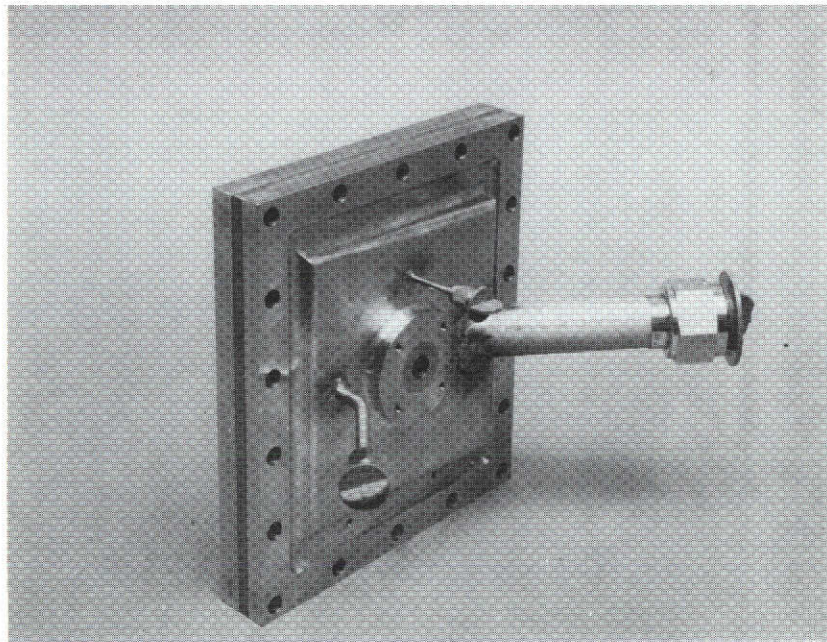
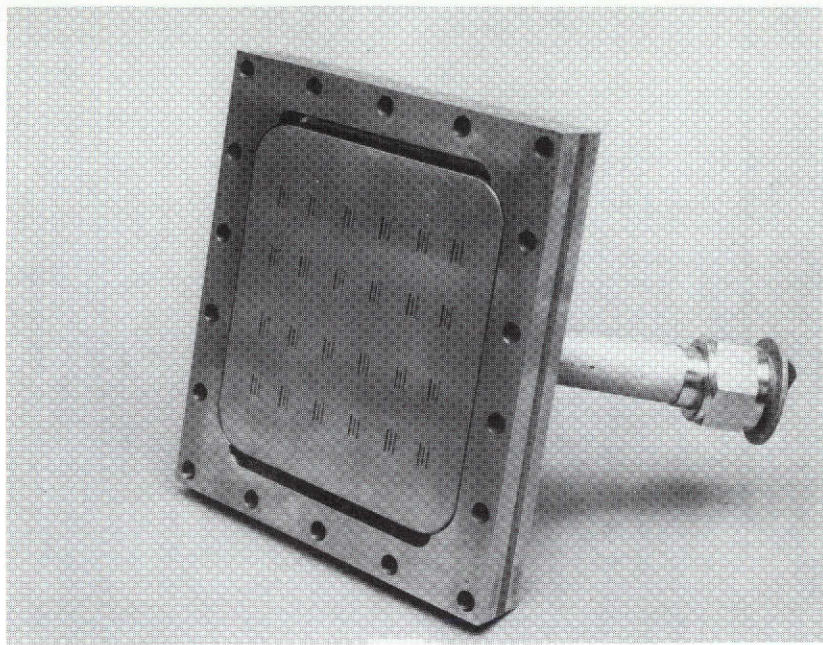


Figure 87. Trislot Injector (Unit No. 1)

Page intentionally left blank

Page intentionally left blank

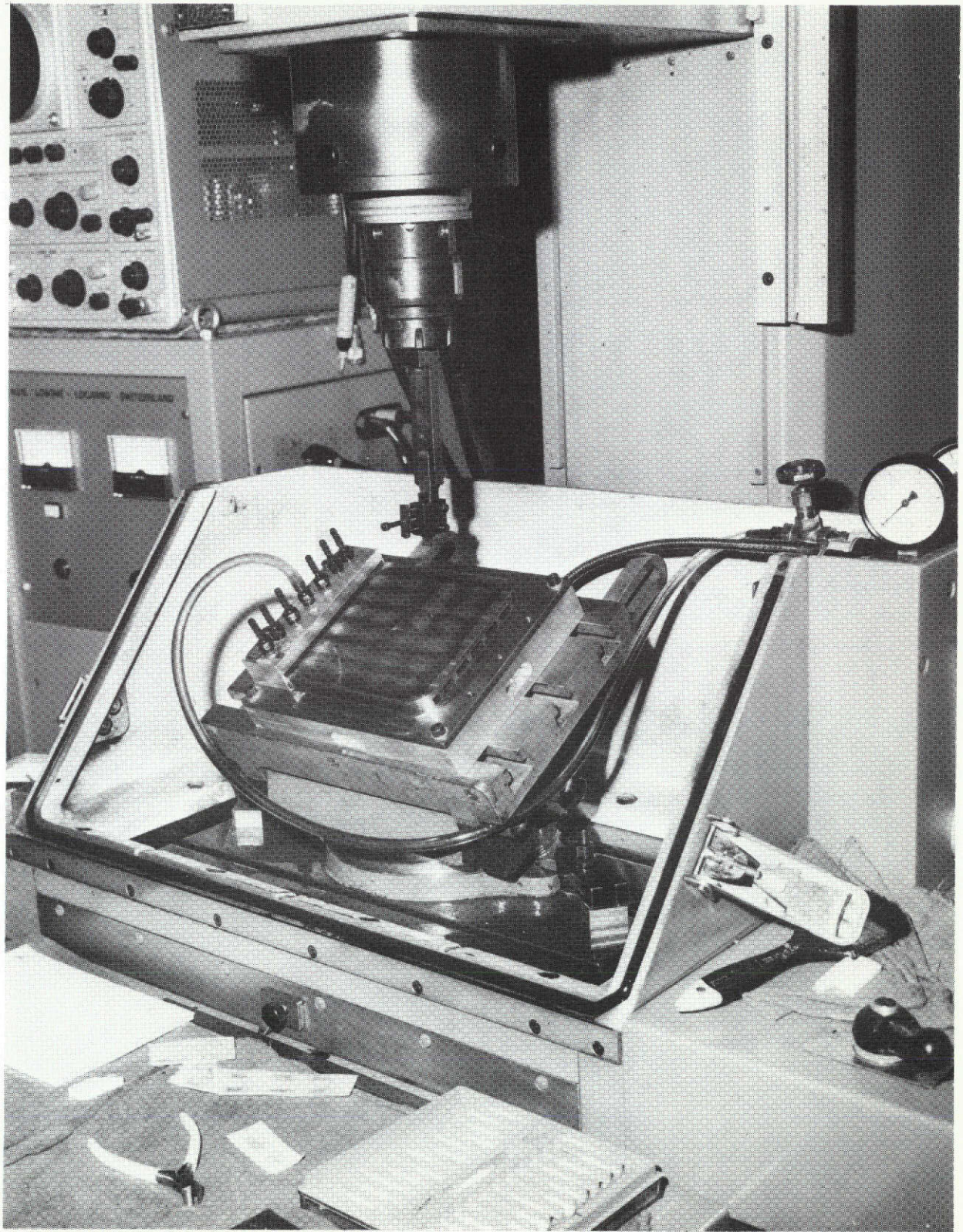


Figure 89. EDM of Injector Elements

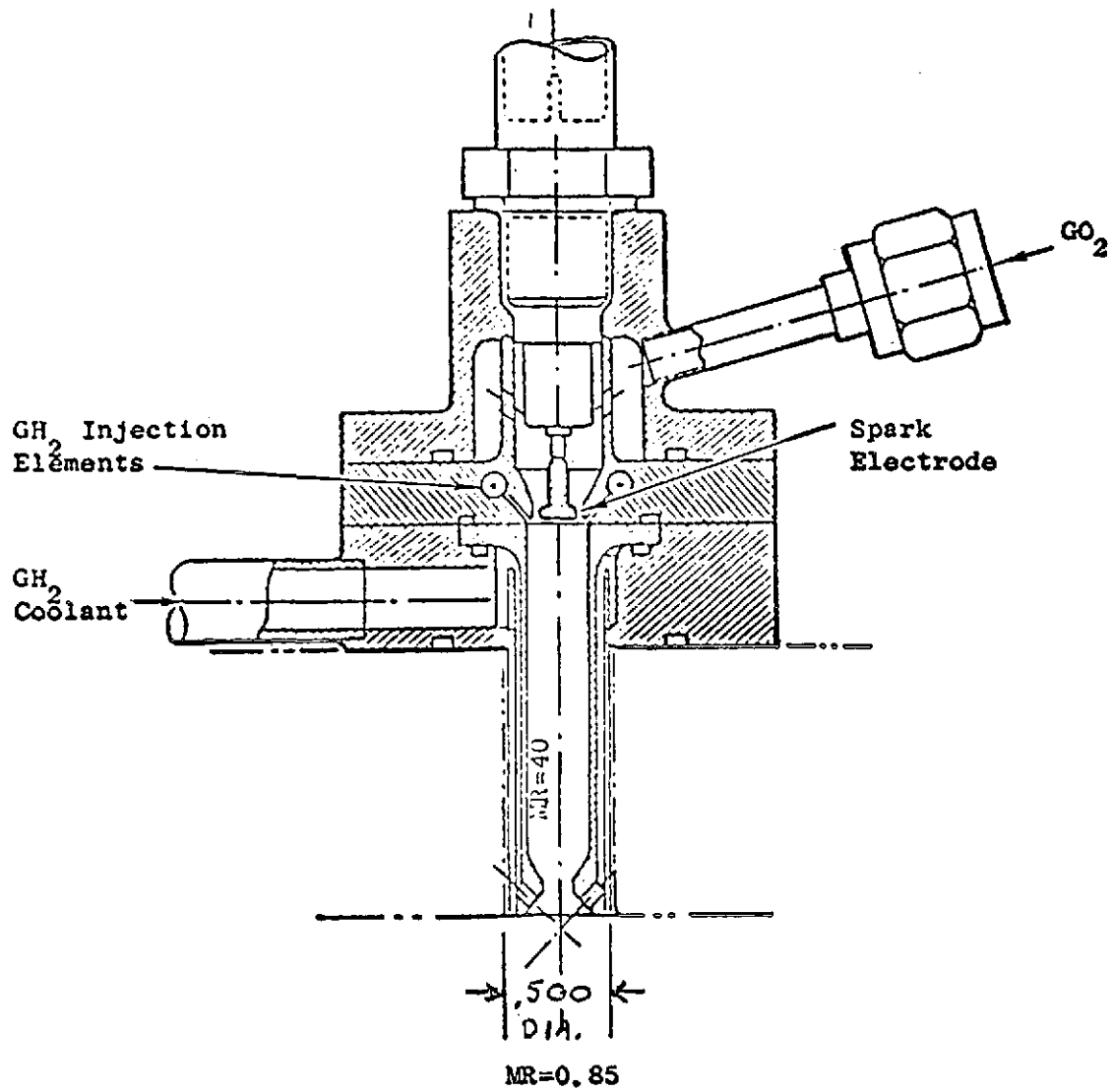


Figure 90. Air Gap Igniter

REACTOR PROPELLANT FLOW CONTROL VALVES

All of the reactor and igniter propellant flow control valves were pneumatically operated bi-propellant ball valves originally designed and used for the Atlas vernier engine system. The valves were modified slightly by increasing the inside diameter of the ball to accommodate the required gaseous oxygen and hydrogen flow rates and the valves were refurbished with new seals and flow checked.

Each bi-propellant ball valve required two Marotta on-off solenoid valves to control the pneumatic flow into the bi-propellant valve actuator.

HYDROGEN CONDITIONER ASSEMBLY CONFIGURATION

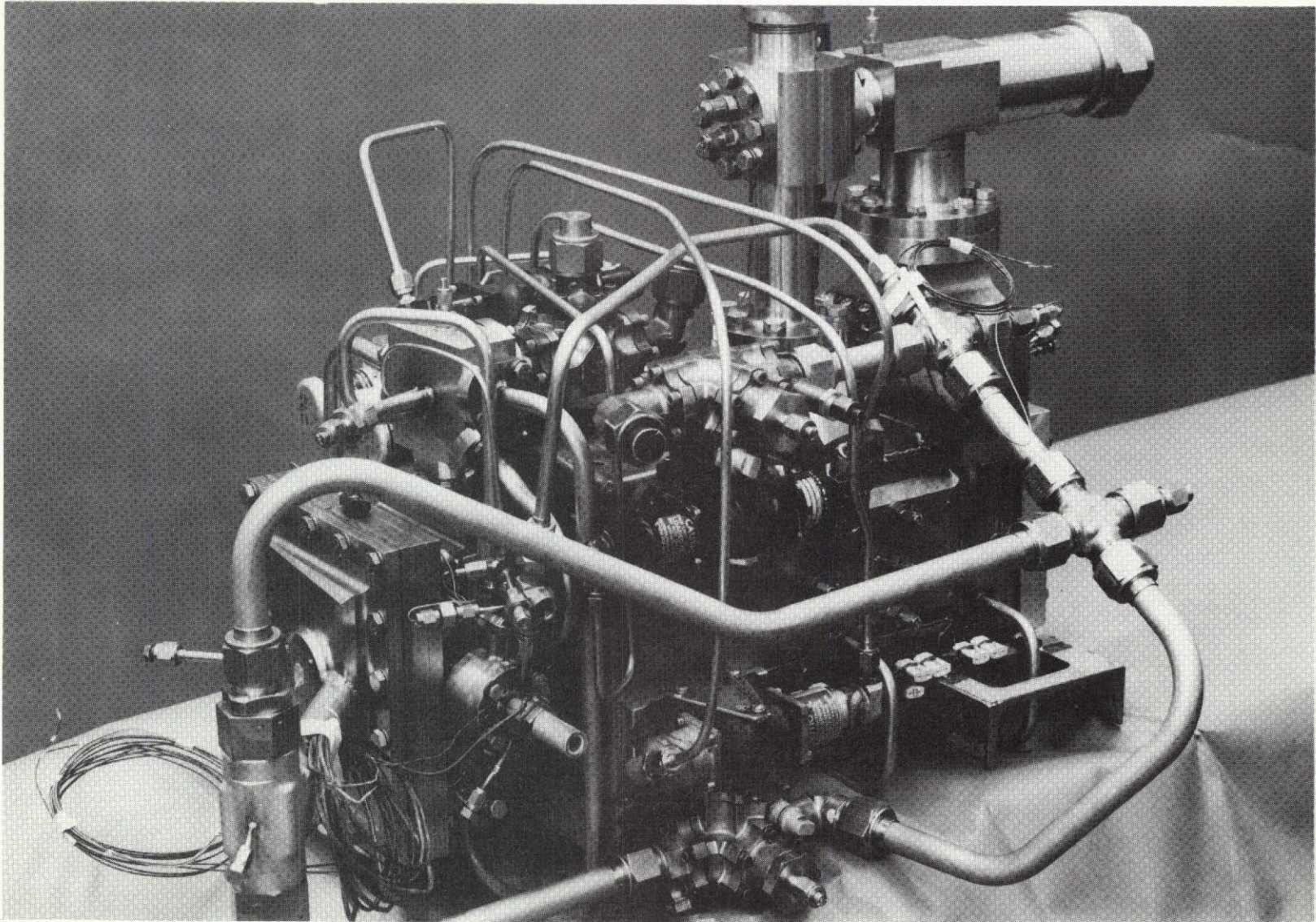
The completed conditioner as shown in Fig. 91 and 92 consists of the conditioner subassembly, the injector, the igniter, injector flow control valves, the coolant by-pass valve, the associated plumbing, and instrumentation which consisted of thermocouples, static and velocity pressure ports. The entire assembly was mounted on two steel channels for ease of handling and ease of mounting in the test stand.

A total of 50 thermocouples, were installed, and a total of 36 pressure ports were located at critical locations on the conditioner. A list of the thermocouples and their locations is shown below:

- 16 thermocouples in the center baffle.
- 6 thermocouples in the hot gas exit passages.
- 7 thermocouples to monitor the coolant exit temperature from each baffle.
- 10 thermocouples in the conditioner side walls.
- 3 at the injector face.
- 1 to measure coolant inlet temperature.
- 1 to measure total coolant outlet temperature.
- 1 to measure gaseous hydrogen inlet temperature at the valves.

Page intentionally left blank

Page intentionally left blank



1ST62-5/16/72-C1F

Figure 92. Completed Hydrogen Conditioner Assembly

- 1 to measure gaseous oxygen.
- 1 on the igniter.
- 2 to measure injector hydrogen inlet temperature.
- 1 combustion gas temperature.

After assembly the unit was proof pressure tested to verify structural integrity and leak tightness. The liquid hydrogen side of the conditioner was proof pressure tested at ambient conditions and cryogenic conditions (using liquid nitrogen) to 2000 psig. The hot gas side was pneumatically pressure tested to 450 psig.

CONDITIONER TEST EFFORT

The hydrogen conditioner was hot fire tested over a range of operating conditions. The primary goal of the test effort was to verify that the concept was not duty cycle limited and to establish a strong technology base for the concept.

A review of the test effort, post test data analysis and post test hardware evaluation is presented in the following sections.

FACILITY

The thermal conditioner was tested at CTL-IV, Cell 29B area of the Santa Susana Field Laboratory. This facility was specifically designed for gaseous oxygen/gaseous hydrogen test firings with ambient temperature and temperature conditioned propellants. Presented is a description of the propellant systems, system controls, and measurement systems.

Propellant Systems

The conditioner was delivered to the test facility as an assembly unit which consisted of the reactor gaseous propellant valves, propellant lines from the reactor valves to the conditioner, liquid propellant bypass mixer, and temperature measurements and orificing on these systems. This unit is shown in Fig. 92 and represented by the simplified schematic in Fig. 93. Figure 94 shows the unit installed in the test facility, and the completed propellant schematic is shown in Fig. 95.

The reactor propellant feed systems consisted of servo controlled liquid propellant, servo controlled gaseous propellant, and mixer systems. These systems were capable of supplying propellant over the full range of propellant temperatures (275 R fuel and 375 R oxidizer to 600 R fuel and oxidizer) at any specified pressure up to 1000 psig. Subsonic

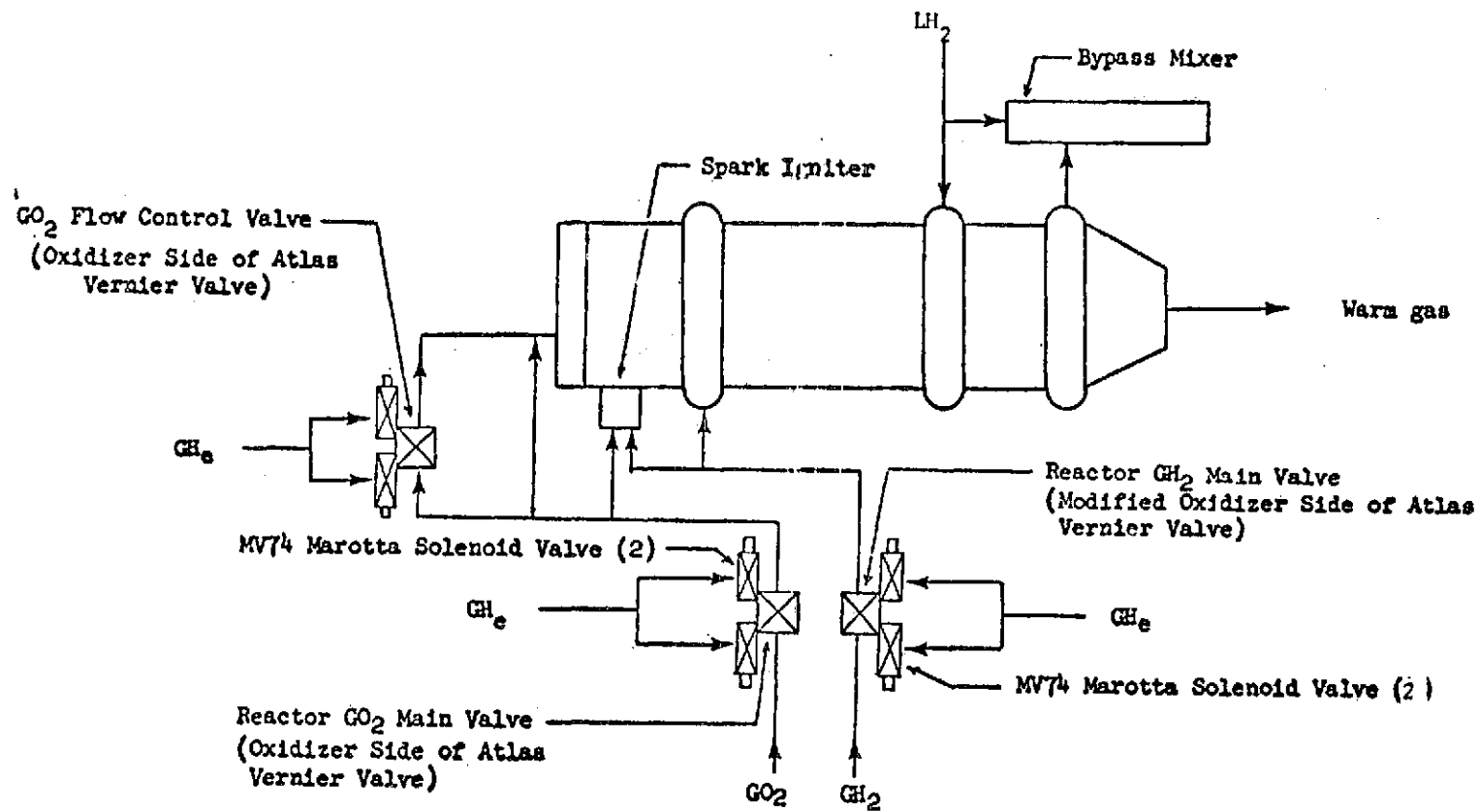
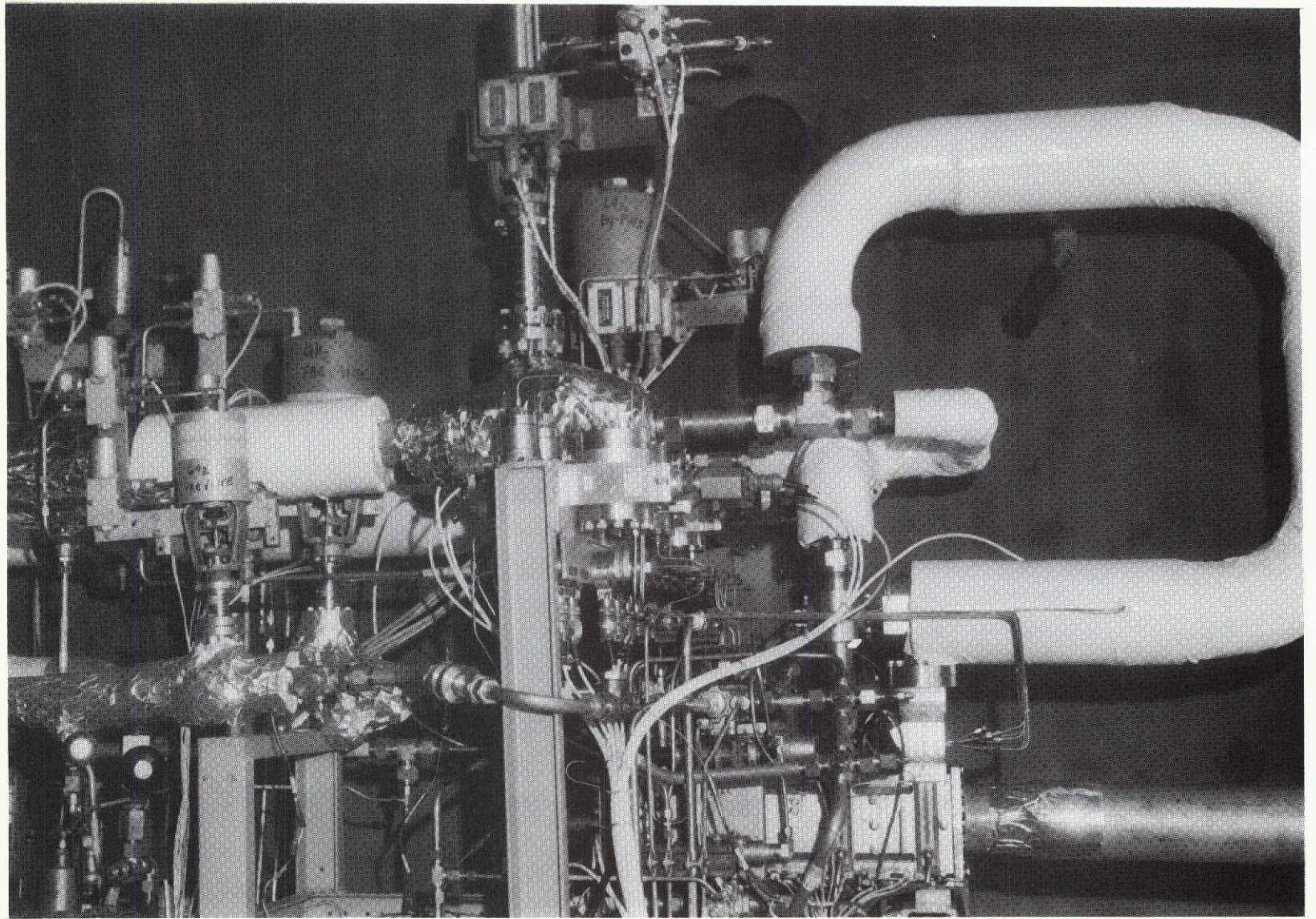
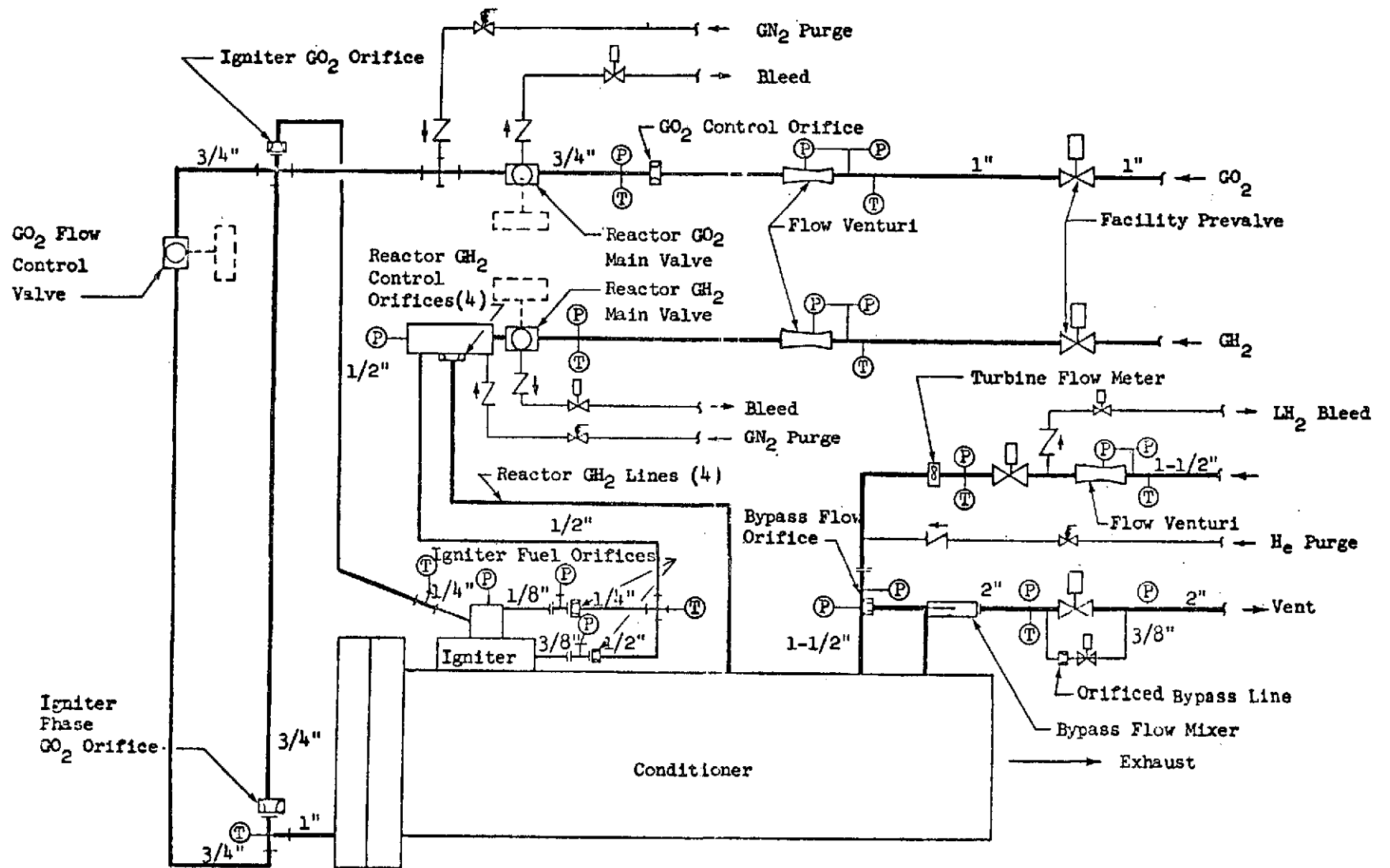


Figure 93. Conditioner Flow Circuits



6DV31-6/21/72-S1D

Figure 94. Thermal Conditioner Installed in Test Facility



170

Figure 95. Propellant Schematic - Facility Setup



venturis were used to measure the total reactor gaseous oxygen and hydrogen flowrates. These venturis had been designed to cover the expected range of operation including mixture ratio variations, temperature variations, and partial flowrates (orificed blowdowns). During propellant blowdowns, the individual circuits were calibrated to define their characteristic resistance. This resistance was used during hot fire tests to determine the flow splits. Flows through the three igniter circuits were determined from previously established igniter characteristics. The air gap torch igniter had been extensively tested during a company-funded program, and its flow characteristics were well established. During a typical operation the flowrate through the igniter was 4 percent of the total reactor flowrate.

The gaseous hydrogen reactor feed system consisted of a single pneumatically actuated ball valve. Downstream of the valve, the fuel was divided into the reactor injector feed, and two air gap igniter feeds. Orifices were placed in the igniter circuits to control flowrate to the igniter injector (igniter core flow) and flowrate to dump cool the igniter body.

The gaseous oxygen reactor feed system consisted of a main valve, and downstream of this valve the flow was split into three circuits as shown in the schematics of Figs. 93 and 95. One circuit fed the igniter and was orificed to obtain the desired igniter core mixture ratio. The remaining two circuits were a parallel feed to the reactor injector which allowed the reactor to operate in low mixture ratio ignition phase and a design mixture ratio mainstage phase. During the ignition phase, all flow went through one leg of the parallel injector feed which was orificed to obtain a partial oxygen flow for low mixture ratio operation. A valve in the remaining leg was closed. At a specified time, this valve was opened, and the full oxygen flow

was developed for mainstage operation. During the actual test program, the ignition phase operation was deleted, and the feed system was modified by removing the parallel leg with the valve and redesigning the orifice in the remaining leg for the full mainstage flowrate.

The facility was designed to initially supply liquid hydrogen as the conditioned propellant, and then the facility was to be converted to supply liquid oxygen. Liquid hydrogen was supplied through a 2" line from a 2000 psig, 1000 gallon run tank. Liquid oxygen was available from a 2" line from a 2000 psig, 600 gallon tank. The propellant system upstream of the conditioner consisted of a subsonic venturi for total flowrate measurement, a redundant turbine flowmeter, and a facility main valve. The assembly contained a bypass mixer section where 60 percent of the liquid flow went through the conditioner baffles and 40 percent of the flow was bypassed. The bypass circuit contained provisions to orifice the flow. The parallel flows were rejoined in a mixer section designed for uniform mixing within the bypass mixer section. The downstream propellant system consisted of a critical flow nozzle to control the total flowrate, a facility valve to be used for propellant pressure lockup tests, and an orificed bypass valve and line to control overpressure during propellant pressure lockup tests. During the initial phases of the test program, the bypass flow was deleted to simplify the test operation by placing a blank orifice in the bypass mixer and the critical flow nozzle was changed for the conditioner baffle flow only ($2.7 \text{ lb}_m/\text{sec}$ nominal). Most of the tests were conducted with no bypass flow.

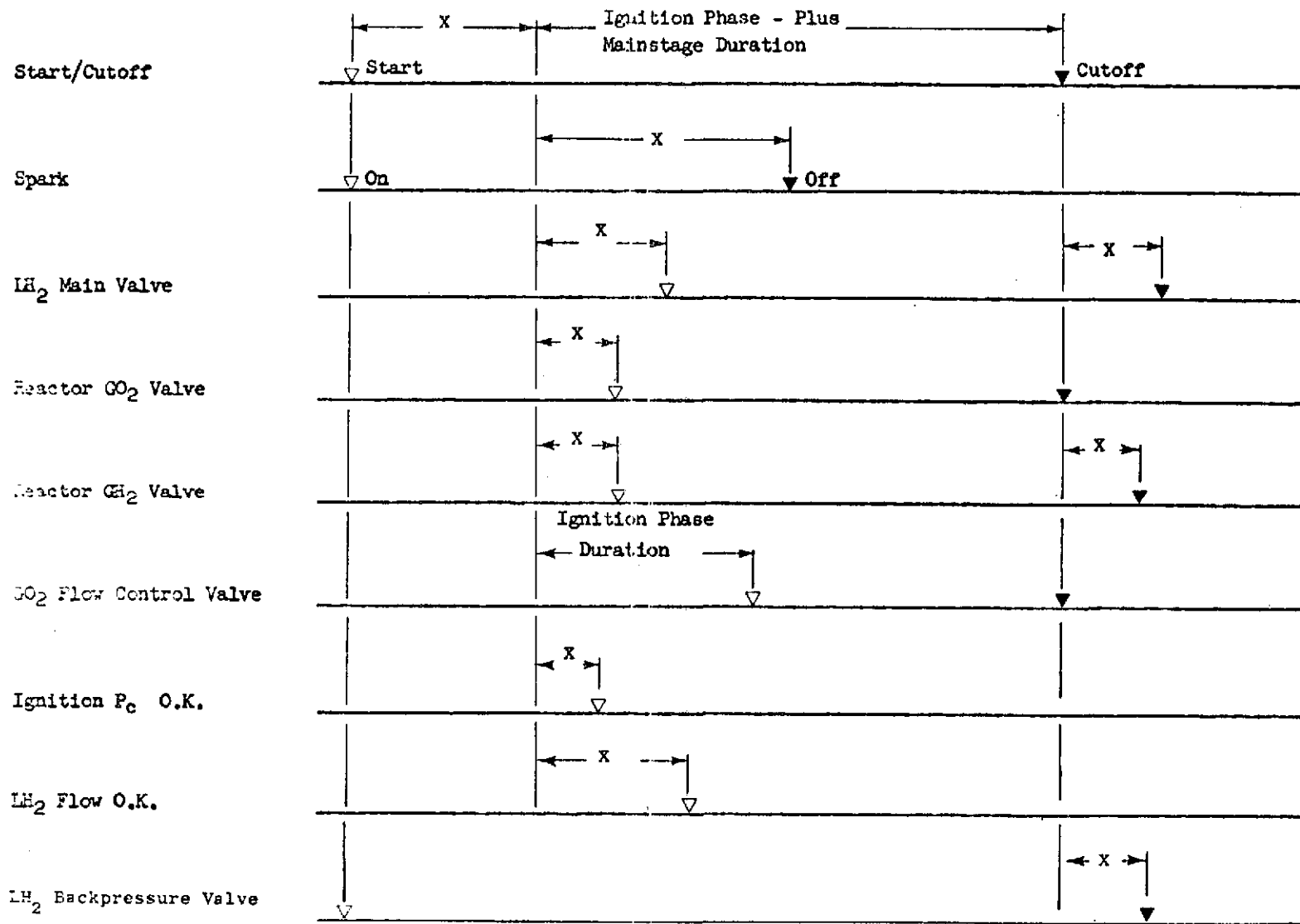
Purges were located immediately downstream of the reactor valves and facility liquid propellant valves. These low pressure purges were turned on prior to testing and locked off automatically during hot fire as the propellant pressures rise. The purges prevented ambient air from entering the conditioner and causing icing post test.

System Control

The sequencing capability is shown schematically in Fig. 96. The start sequence was designed for flexibility of the ignition phase and start of conditioned propellant flow. A safety circuit terminated the test if the targeted reactor chamber pressure was not achieved after a specified time. This served as a check that ignition successfully occurred and that the facility propellant systems were operating satisfactorily and as expected. Another circuit automatically verified that conditioned propellant was flowing and terminated the test if a minimum propellant flowrate was not indicated after a specified time. Both circuits terminated the test any time during mainstage if chamber pressure decreased or propellant flowrate decreased below a specified value. The cutoff allowed the reactor fuel valve to delay while the oxidizer was purged, and this feature prevented an oxidizer rich cutoff due to the trapped volumes downstream of the propellant valves. (An oxidizer rich cutoff would occur whenever the fuel to oxidizer volume ratio downstream of the main valves was less than 16:1). The emergency cutoff was the same as the normal cutoff. The conditioned propellant valve could also be delayed as a precaution during initial checkout tests and/or to simulate any expected propellant conditioning assembly operational mode.

Conditioner Instrumentation

The conditioner was heavily instrumented to allow measurement of sufficient parameters so that a close comparison to predicted operating conditions could be made. This instrumentation was planned to allow for measurement of conditions within the conditioner as well as overall response and heat exchange data. An instrumentation list is presented in Table 17 and includes the feed system parameters reflected in the propellant schematic of Fig. 95. All recorded parameters were recorded on the digital data system. The facility had less recording channels than there was instrumentation on the hardware; therefore, all parameters were not recorded on each test. Parameters required for facility setup were also recorded on Foxboro recorders (DIGR), parameters required for monitoring the conditioner operation during testing were recorded on Brush recorders, and critical response parameters were recorded on the oscillograph.



Times (X) to be specified for each test depending on test objectives.
 System purges to be on during test at specified pressures.

Figure 96. Sequencing Schematic

TABLE 17. APS THERMAL CONDITIONER INSTRUMENTATION

<u>SYSTEM</u>	<u>RECORD</u>	<u>PARAMETER</u>	<u>PURPOSE</u>
HOT GAS	X	Pc	INJECTOR RESISTANCE; EFFECTIVE HOT GAS FLOW DATA LOCAL MR; VERIFICATION OF COMBUSTION; η_{C^*}
	X	Tc	
	X	BAFFLE L-1 GAP EXIT P	HOT GAS FLOW AND MR DISTRIBUTION INDICATION OF U/S FLOW BLOCKAGE
	X	BAFFLE 1-2 GAP EXIT P	
	X	BAFFLE 2-3 GAP EXIT P	
	X	BAFFLE 3-4 GAP EXIT P	
	X	BAFFLE 4-5 GAP EXIT P	
	X	BAFFLE 5-R GAP EXIT P	
	X	BAFFLE L-1 GAP EXIT T	HOT GAS ENTHALPY CHANGE; HOT GAS FLOW AND MR DISTRIBUTION
	X	BAFFLE 1-2 GAP EXIT T	
	X	BAFFLE 2-3 GAP EXIT T	
	X	BAFFLE 3-4 GAP EXIT T	
	X	BAFFLE 4-5 GAP EXIT T	
	X	BAFFLE 5-R GAP EXIT T	

TABLE 17. (Continued)

<u>SYSTEM</u>	<u>RECORD</u>	<u>PARAMETER</u>	<u>PURPOSE</u>
GO ₂	X	VENTURI U/S P	GO ₂ FLOW (TOTAL)
	X	VENTURI U/S T	
	X	VENTURI ΔP	
	X	VALVE U/S P	VALVE RESISTANCE; POSITION (BACK-UP VERIFICATION OF FLOWRATE)
	X	VALVE U/S T	
	X	VALVE D/S P	
	X	INJECTION Pr.	INJECTOR RESISTANCE
	X	INJECTION T	
	X	IGNITER INJECTION P	IGNITER RESISTANCE, GO ₂ IGN FLOWS GO ₂ INJECTOR FLOW
	X	IGNITER INJECTION T	
GH ₂	X	VENTURI U/S P	GH ₂ FLOW (TOTAL)
	X	VENTURI U/S T	
	X	VENTURI ΔP	
	X	VALVE U/S P	VALVE RESISTANCE; POSITION (BACK-UP VERIFICATION OF FLOWRATE)
	X	VALVE U/S T	
	X	VALVE D/S P	
	X	INJECTION T ₁	HEAT INPUT IN COMBUSTOR INJECTOR RESISTANCE
	X	INJECTION T ₂	
	X	INJECTION P	IGNITER CORE AND COOLANT GH ₂ FLOW; INJECTOR GH ₂ FLOW
	X	IGNITER T	
	X	IGNITER CORE INJECTION P	
	X	IGNITER COOL. INJECTION P	

TABLE 17. (Continued)

<u>SYSTEM</u>	<u>RECORD</u>	
LH ₂	X	VENTURI U/S P
	X	VENTURI U/S T
	X	VENTURI ΔP
	X	FLOWMETER U/S P
	X	FLOWMETER T
	X	FLOWMETER OUTPUT
	X	INLET P
	X	BAFFLE NO. 1 OUT. P
	X	BAFFLE NO. 2 OUT. P
	X	BAFFLE NO. 3 OUT. P
	X	BAFFLE NO. 4 OUT. P
	X	BAFFLE NO. 5 OUT. P
	X	BAFFLE NO. 1 OUT. VEL. P
	-	BAFFLE NO. 2 OUT. VEL. P
	XNR	BAFFLE NO. 3 OUT. VEL. P
	-	BAFFLE NO. 4 OUT. VEL. P
	X	BAFFLE NO. 5 OUT. VEL. P
	X	BYPASS OUT. P
	X	OUT. P
	X	LEFT WALL OUT. T
	X	BAFFLE NO. 1 OUT. T
	X	BAFFLE NO. 2 OUT. T
	X	BAFFLE NO. 3 OUT. T
X	BAFFLE NO. 4 OUT. T	
X	BAFFLE NO. 5 OUT. T	
X	RIGHT WALL OUT. T	
X	MIXER OUT. T	
		U/S P TRANSDUCER CHANGED AFTER TEST 219 PRIMARY LH ₂ TOTAL FLOW
		BACK-UP LH ₂ TOTAL FLOW
		BAFFLE ΔP BAFFLE FLOWRATE
		DETERMINATION OF LH ₂ FLOW IN EACH BAFFLE
		OVERALL (BAFFLE + MIXER) ΔP D/S OF PRESSURE REGULATION SYSTEM
		INDIVIDUAL HEAT INPUT; FLOWRATE; THERMAL RESPONSE
		NO. 4 CONNECTED BACKWARDS THROUGH TEST 219
		OVERALL HEAT INPUT; RESPONSE

TABLE 17. (Continued)

<u>SYSTEM</u>	<u>RECORD</u>	<u>PARAMETER</u>	<u>PURPOSE</u>		
INJECTOR	X	FACE T NO. 1			
	X	FACE T NO. 2			
	X	FACE T NO. 3			
BAFFLE		BAFFLE NO. 1 VENT P	MANIFOLDED TOGETHER; MONITOR LEAKAGE OF LH ₂ OR HOT GAS TO BAFFLE CENTER		
		BAFFLE NO. 2 VENT P			
	X	BAFFLE NO. 3 VENT P			
		BAFFLE NO. 4 VENT P			
		BAFFLE NO. 5 VENT P			
CENTER BAFFLE	X	HOT WALL SURFACE T NO. 1	X = .85 IN.	}	LIFE
	a	2	4.9 IN.		
	a	3	9.9 IN.		
	a	4	12.9 IN.		
	X	5	15.4 IN.		
	-	COLD WALL SURFACE T NO. 1		}	HEAT FLUX DISTRIBUTION
	b	2	2.9 IN.		
	b	3	4.9 IN.		
	b	4	9.9 IN.		
	-	5	12.9 IN.		
	X	6	15.4 IN.		
	X	TOP GAP SURFACE T NO. 1	0.9 IN.	}	INDICATION OF HEATING OR ICING PROBLEMS
	b	2	4.9 IN.		
	x	BOTTOM GAP SURFACE T NO. 1	0.9		
	-	2	4.9 IN.	}	
a	3	14.9 IN.			

TABLE 17. (Concluded)

<u>SYSTEM</u>	<u>RECORD</u>	<u>PARAMETER</u>		<u>PURPOSE</u>
SIDE WALL	-	RIGHT HOT WALL T NO. 1	X = 1 IN.	
	X	RIGHT HOT WALL T NO. 2	X = 5 IN.	SIDE WALL
	X	RIGHT HOT WALL T NO. 3	X = 10 IN.	HEATING
	X	RIGHT HOT WALL T NO. 4	X = 13 IN.	
	X	RIGHT HOT WALL T NO. 5	X = 17 IN.	
	-	LEFT HOT WALL T NO. 1	X = 1 IN.	
	X	LEFT HOT WALL T NO. 2	X = 5 IN.	
	-	LEFT HOT WALL T NO. 3	X = 10 IN.	
	X	LEFT HOT WALL T NO. 4	X = 13 IN.	
	X	LEFT HOT WALL T NO. 5	X = 17 IN.	
	X	RIGHT WALL GAS T	X = 13 IN.	GAS T PROFILE;
	X	LEFT WALL GAS T	X = 13 IN.	H ₂ O CONDENSATION;
	X	LEFT WALL GAS P	X = 13 IN.	GAS P PROFILE

To determine the operating characteristics of the thermal conditioner, various instrumentation was installed to monitor hot fluid, cold fluid, and wall parameters. A hot gas thermocouple was installed at the downstream end of each hot gas passage, together with a static pressure tap. This information in conjunction with the combustion temperature and pressure measurements upstream of the baffle was used to determine the hot gas heat loss and pressure drop in each of the six hot gas passages. In addition, hot gas temperature and pressure was measured just downstream of the coolant inlet manifold, to help verify the predicted heat flux distribution. The hot gas thermocouple located in the combustor upstream of the baffles served as a backup check on the injector mixture ratio, although it should be remembered that this is only an approximation since small mixture ratio differences across the injector face can result in the thermocouple indicating a mixture ratio other than the average value, depending on the thermocouple location and injector characteristics.

Cold fluid inlet conditions were determined with upstream pressure, temperature and flowrate readings. Downstream measurements included thermocouples, and both static and total pressure measurements at the exit of each baffle. A number of baffle outlet pressure instrumentation lines on the conditioner assembly had become plugged during a braze operation. Baffle outlet total pressures were limited to three baffles, and baffle outlet static pressures (individual baffle flowrate) were limited to two baffles. The purpose of these measurements was to obtain a coolant pressure drop through the conditioner as well as the flowrate through each baffle; the flowrate plus the temperature rise of the hydrogen in each baffle then gave the heat input distribution from baffle to baffle. Instrumentation downstream of the conditioned propellant mixer measured both the overall pressure drop and the overall conditioned propellant discharge temperature.

Both hot wall and cold wall temperature measurements were made. The cold wall temperatures were monitored at several locations behind a downpass channel, with one set of measurements on a U-baffle and another set on a wall baffle. These were located three or four channels in from the edge; far enough to avoid edge effects while still facilitating installation of the thermocouples. Based on theoretical considerations, the channel closeout temperature at steady-state is very close to the coolant bulk temperature at that point. The purpose of these measurements, then, was to obtain a coolant temperature profile, and thereby deduce the hot gas heat flux profile. A downpass channel was preferred since it is more indicative of the heat input (the uppass channel transfers heat to the downpass channel as a result of the temperature difference of the fluid in adjacent channels flowing in opposite directions). Both the U-baffle and wall baffle were instrumented since the hot gas gap, and thus the heat flux, will be different at the leading edge (there is no taper to the side plate, as there is in the forward part of the U-baffles).

Hot wall temperature measurements were monitored on the U-baffles and wall baffle surface (flush mounting) to obtain local heat flux data (to verify backwall temperature measurements) and to verify predicted operating thermal characteristics. Between the coolant inlet and outlet manifolds, this instrumentation also indicated the effect of condensation on the wall, give an indication of the range over which it is occurring, and the resulting heat flux.

Other areas of interest in the conditioner which were monitored are as follows: one area to be monitored is the U-baffle cover plate (at the top and bottom of each baffle). Temperature readings at the forward end gave an indication of the heat flux to which the baffle cover plate was exposed; instrumentation at the back end indicated whether an icing problem exists between the baffle and the outer wall. In addition, temperature measurements were made on the injector face to verify that no heating problem exists here.

TEST PLAN

The planned test effort was initiated with liquid hydrogen as the conditioned propellant, and the proposed test matrix is presented in Table 18 . The facility/hardware was then to be converted for liquid oxygen as the conditioned propellant, and a similar test effort was to be conducted. These test series would characterize the conditioner thermal operation and response as a function of mixture ratio, reactor flowrate, reactor inlet temperature, and propellant sequencing.

Each matrix consisted of (1) propellant blowdowns, (2) ignition phase only tests (3) mainstage tests with ambient temperature propellants, and (4) mainstage tests with 375 R oxygen and 275 R hydrogen. These matrices reflected a step-by-step approach to achieve the desired data with a minimum of risk. Initial tests were to be conducted with ambient temperature reactor propellant for simpler facility operation. Testing was to progress toward the desired operation of cold reactor propellants and the conditioned propellant sequenced on with mainstage.

A comprehensive propellant blowdown series was required because of the complex flow circuits of the igniter/conditioner. Individual circuits of the conditioner were to be calibrated by alternately placing blank orifice fittings in the lines.

Initial checkout tests (Series II) were to be conducted by establishing and verifying liquid hydrogen flow prior to ignition phases. During these ignition phases only tests, initial thermal characteristics will be assessed at the ignition phase mixture ratio of 0.5 o/f.

TABLE 18. TEST MATRIX - LH₂ CONDITIONER

Test Phase	Variables	No. of Tests	Duration - Sec		LH ₂ Sequence-ms		Results	
			Ignition Phase	Mainstage	Ignition Phase	Mainstage		
I Propellant Blowdowns (Ambient reactor propellants)	Reactor GO ₂ System (4) Reactor CH ₄ System (3) LH ₂ System (3)	3 pts per setup	Stabilized		-	-	Calibrate flow cir- cuits, Facility/hardware response	
II Ignition Phase (Ambient re- actor propel- lants)	Ignition Phase Duration (3)	3	0.5 to 5	0	On & Veri- fied	-	Checkout Initial data with ignition phase MR	
III Conditioner Operation with Ambient Tem- perature Re- actor Propel- lants	Nominal Flows	1	0.5	0.5	On	On	Checkout with m/s planned inspection	
	Mixture Ratio (3) Reactor Flow (3)	9	1.5	5	On	On	Effect of reactor W & MR Effect of LH ₂ W & MR	
	Nominal Flows	1	0.5	0.5	Off	50 ms Lead	Checkout test with uncooled ignition phase Planned inspection	
	Ignition Phase Duration (3)	3	0.5 to 1.5	5	Off	50 ms Lead	Conditioner response Effect of ignition phase duration	
	Pulse Widths Nominal Flows	10 (pulses)	10 (pulses)	0.5	2 On 2 Off	On	On Entire Pulse Duty Cycle	Effect of pulse on/ off time on thermal response
		10 (pulses)	10 (pulses)	0.5	2 On 2 Off	Off	50 ms Lead	
5 (pulses)		5 (pulses)	0.5	2 On 5 Off	Off	50 ms Lead		
5 (pulses)		5 (pulses)	0.5	2 On 10 Off	Off	50 ms Lead		

TABLE 18. (Concluded)

Test Phase	Variables	No. of Tests	Duration - Sec		LH ₂ Sequence-m/s		Results
			Ignition Phase	Mainstage	Ignition Phase	Mainstage	
III (Cont)	Mixture Ratio (3) Nominal Flows	3	1.5	5	On	On	Effect of reactor W & MR Repeat Tests with b instrumentation
	Cutoff with System Pressure Locked up Nominal Flow and MR	3	0.5	5	Off	50 ms Lead	Effect of Residual Heat
	Nominal Flows	3	0.2	0	Off	-	Demonstrate vacuum start
IV Conditioner Operation with 275R CH ₂ and 375R GO ₂	Mainstage Duration (2) Nominal Flows	2	0.5	0-1	On	On	Checkout Test Verify facility operation
	Mixture Ratio (3) Nominal Flows	3	1.5	5	On	On	Effect of reactor MR and inlet tem- perature
	Ignition Phase (3)	3	0.5 to 1.5	5	Off	50 ms Lead	Conditioner response Effect of sequence
	Mixture Ratio (3) Nominal Flows	3	1.5	5	On	On	Repeat mixture ratio tests
	High (TBD) Mixture Ratio (3)	3	1.5	5	On	On	High MR operation Planned Inspection

Test series III was to be conducted with ambient temperature reactor propellants. The first test was a short duration checkout test at the nominal flow condition followed by a visual inspection to verify hardware integrity. Initial tests were to obtain steady-state data with a minimum risk sequence where the conditioned propellant is on to provide cooling during the ignition phase. The conditioner was to be orificed for the nominal conditions with an ignition phase mixture ratio of 0.5:1 o/f when the mainstage mixture ratio is 0.85:1 o/f. Steady-state data was to be obtained for ignition phase and mainstage as a function of reactor mixture ratio, and reactor flow. These parameters were to be varied by approximately 10 percent from nominal. Cycle tests were to be conducted to determine conditioner response as a function of off-times. Off-times were to be varied from 2 to 10 seconds. These tests included "worst case" thermal cycle conditions where the liquid propellant flow remained on during the off-period. Tests were to be conducted to determine thermal soakback and effect of residual heat on trapped conditioned propellant. The hydrogen downstream back pressure valve was to be sequenced closed at cutoff, and the propellant trapped at its nominal pressure. A bypass valve could be used to prevent the trapped propellant pressure from becoming excessive.

Series IV was to be conducted with the reactor propellants conditioned to 375 R oxygen and 275 R hydrogen. Checkout tests would be conducted to verify the operation using the facility propellant condition systems. The effects of reactor mixture ratio and propellants sequencing would be ascertained in test series similar to ambient temperature series. The test matrices for these variables have been abbreviated since the basic trends will have been established during ambient temperature tests. Based on the results, an upper limit of mixture ratio would be selected, and a high mixture ratio test series would be conducted.

TEST PROGRAM

The test program generally followed the test plan as previously outlined. Test series which were conducted using liquid hydrogen as the conditioned propellant included (1) propellant blowdowns and system calibrations, (2) ignition phase only tests, and (3) mainstage tests with ambient temperature reactor propellants. During the course of conducting these series, additional tests were conducted with objectives related to ignition of the reactor propellants, and variables investigated included the air gap igniter mixture ratios (core and overall) and flow-rate and injector pattern. Testing was terminated at this point in the planned program due to distortion of the baffle leading sections with a resulting reduction in the effective baffle gap hot gas flow area. No tests were conducted using temperature conditioned reactor propellants, and no tests were conducted using liquid oxygen as the conditioned propellant. A summary of the test program is shown in Tables 19 and 20. A total of 85 tests were conducted with an accumulated reactor burn time of 197 seconds. This summary does not include no-ignition tests or cold flow calibration tests.

Summary of Tests

Test results are presented in Table 21 in chronological order. The initial effort was a comprehensive series of propellant blowdowns. Individual circuits were calibrated by alternately placing blank orifices in parallel circuits. Characteristic flow resistances were determined for each section of the flow circuits such as propellant valves, valve to injector feed system, injector, and total conditioner baffle section.

TABLE 19. LH₂ CONDITIONER TEST SUMMARY

● TOTAL NUMBER OF TESTS	85
IGNITION ONLY	23
HEAT EXCHANGE/RESPONSE TESTS	62
● ACCUMULATED DURATION (Reactor Burn Time), sec	197
● RANGE OF TEST CONDITIONS	
REACTOR MIXTURE RATIO, o/f	0.70 - 0.95
REACTOR FLOWRATE, lb/sec	0.73 - 1.07
LH ₂ FLOWRATE, lb/sec	2.32 - 4.08
TEST DURATION, sec	0.5 - 30.0

TABLE 20. LH₂ CONDITIONER TEST MATRIX

●	IGNITION/RESPONSE DATA _____	13 TESTS
	DURATION	0.5 sec
	MIXTURE RATIO RANGE	0.70 to 0.93 o/f
	LH ₂ FLOWRATE	2.36 to 2.82 lb/sec
●	BASIC HEAT EXCHANGE DATA _____	9 TESTS
	DURATION	2.0 to 5.0 sec
	MIXTURE RATIO RANGE	0.90 to 0.94 o/f
	LH ₂ FLOWRATE	2.32 to 3.11 lb/sec
●	"WORST CASE" PULSE DATA _____	9 TESTS
	DURATION	3 sec on/ 2 sec off
	MIXTURE RATIO RANGE	0.70 to 0.92 o/f
	LH ₂ FLOWRATE	2.61 to 3.23 lb/sec (continuous)
●	NOMINAL PULSE DATA _____	19 TESTS
	DURATION	3 sec on/ 2 sec off
	MIXTURE RATIO RANGE	0.93 to 0.95 o/f
	LH ₂ FLOWRATE	2.92 to 3.79 lb/sec
●	SIMULATED MISSION DUTY CYCLE _____	11 TESTS
	DURATION	3-5 sec on/ 5 sec-5 min off
	MIXTURE RATIO	0.90 to 0.95 o/f
	LH ₂ FLOWRATE	3.19 to 4.08 lb/sec
●	DURATION CAPABILITY DEMONSTRATION _____	1 TEST
	DURATION	30 sec
	MIXTURE RATIO	0.87 o/f
	LH ₂ FLOWRATE	3.40 lb/sec

62 TOTAL TESTS

TABLE 21. CONDITIONER TEST RESULTS

TEST	TEST OBJECTIVE	REACTOR CONDITIONS			CONDITIONED PROPELLANTS			NO. OF TESTS	DURATION SEC	REMARKS
		\dot{W} LB/SEC	M.R.	P_c PSIA	\dot{W} LB/SEC	$T_{OUT R}$	ΔQ BTU/SEC			
--	COLD FLOW CALIBRATION	--	--	--	--	--	--	20	--	ALL CIRCUITS CALIBRATED
I&II	IGNITION TEST	0.89	0.53	--	--	--	--	8	0.3 TO 3.6	IGNITER LIT NO REACTOR IGNITION
MODIFY INJECTOR BY PLUGGING FILM COOLANT HOLES ADJACENT TO IGNITER										
III	IGNITION TEST	0.97 TO 1.07	0.53 TO 1.00	--	--	--	--	9	0.5	IGNITER DID NOT LIGHT
IV	IGNITION TEST	1.06	0.85 TO 1.00	--	--	--	--	14	0.5	IGNITER LIT ON 5 TEST NO REACTOR IGNITION.
EVALUATE NO. 1 INJECTOR										
V	IGNITION TEST	0.89 TO 1.01	0.53 TO 0.75	198	2.80	285	2220	10	0.5	SPORADIC IGNITION OF IGNITER AND REACTOR IGNITER LIT ON 4 TESTS
NO. 1 INJECTOR UNSUITABLE - INCOMPATIBLE WITH CONDITIONER WALLS - USE NO. 2 INJECTOR										
VI	IGNITION & RESPONSE	0.80 TO 1.00	0.56 TO 0.86	164 TO 217	2.36 TO 2.82	266 TO 324	2120 TO 2370	11	0.5 TO 0.9	ON 2 TESTS REACTOR DID NOT LIGHT

TABLE 21.(Continued)

TEST	TEST OBJECTIVE	REACTOR CONDITIONS			CONDITIONED PROPELLANTS			NO. OF TESTS	DURATION SEC	REMARKS
		W LB/SEC	M.R.	P _c PSIA	W LB/SEC	T _{OUT} R	ΔQ BTU/SEC			
VII-A	HEAT EXCHANGE DATA	0.79 TO 1.07	0.79 TO 0.93	197 TO 250	2.44 TO 2.85	281 TO 394	2220 TO 2540	9	2.0 TO 5.0	ON 2 TESTS REACTOR DID NOT LIGHT
VII-B	WORST CASE PULSING	0.80 TO 0.97	0.70 TO 0.92	224 TO 320	2.61 TO 3.23	196 TO 295	1641 TO 2270	12	3.0 ON 2.0 OFF	ON 1 TEST HAD CUT @ 0.5 SEC. ON 3 TESTS REACTOR DID NOT LIGHT LH ₂ ON CONTINUOUSLY
VIII-A	HEAT EXCHANGE DATA	0.89 TO 0.92	0.90 TO 0.94	238 TO 297	2.32 TO 3.11	230 TO 388	1890 TO 3090	5	0.5 TO 5.0	ALL TESTS AT 5 SEC DURATION EXCEPT ONE AT 0.5 SEC
VIII-B	PULSE DATA	0.84 TO 0.90	0.92 TO 0.95	266 TO 310	2.95 TO 3.79	194 TO 245	1940 TO 2260	19 24	3.0 ON 2.5 & 10 OFF	NOMINAL 3 SEC ON/2 SEC OFF PULSING. LH ₂ CYCLED ON AND OFF WITH REACTOR GO ₂ FLOW
IX-A	IGNITION CHECK	0.88	0.79	343	5.51	97	740	1	1.0	CROSS CHECK ON IGNITION PARAMETERS
IX-B	HEAT EXCHANGE DATA	0.85	0.95	316	2.64	241	1820	1	5.0	BASIC HEAT EXCHANGE DATA

TABLE 21. (Concluded)

TEST	TEST OBJECTIVE	REACTOR CONDITIONS			CONDITIONED PROPELLANTS			NO. OF TESTS	DURATION SEC	REMARKS
		\dot{W} LB/SEC	M.R.	P_c PSIA	\dot{W} LB/SEC	T_{OUT} R	ΔQ BTU/SEC			
X-A	SIMULATED MISSION DUTY CYCLE	0.75 TO 0.85	0.90 TO 0.95	308 TO 370	3.19 TO 4.08	176 TO 219	1670 TO 1900	5	5.0 ON 10 SEC TO 5 MIN OFF	VARIED OFF TIMES TO VERIFY CONDITIONER NOT DUTY CYCLE LIMITED
X-B	DURATION TEST	0.73	0.87	382	3.40	219	1570	1	30	EVALUATE DURATION CAPABILITY
X-C	HEAT EXCHANGE DATA	0.81	0.92	342	2.87	227	1820	1	5	BASIC HEAT EXCHANGE DATA

These characteristic resistances were monitored throughout the test effort, and as expected, there was no change in the flow characteristics of the individual components and feed systems including the conditioned propellant/baffle section. The only resistance which varied during testing was the effective baffle hot gas flow area.

During the initial test effort, the igniter failed to ignite the reactor propellants. During test series I and II, as shown in Table 21, the igniter operated successfully on each test as indicated by the igniter internal chamber pressure and by a temperature rise indicated by the reactor combustion temperature thermocouple located near the path of the igniter flow. This igniter assembly had been used during the solid wall conditioner checkout test series with complete success, and the reactor propellants ignited on every test during this series. A major difference in the igniter/reactor configuration between the solid wall and conditioner tests was the injector pattern. The injector unit #2 used on the conditioner tests was a modified version of unit #1 which was used on the solid wall hardware. During the solid wall test program, localized erosion of the reactor side walls was experienced and therefore, unit #2 injector was fabricated where the tri-slot elements adjacent to the side walls was deleted and replaced with fuel film coolant slots.

The injector (unit #2) was modified by plugging the two fuel film coolant slots immediately adjacent to the side wall mounted igniter since there was a possibility that the film coolant was mixing with the igniter flow. This would lower the temperature of the igniter flow below that required for ignition. Series III and IV were conducted in which the igniter operated on 5 tests but the reactor again failed to ignite. During many of the tests, the igniter failed due to a faulty spark cable connection which was difficult to detect.

Failure to ignite the reactor propellants was a perplexing problem since the igniter was the same unit used successfully during the solid wall test program and the injector was similar to unit #1. The difference in the injector patterns was shown previously. As a reference test series, the solid wall configuration was duplicated by installing unit #1 injector on the conditioner assembly and orificing the air gap igniter to duplicate the same igniter flowrate, core mixture ratio, and overall mixture ratio that was used during the solid wall test effort. One difference which could not be rectified was that the cooled conditioner assembly has a higher unignited backpressure (chamber pressure) than the heat sink solid wall hardware due to the presence of cooled baffles. The reactor ignited on one test of four. This test was of 0.5 seconds duration. During the other tests conducted during this series, the igniter failed due to the faulty spark cable connector. The faulty connector was discovered and repaired for subsequent testing, and no further igniter failures were experienced. Post test inspection of the conditioner indicated heated areas on the reactor side walls which was the result of the single 0.5 second test with unit #1 injector. The pattern of the heated areas was remarkably similar to the erosion pattern which occurred on the solid wall assembly. Thus, injector unit #1 was unsuitable for further testing due to potential overheating of the reactor side walls, and injector #2 was reinstalled for all subsequent test effort.

The results of these tests indicated that ignition of the reactor propellants was sensitive to distribution of the igniter high temperature core flow, the intermixing of the core flow and the igniter dump coolant flow, and the proximity of the injector elements to the igniter flow. In the next test series VI, the initial ignition phase mixture ratio was successively increased to higher and more ignitable mixture ratios. The results showed that a reactor mixture ratio of 0.9:1 o/f or higher was required for repeated ignitions. The ignition phase concept was eliminated since these test results show that a low mixture ratio start was not required or desired for the conditioner assembly.

Test series VII obtained heat exchange data as a function of reactor mixture ratio and flowrate. Seven data tests were conducted plus three tests where the reactor did not ignite at relatively low reactor mixture ratios (less than 0.9:1 o/f). A "worst case" pulse duty cycle test series was also conducted where the liquid hydrogen flow remained on during the 2 second off period. The first attempt at this pulse series was terminated at the end of two cycles due to a facility sequence malfunction. The planned series of ten pulses was then conducted during which there were three pulses in which the reactor did not ignite.

Test series VIII obtained conditioner thermal data as a function of liquid hydrogen flowrate. Pulsing data was obtained where the conditioned propellant was shutoff during the reactor off periods. Pulsing capability was demonstrated with an on time of 3 seconds and off times of 2, 5, and 10 seconds.

As a cross check on ignition parameters, series IX was conducted at a low reactor mixture ratio, and ignition did not occur. When the reactor mixture ratio was increased above 0.9:1 o/f, successful ignition occurred. This was the same results experienced on past testing.

Series X was a simulated mission duty cycle where the on-time was 5 seconds and the off-time was varied from 10 seconds to 5 minutes. This series was concluded with a 30 second duration test which demonstrated extended duration capability.

Series XI objective was to evaluate conditioner thermal soakback by locking up the conditioned hydrogen propellant when the reactor mainstage was terminated. Thermal soakback data was to be monitored for several minutes after cutoff of the reactor. However, several seconds after reactor cutoff, a facility fire occurred, and the test was aborted; therefore, lockup capability was not demonstrated.

Reactor and conditioned propellant flow conditions on each test as well as test results and objectives are listed in Table 22 .

During the cold conditioner test program, 85 tests were conducted, and 197 seconds of hot-fire duration was accumulated. Thermal and response data was obtained which established a technology base for a highly efficient, baffle type propellant heat exchanger with integral reactor. Data obtained over a range of conditioned propellant and reactor flow conditions verified the analytical design techniques used for designing baffle type conditioners.

Data was obtained on the ignition and operation of the reactor over a range of reactor and igniter operating conditions including mixture ratios, flowrates, and propellant sequencing. Ignition of the reactor was smooth and rapid, and the data indicated that there were no detonations or overpressures during the ignition process. Further effort is required to evaluate conditions required for reliable ignition. This effort should further evaluate distribution of the igniter effluent relative to the injector face and elements and igniter/injector operating conditions at ignition including igniter mixture ratios and flowrate, and injector mixture ratio.

The reactor operated stably and the data showed that there were no chugging or indication of acoustic instabilities. During the early phases of testing, the reactor operated predictably, and the reactor chamber pressure and combustion temperature obtained the expected values during both unignited and ignited conditions. As testing progressed, anomalies occurred in the reactor operation. The reactor chamber pressure became

TABLE 22. LH₂ THERMAL CONDITIONER TEST CONDITIONS

Test No.	Test Sub.	Reactor		Igniter			Reactor PC (min)	Condenser Equipment				Ignition Duration (Sec)	Mixture Duration (Sec)	Ignition		No. of Tests	Objective	Comments
		W (W/hr)	MR (1/5)	W (W/hr)	MR _{1,101} (1/5)	MR _{1,102} (1/5)		W (W/hr)	Test (R)	P ₁ (psia)	ΔH (Btu/lb)			Igniter	Reactor			
147-148	C-114	-	-	-	-	-	-	-	-	-	-	Stabilized	-	-	-	4	50% Calibration, 4 Flows	Maintenance and ignition glass circuits
149-149	-	-	-	-	-	-	-	-	-	-	-	-	-	-	-	4	60% Calibration, 4 Flows	No bypass circuit
149-149	-	-	-	-	-	-	-	-	-	-	-	-	-	-	-	4	40% Calibration, 4 Flows	Full bypass circuit
149-152	-	-	-	-	-	-	-	-	-	-	-	-	-	-	-	4	50% Calibration, 4 Flows	Side walls only
152-155	-	-	-	-	-	-	-	-	-	-	-	-	-	-	-	4	60% Calibration, 4 Flows	All circuits open
157-160	I	0.77	0.53	0.071	1.1	30	-	-	530	-	-	0.3-3.0	0	Yes	No	4	Checkout	
161-164	II	0.87	0.57	0.071	1.1	30	-	-	1400	-	-	0.5	0.5-5	Yes	No	4	Checkout	
165-168	III	0.89	0.57	0.071	1.1	30	-	-	1040	-	-	0.5	0.5-2	No	No	4	Ignition Investigation	
169	-	1.07	0.75	0.093	1.7	48	-	-	1040	-	-	0	0.5	No	No	1	With Mod. #2	
170	-	1.03	0.90	0.090	1.9	51	-	-	1040	-	-	0	0.5	No	No	1	Injector	
171	-	1.00	0.95	0.097	2.0	54	-	-	1040	-	-	0	0.5	No	No	1		
172	-	0.97	1.00	0.097	2.1	57	-	-	1040	-	-	0	0.5	No	No	1		
173	-	0.97	1.00	0.097	2.1	57	-	-	1040	-	-	0	0.5	No	No	1		
174-175	IV	1.06	0.95	0.065	1.0	26	-	-	1040	-	-	0	0.5	No	No	1	Ignition Investigation	GM ₂ /GN ₂ Simulated Flows
176	-	1.06	0.94	0.065	1.7	29	-	-	1040	-	-	0	0.5	No	No	1	With Mod. #2	
177-178	-	1.06	1.00	0.065	1.1	31	-	-	1040	-	-	0	0.5	No	No	2	Injector Mixture	
179	-	1.06	1.00	0.065	1.1	31	-	-	1040	-	-	0	0.5	No	No	1	Injector And Mixture	GM ₂ /GN ₂ Simulated Flows
180	-	1.06	0.95	0.065	1.0	26	-	-	1040	-	-	0	0.5	Yes	No	1	Injector Operation	Increased spark voltage
181	-	1.06	0.94	0.065	1.1	29	-	-	1040	-	-	0	0.5	Yes	No	1		
182	-	1.06	0.94	0.065	1.1	29	-	-	1040	-	-	0	0.5	No	No	1		
183-184	II	1.06	1.00	0.065	1.1	31	-	-	1040	-	-	0	0.5	No	No	2		
185-187	-	1.06	1.00	0.065	1.1	31	-	-	1040	-	-	0	0.5	Yes	No	3		
188-189	V	0.89	0.53	0.071	1.1	30	-	-	1430	-	-	0.5	0	Yes	No	2	Ignition Investigation	
190	-	0.96	0.63	0.079	1.4	37	198	2.94	285	1450	2220	0.5	0	Yes	Yes	1	With #1 Injector	0.3 seconds of hot-fire
191	-	0.96	0.65	0.079	1.4	37	-	-	1430	-	-	0.5	0	Yes	No	1		
192-197	-	1.01	0.75	0.086	1.6	43	-	-	1430	-	-	0.5	0	No	No	6		Various preflight sequencing
198	VI	0.86	0.52	0.072	0.8	16	-	-	1430	-	-	0.5	0	Yes	No	1	Ignition Investigation With	
199	-	0.81	0.73	0.075	1.2	23	167	2.59	219	1427	2180	0.5	0	Yes	Yes	1	#2 Mod. Injector	
200	-	0.81	0.75	0.075	1.2	24	164	2.78	278	1484	2180	0.5	0	Yes	Yes	1	And Lower Igniter	
201	-	0.80	0.86	0.075	1.4	27	171	2.36	344	1308	2283	0.5	0	Yes	Yes	1	W & MR's	
202	-	0.81	0.85	0.075	1.4	27	170	2.63	277	1418	2270	0.5	0	Yes	Yes	1		
203	-	0.80	0.81	0.075	1.3	25	171	2.67	292	1473	2280	0.5	0	Yes	Yes	1		
204	-	0.83	0.67	0.074	1.1	20	174	3.70	209	1409	-	0.5	0	Yes	No	1		
205	-	0.82	0.78	0.075	1.3	27	171	2.88	270	1427	2250	0.5	0	Yes	Yes	1		
206	-	0.81	0.82	0.079	1.3	25	166	2.72	266	1431	2130	0.5	0	Yes	Yes	1		
207	-	1.00	0.73	0.086	1.3	25	177	2.60	305	1437	2170	0.5	0	Yes	Yes	1		
208	-	0.81	0.78	0.076	1.3	24	172	2.73	277	1433	2180	0.5	0	Yes	Yes	1		
209	VII A	1.10	0.79	0.077	0.8	18	176	2.96	311	1490	-	0	0.5	Yes	No	1	Checkout	
210	-	1.06	0.79	0.077	0.8	15	175	3.12	278	1487	-	0	0.5	Yes	No	1		
211	-	0.90	0.83	0.072	1.0	17	177	2.67	325	1502	2540	0	0.5	Yes	Yes	1		
212	-	0.92	0.85	0.075	0.7	17	200	2.56	249	1494	2290	0	2	Yes	Yes	1		
213	-	0.97	0.71	0.075	0.9	17	228	2.78	271	1467	2340	0	5	Yes	Yes	1	Condenser Data	
214	-	1.00	0.89	0.079	0.9	17	166	4.21	172	1453	-	0	0.5	Yes	No	1		
215	-	0.77	0.81	0.036	0.9	16	160	2.44	394	1420	2840	0	0.5	Yes	Yes	1	Low Reactor Flow Data	Low P ₂ Cut
216	-	0.87	0.73	0.071	0.9	18	191	2.61	281	1336	2220	0	5	Yes	Yes	1		
217	-	1.07	0.92	0.079	0.9	17	250	2.95	287	1550	2480	0	5	Yes	Yes	1	High Reactor Flow Data	
218-1	VII B	0.80	0.70	0.070	0.8	14	233	2.61	275	1460	2270	0	2	Yes	Yes	1	Pulsing - 2 sec off time	
219-2	-	0.91	0.70	0.072	1.0	17	179	2.96	229	1400	1910	0	0.5	Yes	Yes	1	LH ₂ flowing during off	Low P ₂ Cut
219-1	-	0.92	0.90	0.072	0.9	17	273	2.78	266	1452	2140	0	3	Yes	Yes	1	Pulsing 3 sec off time	
219-2	-	0.97	0.90	0.075	0.9	17	224	2.70	276	1420	2220	0	3	Yes	Yes	1	LH ₂ flowing during off time	
219-3	-	0.93	0.90	0.075	0.9	17	275	2.77	255	1407	2050	0	3	Yes	Yes	1		
219-4	-	0.97	0.91	0.078	1.0	17	204	5.71	90	1177	671	0	3	Yes	No	1		
219-5	-	0.91	0.92	0.072	0.9	17	285	2.86	241	1385	1965	0	3	Yes	Yes	1		
219-6	-	0.88	0.89	0.070	0.9	16	320	3.23	196	1370	1641	0	3	Yes	Yes	1		
219-7	-	0.93	0.92	0.072	0.9	17	262	2.80	254	1373	2067	0	3	Yes	Yes	1		
219-8	-	0.87	0.89	0.070	0.9	16	327	3.12	209	1379	1753	0	3	Yes	Yes	1		
219-9	-	0.98	0.91	0.075	0.9	17	246	6.08	54	1145	573	0	2	Yes	No	1		
219-10	VIII A	0.89	0.75	0.071	1.0	19	225	6.13	82	1130	517	0	2	Yes	No	1		
220	-	0.94	0.90	0.087	1.6	31	238	2.61	328	1562	3090	0	0.5	Yes	Yes	1	Checkout	
221	-	0.92	0.91	0.086	1.6	30	283	3.03	242	1512	2080	0	5	Yes	Yes	1	Normal Condenser	
222	-	0.89	0.93	0.085	1.6	30	294	3.11	230	1509	2050	0	5	Yes	Yes	1		
223	-	0.90	0.93	0.086	1.6	31	293	2.60	251	1351	1990	0	5	Yes	Yes	1	Normal LH ₂ Flow	
224	-	0.89	0.94	0.086	1.6	31	287	2.32	275	1337	1880	0	5	Yes	Yes	1	Normal LH ₂ Flow	
225	VIII B	0.89	0.94	0.085	1.6	31	298	2.90	242	1467	2079	0	3	Yes	Yes	1	Pulsing demonstration	Malfunction cut
226-1	-	0.89	0.95	0.085	1.6	31	295	3.02	274	1469	2040	0	3	Yes	Yes	1	3 sec on/2 sec off	
226-2	-	0.87	0.94	0.085	1.6	31	296	2.97	237	1460	2070	0	3	Yes	Yes	1		
226-3	-	0.87	0.91	0.083	1.5	31	302	3.05	227	1452	2000	0	3	Yes	Yes	1		Cut, facility fire
227-1	-	0.87	0.94	0.085	1.6	31	297	3.24	245	1501	2210	0	3	Yes	Yes	1		
227-2	-	0.89	0.95	0.086	1.6	31	292	3.22	233	1500	2160	0	3	Yes	Yes	1		
227-3	-	0.90	0.95	0.085	1.6	31	292	3.27	227	1571	2140	0	3	Yes	Yes	1		
227-4	-	0.90	0.93	0.086	1.6	31	290	3.27	222	1537	2170	0	3	Yes	Yes	1		
227-5	-	0.89	0.94	0.085	1.6	31	292	3.32	230	1505	2190	0	3	Yes	Yes	1		
227-6	-	0.87	0.95	0.086	1.6	31	291	3.33	227	1507	2170	0	3	Yes	Yes	1		
227-7	-	0.89	0.94	0.086	1.6	31	285	3.17	228	1512								

increasingly higher indicating a decrease in the effective hot gas flow area. This anomaly first became evidenced during the "worst case" cycle testing and became more prevalent as testing progressed. Typically chamber pressure would step up in value randomly during a test and sometimes occurred several times in a test. Reactor total flowrate would decrease as the chamber pressure increased. On some tests, the effective hot gas flow area decreased to less than one half of its nominal value. The major cause of the phenomenon is attributed to the distortion of the baffle leading section due to thermal stresses. Further effort should be directed toward improving the injector distribution to avoid thermal imbalance while maintaining capability with the reactor side walls.

POST TEST THERMAL ANALYSIS

The test hardware was primarily designed to condition hydrogen at the nominal mixture ratio over a range of reactant hydrogen inlet temperature. The hardware was expected, however, to be capable of conditioning either hydrogen or oxygen over a range of mixture ratios well above the nominal design value, based on the theoretical pre-test analysis. The primary goal of the test program was to verify the theoretical results and to be able to account for all the heat within 5%. The test program was expected to verify the amount of heat transferred, indicating whether the conditioner was sufficiently long to extract the required heat; to verify reactant and conditioned propellant be achieved within 1/2 second after initiation of flow; that the conditioner could operate on any duty cycle; that the conditioner could satisfactorily operate at off-design conditions; to verify the feasibility of the overall design concept; to verify the planned control method and control requirements; to determine the best start sequences; and to verify the injector pattern design in terms of performance and heat distribution.

Most of the goals were met. The thermal response met or exceeded specifications; the instrumentation was sufficient to determine the heat distribution and account for the total heat distribution within 5%; the conditioner was operated over a wide range of duty cycles; pressure drops were measured and variations from the theoretical were accounted for; except for a partial collapse of one baffle and a small amount of bending at the forward end of the baffles-- where they are unsupported-- the baffles showed no damage and no overheating. Because of damage to one of the baffles (which was determined to be minor after the hardware was disassembled and inspected) and because of faulty hot gas wall thermocouples on the instrumented baffle which read much higher than expected temperatures (later analysis showed them to be reading the hot gas temperature) many of the off-design conditions were not run. This was the reason that higher mixture ratios were not attempted. It was also the reason no oxygen conditioner tests were attempted, since the oxygen tests would run with higher wall temperatures and it was undesirable to risk the chance of oxygen leaking to the hot gas through the damaged baffle, which could cause even more local damage.

Overall Results

This section covers the overall thermal balance and the upstream hot gas chamber pressure results. In addition, the thermal efficiency is related to combustion efficiency.

Of the two fluids in the conditioner, the conditioned hydrogen is the only one which measures an overall outlet temperature; the hot gas has six individual outlet temperatures, and in order to obtain the heat released from the hot gas it is first necessary to determine the hot gas flow distribution and mixture ratio distribution. Consequently all of the heat exchange rates are based on the conditioned hydrogen flowrate, inlet temperature, and outlet temperature at the mixer. This is shown in Figure as a function of hot gas flow rate. Since mixture ratio varied little from test to test, this is not shown as a parameter. The solid points are the early tests with durations of about 0.5 seconds; they tend to show somewhat higher heat exchange rates due to the mixer not having cooled down to steady state operation within the test duration. As would be expected, a good correlation exists between the total heat input and the reactor flowrate. However, the nominal heat input was never achieved because of 1) only one test was run at the nominal hot gas flowrate (100% combustion), and none were run over this value; and 2) reduced combustion efficiency, which will be discussed shortly. The actual duty cycle seemed to have little effect on the heat input.

In order to determine the thermal efficiency of the conditioner, and noting from Figure 97 that the heat input is approximately proportional to the reactor flowrate, a parameter was calculated which represents the heat input to the hydrogen divided by the reactor flowrate (or hot gas enthalpy drop) for a particular test divided by the same quantity determined based on the theoretical predictions of 2800 Btu/sec transferred with a reactor flowrate of 1.08 lb/sec. This is shown as a function of test number in Figure 98; it is noted that many of the early ignition tests between tests 157 and 199 are omitted. As in the previous figure, the early short duration tests had not reached steady state and thus showed high values of heat input compared to the later longer duration tests. The later tests showed heat exchange efficiencies between 80 and 100 percent, again with no apparent effect of duty cycle.

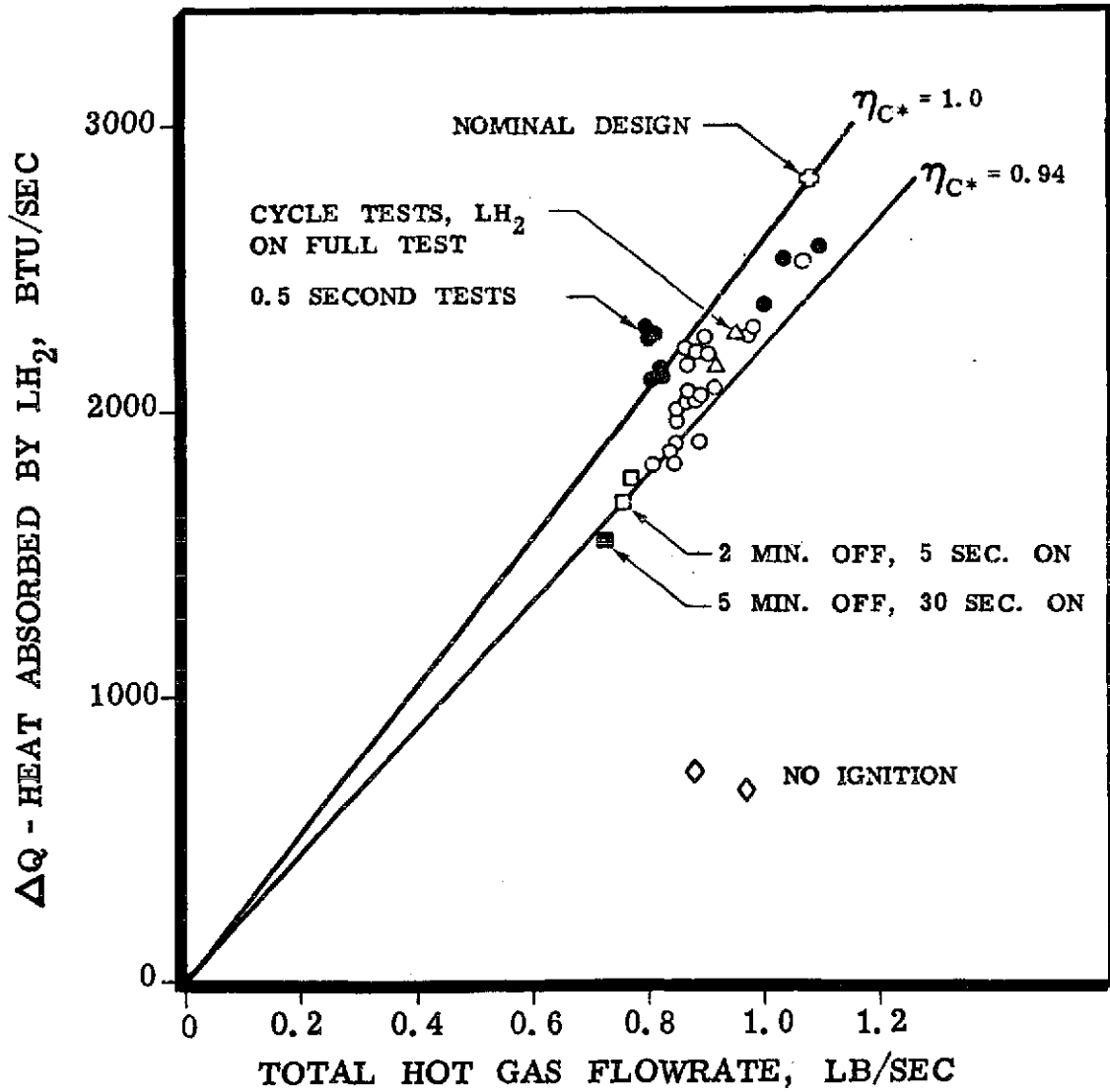


Figure 97. Heat Input to Conditioned Hydrogen Versus Hot Gas Flowrate, Tests 201-236, O₂/H₂, Ambient Propellants

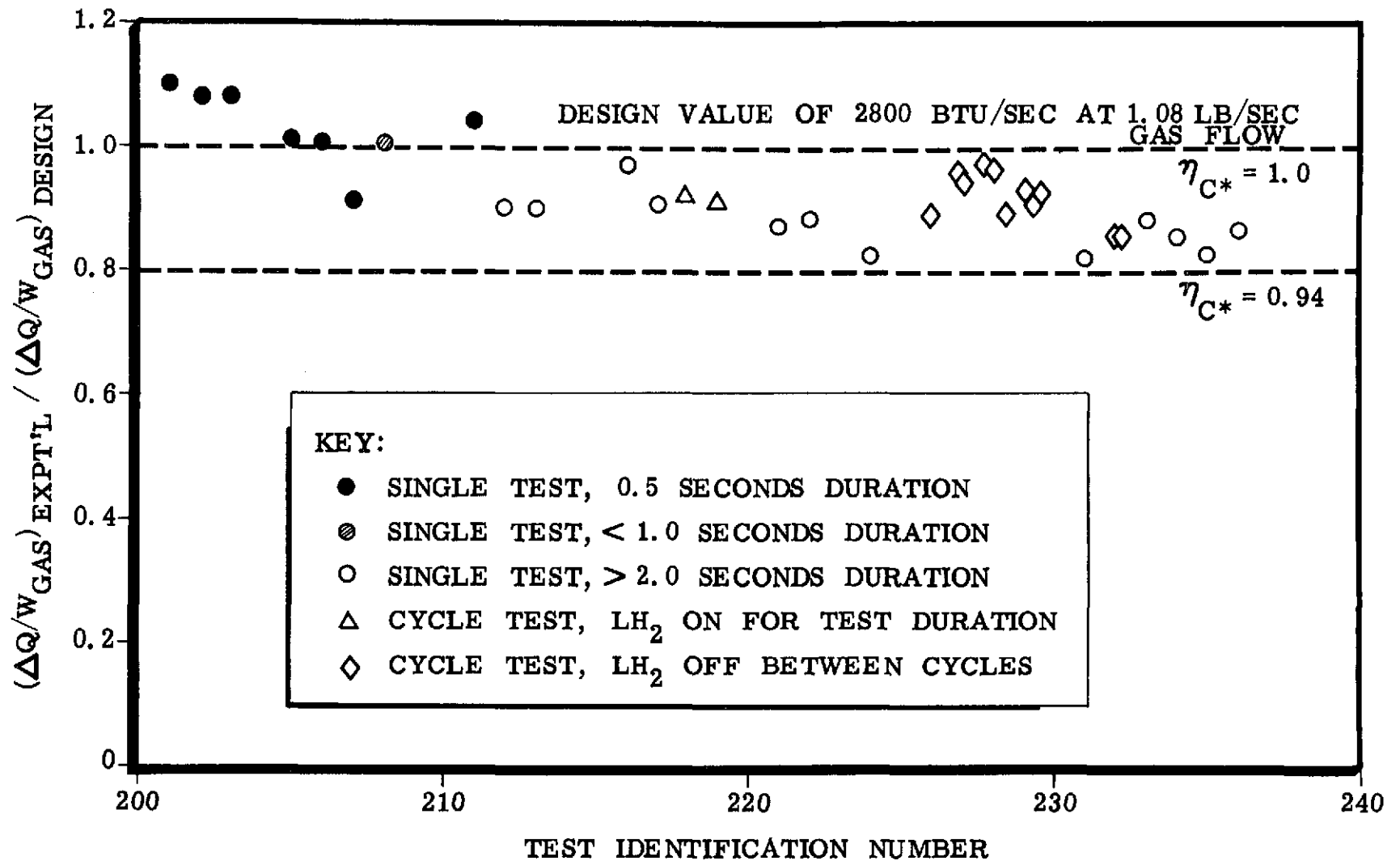


Figure 98. APS Thermal Conditioner Heat Input Parameter Versus Test Number, Q Based on LH₂ Flowrate and Mixer Outlet Temperature Propellants Injected at Ambient Temperature

The experimental combustion efficiency was determined from the experimental combustion temperature, using the relation:

$$\eta_{c*} = (T_{\text{experimental}} / T_{\text{theoretical}})^{0.5}$$

where the theoretical combustion temperature is based on the experimental mixture ratio and reactor hydrogen injection temperature. This may not be the most ideal way to measure combustion efficiency, but it was the most practical. Since the combustion temperature is probably not uniform across the face of the injector, this measurement may be somewhat sensitive to the actual location of the hot gas thermocouple. The resulting combustion efficiency is shown in Figure 99 as a function of core mixture ratio. The core mixture ratio differs from the overall mixture ratio in that the injector has edge film cooling slots, and in addition the igniter is normally running at a different mixture ratio than the injector. The core mixture ratio is thus 19/16 times the overall injector mixture ratio. The core mixture ratio is the desired value since this is where the hot gas thermocouple is located. As shown in Figure 99, the experimental combustion efficiency is between 90 and 100 percent, with most of the data between 93 and 97 percent. The solid points are the early short duration tests of approximately 0.5 second duration; as would be expected, these show similar values to the longer duration tests.

In order to relate the combustion efficiency to reduced thermal efficiency, the combustion efficiency was selected, and the combustion temperature determined using the correlation above. This reduced combustion temperature was then used to determine the available energy for a particular mixture ratio and outlet temperature. The result is shown in Figure 100 as a ratio of available energy to that available with 100 percent combustion efficiency. The analysis was performed for three conditions: (1) an outlet temperature of 750R at a mixture ratio of 1.10; (2) 750R at a mixture ratio of 0.85, and (3) 1000R at a mixture ratio of 1.0. In this case, the mixture ratio represents the overall hot gas mixture ratio. The first two cases represent nominal conditions with cold and warm reactor hydrogen respectively; the last case is to show the sensitivity of the hot gas outlet temperature. Within the range of interest there is little difference between the three cases. Superimposed

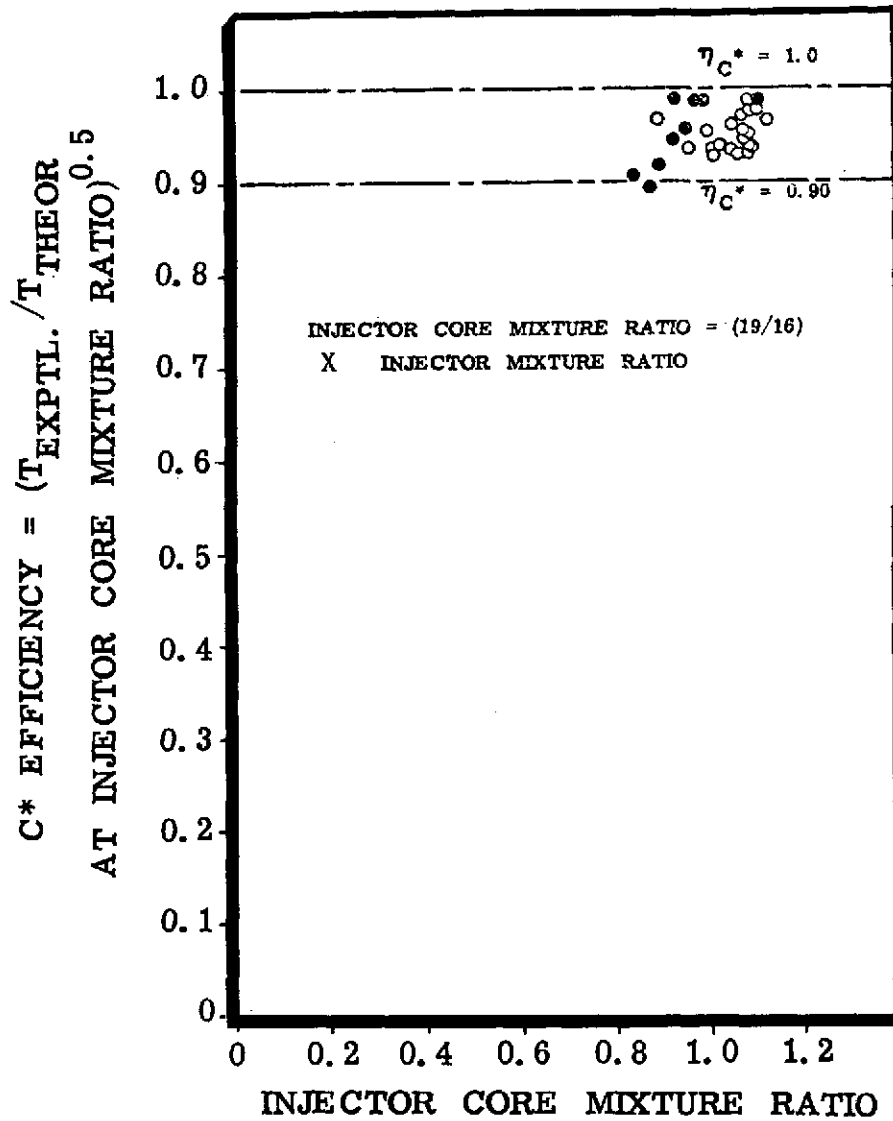


Figure 99. Experimental Combustion Efficiency Versus Mixture Ratio O_2/H_2 , Injector Number 2

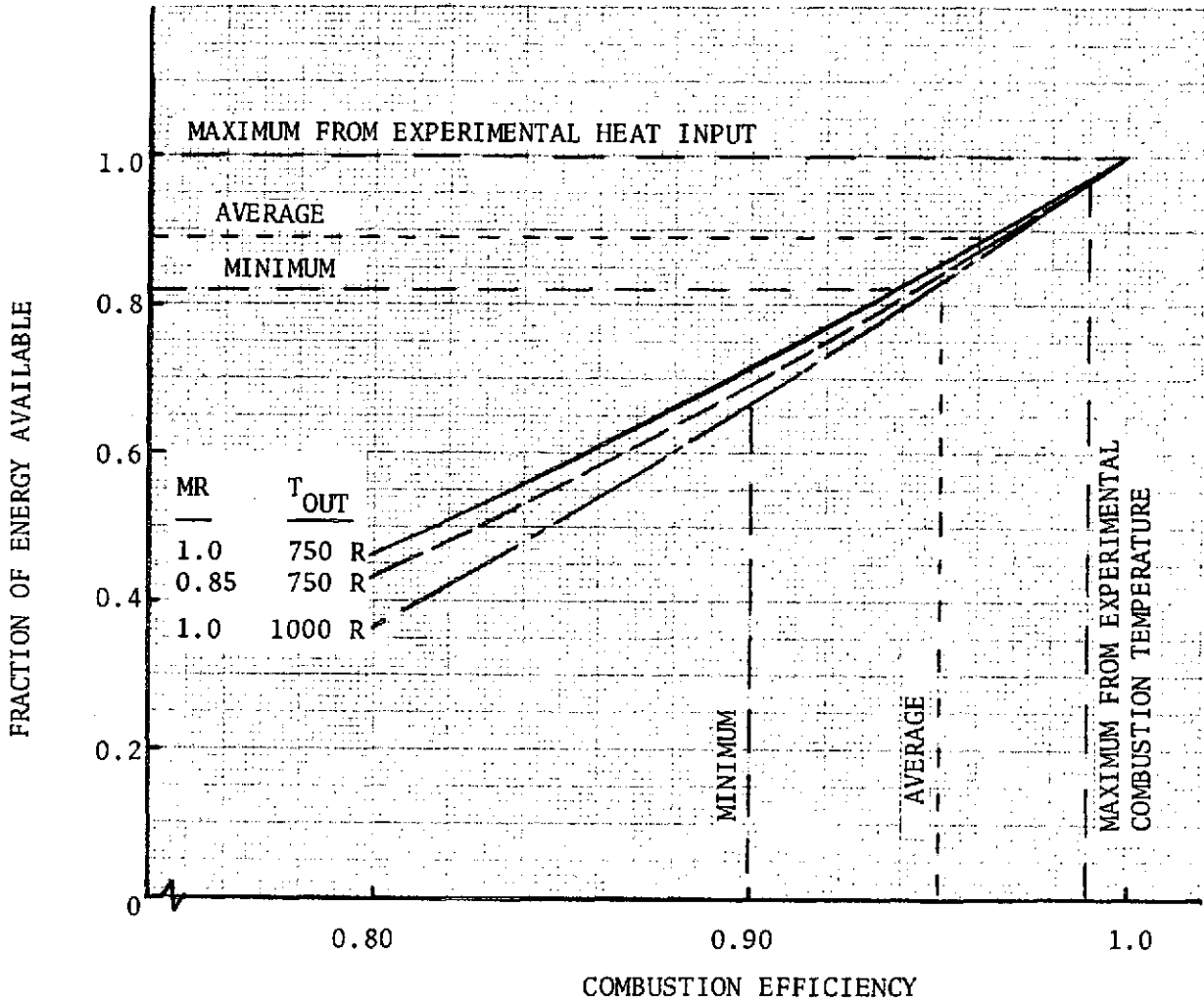


Figure 100. Fraction of Available Energy Versus Combustion Efficiency O_2/H_2 , 600 R Injection Temperature

on Figure 100 is the experimental fraction of available energy efficiency from Figure 99 . It is seen that this fraction as measured by the heat input to the hydrogen for a given reactor flowrate and the average combustion efficiency as measured by the combustion temperature compare very well. They indicate a combustion efficiency of 95-96 percent with a corresponding reduction in available energy to 85-89 percent of theoretical. It would thus appear that the method for determining combustion efficiency is reasonable, and furthermore that the reduced heat input can be accounted for completely by the reduced combustion efficiency.

The range of conditioner operation compared to the required range of operation is shown in Figure 101 . In this figure, the conditioned hydrogen outlet temperature is shown as a function of heat input for five different cases: 1) 3 lb/sec flow, 70R inlet temperature; 2) 4.5 lb/sec., 70R; 3) 4.5 lb/sec, 55R (nominal case); 4) 4.5 lb/sec, 40R; and 5) 5.95 lb/sec, 40R inlet temperature (maximum heat input). Superimposed on this figure is the range of experimental heat inputs. The experimental heat input is capable of conditioning from 3 to over 4.5 lb/sec to the required outlet temperature. The upper heat input range, as indicated earlier, would have required higher reactor flowrates and/or mixture ratios, and these were not run as a result of faulty hot wall thermocouple measurements. However, over half of the required heat input band was covered experimentally.

Chamber Pressure

The measured hot gas chamber pressure is a function of the flow area, flowrate, mixture ratio, and exit temperature. Since everything is experimentally measured except for the flow area, this parameter can be determined experimentally. Assuming that the minimum flow area occurs at the conditioner exit - either due to thermal distortion or icing - it is necessary to calculate the total pressure at the conditioner exit. It is noted that the experimental exit pressures are static pressures, and that their readings are sensitive to local and upstream obstructions so that they are not necessarily a good indication of the local total pressure. The method of determining the ratio of upstream to downstream total pressure is covered in Appendix D. For a given geometry, it is seen that the pressure ratio is basically a function of the total temperature ratio. The numerical constant involved is based on the theoretical pressure profile determined for the nominal operating condition.

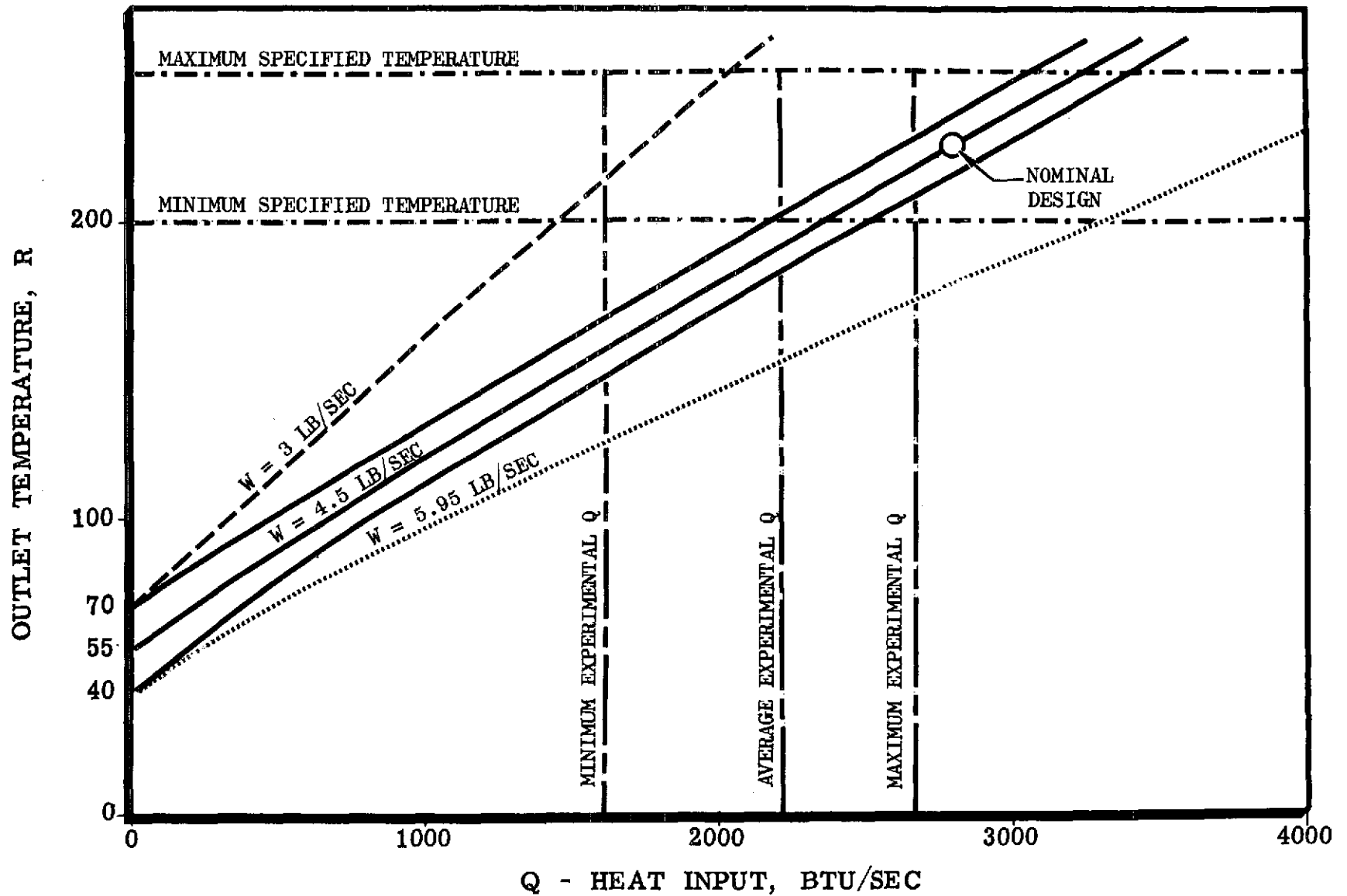


Figure 101. Liquid Hydrogen Outlet Temperature Versus Heat Input, LH₂ Flowrate and Inlet Temperature, P_{OUT} = 1500 psia

The resulting pressure ratio is shown in Figure 102 as a function of the hot gas exit temperature and mixture ratio; the latter determines the upstream total temperature. In this manner the effective hot gas flow area can be determined. The nominal flow area is based on the measured hot gas gaps at the exit plane.

The ratio of the effective flow area to the nominal flow area is shown in Figure 103 as a function of the ratio of the reactor flow to the conditioned hydrogen flow. It is noted that this ratio of flowrates is the primary factor which controls the local wall temperature, and thus it is this factor which should determine if icing is going to occur. Consequently if the area reduction is due to ice formation, one would expect a good correlation between flow area reduction and the ratio of flowrates. However, in studying Figure 103 it appears that the principal variable influencing the reduction in flow area is the test number. It is seen that tests 201-217 have essentially the nominal flow area; it is also seen that tests 221-229 have about a uniform flow area about 65% of the nominal area. The only points which may have an area reduction due to icing are the bottom left hand three points, which have the lowest reactor flowrates.

The same effect is shown as a function of test number in Figure 104. It is again seen that the first tests through test 216 have a calculated area equal to the measured flow area; this is not just due to short duration runs, since all tests after test 210 have durations in excess of 2 seconds. The first reduction in hot gas flow area occurs at test 218, where two cycles were run with the conditioned propellant on throughout the test. The major reduction in flow area occurred at test 219, which consisted of 10 cycles, again with the liquid hydrogen flow on both with and without the reactor flow, for the full test duration. This was the last test series in which the liquid hydrogen was flowed without any reactor flow. As a result very minor changes in effective hot gas area occurred from tests 220 to 232, in spite of several different duty cycles being run. Tests 233-235 had lower hot gas flow areas, and this could have been due to icing since the hot gas flowrates were lower. This apparently was not a "permanent" change since the flow area came back from 60% to about 70% of nominal value. It is noted that when the area reduction occurred at test 219, that test 220 started a new test day; yet the flow area remained unchanged between tests 219 and 220.

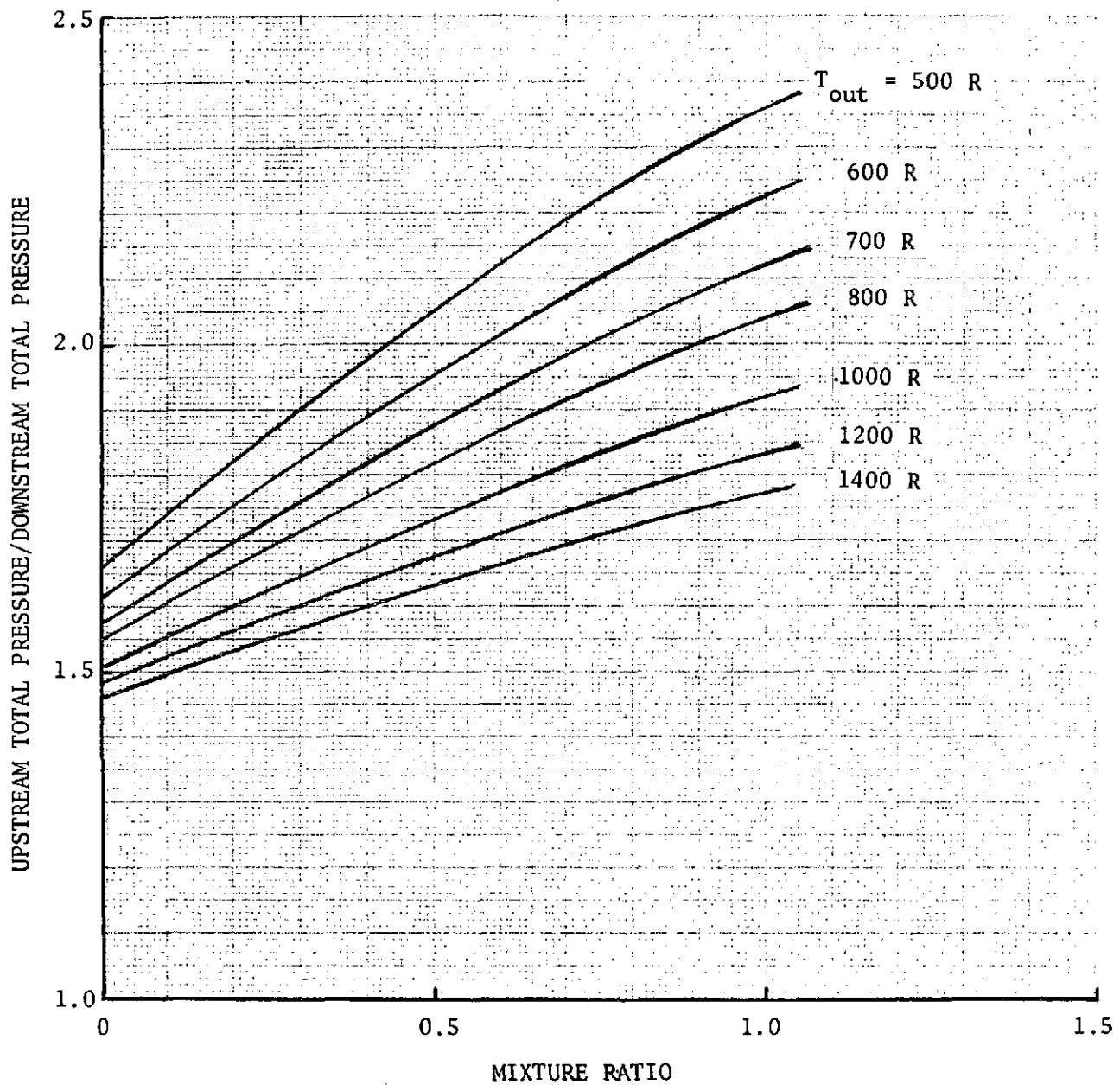


Figure 102. Predicted Total Hot Gas Pressure Ratio Versus Hot Gas Exhaust Temperature and Mixture Ratio with a Sonic Exit O_2/H_2 Propellants

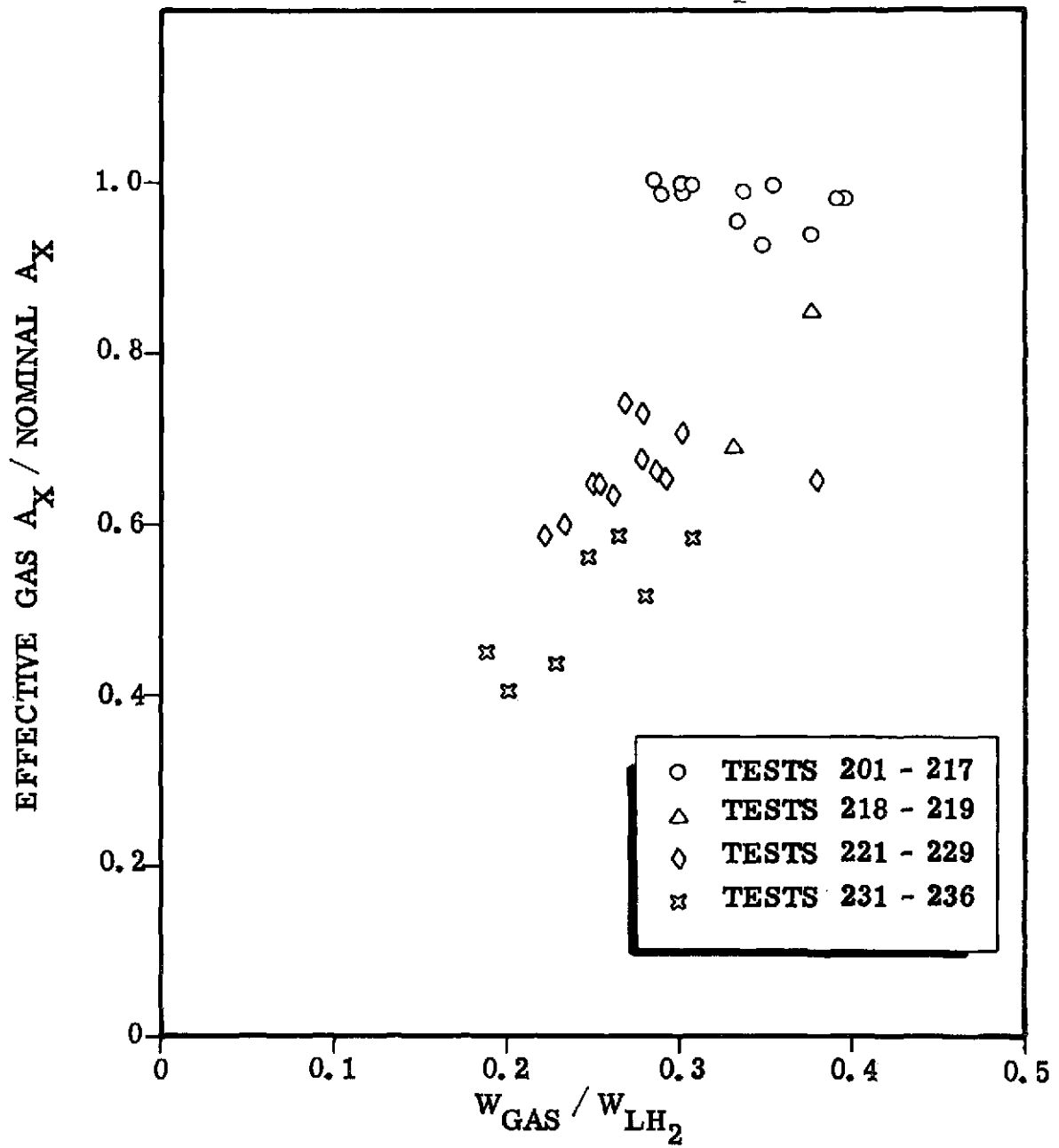


Figure 103. Relative Hot Gas Flow Area Versus Ratio Hot Gas Flow to LH₂ Flow

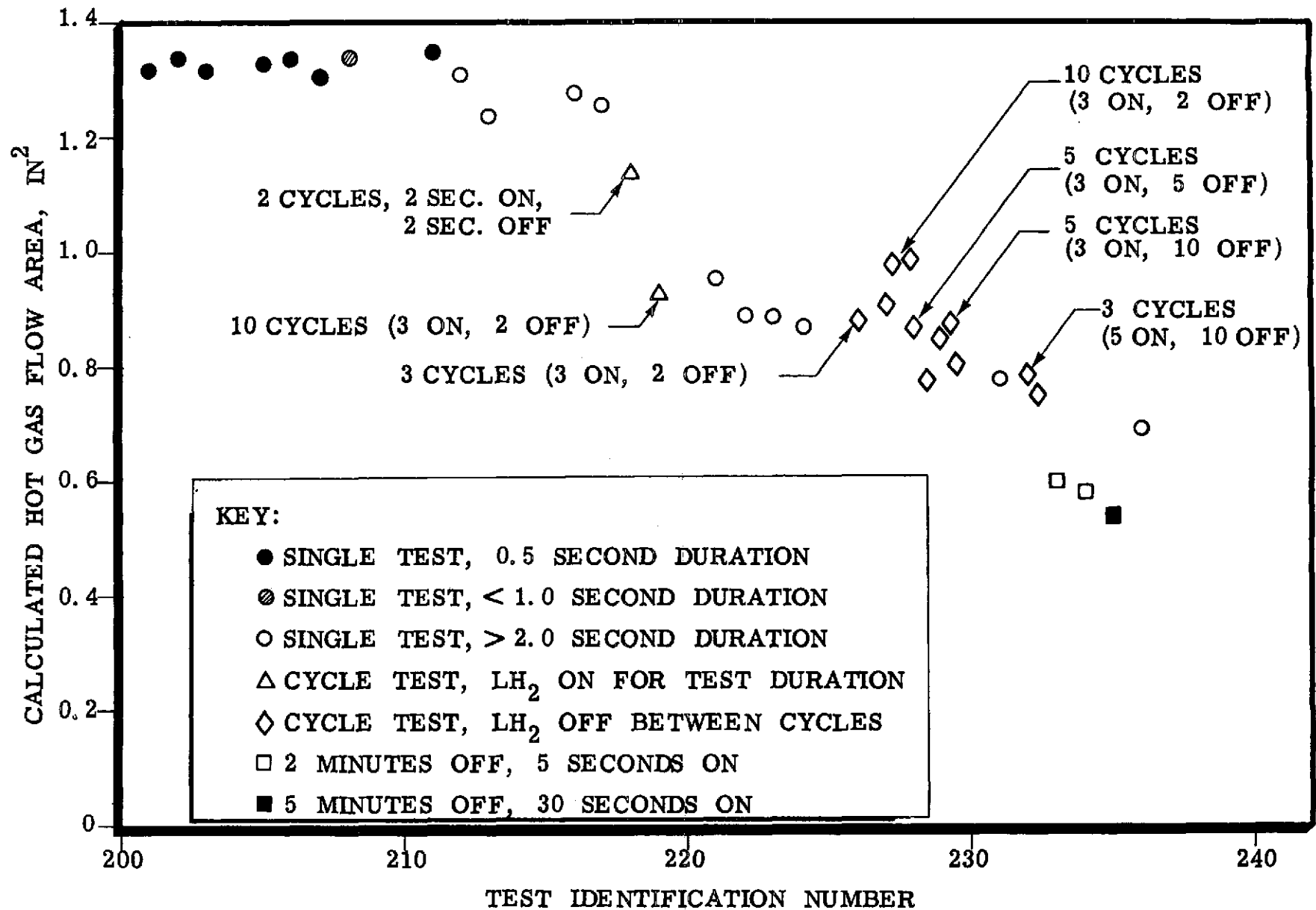


Figure 104. APS Thermal Conditioner Effective Hot Gas Flow Area Versus Test Number

Consequently, it is concluded that while the conditioner withstood a wide range of operational duty cycles, the reduction in area is due to the very severe cycling tests where the liquid hydrogen was left on throughout the test duration, resulting in very rapid changes to the wall temperatures. Had these tests not been run, it is believed that the chamber pressure would have been close to nominal. Incidentally, the method in which the calculated hot gas flow area depends on the experimental chamber pressure and theoretical hot gas pressure profile is a good indication that the predicted pressure drop was experimentally verified, since the calculated flow areas match the measured areas for the early tests.

The overall operational conclusions are that: 1) the injector has a 95-96 percent combustion efficiency, which is sufficient to completely account for the 85-89 percent thermal efficiency; 2) the heat exchange efficiency is not a function of duty cycle and is not affected by apparent baffle distortion; and 3) that the apparent baffle distortion occurred only during the most severe cycling tests where the liquid hydrogen was run for the full test duration. It is also concluded that the observed reduction in area is not due to icing primarily, except for maybe three tests at the end, so that ice formation is not a problem at normal operating conditions.

Thermal Response

The contract requirement was that conditioned propellants must be supplied within 0.5 seconds after the initiation of flow. Following are a number of figures showing thermal response under a range of conditions including with no ignition, and response from both ambient temperature and liquid hydrogen temperatures. Cycling tests are also shown to indicate the repeatability of the data.

The thermal transient for one of the early tests is shown in Figure 105. Test 164 was run at a mixture ratio of 0.8 with no ignition. Consequently, it is useful for studying how rapidly the hardware chills. The liquid hydrogen was introduced approximately 0.4 seconds after the hot gas flow, and the mixer outlet temperature reached a nominal 230R with 5 lb/sec conditioned propellant approximately 0.4 seconds later. This indicates that the hardware will meet the required thermal response. It is also seen that the baffle outlet temperature responded faster than the mixer, because of

MR = 0.8
NO IGNITION

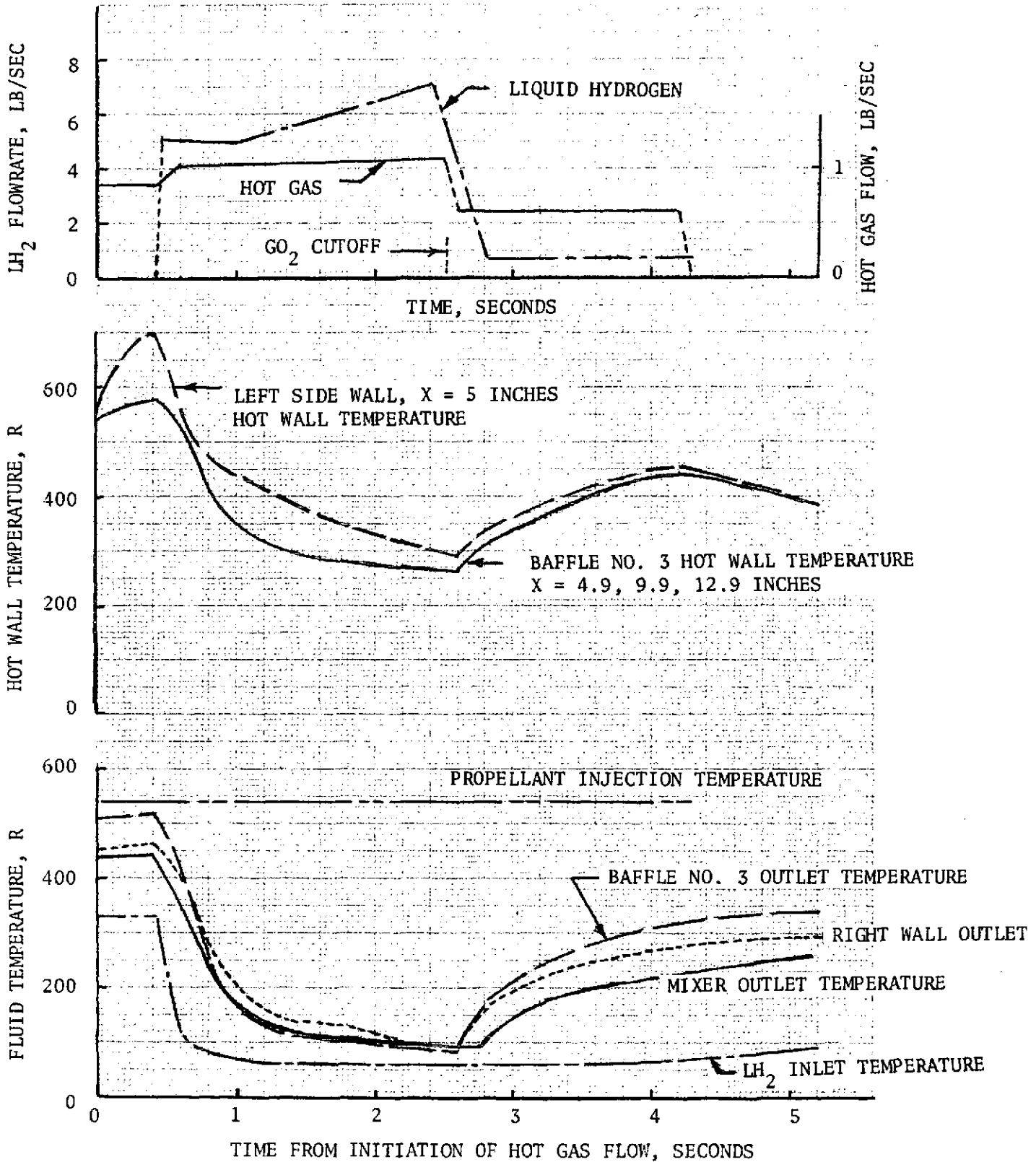


Figure 105. Test 164 Thermal Response

additional thermal mass in the latter. In addition, the baffle responded somewhat faster than the sidewalls due to the large mass of the backup structure in the sidewalls.

A comparison of the theoretical and experimental thermal transients are shown in Figure 106 for test 213. It is seen that steady state conditions were reached in about 0.5 seconds. It is also seen that the hydrogen outlet temperature transient can be predicted very well. A comparison of the baffle hot wall temperature 5 inches from the leading edge indicates that the experimental temperature was about 400R higher than the theoretical value. The probable reason for this is the thermocouple was reading essentially the hot-gas temperature rather than the wall temperature, as shown in the temperature profiles presented in Fig. 114 through 118. Here it can be seen that many of the experimental hot wall thermocouple measurements compare very well with the predicted and experimental hot-gas temperatures. This can occur if the thermocouple is projecting into the hot-gas stream rather than mounted flush with the baffle surface.

The thermal response for test 221 is shown in Figure 107. Again, the conditioned hydrogen outlet temperature easily reached the required operating temperature in 0.5 seconds, even though it took longer to attain steady state conditions. The injector face took 3-4 seconds to reach steady state due to its copper wall construction; its slower response did not influence the response of the conditioned propellant. The two baffle hot wall temperatures appear to read approximately hot gas temperatures; one had a very fast response, indicating it was probably projecting into the gas stream from the beginning of the test. The other thermocouple had a very slow response, indicating it was probably not fastened securely to the wall but was reading hot gas temperature by the end of the test.

The thermal response for test 222 is shown in Figure 108. The baffle hot wall and injector face temperatures show the same trend as in the previous test. In addition, the heat input to the conditioned hydrogen took about 1½ seconds to stabilize, mostly due to mixer response; again, it was not necessary to reach steady state in 0.5 seconds, it was only required to

$W_{LH_2} = 2.767 \text{ LB/SEC}$
 $W_{GAS} = 0.973 \text{ LB/SEC}$
 $MR = 0.910$

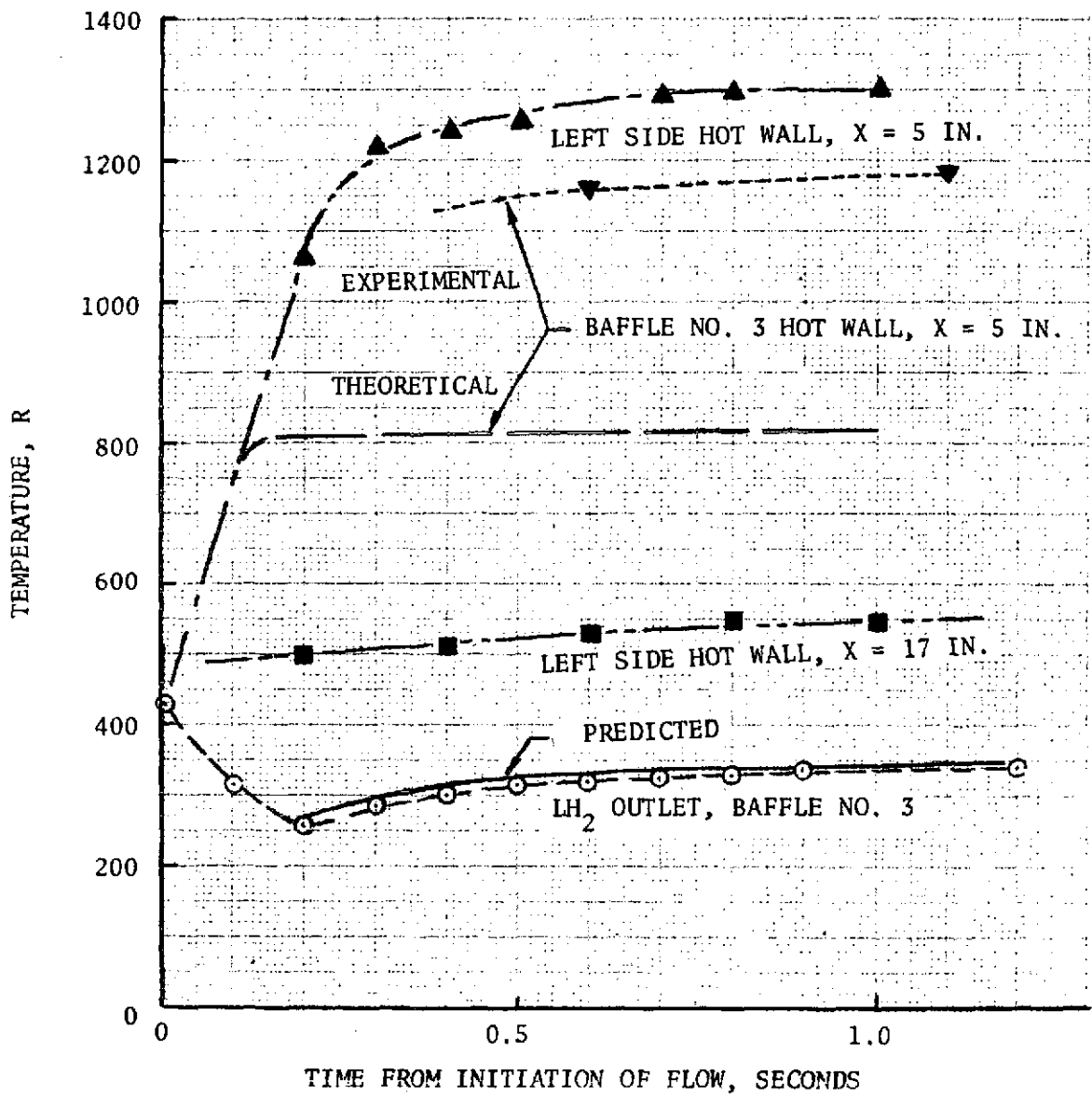


Figure 106. Test 213 Thermal Transients

MR = .910, $\dot{w}_{GAS} = 0.917$ LB/SEC

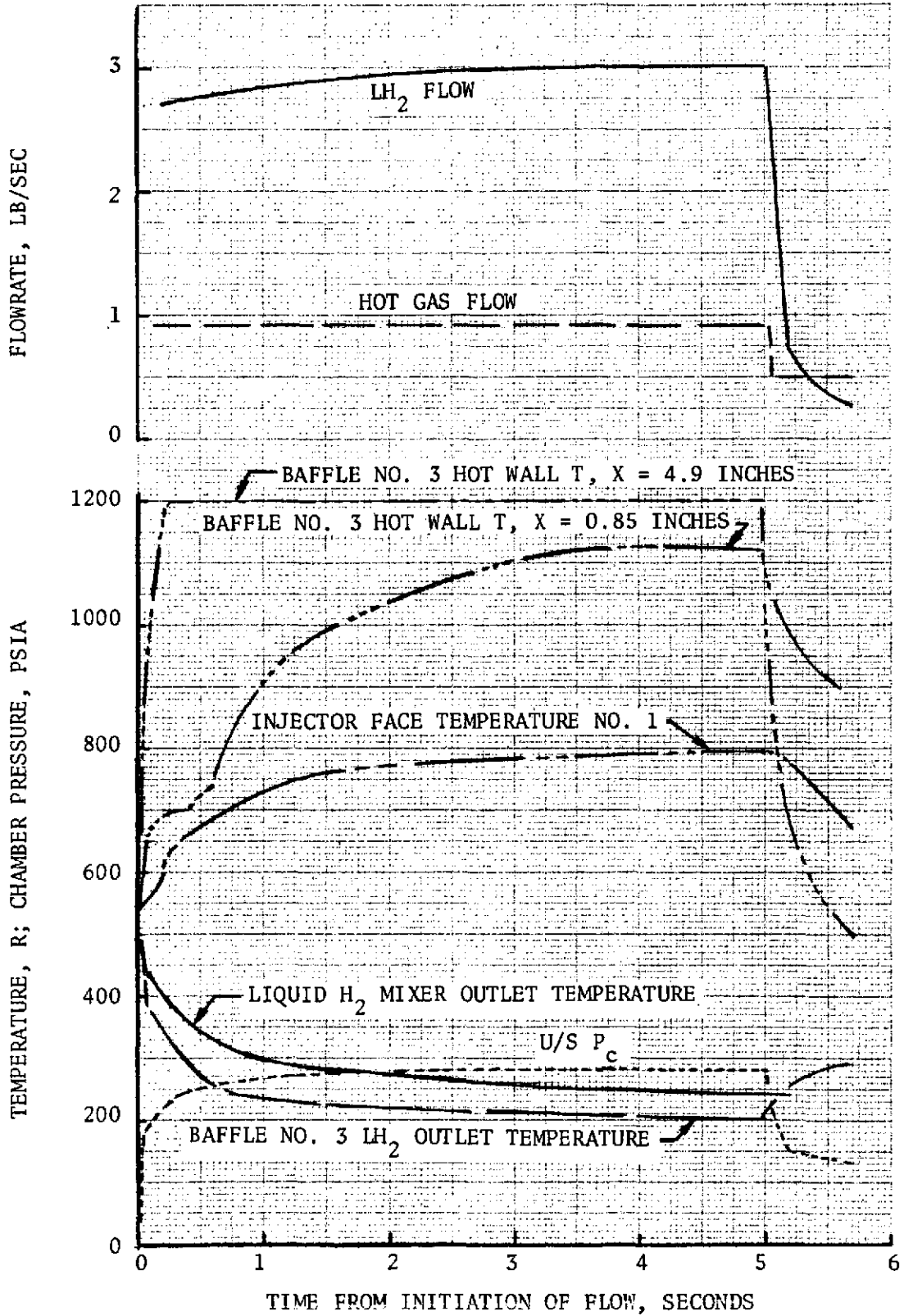


Figure 107. Test 221 Thermal Response

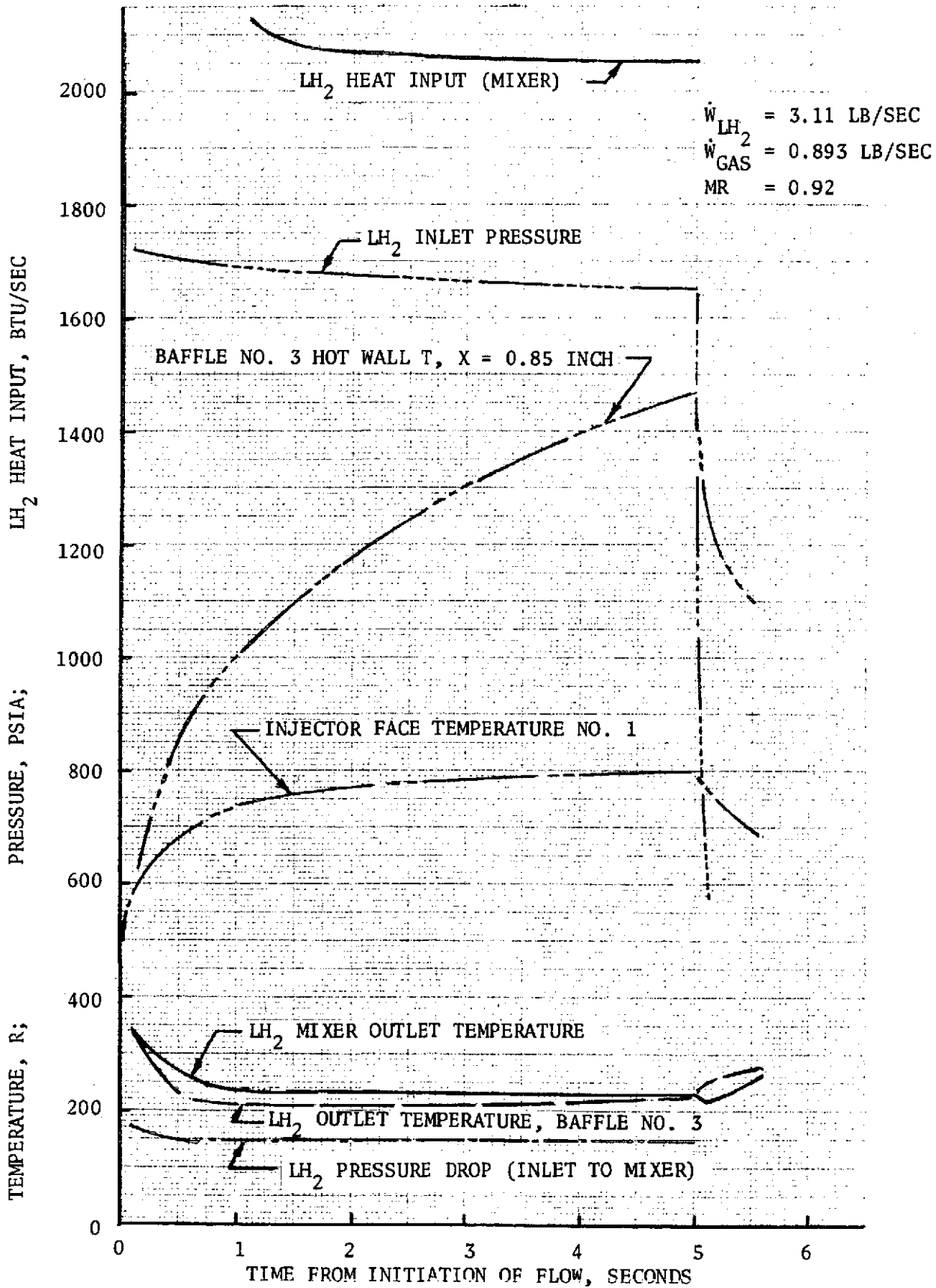


Figure 108. Test 222 Thermal Response

enter the required operating range at this time. It is also seen that the liquid hydrogen inlet pressure decayed slowly throughout the test (due to the tank pressurization system) but that the pressure drop through the conditioner was constant.

The thermal transient for the long-duration test, test 235, is shown in Fig. 109 in order to show that various parameters are stable during the test. Between 1 and 2 seconds into the test, the liquid hydrogen flow increased; this caused a drop in the mixer outlet temperature and may have caused an increase in chamber pressure due to icing. Icing would be expected since less than 75% of the nominal hot gas flow was present with nearly 50% excess liquid hydrogen flow within the conditioner. After this time most of the parameters are essentially constant for the remainder of the test, with the exception of the liquid hydrogen flow which started to decrease half way through the run, due to the tank pressurization system.

Thermal transients for two of the cycling tests are shown in Figures 110 and 111. The first figure shows the first half of the ten cycles in test 219; it will be remembered that this test had liquid hydrogen flowing for the full test duration. It is seen that: (1) the initial cycle starts from ambient conditions; (2) no ignition occurred in the fourth cycle; (3) the thermal response satisfied the requirements for each cycle, including the one following the no ignition cycle; (4) the baffle outlet temperature consistently responded faster than did the mixer outlet temperature, as previously observed in test 164; (5) the liquid hydrogen flowrate was consistent from cycle to cycle, being controlled by the hot gas heat input (hot gas flowrate and mixture ratio). The remaining four cycles (not shown) are essentially the same as the first six, except that ignition did not occur on cycles 9 and 10.

The second cycling test for which thermal transients are shown is test 229, Figure 111. This test consisted of 5 cycles, with 3 seconds on and 10 seconds off. The reactor and conditioned propellants came on

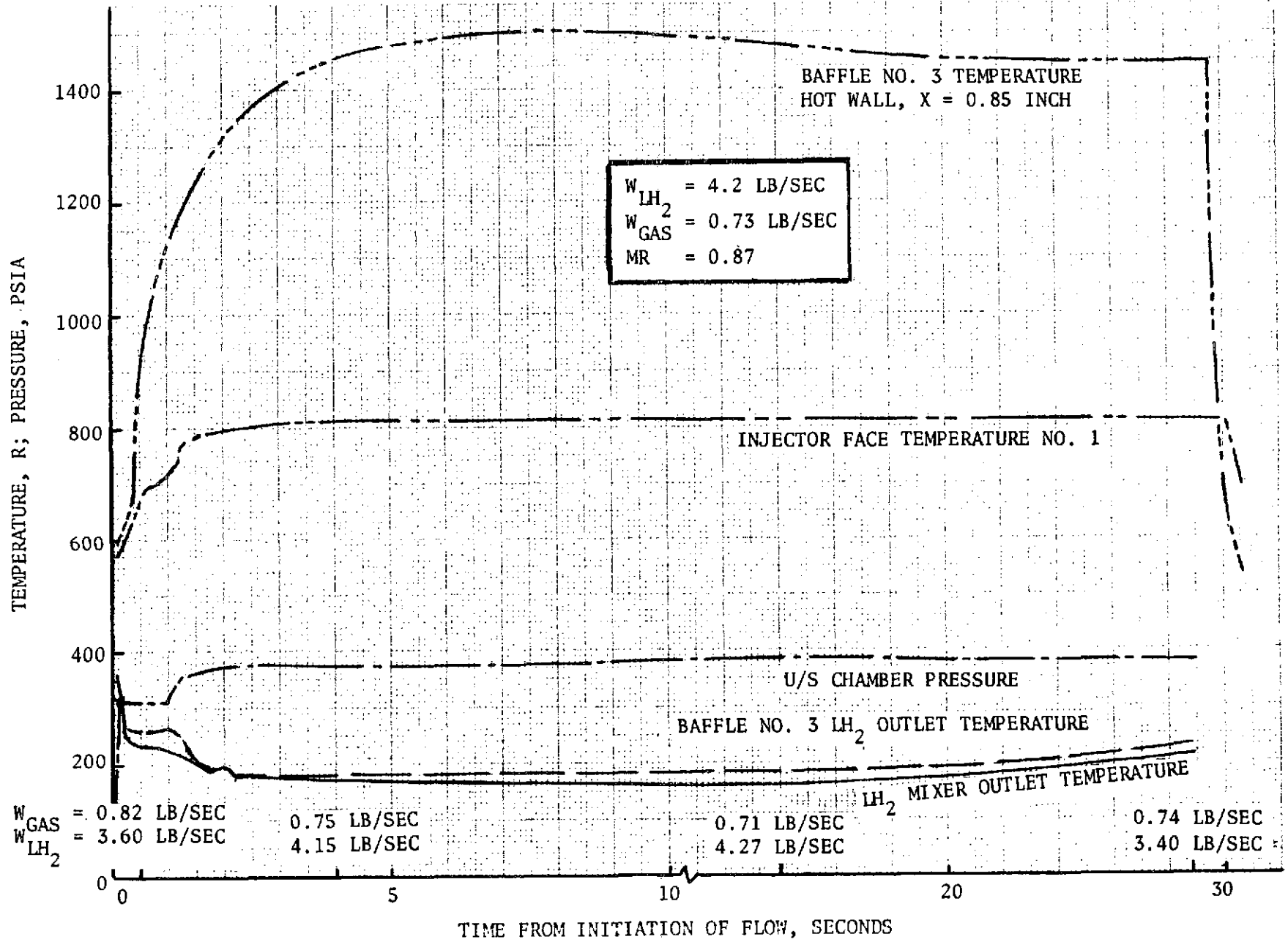


Figure 109. Test 235 Transient Response

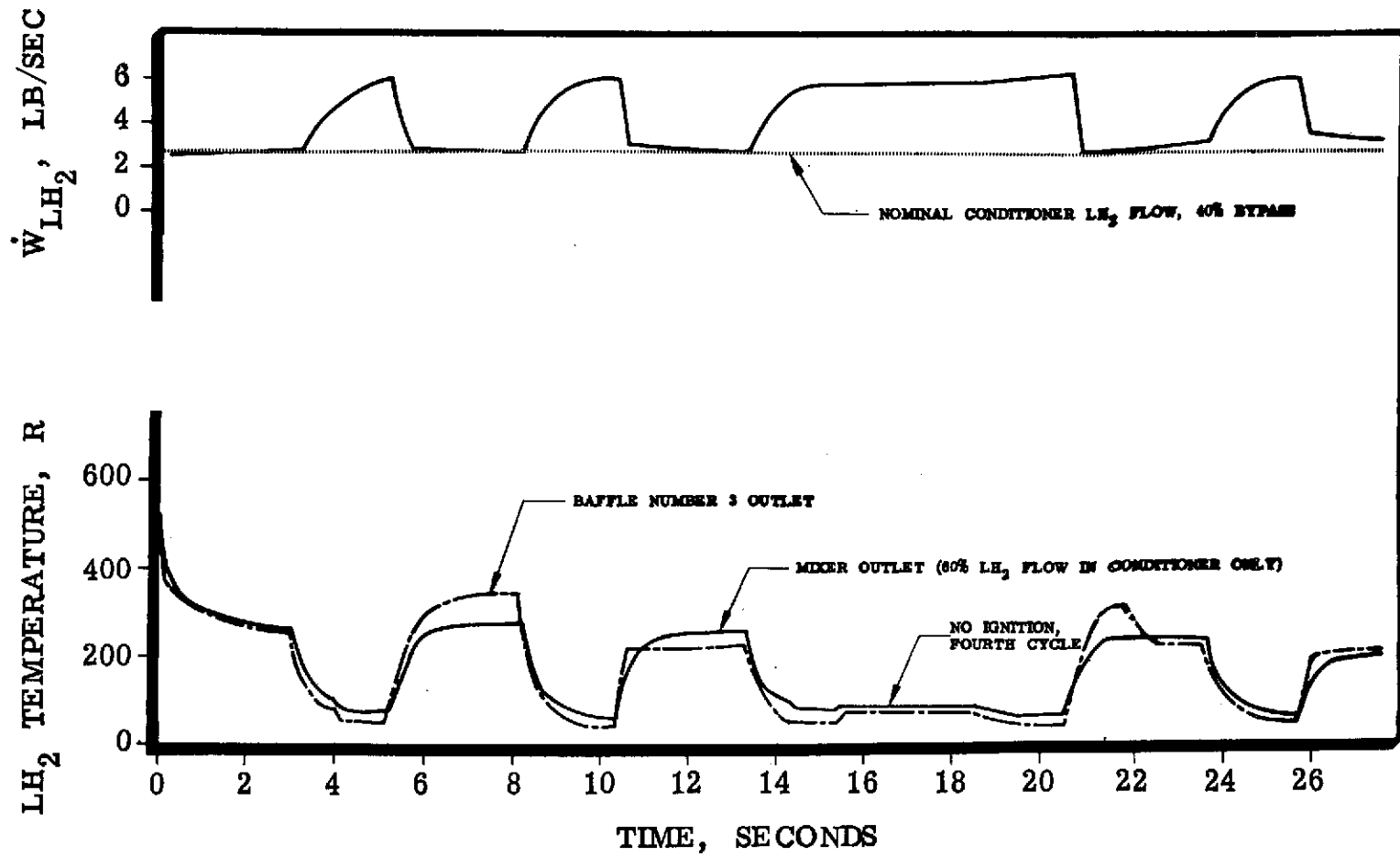


Figure 110. Test 219 LH₂ Exit Temperature and Flowrate Response [MR = 0.91 O₂/H₂ (Ambient Temperature), First 6 of 10 Cycles (3 Seconds On, 2 Seconds Off); Remainder of Cycles Identical]

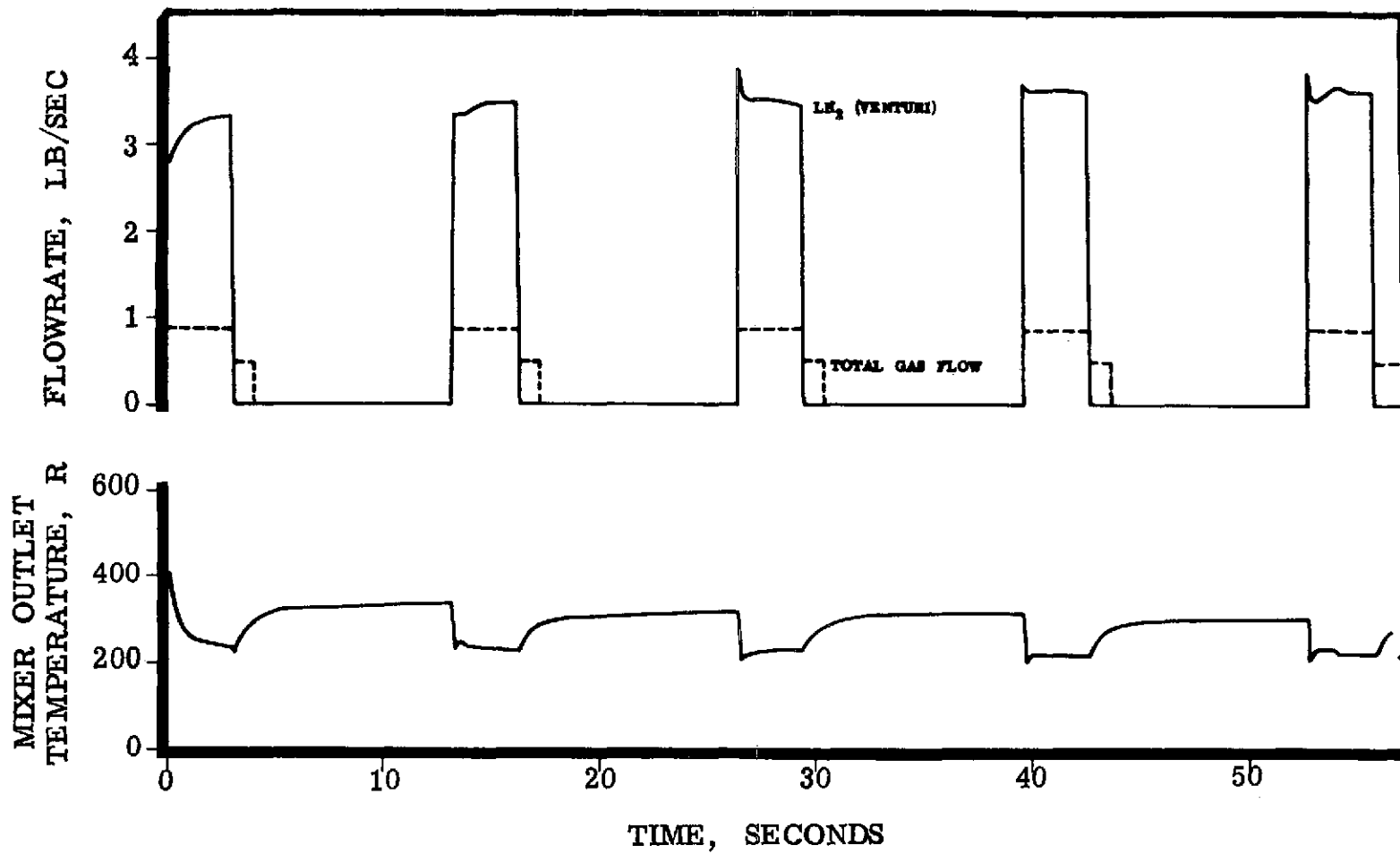


Figure 111. Test 229 LH₂ Outlet Temperature and Flowrate Response [MR = 0.95 O₂/H₂ (Ambient Temperature), 5 Cycles (3 Seconds On, 10 Seconds Off)]

together; the reactor oxygen and conditioned hydrogen were turned off 3 seconds later, and the reactor hydrogen was shut off 1 second after the other two. All cycles ignited properly. As in test 219, the hot gas flow was the same for each cycle, resulting in the same heat input for each cycle, the same conditioned hydrogen flowrate for each cycle, and the same conditioned propellant outlet temperature for each cycle; in other words, the conditioned propellant flow conditions were repeatable from cycle to cycle, being controlled by the heat input to the conditioner.

A cursory look at the effect of wall thickness increase in thermal response increase using one-dimensional tables gave the following results. Two extreme cases were considered. The first considered nominal liquid hydrogen flow at a temperature of 60 R, with no hot gas flow and initially ambient hardware. The time it took to heat the wall temperature adjacent to the conditioned propellant to about 300 R was essentially independent of wall thickness. The second case considered the nominal hot gas flow with no conditioned hydrogen, with an initial wall temperature of 60 R. The time it took to heat the wall surface adjacent to the conditioned propellant was proportional to the wall thickness. Consequently it is concluded that with both reactor and conditioned propellants flowing, the wall response will be less than proportionally sensitive to wall thickness, and that small variations in wall thickness should have no appreciable effect on conditioner response.

In summary, it can be concluded that: (1) the conditioned propellant temperature came into its operating range within 0.5 seconds, as required; (2) there was a rapid buildup in flowrate and pressure; (3) the experimental response compared favorably with the predicted response; (4) the side plate response was slower than the baffle response due to the heavy backup structure; (5) the mixer response was slower than the baffle response due to heavy instrumented

exit manifolds and partial optimization of the mixer for response; (6) the response would be faster with the nominal hot gas flowrate; (7) the injector face required about 3 seconds to reach steady state; (8) the conditioner flows were stable; and (9) the liquid hydrogen flow was repeatably controlled by the hot gas flowrate and mixture ratio for a given liquid hydrogen inlet pressure and temperature.

Detailed Baffle Heat Transfer Analysis

The previous section covered the overall transient and steady state operation of the thermal conditioner. The first part of this section will discuss the hot gas mixture ratio and flowrate distribution within the conditioner, as well as the distribution of the conditioned propellant flow and the heat input distribution. The second part will use this flow distribution to analyze the baffle temperature distribution and to determine if the experimental results can be predicted.

The basic variables to be determined are the hot gas flow distribution, mixture ratio distribution, and combustion efficiency distribution for each of the hot gas passages. In addition the conditioned propellant distribution for each baffle and side plate must be determined. To determine the validity of the analysis, a number of checks are employed. The first four conditions are that the appropriate individual components must add up to (1) the total conditioned propellant flow; (2) the total heat input; (3) the total reactor hydrogen flow; and (4) the total reactor oxygen flow. In addition, (5) the overall hot gas flow area should match the individual areas; (6) the calculated individual hot gas flow areas should correspond to the measured individual hot gas gaps; and (7) there should be a reasonable match between the heat input to a given baffle and the heat rejected from the adjacent hot gas passages. If all of these conditions can be satisfied, it is felt that the various distributions have been determined with sufficient accuracy.

A major part of the conditioner instrumentation was utilized to determine the various flow distributions, as seen in Table 23 . Because of the complexity of the analysis, consideration was given to writing a computer program to determine the required parameters. However, due to the shortness of time

TABLE 23. INSTRUMENTATION USED TO DETERMINE FLOW DISTRIBUTION

● LH ₂ FLOWRATE (overall)	{ Venturi U/S Temperature Venturi U/S Pressure Venturi ΔP
● LH ₂ FLOWRATE (individual)	{ 7 LH ₂ Baffle Outlet Temperatures 1 LH ₂ Inlet Temperature 1 Inlet Pressure 1 Outlet Pressure
● LH ₂ HEAT INPUT (overall)	{ Overall LH ₂ Flow Mixer Outlet Temperature Mixer Outlet Pressure Inlet Temperature Inlet Pressure
● LH ₂ HEAT INPUT (individual)	7 Individual Flowrates: { LH ₂ Baffle Outlet Temp. 1 LH ₂ Inlet Temp.
● HOT GAS: ● Total GH ₂ Flow:	{ U/S Venturi Temperature U/S Venturi Pressure Venturi ΔP
● Total GO ₂ Flow:	{ U/S Venturi Temperature U/S Venturi Pressure Venturi ΔP
● Total Mixture Ratio	
● Core Mixture Ratio	{ Igniter Fuel Core Inlet Pressure Igniter Contour Inlet Pressure Igniter Fuel Injection Temperature Film Cool Slots on Injector Face
● Chamber Pressure	
● 6 Gas Outlet Temperatures	
● 6 Gas Outlet Static Pressures	

available, and because it was not yet known which instrumentation was good and which could not be relied on, it was decided to do the analysis by hand.

Conditioned Hydrogen Flow Distribution

The easiest flow distribution to determine is the conditioned hydrogen flow. The various baffle and side plate resistances were determined by individual water flow calibration; this is shown in Figure 112. The top and bottom plates, which account for about 5% of the flow are not included in the figure.

The individual conditioned hydrogen flowrates could then be determined from the baffle resistance, the baffle pressure drop, and the average density based on the average temperature and pressure within the baffle or side plate.

$$W_{H_2} = \frac{\sqrt{\rho_{AV} \Delta P}}{K}$$

Where W_{H_2} = Venturi LH₂ Flowrate, lb/sec

ρ_{AV} = Average Density³ Based on Average Temperature and Pressure, lb/ft

ΔP = LH₂ Pressure Drop, psi

K = Determined From Water Calibration Tests, in Consistent Units

Upstream Pressure = LH₂ Venturi Upstream Pressure (except prior to test 220 had bad Transducer, so LH₂ F/M Pressure Used)

Downstream Pressure = Mixer Inlet Pressure

Upstream Temperature = LH₂ F/M Temperature

Downstream Temperature = Baffle Exit Temperature

The individual values of K used were:

<u>Location</u>	<u>Left Wall</u>	<u>Baffle 1</u>	<u>2</u>	<u>3</u>	<u>4</u>	<u>5</u>	<u>Right Wall</u>
K	72.0	34.1	34.1	34.7	35.2	34.1	72.0

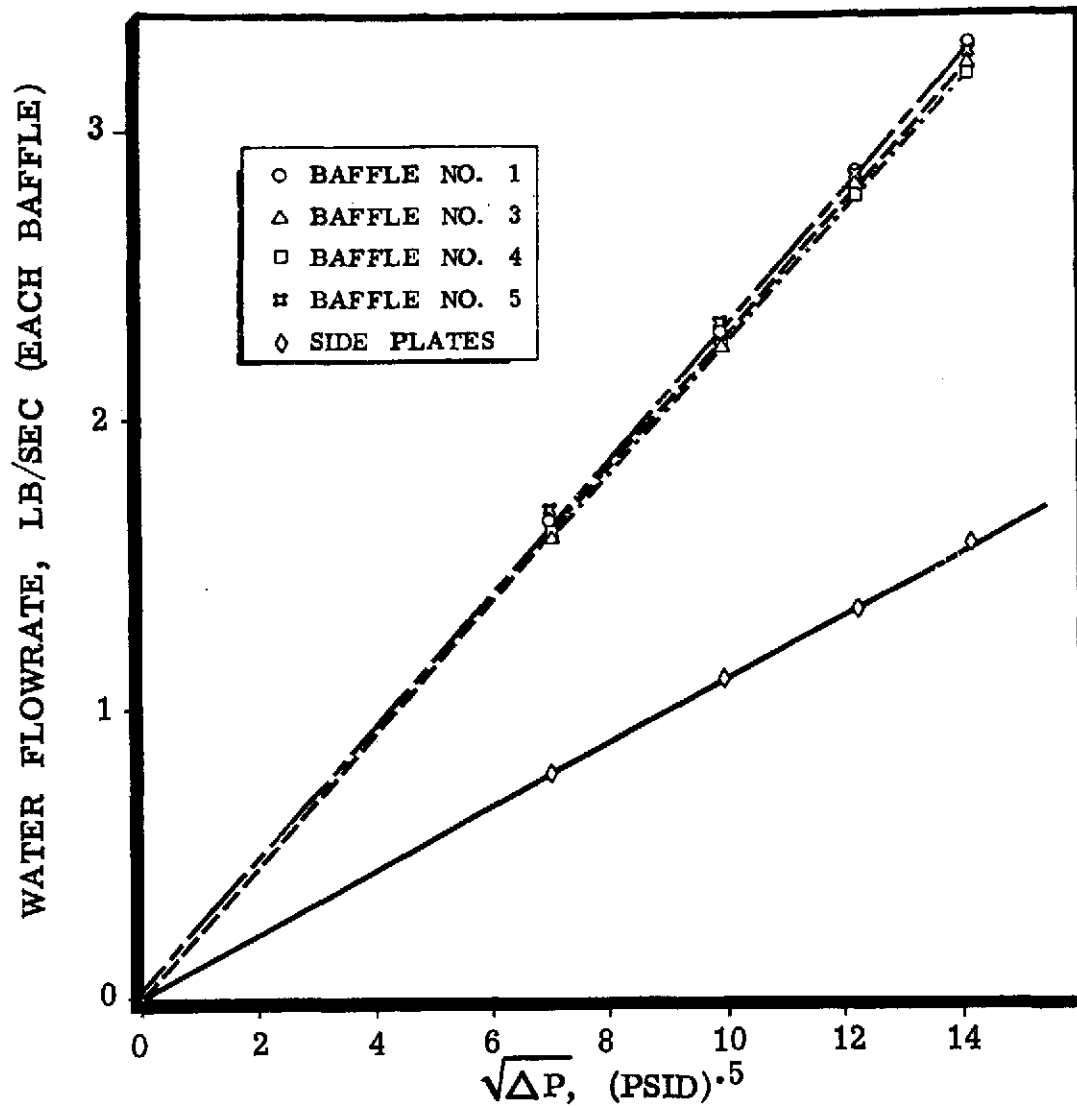


Figure 112. Water Calibration of APS Thermal Conditioner Baffles

Having determined the conditioned hydrogen flow for each side plate and baffle, the heat input for each can be evaluated using the flowrate, and the individual inlet and outlet temperatures. The resulting heat input distribution is shown in Table 24 for a number of tests; the proportional heat input for the same tests is shown in Table 25 . It is noted that each side wall should have only half the heat input of each baffle since the baffle has twice the surface area. For the early tests through test 219, baffles 1-4 have a nearly uniform heat input. The heat input to baffle No. 5 was somewhat lower, and the heat input to the right side wall was very low; by comparison the heat input to the left side wall (away from the igniter) was much higher than expected, considering the amount of film cooling present at that edge of the injector.

Following the liquid hydrogen cycling tests (Test 219), a change in the heat distribution occurred. The left side wall had a somewhat reduced heat input, whereas the heat input to the right side wall was increased considerably.

Since the No. 5 baffle also showed some increase in heat input, it would indicate a considerable change in the heat input from the hot gas passage closest to the igniter. A later discussion of the data presents evidence that no combustion occurred in this passage on the early tests; why this should occur is not known, but it indicates further development work is required in connection with the injector. The heat input to baffle No. 1 is quite consistent throughout the test series; baffles 2 and 3 show some decrease in heat input following test 219, and baffle No. 4 in general shows no change with the exception of about three tests where higher heat inputs were measured.

In studying the results it is noted that there are four film cooling slots on the left side of the injector, while the right side only has two slots to improve the ignition characteristics. In studying test 230, in which no ignition occurred, it is noted that the reason why the heat input determined from the calculated flow distribution is only 49% of the overall heat input as measured at the mixer exit is that the mixer has not reached steady state conditions within the test duration; since the liquid hydrogen temperature rise is relatively small, this results in a large error. It is also interesting to note that except for the side plates, the heat input distribution with or

TABLE 24. TYPICAL HEAT INPUT DISTRIBUTIONS

TEST	M.R.	W _{GAS} LB/SEC	W _{LH₂} LB/SEC	Q _L	Q ₁	Q ₂	Q ₃ BTU	Q ₄ /	Q ₅ SEC	Q _R	Q _{CALC}	$\frac{Q_{CALC}}{Q_{EXPTL}}$
202	.847	.809	2.626	194	379	383	396	483*	305	131	2271	1.0
213	.910	.973	2.767	169	377	405	436	405*	270	45	2107	.95
217	.921	1.072	2.847	187	409	440	469	440*	352	94	2391	.95
219(2)	.903	.968	2.699	158	369	397	424	391*	297	50	2086	.95
221	.910	.917	3.026	80	272	249	271	394	439	223	1928	.93
222	.926	.893	3.110	61	273	279	308	392	423	217	1964	.97
224	.935	.887	2.324	87	276	270	290	460	346	89	1817	.96
226(1)	.947	.887	3.017	95	290	250	271	491	377	100	1875	.94
227(1)	.940	.887	3.184	106	303	266	277	338	371	237	1898	.88
227(8)	.941	.885	3.391	155	380	276	297	359	399	219	2084	.95
228(1)	.954	.870	3.393	107	312	266	280	331	370	239	1904	.88
228(5)	.935	.848	3.782	47	268	267	292	337	370	221	1803	.95
229(1)	.942	.870	3.311	108	302	254	274	327	366	234	1863	.91
229(3)	.950	.870	3.462	77	280	244	269	501	390	112	1872	.95
229(5)	.949	.849	3.606	69	277	282	302	339	367	218	1854	.95
235	.884	.725	3.566	27	250	229	260	376	228	72	1494	.90
236	.916	.810	2.872	96	303	259	272	331	227	126	1614	.90
No Ignition Test 230	.786	.884	5.507	40	59	47	52	70	47	41	355	.49

* Best Estimate; Baffle No. 4 thermocouple connected backwards through Test 219.

TABLE 25. PROPORTIONAL HEAT INPUT DISTRIBUTION TO BAFFLES

TEST	Q_L/Q_{TOTAL}	Q_1/Q_{TOTAL}	Q_2/Q_{TOTAL}	Q_3/Q_{TOTAL}	Q_4/Q_{TOTAL}	Q_5/Q_{TOTAL}	Q_R/Q_{TOTAL}
	PERCENT						
202	8.5	16.7	16.9	17.4	21.3*	13.4	5.8
213	8.0	17.9	19.2	20.6	19.2*	12.8	2.1
217	7.8	17.1	18.4	19.6	18.4*	14.7	3.9
219(2)	7.6	17.7	19.0	20.3	18.7*	14.2	2.4
221	4.2	14.1	12.9	14.1	20.6	22.8	11.6
222	3.1	13.9	14.2	15.7	20.0	21.6	11.0
224	4.8	15.2	14.9	16.0	25.3	19.0	4.9
226(1)	5.1	15.5	13.3	14.5	26.1	20.1	5.3
227(1)	5.6	16.0	14.0	14.6	17.8	19.5	12.3
227(8)	7.4	18.2	13.2	14.2	17.2	19.1	10.0
228(1)	5.6	16.4	14.0	14.7	17.4	19.4	12.5
228(5)	2.6	14.9	14.8	16.2	18.7	20.5	12.2
229(1)	5.8	16.2	13.6	14.7	17.5	19.6	12.5
229(3)	4.1	15.0	13.0	14.4	26.8	20.8	6.0
229(5)	3.7	14.9	15.2	16.3	18.3	19.8	11.7
235	1.8	16.7	15.3	17.4	25.1	15.2	4.8
236	5.9	18.8	16.0	16.8	20.5	14.0	7.8
No Ignition							
230	11.1	16.5	13.1	14.6	19.7	13.2	11.6
Ideal	8.3	16.7	16.7	16.7	16.7	16.7	8.3

* Best Estimate; Baffle No. 4 thermocouple connected backwards through Test 219

without ignition is about the same; the side plates have somewhat more heat input probably because they have additional thermal mass and thus take longer to reach steady state.

In summary, it would appear that the heat input distribution for baffles 1-4 is fairly uniform throughout the test series. The inconsistencies tend to show up primarily in the side plates and the 5th baffle. These inconsistencies are partly a result of the film cooling distribution from the injector face and partly due to apparently inconsistent ignition characteristics whereby not all injector elements light off for each test. This undoubtedly affects the measured combustion efficiency and thermal efficiency of the conditioner. In addition, it is interesting to note that for the later tests the same heat input distribution is observed as was seen on the solid wall tests -- namely, that more heat is input to the two baffles adjacent to the igniter than to the others. This was true on the solid wall tests with or without the igniter on. This may indicate further work is required with the injector pattern to obtain more uniform heating rates; in addition further work is required to attempt to eliminate the film cooling slots on the injector in order to achieve more uniform heating without overheating the side walls near the injector.

Additional work definitely appears needed to improve the ignition characteristics of the injector. Finally, it appears that the severe liquid hydrogen cycling tests (Tests 218-219) resulted in some permanent change which changed the heat balance within the conditioner; this was minor except at the two side plates.

Hot Gas Distribution

The determination of the hot gas flow distribution is considerably more difficult than for the conditioned propellant flow distribution. Not only must the flow distribution be determined, but because of the non-uniform mixture ratio distribution across the injector face, the mixture ratio distribution and combustion efficiency distribution must also be determined. This amounts to 18 unknowns. Several methods of solution were attempted. The method finally selected was based on assuming that the center hot gas passages were at the injector core mixture ratio, with the right hand passage being reduced somewhat by injector film cooling while also being affected by the igniter. In order to achieve the required heat input to the left hand hot gas passage for the early tests, it was necessary to assume a

mixture ratio for the first two left hand passages equal to an average value (4 oxygen elements, 12 hydrogen elements). In addition it was assumed that each injector slot for a given propellant had equal flow.

The combustion efficiency was determined based on that required to yield a heat balance between the heat given up by the gas and that absorbed by the liquid hydrogen. This resulted in selecting a value of 94% for the center passages. It is noted that for 100% film cooling, it would be reasonable to assume a combustion efficiency of 100%; in this manner a value of 97% was arrived at for the two left hand passages, where the one next to the wall would be 100% and the next 94%, these being assumed to be fully mixed together prior to contact with the baffles. A slightly higher combustion efficiency was assumed for the right wall for several reasons: (1) less film cooling (results in a decrease); (2) presence of the igniter (assumed high efficiency); and (3) this was required to achieve the required heat input to the right wall for several tests. A summary of the mixture ratio and combustion efficiency distribution used for the analysis is given below:

Baffle	Left -	1	1-2	2-3	3-4	4-5	5	- Right
Mixture Ratio		0.8	0.8	1.05	1.05	1.05	0.9	
C* Efficiency		.97	.97	.94	.94	.94	.98	

Slight modifications to the mixture ratio and combustion efficiency distribution were made to achieve the best balance for each test examined. To determine the hot gas flow distribution, it is necessary to know the gas inlet temperature, outlet temperature, and heat input in addition to the mixture ratio. The hydrogen injection temperature, in conjunction with the mixture ratio and combustion efficiency determine the combustion temperature. Each hot gas outlet temperature is measured, and these were assumed to be correct. The exit enthalpy is a function of the mixture ratio, exit temperature, and exit pressure (if condensation occurs). A first estimate of the heat input to each hot gas passage was made by assuming that each of the 4 center passages had a heat input equal to an average of the heat input for the two adjacent baffles; the two side gas passages were assumed to have a heat input equal to twice that for the adjacent side plate. Again this was used for a first cut, but gave remarkably good results.

By using the heat input as determined above, and by determining the hot gas enthalpy decrease along the baffle by using data such as presented in Figure 113 , the hot gas flow for each passage is readily determined.

To determine if the solution is valid, the separate liquid hydrogen flowrates are added up and compared to the venturi flowrate (remembering that about 4-5% goes through the top and bottom plates of the conditioner); the total reactor hydrogen flowrate measured at the venturi is compared to the total from the calculated flow distribution; the same is done for the oxygen flow through the reactor; and the total heat input based on the liquid hydrogen flowrate, inlet temperature, and mixer outlet temperature is compared to that determined from the calculated liquid hydrogen flow distribution, and hot gas distribution. Minor modifications in mixture ratio or combustion efficiency may be required to improve the balance, although little modification was found necessary using the above assumptions.

As a final check on the hot gas flow distribution, the individual hot gas gaps were calculated based on the calculated hot gas flowrate distribution, and determining the exit hot gas mass velocity from the calculated mixture ratio distribution, the calculated total pressure at the exit of each passage based on the experimental chamber pressure, and using the experimental hot gas exit temperature. The flowrate and the mass velocity determine the gas flow area for each passage, and knowing the height of the passage, the effective hot gas passage width is determined. These calculated values are compared to the total calculated gas flow area discussed in an earlier section, and they were also compared to the measured exit gas gaps. If the solution meets all of these stringent conditions, it is probably valid. In some cases, the calculated gas gaps are less than the experimental measurements. This could be due to calculational errors (use of wrong total pressure) but probably not since the sum of the individual areas compares well with the overall calculated area. This difference is probably due to either thermal distortion reducing the gas area or due to icing.

These principles were applied to test 213 as being representative of the early tests and test 222 for the later tests. These are summarized in Tables 26 and 27 respectively. Studying test 213, the heat input distribution to the baffles indicates very low heat input to the right side wall. The total

MR = 1.0

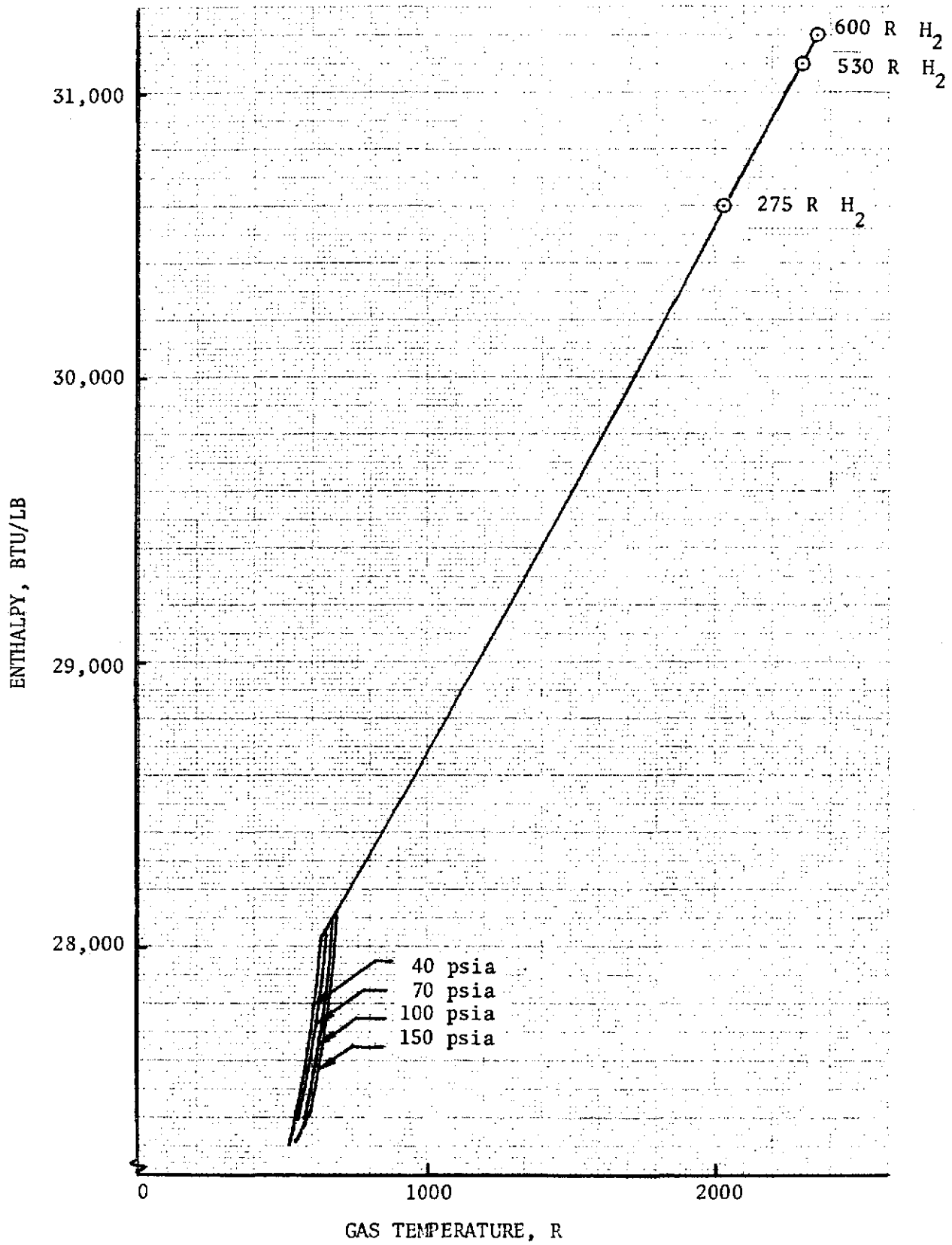


Figure 113. O_2/H_2 Enthalpy Versus Temperature

TABLE 26. TEST 213 FLOW DISTRIBUTION ANALYSIS

OPERATING CONDITIONS

$W_{LH_2} = 2.767$ lb/sec

$W_{GH_2} = .509$ lb/sec

$W_{GO_2} = .464$ lb/sec

$\Delta Q_{mixer} = 2216$ Btu/sec

$P_c = 227$ psia

LH₂ INLET Pr = 1651 psia (flowmeter) at

MIXER Pr = 1509 psia

INLET T = 52°R

MIXER T = 230°R

INJECTOR CORE ELEMENT MR = 1.08

BAFFLE	Left	1	2	3	4 _(calc)	5	Right
LH ₂ T _{out} ' °R	269	286	308	339	(320)	206	102
W _{LH₂} ' lb/sec	.212	.435	.422	.399	(.402)	.497	.303
ΔH, Btu/lb	797	866	958	1094	(1006)	543	149
LH ₂ ΔQ, Btu/sec	169	377	405	436	(405)	270	45

Calculated $W_{LH_2} / W_{LH_2 \text{ venturi}} = 0.96$ (leaves 4% for top & bottom plate)

Calculated $\Delta Q / \text{Mixer } \Delta Q = 0.952$ (within 5%)

NOT GAS MR	0.8	0.8	1.08	1.08	1.08	0.9
η_{C^*}	.97	.97	.94	.94	.94	0
Measured T _{exit} ' °R	650	646	800	1018	694	324
ΔH, Btu/lb	2490	2490	2460	2090	2640	559
ΔQ*, Btu/sec	338	418	442	360	450	90
W _{gas} ' lb/sec	.136	.168	.180	.172	.170	.161
D/S P _{exptl} ' psia	123	112	14	128	0	17
D/S P _{total, calc} ' psia	109	109	109	118	105	126
G*, lb/in. ² -sec	.805	.805	.780	.749	.807	.988
A _{x calc} ' in. ²	.169	.219	.231	.230	.210	.163
δ _{gap calc} ' in.	.033	.043	.045	.045	.041	.032
δ _{measured} ' in.	.028	.042	.045	.038	.045	.038
δ _{calc} / δ _{measured}	1.18	1.02	1.0	1.18	.91	.84

$\Delta Q^* / \Delta Q_{mixer} = .95$; $W_{GH_2 \text{ calc}} / W_{GH_2 \text{ exptl}} = .99$; $W_{GO_2 \text{ calc}} / W_{GO_2 \text{ exptl}} = 1.04$

$A_{x \text{ calc}} / A_x \text{ from } P_c = 1.22 / 1.24 \text{ in.}^2 = .985$

The above balance indicates:

- 1) A good estimate can be made for the heat input to baffle #4.
- 2) Apparently no combusted gases passed between baffle #5 & right wall.
- 3) Principal reason for flow & heat input distribution is effective flow area variation resulting from baffle thermal distortion.
- 4) All heat input & flowrates satisfactorily accounted for.

TABLE 27. TEST 222 ANALYSIS

OPERATING CONDITIONS

W_{LH_2} = 3.110 lb/sec	LH_2 INLET Pr = 1651 psia
W_{GO_2} = .429 lb/sec	MIXER Pr = 1509 psia
W_{GH_2} = .463 lb/sec	INLET T = 52°R
ΔQ = 2013 Btu/sec	MIXER T = 230°R
P_c = 294 psia (injector end)	

INJECTOR CORE MR = 1.06

BAFFLE	Left	1	2	3	4	5	Right
LH_2 T _{out} , °R	110	190	200	218	292	313	348
W_{LH_2} , lb/sec	.321	.554	.542	.510	.436	.429	.193
ΔH , Btu/lb	191	493	533	604	900	986	1128
ΔQ , Btu/sec	61	273	289	308	392	423	217

CALCULATED LH_2 FLOW FROM BAFFLE RESISTANCE = 2.985 lb/sec (96%)
 THIS LEAVES 4% FOR TOP AND BOTTOM PLATE
 TOTAL CALCULATED Q = 1964 Btu/sec (97.5%) ∴ accounted for within 5%

HOT GAS MR	=	0.8	0.8	1.05	1.05	1.05	0.9
η_{C^*}	=	.97	.97	.94	.94	.94	.98
EXIT TEMP, °R	=	708	765	600	1193	607	973
ΔH , Btu/lb	=	2380	2300	2660	1780	2660	2200
ΔQ , Btu/sec	=	270	281	299	350	408	428
W_{gas} , lb/sec	=	.113	.122	.112	.197	.153	.194
D/S P_{exptl} , psia	=	153	116	41	148	57	163
D/S $P_{total calc}$, psia	=	144	143	131	159	131	153
Molecular Weight	=	3.63	3.63	4.13	4.13	4.13	3.83
G^* , lb/in ² -sec	=	1.02	.973	1.02	.924	1.02	.948
Gas A_x , in. ²	=	.111	.125	.110	.213	.151	.205
δ_{cal} (gas gap), in.	=	.0217	.0246	.0216	.0418	.0295	.0401
$\delta_{measured}$, in.	=	.028	.042	.045	.038	.045	.038
$\delta_{calc}/measured$	=	.78	.59	.48	1.1	.66	1.06

$$\Delta Q^*/\Delta Q_{mixer} = .993; W_{GH_2 calc}/W_{GH_2 exptl} = .99; W_{GO_2 calc}/W_{GO_2 exptl} = 1.01$$

Hot gas calc. area/ calc. area from $P_c = .915 \text{ in.}^2 / .892 \text{ in.}^2 = 1.02$

The only discrepancy is in the very low heat input to the left wall. Probable cause of small effective flow areas in passages 1, 2, 3, & 5 is thermal distortion of baffle.

of the calculated hydrogen flowrates compares within 4% of the measured venturi flowrate, leaving about 4% for the top and bottom plates as expected. The calculated heat input from the calculated hydrogen flow distribution compares within 5% with the heat input to the conditioned hydrogen as measured at the mixer outlet. While determining the hot gas enthalpy drop of the hot gas, it was noticed that a very low temperature was measured at the exit of the right hand hot gas passage. This would indicate either a very large enthalpy drop with corresponding large heat input or very low flow through this passage with considerable icing, or else no combustion in this passage with little icing. With the former assumption no reasonable heat balance could be achieved that would satisfy all of the propellant flowrates as well. By comparison, the assumption of no combustion satisfied the total heat input and the individual propellant flowrate totals, and gave results consistent with the low heat input to the right wall. In addition, although the calculated hot gas gaps do not exactly match the measured values, they are fairly good, and the sum of the individual areas is very close to that calculated from the overall flowrate and chamber pressure. It can be concluded, then, that the hot gas flow distribution does meet all of the required checks; that all of the heat input and the various flowrates are satisfactorily accounted for; that the heat input distribution to the baffles is accounted for by injector mixture ratio distribution variations in hot gas gap between baffles, and the lack of combustion in the right hand hot gas passage.

Applying the same analysis to Test 222, it is seen that the heat input is accounted for within 3% and all of the flowrates are accounted for within 1%. In addition the total hot gas flow area is accounted for within 2%. The right hand baffles are receiving more heat input than the left hand baffles (same as on the solid wall tests), and combustion is occurring in all gas passages. As in all the other tests, the hot gas temperature from the center passage is considerably higher than most; by the time this was discovered it was too late to determine if the correct thermocouple had been installed. A look at the hot gas passage widths shows that those for gaps 1-2, 2-3, and 4-5 are considerably less than the measured exit gaps. The first reaction is that this is due to severe icing. Some icing would be expected, since 15% more liquid hydrogen flow and only 85% of the hot gas flow is present (compared to nominal). Some of the reduction in area, however, is probably due to baffle distortion, resulting in a reduced area at some point upstream of the exit. As discussed earlier, this is suspected due to the

consistently high chamber pressure measurements on all tests following test 219, indicating a more permanent change than icing would indicate.

A summary of the hot gas outlet temperatures is tabulated in Table 28 for each cycle of each test. Several no ignition tests (based on the combustion thermocouple measurement) such as tests 204, 209, 210, 214, and some cycles of test 219 are tabulated to show the experimental values under such conditions and to show the consistency of the measurements. The measurements for the first four tests listed above indicated the temperatures lie between 370-500R with about a 70R difference between the left and right passages.

For these same tests the left side consistently reads the higher temperature, with a fairly consistent decrease toward the right-hand side. For the last two cycles in test 219, the two hot gas passages adjacent to the side walls had very low exit temperatures in the range of 220-250R. In fact these very low temperatures in the right hand gas passage were measured for the last six cycles of test 219, indicating that no combusted gas was flowing through this passage. Even for many of the earlier tests, this gas passage registered much lower exit temperatures than the others, and this is confirmed by the conditioned hydrogen enthalpy rise in the right hand side plate as further indication of the lack of combusted gases in this passage. This is no longer the case following test 219, however.

With nearly no exceptions, the hot gas passage between baffles 3 and 4 registered considerably higher temperatures at the exit than did the other passages (except for the no ignition tests). The first reason to be suspected is that the wrong type of thermocouple was installed in this particular passage. However, agreement of the thermocouples in the tests without ignition coupled with a few high temperature measurements in adjacent passages (Tests 219-1, 220, 223, and 224) tended to imply this temperature reading may be real. This type of condition would be expected if this passage had (1) higher mixture ratios than nominal; (2) a greater than nominal hot gas flowrate with a corresponding decrease in the enthalpy change; (3) a larger hot gas gap with an appreciably reduced hot gas mass velocity and heat transfer coefficient, resulting in less heat removed from the gas. The first two explanations are more feasible than the third, since an analysis with the computer model indicated that the high exit temperature could not be achieved theoretically even using

TABLE 28. HOT-GAS OUTLET TEMPERATURE DISTRIBUTION*

Test	Gap L-1	Gap 1-2	Gap 2-3	Gap 3-4	Gap 4-5	Gap 5-R (Igniter)	Notes	
199	610	525	628	851	581	479	0.5-second tests	
200	597	585	625	829	535	448		
201	606	617	639	986	637	479		
202	601	615	640	970	639	460		
203	588	614	643	945	643	461		
204	444	425	411	420	396	371		No ignition
205	577	581	639	789	582	419		
206	559	580	633	690	597	417		
207	599	625	677	938	677	474		
208	579	606	649	882	653	449		0.8-second test
209	489	504	480	447	493	510	No ignition indicated	
210	474	471	450	443	460	497	No ignition indicated	
211	630	622	655	1080	651	471		
212	634	649	752	1041	745	455		
213	650	648	796	1014	699	325	5-second test	
214	440	408	409	435	381	370	No indicated ignition	
215	630	555	627	900	621	532	Low P_c cut	
216	637	625	822	958	832	590		
217	656	671	855	1076	650	310		
218-1	560	875	765	943	918	559	LH ₂ on full test duration	
218-2	499	569	662	1032	572	487		
219-1	550	1016	731	1143	1009	573	LH ₂ on full test duration	
219-2	619	788	653	1119	876	443		
219-3	649	866	568	1196	665	313		
219-4	396	373	409	455	354	280	No ignition	
219-5	486	891	556	1172	669	235		
219-7	549	768	670	1124	651	225		
219-9	246	385	377	454	336	225	No ignition indicated	
219-10	237	384	365	441	321	220	No ignition indicated	
220	608	565	967	592	1223	662	0.5-second test	
221	584	967	573	1256	711	1000	5-second test	
222	620	766	591	1194	607	972		

*All measurements in degrees Rankine

TABLE 28. (Concluded)

Test	Gap L-1	Gap 1-2	Gap 2-3	Gap 3-4	Gap 4-5	Gap 5-R (Igniter)	Notes
223	663	683	582	1268	693	1030	
224	677	792	574	1192	1027	616	
225	681	824	560	1274	604	991	
226-1	682	764	575	1198	963	528	No flow between cycles
226-2	682	754	555	1229	599	947	No flow between cycles
227-1	625	1024	591	1328	710	964	
227-2	581	985	575	1275	925	577	
227-3	670	820	581	1338	662	929	
227-4	672	737	590	1330	722	931	
227-5	670	723	579	1320	674	916	
227-6	667	768	604	1317	680	904	
227-7	664	715	604	1311	700	907	
227-8	648	678	639	1309	683	888	
227-9	655	842	608	1307	656	666	
227-10	447	871	636	1255	657	876	
228-1	608	993	572	1348	680	864	
228-2	570	610	570	1354	734	874	
228-3	388	750	578	1277	957	592	
228-4	352	716	595	1318	638	842	
228-5	329	672	599	1306	646	854	
229-1	649	808	571	1363	658	869	
229-2	665	671	578	1350	666	873	
229-3	660	704	582	1280	900	580	
229-4	669	691	580	1324	616	837	
229-5	673	676	585	1308	629	815	
230	441	408	449	543	444	392	No ignition indicated
231	367	746	631	1348	727	901	
232-1	482	673	588	1342	686	879	
232-2	356	770	588	1249	886	631	
232-3	333	678	620	1290	648	853	
233	368	673	603	1301	634	660	
234	359	675	597	1292	626	630	
235 (end)	461	671	581	1180	655	660	
236	597	953	660	1411	791	657	

appreciably reduced values of the heat transfer coefficient. Because the thermocouples had been removed by the time this phenomenon had been noticed, there was no way to verify whether the correct thermocouple had been installed.

For the later tests the thermocouple adjacent to the right side wall registered temperatures equal to or exceeding the average value, whereas that adjacent to the left side wall (away from the igniter) read either near nominal or much lower than nominal, indicating that possibly only film coolant or uncombusted gases were flowing through this passage at times.

One phenomenon of considerable interest is that on certain tests the right hand passage read a higher exit temperature than the adjacent passage, while in some tests this situation was reversed. This occurred in tests 220, 224, 226-1, 227-2, 228-3, 229-3, 232-2, and 236. Since the highest exit temperature would normally be associated with the higher flowrate and the larger gas gap, this would tend to indicate that either the number 5 baffle was moving from side to side (not during a test, but between tests or cycles) or else either the 4th or 5th baffle is bending to a greater or lesser extent or in an inconsistent manner to cause the relative dimensions of the two hot gas passages to change. This would also tend to indicate that at least one of the baffles was bent at the forward end as early as test 220 or 221, implying that the damage was done either during the severe cycling tests of 218-219, or due to the lack of uniform ignition of the injector.

In studying the hydrogen outlet temperature from baffle no. 3 during the cycling tests of test 219, it was noticed that a higher outlet temperature was achieved for the first two tests than for the next four tests shown in Figure 110. In order to explain this occurrence, the hot gas flow areas were calculated and tabulated along with the individual hydrogen enthalpy rises in each baffle (except in the 4th baffle with its improperly connected exit thermocouple) and the propellant flowrates and flow ratios; these are presented in Table 29 .

TABLE 29. CORRELATION BETWEEN GAS FLOW AREA
AND LH₂ ENTHALPY RISE, TEST 219

Cycle	1	2	3	4	5	6	7	8
A _{x Gas} , in. ²	0.946	1.26	0.99	*	0.93	0.78	1.03	0.76
LH ₂ ΔH _L , Btu/lb	338	756	787	115	740	93	336	146
LH ₂ ΔH ₁ , Btu/lb	636	874	931	87	941	381	646	555
LH ₂ ΔH ₂ , Btu/lb	673	971	531	53	539	421	1027	536
LH ₂ ΔH ₃ , Btu/lb	742	1103	591	47	617	571	1196	609
LH ₂ ΔH ₅ , Btu/lb	802	643	726	44	543	503	439	489
LH ₂ ΔH _R , Btu/lb	317	175	335	16	153	120	101	97
\dot{w}_{gas} , lb/sec	0.919	0.968	0.933	0.971	0.912	0.868	0.933	0.869
\dot{w}_{LH_2} , lb/sec	2.78	2.70	2.79	5.81	2.86	3.21	2.80	3.12
$\dot{w}_{\text{gas}}/\dot{w}_{\text{LH}_2}$	0.330	0.358	0.334	0.167	0.320	0.270	0.333	0.278

*No ignition

It is seen that the highest flow areas appear to exist in the second and seventh cycle; the highest heat inputs to baffles 2 and 3 occur on these cycles. Cycles 6 and 8 have the smallest reactor flow area; these two cycles also have the smallest reactor flow relative to the conditioned hydrogen flow, indicating icing is more likely to occur and furthermore less enthalpy gain of the conditioned hydrogen is to be expected. Ignoring the fourth cycle, which failed to ignite, the sixth cycle has the lowest heat inputs in all baffles except the right hand side plate (which consistently ran with a very low heat input probably due to lack of ignition in this passage). During the eighth cycle, the baffles show anywhere from appreciably lower heat input than normal (baffle 1 and the left side wall) to very little decrease (baffles 2, 3, 5, and the right wall).

Due to the reduced heat input in the left hand baffles associated with the reduced reactor flowrate, it would appear that icing occurred in this area since this has the effect of reducing both flow area and surface area. The region next to the right side wall may not be affected due to the lack of combustion and thus the lack of water formation.

It is also interesting to note that the total reactor flow area changed considerably from cycle to cycle, varying from almost the 1.33 in² value of the early tests to less than the 0.956 in² representative of test 221. This change must be due to either a variable

ice formation pattern or else due to bending of the baffles. Cycles 6 and 8 probably have a combination of both. It is at least apparent that the reduction in area for cycles 6 and 8 is not permanent as a recovery is made after each of these cycles. However, due to the persistence of reactor flow area in the range of 0.9 to 1.0 in² which is within 10% of that typical of the later tests, and due to the apparent lack of either flow area reduction or surface area reduction due to icing on the earlier tests, it would appear that either baffle distortion occurred early in the test (or possibly in test 218, which was also a cycling test) and/or more ice formation occurred on shutdown due to the liquid hydrogen being flowed for the full test duration.

Comparison of Theoretical and Experimental Parameters

In order to verify the capabilities of the computer model to predict what was occurring inside of the conditioner, several tests were selected for analysis. Heat transfer coefficients were determined the same way as in the earlier theoretical studies, and the same baffle geometries were used. The computer model for the baffles was modified, however, in order to analyze two counterflow liquid hydrogen passages with different hot gas boundary conditions on each side of the baffle (the previous model assumed identical hot gas conditions on each side of the baffle).

A comparison of the predicted and experimental conditioned hydrogen outlet temperature, hot gas outlet temperature, and heat input is presented for tests 213, 222, and 236 in Tables 30 to 32, respectively.

TABLE 30. COMPARISON OF PREDICTED AND EXPERIMENTAL PARAMETERS - TEST 213

OPERATING CONDITIONS:

MIXTURE RATIO = 0.911
 GAS FLOW = 0.972 LB/SEC
 LH₂ FLOW = 2.776 LB/SEC
 HEAT INPUT = 2198 BTU/SEC
 TEST DURATION = 5 SECONDS

LOCATION	LEFT WALL	BAFFLE NO. 1		BAFFLE NO. 3		BAFFLE NO. 5		RIGHT WALL
LH ₂ OUTLET T, R								
THEORETICAL	271	261		340		209		120
EXPERIMENTAL	269	285		339		206		102
HOT GAS OUTLET T, R								
THEORETICAL	704	650	690	836	820	741	318	275
EXPERIMENTAL	650	650	647	800	1018	694	324	324
HEAT INPUT, BTU/SEC								
THEORETICAL	164	340		432		268		59
EXPERIMENTAL	169	377		436		270		45
Q_{EXPERL}/Q_{THEOR}	1.03	1.11		1.01		1.01		0.77
$\delta_{CALC}/\delta_{MEASURED}$	1.18	1.18	1.02	1.0	1.18	0.91	0.84	0.84

TABLE 31. COMPARISON OF PREDICTED AND EXPERIMENTAL PARAMETERS - TEST 222

OPERATING CONDITIONS:

MIXTURE RATIO = 0.925
 GAS FLOW = 0.892 LB/SEC
 LH₂ FLOW = 3.110 LB/SEC
 HEAT INPUT = 2013 BTU/SEC
 TEST DURATION = 5 SECONDS

LOCATION	LEFT WALL	BAFFLE NO. 1		BAFFLE NO. 3		BAFFLE NO. 5		RIGHT WALL	
LH ₂ OUTLET T, R	THEORETICAL	194	212		267		316		359
	EXPERIMENTAL	110	190		218		313		348
HOT GAS OUTLET T, R	THEORETICAL	561	600	627	636	816	660	796	828
	EXPERIMENTAL	620	708	765	600	1193	607	973	972
HEAT INPUT, BTU/SEC	THEORETICAL	161	334		410		430		227
	EXPERIMENTAL	61	273		308		423		217
Q _{EXPTL} /Q _{THEOR}	0.38	0.82		0.75		0.98		0.96	
δ _{CALC} /δ _{MEASURED}	0.78	0.78	0.59	0.48	1.10	0.66	1.06	1.06	

TABLE 32. COMPARISON OF PREDICTED AND EXPERIMENTAL PARAMETERS - TEST 236

OPERATING CONDITIONS :

MIXTURE RATIO = 0.916
 GAS FLOW = 0.810 LB/SEC
 LH₂ FLOW = 2.872 LB/SEC
 HEAT INPUT = 1808 BTU/SEC
 TEST DURATION = 5 SECONDS

LOCATION	LEFT WALL	BAFFLE NO. 1		BAFFLE NO. 3		BAFFLE NO. 5		RIGHT WALL
LH ₂ OUTLET T, R								
THEORETICAL	219	245		300		247		258
EXPERIMENTAL	171	247		226		187		218
HOT GAS OUTLET T, R								
THEORETICAL	406	485	635	585	894	608	790	556
EXPERIMENTAL	597	597	953	660	1411	546	657	657
HEAT INPUT, BTU/SEC								
THEORETICAL	135	320		436		356		158
EXPERIMENTAL	102	321		289		227		133
Q _{EXPTL} /Q _{THEOR}	0.76	1.0		0.66		0.64		0.84
δ _{CALC} /δ _{MEASURED}	0.50	0.50	0.64	0.38	1.18	0.45	0.42	0.42

Test 213 was selected as the first 5 second test. This is before the severe cycling tests, when the theoretical and experimental chamber pressures were consistent. For clarity, only the results for the odd-numbered baffles are presented, along with the side plates. The results indicate for Test 213 that the liquid hydrogen outlet temperature can be predicted within a few degrees, and that the heat input can be predicted within 1-10% except for the right side plate, where no apparent combustion occurred. For this side plate the heat input was over-predicted by 15 Btu/sec. In addition, the hot gas outlet temperatures match quite well, the error being mostly due to difficulty of the computer program in iterating for the outlet temperature in a region where the water is condensing on the hot gas side. The really important parameter of the three, however, is the heat input, since this is the job the baffles are designed to perform; the outlet temperatures can be readily verified by hand if the heat input is known. The excellent comparison between the experimental and theoretical results also indicates the validity of the method by which the hot gas flowrate, mixture ratio, and combustion efficiency distribution were determined.

Tests 222 and 236 are representative of tests run after the severe liquid hydrogen cycles of test 219, following which an apparently permanent rise in chamber pressure was noted. The result is that the heat input can no longer consistently be predicted within 10% for each baffle. Some of this may be due to loss of surface area resulting from icing. It is noted, however, that the reduction in heat input is much less than the reduction in the apparent hot gas flow area or gas gap. If the gas area blockage was due only to icing, this would result in a proportionate decrease in surface area and a nearly proportionate decrease in heat input. Since this is not the case, it must be concluded that the primary reduction in gas flow area is due to thermal distortion resulting from the severe cycling tests, with icing being a possible secondary phenomenon.

To determine the validity of the third baffle hot wall and back wall thermocouple measurements, the experimental values were compared to the theoretically predicted ones (from the computer model). This has been done for Test 213 in Fig. 114 and 115. It is seen that all except the first hot wall thermocouple is very close to the predicted hot gas temperature, and within 200F of the interpolated experimental hot gas temperature based on the combustion

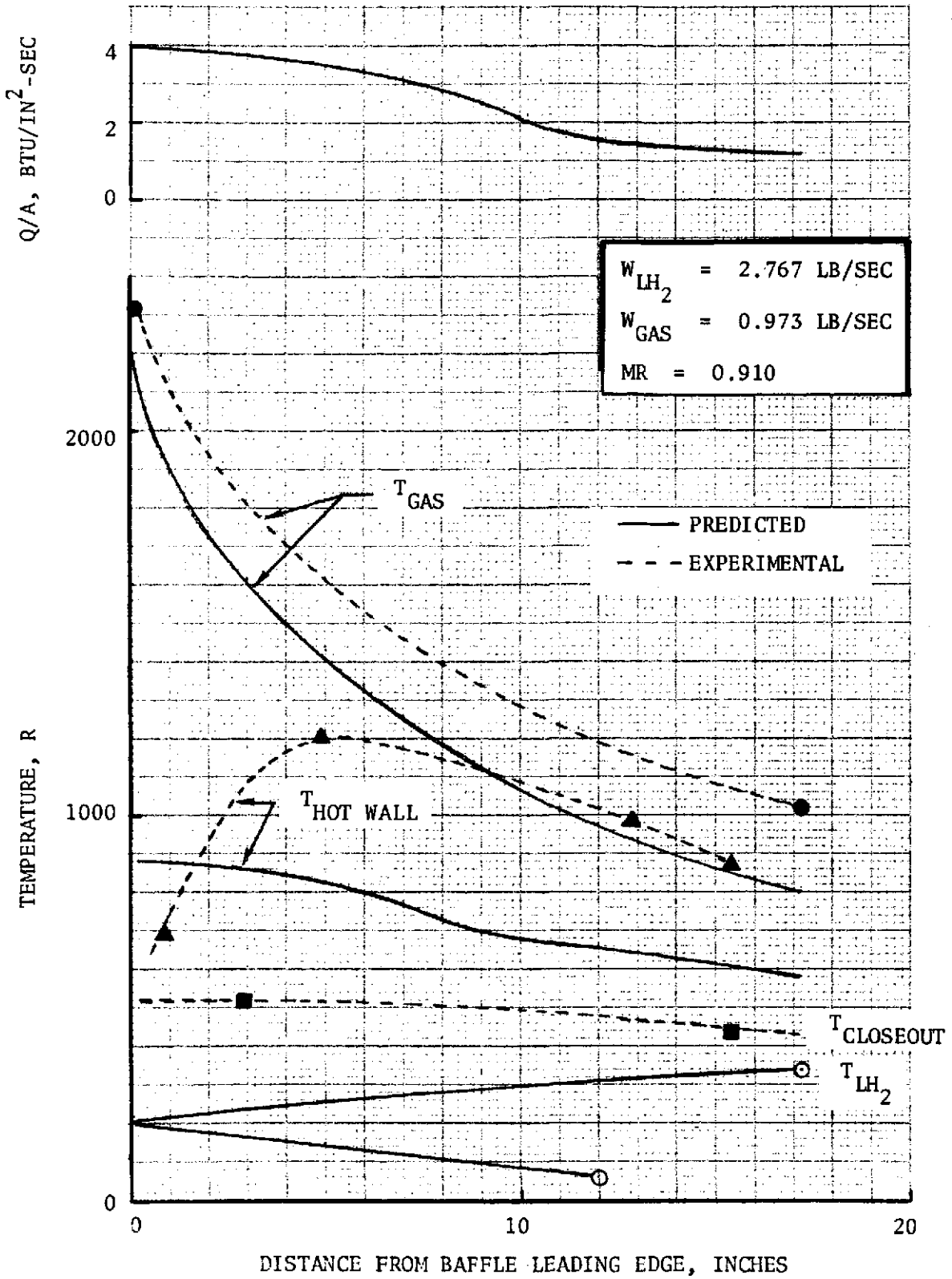


Figure 114. Baffle No. 3 Temperature Profiles, Test 213

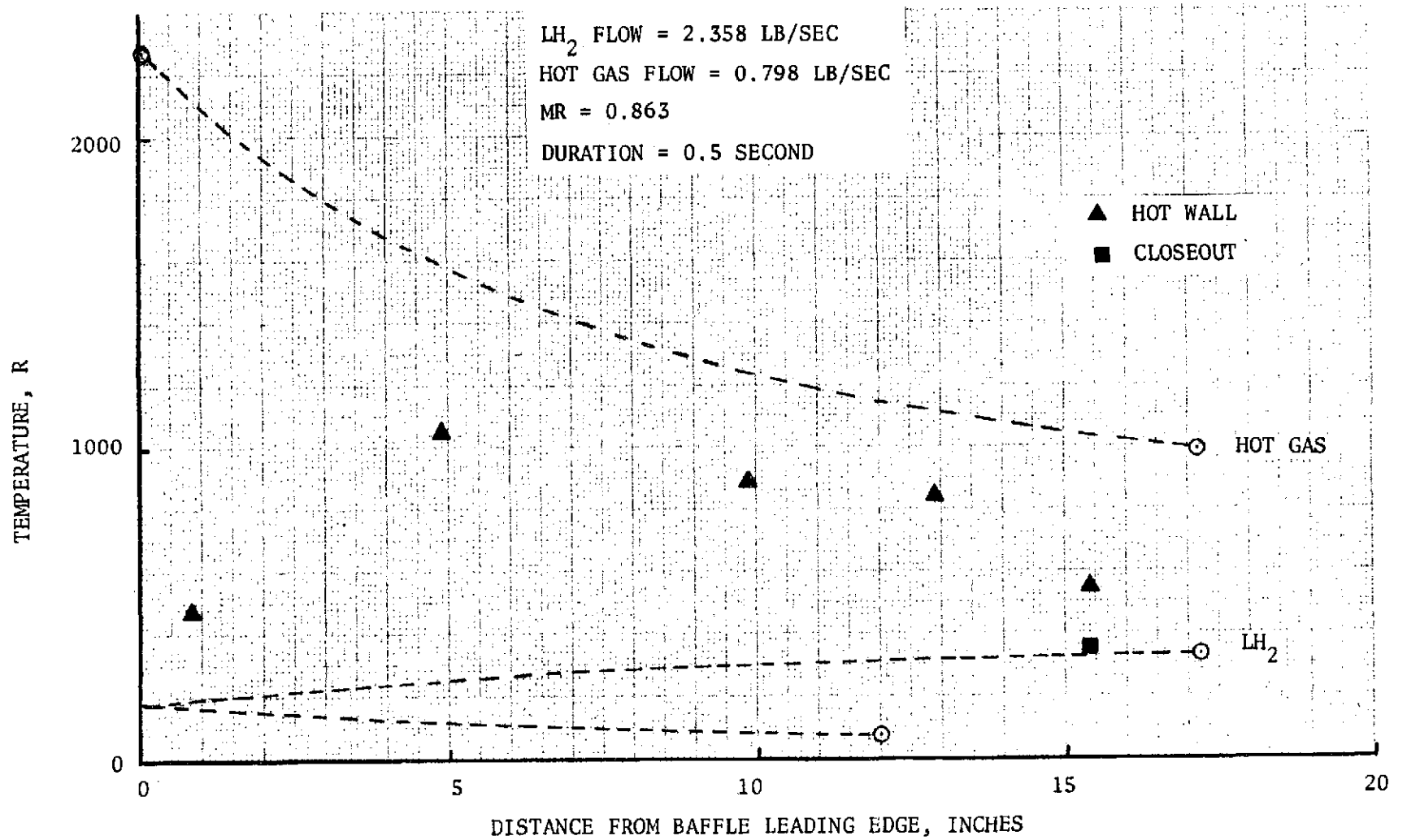


Figure 115. Experimental Temperature Profiles, Test 201, Baffle No. 3

temperature and the measured exit temperature. These temperatures are about 400F higher than the predicted value, leading to the conclusion that the thermocouples probably are measuring the hot gas temperature, or close to it. On the other hand, the back wall thermocouples, which should measure the downpass liquid hydrogen temperature, read approximately ambient temperature, thereby raising the question of whether they are attached to the back wall or even if the thermocouples are intact or possibly shorted out at another location. The same results appear to be true for the last test, Test 236, shown in Figure 116. At this point it was decided to look at Test 201, one of the early tests. The results are somewhat inconclusive for the center three thermocouples, but the first and last hot wall thermocouples appear to be reading the hot wall temperature. The one recorded back wall temperature also appears to be reading the conditioned hydrogen temperature as expected. Unfortunately there were insufficient data channels to record more of the thermocouple data from the early tests. As a result it is questionable whether it is worthwhile instrumenting the baffles themselves, considering the expense, the doubtful data, and noting that it was the instrumented baffle which partially collapsed. It is possible that valid data could be obtained by relocating the thermocouples, using heavier thermocouple wire, a different type of thermocouple, or some other means. It should be remembered that having to put the thermocouples through a braze cycle did not improve their life capability. Furthermore, the large number of unplanned ignition tests run prior to obtaining heat transfer data did not help the thermocouples either.

The results of a similar analysis of the side plates is presented in Figures 117 and 118 for tests 201 and 213 respectively. For test 201, the hot wall thermocouples on the left side plate appear to be reading the hot gas temperature, whereas those on the right are probably reading the hot wall temperature. These results seem to be verified in test 213, except that the one functioning thermocouple may be reading the hot gas temperature since there was no apparent ignition in the right hand gas passage. By the end of the test program, none of the side plate thermocouples were functioning correctly.

One of the questions raised upon examination of the hardware after test 236 was: what caused the 4th baffle to bend? One theory was that if a difference in hot wall temperatures between adjacent sides of the baffle exceeded about 300F

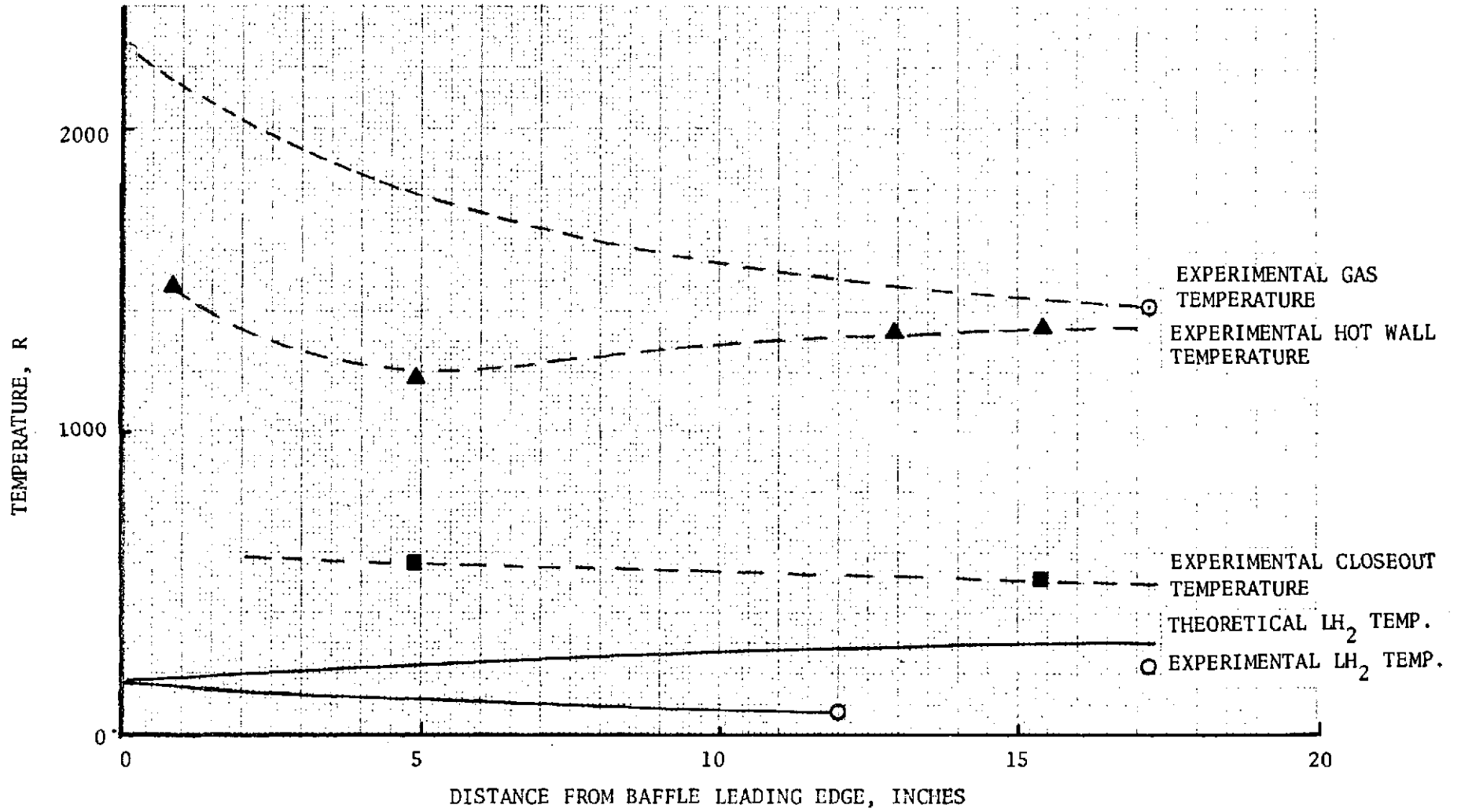


Figure 116. Experimental Temperature Profiles, Test 236, Baffle No. 3

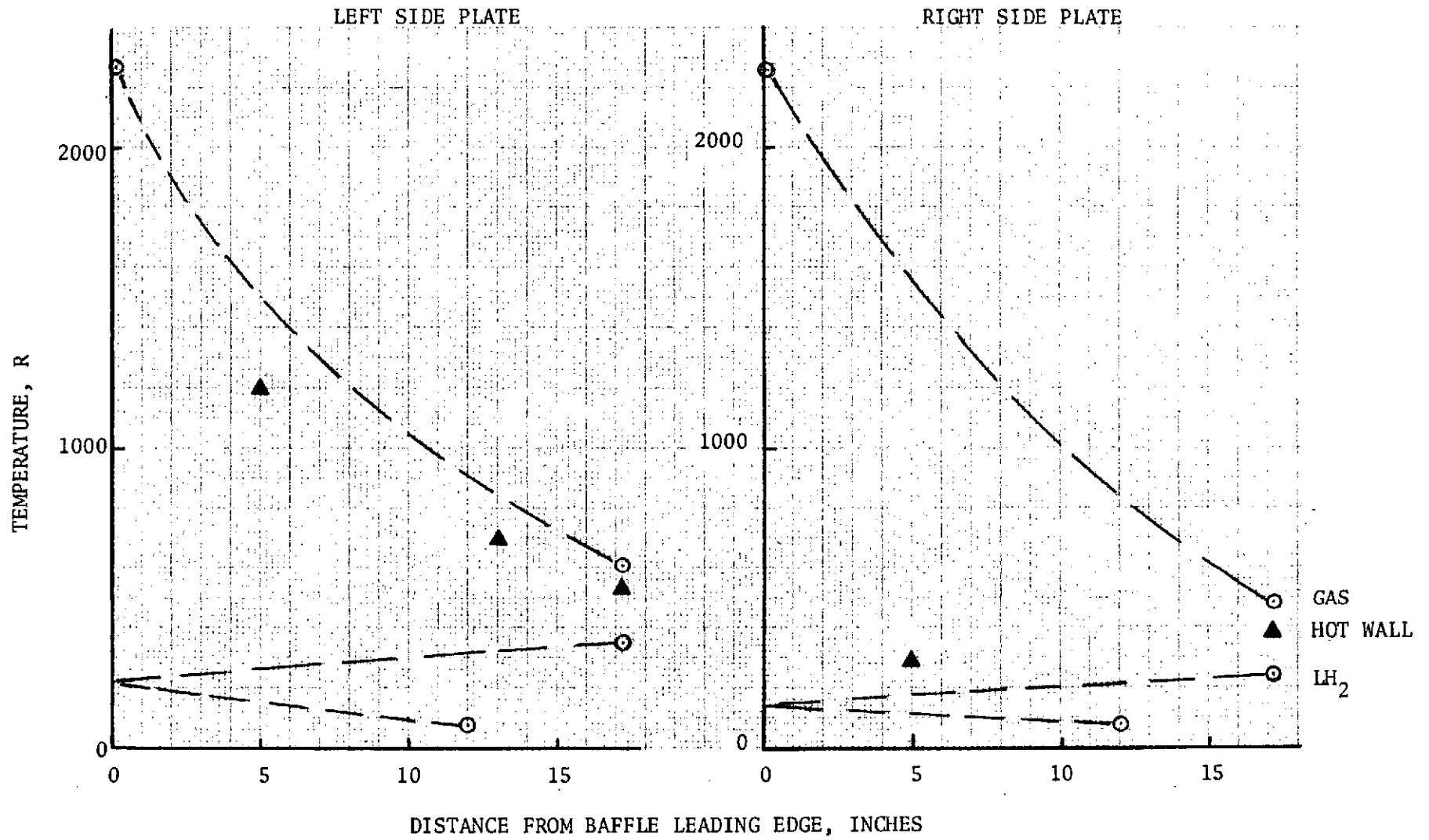


Figure 117. Experimental Side Plate Temperature Profiles, Test 201

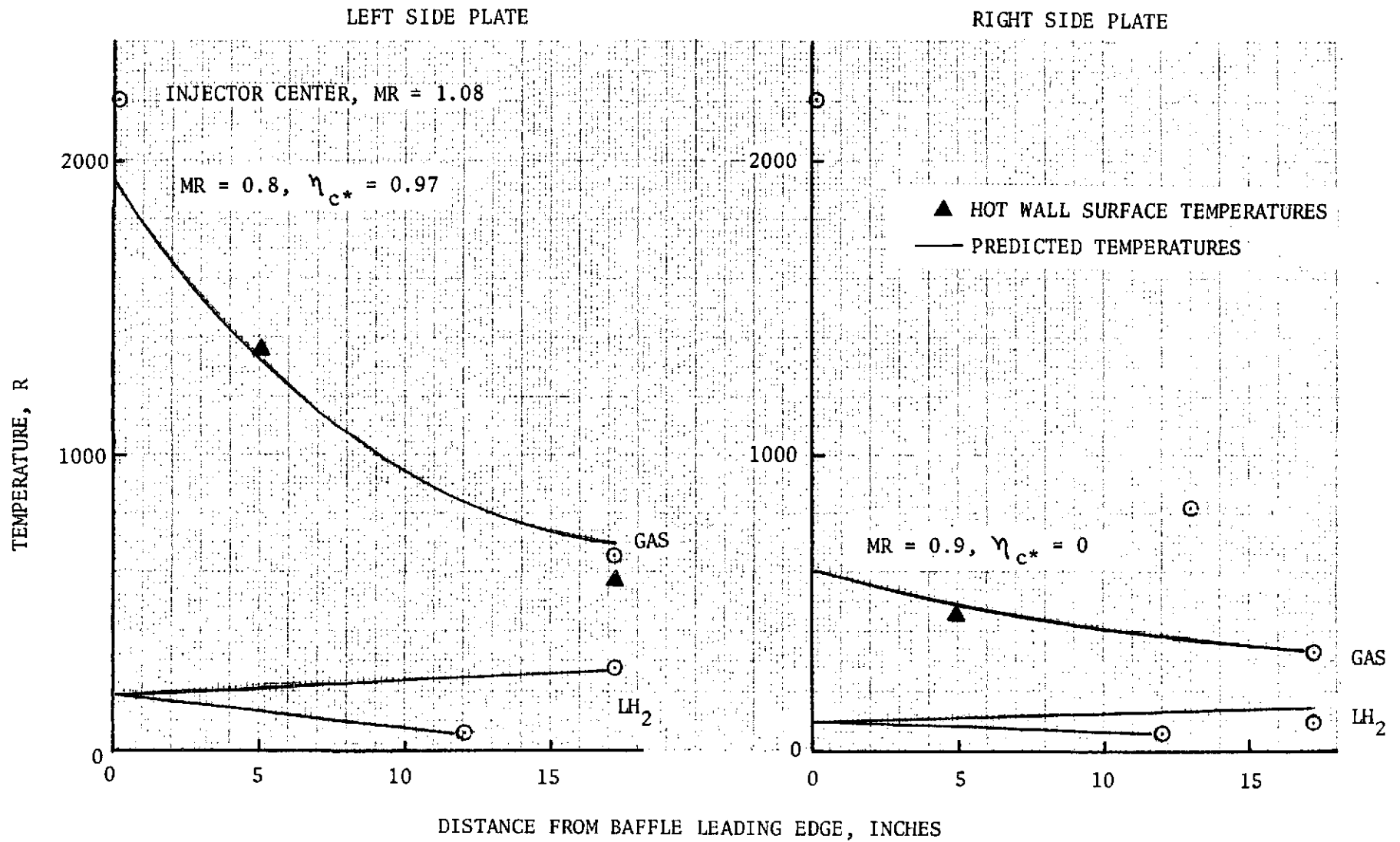


Figure 118. Experimental Side Plate Temperature Distributions, Test 213

a permanent deformation could result. To determine if this was possible, the theoretical computer baffle model was utilized to predict the temperature gradients around the odd-numbered baffles for tests 213, 222, and 236. The resulting hot wall temperature profiles are shown in Figures 119 to 121, respectively. For test 213, symmetrical heating conditions exist on the 3rd baffle. The first baffle has a maximum difference in hot wall temperature of about 70 F. The maximum predicted temperature gradient occurs on baffle No. 5 because of the apparent lack of combustion in the gas passage next to the side plate. In this case a maximum difference in the hot wall temperature on opposite sides of the baffle is 500-600 F, more than enough to cause bending of the baffle. By comparison, the other two tests studied show temperature differences up to 200 F, but none as severe as the 500-600 F discussed above. As a result it is quite possible that the failure to light the injector properly in the early tests resulted in the bending of the baffles.

Based on the solid wall heat flux distribution discussed in the next section, the maximum differential heat flux between adjacent baffles is in the range of 0.5 to 1.0 Btu/in²-sec. This can also be considered the difference in heat flux between one side of the baffle and the other. This difference in heat flux results in a difference in baffle hot wall temperature of 80-160 R based on Figure 122, which is theoretically insufficient to cause the baffle leading edge to bend with a permanent set.

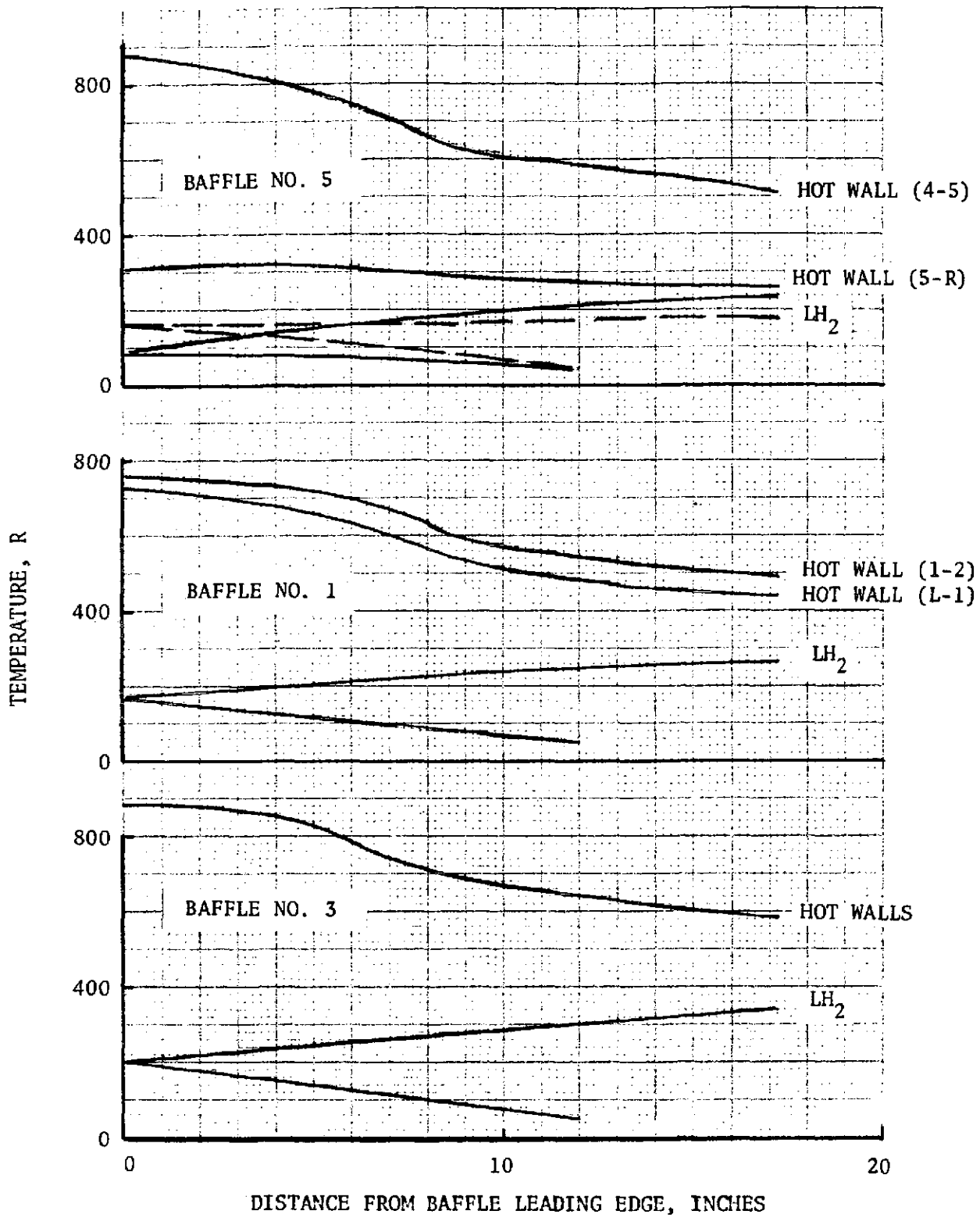


Figure 119. Predicted Baffle Temperature Profiles, Test 213

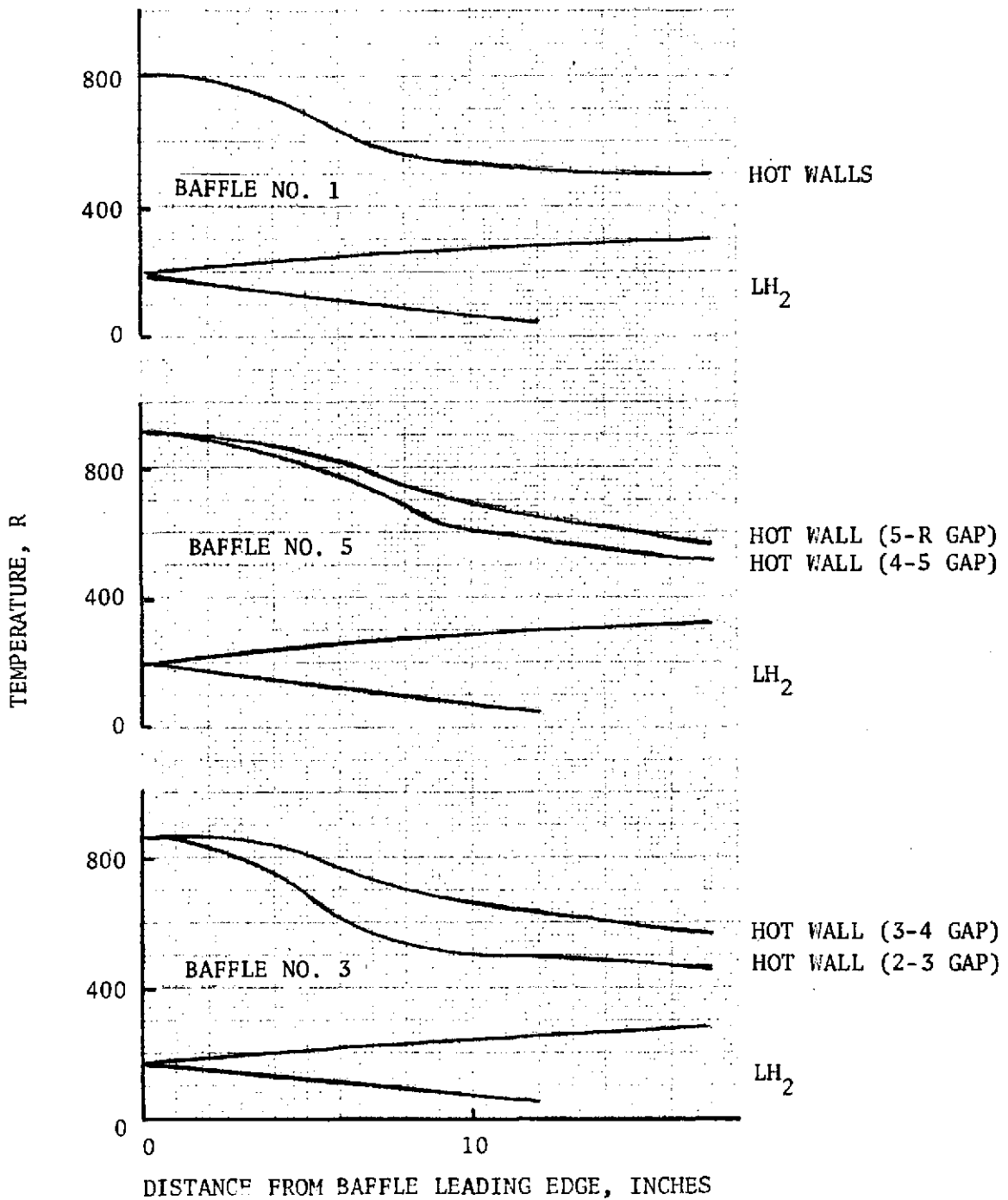


Figure 120. Predicted Baffle Hot Wall and LH₂ Temperature Profiles, Test 222

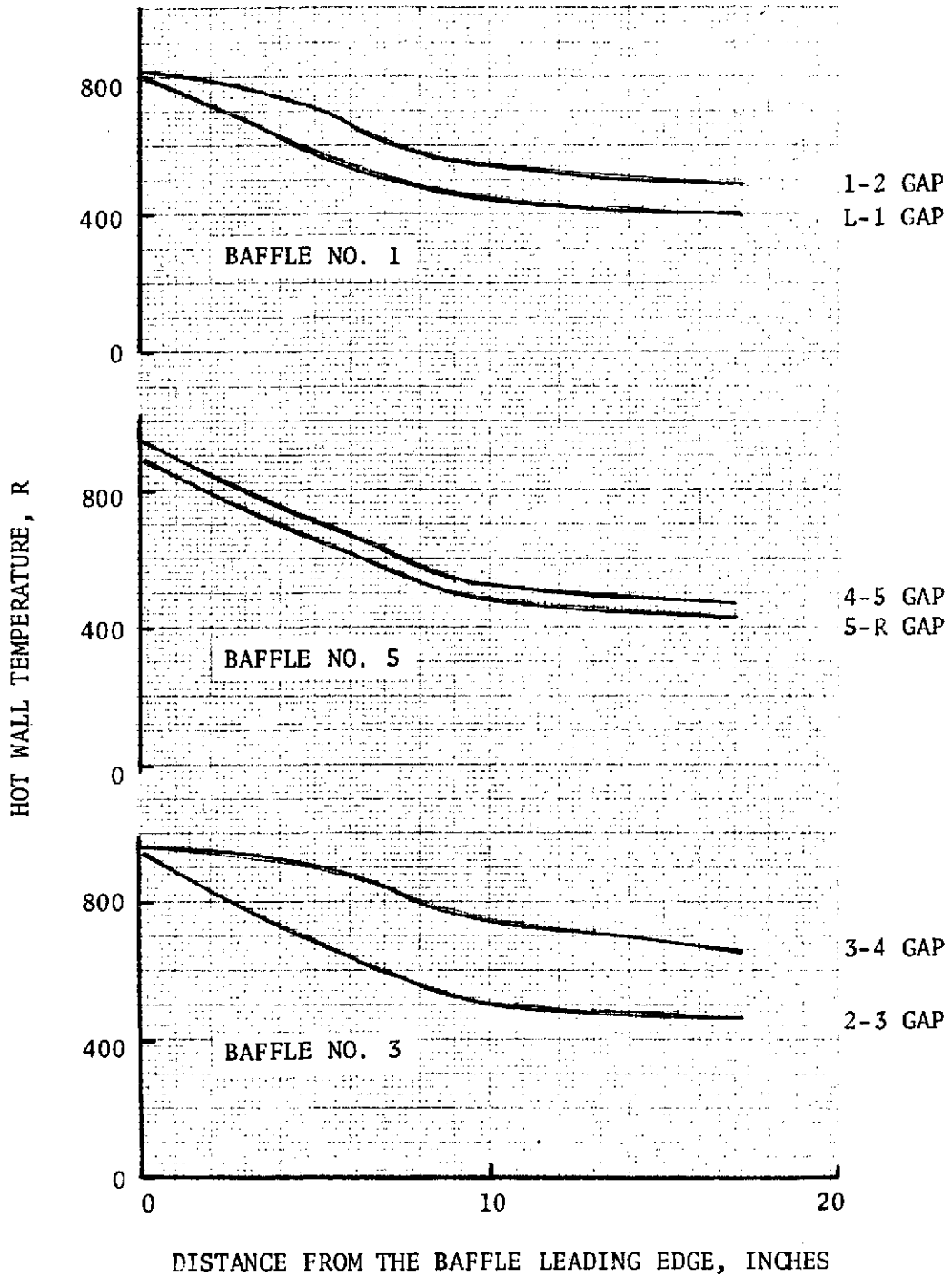


Figure 121. Predicted Baffle Hot-Wall Temperature Profiles, Test 236

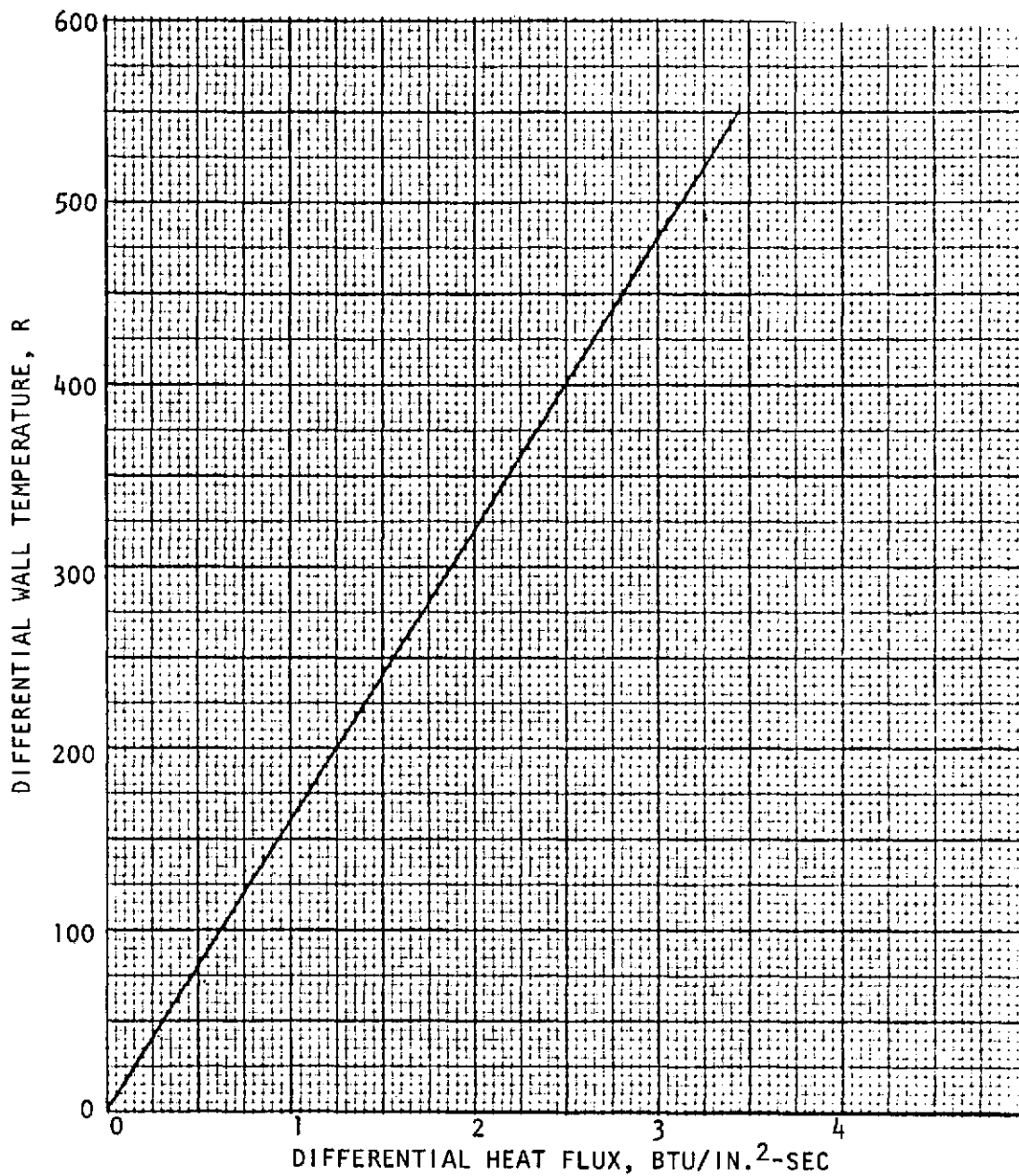


Figure 122. Predicted Effect of Differential Heat Flux on Both Sides of the Baffle on the Differential Hot-Wall Temperature

Liquid Hydrogen Pressure Drop

The contract specified a conditioned propellant pressure drop of 100 psi at nominal conditions. The hardware was designed for 75 psi pressure drop at nominal conditions, with 2.7 lb/sec of hydrogen through the conditioner. This was to leave some pressure drop for the mixer with some leeway for tolerance effects. The actual experimental pressure drops came out appreciably higher. To verify the results, the baffles were water flowed following the test series to determine the individual baffle resistances. Using this information, a detailed water pressure drop calculation through the baffle was made. Two roughnesses were assumed: 75 and 200 microinches. The result is shown in Table 33. The experimental pressure drop with 3 lb/sec per baffle was 170 psi; the theoretical pressure drops were 106 and 119 psi for 75 and 200 microinches respectively. This represents an error of 60% and 43% respectively; this is approximately the same error observed while flowing hydrogen during the test program. It is very unusual for pressure drop predictions to be in error by this much, especially for water. The most probable explanation is that the passages have either a larger roughness and/or the passages have a smaller cross-sectional area than nominal. For example, decreasing the channel height and width 10% will result in a 60% increase in pressure drop. Doubling the roughness only results in approximately a 15% increase in pressure drop.

TABLE 33. PRELIMINARY BAFFLE ΔP ANALYSIS

●	WATER FLOW = 3 lb/sec/BAFFLE		
●	MAX. INLET MANIFOLD (flow thru full length)	.92" x .42" x 5.1"	0.76 psi
●	INLET ORIFICE (manifold → baffle)	52 x .050" x .400" vel. hd.	0.30 psi
		<u>75 μin.</u>	<u>200 μin.</u>
●	FRICITION LOSS 52 - .050" x .076" PASSAGES	92.1	104.0
●	TRANSITION LOSS .050" → .090" PASSAGES (1 V. H.)	5.7	5.7
●	FRICITION LOSS 52 - .090" x .076" PASSAGES	4.2	4.7
●	EXIT VEL. HD. 52 - .090" x .076" PASSAGES	2.6	2.6
●	OUTLET ORIFICE (baffle-man.) VEL. HD. - 52 x .090" x .400"		0.09 psi
●	MAX. OUT MANIFOLD = 1.20" x .42" x 5.1" high		<u>0.50 psi</u>
	Calc. Baffle ΔP , psi	<u>104.6</u>	<u>117.0</u>
		<u>1.6</u>	<u>1.6</u>
	Calc. ΔP with manifolds, psi	106.2	118.6
●	EXPERIMENTAL ΔP = 170 psi		

Post-test hardware inspection indicated that the coolant passages were within 0.002 in. of the nominal dimension where checked. This amounts to approximately a 4% error in the dimension, which can result in approximately a 22% error in pressure drop. This does not take into account possible rounding in the corners of the passage, nor does it take into account the possibility of the few locations checked being representative of the whole baffle. Measurements of the channel roughness were not made, but they appear to be in the neighborhood of 300 microinches. This is higher than normal because of the EDM machining method used. Assuming this roughness, this would represent another 22% increase in pressure drop over the original design. Together, this represents an increase of 50% over the original design analysis; this would account for the large difference between theoretical and experimental results.

In a future design, the large roughness value can readily be taken into account when designing the baffle channel geometry. Now that the type of tolerances to be expected is known, they can also be taken into account in the next design.

Thermal Efficiency of Conditioner

The theoretical thermodynamic efficiency of the conditioner is equal to the hot gas enthalpy loss to the nominal exit temperature divided by the enthalpy loss to the minimum available exit temperature. This minimum temperature would be the liquid hydrogen inlet temperature (for the hydrogen conditioner) for a counterflow heat exchanger, or the hydrogen outlet temperature (225R with no bypass) for a parallel flow heat exchanger. The selected heat exchanger is basically of the latter design. However, the operating requirements for the heat exchanger is that the hot gas temperature cannot drop below the freezing temperature of the water trapped within the combustion products in order to avoid bulk icing. This limits the minimum available hot gas temperature for the design to 32F (492R). Using the hot gas enthalpy as a function of temperature as shown in Figure 113 for a mixture ratio of 1.0, with the nominal reactor hydrogen injection temperature of 275R results in a theoretical combustion temperature of 2060R. The resultant enthalpy loss to the nominal gas exit temperature of 750R is 2360 Btu/lb. The available enthalpy going down to 492R exit temperature is about 3380 Btu/lb, resulting in a thermodynamic efficiency of about 70%. This was deemed satisfactory for this

design since the requirement was that the system weight be minimized. The thermal efficiency can readily be increased by increasing the operating mixture ratio (combustion temperature). For example, at a mixture ratio of 3 with a combustion temperature of about 4460 R, the efficiency increases to 89% for a design outlet temperature of 750 R, or 74% for an outlet temperature of 1000 R.

Experimental Thermal Efficiency

The experimental thermal efficiency compares the heat transferred in the as-built hardware to the theoretically available heat for transfer. Due to tolerance effects the hardware was not built to exactly nominal dimensions. Also, the injector did not produce 100% combustion or a uniform flow and mixture ratio distribution. These will be discussed in terms of how they relate to the experimental efficiency.

Based on the early tests, the calculated hot gas flow area (based on chamber pressure, mixture ratio, and total gas flow) was very close to the measured area, indicating that the calculated pressure drops are correct and that the gas flow area was close to nominal. As a result this should have no effect on the as manufactured thermal efficiency.

The slightly smaller conditioned hydrogen channel dimensions and increased surface roughness had little influence on the surface area but did increase the coolant side heat transfer coefficient, resulting in cooler walls and more heat transferred for a given flowrate. Based on the theoretical results presented previously, showing the effect of conditioned hydrogen flowrate on heat input, increasing the hydrogen flow from 4.5 to 5.95 lb/sec results in only a 3% change in the heat input. This change in flow represents a 32% change in mass velocity, whereas the increased pressure drop can be accounted for by approximately an 8% increase in mass velocity with about the same equivalent increase due to roughness. With half the increase in mass velocity, the 50% increase in pressure drop could produce about a 1½% increase in efficiency. Even this is too high, since an increased hydrogen flow used in the analysis reduces the hydrogen outlet temperature and increases the temperature potential and heat input; this does not occur in a system where nothing has changed except for the pressure drop. Consequently it is concluded that the large increase in the conditioned hydrogen pressure

drop over the design value causes about a 1% increase in thermal efficiency in the as-built hardware. This result is not too surprising, as previous parametric studies showed that the wall temperatures are not very sensitive to variations in hydrogen mass velocity. Another aspect of having a high conditioned hydrogen pressure drop is that it would stabilize the hydrogen flow system, so that instabilities would be less likely to show up. This is true for a given hydrogen flowrate. However, if the as-built design were operated with a reduced flow in order to achieve the correct pressure drop, the hydrogen system would be less stable due to the higher hydrogen outlet temperature and thus reduced exit density. This could easily have been checked by increasing the hydrogen bypass for one or two tests. This was not done, however, as indicated earlier, because of high erroneous hot wall temperature readings from the baffle thermocouples.

The injector mixture ratio distribution as well as the completeness of combustion affected the measured conditioner efficiency. Based on earlier discussions, the experimental data indicated a combustion efficiency of 95-96%; this resulted in reducing the thermal efficiency 11-15% based on theoretical considerations.

The effect of a few thousandths variation in the various hot gas gaps appeared to have little effect on the heat transferred to a baffle, based on data for the early tests (prior to Test 218). The two side passages were measured to be 0.010-0.020 less than the center hot gas passage widths; yet for the early tests the left side wall had nearly the same heat input as the baffles (considering that the side wall only has half the area). On the later tests the right side wall had some very appreciable heat inputs on several tests. This appears to strengthen the argument that the hot gas gap distribution has little effect on the conditioner performance. This is at least partly accounted for by the design, where each baffle is exposed to two hot gas passages, thereby averaging out differences in the gas gaps. The narrower gaps will carry less hot gas flow, and will thus tend to ice sooner. However, near the nominal operating point icing does not seem to be an operational problem, based on the test results; this was shown both by the insensitivity of gas flow area to the ratio of hot gas to conditioned hydrogen flowrates, and by comparing the calculated hot gas flow area for the early tests to the directly measured dimensions of the gas flow passages.

The experimental thermal efficiency compares the heat transferred for a given hot gas flowrate in the as-built hardware to the heat which should theoretically have been transferred for that flowrate. This represents the amount the theoretical efficiency presented above is reduced from the design value. The experimental efficiency can be represented as a hot gas enthalpy ratio:

$$\eta_{\text{experimental}} = \Delta H_{\text{measured}} / \Delta H_{\text{design}}$$

This parameter is presented as a function of test number in Fig. 98. The experimental range is between 0.8 and 1.0, with an average of about 0.89. This can be accounted for completely by the measured combustion efficiency of about 95-96%, as shown in Fig. 100.

In reviewing the hot gas outlet temperature data, it is noted that several of the thermocouples measure temperatures appreciably less than the nominal 750 R for many of the tests. The hot gas passage between baffles 3 and 4 is the only one that consistently reads appreciably greater than the design value. This again indicates that the lower than expected heat input to the baffles is not due to the baffle design or due to tolerances built into the hardware. It indicates that the baffles are trying to extract the available heat, but that a reduced heat was available because of the reduced injector efficiency (100% combustion efficiency was assumed for the original design analysis). While the assumption of 100% combustion may not have been entirely realistic, the net effect on the design would have been minor. It would have been compensated for by increased gas flow and/or increased mixture ratio, which could also have been accomplished after the hardware had been built. The only effect on the hardware itself may have been small adjustments to the injector orifices to accommodate the different reactor flow, and slightly larger hot gas flow area in order to maintain the same chamber pressure. These can be considered as refinements to the basic design.

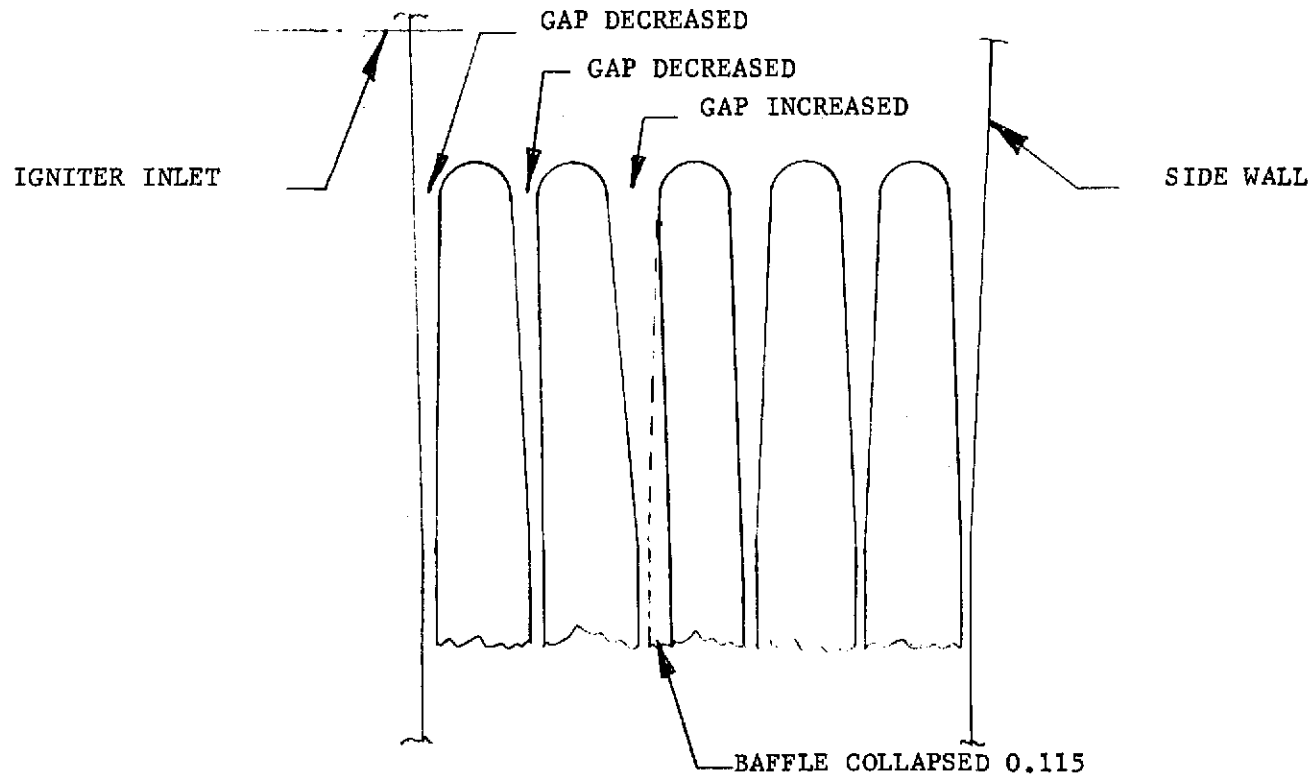
POSTTEST HARDWARE EVALUATION

Following the first series of igniter only tests, the injector assembly was removed from the conditioner for visual inspection of the baffle assemblies and the conditioner walls. There was no evidence of any overheating or hot spots in the conditioner assembly. The injector assembly was reinstalled to the conditioner and no further internal inspection of the conditioner assembly was performed until completion of all hot fire tests planned for hydrogen.

Upon disassembly of the injector assembly from the conditioner subsequent to all hot fire tests, it was again noted there was no evidence of baffle or conditioner wall overheating, but it was noted that the leading or forward ends of the baffles had deflected from their initial position, causing a pronounced variation in hot gas gaps, and that the center or instrumented baffle collapsed in the region where the baffle honeycomb had been removed for thermocouple installation. Fig. 123 is a sketch of the baffle position and location of the baffle collapse after test; Fig. 124 shows the actual hot gas gap dimensions before and after test; and Fig. 125 denotes the region of baffle collapse.

Subsequent to removal of each baffle assembly from the conditioner, each baffle was water-flow calibrated to ascertain any variation in coolant channel geometry. All five baffle assemblies flowed within +2% of each other at several pressure drop measurements.

The collapsed or center baffle was sectioned at the forward edge, as shown in Fig. 126. The coolant channels showed no evidence of distortion and the channel dimensions were well within the drawing tolerances. A chart of the channel cross-section dimensions per drawing, as fabricated, and posttest is shown on the next page.



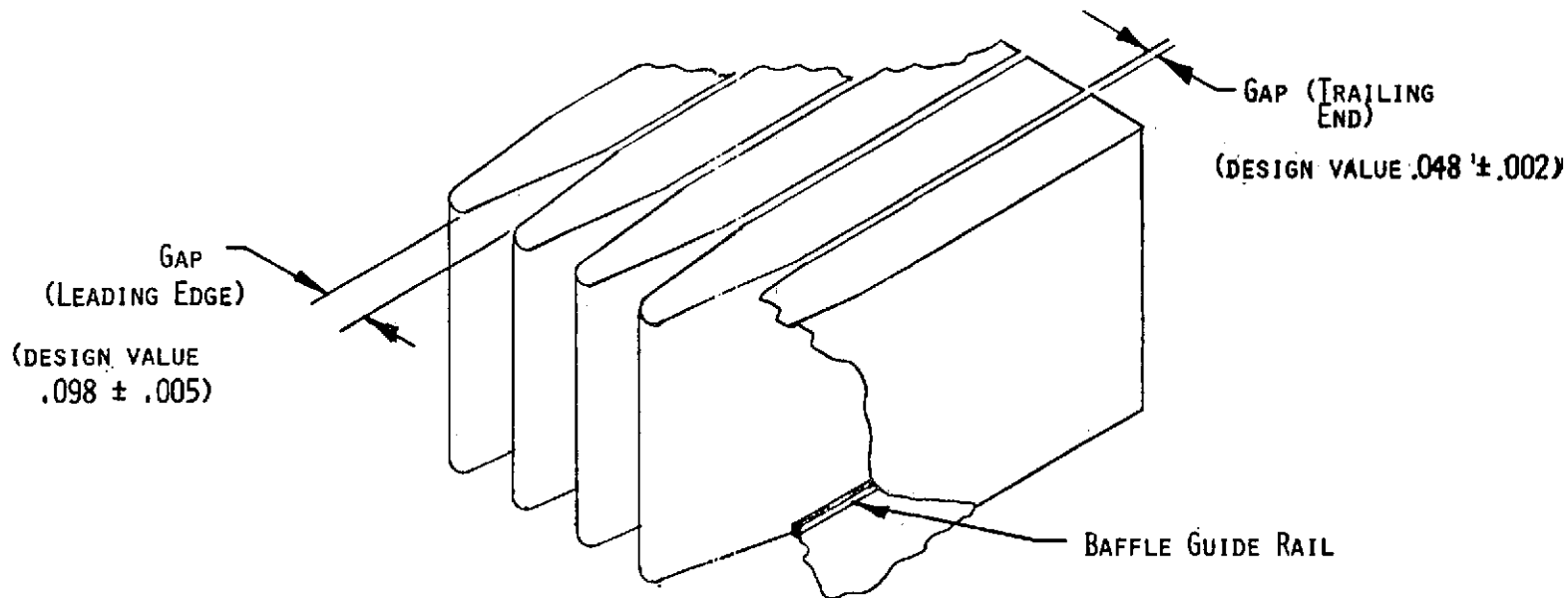
1. POSSIBLE CAUSE OF DAMAGE

- A. THERMAL
- B. PRESSURE

2. TO CAUSE PERMANENT DAMAGE

- A. Δt ACROSS THE BAFFLE MUST BE GREATER THAN 350 DEGREES
- B. Δp ACROSS THE BAFFLE MUST BE 100 psi @ AMBIENT CONDITIONS TO 65 psi @ 800 F

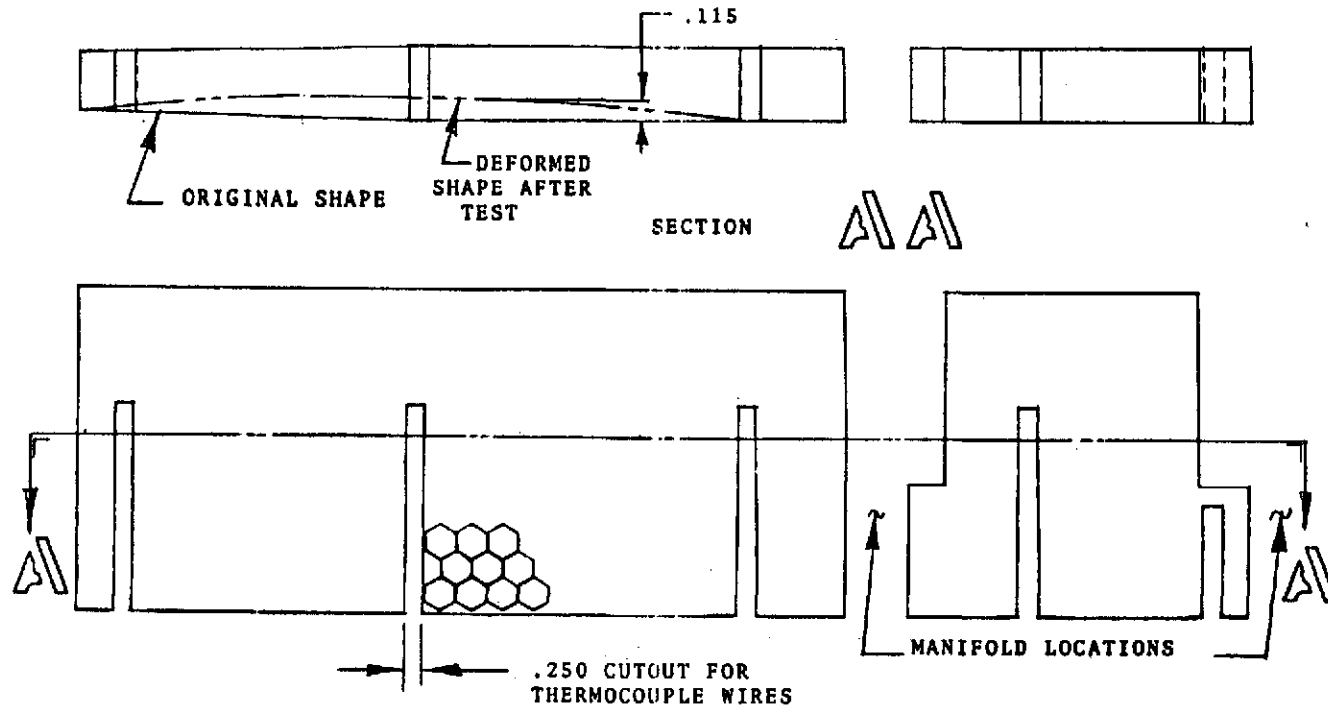
Figure 123. Hydrogen Conditioner, Unit No. 1, Baffle Deflection



LEADING EDGE GAP		
GAP NO.	GAP (INCHES)	
	PRE TEST	POST TEST
1	.060	.065
2	.090	.085
3	.077	.080
4	.083	.150
5	.090	.040
6	.054	.034

TRAILING EDGE GAP		
GAP NO.	GAP (INCHES)	
	PRE TEST	POST TEST
1	.031	.031
2	.046	.046
3	.053	.053
4	.038	.038
5	.053	.053
6	.040	.040

Figure 124. Hot-Gas Gap Dimensions



- 1. BASED ON HONEYCOMB CORE BUCKLING, PRESSURE REQUIRED FOR BUCKLING = 400 PSI.

Figure 125. Sketch of Honeycomb Cutout

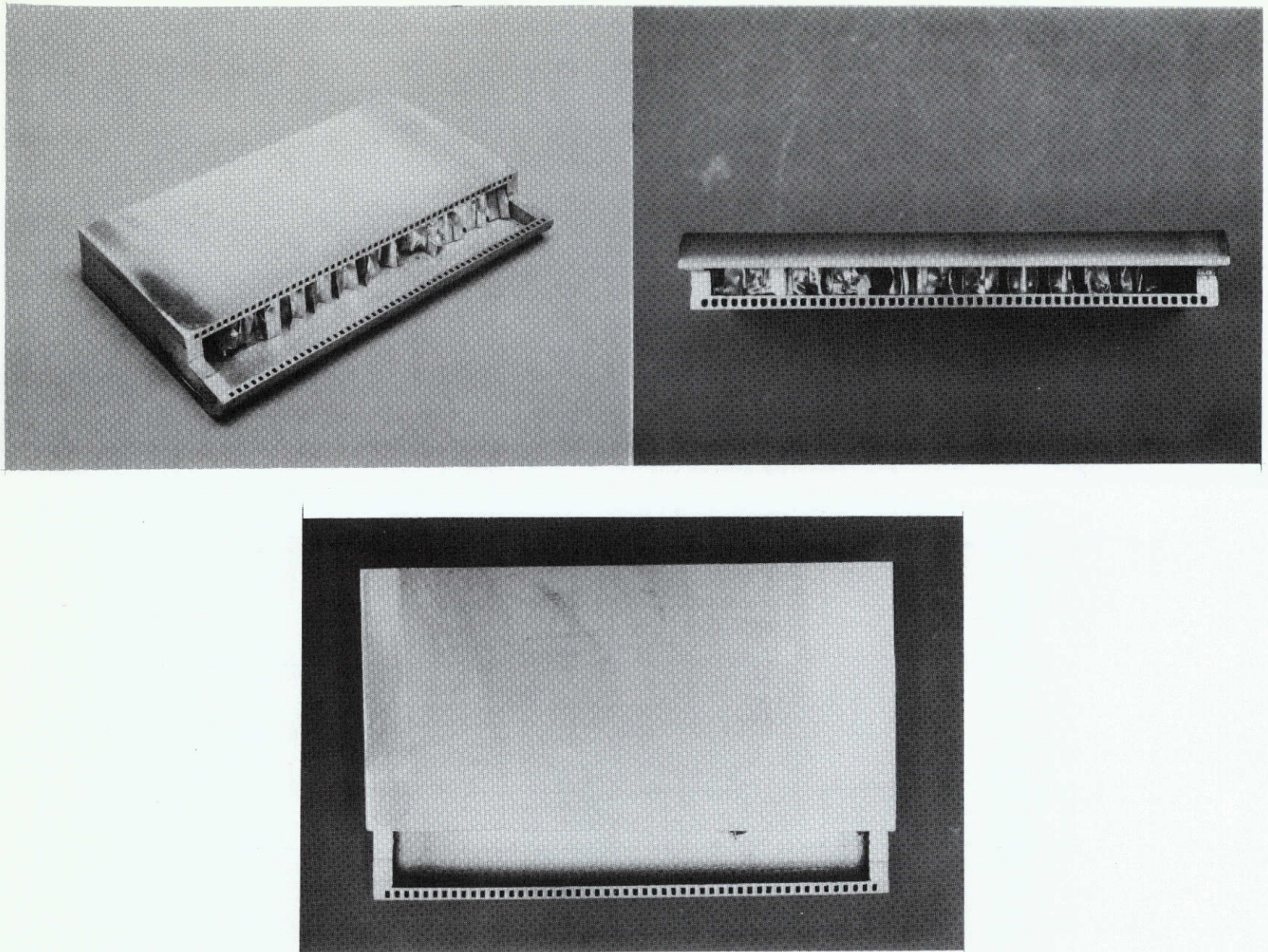


Figure 126. Sections of Instrumented Baffle

	<u>Design</u>	<u>As Fabricated</u>
Width	.050 <u>+</u> .002	.050 <u>+</u> .001
Depth	.075 <u>+</u> .004	.072 <u>+</u> .002

The sectioned portion of the baffle assembly verified the brazing technique used for the braze joint of the Haynes 188 to the 304L stainless indicated an exceptionally good bond with good braze fillets in the channels. The 347 stainless honeycomb to the 304L stainless closure was also well brazed with a very clean and shiny surface, indicating that the hydrogen purging technique used was well adapted to this configuration.

Each of the conditioner side walls as well as the top and bottom wall showed no evidence of overheating or distortion as evidenced by the fact that the post-test internal box dimensions of the conditioner were within .005 inch of their original value.

An analysis of the buckled baffle assembly indicated the possible cause of failure to be either temperature variation from one side to the other or excessively high pressure in the combustion portion of the conditioners. To determine an absolute value and the variation in pressure to collapse a baffle with some honeycomb structure removed in comparison to a baffle without any honeycomb removed, two sample panel assemblies as shown in Fig. 127 through 129. were fabricated in a manner similar to that used in the conditioner baffle construction. After fabrication of the two samples, each sample was hydraulically crushed to failure as shown in Fig. 130 and 131. The -003 specimen (without cutout) failed at 1450 psi and the -005 specimen (with a .250 cutout) failed at 1250 psi. These high values strongly indicate that pressure alone was not the cause of the conditioner baffle failure.

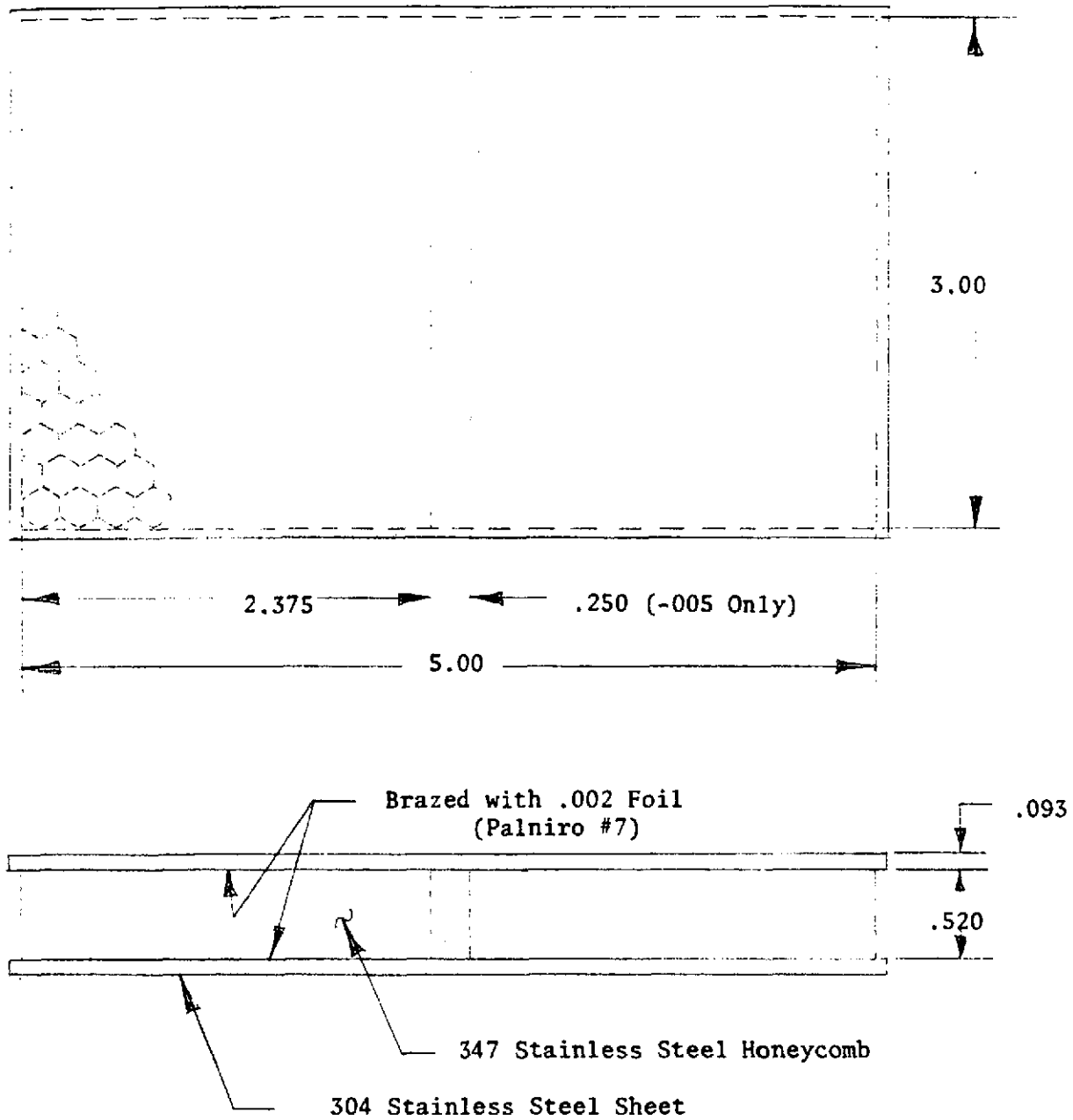
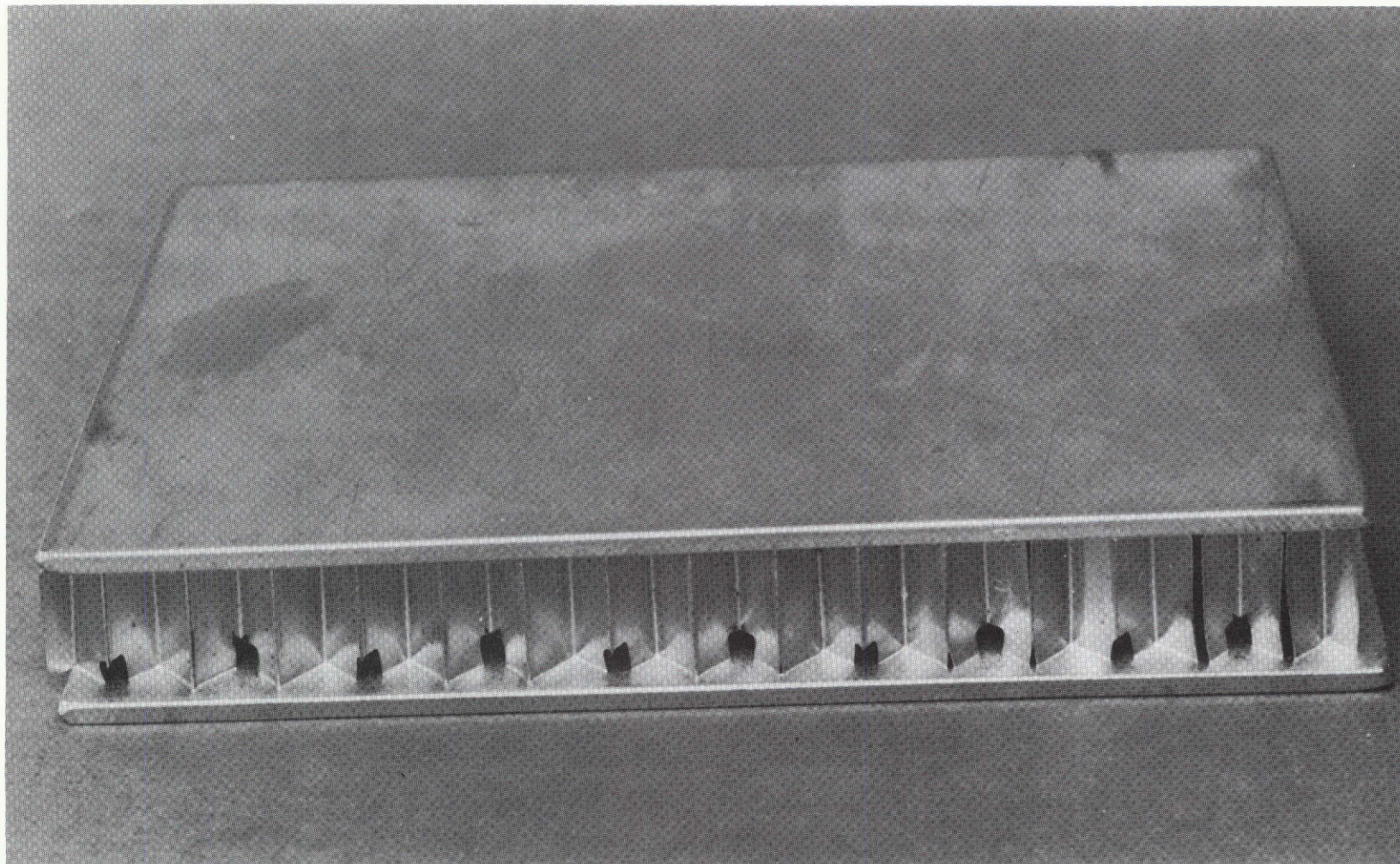
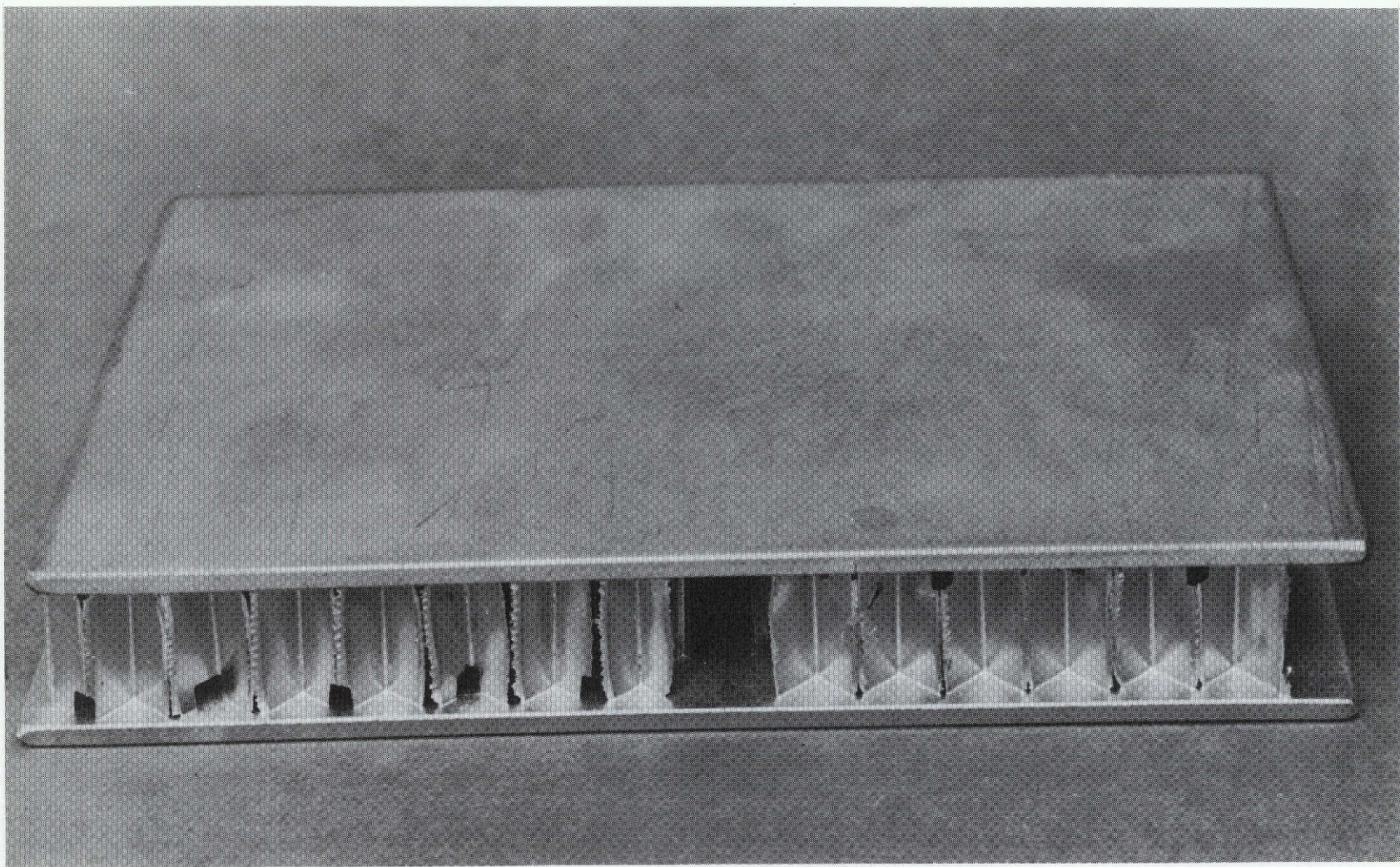


Figure 127. Baffle-Buckling Test Specimen (-003 Specimen Without Cutout) and (-005 Specimen With 0.250 Cutout)



5AG49-1/3/73-C1A

Figure 128. As Fabricated -003 Sample Baffle (No Cutout in Honeycomb)



5AG49-1/3/73-C1B

Figure 129. As Fabricated -005 Sample Baffle (With Cutout in Honeycomb)

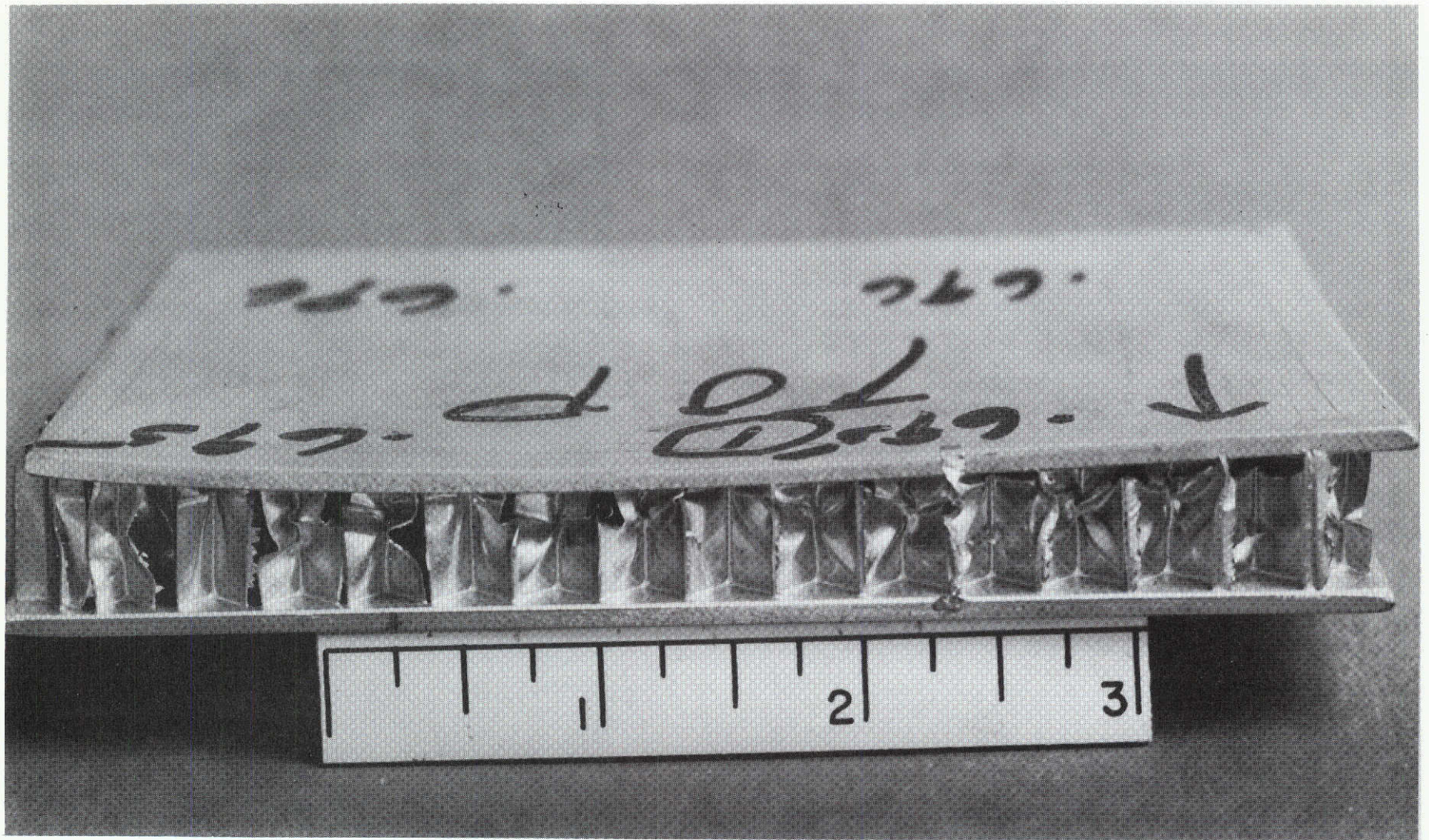
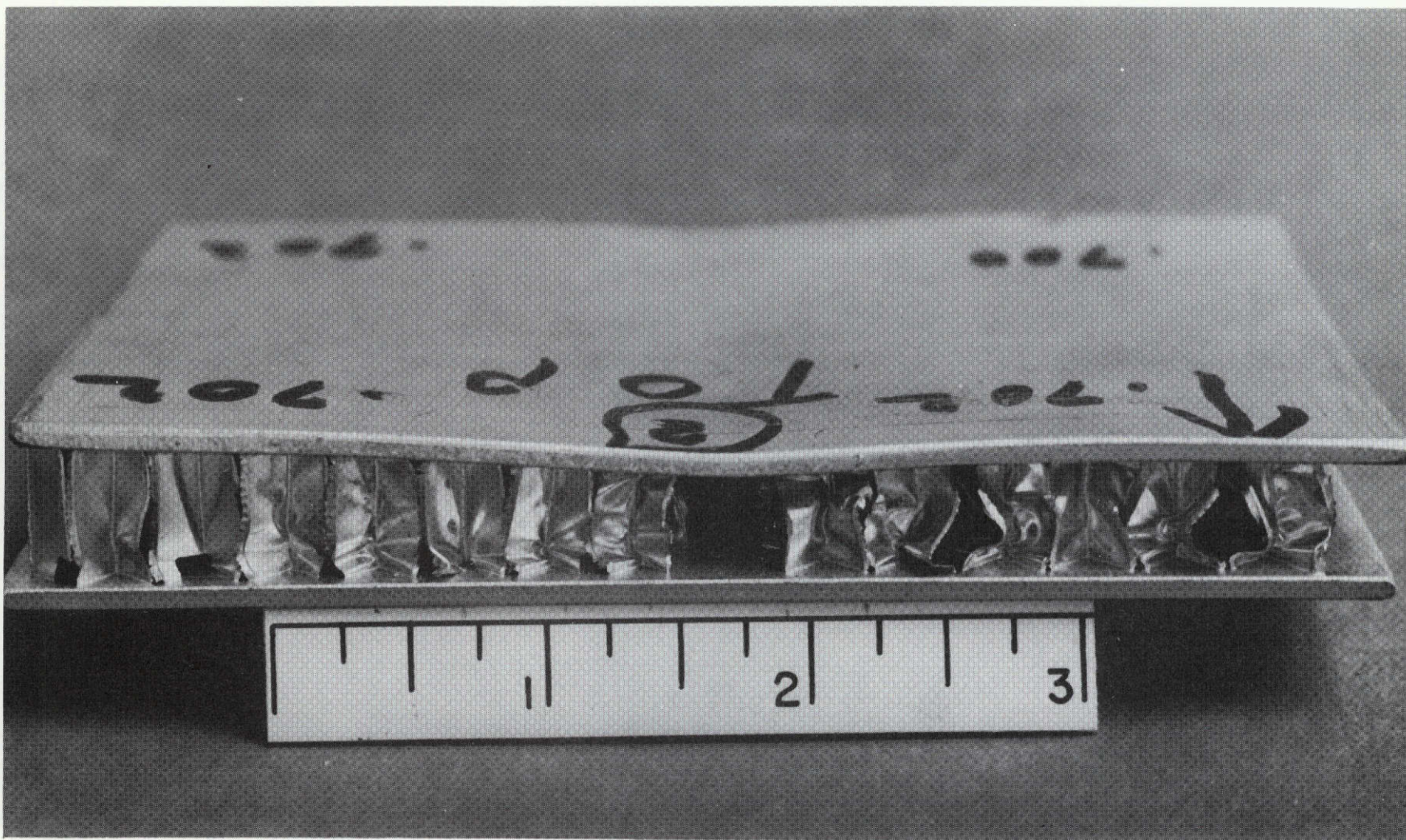


Figure 130. -003 Sample Baffle After Collapse at 1450 psig

5AG49-1/4/73-C1A



5AG49-1/4/73-C1B

Figure 131, -005 Sample Baffle After Collapse at 1250 psig

TECHNOLOGY DEVELOPMENT

A technology task was conducted to determine the injector mixture ratio and heat flux distribution, and to determine the effect of the igniter on the combustor and baffle heat fluxes. For this purpose an uncooled piece of hardware was designed, built and tested using the injector and igniter that was planned for the full size hardware. The nose section of each of the five baffles was simulated, with the nominal hot gas gap. Baffle instrumentation included hot wall thermocouples at the stagnation point and within the gap on each baffle to give an indication of the heat flux distribution from left to right and from top to bottom. An additional hot wall thermocouple was located in the side wall across from the igniter to determine the effects of the injector and igniter on the local heat flux. In addition, the injector face itself had three face thermocouples to verify that it was operating at a satisfactory temperature. A schematic of the hardware and associated instrumentation is shown in Fig. 132 and 133 while a photograph of the solid wall conditions is shown in Fig. 134. Another purpose of the solid wall chamber was to verify the ignition and start characteristics of the side-mounted igniter.

This effort was concentrated on experimentally verifying the compatibility of the trislot reactor injector and the side mounted igniter. This was accomplished through a series of hot firing tests of the injector and igniter assembly in a solid wall chamber.

The injector shown previously in Fig. 88, incorporated trislot injection elements with elements arranged in a rectangular pattern and aligned in such a manner that they are aligned with the hot gas passages between the simulated heat exchange baffles.

INJECTOR THERMAL ANALYSIS

A steady state thermal analysis of the trislot injector face was performed at nominal operating conditions ($MR = 1$, $T_c = 1600F$, $T_{H_2} = 275R$, $T_{O_2} = 375R$). For this purpose an area consisting of 1/2 injector element in width and 1/2 the

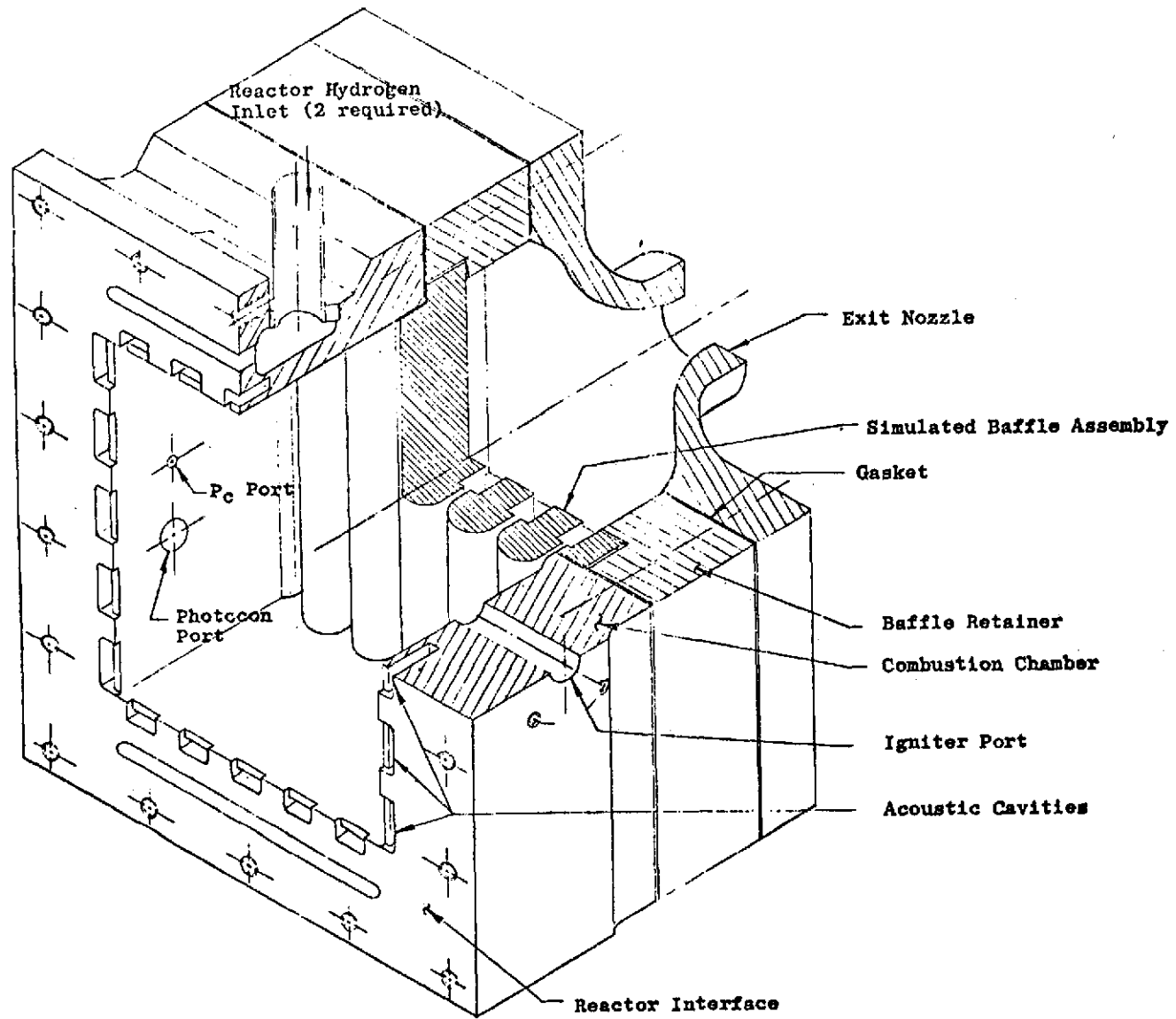


Figure 132. Solid Wall Chamber

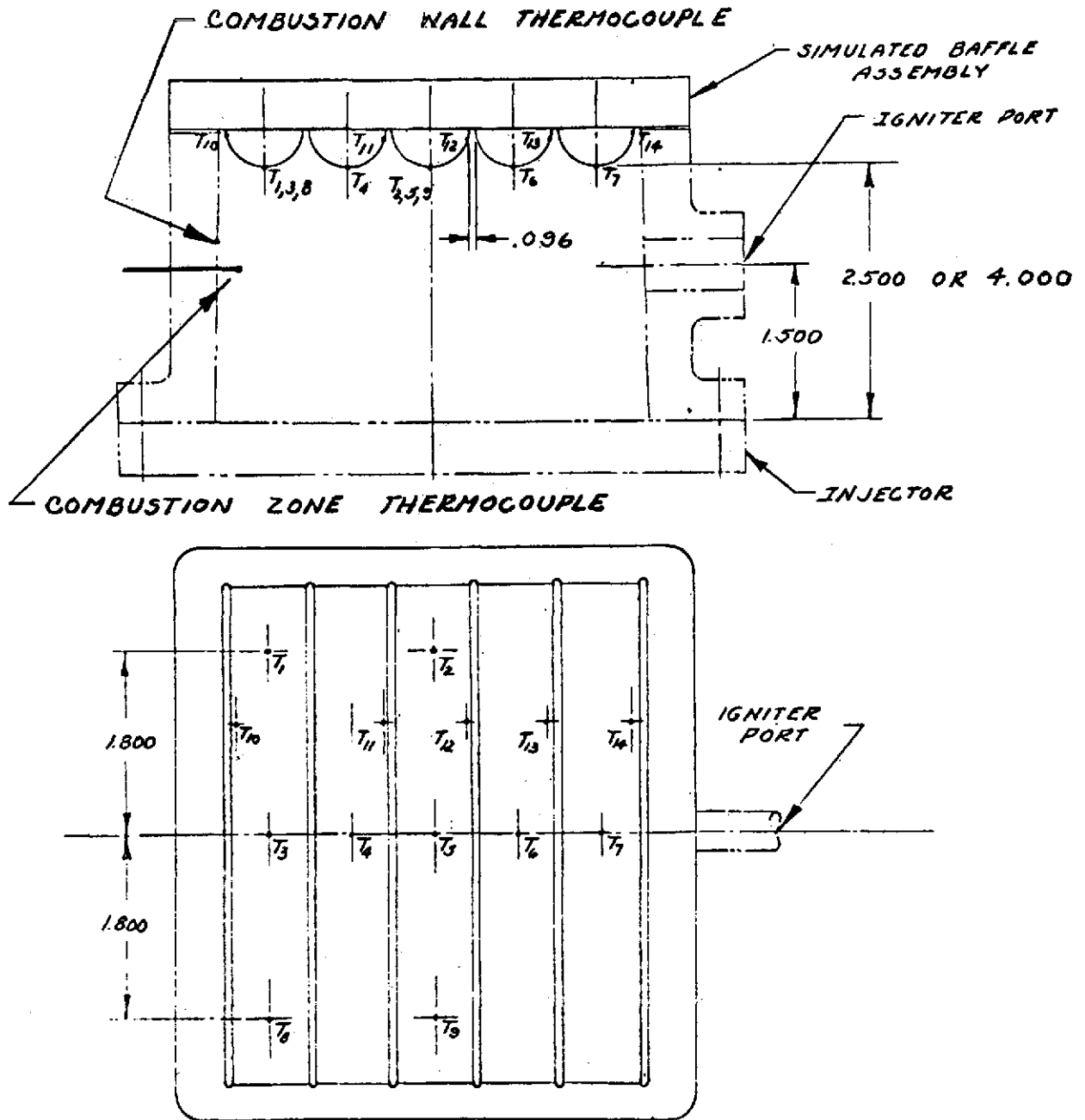


Figure 133. Uncooled Dummy Baffle Thermocouple Locations

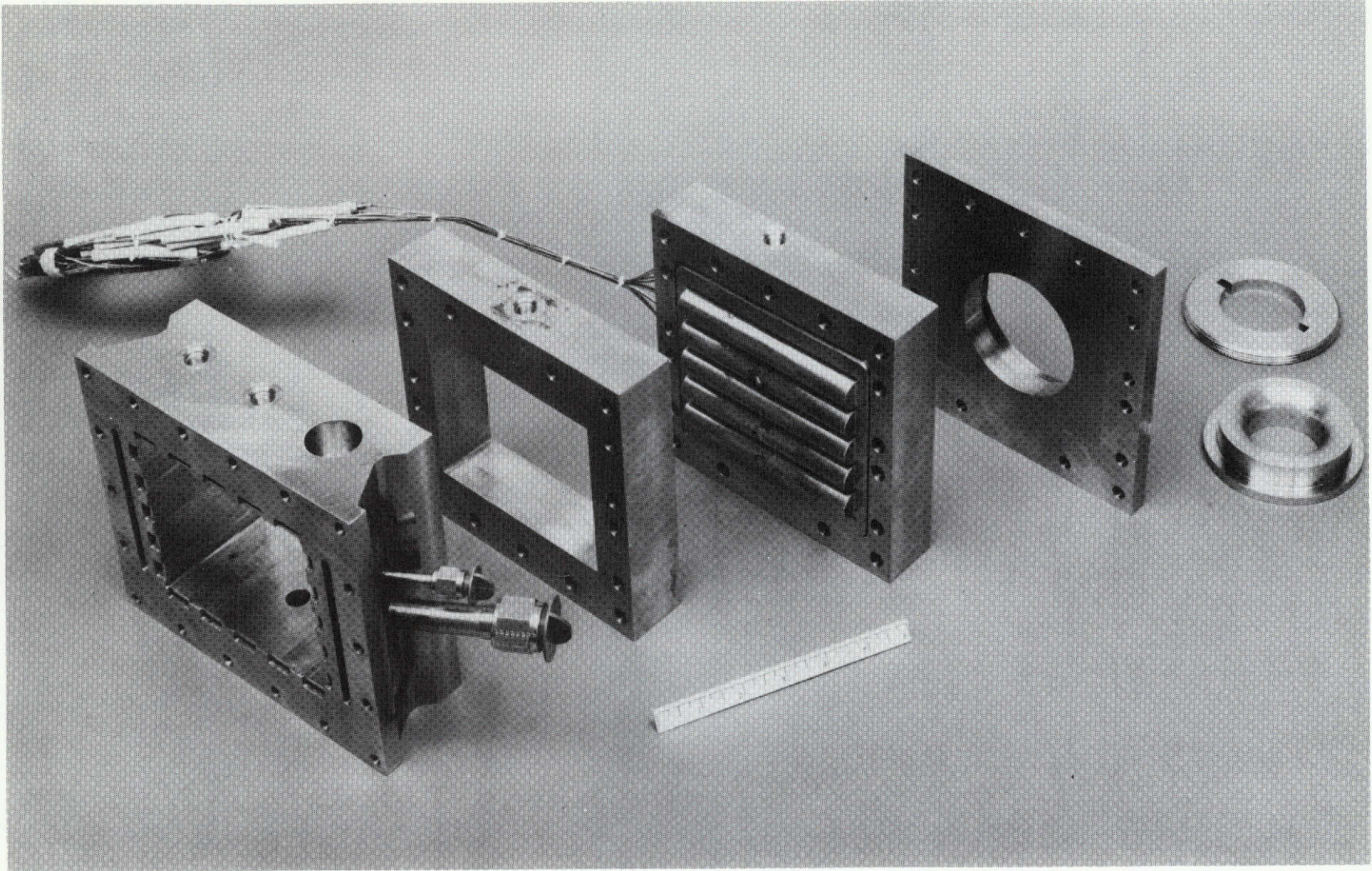


Figure 134. Solid Wall Conditioner

1ST52-11/5/71-C1B

injector face in length, and the depth of the copper face plate was programmed for the HEATING program. Two hot gas heat transfer coefficients were analyzed: one represents the value in the combustor upstream of the baffle, and the second one represents twice this heating rate. These represent heat fluxes of about 0.8 and 1.6 Btu/in²-sec respectively. Furthermore, both of these values are expected to be conservative, the maximum heat flux analyzed being 40 percent of the maximum heat flux in the conditioner. For the same combustor mass velocities, data from Ref. 3 indicated lower heat fluxes than assumed here. Results are shown in Fig. 135 and 136 for the low and high heat flux cases respectively. At the lower heat flux, heated face temperatures range from a predicted low of 3F to a high of about 180F. The temperature drop across the copper from the heated surface to the hydrogen feed passage is only about 20F. At the higher heat flux condition, the face temperatures ranged from a low of 100F to a high of about 440F. These temperatures are acceptable for OFHC copper, and no overheating problems are foreseen. As expected, highest temperatures occur at the injector centerline, since because of the symmetrical hydrogen feed system there is presumably no hydrogen flowing in the feed passages in this region. It is noted that while there tends to be relatively strong temperature gradients in the direction of hydrogen flow through the feed passage, there is a much smaller temperature gradient in the other direction (midway between elements to the element centerline).

Somewhat higher face temperatures can be expected with higher propellant injection temperatures. Verification of these predicted temperatures were obtained during the test program through direct temperature measurements on the injector face.

$T_{H_2} = -185F (275R)$	$G = .125 G_{H_2}$ ELEMENT $.76 \text{ INCH} < Y < 1.96 \text{ INCH}$
$T_{O_2} = -85F (375R)$	$G = 0$ $Y > 1.96 \text{ INCH}$
$T_{H_C} = 1600F (2060R)$	$(h_c) \text{ SLOT} = .00865 \text{ BTU/IN}^2 - \text{SEC} - F$
H_2 FEED PASSAGE ($0 < x < .3 \text{ INCH}$)	$(h_c) \text{ SLOT} = .0030 \text{ BTU/IN}^2 - \text{SEC} - F$
$G = .25 G_{H_2}$ ELEMENT $0 < Y < .76 \text{ INCH}$	$h_g = .00058 \text{ BTU/IN}^2 - \text{SEC} - F$

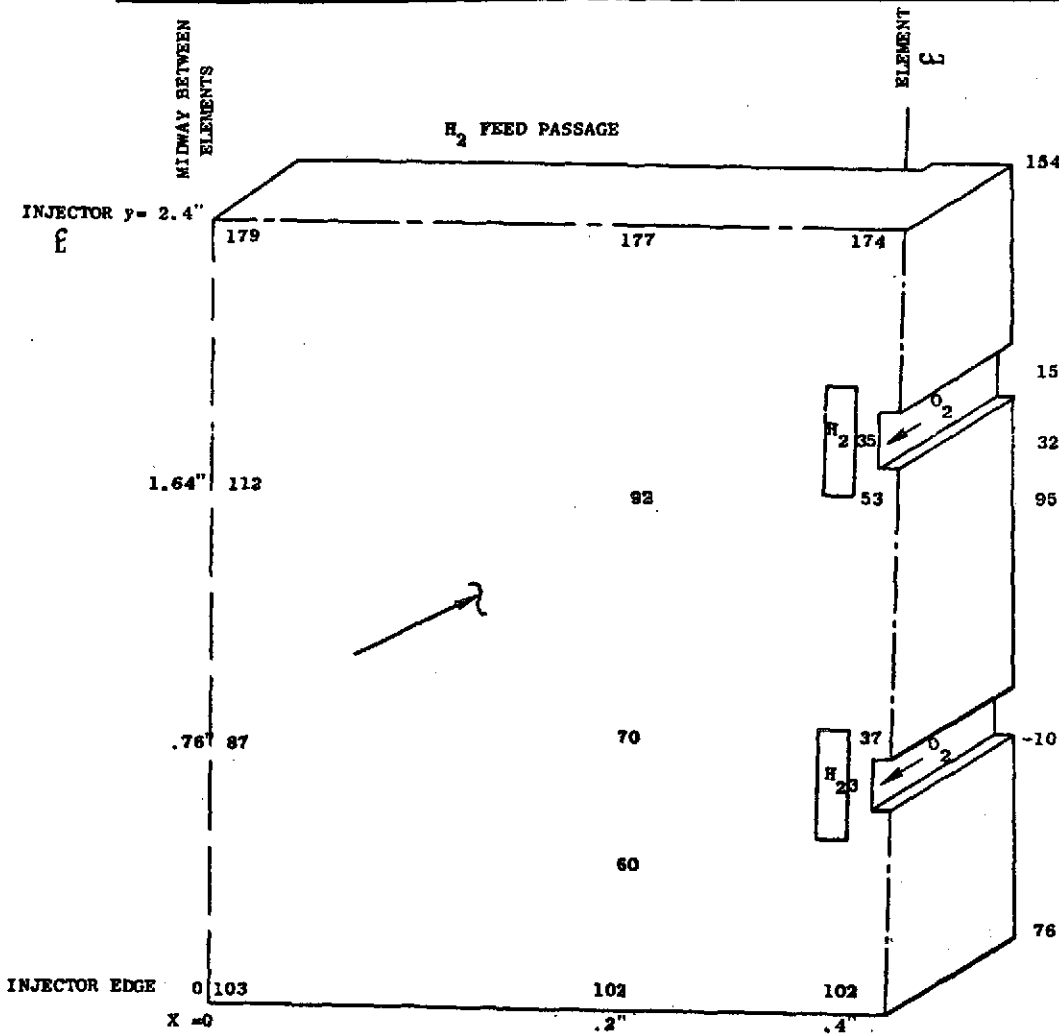


Figure 135. H₂ Conditioner - Injector Face Temperature (Nominal Heat Flux) (Injector End Combustor Heat Flux)
 Q/A ~0.8 Btu/in.²-sec, MR = 1, W_{HG} 1.2 lb/sec

$T_{H_2} = 185F (275R)$	$h_{c_{slot}} = 0.00865 \text{ BTU/IN}^2\text{-SEC-F}$
$T_{O_2} = -85F (375R)$	$h_c = 0.0030 \text{ BTU/IN}^2\text{-SEC-F}$
$T_{HG} = 1600F (2060R)$	$h_g = 0.0012 \text{ BTU/IN}^2\text{-SEC-F}$
$H_2 \text{ FEED PASSAGE } (0 < X < 0.3 \text{ IN.})$	$Q/A_{FACE} \sim 2 \text{ } Q/A_{COMBUSTOR} \sim$
$G = 0.25 \text{ G/ELEMENT } 0 < Y < 0.76 \text{ IN.}$	$1.6 \text{ BTU/IN}^2\text{-SEC}$
$G = 0.125 \text{ G/ELEMENT } 0.76 \text{ IN.} < Y < 1.96 \text{ IN.}$	$MR = 1$
$G = 0$	$Y > 1.96 \text{ IN. } W_{HG} = 1.2 \text{ LB/SEC}$

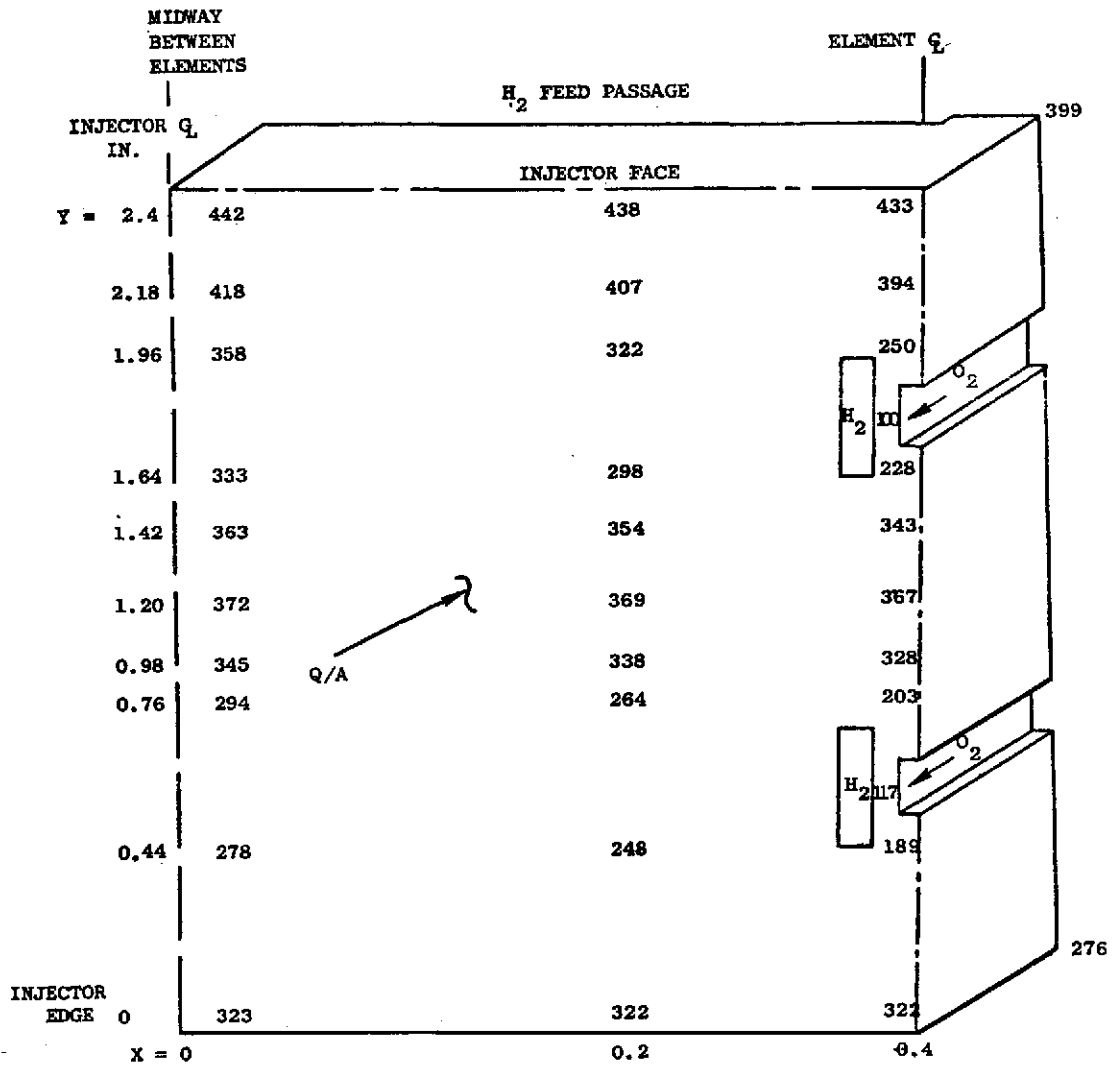


Figure 136. H₂ Conditioner Injector Face Temperatures (Peak Heat Flux)

TEST RESULTS

A total of 54 tests was conducted on the solid wall conditioner, including 42 mainstage tests and 12 ignition only tests for an accumulated duration of 126 seconds. These tests were conducted over a range of propellant temperatures, chamber pressures and mixture ratios as summarized below.

Solid Wall Conditioner Tested 54 Times

12 - Ignition Only Tests

42 - Mainstage Tests

Range of Conditions Tested

Chamber Pressure, Psia	71 - 301
Reactor Mixture Ratio	
Ignition Phase	0.43 to 2.26
Mainstage	0.73 to 3.28
Igniter Mixture Ratio(at Ignition)	0.2 to 1.0
Hydrogen Temperature, R	530 - 184
Oxygen Temperature, R	530 - 234
Duration, Sec	
Ignition Phase	0 to 1.5
Mainstage	0 to 8.4
Accumulated Duration, Sec	126

A compilation of test parameters is presented in Table 34.

Ignition was achieved on all tests except one very low (0.4) mixture ratio test. The wide ranges of flowrates and propellant temperatures over which the torch igniter is operable were thus demonstrated. The igniter was in excellent condition after the test series.

FOLDOUT FRAME

TABLE 34. TEST RESULTS

** Test No.	Duration, Seconds	P psia	Total Flowrate lb/sec	Mixture Ratio			Purpose
				Total	Injector	Igniter	
1 (Ign)	1.0	122	0.71	0.55	0.56	0.32	Ignition Only Test Ignition/Mainstage Tests
2 (Ign)	1.0	148	0.79	0.58	0.59	.35	
2 (MS)	2.0	176	0.87	0.75	0.78	.14	
3 (Ign)	1.0	149	0.79	0.67	0.69	.39	
3 (MS)	2.0	181	0.88	0.85	0.89	.17	
4 (Ign)	1.0	218	1.08	0.76	0.79	.16	
4 (MS)	2.0	241	1.16	0.89	0.93	.20	
5 (Ign)	1.0	194	1.04	0.60	0.61	.37	
5 (MS)	0.5	232	1.13	0.72	0.76	.11	
6 (Ign)	1.0	142	0.80	0.57	0.58	.35	
6 (MS)	1.8	174	0.88	0.73	0.73	1.10	
7 (Ign)	0.8	195	1.04	0.69	0.71	.40	
7 (MS)	1.9	241	1.17	0.88	.88	1.17	
8 (Ign)	0.9	144	0.78	0.66	.67	.39	
8 (MS)	1.9	177	0.87	0.83	.83	1.15	
9 (Ign)	0.9	222	1.25	0.54	.65	.43	
9 (MS)	1.9	271	1.39	0.83	.83	1.20	
10 (Ign)	0.9	142	1.29	0.71	.72	.40	
10 (MS)	1.4	283	1.44	0.90	.90	1.25	
11 (Ign)	0.9	244	1.28	0.69	.70	.43	
11 (MS)	1.4	301	1.44	0.89	.89	1.19	
12 (Ign)	0.9	176	0.76	0.85	.88	.48	
12 (MS)	1.2	180	0.86	1.08	1.06	-	
13 (Ign)	0.9	200	1.02	0.85	.87	.48	
13 (MS)	1.9	241	1.15	1.07	1.05	-	
14 (Ign)	0.9	222	1.14	0.86	.88	.49	
14 (MS)	1.8	279	1.28	1.08	1.13	-	
15 (Ign)	0.3	99	0.69	0.73	0.74	0.48	
15 (MS)	3.0	156	0.85	.72	0.73	.39	
16 (Ign)	0.3	141	0.77	.55	0.55	.49	
16 (MS)	3.0	220	1.14	.83	0.85	.38	
17 (Ign)	0.3	97	0.45	.65	0.66	.46	
17 (MS)	3.0	154	0.78	1.03	1.05	.48	
18 (Ign)	0.3	154	0.73	.63	.64	.49	
18 (MS)	3.0	236	1.17	1.09	1.11	.51	
19 (Ign)	0.3	103	0.48	.69	.69	.49	
19 (MS)	1.0	153	0.80	1.32	1.35	.64	
20 (Ign)	0.3	153	0.70	.84	.85	.77	
20 (MS)	1.0	228	1.15	1.46	1.49	.69	
21 (Ign)	0.3	103	0.51	.42	.43	.27	
21 (MS)	2.0	152	0.79	.80	.83	.28	
22 (Ign)	0.3	102	0.46	.61	.62	.36	
22 (MS)	2.0	153	0.77	1.01	1.04	.37	
23 (Ign)	0.3	155	0.70	.57	.58	.37	
23 (MS)	2.0	239	1.17	1.04	1.07	.38	
24 (Ign)	0.3	104	0.44	.72	.73	.44	
24 (MS)	1.0	148	0.77	1.27	1.34	.35	
25 (Ign)	0.3	154	0.66	.86	.88	.49	
25 (MS)	1.0	225	1.14	1.31	1.34	.54	
26 (Ign)	0.3	112	0.34	2.02	2.22	0.54	
26 (MS)	2.0	152	0.91	0.69	0.70	.49	
27 (MS)*	2.2	220	1.06	0.74	.75	.46	
28 (Ign)	0.3	91	0.49	0.74	.75	.60	
28 (MS)	2.0	157	0.80	1.28	1.30	.59	
29 (Ign)	0.3	138	0.73	0.76	.76	.60	
29 (MS)	2.0	235	1.20	1.37	1.40	.59	
30 (Ign)	0.3	99	0.49	0.73	0.73	.74	
30 (MS)	2.0	162	0.80	1.70	1.73	.77	
31 (Ign)	0.3	94	0.52	0.50	0.50	.50	
31 (MS)	2.0	159	0.83	1.08	1.10	.48	
32 (Ign)	0.2	116	0.52	1.0	1.04	.41	
32 (MS)	2.1	236	1.26	1.11	1.13	.49	
33 (Ign)	0.3	96	0.53	0.52	0.53	.42	
33 (MS)	2.0	160	0.85	1.05	1.08	.38	
34 (Ign)	0.3	59	0.29	1.19	1.21	.79	
34 (MS)	0.5	85	0.44	1.75	1.80	.73	
35 (Ign)	0.2	48	0.22	2.19	2.26	1.02	
35 (MS)	0.6	71	0.36	3.15	3.28	1.12	
36 (Ign)	0.3	130	0.75	0.51	0.52	.41	
36 (MS)	8.4	236	1.27	0.99	1.02	.36	

Igniter/Mainstage - Igniter
Shutoff During Mainstage

Ignition/Mainstage Tests
T_o = 398 - 442R
T_f = 215 - 367R

Ignition/Mainstage Tests
T_o = 307 - 445R
T_f = 184 - 425R

FOLDOUT FRAME

* No ignition phase

** Test number start with 1 commencing with the start of each calendar year

Combustion was acceptably stable during all conditions. Only during tests with the coldest propellants did occasional low amplitude ± 15 psi oscillations occur at approximately 11 khz for periods of a few tenths of a second. These oscillations would not be damaging to the cooled conditioner and occurred in the configuration of the solid wall conditioner which had no acoustic cavities. It was thus concluded that the cooled conditioner would not require acoustic cavities.

SOLID WALL BAFFLE DATA ANALYSIS

Heat transfer data on the solid wall chamber was obtained from one Chromel-Alumel (C/A) thermocouple in the combustor opposite the igniter, nine Iron-Constantan (I/C) thermocouples located at the baffle stagnation point, and five C/A thermocouples located on the baffle near the hot gas gap (Fig. 133). All thermocouples were attached to the hot gas surface. Heat flux data was determined from the transient temperature-time data, comparing the experimental results with theoretical values. If the chamber were run sufficiently long to attain steady state, the thermocouples would register the local combustion temperature and thus give an indication of the local mixture ratio and/or combustion efficiency. This was not done, however, as it was undesirable to jeopardize the hardware before obtaining the required data.

To obtain experimental heat transfer coefficients, it was first necessary to perform a theoretical analysis using the hardware geometry and material in order to obtain theoretical temperature-time plots over a range of heat transfer coefficients. For convenience, a standard dimensionless temperature parameter was used; the numerator of which is the temperature rise of the wall surface at any given time, while the denominator is the difference between the hot gas temperature and the initial wall temperature. Time is measured from the start of ignition. The required temperature-time data is obtained from the Astrodata system used to record test data, with the reference time at which ignition occurs being determined from synchronized Brush recorder traces. For the dimensionless temperature parameter, the initial hardware temperature is

determined from the temperature trace on the Brush recorder, and the combustion gas temperature is based on the mainstage total mixture ratio (igniter plus injector). While this does not give quite the correct heat transfer coefficient during the ignition phase, the error in heat flux is small.

Typical plots of the temperature-time traces from which the heat transfer rates were determined are shown in Figures 137 and 138. Due to the sensitivity of the results at small values of time, these values usually differ somewhat from those at later times due to small errors in initial hardware temperature and initial time. Similarly, errors can occur at high values of time, since the correspondence of experimental and theoretical curves depends on the value of the combustion temperature used in reducing the data.

Examination of the transient temperature data indicated that ignition heat fluxes could be obtained in one second of transient operation, and mainstage heat fluxes were obtained in another 1-1/2 - 2 seconds of operation. Also, mainstage data could be obtained in a shorter duration if the ignition phase was reduced in duration.

The experimental baffle stagnation heat flux is shown as a function of hot gas flowrate in Fig. 139 for tests 556 and 567-570 (ignition MR=0.52, mainstage MR=0.72). For clarity, the last two tests at higher mixture ratio were omitted from this figure. It is noted that thermocouple 3 was not functioning, and thermocouple 2 is probably not reading correctly. Of the remaining thermocouples, those at locations 1, 4, 5, and 8 have the same ignition heat flux, and those at 1, 4, 5, 8 and 9 have the same mainstage heat flux. The heat flux at thermocouple 6 (2nd baffle from the igniter) has stagnation point heat fluxes approximately 50 percent higher than the "nominal" experimental value, although lower than the design value. Thermocouples 7 and 14 show somewhat different behavior than the rest, although the peak values measured do not differ much from those at 6 and 13, respectively. This may be due to the proximity of the igniter.

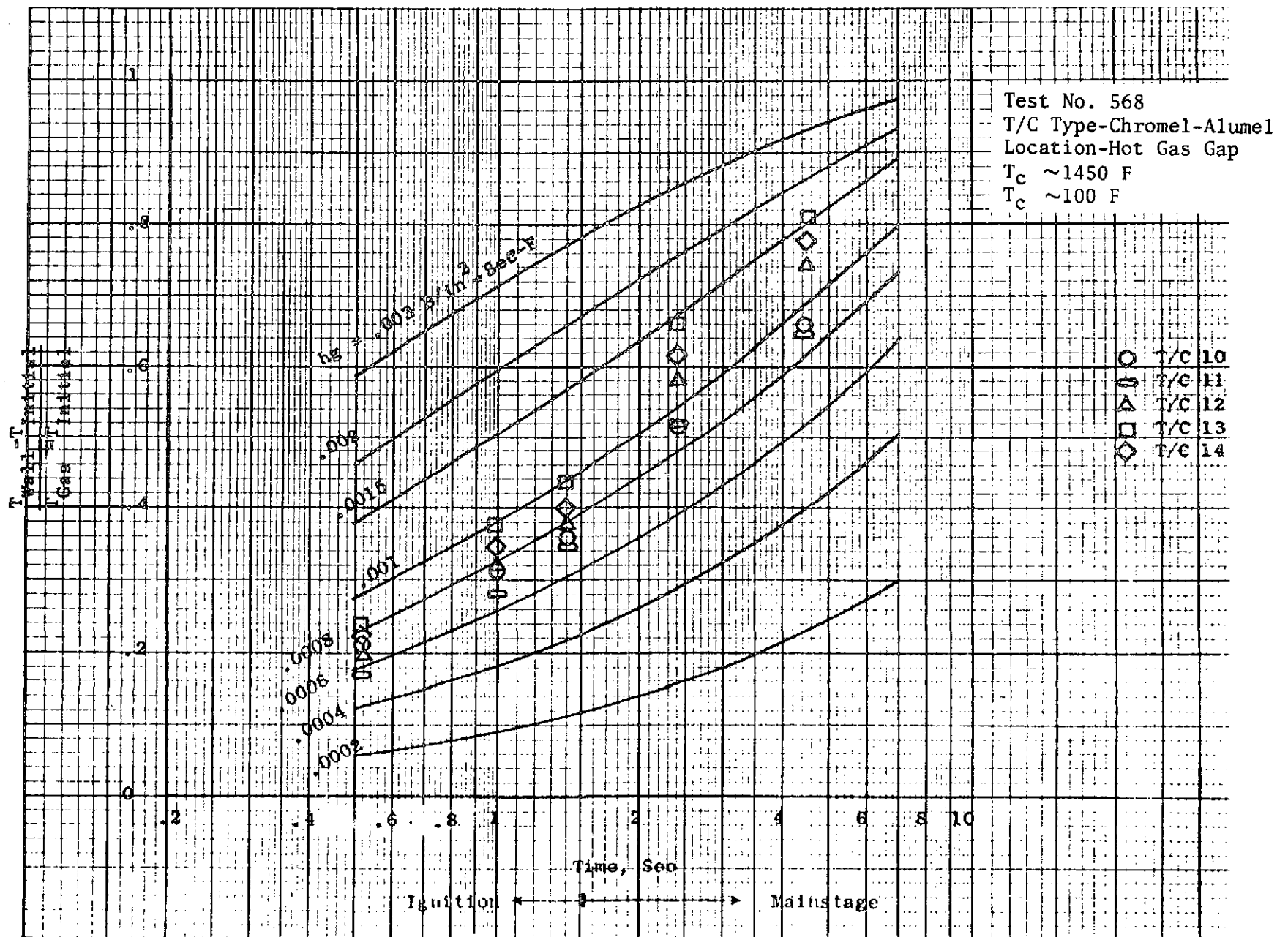


Figure 137. Uncooled Workhorse Dummy Baffle Hot Wall Thermal Response (347 CRES, $K \sim 0.26 \times 10^{-5}$ Btu/in.-sec-F, $\alpha \sim 0.009$ in.²/sec)

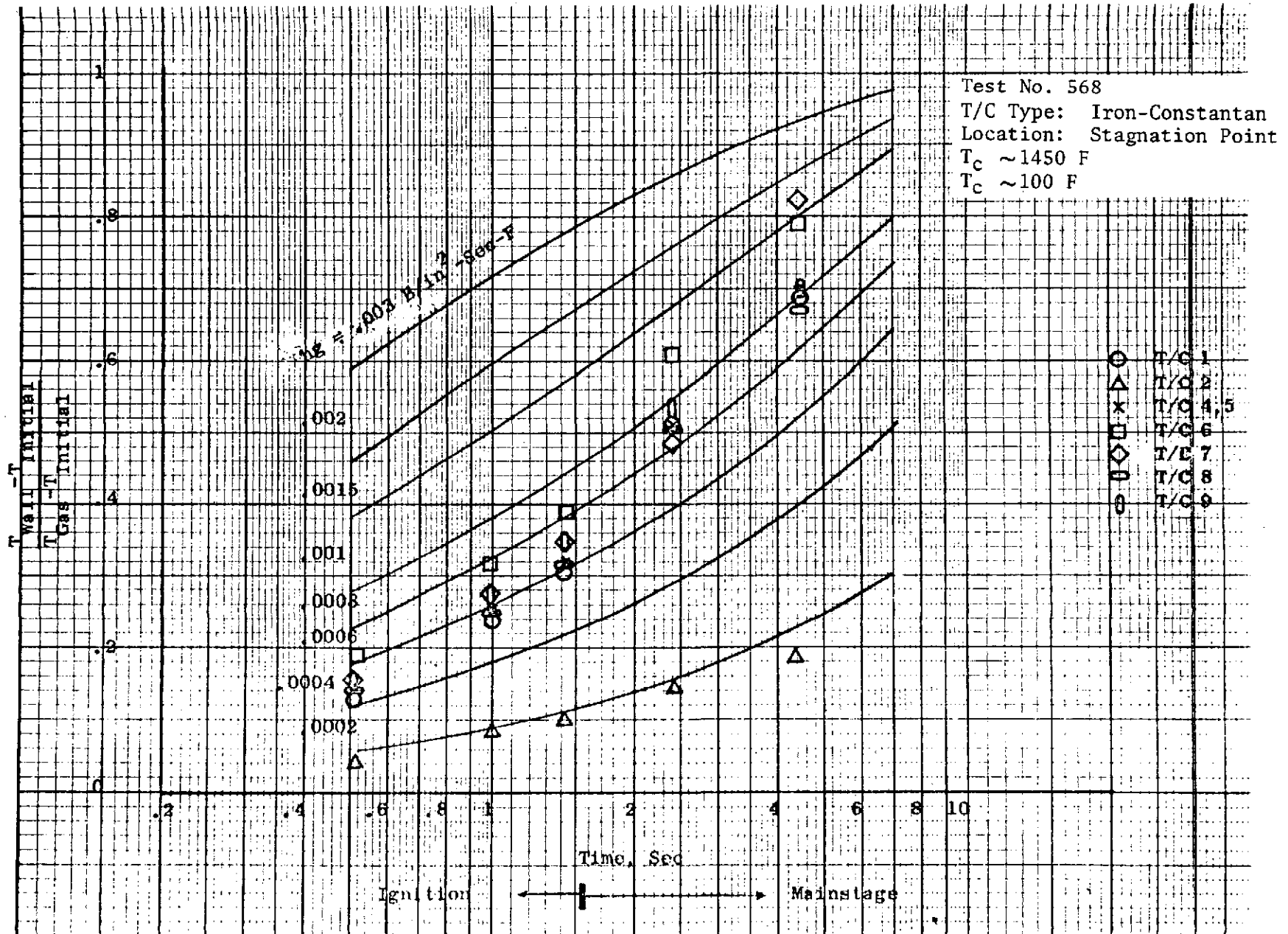


Figure 138. Uncooled Workhorse Dummy Baffle Hot Wall Thermal Response (347 CRES, $K \sim 0.26 \times 10^{-3}$ Btu/in.-sec-F, $\alpha \sim 0.009$ in.²/sec)

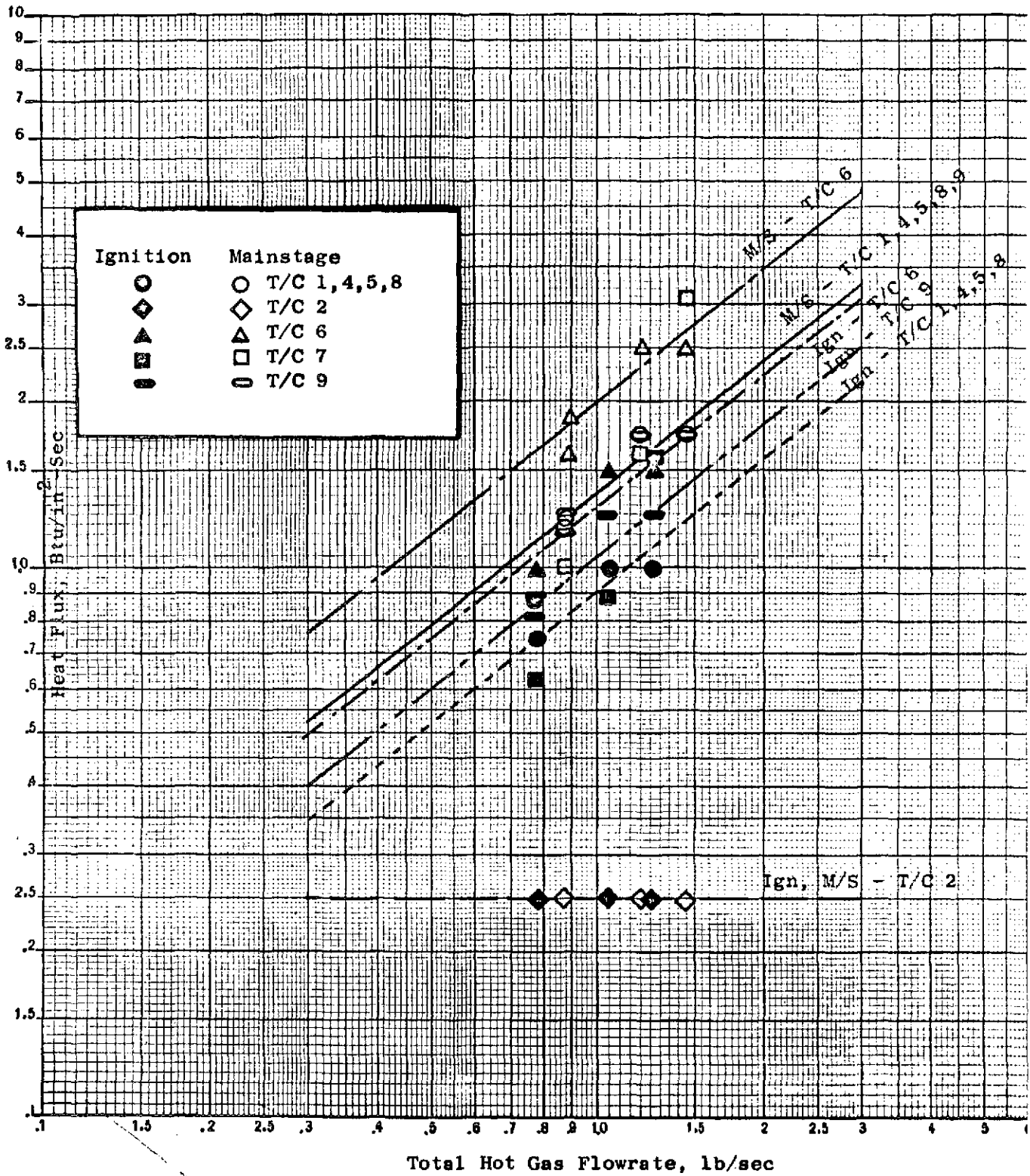


Figure 139. Experimental Baffle Stagnation Point Heat Flux Versus Flowrate (GOX/GH₂ T = 530 R, MR = 0.52 Ign., MR = 0.73 M/S, T_{Wall} = 200 F)

Results for the baffle thermocouples located near the hot gas gap are shown in Fig. 140, in terms of heat flux vs. gas flowrate. It is noted that thermocouple 14 is located in the gap adjacent to the igniter, that the gap in which thermocouple 10 is located was somewhat restricted by the seal used between the space and the baffles (resulting in possibly low readings), and that both of these thermocouples are located closer to the minimum hot gas gap than thermocouples 11, 12 and 13. As a result lower heat flux measurements from 11, 12 and 13 would be expected. In addition, thermocouple 11 ceased operating after test 568. The results indicate that thermocouples 10 and 11 read the lowest heat flux, with the heat flux steadily increasing as the igniter is approached. This trend occurs during both ignition and mainstage.

In comparing the stagnation point and the hot gas gap heat flux trends, it is noted that the stagnation heat flux is lower than that in the gap (by about 20 percent). Furthermore, both indicate a heat flux dependence on flowrate to the 0.8 power, typical of turbulent flow.

The reason for this at the stagnation point, where laminar flow usually exists, is that the diameter Reynolds number is high at this point - about 10,000; as a result the flow turns turbulent near the baffle leading edge, and with the higher conductivity braze spots covering the thermocouples, the thermocouples cannot distinguish the small area of laminar flow from the much greater area of turbulent flow.

Using a mixture ratio range of .86, a curve of heat flux vs mixture ratio was developed for a constant flowrate of 1.0 lb/sec. The results are shown in Fig. 141. It is noted that mixture ratios of 0.53 and 0.63 are during ignition, and the two higher mixture ratios are at mainstage. The theoretical value for thermocouple 11, 12, and 13 falls between the experimental values for 12 and 13, with thermocouple 11 being somewhat lower. The theoretical value for thermocouple 10 and 15 is about 50 percent higher than the experimental values at the lowest mixture ratios, but only about 15 percent higher than thermocouple 15 at the highest mixture ratio. As indicated earlier, thermocouple 10 was probably reading low due to a blockage of that hot gas gap.

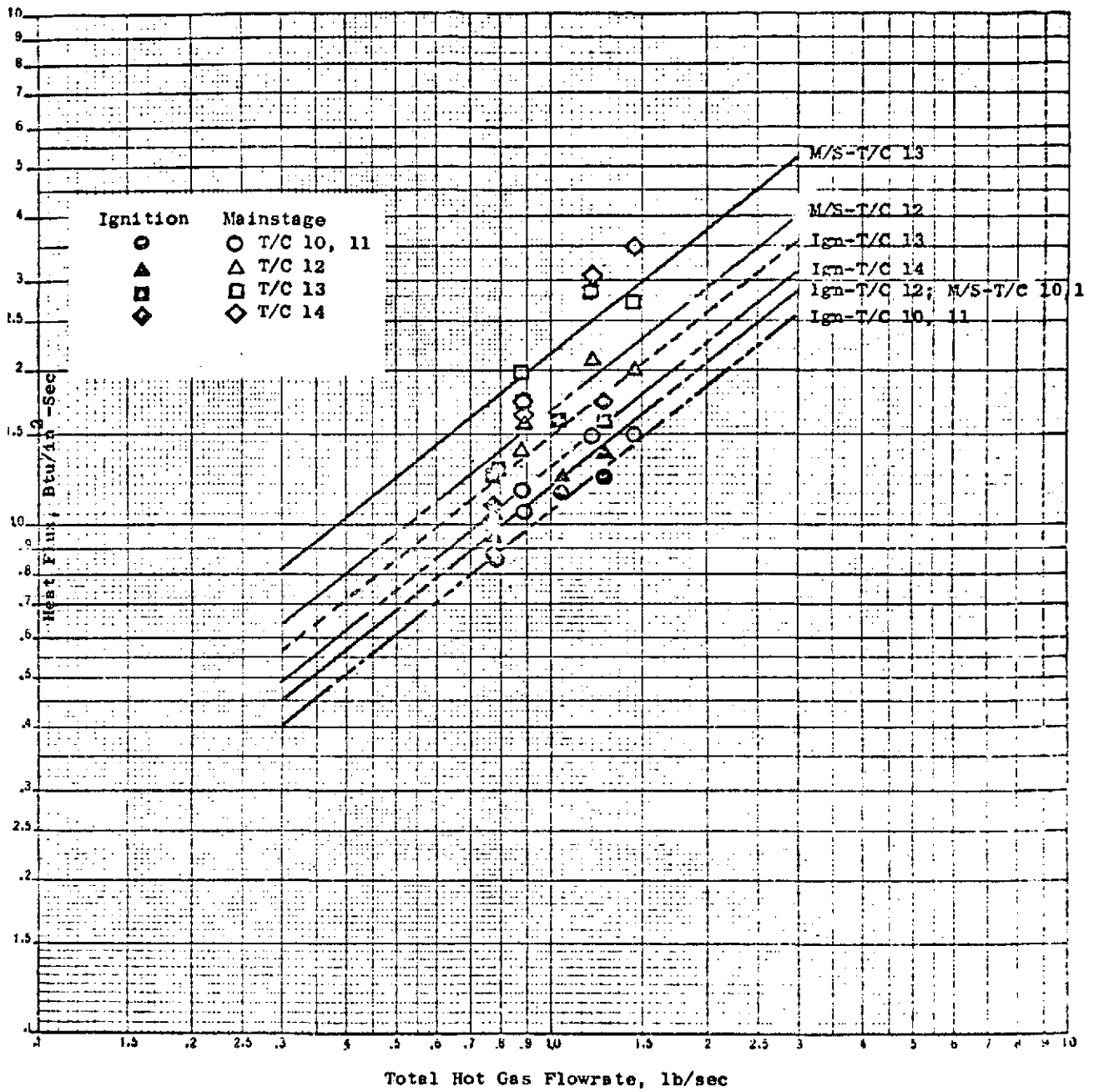


Figure 140. Experimental Dummy Baffle Heat Flux in Gap vs Flowrate
 (GOX/GH₂, T = 530 R, MR = 0.52 Ignition, MR = 0.73 M/S,
 T_{wall} = 200 F)

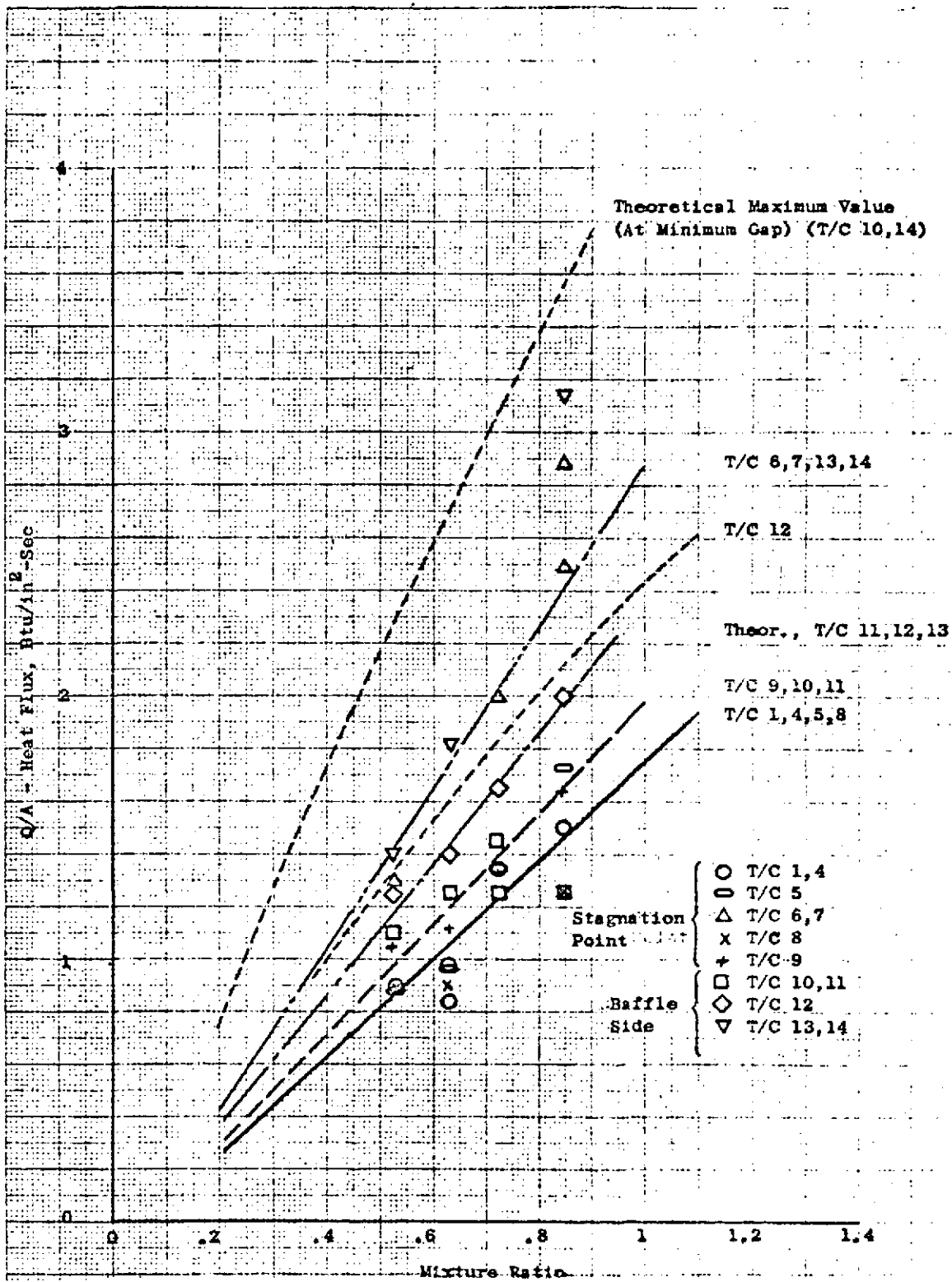


Figure 141. Experimental Dummy Baffle Heat Flux vs Mixture Ratio
 (GOX/GH₂ (540 R), W_{gas} = 1.0 lb/sec, T_{wall} = 200 F)

In conclusion, considering the difficulty in obtaining transient temperature data at the hot gas surface and the considerable number of variables which affect the results, the agreement between theoretical and experimental values is sufficiently close to indicate that the baffle should operate about as designed, with no problems at the stagnation point or in the hot gas gap.

Several items were corrected and/or changed in the next series of tests (Tests 002-036). Aside from removing the restriction to the hot gas gap in which thermocouple 10 was located, the spacer between the baffle and the injector was removed, to give an indication of whether the spacer is required or not. In addition, tests were run with the igniter turned off during mainstage, to determine its effect on the operation of the baffles. Also, tests were run over a wider range of mixture ratio, to indicate what can be expected with the cooled hardware at higher mixture operation.

Experimental heat flux is shown in Figures 142 and 143 as a function of the total hot gas flowrate for the baffles. Figure 142 is for tests 007-011, where the igniter was shutoff during mainstage operation. By comparison, Fig. 143 shows the results for some of the cold propellant injection conditions (with the igniter on during mainstage). A comparison of these two figures indicate that the measured heat fluxes as a function of flowrate are about the same, although the mixture ratios are different. The data shows higher heat fluxes at higher mixture ratio and lower heat fluxes with lower combustion temperature, as expected.

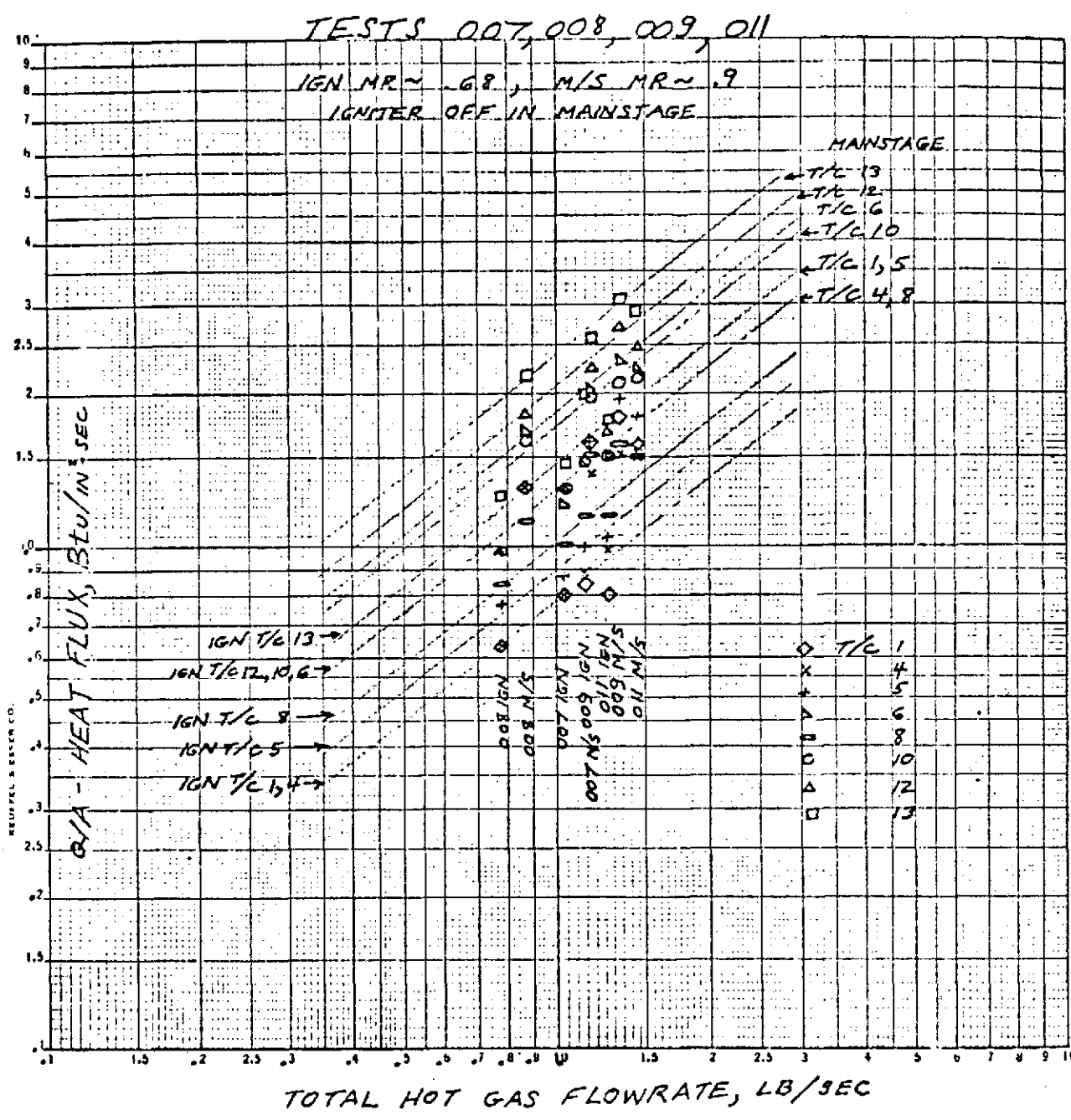


Figure 142. Baffle Heat Flux Values

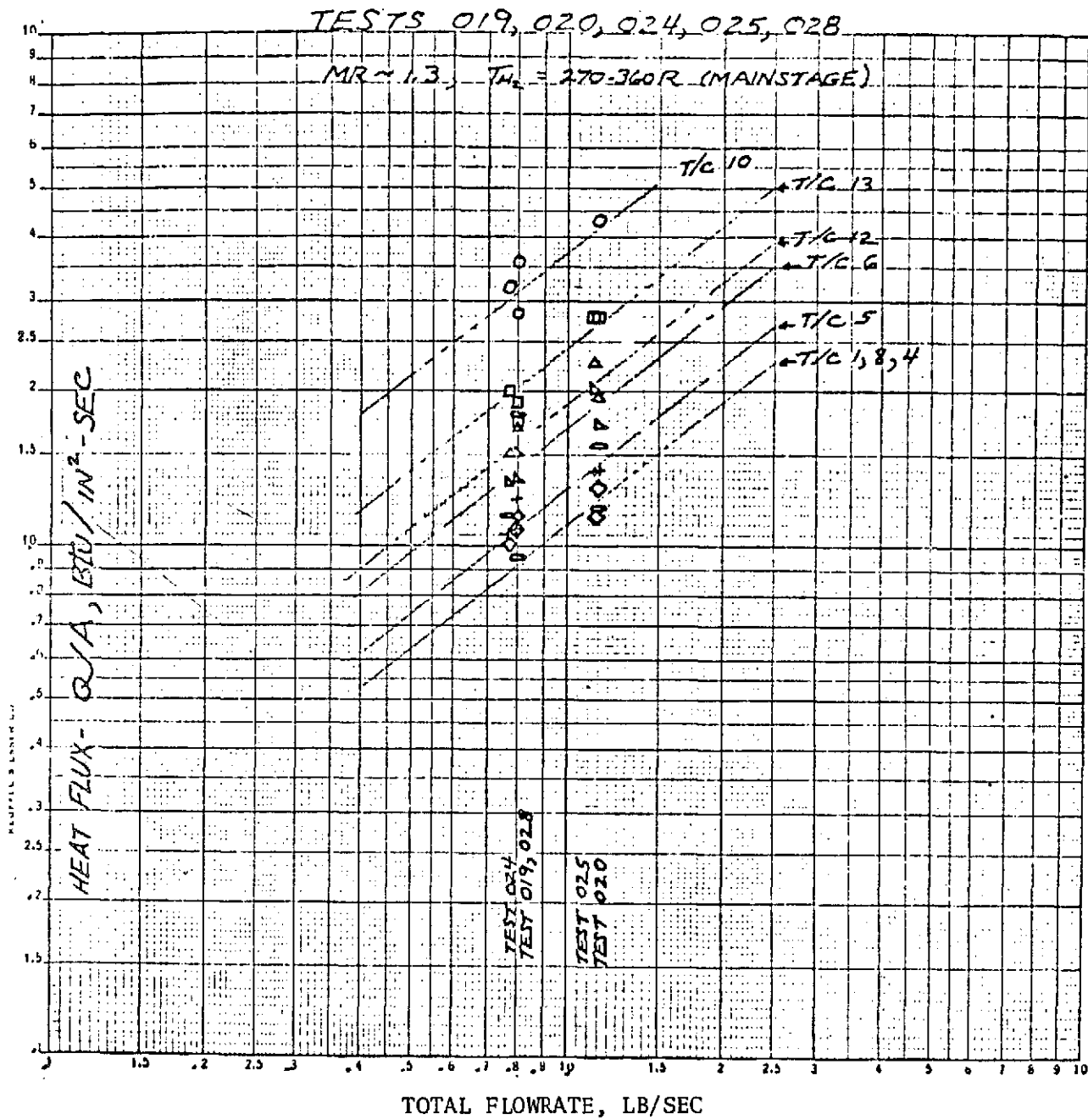


Figure 143. Baffle Heat Flux Values (Ignition on During Mainstage)

Starting with test 018, thermocouple 10 (side mounted baffle thermocouple farthest from the igniter) began to indicate higher heat fluxes than normal. Since this test was not at severe conditions (total flow-rate of 1.17 lb/sec, mixture ratio of 1.09), and the previous test was at even less severe conditions, it is uncertain what caused this change. It is noted that it was expected that thermocouples 10 and 14 would register a higher heat flux due to being mounted closer to the smallest part of the hot gas gap. It is not known whether anything changed to increase the heat flux at this point, or whether enough braze was eroded from the thermocouple over the previous tests so that the thermocouple tip was no longer attached to the wall, allowing a faster thermal response and thus indicating a higher heat flux. In any case, the peak heat fluxes as measured by T/C 10 after test 018 are slightly less than the predicted peak heat fluxes at the forward end of the baffle, and thus no problems are foreseen with the cooled conditioner.

EXPERIMENTAL COMBUSTOR HEAT FLUX

A thermocouple was attached to the hot gas wall in the combustor opposite the igniter. Typical transient temperature curves for tests 556 and 567-572 are shown in Fig. 144. The resulting heat transfer coefficients are in the range of .002-.004 Btu/in²-sec-F. This results in roughly a factor of 4 higher heat transfer coefficient in this region at the nominal operating point with ambient temperature propellants than was predicted with the Bartz simplified equation.

Data are shown in Fig.145 for tests 002-014 with ambient temperature propellants, and in Fig.146 for tests 014-024 for colder temperature propellants. Variations in flowrate, mixture ratio, and injection temperature seem to have little effect on the heat transfer coefficient in this region. The igniter also has little effect. Whether this is real or due to a faulty thermocouple installation is not definitely known. However, the heat fluxes are higher than theoretically predicted with the simplified Bartz pipe flow equation, and are being used in the analysis of the cooled hardware.

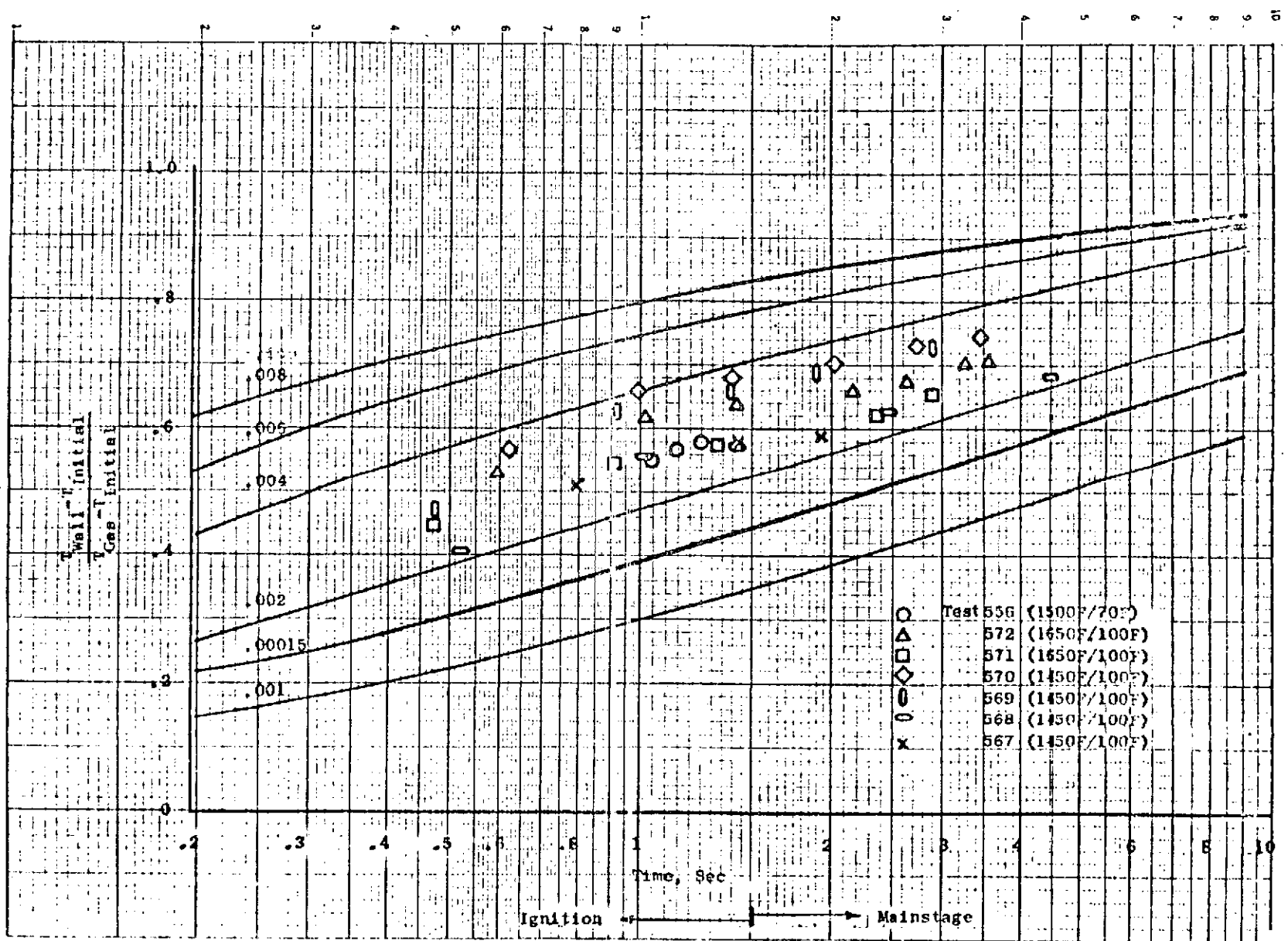


Figure 144. Uncooled Workhorse Combustor Thermal Transients 0.5-Inch Thick, 347 CRES

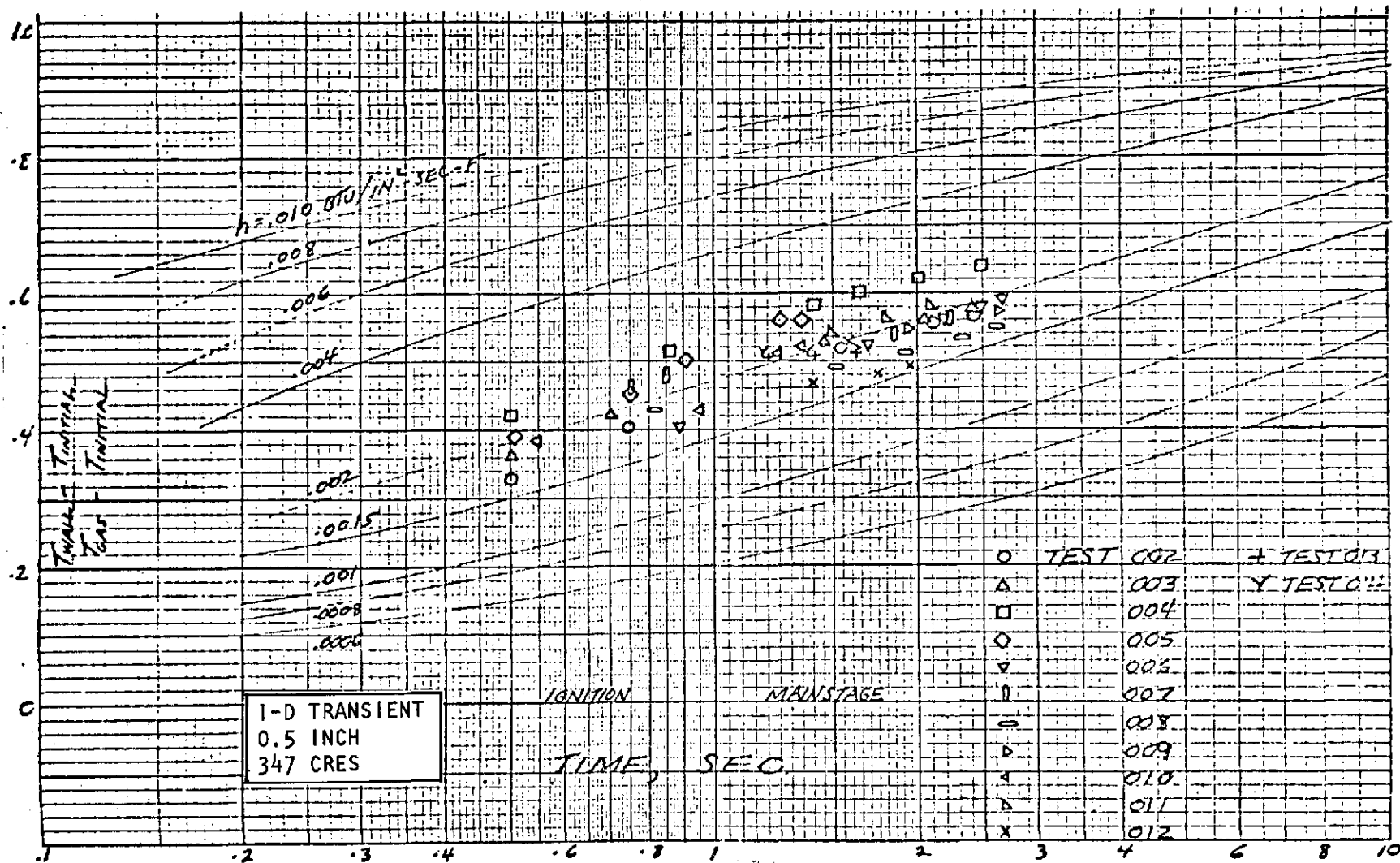


Figure 145. Combustor Wall Thermocouple, Tests 002 Through 014, Theoretical Combustion Temperature

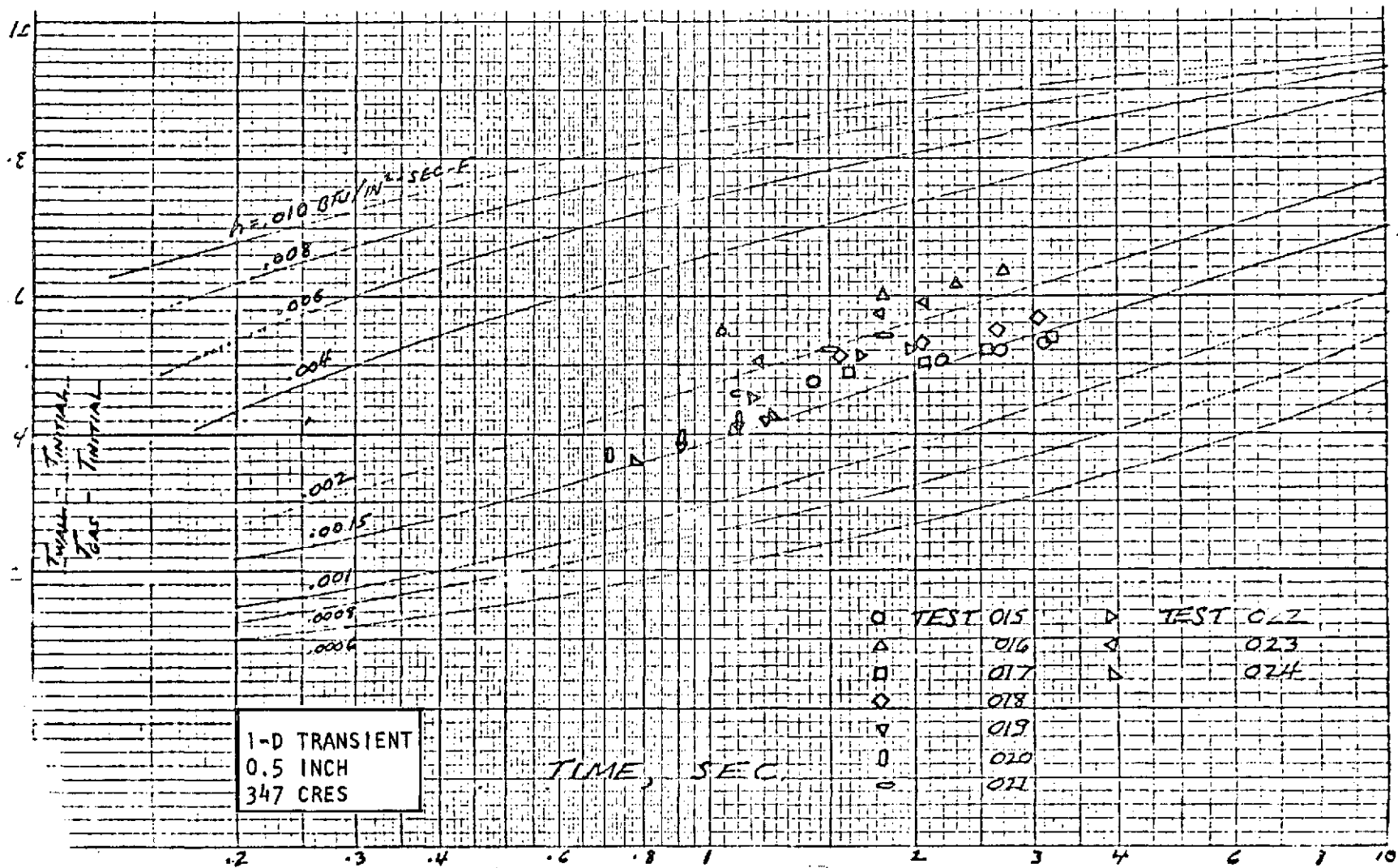


Figure 146. Combustor Wall Thermocouple, Tests 015 Through 025, Theoretical Combustion Temperature

The result of the higher heat flux is to increase the predicted mid channel gas wall temperature of 660 F, and a mid-land value of 1070 F at a MR=1 with ambient propellants. This is based on the channel height being reduced from .117 inch to .077 inch (this adds more margin to the mid-channel, although it has little effect on the mid-land temperature). In spite of the increased heat flux measured, the combustor can easily operate at the design condition.

It is noted that the side walls tend to run at a higher temperature than do the top and bottom walls due to the difference in land width - 0.2 inch vs 0.1 inch, even though both have the same hot gas wall thickness, channel width and channel height.

INJECTOR THERMAL RESPONSE

The thermal response of the injector as measured by the thermocouple located at the injector center are shown in Figures 147 through 150. Results for the first series of tests (567-572) are shown in Fig. 147. Results indicate that it takes 2-3 seconds for the copper face to reach steady-state temperatures. The peak measured temperature was about 600 F, and it occurred with the maximum injector flowrate. Figure 148 shows the same results for tests 006-011 with the igniter off during mainstage. As in the previous test series, both ambient oxygen and hydrogen were used, and the results are about the same. Tests 015 to 025 results are shown in Fig. 149. In this case, the response time has been reduced to 1-2 seconds, and the steady-state injector face temperatures are lower due to the lower injection temperatures. A cross-plot of the data for these last tests is presented in Fig. 150. This figure has three separate plots; injector face temperature as a function of total flowrate, the difference between injector face temperature and hydrogen injection temperature vs flowrate, and also as a function of mixture ratio.

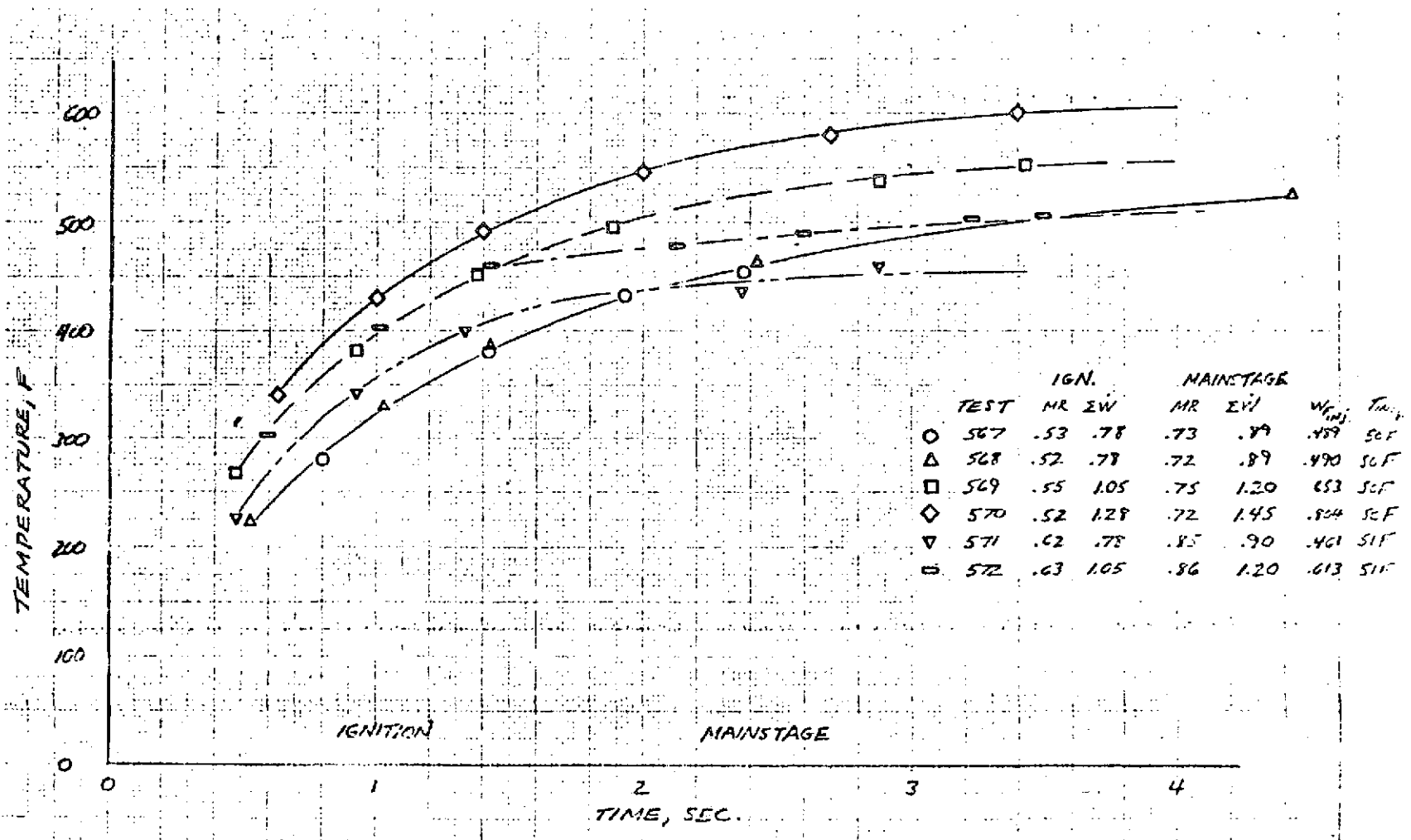


Figure 147. Injector Center Thermocouple Transients, Tests 567 Through 572

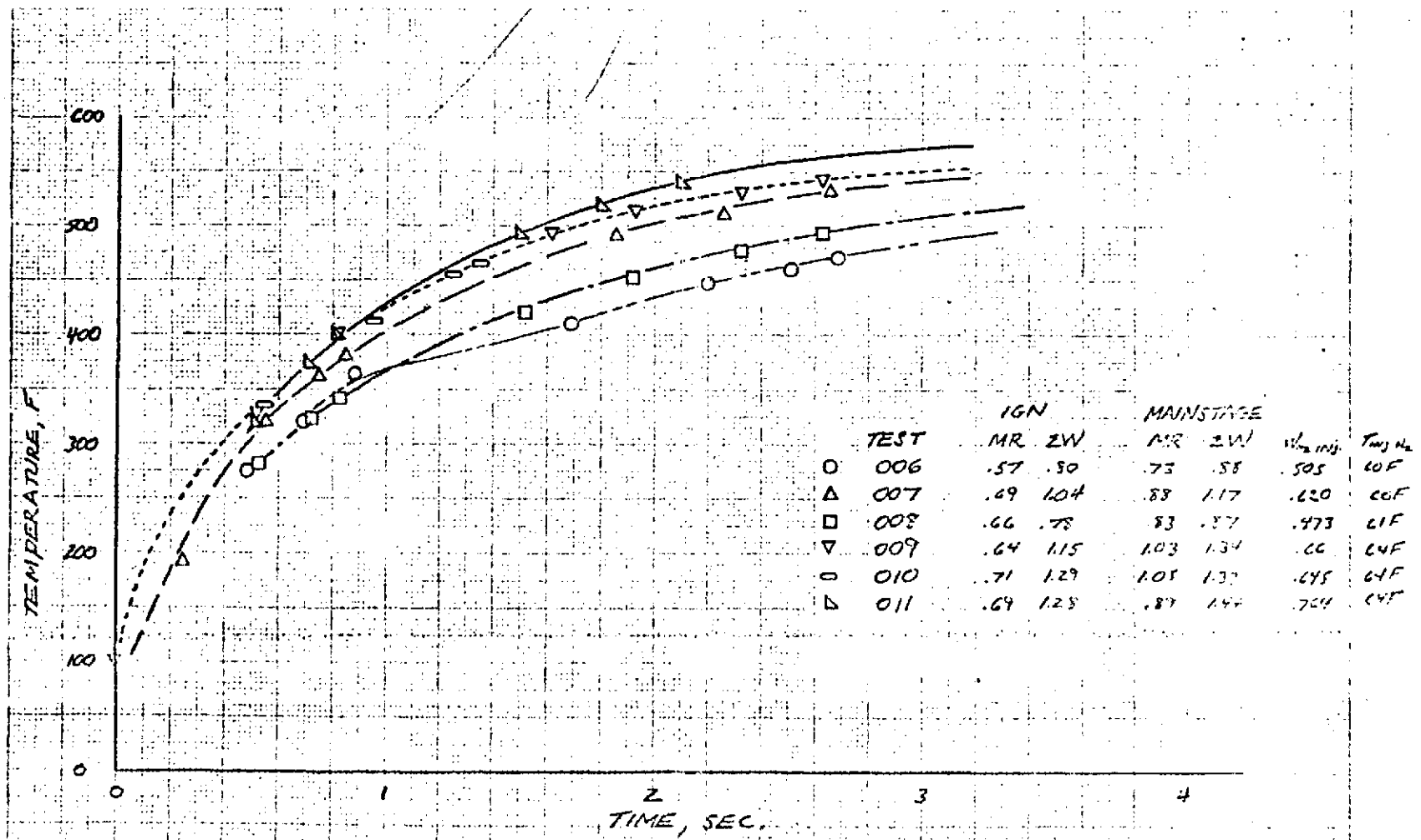


Figure 148. Injector Center Thermocouple Transients, Tests 006 Through 011, Igniter Off During Mainstage

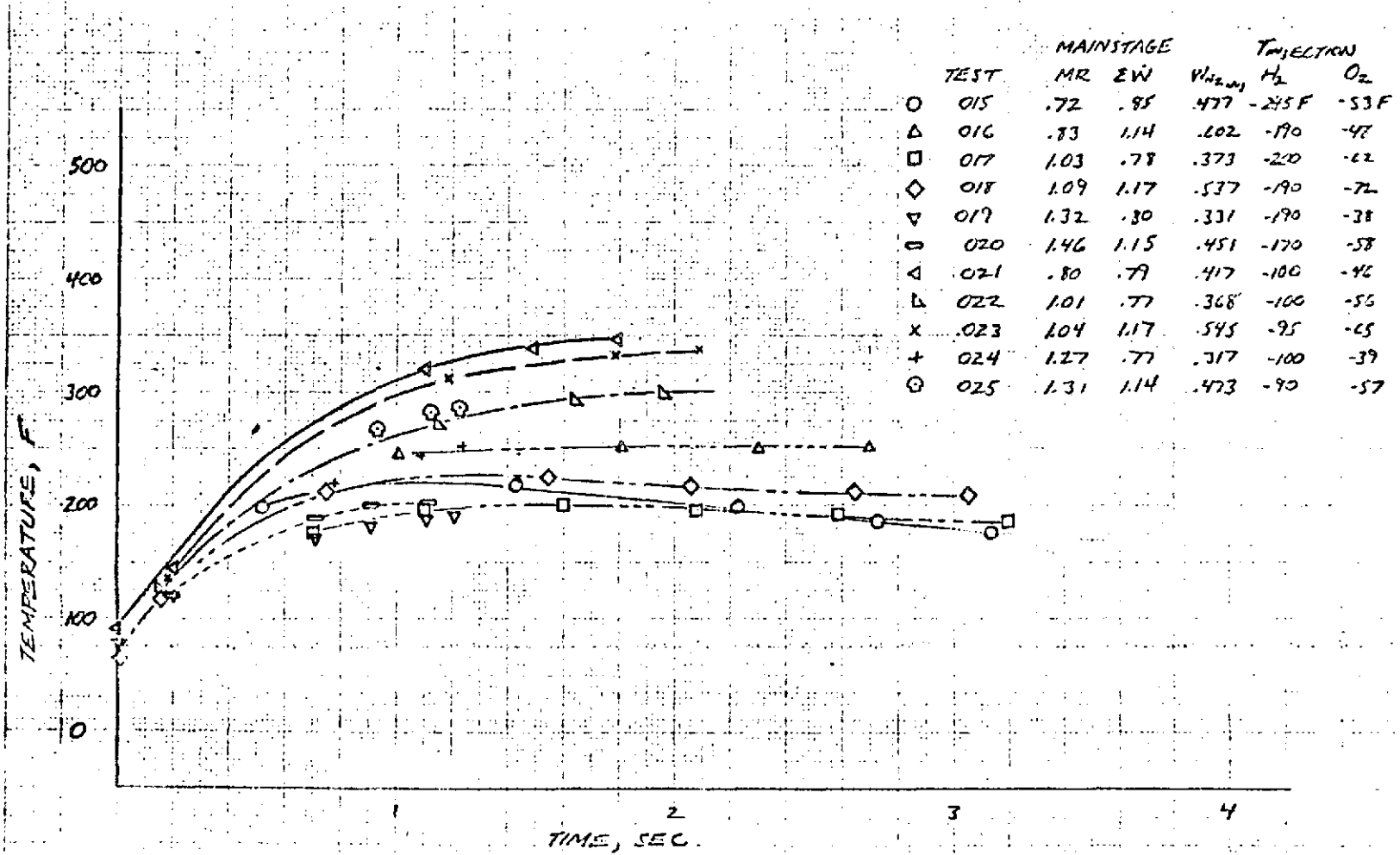


Figure 149. Injector Center Thermocouple Transients, Tests 015 Through 025

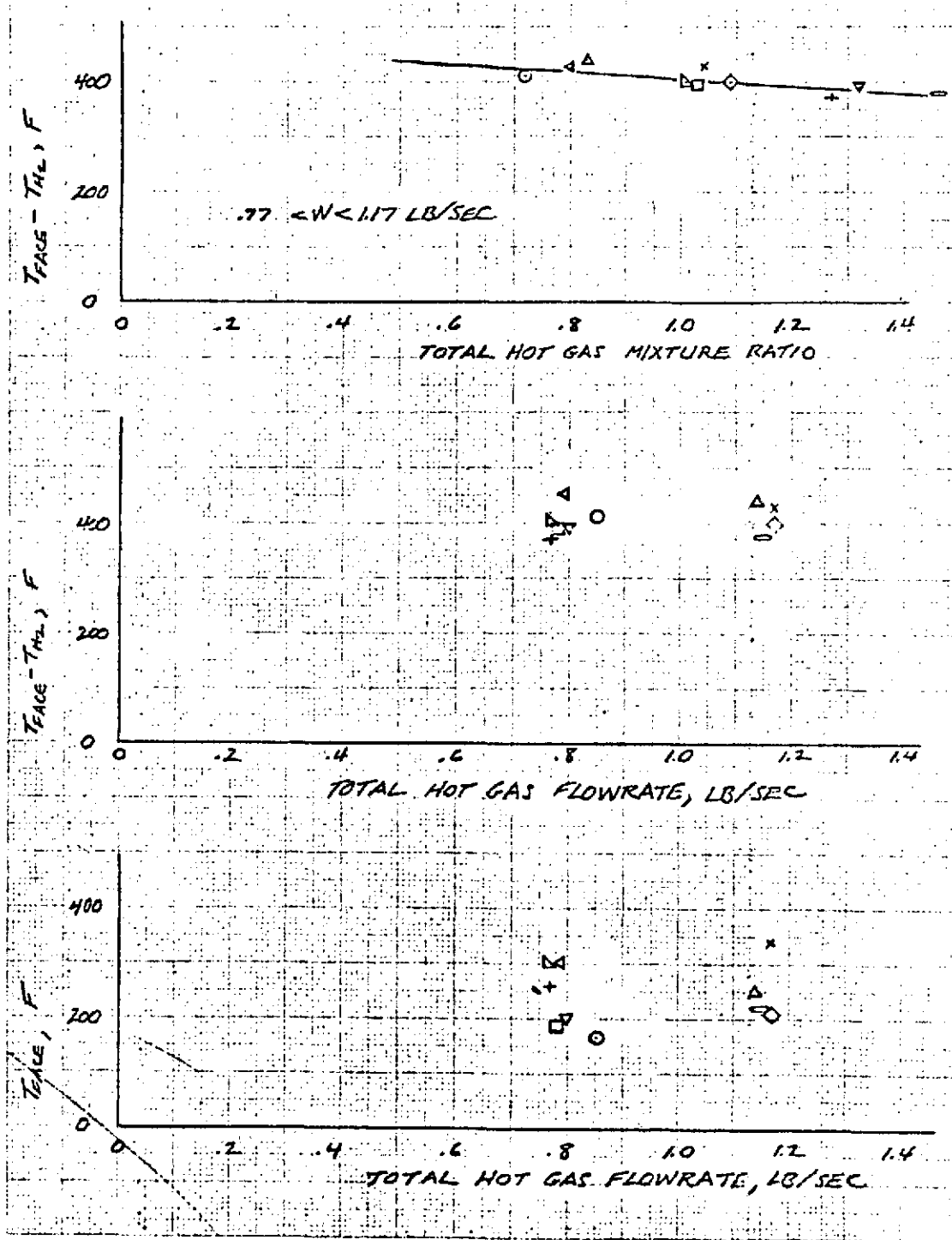


Figure 150. Injector Center Face Temperatures, Steady-State Mainstage, Tests 015 Through 024

The last correlation was also the best, and indicated for this series of tests that the injector face temperature went up in proportion to the hydrogen injection temperature increase, and that the face temperature was independent of hot gas flowrate and a very weak function of mixture ratio. The data actually indicates a slight decrease in temperature with increasing mixture ratio, which may be indicative of reduced recirculation on the injector face due to the decreasing hydrogen injection velocity.

Inspection of the hardware after the last test (036) indicated localized erosion patterns in the combustor; these did not cover the combustor wall thermocouple. It is not known exactly when this happened, but it is strongly suspected of having occurred in the last test. Although the duration was 8-1/2 seconds, the overall mixture ratio was only 1.0, with a combustion temperature under 1800 F. This condition alone would not indicate that erosion could take place. However for the first 3.5 seconds of the test, the oxygen flow was oscillating, due to two-phase flow passing through the upstream oxidizer control venturi. At this point the oxygen temperature dropped and the oxidizer flow stabilized; in the meantime the hydrogen flow was slowly decreasing due to a rise in hydrogen temperature, resulting in an increasing mixture ratio. It is suspected that the oscillating oxygen flow during the two-phase operation could have resulted in abnormal mixture ratio distributions, with the subsequent erosion. The last part of the test also probably had two-phase flow in the upstream venturi, but the flow was stable.

Typical distribution of the heat flux across the baffles is shown in Fig. 151. The results showed that with the igniter either on or off during mainstage, the heat flux reaches a peak on the second baffle from the igniter. This is true both at the stagnation point and in the hot gas gap. The reason for this was not finalized; however, it was undoubtedly caused by a non uniform distribution of the hot gases.

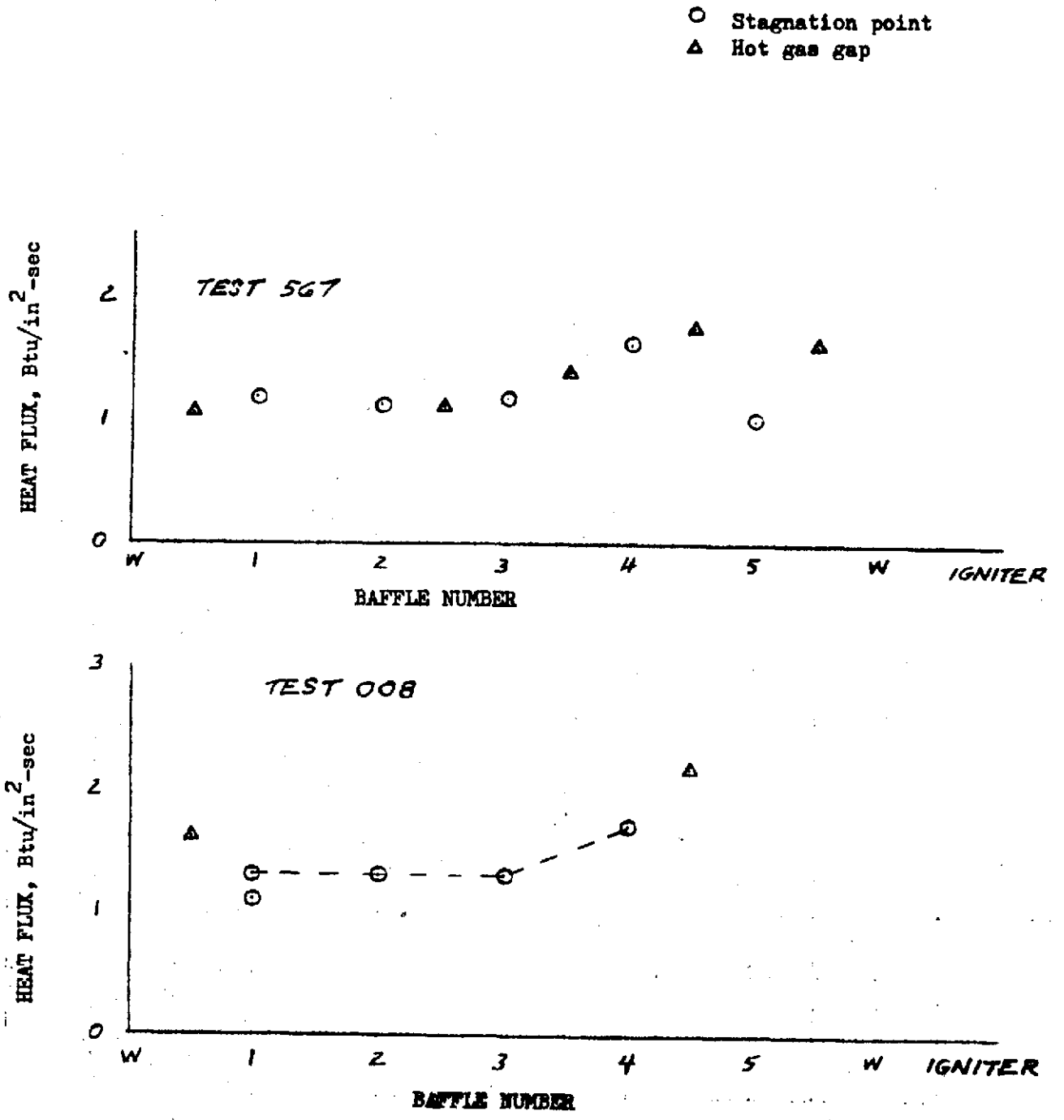


Figure 151. Typical Heat Flux Distribution on the Baffles (Mainstage)

CONCLUSIONS

Review of the test data and subsequent thermal analysis has resulted in formulation of the following conclusions relative to the technology task and its impact on the cooled conditioner design and test efforts.

1. The concept of using a tri-slot injector and side mounted torch igniter close coupled to the heat exchanger baffles is feasible. The effluent from the side mounted torch igniter mixes well with the main flow and does not impinge on the opposite wall. Also, the use of the oxygen flow control valve to maintain low mixture ratios during the ignition phase of operation is valid.
2. Separate ignition valves are not required; all flow can be controlled by the main propellant valves.
3. Reliable ignition and stable combustion can be expected over the entire range of expected operating conditions.
4. Peak heat flux values on the baffles are quite close to predicted, and should present no problem on the cooled conditioner.
5. Combustion zone heat flux is somewhat higher than predicted on the side walls; however well within the capability of the cooled conditioner.
6. Some tests were conducted where the igniter was shut off during mainstage, with no significant effect on combustion zone temperatures.

7. On the last test there was some localized erosion of the side walls of the conditioner, which has been attributed to two phase oxygen flow and reducing hydrogen flow during the test, resulting in erratic injection and localized very high heat fluxes. To alleviate this condition on the cooled conditioner tests with chilled propellants, a larger pre-fire bleed will be used to stabilize temperatures.

8. Since the localized erosion occurred only on the side walls where the injector elements are quite close to the conditioner wall a revision to the second injector was decided upon. The outer row of elements on the side walls were eliminated, leaving a greater gap between elements and conditioner wall. This will reduce localized heat flux in this region while having no detrimental effect on the heat exchange efficiency of the conditioner.

CONCLUSIONS AND RECOMMENDATIONS

The program met its basic objective of establishing a technology base for the baffle type propellant thermal conditioner that was evaluated. The test effort showed that the conditioner was not mission duty cycle limited and is capable of operation over a wide mixture ratio. Use of the flow control valve (demonstrated on the solid wall conditioner) whereby the reactor starts at a low mixture ratio and is automatically sequenced into mainstage conditions by the cold fluid precludes damage to the hardware if the system fails to flow cold fluid on demand. This concept also allows for safe operation of the conditioner at a higher mixture ratio, if desired, to reduce system weight and envelope. Ignition of the reactor propellants over a wide range of propellant temperatures and mixture ratio extremes was demonstrated with the side mounted spark igniter. Operation at high mixture ratio was demonstrated on the IR&D hardware and on the solid wall conditioner. One very attractive feature incorporated into the concept was the use of bypass on the hydrogen to be conditioned. This not only improved the margin against icing but yielded a common conditioner capable of being used to condition either hydrogen (with a 40 percent bypass) or oxygen with 0 to 5 percent bypass.

The thermal characteristics of the conditioner were quite good; demonstrating the capability to deliver conditioned fluid within 1/2 second after start of cold fluid flow.

The experimental efficiency (ratio of measured heat input to hydrogen gas to calculated heat input for these operating conditions) of the conditioner was approximately 90 percent.

Baffle distortion which was experienced during the test program is well understood and requires minor design modifications on any future hardware. These modifications include (1) relocating the guide rails to a plane directly underneath the baffle and extending for the full length of the baffles, and (2) better internal support (honeycomb) especially in any cutout areas such as where instrumentation is located.

It is recommended that additional technology be acquired on this concept to prepare it for development. These additional technology areas are associated with the injector and the ignition system.

Injector technology is required in refining the injector pattern to improve distribution and wall compatibility. This would include, more elements and/or alternate element types.

Ignition technology is required to more thoroughly evaluate the side mounted igniter with the refined injector from above to characterize ignition parameters. Parameters needing characterization include (1) igniter mixture ratio, (2) igniter flow rate, (3) reactor mixture ratio and (4) sequencing.

Exploration is also required to determine the optimum location of the side mounted igniter with respect to the injector face plane.

REFERENCES

1. Friedly, J. C., J. L. Manganaro, and P. G. Kroeger: A Simple Criterion for Predicting Flow Oscillations in Fluid Heat Exchangers Operating Near the Critical Pressure, General Electric Report 68-C-078, March 1968.
2. Tabulation and Analysis of Supercritical Oxygen Heat Transfer Data with Regard to Flow Oscillation, Rocketdyne Report R-8420, 10 February 1971.
3. R. D. Paster; Hydrogen Oxygen APS Engines NASA CR 120805 (unpublished to date)

APPENDIX A

SYSTEM BALANCE ANALYSIS

A non-linear system balance program was written to evaluate reactor (hot gas) flow requirements for the hydrogen thermal conditioner. The purpose of this program was to establish reactor flow requirements over the specified range of inlet temperature (275F to 600R for hydrogen and 375R to 600R for oxygen) such that a near constant heat input to the conditioned hydrogen (2800 Btu/sec) was maintained.

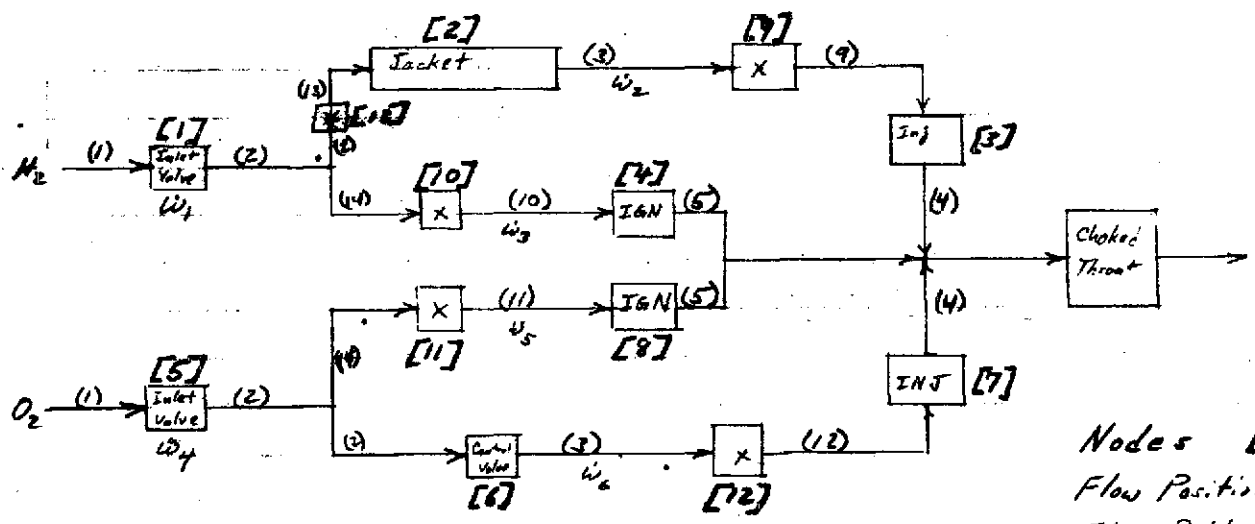
PROGRAM DESCRIPTION

The schematic of the thermal conditioner used in the off-design balance program is shown in Figure A-1. Node numbers are for reference to the output format - a sample of which is included as Figure A-2. Position and path numbers are used internally by the program.

The program basically consisted of:

- (1) two routines to calculate pressure drops (forward or backward) as functions of resistance, pressure, temperature and average density (linear average) for either oxygen or hydrogen using direct substitution iteration and real gas property tables,
- (2) a heat transfer routine containing the equations and empirical relations required to represent the hot gas side heat transfer (easily modified as more knowledge and/or sophistication dictate),

FIGURE A-1. THERMAL CONDITIONER BALANCE PROGRAM SCHEMATIC



Nodes [#]
 Flow Positions (#)
 Flow Paths (#)

00001
00002
00003
00004
00005
00006
00007
00008
00009
00010
00011
00012
00013
00014
00015
00016
00017
00018
00019
00020
00021
00022
00023
00024
00025
00026
00027
00028
00029
00030
00031
00032
00033
00034
00035
00036
00037
00038
00039
00040
00041
00042
00043
00044
00045
00046
00047
00048
00049
00050
00051
00052
00053
00054
00055
00056
00057
00058
00059
00060
00061
00062
00063
00064

FIGURE A-2. TYPICAL OUTPUT FORMAT

CONTROL REQUIREMENTS

HYDROGEN THERMAL CONDITIONER

H2= 294.9 PSIA 275.0 DEG R 0.613 LBM/SEC
 O2= 326.6 PSIA 375.0 DEG R 0.613 LBM/SEC
 PC= 240.0 PSIA MR= 1.000 O/F CHAMBER FLOW= 1.226 LBM/SEC
 COMBUSTION TEMPERATURE= 2034.2 DEG R
 IGNITOR: MR= 1.000 O/F FLOW= 0.240 LBM/SEC

INJECTOR HYDROGEN FLOW

NODE	DELTA-P	DELTA-T	R0-IN	R0-OUT	RESISTANCE	FLOW
1	6.55	0.00	1.99E-01	1.95E-01	3.4665	0.613
13	13.55	0.00	1.95E-01	1.86E-01	10.8500	0.493
2	10.89	30.00	1.86E-01	1.61E-01	7.7562	
9	0.00	0.00	1.61E-01	1.61E-01	0.0000	
3	24.00	0.00	1.61E-01	1.46E-01	15.8627	

INLET PRESSURE=294.9 INLET TEMPERATURE=275.0

INJECTOR OXYGEN FLOW

NODE	DELTA-P	DELTA-T	R0-IN	R0-OUT	RESISTANCE	FLOW
5	7.66	0.00	2.76E+00	2.69E+00	56.3270	0.613
6	15.08	0.00	2.69E+00	2.56E+00	167.0037	0.493
12	39.91	0.00	2.56E+00	2.20E+00	420.0000	
7	24.00	0.00	2.20E+00	1.99E+00	217.7476	

INLET PRESSURE=326.6 INLET TEMPERATURE=375.0

IGNITOR HYDROGEN FLOW

NODE	DELTA-P	DELTA-T	R0-IN	R0-OUT	RESISTANCE	FLOW
1	6.55	0.00	1.99E-01	1.95E-01	3.4665	0.613
10	24.44	0.00	1.95E-01	1.78E-01	330.0000	0.120
4	24.00	0.00	1.78E-01	1.62E-01	297.1941	

IGNITOR OXYGEN FLOW

NODE	DELTA-P	DELTA-T	R0-IN	R0-OUT	RESISTANCE	FLOW
5	7.66	0.00	2.76E+00	2.69E+00	56.3270	0.613
11	54.99	0.00	2.69E+00	2.20E+00	10280.0000	0.120
8	24.01	0.00	2.20E+00	1.99E+00	3675.3469	

FIGURE A-2. TYPICAL OUTPUT FORMAT

(3) a general iteration routine, and

(4) an output routine.

These parts can be arranged in various ways depending upon the results desired. For example, in generating the regulator pressure requirements (for constant heat output) presented in the main body of this report, the system must be analyzed backwards - from the combustion chamber to the inlets. However, in analyzing the effect of regulator pressure keeping tolerance, the system must be stepped through from inlet to chamber with the choked exit providing the necessary constraint. This variety of logic patterns needed is the reason no "hard" (i.e., permanent IBM) version of the program exists. Instead, a number of modified versions are stored on the GE-440 Timeshare System.

An example of the logic and backup equations of the version of the program used to generate the regulator pressure vs inlet temperature requirements presented earlier is given as Table A-1.

The program is given a set of inlet temperatures, assumed flowrates, and assumed inlet pressures. The inlet pressures are then perturbed (equal percentage amounts and in opposite directions as this represents the worst case), and pressure drops and flow splits are calculated to determine the chamber pressure. Real gas properties are used. Combustion temperature and reactor exit temperatures are then determined by use of various heat transfer relations and the assumption of a choked exit. Reiteration of the feed system flow splits is performed at this point to account for changes in the heat input (and consequently, the pressure drop) to the reactor

TABLE A-1

LOGIC SEQUENCE FOR GENERATING CONTROL REQUIREMENTS

1. Set: combustion temperature, outlet temperature, total heat output, total conditioner exit area, jacket temperature rise per pound/second of H_2 in jacket, γ .
2. Assume: MR, P_c , flows in O_2 and H_2 igniter and injector lines.
3. Input: inlet temperatures
4. Calculate injection enthalpy accounting for H_2 jacket and igniter flows and O_2 flows.
5. Calculate mixture ratio needed to yield fixed combustion temperature with calculated injection enthalpy.
6. Does calculated MR agree (within ± 0.0001) with assumed MR?
 If "No" then use calculated MR as assumed MR,
 Recalculate flows and go to "4"
 If "Yes" go on
7. Calculate C_p as function of MR
8. Calculate flow required to maintain total Q at design level
9. Does calculated total flow agree (within 0.000001) with assumed flow?
 If "No" then use calculated flow as assumed flow, recalculate jacket flow split, and go to "4"
 If "Yes" go on
10. Calculate total pressure at exit with fixed exit temperature, γ , and area and known total flow and molecular weight
11. Calculate exit static pressure and temperature from Mach relations at fixed γ and $M = 1$.
12. Find static density at exit from perfect gas law
13. Using fixed ratio of static to total temperature at start of converging tubes find static temperature there
14. Assume static density at "13" is same as at exit
15. Calculate ΔP in tubes to exit using linear average of static densities
16. Find P_c from $P_c = P_{exit_{total}} + \Delta P$
17. Assume static pressure at start of convergence is $0.9 P_c$
18. Find static density at "13" from perfect gas laws

TABLE A-1 (CONT)

19. Does static density calculated agree with (within 0.0001) static density assumed?
If "No" then use calculated density as assumed density and go to "15"
If "Yes" go on
20. Does calculated P_c agree with (within 0.02) assumed P_c ?
If "No" then use calculated P_c as assumed P_c and go to "4"
If "Yes" go on
21. Assign exit pressure from all lines as P_c
22. Assign exit temperatures of O_2 liner and H_2 igniter line as inlet temperatures
23. Assign exit temperature of H_2 injector line as inlet temperature plus ΔT in jacket
24. Find exit densities for the four lines from real gas property tables
25. Back calculate pressure drops and find pressure just downstream of H_2 inlet valve
 - a) through injector line
 - b) through igniter line
26. Do pressures from 25a and 25b agree (within 0.05)?
If "No" then adjust flow split and go to "4"
If "Yes" go on
27. Back calculate pressure drops and find pressures just downstream of O_2 inlet valve
 - a) through injector line
 - b) through igniter line
28. Do pressures from 27a and 27b agree (within 0.05)?
If "No" then adjust flow split and go to "27"
If "Yes" go on
29. Calculate pressure drops across inlet valves and find required inlet pressures for O_2 and H_2 lines
30. Print results
31. GO TO "3"

Equations used in various steps:

$$4. \quad h_{f_{H_2}} = 1.18 + (1.44/350) (T_{H_2, AVG} - 250) + h_{f_{O_2}}$$

$$\text{where } T_{H_2, AVG} = \left\{ T_{H_2, in} + \Delta T_{H_2, in} \left(\frac{\dot{w}_{O_2, in}}{\dot{w}_{H_2, in}} \right) \right\} (\dot{w}_{O_2, in}) + T_{H_2, out} \dot{w}_{H_2, out} / \dot{w}_{H_2}$$

$$h_{f_{O_2}} = \left\{ \left[(h_{f_{O_2}})_{250} - (h_{f_{O_2}})_{162} \right] \dot{w}_{O_2} \right\} / [\dot{w}_{H_2} (898.86)]$$

$$5. \quad MR = -0.286966 + 5.13854 \times 10^{-4} (T_0) + 2.96261 \times 10^{-8} (T_0)^2 \\ - 0.144405 h_{f_{H_2}} - 2.76646 \times 10^{-4} (h_{f_{H_2}})^2$$

$$7. \quad C_p = 0.1 T_0 + [2.2182 + 3.4628 MR - 9.72166 MR^2 + 7.55 MR^3 \\ - 1.8333 MR^4] = C_1 T_0 + C_2$$

$$8. \quad Q = \dot{w} \int_{exit}^{inlet} C_p dT$$

$$\dot{w}_{needed} = Q_{design} / \int_{exit}^{inlet} C_p dT$$

$$\dot{w}_{needed} = Q_0 / [(C_1/2) (T_0 - T_{exit})^2 + C_2 (T_0 - T_{exit})]$$

$$10. \quad MW = 2.026 (1 + MR)$$

$$P_{exit} = (\dot{w}/A_{exit}) \left[\frac{1545}{32.174} \frac{T_{exit}}{MW} \right]^{0.5} \left[\frac{1}{(\gamma)^{0.5} \left(\frac{2}{\gamma+1} \right)^{(r+1)/2(r-1)}} \right]$$

$$\gamma = 1.38$$

$$11. \quad P_{exit} = P_{0, exit} / \left[1 + \frac{\gamma-1}{2} M^2 \right]^{r/(r-1)}$$

$$T_{0, exit} = T_{0, in} / \left[1 + \frac{\gamma-1}{2} M^2 \right]$$

TABLE A-1 (CONT)

$$12. \quad P_{\text{EXIT}} = \left(\frac{144}{1545} \text{ MW} \right) \left(\frac{P_{\text{EXIT}}}{T_{\text{EXIT}}} \right)$$

$$13. \quad T_{\text{chamber end}} = 0.976 T_c$$

$$15. \quad \Delta P = \Delta P_{\text{Design}} \left(\frac{\dot{W}}{\dot{W}_{\text{Design}}} \right)^2 \left[\frac{P_{\text{AVG, DESIGN}}}{(P_{\text{EXIT}} + P_{\text{CHAMBER END}})/2} \right]$$

$$16. \quad P_{c_T} = P_{\text{EXIT}} + \Delta P$$

$$17. \quad P_{c_s} = 0.9 P_{c_T}$$

$$18. \quad P_{\text{CHAMBER END}} = \left(\frac{144}{1545} \right) \text{ MW} \left(\frac{P_{c_s}}{T_{\text{chamber END}}} \right)$$

$$25., 27., 29. \quad \Delta P = \frac{K \dot{W}^2}{(P_{\text{IN}} + P_{\text{OUT}})/2}$$

TABLE A-2
PROGRAM LISTING

TCBAL4 21:04 NR T/S 4 OCT, 1971

```

100SLIB,H2HS,,B072
200SLIB,XYHS,,B072
300 DIMENSION XI(15),DP(15),DT(15)
400 DIMENSION DR(15),DOR(15),ROR(15),F(15)
500 DIMENSION J(15)
600 COMMON R(20),W(10),PH(20),P0(15),TH(20),T0(15),RH(15),R0(15),CN(17)
700 CALL OPENF(1,"BALIN2",2,"G291")
800 CALL OPENF(5,"TC0N2",7)
900 CS=119.65
1000 CON=3.963353E-2
1100 NI=0
1200 TC=2023.3
1300 QD=2778.379518
1400 QD=QD*((0.11/2000.)*(TC**2-750.**2)+1.67574*(TC-750.))
1500& /((0.11/2000.)*(2026.9**2-750.**2)+1.67574*(1276.9))
1600 XT01=750.
1700 C3=1.67574
1800 WX3=0.0
1900 WX1=0.02
2000 WX2=0.0
2100 WX4=0.02
2200 DO 5 I=1,15
2300 5 J(I)=I
2400 READ (1,)(R(I),I=1,20)
2500 10 READ (1,)(XI(I),I=1,11)
2600 PRINT,"T"
2700 PE1=240.
2800 DELTAT=13.
2900 PC=240.
3000 W(1)=0.595
3100 W(4)=0.595
3200 W(2)=0.5657
3300 W(6)=0.5657
3400 W(3)=0.0293
3500 W(5)=0.0293
3600 CALL @XYHS(14.7,162.,0.,XH01,S1,NI,D1)
3700 12 DO 15 I=1,15
3800 PH(I)=0
3900 TH(I)=0
4000 P0(I)=0
4100 15 T0(I)=0
4200 T0(I)=XI(I)
4300 XMR=1.0
4400 WTC=1.19
4500 DO 370 J1=2,9
4600 TH(I)=XI(J1)
4700 IF (TH(I)..EQ.0) GO TO 370
4800 PRINT,"A"
4900 1405 CALL @XYHS(PC,T0(I),0.,XH02,S1,NI,D1)
5000 300 CONTINUE
5100 XH03=(W(4)*(XH02-XH01)/892.86)/W(1)
5200 XMW=2.016*(1+XMR)

```

```

5300 GO=(1545./32.174)
5400 G1=SQRT(1.38)*(0.840336)**(2.38/.76)
5500 A1=1.417206891
5600 A1=A1*(1.19/1.226)
5700 A1=A1*SQRT(TC/2034.2)
5800 1410 TEMP=(TH(1)+DELTAT*(0.5657/W(2)))*W(2)
5900 TEMP=(TEMP+TH(1)*W(3))/W(1)
6000 XHF=-1.18+(1.44/350.)*(TEMP-250.)
6100 XHF=XHF+XH03
6200 XMR2=-.286966+5.13854E-4*TC+2.96261E-8*TC**2
6300& -.144405*XHF-2.76646E-4*XHF**2
6400 IF (ABS(XMR2-XMR).LT.0.0001) GO TO 310
6500 W(1)=WTC/(1+XMR2)
6600 W(4)=WTC-W(1)
6700 W(2)=W(2)*(1+XMR)/(1+XMR2)
6800 W(3)=W(1)-W(2)
6900 XMR=XMR2
7000 GO TO 300
7100 310 C1=0.11/1000.
7200 C2=3.41+15.217*XMR-169.19*XMR**2+627.992*XMR**3
7300& -1200.95*XMR**4+1303.76*XMR**5-809.766*XMR**6
7400& +267.562*XMR**7-36.3596*XMR**8
7500 W(7)=(1.19)*((C1*TC+C3)/(C1*TC+C2))**(.7)
7600 CC1=0D/W(7)-(C1/2.)*TC**2-C2*TC
7700 CC2=C2
7800 CC3=C1/2.
7900 XT0=(-CC2+SQRT(CC2**2-4.*CC3*CC1))/(2.*CC3)
8000 620 IF (ABS(W(7)-WTC).LT.1E-6) GO TO 1420
8100 W(1)=W(7)/(1+XMR)
8200 W(4)=W(7)-W(1)
8300 W(2)=W(2)*W(7)/WTC
8400 W(3)=W(1)-W(2)
8500 WTC=W(7)
8600 QREL=((C1*TC+C2)/(C1*TC+C3))*(WTC/1.19)**0.66
8700 DELTAT=(13.)*QREL
8800 GO TO 300
8900 1420 XP0=(WTC/A1)*SQRT(G0*XT0/XMW)/G1
9000 XP0S=XP0/(1.19**(.38/.38))
9100 XT0S=XT0/(1.19)
9200 R0T=((144.)*XMW/(1545.))*(XP0S/XT0S)
9300 TCS=0.976*TC
9400 R0TC=R0T
9500 R0TC1=R0T
9600 1430 DELP=((C5*C0N)*(WTC/1.19)**2)/((R0TC+R0T)/2)
9700 PC2=XP0+DELP
9800 PC2S=0.9*PC2
9900 R0TC=((144.)*XMW/(1545.))*(PC2S/TCS)
10000 IF (ABS(R0TC-R0TC1).LT.1E-6) GO TO 1433
10100 R0TC1=R0TC
10200 GO TO 1430
10300 1433 IF (ABS(PC-PC2).LT.0.02) GO TO 1435
10400 PC=PC2
10500 GO TO 1405
10600 1435 TH(4)=(TEMP*W(1)-TH(1)*W(3))/W(2)
10700 T0(2)=T0(3)=T0(11)=T0(12)=T0(5)=T0(4)=T0(1)
10800 TH(5)=TH(1)
10900 P0(4)=P0(5)=PH(4)=PH(5)=PC
11000 CALL PHR0(PH(4),TH(4),0.,RH(4),0,PV,CN)
11100 CALL PHR0(PH(5),TH(5),0.,RH(5),0,PV,CN)
11200 CALL OXYDEN(P0(4),T0(4),0.,R0(4),0)
11300 CALL OXYDEN(P0(5),T0(5),0.,R0(5),0)
11400 CALL HP(4,9,4,3,2,4,9,4,9)
11500 CALL HP(9,3,9,9,2,9,3,9,3)
11600 CALL HP(5,10,5,4,3,5,10,5,10)
11700 K2=RH(3)
11800 PH(13)=PH(3)+R(2)*W(2)**2/RH(2)

```

TABLE A-2 (CONT)

```

11900 TH(13)=TH(1)
12000 1437 CALL PHR( PH(13),TH(13),0.,RH(13),0.,PV,CN)
12100 IF (ABS(X2-RH(13)).LT.1E-8) GO TO 1439
12200 PH(13)=PH(3)+R(2)*W(2)**2/((RH(3)+RH(13))/2)
12300 X2=RH(13)
12400 GO TO 1437
12500 1439 CALL HP(13,2,13,13,2,13,2,13,2)
12600 CALL HP(10,14,10,10,3,10,14,10,14)
12700 IF (ABS(PH(2)-PH(14)).LT.0.05) GO TO 330
12800 CALL XITER(PH(2),PH(14),WX3,WX1,WX)
12900 IF (PH(2).LT.PH(14)) GO TO 320
13000 W(2)=W(2)-WX
13100 W(3)=W(3)+WX
13200 GO TO 1410
13300 320 W(2)=W(2)+WX
13400 W(3)=W(3)-WX
13500 GO TO 1410
13600 330 CALL HP(2,1,2,1,1,2,1,2,1)
13700 W(6)=W(6)*W(4)/0.5950
13800 W(5)=W(4)-W(6)
13900 340 CALL OP(4,12,4,7,6,4,12,4,12,1)
14000 CALL OP(12,3,12,12,6,12,3,12,3,1)
14100 CALL OP(3,2,3,6,6,3,2,3,2,1)
14200 CALL OP(5,11,5,8,5,5,11,5,11,1)
14300 CALL OP(11,14,11,11,5,11,14,11,14,1)
14400 IF (ABS(P0(2)-P0(14)).LT.0.05) GO TO 360
14500 CALL XITER(P0(2),P0(14),WX2,WX4,WX)
14600 IF (P0(2).LT.P0(14)) GO TO 350
14700 W(6)=W(6)-WX
14800 W(5)=W(5)+WX
14900 GO TO 340
15000 350 W(6)=W(6)+WX
15100 W(5)=W(5)-WX
15200 GO TO 340
15300 360 CALL OP(2,1,2,5,4,2,1,2,1,1)
15400 WIGN=W(5)+W(3)
15500 XMR1=W(5)/W(3)
15600 DO 1630 I=1,5
15700 1630 WRITE (5,2300)
15800 WRITE (5,2870)
15900 WRITE (5,2300)
16000 IF (XI(10).EQ.1) GO TO 1600
16100 WRITE (5,2000)
16200 GO TO 1700
16300 1600 WRITE (5,2100)
16400 1700 IF (XI(11).EQ.1) WRITE (5,2600)
16500 WRITE (5,2300)
16600 WRITE (5,2200)PH(1),TH(1),W(1)
16700 WRITE (5,2210)P0(1),T0(1),W(4)
16800 WRITE (5,2220)PC,XMR,WTC
16900 WRITE (5,2700)TC
17000 WRITE (5,2800)XMR1,WIGN
17100 WRITE (5,2300)
17200 DR(1)=RH(1)
17300 DR(2)=RH(13)
17400 DR(3)=RH(9)
17500 DR(4)=RH(10)
17600 DR(5)=R0(1)
17700 DR(6)=R0(2)
17800 DR(7)=R0(12)
17900 DR(8)=R0(11)
18000 DR(1)=RH(2)
18100 DR(2)=RH(3)
18200 DR(3)=RH(4)
18300 DR(4)=RH(5)

```

TABLE A-2 (CONT)

TABLE A-2 (CONT)

```

18400 DOR(5)=R0(2)
18500 DOR(6)=R0(3)
18600 DOR(7)=R0(4)
18700 DOR(8)=R0(5)
18800 F(1)=W(1)
18900 F(2)=F(3)=W(2)
19000 F(4)=W(3)
19100 F(5)=W(4)
19200 F(6)=F(7)=W(6)
19300 F(8)=W(5)
19400 D0 1610 I=1,15
19500 1610 R0R(I)=R(I)
19600 IF (XI(8).NE.1) G0 T0 1620
19700 DP(6)=DP(7)=DT(6)=DT(7)=DR(6)=DR(7)=0.0
19800 DOR(6)=DOR(7)=R0R(6)=R0R(7)=F(6)=F(7)=0.0
19900 DP(12)=DT(12)=D0R(12)=DR(12)=R0R(12)=F(12)=0.0
20000 1620 DP(9)=PH(3)-PH(9)
20100 DP(10)=PH(2)-PH(10)
20200 DP(11)=P0(2)-P0(11)
20300 DP(12)=P0(3)-P0(12)
20400 DP(13)=PH(2)-PH(13)
20500 DT(9)=DT(10)=DT(11)=DT(12)=0.0
20600 DT(13)=TH(13)-TH(2)
20700 DR(9)=RH(3)
20800 DR(10)=RH(2)
20900 DR(11)=R0(2)
21000 DR(12)=R0(3)
21100 DR(13)=RH(2)
21200 D0R(9)=RH(9)
21300 D0R(10)=RH(10)
21400 D0R(11)=R0(11)
21500 D0R(12)=R0(12)
21600 D0R(13)=RH(13)
21700 F(9)=W(2)
21800 F(10)=W(3)
21900 F(11)=W(5)
22000 F(12)=W(6)
22100 F(13)=W(2)
22200 DP(1)=PH(1)-PH(2)
22300 DP(2)=PH(13)-PH(3)
22400 DP(3)=PH(9)-PH(4)
22500 DP(4)=PH(10)-PH(5)
22600 DT(1)=TH(2)-TH(1)
22700 DT(2)=TH(3)-TH(13)
22800 DT(3)=TH(4)-TH(9)
22900 DT(4)=TH(5)-TH(10)
23000 DP(5)=P0(1)-P0(2)
23100 DP(6)=P0(2)-P0(3)
23200 DP(7)=P0(12)-P0(4)
23300 DP(8)=P0(11)-P0(5)
23400 DT(5)=T0(2)-T0(1)
23500 DT(6)=T0(3)-T0(2)
23600 DT(7)=T0(4)-T0(12)
23700 DT(8)=T0(5)-T0(11)
23800 WRITE (5,2810)
23900 WRITE (5,2300)
24000 WRITE (5,2400)
24100 WRITE (5,2500)J(1),DP(1),DT(1),DR(1),D0R(1),R0R(1),F(1)
24200 WRITE (5,2500)J(13),DP(13),DT(13),DR(13),D0R(13),R0R(13),F(13)
24300 WRITE (5,2500)J(2),DP(2),DT(2),DR(2),D0R(2),R0R(2)
24400 WRITE (5,2500)J(9),DP(9),DT(9),DR(9),D0R(9),R0R(9)
24500 WRITE (5,2500)J(3),DP(3),DT(3),DR(3),D0R(3),R0R(3)
24600 WRITE (5,2850)PH(1),TH(1)
24700 WRITE (5,2300)
24800 IF (XI(8).EQ.1) G0 T0 1800
24900 WRITE (5,2820)

```

```

25000 WRITE (5,2300)
25100 WRITE (5,2400)
25200 WRITE (5,2500)J(5),DP(5),DT(5),DR(5),DOR(5),ROR(5),F(5)
25300 WRITE (5,2500)J(6),DP(6),DT(6),DR(6),DOR(6),ROR(6),F(6)
25400 WRITE (5,2500)J(12),DP(12),DT(12),DR(12),DOR(12),ROR(12)
25500 WRITE (5,2500)J(7),DP(7),DT(7),DR(7),DOR(7),ROR(7)
25600 WRITE (5,2850)PO(1),TO(1)
25700 WRITE (5,2300)
25800 1800 WRITE (5,2830)
25900 WRITE (5,2300)
26000 WRITE (5,2400)
26100 WRITE (5,2500)J(1),DP(1),DT(1),DR(1),DOR(1),ROR(1),F(1)
26200 WRITE (5,2500)J(10),DP(10),DT(10),DR(10),DOR(10),ROR(10),F(10)
26300 WRITE (5,2500)J(4),DP(4),DT(4),DR(4),DOR(4),ROR(4)
26400 WRITE (5,2300)
26500 WRITE (5,2640)
26600 WRITE (5,2300)
26700 WRITE (5,2400)
26800 WRITE (5,2500)J(5),DP(5),DT(5),DR(5),DOR(5),ROR(5),F(5)
26900 WRITE (5,2500)J(11),DP(11),DT(11),DR(11),DOR(11),ROR(11),F(11)
27000 WRITE (5,2500)J(8),DP(8),DT(8),DR(8),DOR(8),ROR(8)
27100 WRITE (5,2300)
27200 WRITE (5,2880)XT0
27300 WRITE (5,2890)QREL
27400 WRITE (5,2300)
27500 PRINT,"DP-3=",DP(3)," DP-4=",DP(4)
27600 PRINT,"DP-7=",DP(7)," DP-8=",DP(8)
27700 PRINT,"W-H2-IJ=",W(2)," W-H2-IG=",W(3)
27800 PRINT,"W-O2-IJ=",W(6)," W-O2-IG=",W(5)
27900 PRINT,"PC=",PC," TC=",TC
28000 WDOT=W(1)+W(4)
28100 PRINT,"MR=",XMR," W-DOT=",WDOT
28200 PRINT,"P1-H2=",PH(1)," T1-H2=",TH(1)
28300 PRINT,"P1-O2=",PO(1)," T1-O2=",TO(1)
28400 PRINT,"C1=",C1," C2=",C2
28500 PRINT,"W-H2=",W(1)," W-O2=",W(4)
28600 PRINT,"T-EXIT=",XT0
28700 PRINT,"JACKET RELATIVE Q/A=",QREL
28800 IF (XI(11).EQ.1) GO TO 1820
28900 DO 1810 I=1,14
29000 1810 WRITE (5,2300)
29100 GO TO 1840
29200 1820 DO 1830 I=1,22
29300 1830 WRITE (5,2300)
29400 1840 WRITE (5,2860)
29500 370 CONTINUE
29600 GO TO 10
29700 2000 FORMAT(19X,"HYDROGEN THERMAL CONDITIONER")
29800 2100 FORMAT(19X,"OXYGEN THERMAL CONDITIONER")
29900 2200 FORMAT(5X,"H2-",1X,F5.1,1X,"PSIA",2X,F5.1,1X,"DEG R",
30000& 2X,F6.3,1X,"LBM/SEC")
30100 2210 FORMAT(5X,"O2-",1X,F5.1,1X,"PSIA",2X,F5.1,1X,"DEG R",
30200& 2X,F6.3,1X,"LBM/SEC")
30300 2220 FORMAT(5X,"PC=",F6.1,1X,"PSIA",2X,"MR=",F6.3,1X,"O/F",
30400& 2X,"CHAMBER FLOW=",F6.3,1X,"LBM/SEC")
30500 2300 FORMAT(1X)
30600 2400 FORMAT(5X,"NODE",1X,"DELTA-P",1X,"DELTA-T",3X,"R0-IN",
30700& 5X,"R0-OUT",7X,"RESISTANCE",4X,"FLOW")
30800 2500 FORMAT(6X,I2,3X,F6.2,2X,F6.2,1X,1PE9.3,1X,1PE9.3,
30900& 3X,OPF12.4,3X,F7.4)
31000 2810 FORMAT(22X,"INJECTOR HYDROGEN FLOW")
31100 2820 FORMAT(22X,"INJECTOR OXYGEN FLOW")
31200 2830 FORMAT(22X,"IGNITOR HYDROGEN FLOW")
31300 2840 FORMAT(22X,"IGNITOR OXYGEN FLOW")
31400 2850 FORMAT(5X,"INLET PRESSURE=",F5.1,2X,"INLET TEMPERATURE=",

```

TABLE A-2 (CONT)

```

31500&          F5.1)
31600 2860 FORMAT(1X,"-----")
31700 2870 FORMAT(23X,"CONTROL REQUIREMENTS")
31800 2880 FORMAT(5X,"EXIT TEMPERATURE=",F7.1)
31900 2890 FORMAT(5X,"JACKET RELATIVE Q/A=",F7.4)          TABLE A-2 (CONT)
32000 2600 FORMAT(23X,"IGNITER FLOW ONLY")
32100 2700 FORMAT(5X,"COMBUSTION TEMPERATURE=",F7.1,1X,"DEG R")
32200 2800 FORMAT(5X,"IGNITOR: MR=",F6.3,1X,"O/F",2X,"FLOW=",F7.4,
32300&          1X,"LBM/SEC")
32400 19 END
32500 SUBROUTINE HP(I1,I2,I3,I4,I5,I6,I7,I8,I9)
32600     COMMON R(20),W(10),PH(20),P0(15),TH(20),T0(15),RH(15),R0(15),CN(17)
32700 10 PH(I2)=PH(I3)+R(I4)*W(I5)**2/RH(I6)
32800 20 CALL PHR0(PH(I7),TH(I8),0.,RH(I7),0,PV,CN)
32900     IF (ABS(X-RH(I7)).LT.1E-8) GO TO 30
33000     PH(I2)=PH(I3)+R(I4)*W(I5)**2/((RH(I7)+RH(I1))/2)
33100     X=RH(I7)
33200     GO TO 20
33300 30 TH(I9)=TH(I8)
33400     RETURN
33500 END
33600 SUBROUTINE OP(I1,I2,I3,I4,I5,I6,I7,I8,I9,I0)
33700     COMMON R(20),W(10),PH(20),P0(15),TH(20),T0(15),RH(15),R0(15),CN(17)
33800     IF (I0.EQ.0) GO TO 10
33900     P0(I2)=P0(I3)+R(I4)*W(I5)**2/R0(I6)
34000     GO TO 20
34100 10 P0(I2)=P0(I3)-R(I4)*W(I5)**2/R0(I6)
34200 20 CALL OXYDEN(P0(I7),T0(I8),0.,R0(I7),0)
34300     IF (ABS(X-R0(I7)).LT.1E-8) GO TO 30
34400     IF (I0.NE.0) GO TO 40
34500     P0(I2)=P0(I3)-R(I4)*W(I5)**2/((R0(I7)+R0(I1))/2)
34600     GO TO 50
34700 40 P0(I2)=P0(I3)+R(I4)*W(I5)**2/((R0(I7)+R0(I1))/2)
34800 50 X=R0(I7)
34900     GO TO 20
35000 30 T0(I9)=T0(I8)
35100     RETURN
35200 END
35300 SUBROUTINE XITER(P1,P2,DEL1,X1,X2)
35400     DEL2=P1-P2
35500 20 X2=ABS(X1*DEL2/(DEL2-DEL1))
35600 30 X1=X2
35700     DEL1=DEL2
35800     RETURN
35900 END

```

READY

cooling jacket. The fixed area of the choked exit and the now-known exit temperature are used to predict the chamber pressure required to pass the assumed feed system flowrate. If the two calculated chamber pressures do not agree, the flowrate is changed and the entire analysis is repeated. This procedure continues until the pressures are matched, resulting in a balanced system. The final combustion temperature or exit temperature is compared to a preset limit and, if not matched, the inlet pressures are again perturbed, and the entire procedure is repeated until the limit is reached. A listing of the program is included as Table A-2.

Limits used were a maximum combustion temperature of 2830R (melting point of the material) and a minimum exit temperature of 660R to prevent condensation of water in the exit.

RESULTS

Figure A-3 shows the limits on hydrogen inlet pressure vs hydrogen inlet temperature. The effect of oxygen inlet temperature changes the limits approximately 1 psia; thus, the more stringent limit was taken and oxygen inlet temperature effect on hydrogen pressure requirements was dropped from further consideration. In fact, Figure A-3 shows that a small pressure band exists in which no temperature compensation at all is needed - 296.25 ± 4.25 psia. This would require extremely tight pressure regulation (1.43 percent); however, it totally eliminates any temperature compensation requirements on the hydrogen inlet side.

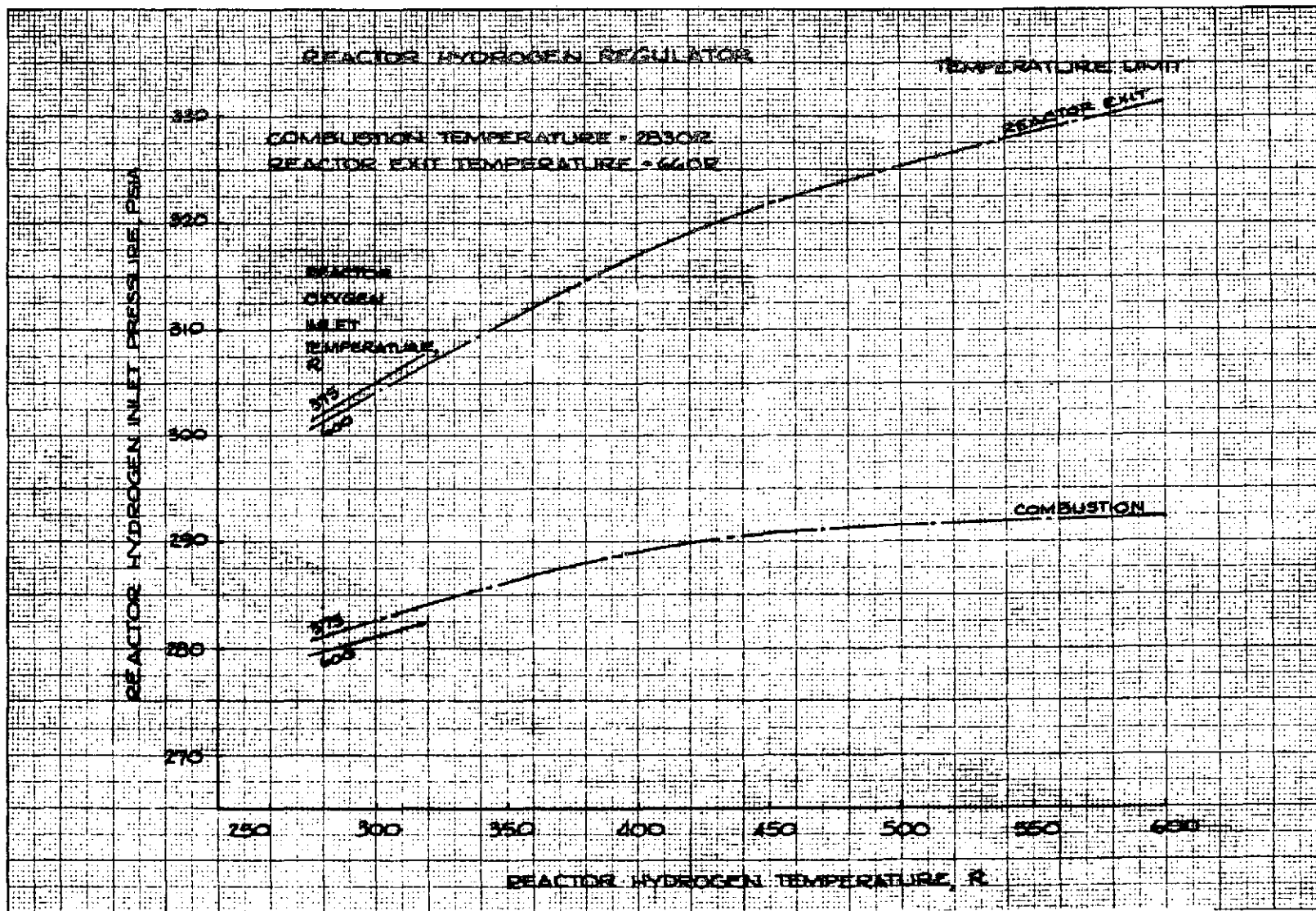


Figure A-3. Hydrogen Thermal Conditioner Control Requirements

However, an examination of Figure A-4 shows that no such possibility exists on the oxygen side - actually, the oxygen inlet pressure should be regulated on both oxygen and hydrogen inlet temperature.

Examination of both Figures A-3 and A-4 indicates that the system can be operated satisfactorily with a nominal operating line centered between limits (and thus temperature compensated) and a pressure regulation of ± 3 percent (Figures A-5 and A-6).

The double temperature compensation for the oxygen inlet can be avoided, by the use of a thermal equalizer located upstream of the pressure regulators. Figures A-7 and A-8 show the inlet pressure vs common inlet temperature requirements for the hydrogen and oxygen inlets, respectively. The hydrogen side is virtually identical with the previous case. The oxygen side is changed appreciably, however. It now even presents a small band in which no temperature compensation at all is required - 303 ± 3.25 psia. Examination of these two figures shows that when a thermal equalizer is used, the system will operate satisfactorily with a centered operating line - with temperature compensation based on only one common temperature for both inlets - and ± 3 percent pressure regulation (Figures A-9 and A-10).

Figures A-11 through A-14 show the range of various operational parameters which result if pressure regulation was maintained within the limits shown in Figures A-3 through A-6. Reactor mixture ratio is shown in Figure A-11, chamber pressure in Figure A-12, flowrate in Figure A-13, and reactor heat output in Figure A-14.

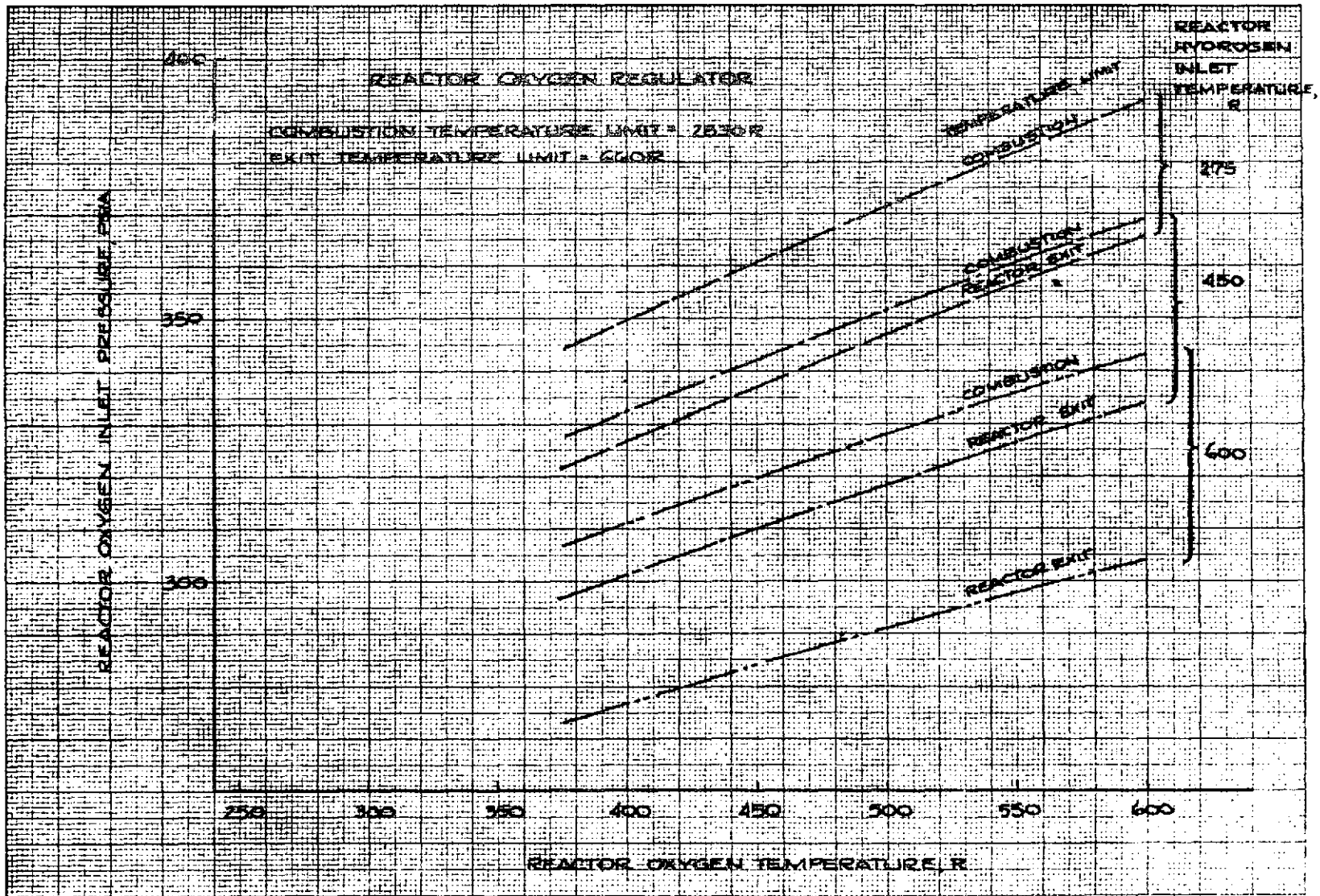


Figure A-4. Hydrogen Thermal Conditioner Control Requirements

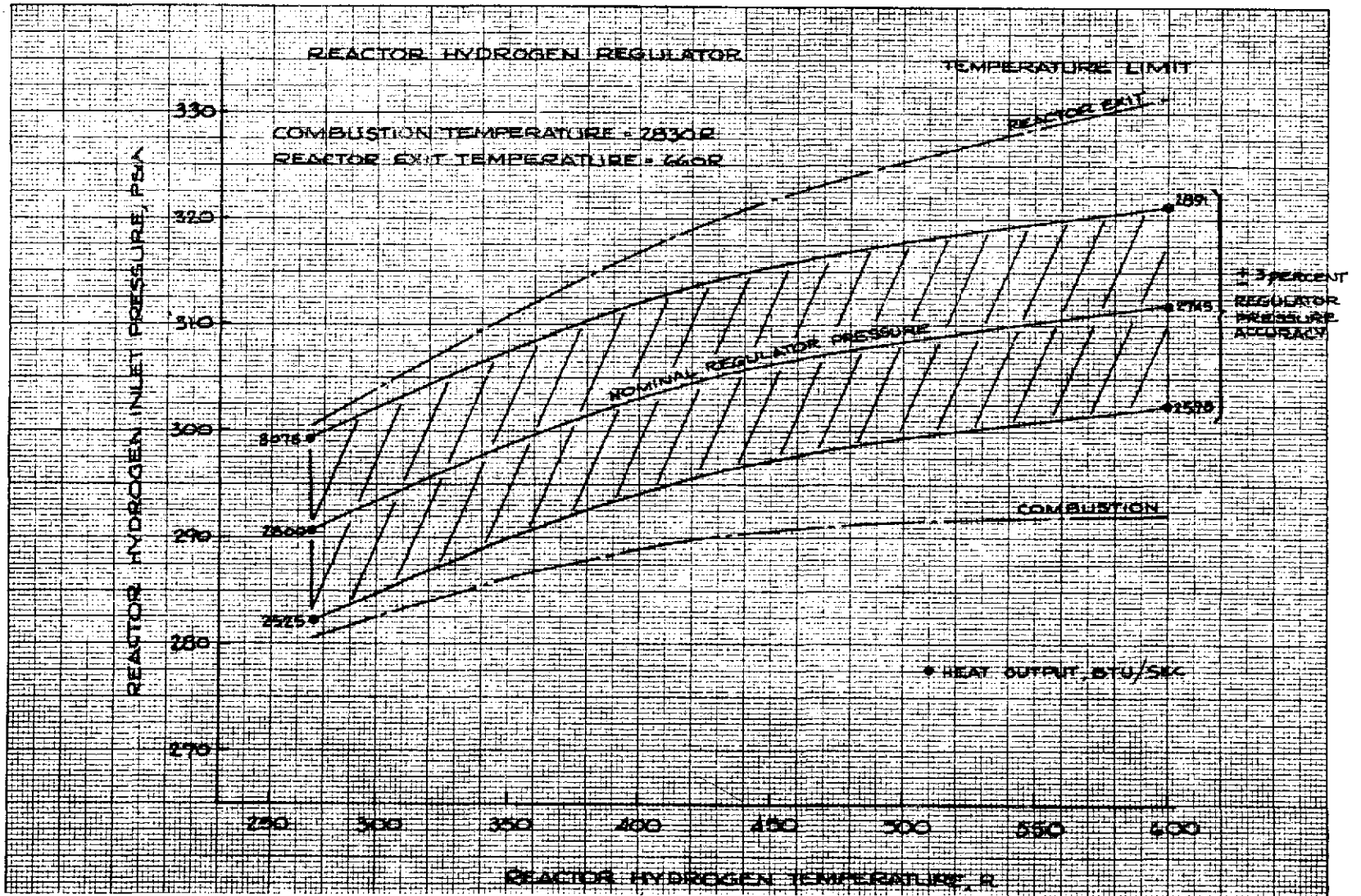


Figure A-5. Hydrogen Thermal Conditioner Control Requirements

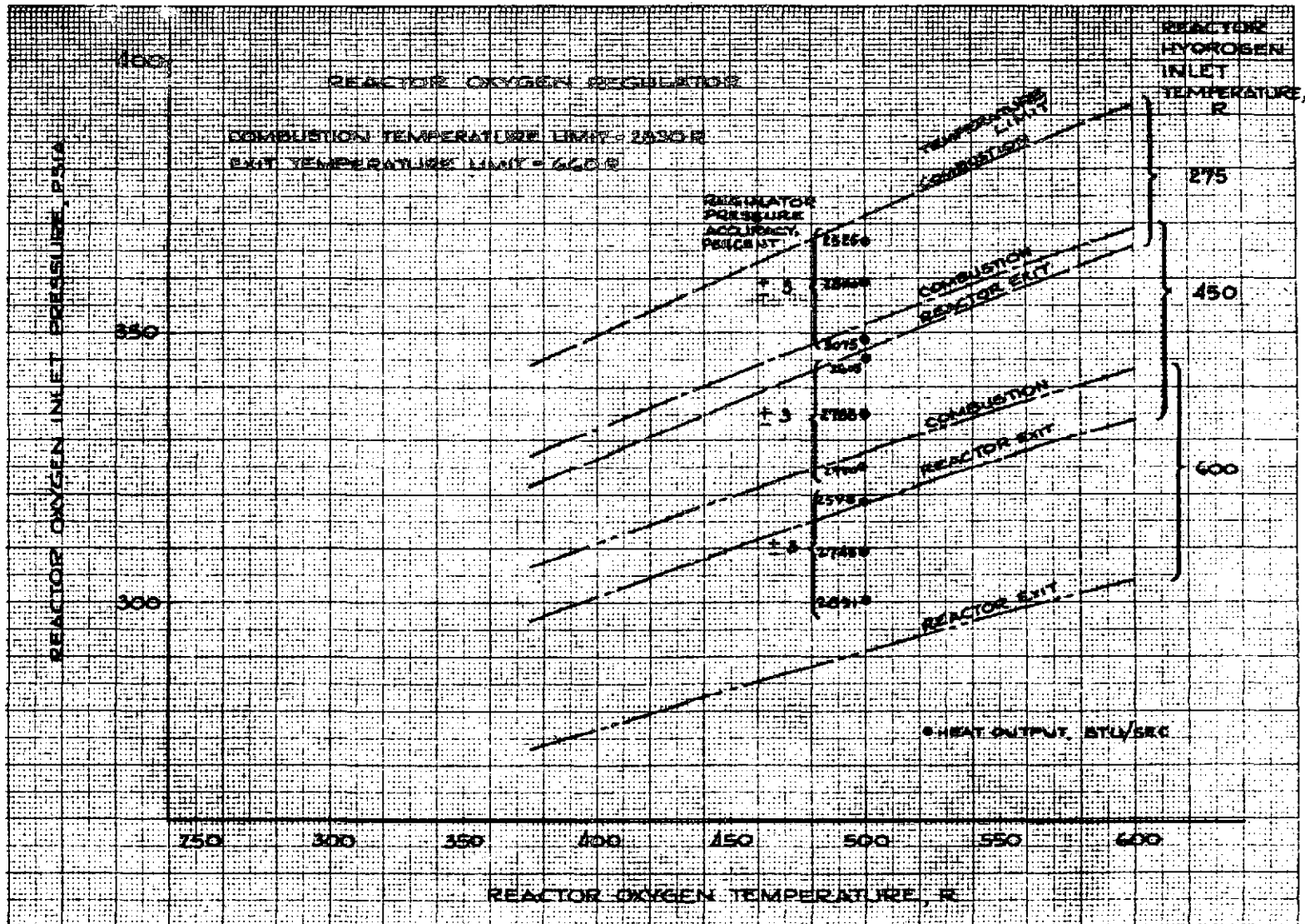


Figure A-6. Hydrogen Thermal Conditioner Control Requirements

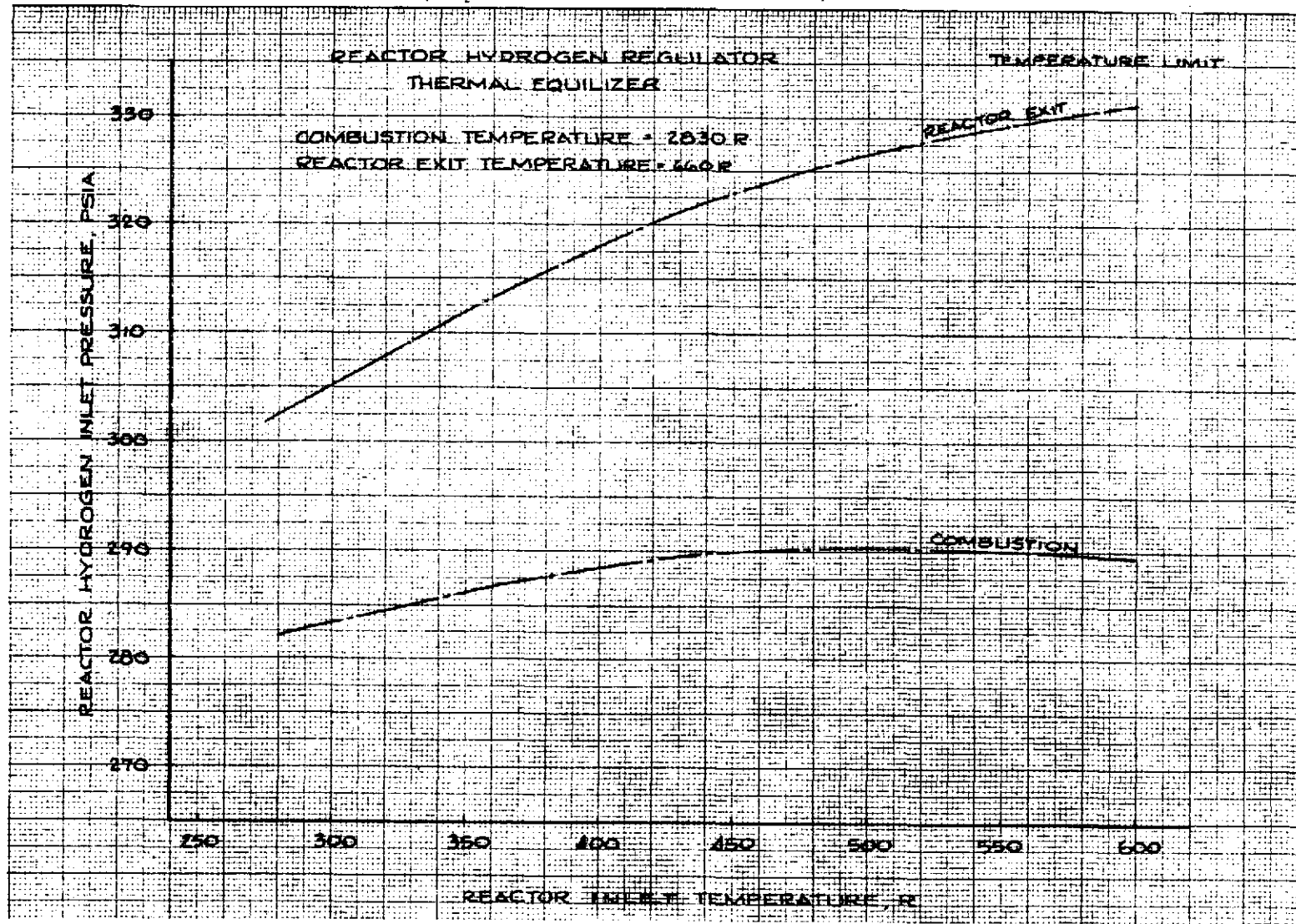


Figure A-7. Hydrogen Thermal Conditioner Control Requirements

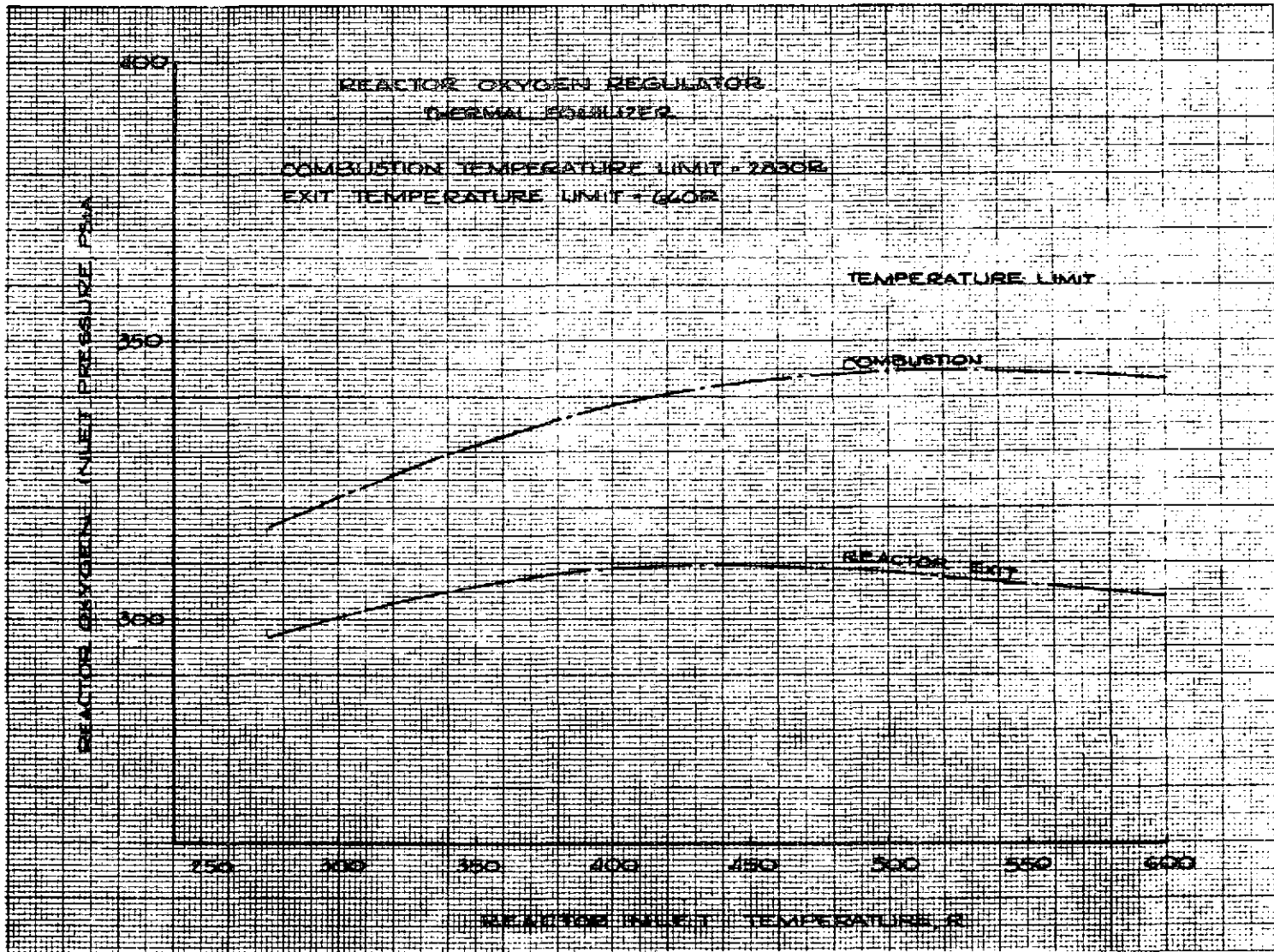


Figure A-8. Hydrogen Thermal Conditioner Control Requirements

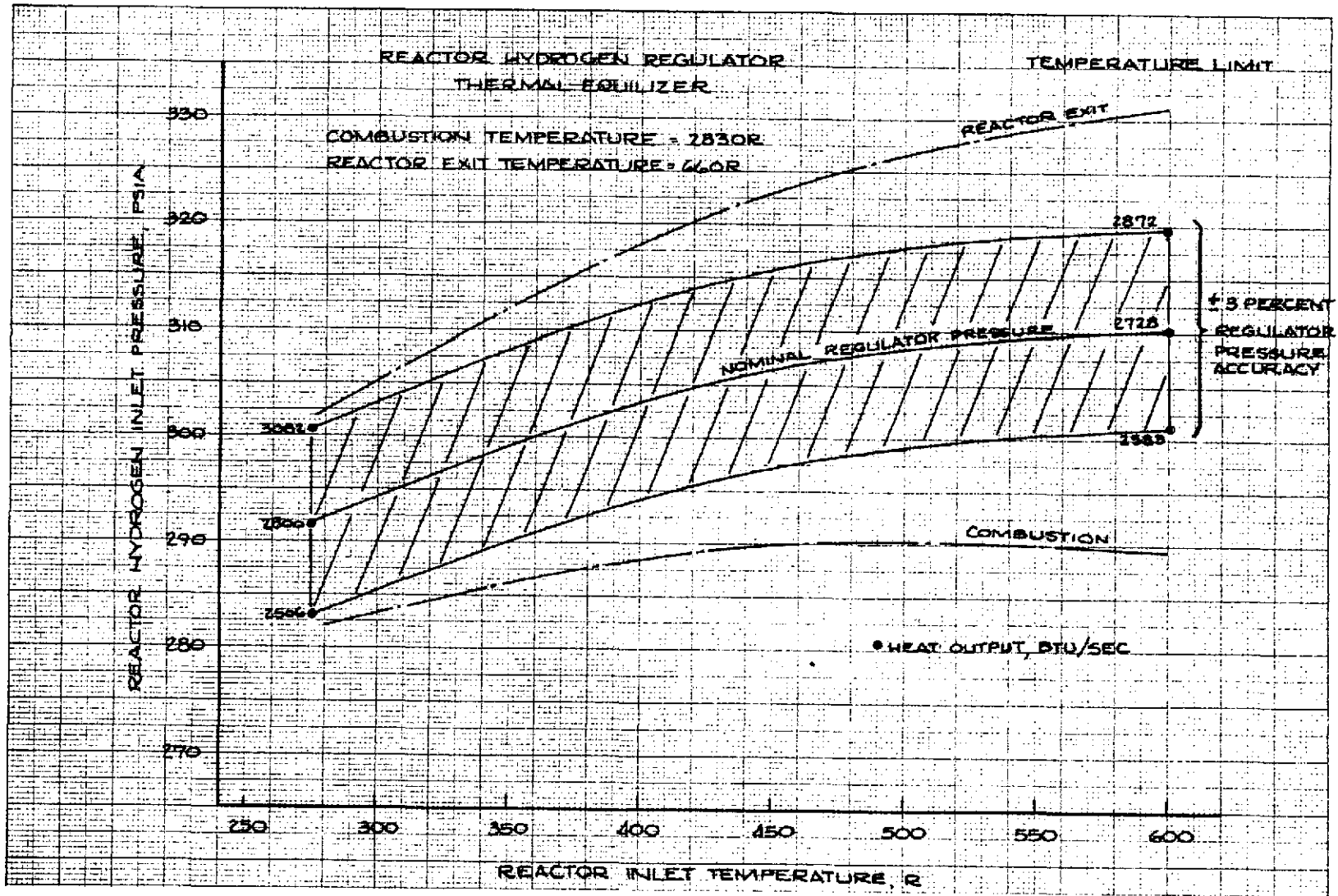


Figure A-9. Hydrogen Thermal Conditioner Control Requirements

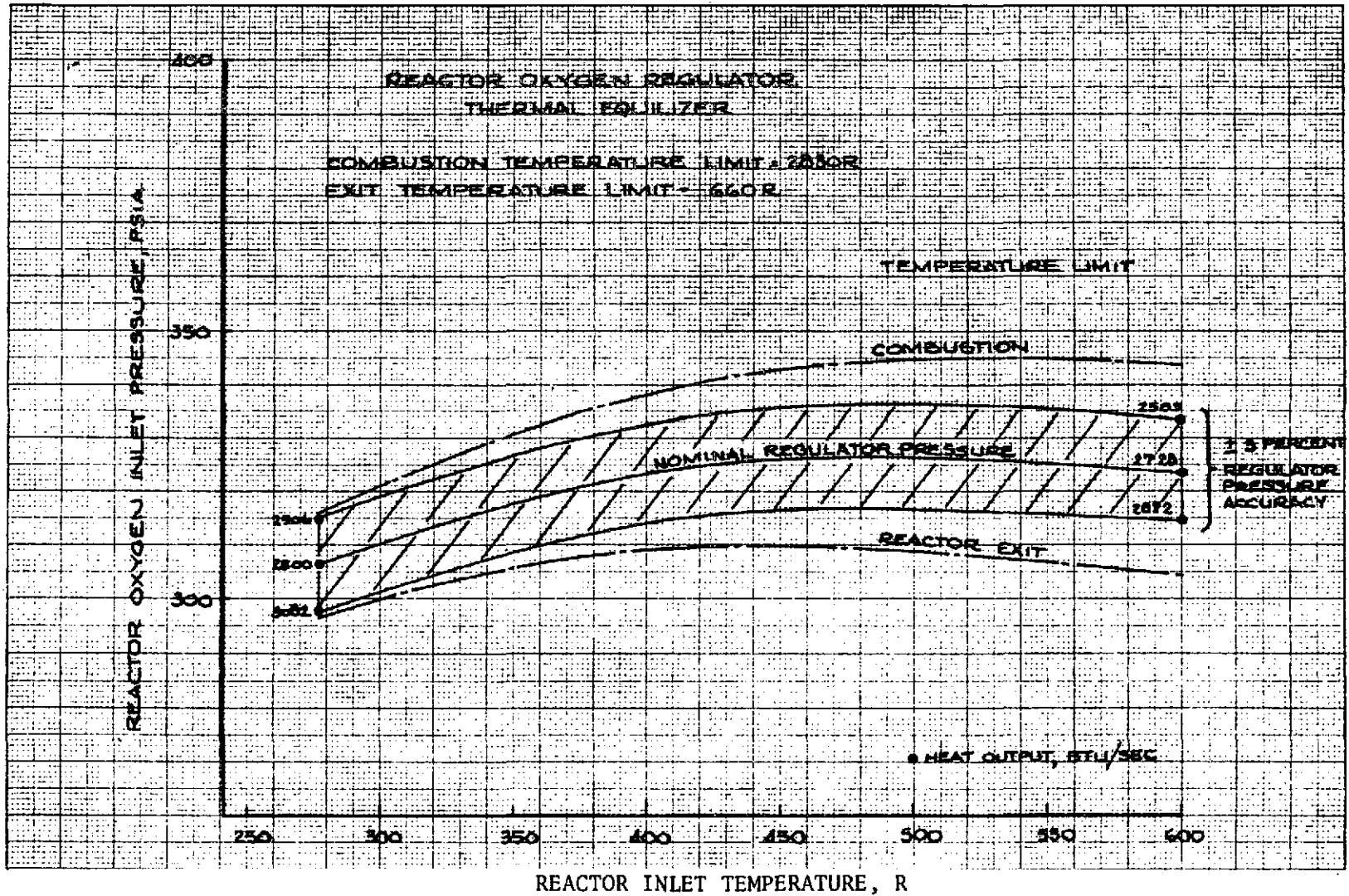


Figure A-10. Hydrogen Thermal Conditioner Control Requirements

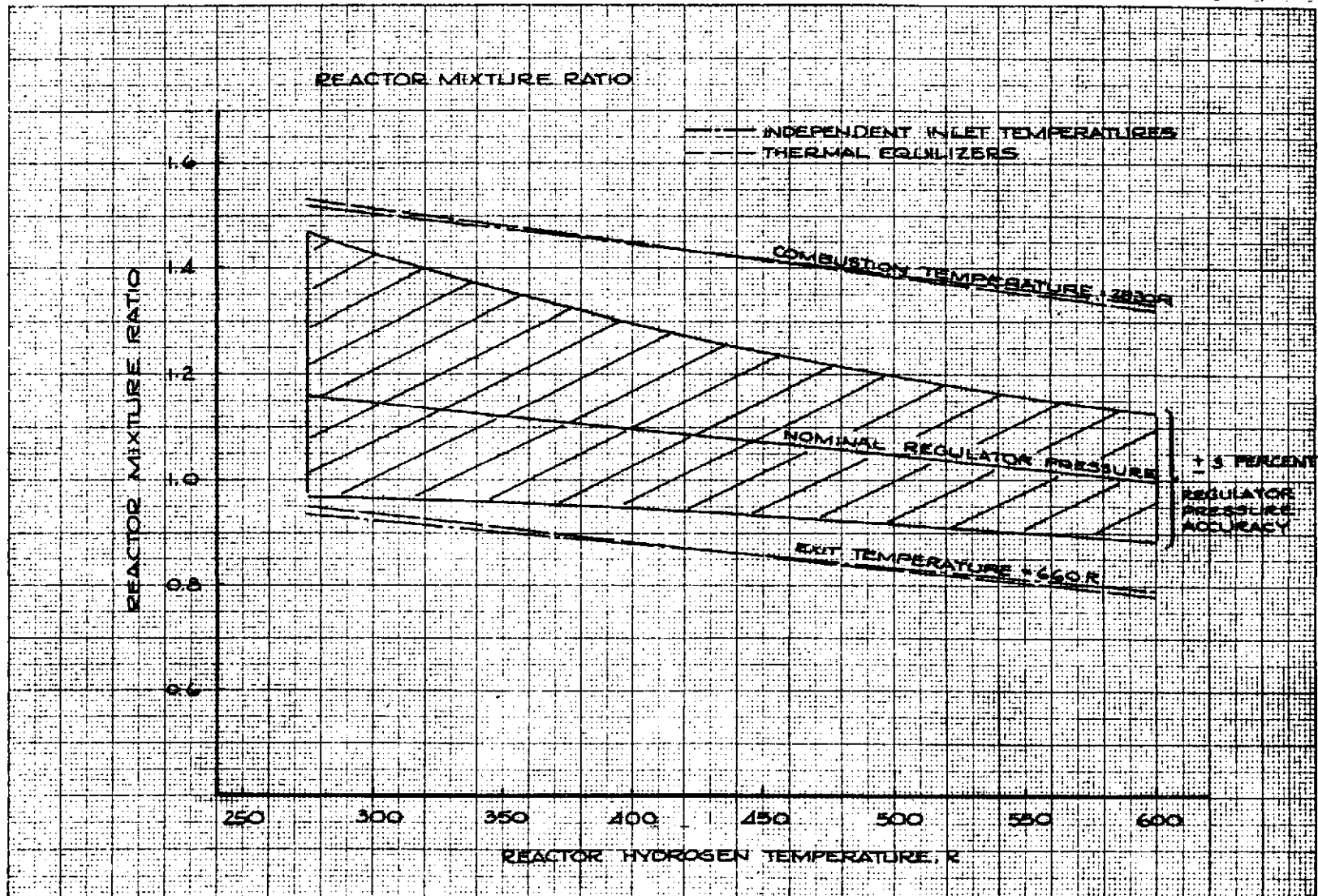


Figure A-11. Hydrogen Thermal Conditioner Control Requirements

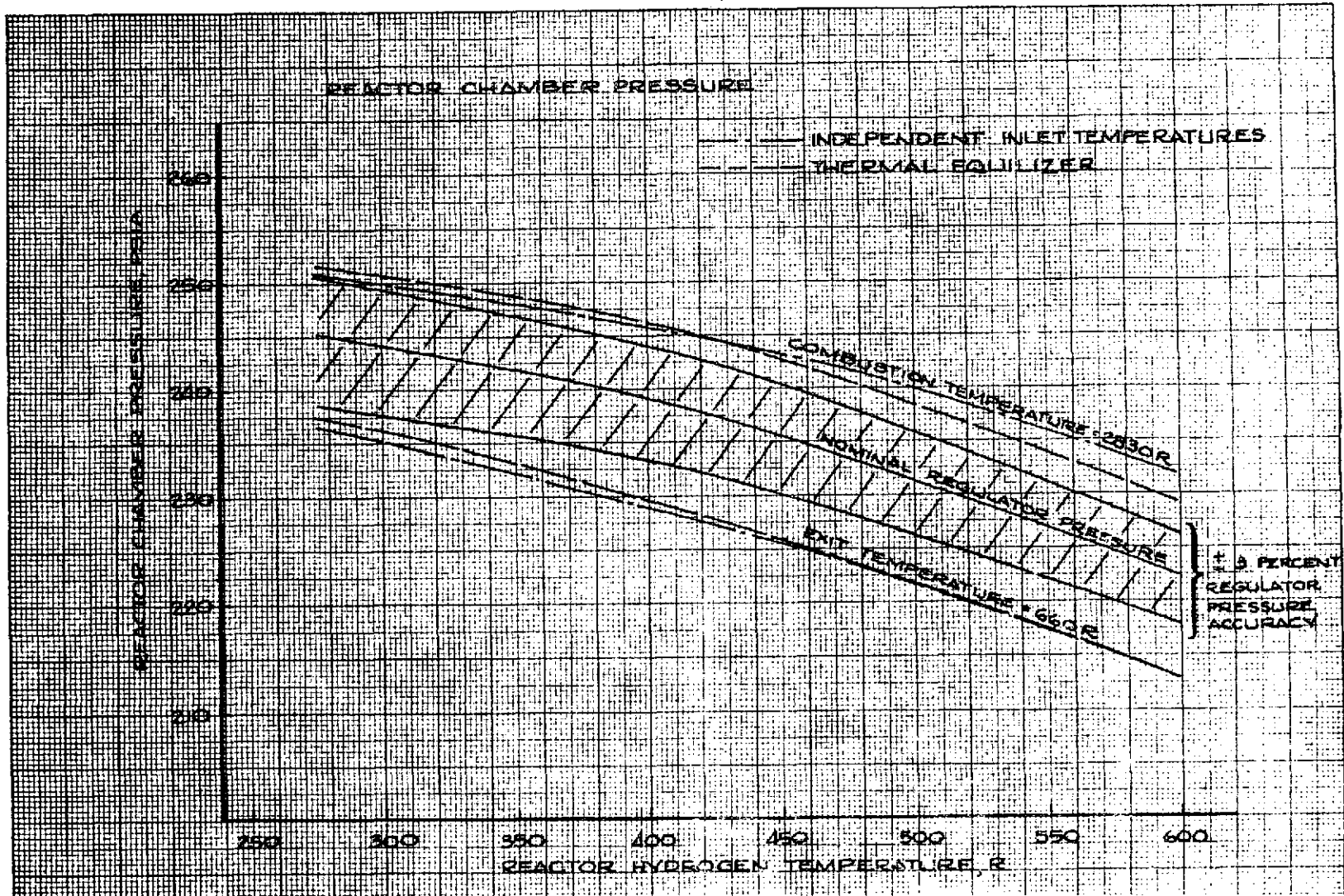


Figure A-12. Hydrogen Thermal Conditioner Control Requirements

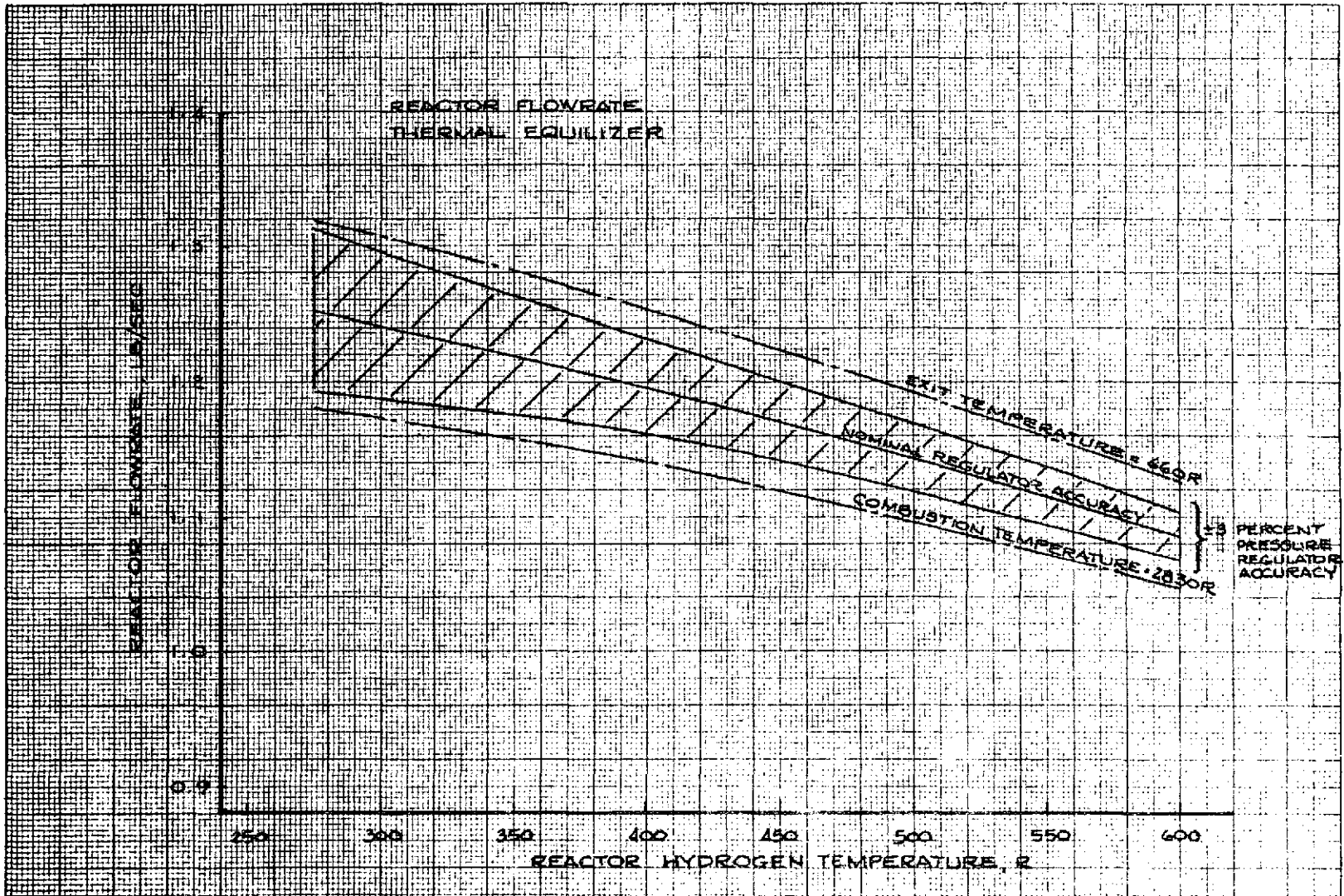


Figure A-13. Hydrogen Thermal Conditioner Control Requirements

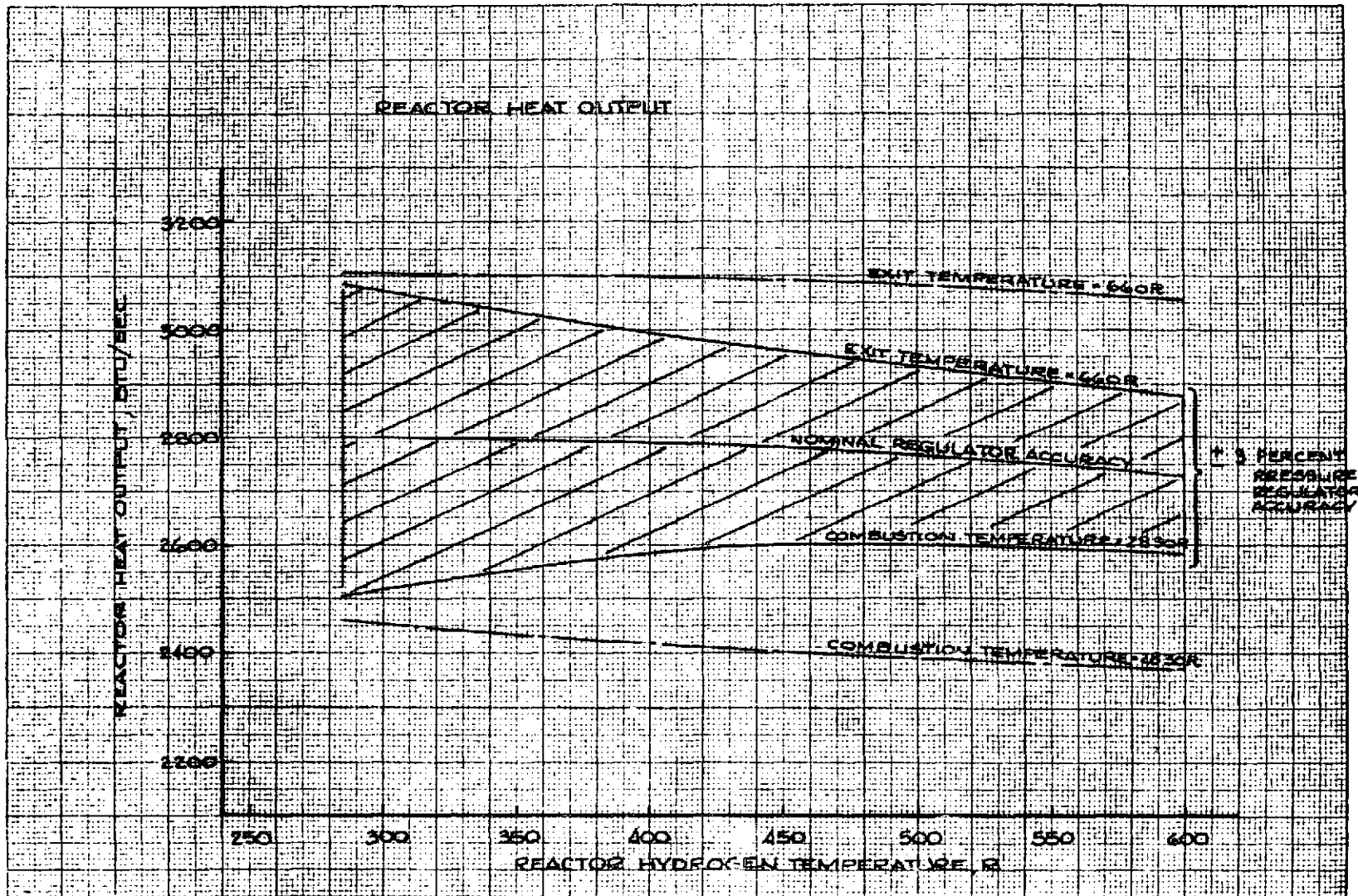


Figure A-14. Hydrogen Thermal Conditioner Control Requirements

APPENDIX B

EVALUATION OF ALTERNATE OXYGEN CONDITIONER CONCEPTS

The baseline oxygen thermal conditioner concept evaluated in this program consisted of a reactor operating at an oxidizer/fuel mixture ratio of 1.0 and a baffle type heat exchanger to transfer the energy from the reactor hot gas to the input cryogenic oxygen. Major factors considered in arriving at the baseline design included:

- Low wall temperature for reliability
- Low coolant pressure loss
- Weight
- Fail-safe operation
- Transient response
- Freezing potential
- Hot gas flow choking limitations
- Oxygen heat flux absorption ability

By far the most critical consideration was for fail safe operation. To ensure this end, alternate cycles for the oxygen conditioner may offer a potentially safer system at a minimum of added system weight. This study was undertaken to consider several alternate cycles for the oxygen conditioner and established a weight for each cycle.

System weights were established for fourteen alternate oxygen conditioner cycles. Weights varied from a high of 5.4 times the baseline weight to half the baseline weight. Weights of the various cycles evaluated are summarized in Table B-1.

Table B-1. Alternate Oxygen Conditioner Cycle Weight Comparison

Cycle		Total Weight* lb	Percent of Baseline
Baseline Cycle	o/f 1	359	Reference
Tridyne	O ₂ /H ₂ /He	1987	540
Tridyne	O ₂ /H ₂ /N ₂	1704	463
Dilution	N ₂	1768	480
Dilution	H ₂ O	954	259
Dilution	He	706	192
Oxidizer Rich	o/f 20:1	1611	438
Heat Sink	Cu	1594	433
Heat Sink	AL	1361	370
Heat Sink	Ni	1197	325
Heat Sink	Be	635	173
Intermediate Fluid	He	617	168
Heat Pipe	H ₂ O	515	140
Recirculation	H ₂ O	235	64
Stoichiometric	o/f 8:1	186	51

* Total weight includes (1) propellant required to condition 4000 lb of oxygen, (2) tank weight required for the propellant and (3) hardware weight of three conditioners (triple redundant systems)

A detailed discussion of these concepts is given in the following paragraphs.

The baseline oxygen conditioner concept and various alternate methods of generating and transferring energy into the oxygen were evaluated to determine feasibility and system weights. The various approaches to generating energy and transferring the energy into the oxygen were first categorized and tabulated (Table B-2). Some of the obviously "too heavy" methods were eliminated. For example advanced fuel cells that weigh 21 lbs per kilowatt were eliminated as an energy source since it would require over 39,800 lbs of fuel cells to supply the 1898 kilowatts of power to condition the oxygen. Eight basic alternate cycles were selected out of the remaining concepts. These eight basic cycles were expanded to 14 by considering more than one fluid (or material in the case of the heat sink cycles) in some of the basic cycles.

Weights of the system components were determined after energy balances were made for each cycle. Reactor and heat exchanger weights were scaled from the required surface areas, propellant weights were determined from the required flow to condition 4000 lbs of oxygen at an oxygen flow rate of 15.6 lbs and the propellant using the exchange factors listed in Table B-3. Other component weight factors (such as turbocompressors) were obtained from Ref. B-1.*

BASELINE OXYGEN CONDITIONER CYCLE

The baseline oxygen conditioner and associated weight is shown in Fig. B-1. It consists of a reactor operating at a mixture ratio of 1.0 a heat exchanger where the hot gas generated by the reactor is used to heat the oxygen, and propellant and propellant tanks that supply the reactor. The baseline conditioner is designed to condition 4000 lbs of oxygen at a rate of 1800 Btu/sec and at an oxygen flowrate of 15.6 lb/sec. The total system weight of 368 lbs includes the weight of 3 reactors and heat exchangers (triple redundant).

*Space Shuttle High-Pressure Definition Study, NAS9-11013, Final Program Review TRW System, 31 March 1971.

TABLE B-2
 APS ALTERNATE CONCEPTS EVALUATION

BASELINE
(REMOVE THE RISK)

- BY DESIGN
 - EXTRUDED HEAT EXCHANGER
 - HEAT EXCHANGER TYPE
- BY ADDED SAFETY FEATURES
 - H₂O DILUTION
 - BYPASS
 - INTERMEDIATE STORAGE

ENERGY GENERATION

- MIXTURE RATIO 1 (FUEL)
- MIXTURE RATIO 120 (OXIDIZER)
- STOICHIOMETRIC MR
 - H₂O, He, N₂ DILUTION
 - RECYCLED FLUID
- ELECTRICAL
 - TURBINE POWERED GENERATOR
- MECHANICAL
 - LOW EFFICIENCY PUMP (RECYCLE)
 - PADDLES
 - COMPRESSION
- CATALYTIC REACTORS
 - O₂
 - HYDRAZINE
 - PEROXIDE
- HEATED CATALYTIC CONVERSION
- THRUSTER HEAT EXCHANGE
- AUTO IGNITION
- TRIDYNE
 - PREMIXED O₂/H₂/N₂, O₂/H₂/He
- LATENT HEAT UTILIZATION
- COMBINATIONS OF ABOVE

ENERGY TRANSFER

- ELECTRICAL HEATERS
- HEAT SINK
 - ACCUMULATOR WALL
 - VEHICLE SKIN
 - SOLID BAR
 - FLUID
- HEAT PIPE
 - INTERMEDIATE FLUID

TABLE B-3

TANK WEIGHT FACTORS

O_2 TANK	0.1	LB/LB	OF	O_2
H_2 TANK	0.5	LB/LB	OF	H_2
H_2O TANK	0.15	LB/LB	OF	WATER
LN_2 (-300 F)	0.3	LB/LB	OF	N_2
GHe (AMBIENT)	9.5	LB/LB	OF	He
GHe COLD (-420 F)	1.0	LB/LB	OF	He
$O_2/H_2/He$ (-77 F)	5.7	LB/LB	OF	$O_2/H_2/He$
$O_2/H_2/N_2$ (-77 F)	0.7	LB/LB	OF	$O_2/H_2/N_2$

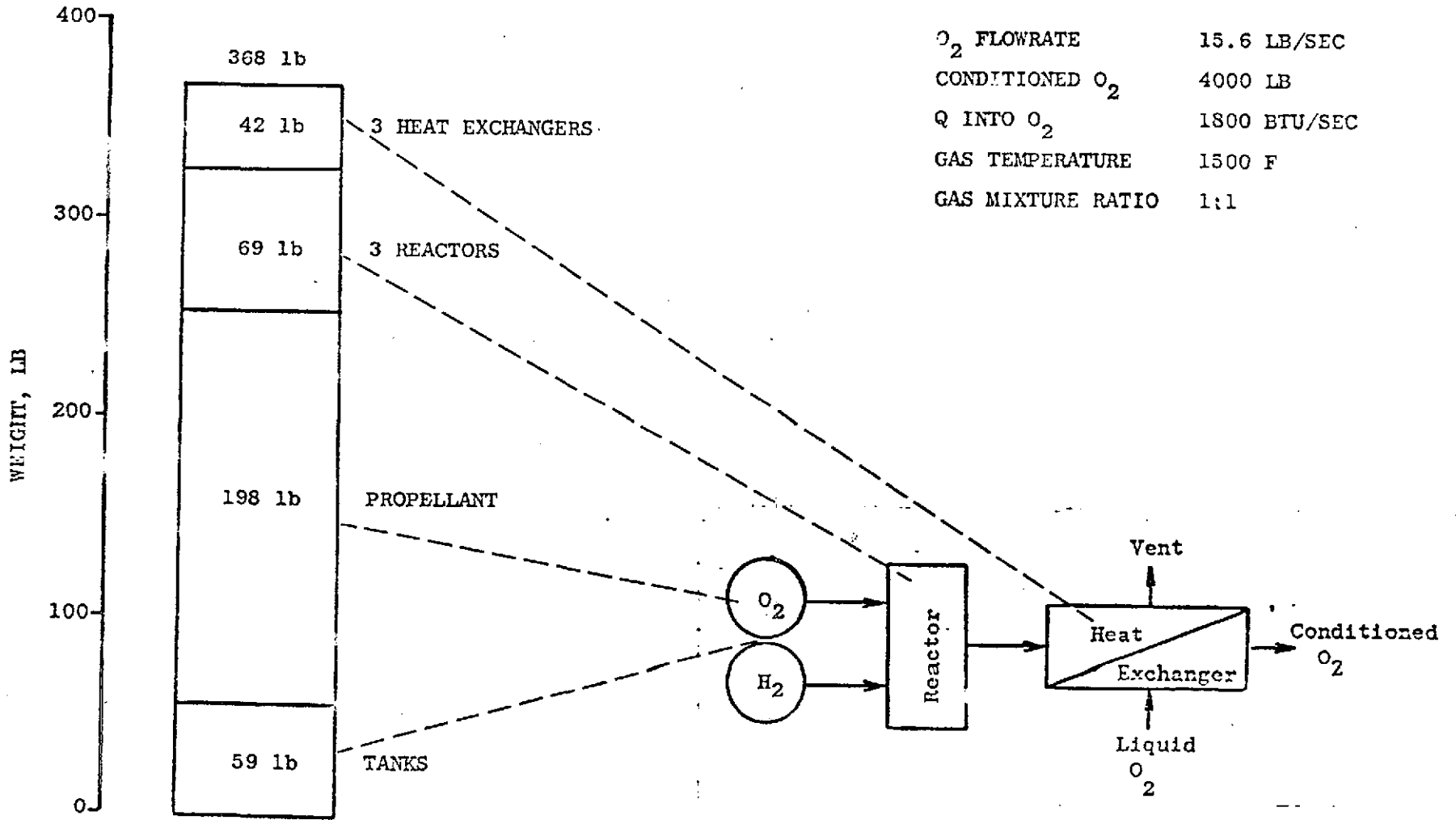


Figure B-1. Baseline Oxidizer Conditioner

The reactor temperature of the baseline conditioner was parametrically varied to determine weight trend with temperature. These trends are shown in Fig. B-2. Weight decreases with increasing temperature due primarily to the reduced propellant and tank weights. Heat exchanger weights decrease only slightly with increased temperature. The baseline conditioner was found to have a sensitivity exchange factor* of -0.08 lb/F .

ALTERNATE OXYGEN CONDITIONER CYCLES

Eight basic conditioner cycles were selected for comparison to the baseline. These were

1. Tridyne Cycle
2. Dilution Cycle
3. Oxidizer Rich Reactor Cycle
4. Heat Sink Cycle
5. Intermediate Fluid Cycle
6. Heat Pipe Cycle
7. Recirculation Cycle
8. Stoichiometric Reactor Cycle

Figure B-3 summarizes the basic cycles considered as alternates for the baseline oxygen conditioner. Each cycle is designed to condition 4000 lb of oxygen at a rate of 1800 Btu/sec and at an oxygen flowrate of 15.6 lb/sec.

Tridyne Cycle (Fig. B-3A)

The tridyne cycle uses a premixed stoichiometric mixture of oxygen and hydrogen, with inert diluent in a reactor. The gases generated in the reactor are used to heat the oxygen in a heat exchanger. Two diluents - He and N_2 were evaluated. The tridyne cycle using $\text{O}_2/\text{H}_2/\text{He}$ weighs 1987 lb while the tridyne cycle using $\text{O}_2/\text{H}_2/\text{N}_2$ weighs 1740 lb. Component weight breakdown of the tridyne He and tridyne N_2 cycles are shown in Fig. B-4 and B-5, respectively. Parametric variation of the reactor temperature is shown in Fig. B-6 for the two cycles. Weight sensitivity to temperature variation is -1.10 lb/F for the He system and -1.30 lb/F for the N_2 system.

* Sensitivity - $\Delta \text{ weight} / \Delta \text{ reactor temperature}$

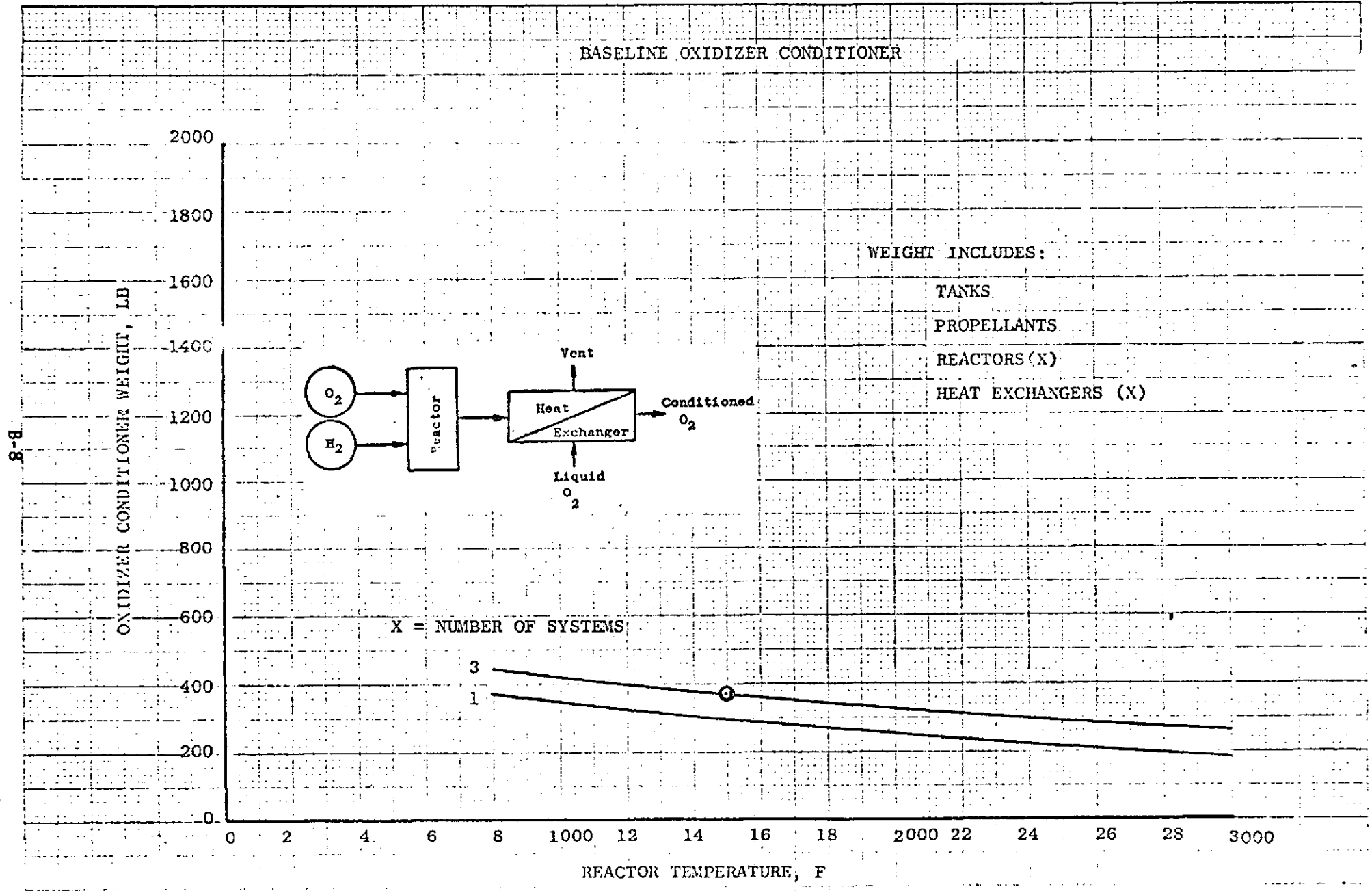
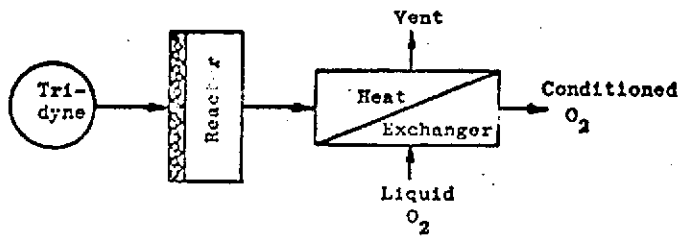
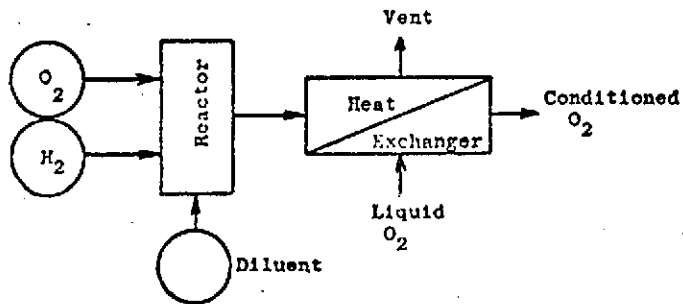


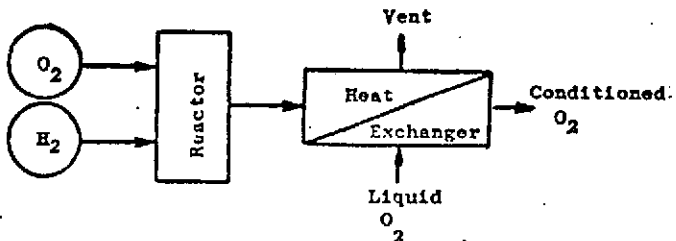
Figure B-2.



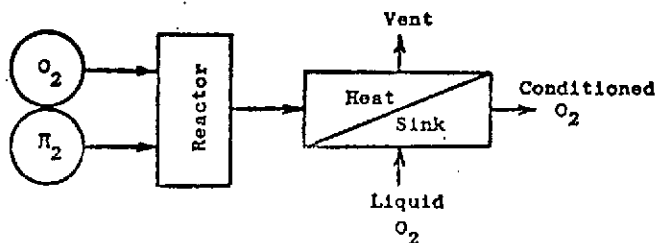
A. TRIDYNE



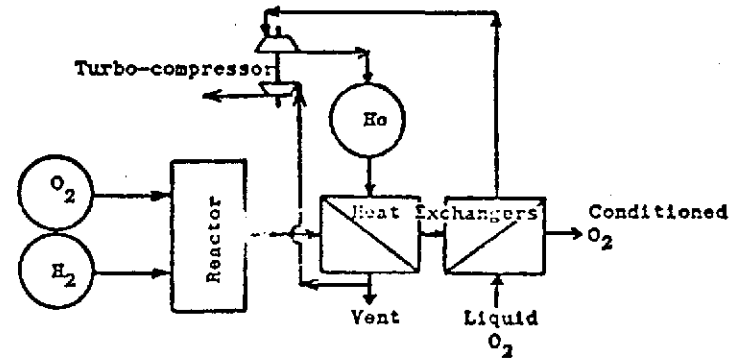
B. DILUTION



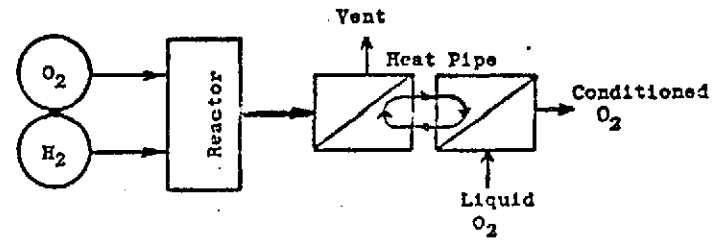
C. OXIDIZER RICH REACTOR



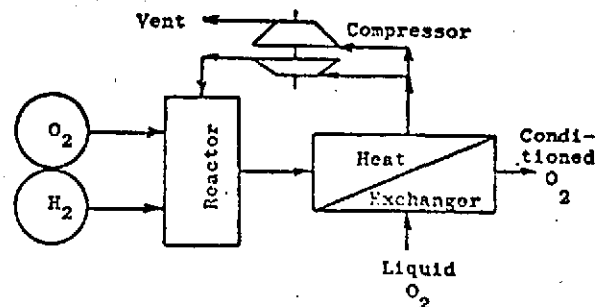
D. HEAT SINK



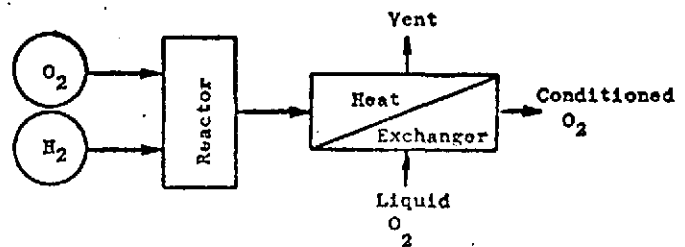
E. INTERMEDIATE FLUID



F. HEAT PIPE



G. RECIRCULATION



H. STOICHIOMETRIC REACTOR

Figure B-3. Alternate Oxidizer Conditioner Cycle

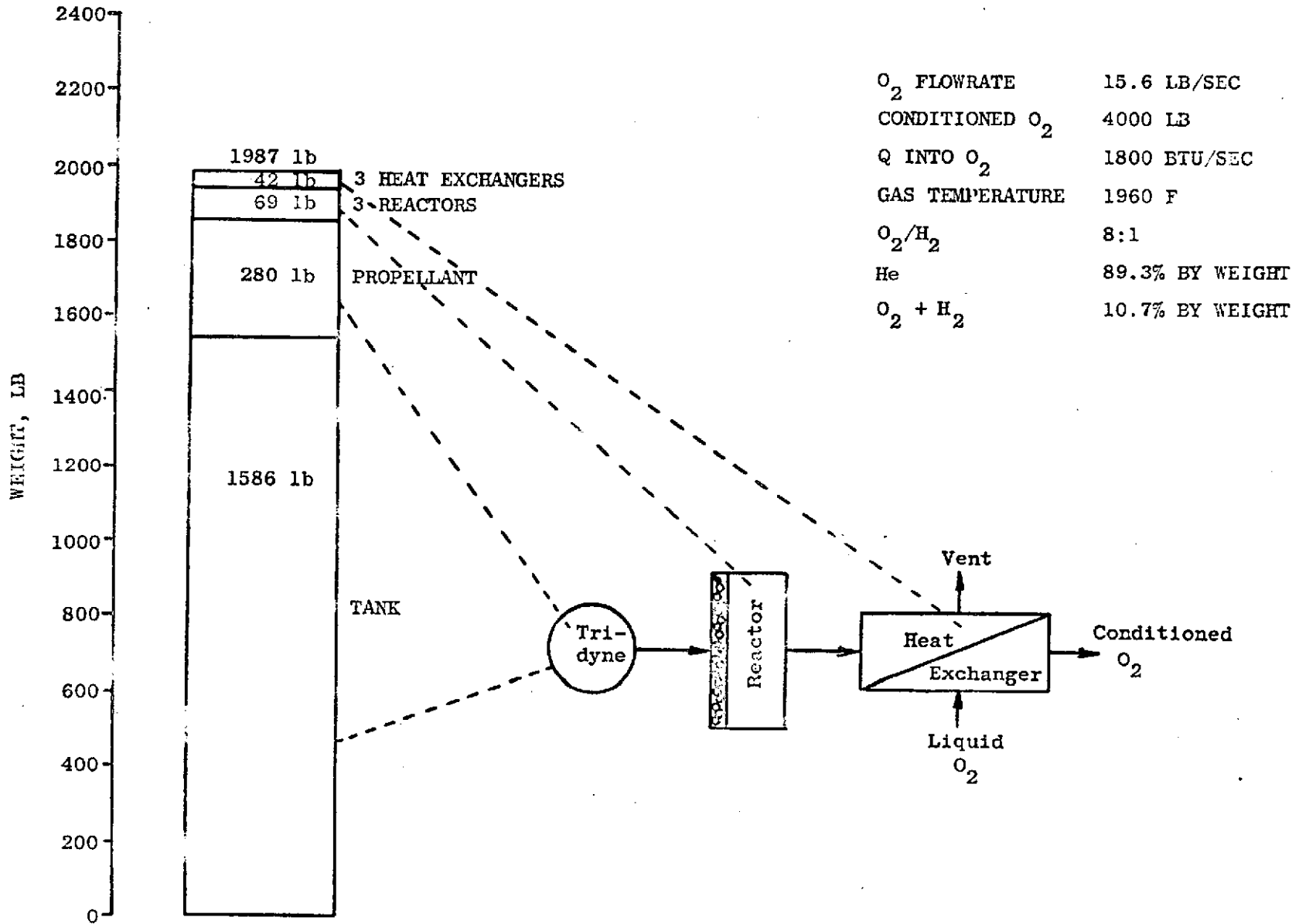


Figure B-4. O₂/H₂/He Tridyne Conditioner

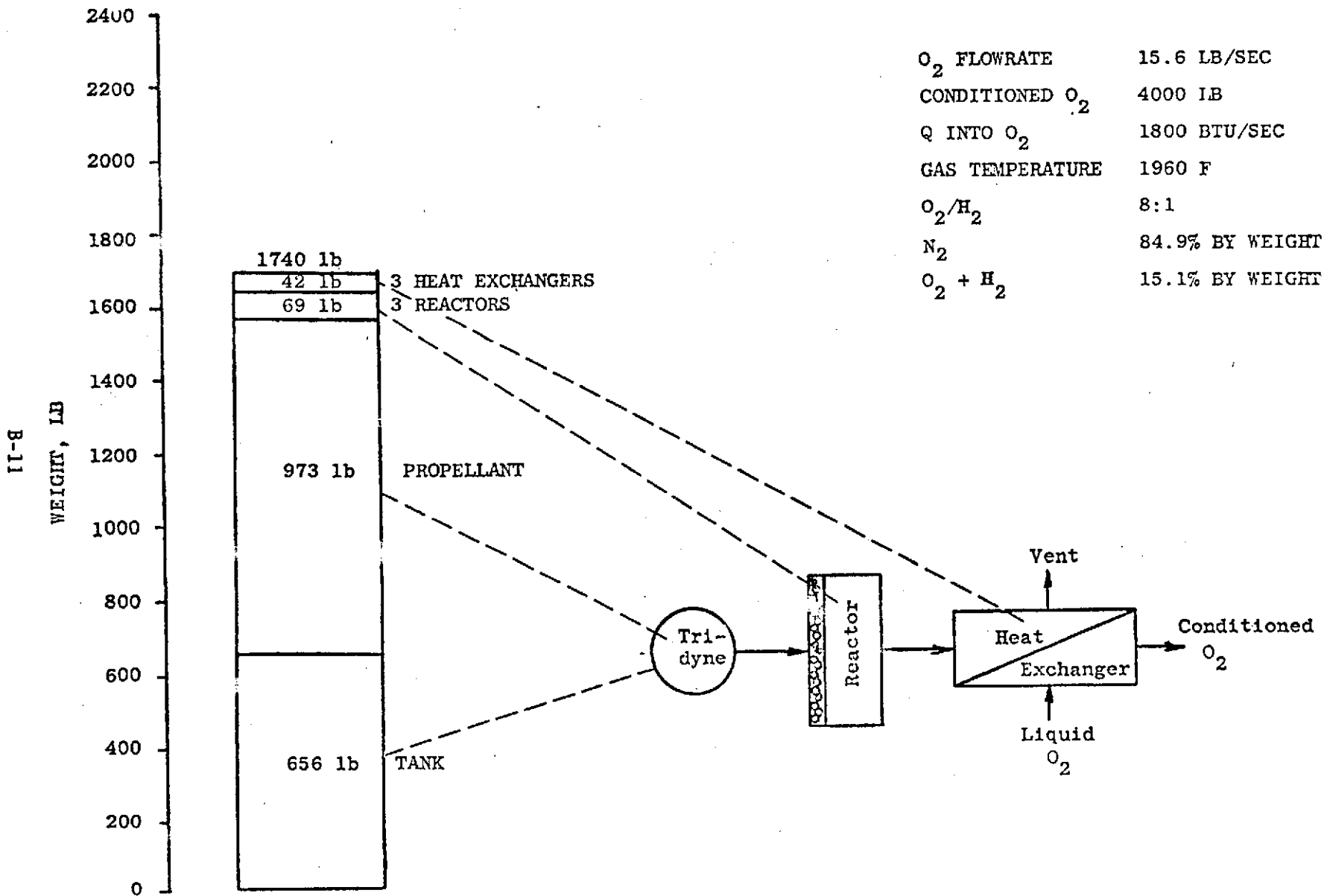


Figure B-5. $O_2/H_2/N_2$ Tridyne Conditioner

B-12

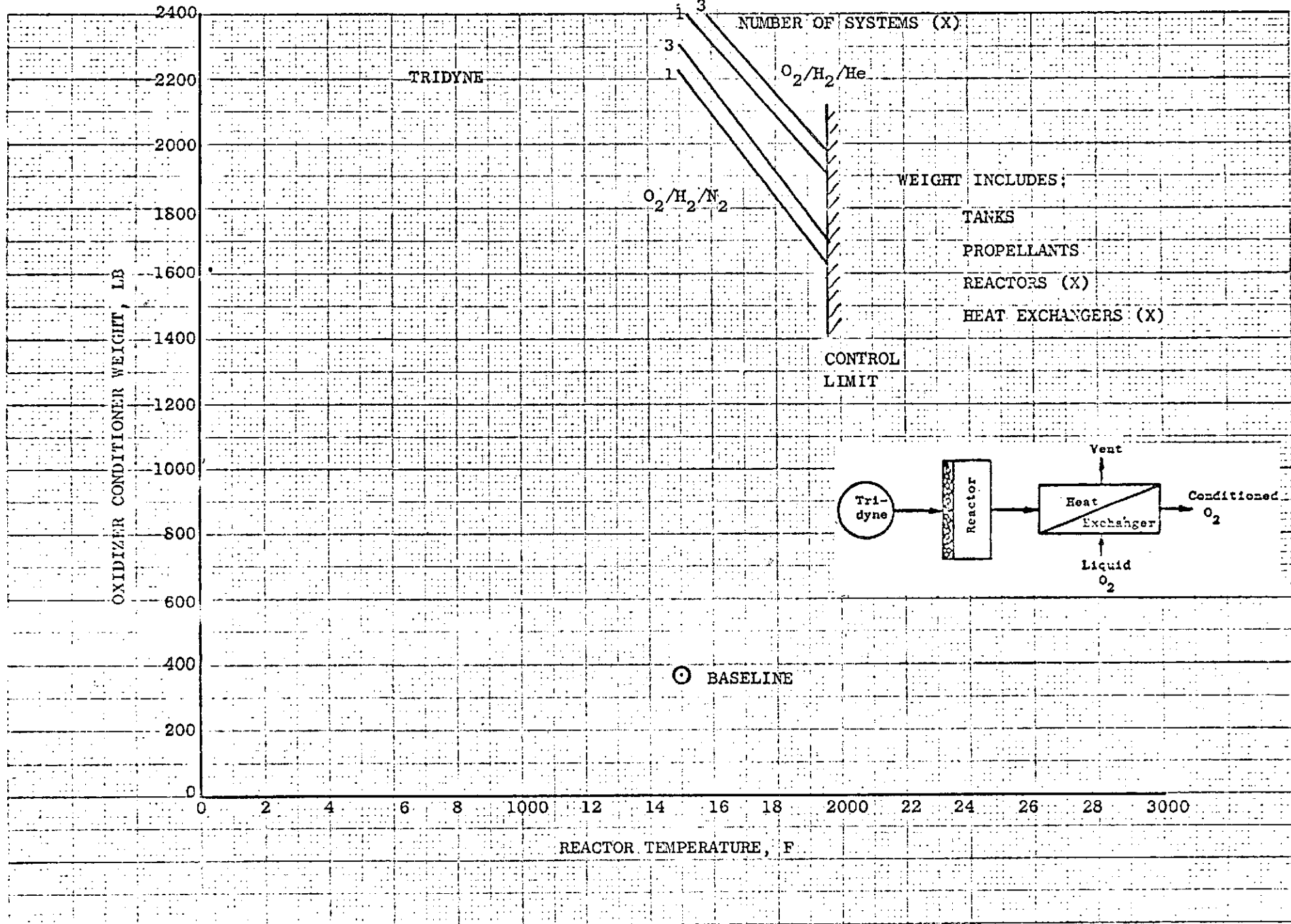


Figure B-6

Since the propellants are premixed and stored in a single propellant tank the exact mixture ratio of the propellants will be known. This would allow for a higher temperature control limit since the combustion temperature will be known exactly (based on the premixed propellant mixture). Thus for the same maximum reactor temperature the nominal reactor temperature can be higher for the tridyne cycles.

Dilution Cycle (Fig. B-3B)

The dilution cycle uses a stoichiometric mixture of oxygen/hydrogen diluted by a third fluid in the reactor to generate gases to condition the oxygen flow. Three fluids were evaluated as diluents - N_2 , He and H_2O . Component weights for the H_2O and He dilution cycles are shown in Fig. B-7 and B-8, respectively. Total weight for the N_2 , H_2O and He dilution cycles were 1768, 954, 706 lb, respectively. Parametric weight trends with reactor temperature are shown in Fig. B-9 for the three dilution cycles. A control temperature limit of 1550 F was established for the cycles since mixture ratios of the propellants must be controlled.

Oxidizer Rich Reactor Cycle (Fig. B-3C)

The oxidizer rich reactor cycle uses the same components as the baseline cycle except the reactor is run oxidizer rich (o/f = 120:1). Weight of this cycle was found to be considerably higher (1611 lb) than the baseline due to the large amount of propellant required for the reactor. This was due to the low specific heat (C_p) of the oxidizer rich gases. Component weights of the oxidizer rich reactor cycle are shown in Fig. B-10. Parametric variation of weight with reactor temperature is shown in Fig. B-11.

Heat Sink Cycle (Fig. B-3D)

Heat sink cycle consists of a metallic heat sink and a reactor to heat the heat sink. Once the heat sink is heated the reactor is turned off and the oxygen is allowed to flow through the heat sink to pick up heat. Four

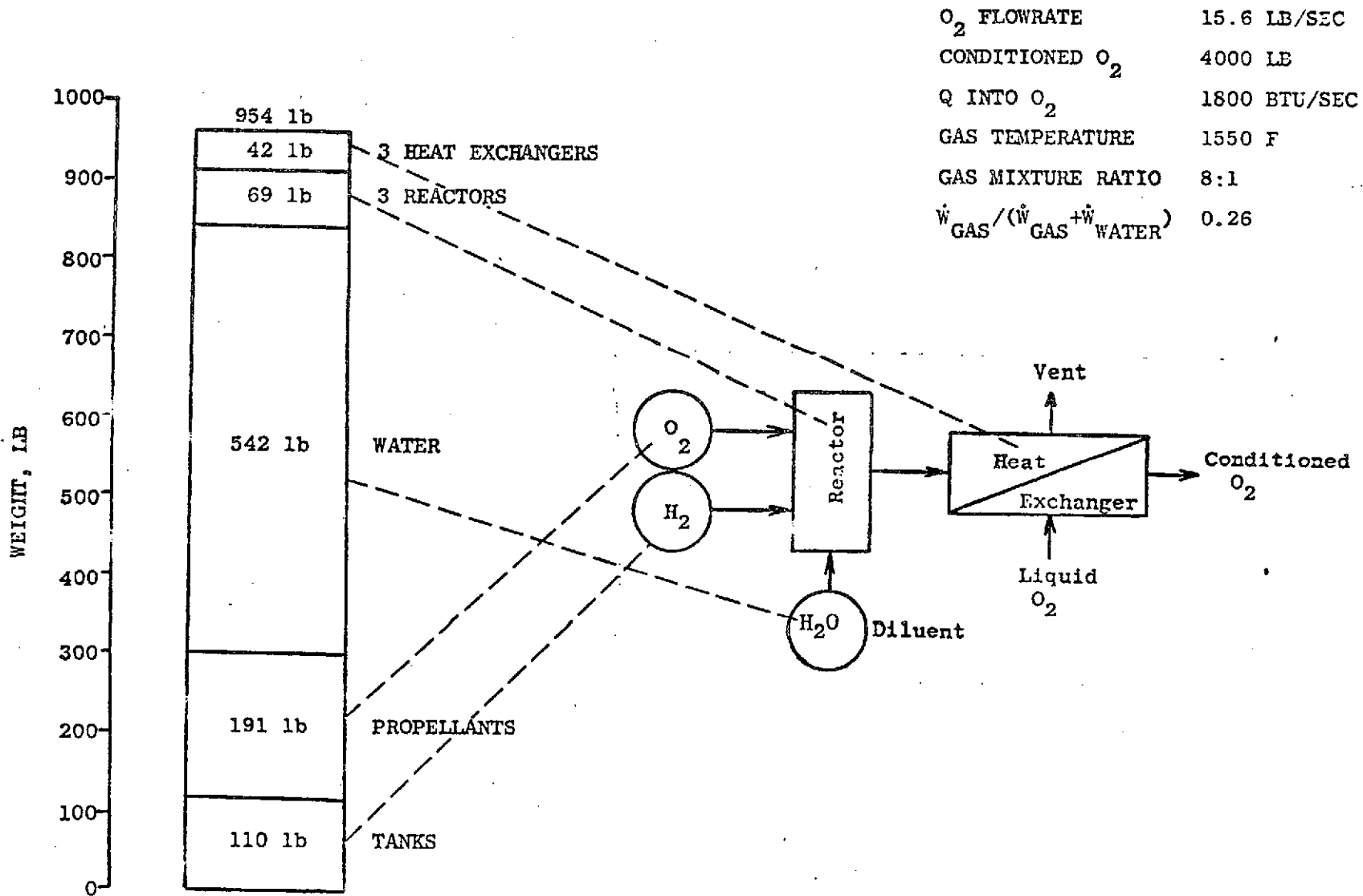


Figure B-7. Stoichiometric O/F with Water Dilution

B-15

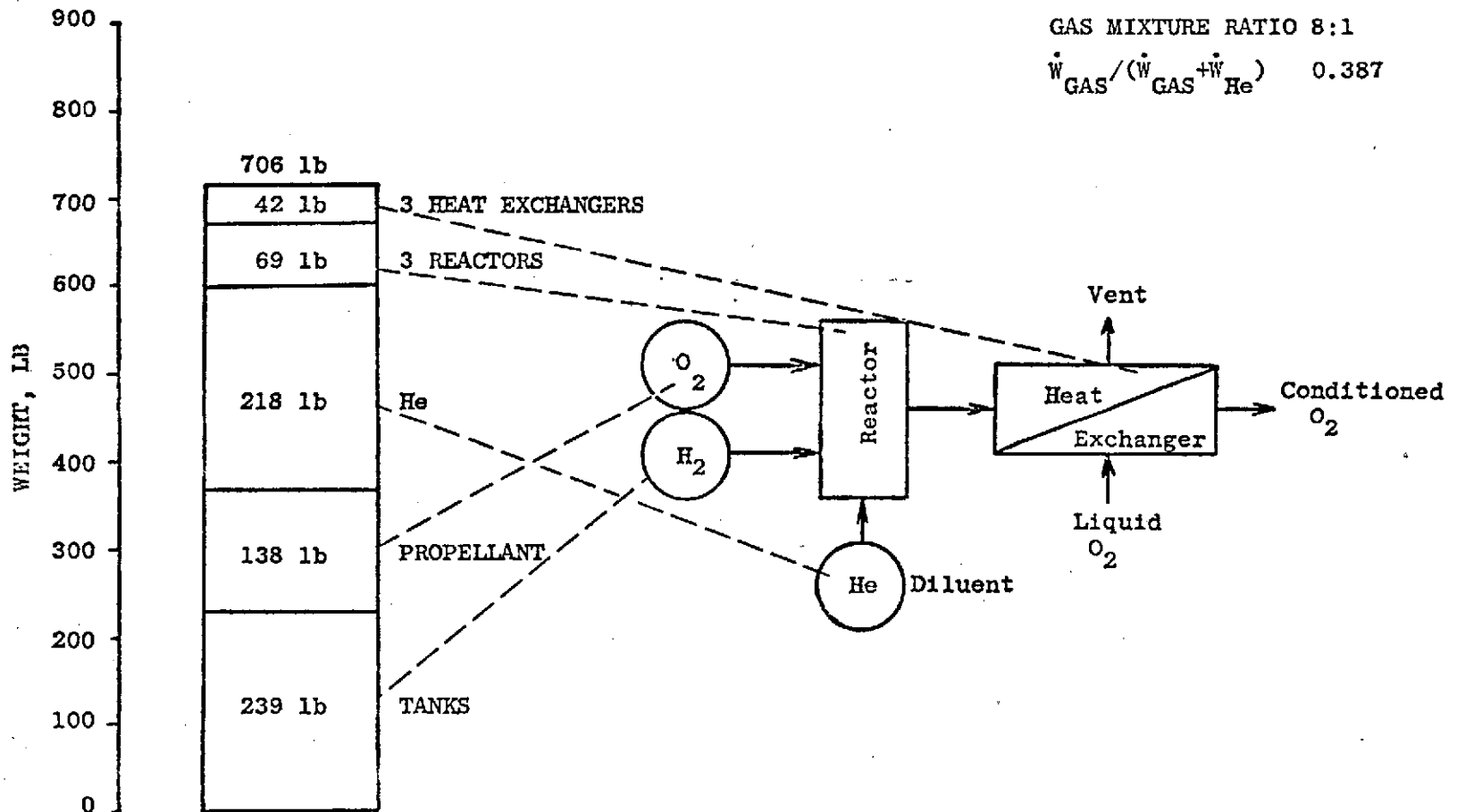


Figure B-8. Stoichiometric O/F with Helium Dilution

B-16

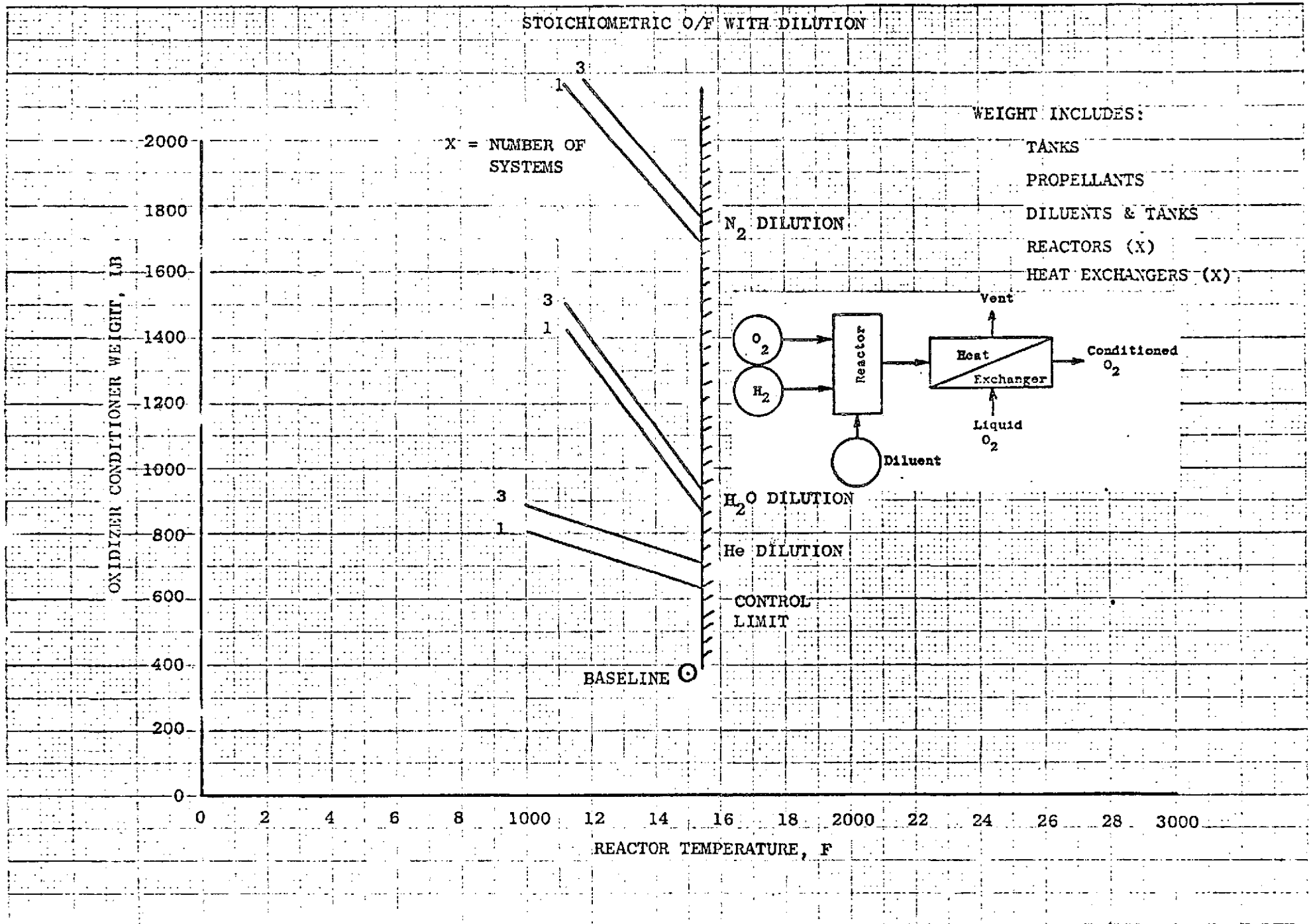


Figure B-9

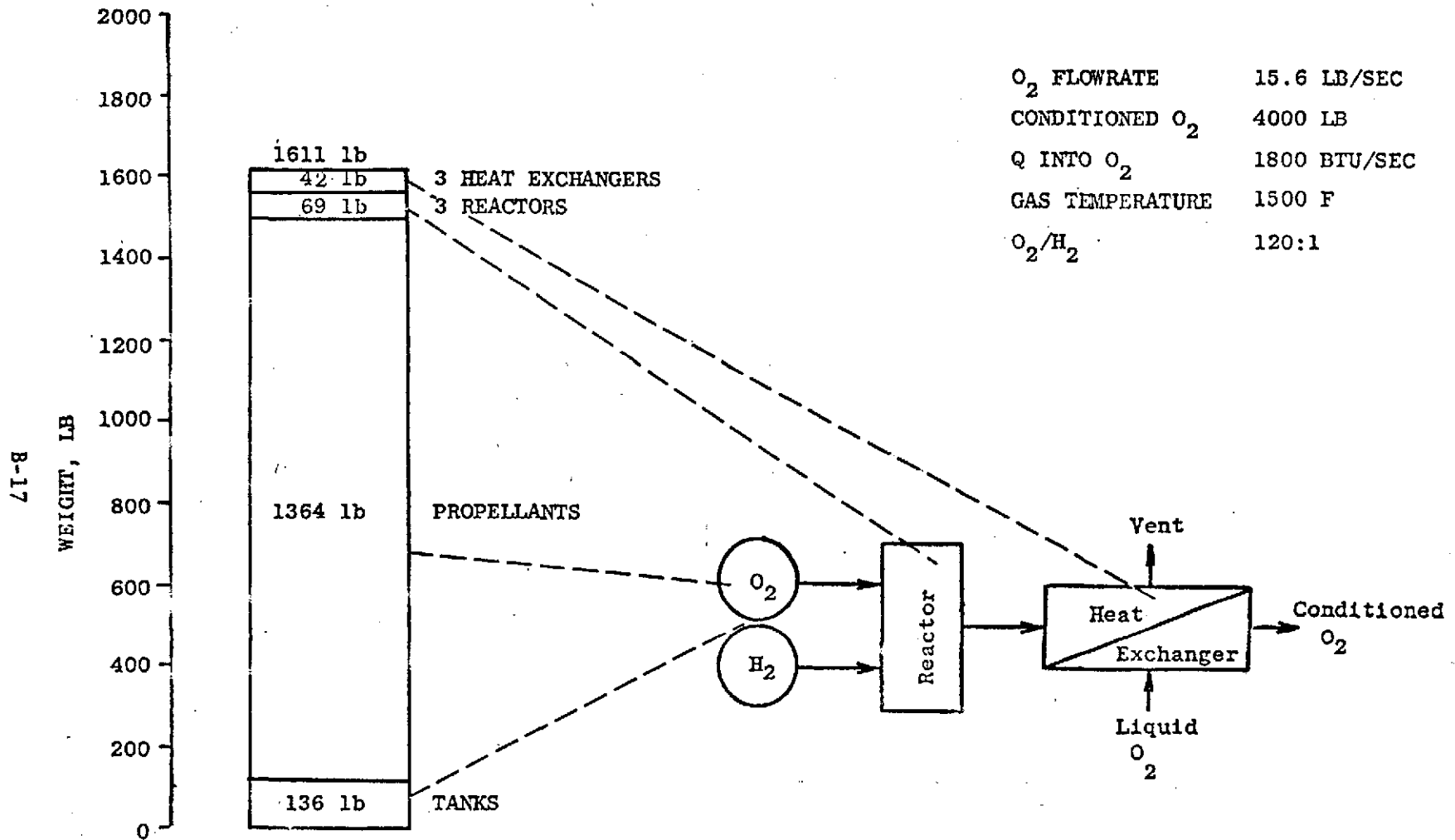


Figure B-10. Oxidizer Rich Reactor

B-18

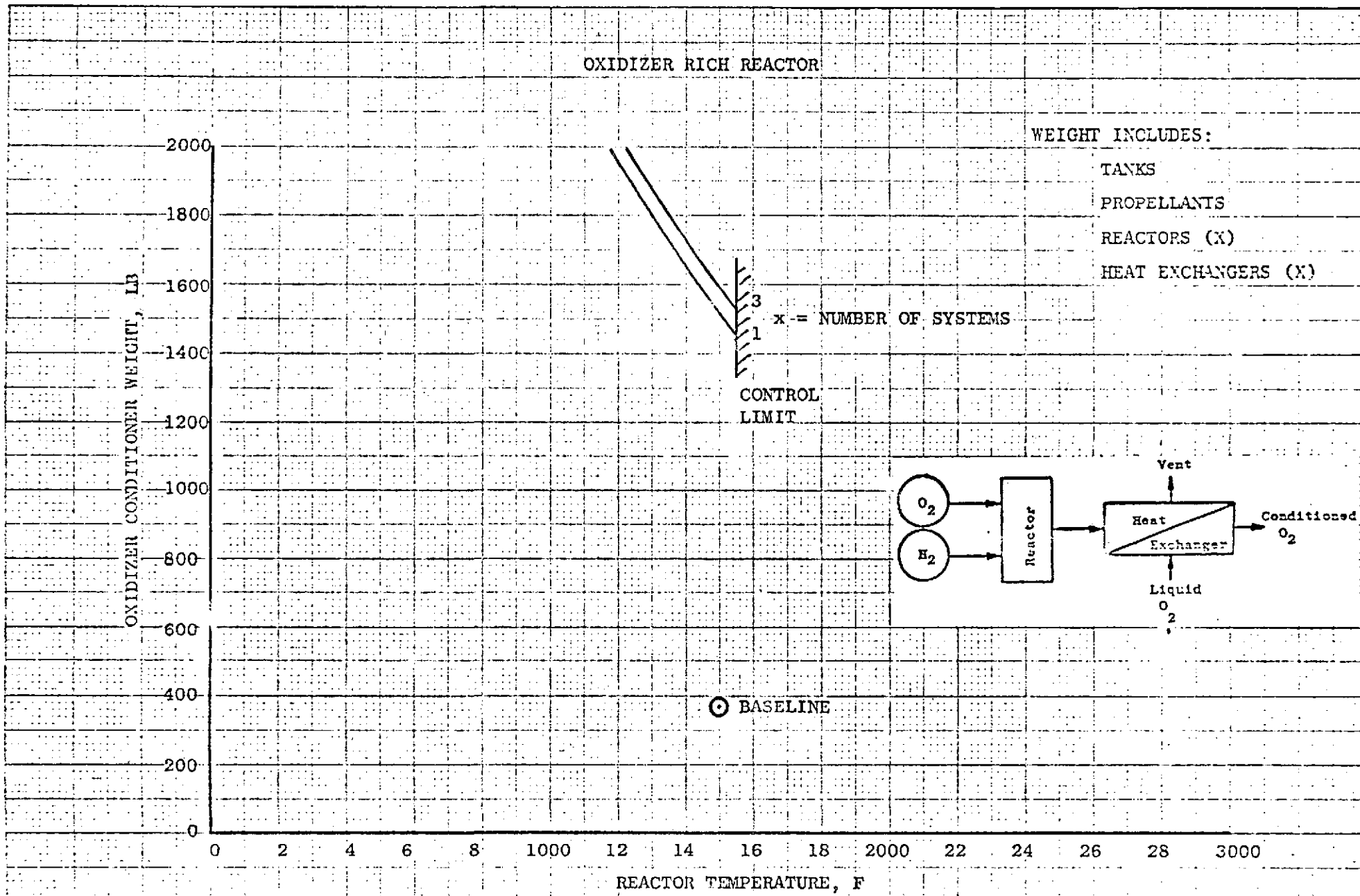


Figure B-11

materials were evaluated as heat sinks; copper, aluminum, nickel, and beryllium. Heat sinks were sized to provide heat storage for 25.6 seconds of operation ($25.6 \text{ sec} \times 1800 \text{ Btu/sec} = 0.46 \times 10^5 \text{ Btu}$). Weights of the Cu, Al, Ni and Be heat sink cycles are 1594, 1361, 1197, and 635 lb, respectively. These weights can be reduced considerably if only one heat sink is required instead of 3. Component weights for the Cu, Al, Ni and Be heat sink cycles are shown in Fig. B-12, B-13, B-14 and B-15, respectively. Parametric variation of initial heat sink temperatures are shown in Fig. B-16 through B-19.

Intermediate Fluid Cycle (Fig. B-3E)

Helium was evaluated as an intermediate fluid between the hot combustion gas and the cold oxygen. The helium is circulated via a turbocompressor which compresses the helium after it has conditioned the oxygen. After compression the helium is circulated through the hot gas heat exchanger where it is heated. The compressor is driven by exhaust gases from the gas/helium heat exchanger. Component weights are summarized in Fig. B-20. Parametric weight variations with reactor temperature variations are shown in Fig. B-31.

Heat Pipe Cycle (Fig. B-3F)

The heat pipe cycle utilizes a hollow metallic pipe lined with a metallic wick material saturated with a fluid to transfer the heat generated in the reactor to the oxygen flowing in a heat exchanger. Water was evaluated as the heat pipe fluid although other fluids such as liquid metals, helium, etc. can be used. One end of the heat pipe constitutes the evaporator where heat is introduced, the other end constitutes the condenser where heat is removed. The heat introduced through the evaporator wall evaporates the fluid in the wick. The vapor travels to the condenser under the pressure differential between evaporator and condenser. Heat removed at the condenser end causes the vapor to condense. The fluid then returns to the evaporator by means of the capillary action of the wick. Because the evaporation and condensation occur at a constant temperature the heat is conducted from one end of the pipe to the other at a very low temperature differential. This represents an effective thermal conductivity many times that of the metallic pipe.

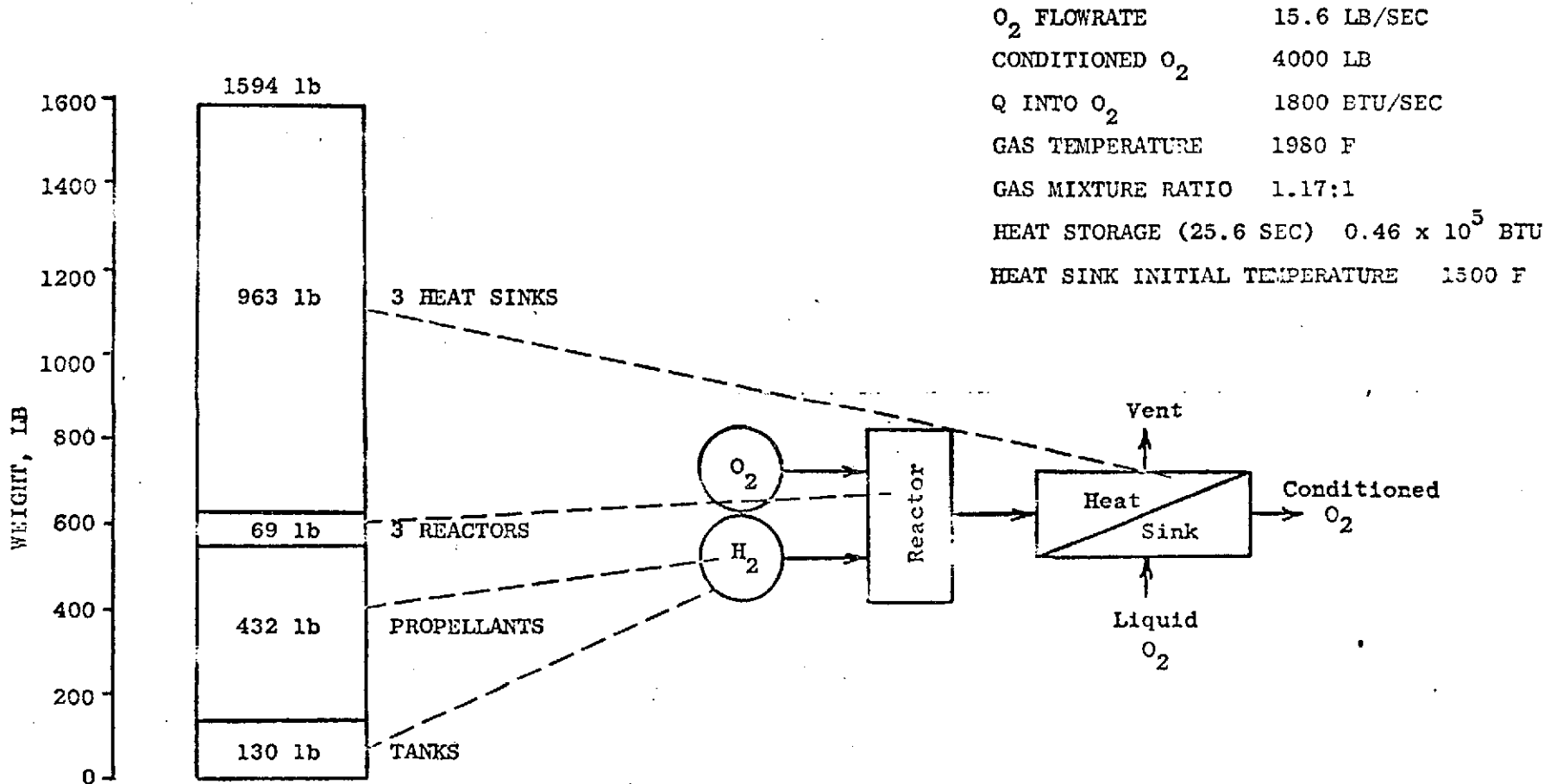


Figure B-12. Copper Heat Sink Conditioner

B-21

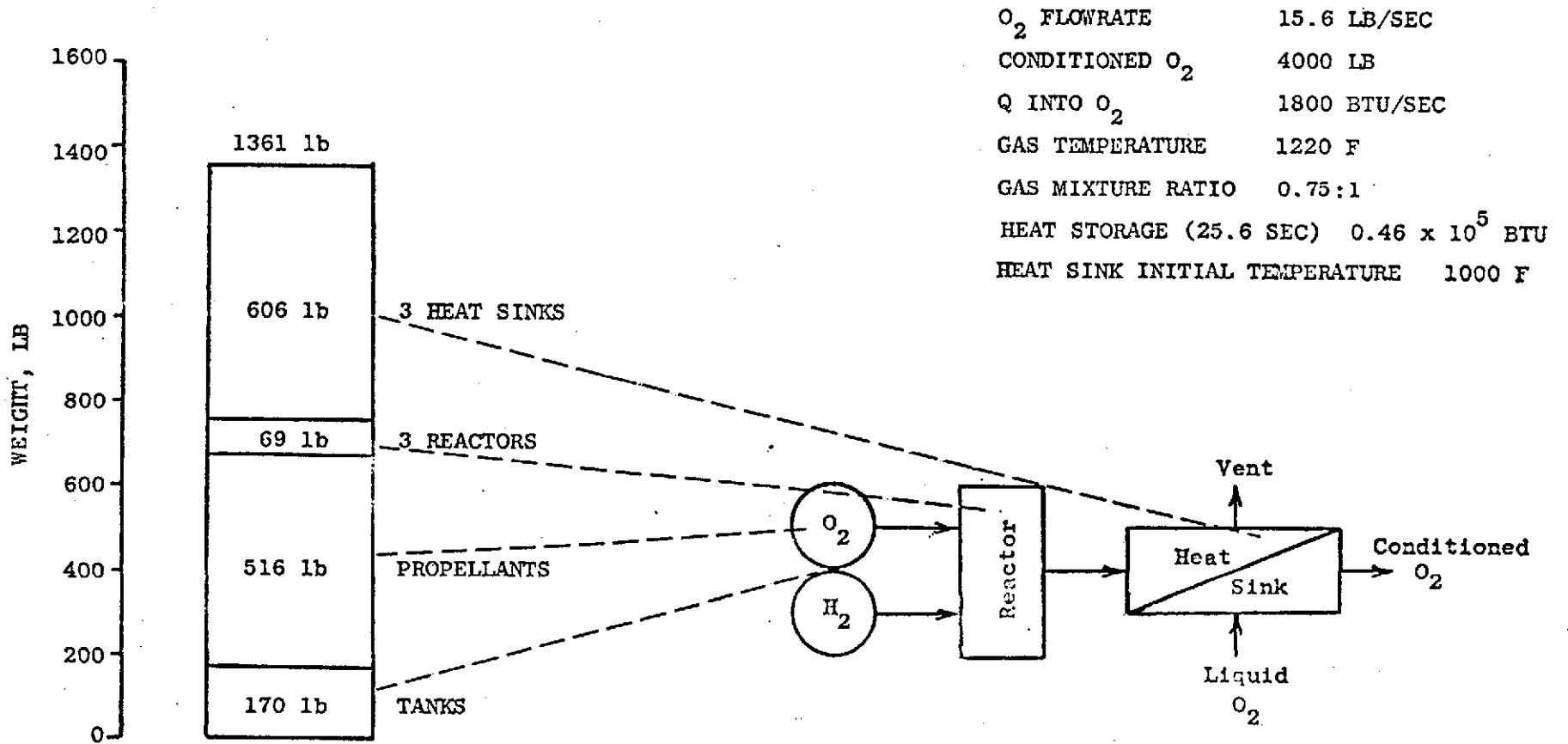


Figure B-13. Aluminum Heat Sink Conditioner

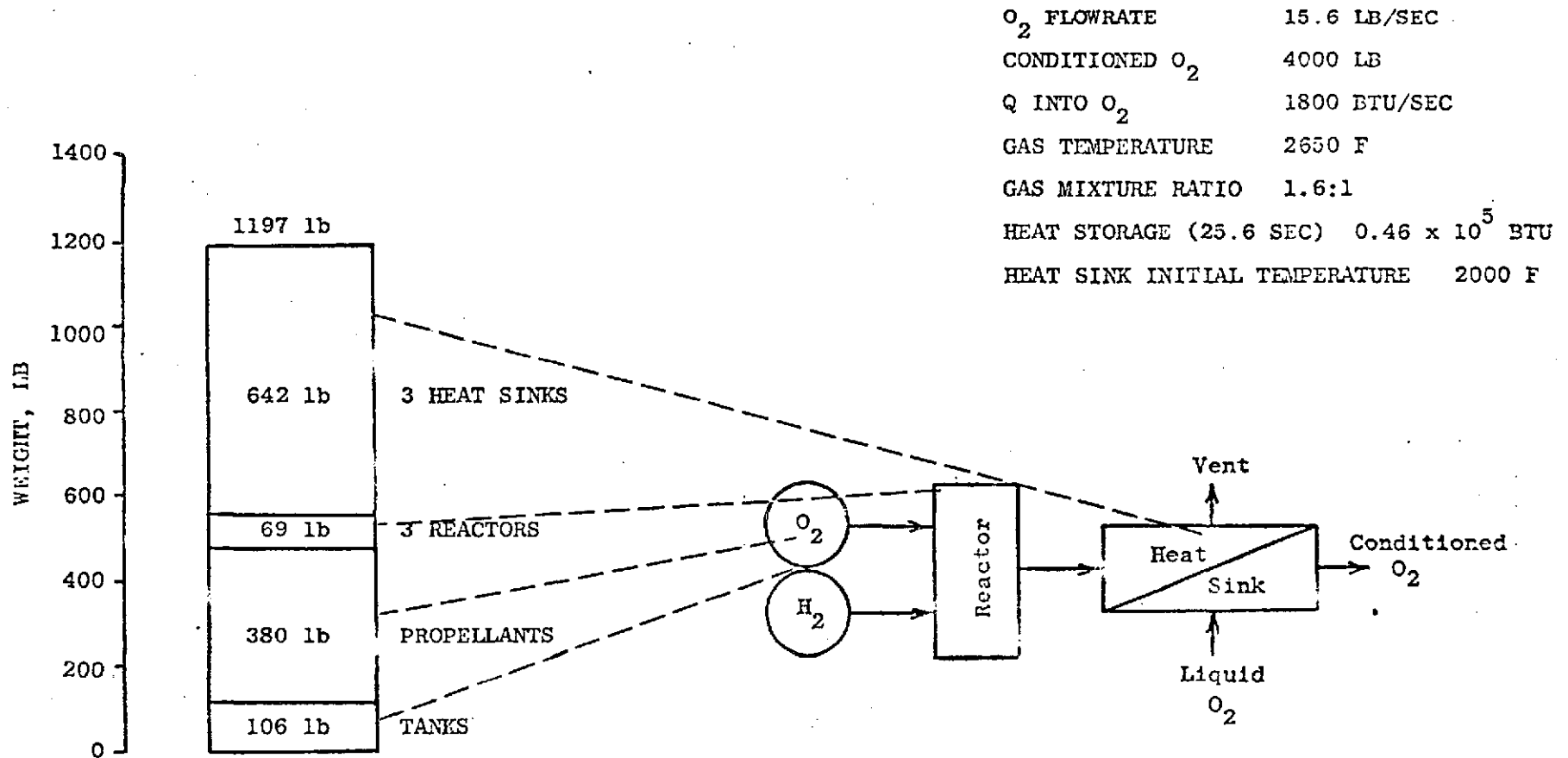


Figure B-14. Nickel Heat Sink Conditioner

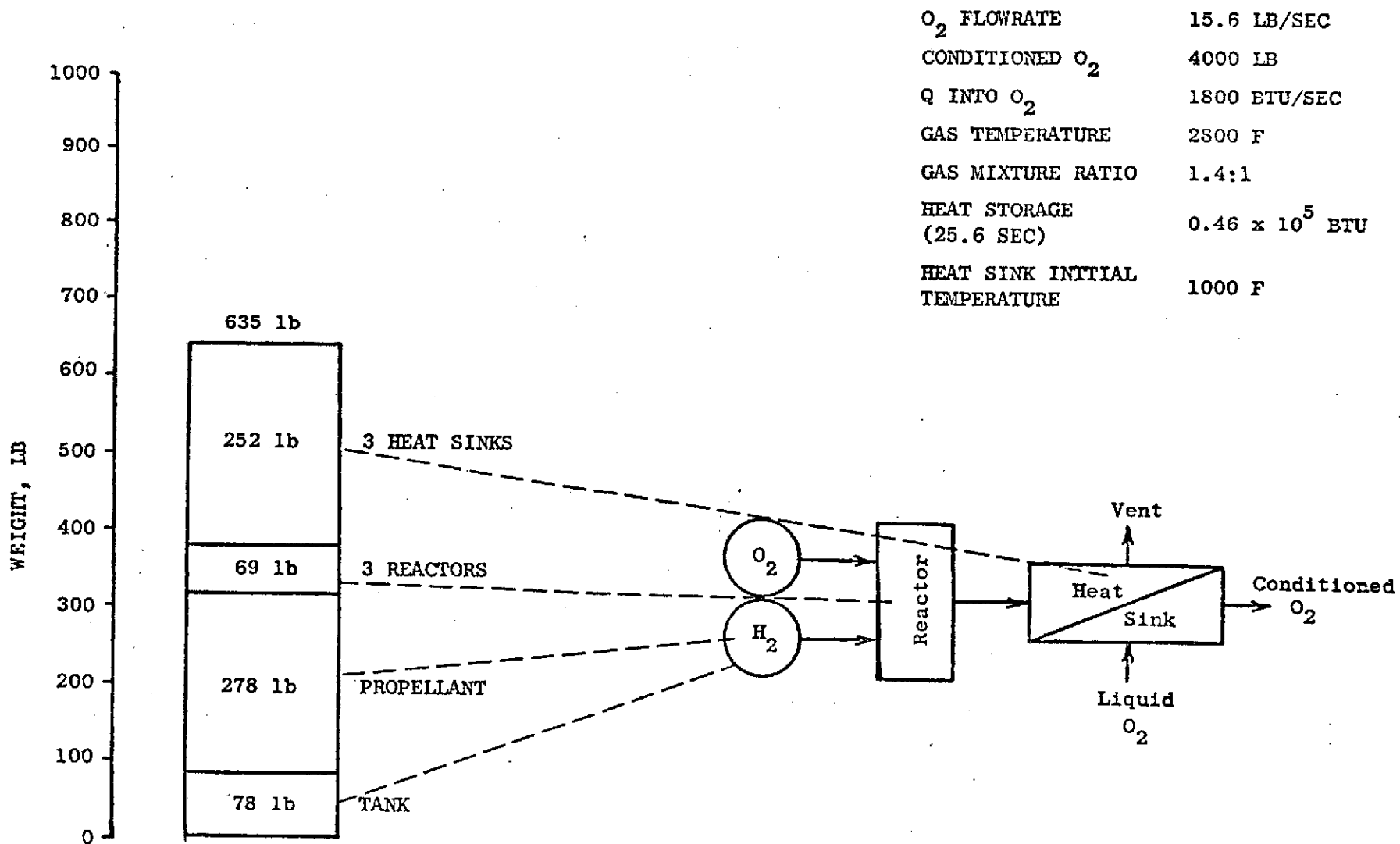


Figure B-15. Beryllium Heat Sink

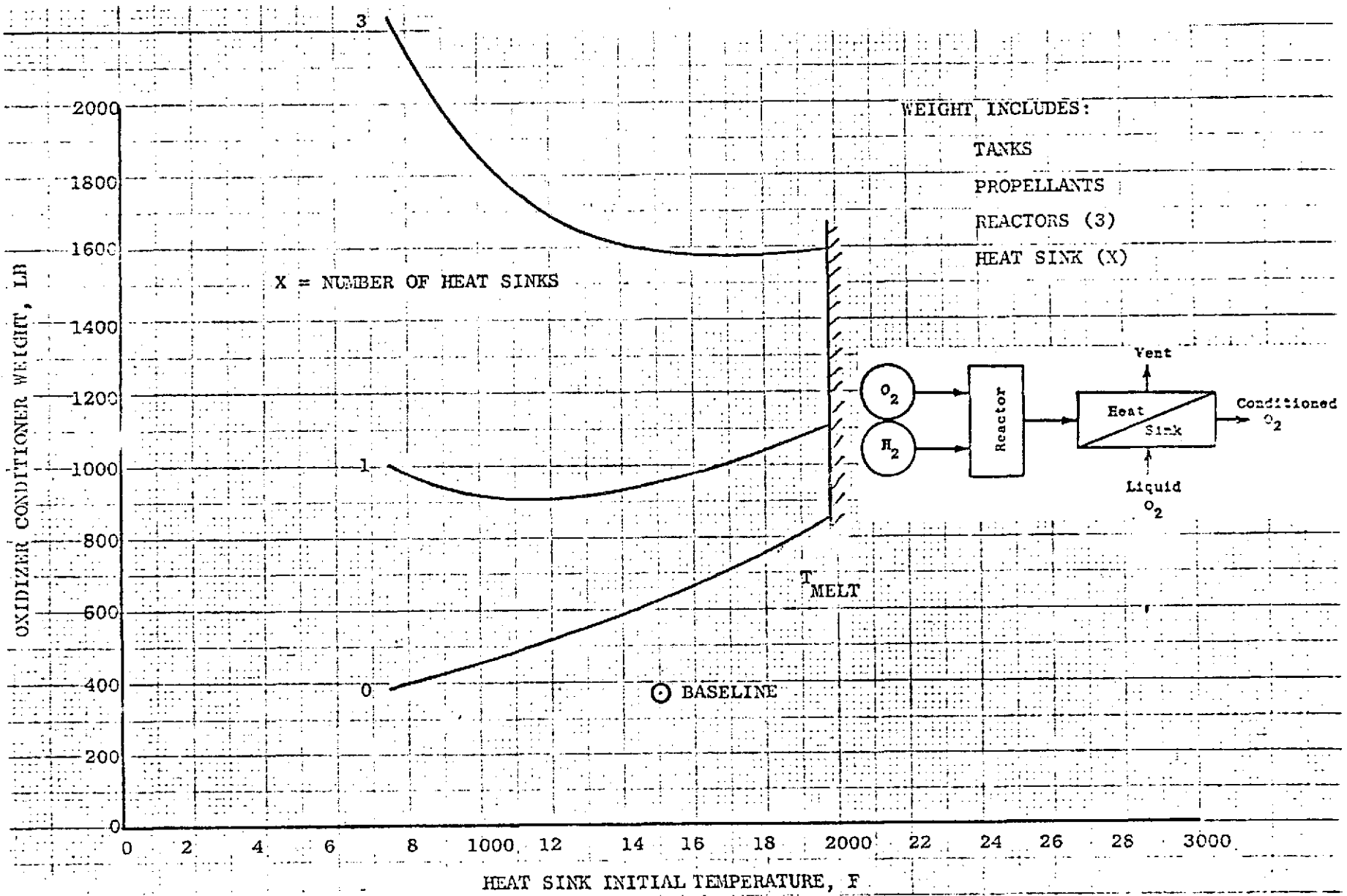


Figure B-16. Copper Heat Sink

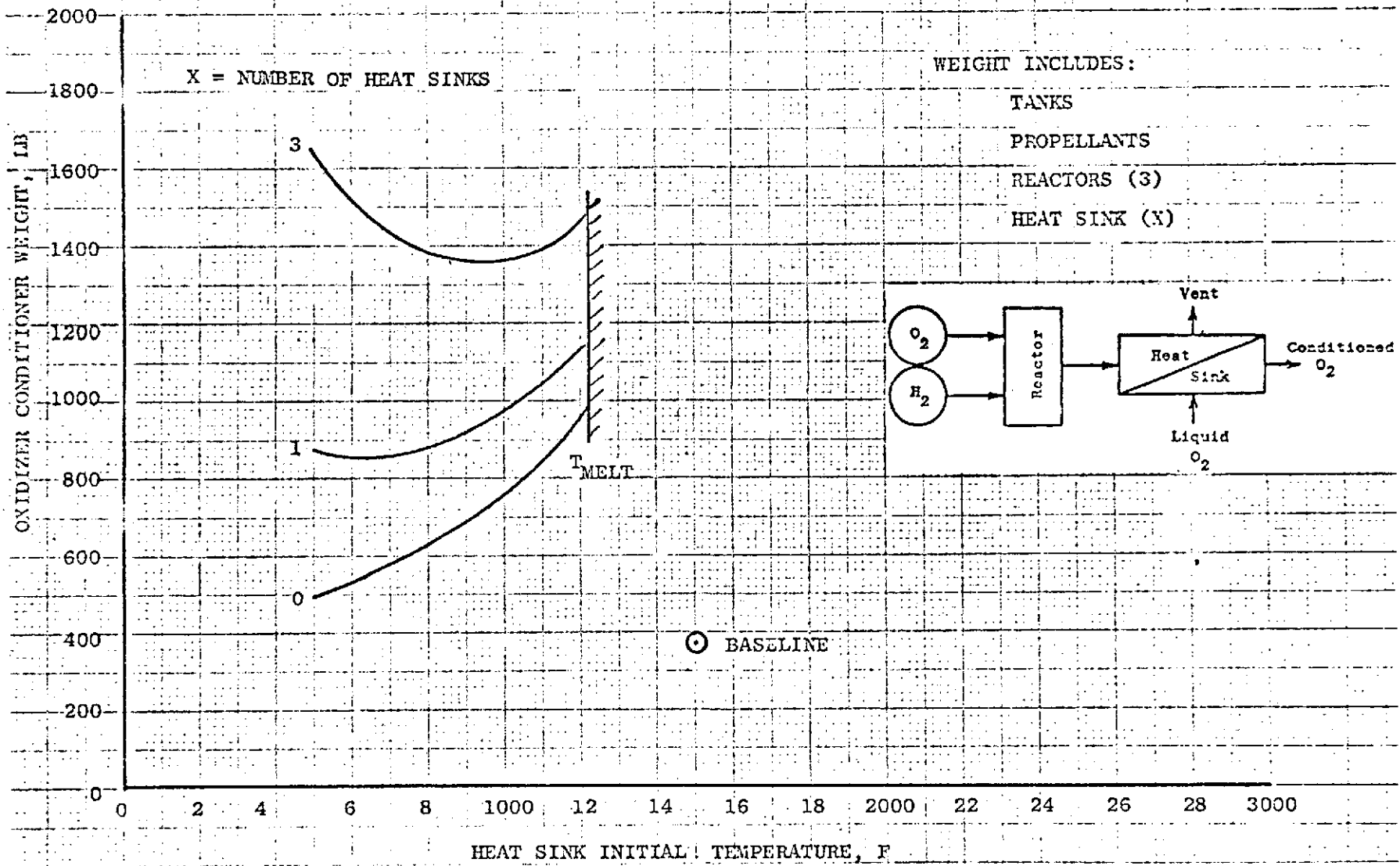


Figure B-17. Aluminum Heat Sink

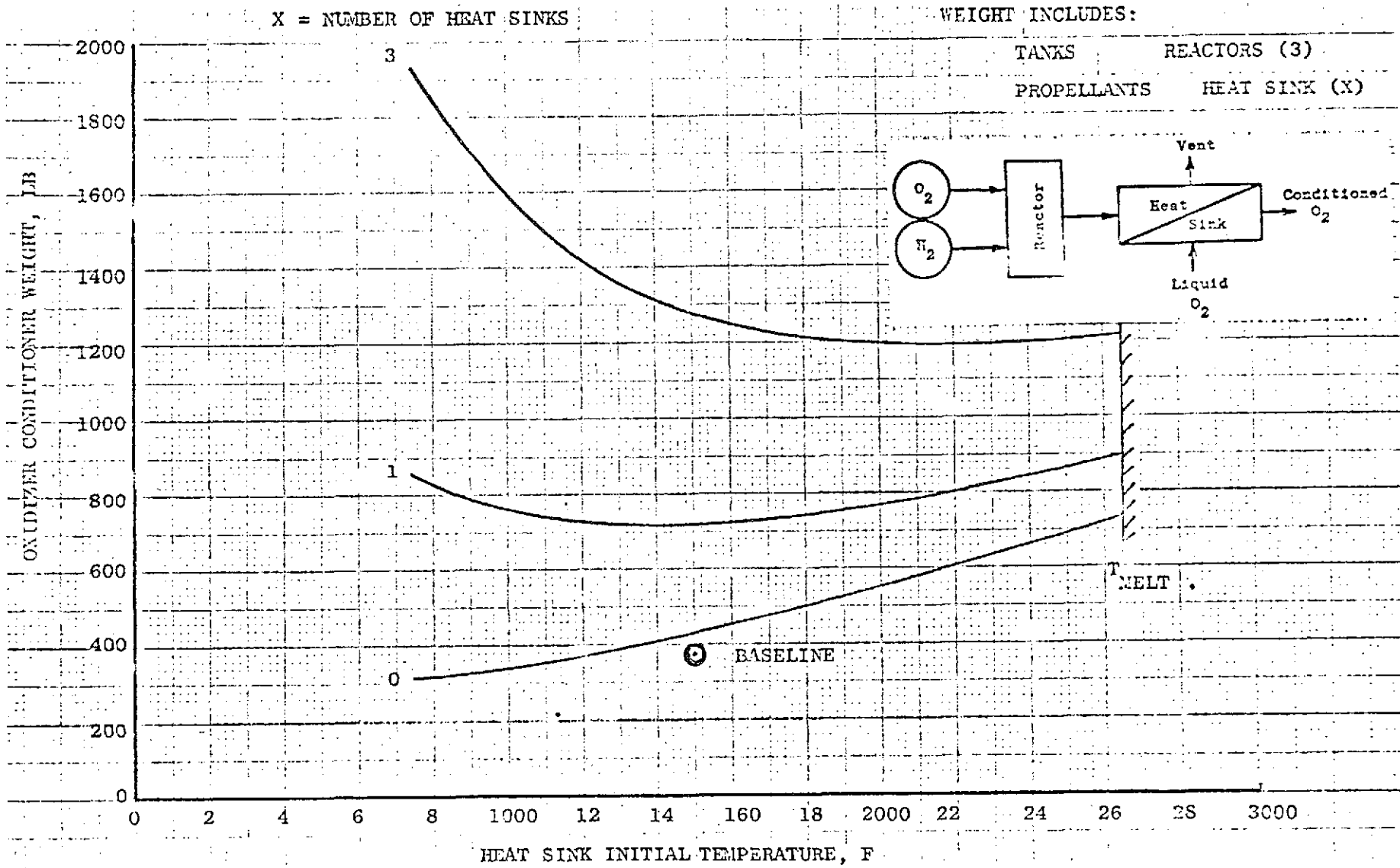


Figure B-18. Nickel Heat Sink

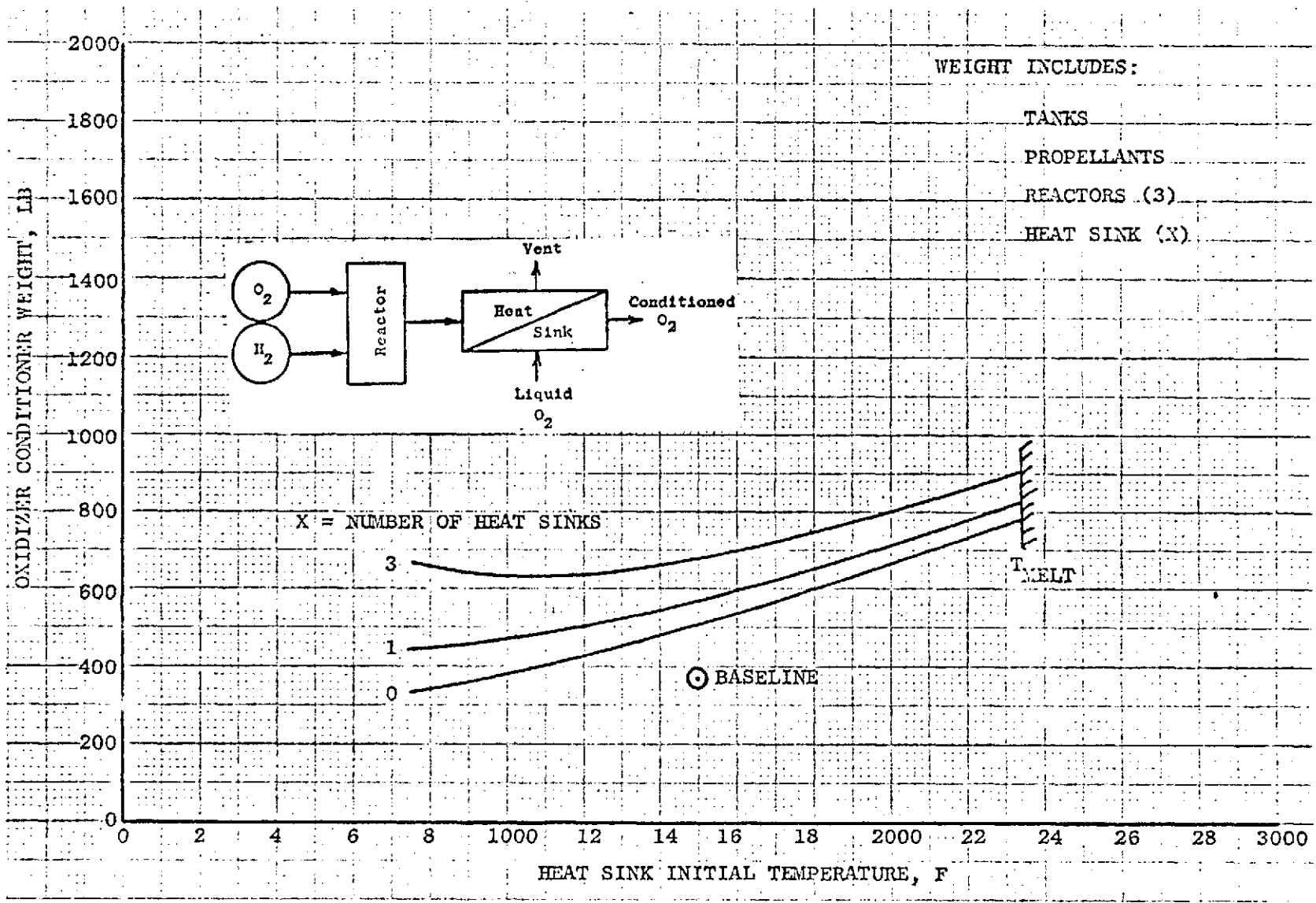


Figure B-19. Beryllium Heat Sink

O_2 FLOWRATE 15.6 LB/SEC
 CONDITIONED O_2 4000 LB
 Q INTO O_2 1800 BTU/SEC
 REACTOR TEMPERATURE 1500 F
 GAS MIXTURE RATIO 1:1

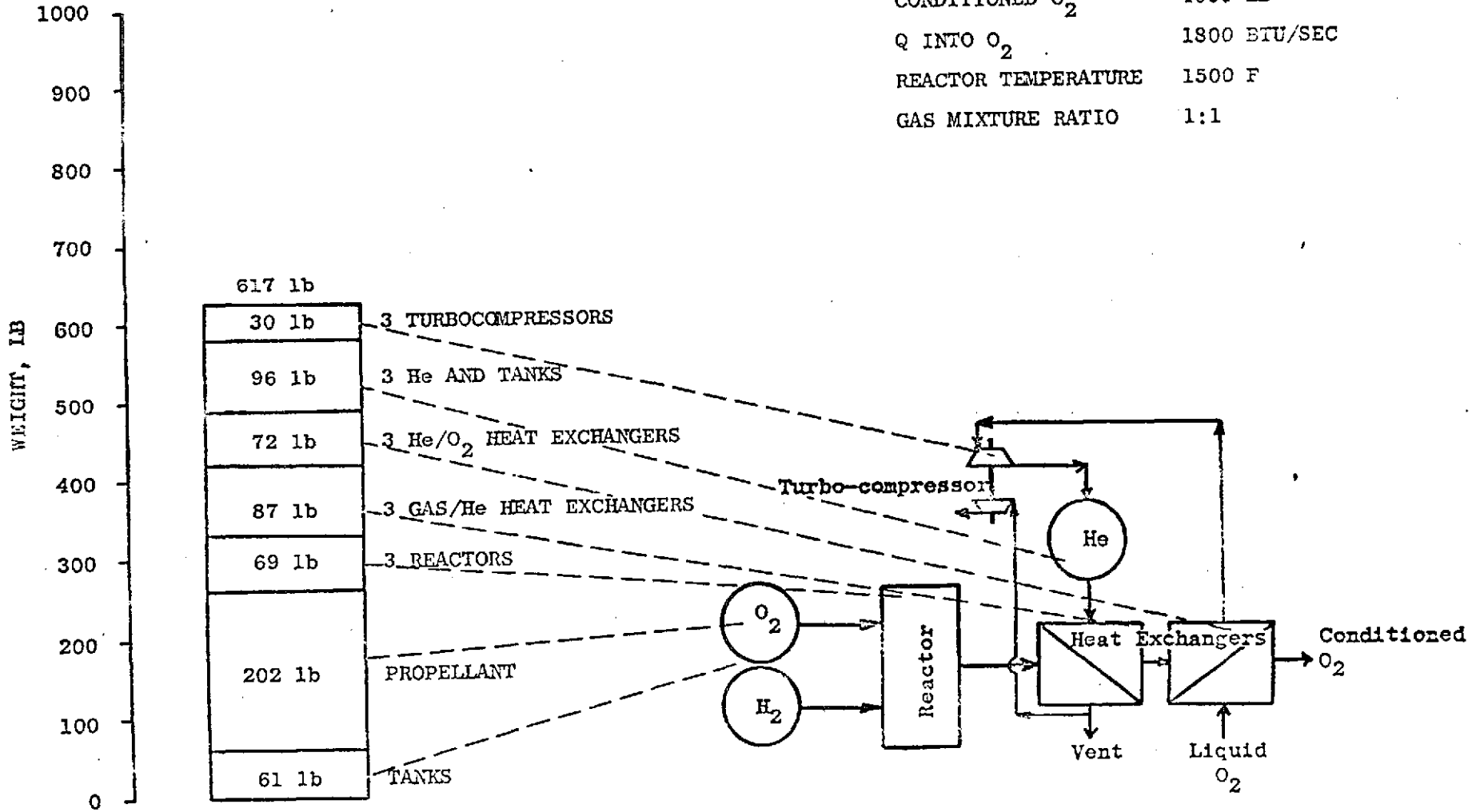


Figure B-20. Intermediate Fluid (Recycled He)

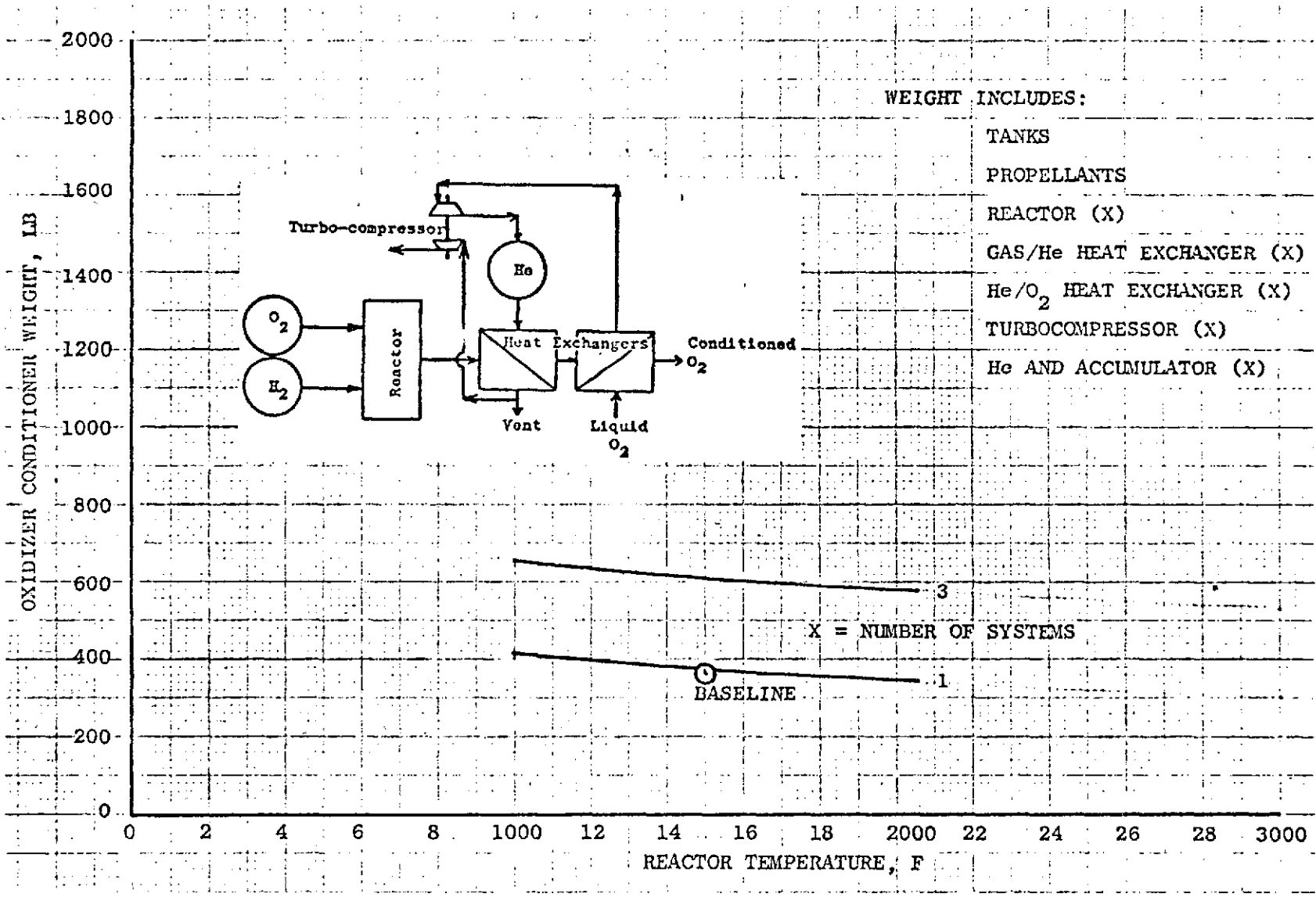


Figure B-21. Intermediate Fluid Conditioner (Helium)

Component weights of the heat pipe conditioner are shown in Fig. B-22. Parametric variation of weight with reactor temperature variation is shown in Fig. B-23.

Recirculation Cycle (Fig. B-3G)

The recirculation cycle utilizes a stoichiometric mixture of oxygen and hydrogen in a reactor. The gases are then diluted with water that has been recycled from the heat exchanger exhaust via a compressor. Since the stoichiometric combustion of oxygen and hydrogen generates water, no auxiliary water supply is required. Component weight of the recirculation cycle is shown in Fig. B-24. The cycle utilizes considerable less propellant since combustion takes place at a mixture ratio of 8:1 where the heat capacity is much greater than at the baseline mixture ratio of 1:1. Conditioner weight variation with reactor temperature is shown in Fig. B-25. Weight variation of this cycle with reactor temperature is minimal since the reactor temperature depends only on the amount of water that is recycled.

Stoichiometric Reactor Cycle (Fig. B-3H)

The stoichiometric reactor cycle utilizes the baseline cycle with a reactor that combusts oxygen and hydrogen stoichiometrically. Component weights of the cycle are shown in Fig. B-26 where they are also compared with the baseline cycle weights. The stoichiometric cycle weight is half that of the baseline due mostly to the reduced propellant requirements. Variation of the conditioner weight with mixture ratio is shown in Fig. B-27.

CYCLE COMPARISONS

Weight comparison of the 14 cycles evaluated are shown in Fig. B-29. All cycles with the exception of the recirculation cycle and the stoichiometric reactor cycle weigh considerable more than the baseline cycle. The lightest weight cycle is the stoichiometric reactor cycle (186 lb) while the heaviest cycle is the helium tridyne cycle (1987 lb).

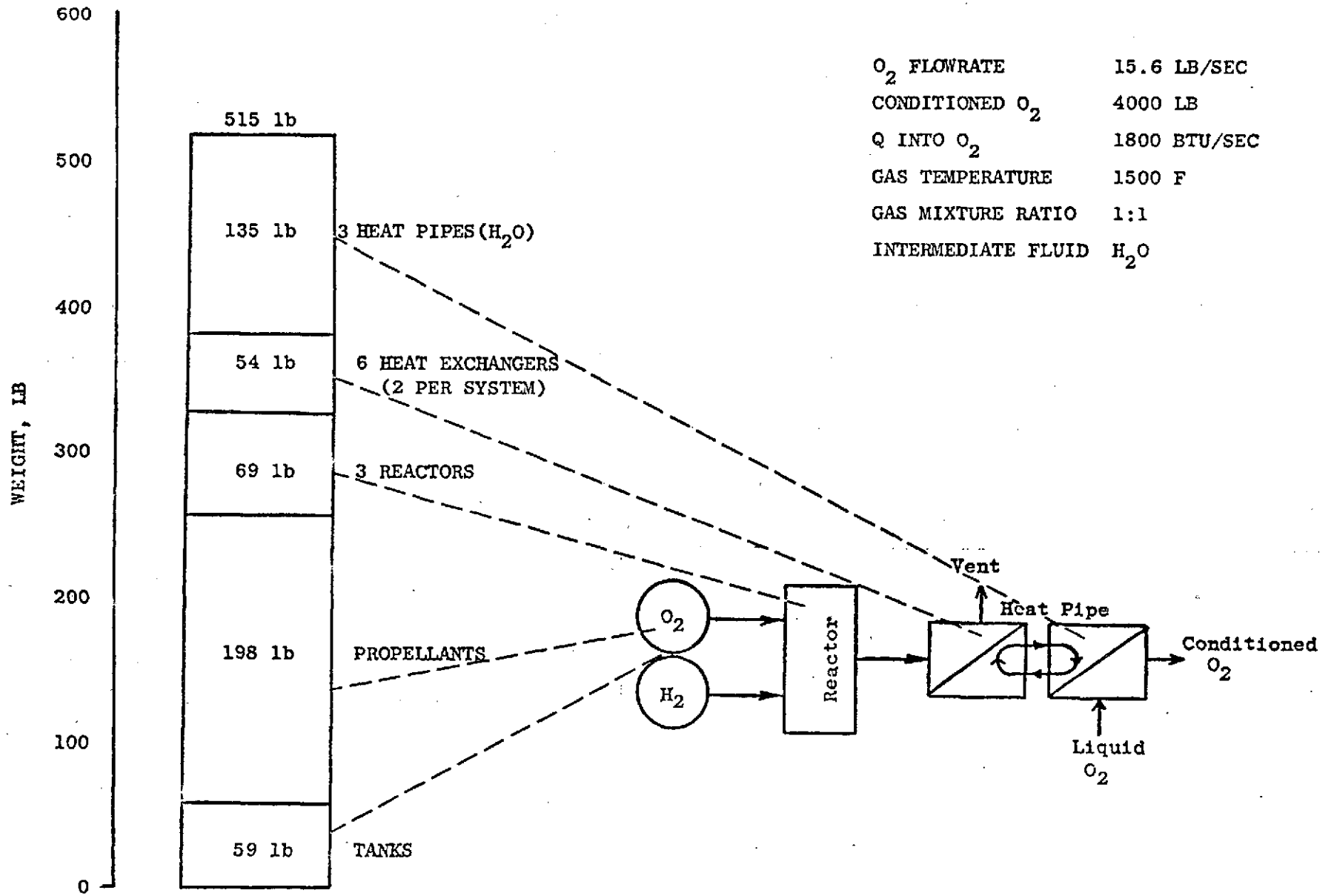


Figure B-22. Heat Pipe (H_2O) Conditioner

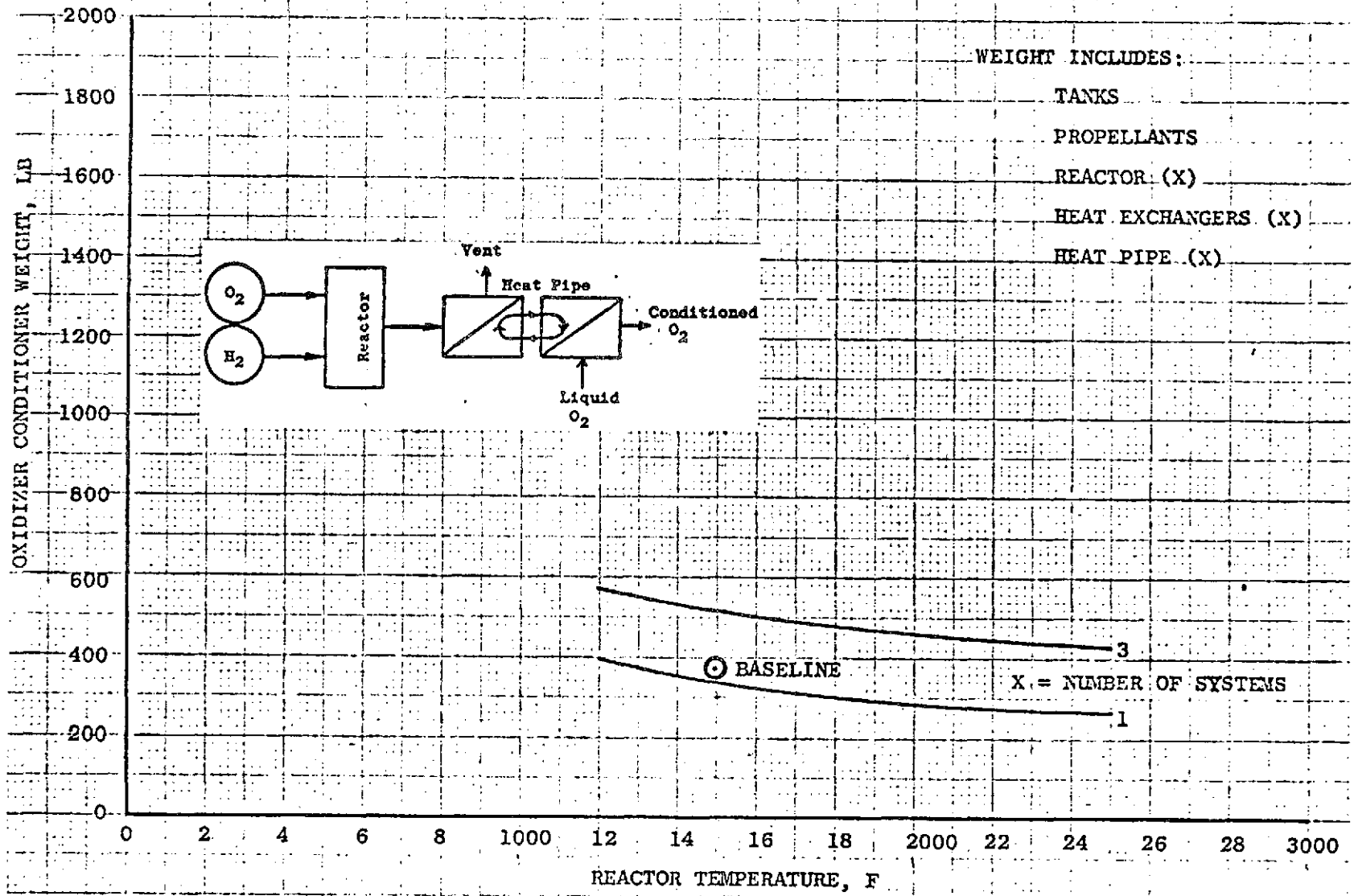


Figure B-23. Heat Pipe (H₂O) Conditioner

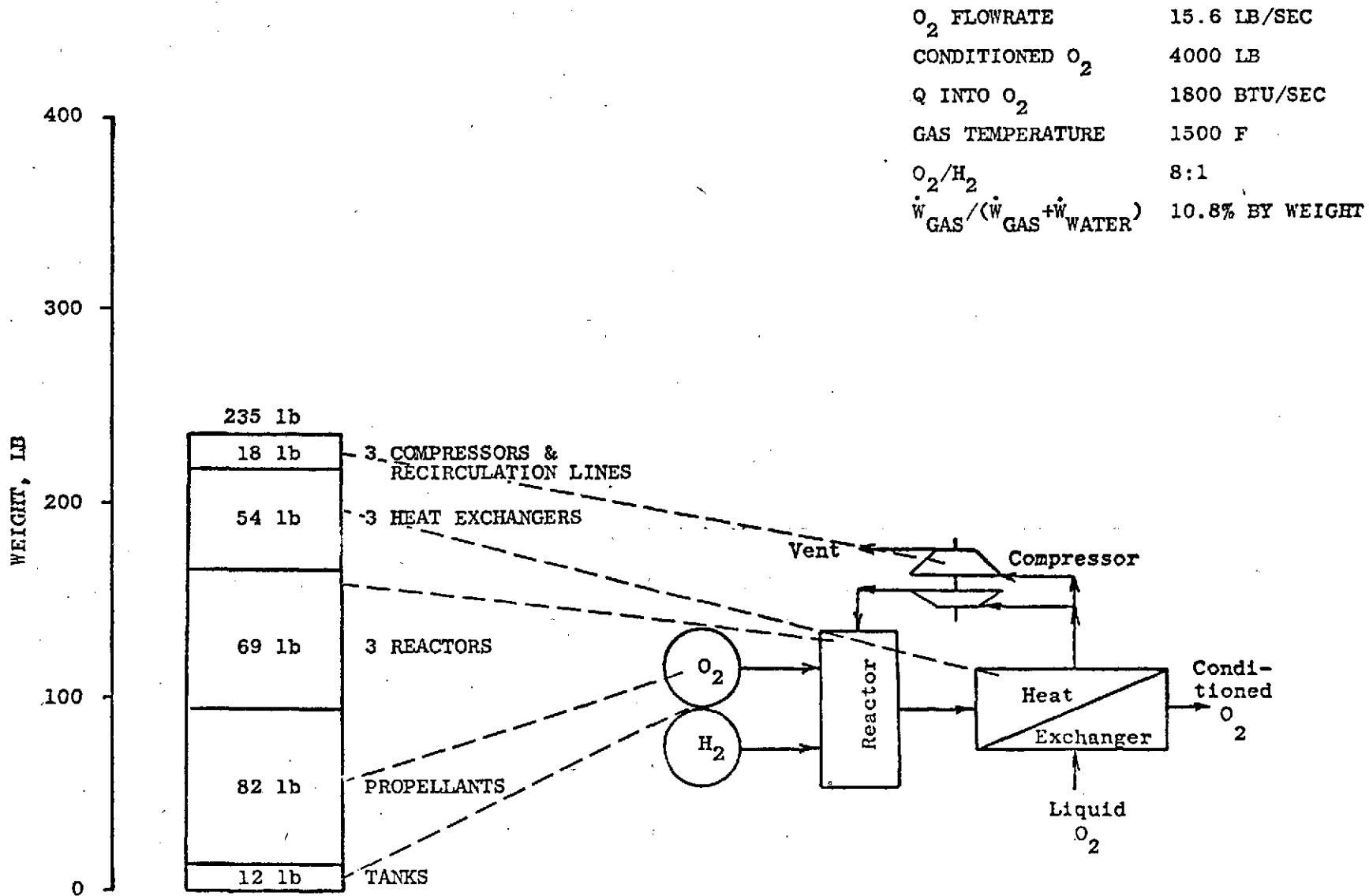


Figure B-24. Stoichiometric O_2/H_2 with H_2O Recirculation

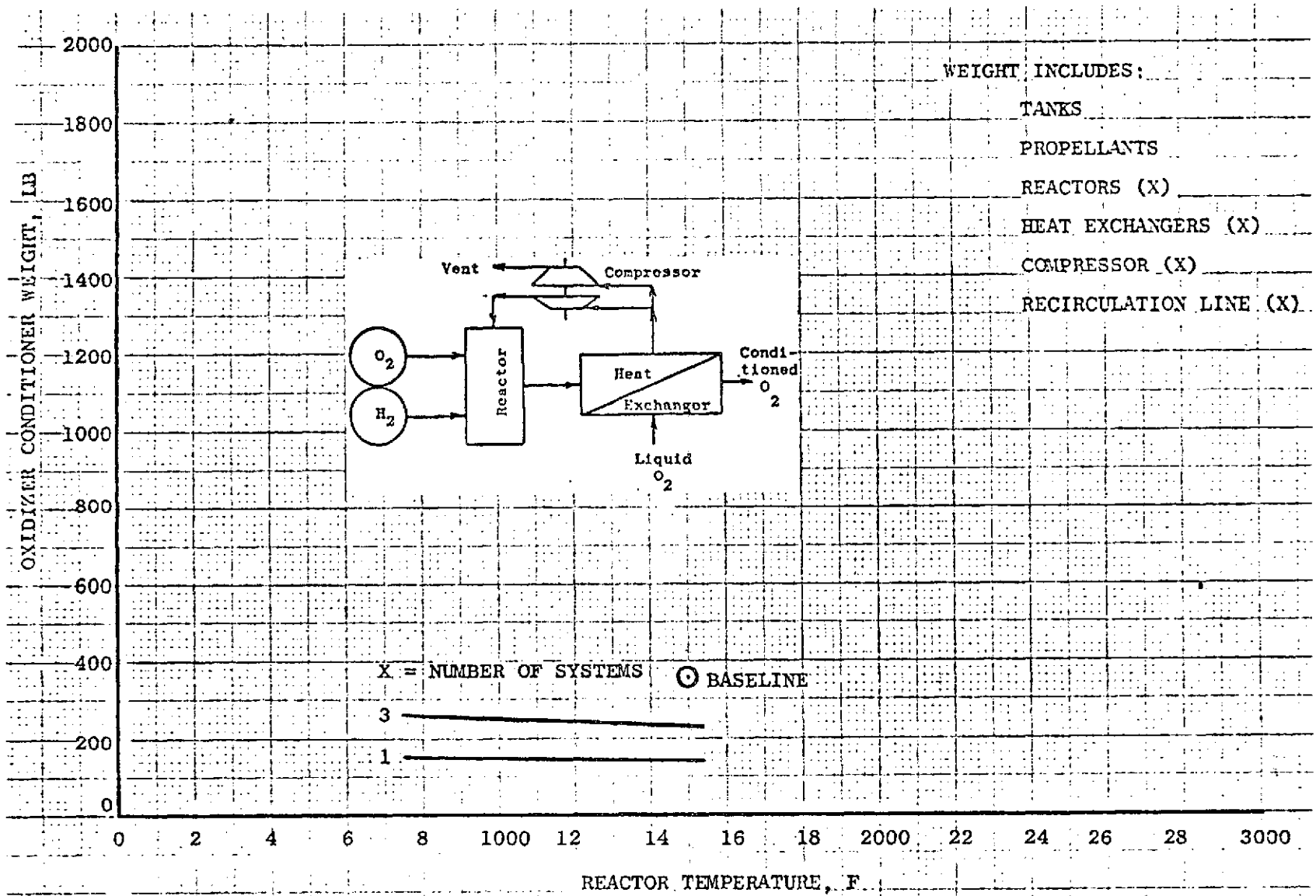


Figure B-25. Stoichiometric O₂/H₂ With H₂O Recirculation

B-35

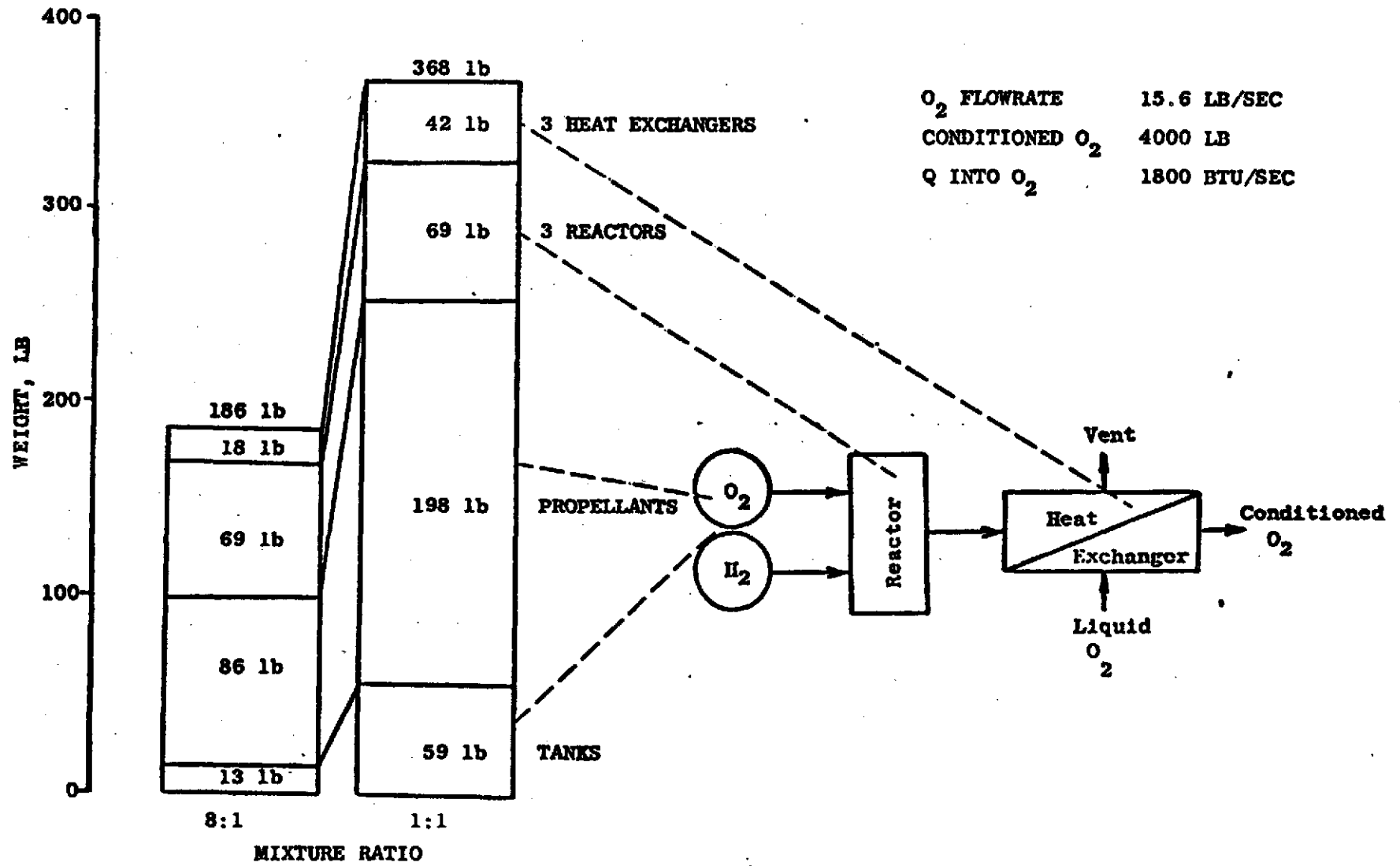


Figure B-26. Baseline Oxidizer Conditioner

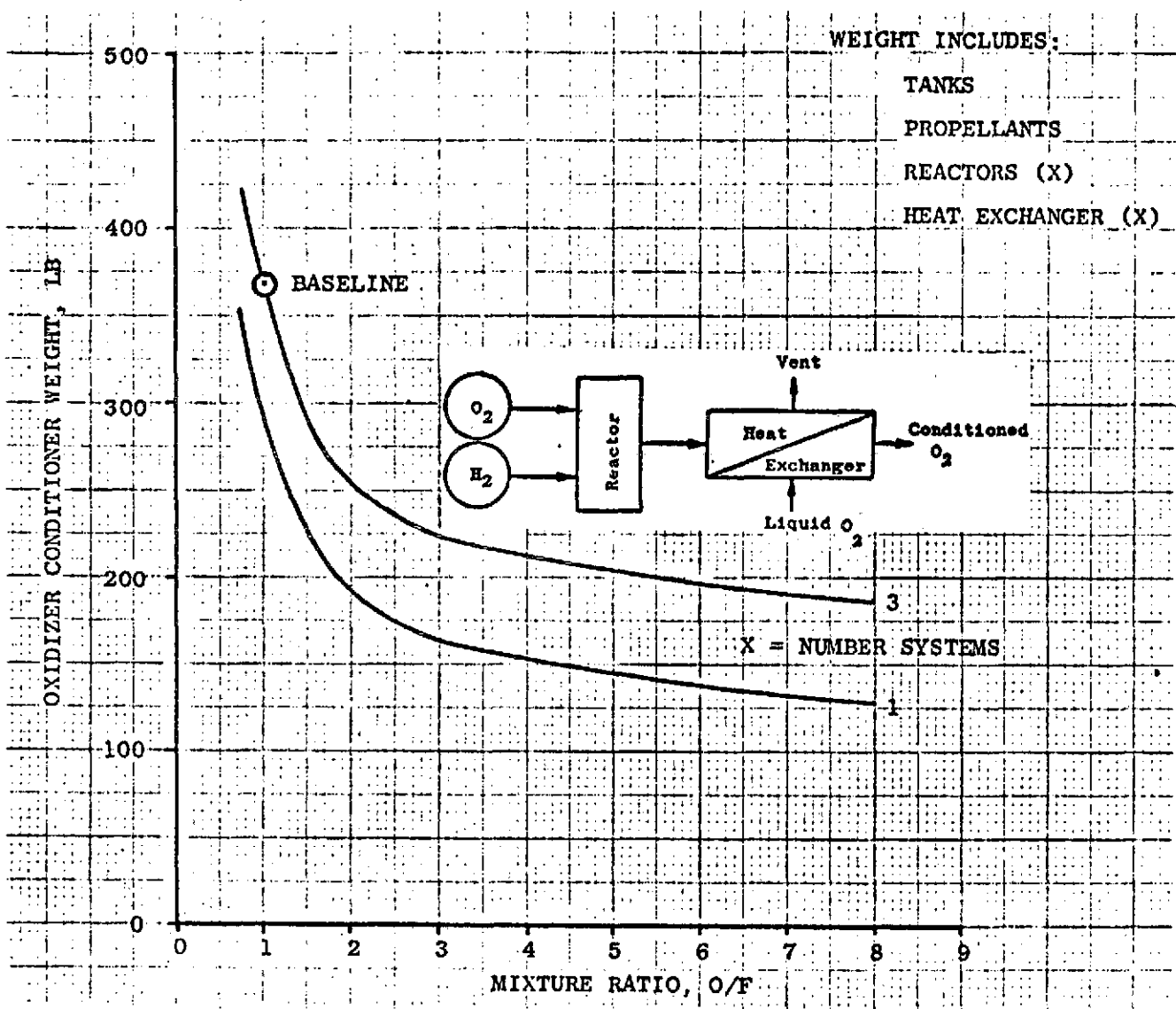


Figure B-27. Oxidizer Conditioner Weight Versus Mixture Ratio

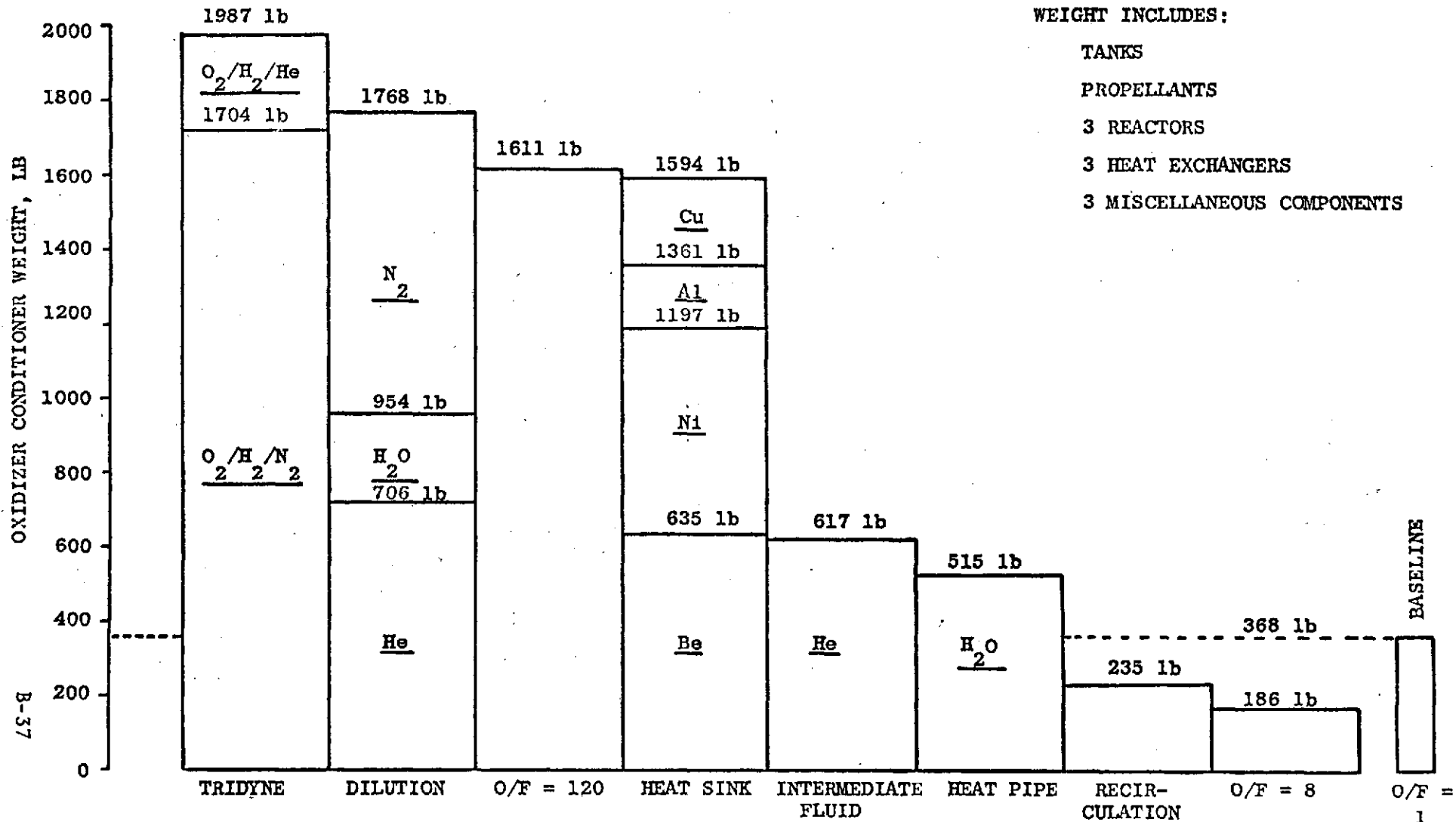


Figure B-28. System Weight Comparison

Table B4 tabulates the cycle weights and weight sensitivities to reactor temperature.

Table B-4. Alternate Oxidizer Conditioner Cycle Weight and Sensitivity* Comparison

Cycle		Total Weight** lb	Sensitivity lb/F
Baseline Cycle	o/f = 1	368	-0.08
Tridyne	O ₂ /H ₂ /He	1987	-1.10
Tridyne	O ₂ /H ₂ /N ₂	1704	-1.30
Dilution	N ₂	1768	-1.17
Dilution	H ₂ O	954	-1.37
Dilution	He	706	-0.33
Oxidizer Rich	o/f = 120:1	1611	-1.10
Heat Sink	Cu	1594	***
Heat Sink	Al	1361	***
Heat Sink	Ni	1197	***
Heat Sink	Be	635	***
Intermediate Fluid	He	617	-0.10
Heat Pipe	H ₂ O	515	-0.18
Recirculation	H ₂ O	235	-0.03
Stoichiometric	o/f = 8:1	186	-0.10

* Sensitivity = Δ Weight / Δ Reactor Temperature

** Total weight includes (1) propellant required to condition 4000 lb of oxygen, (2) tank weight required for the propellant and, (3) hardware weight of three conditioners (triple redundant system)

*** Reactor temperature not varied

CONCLUSIONS AND RECOMMENDATIONS

The 14 alternate cycles evaluated were considered to be independent systems for conditioning the oxidizer propellant. Further evaluation of the alternate cycles should be made considering the entire APS as well as vehicle system effects. For example, a heat sink cycle could eventually be lighter if only 1 heat sink was used instead of 3, or if the heat sink was part of the vehicle structure. Thus, the overall system weight could be lower by the integration of components of the cycle with some other part of the APS or vehicle.

Further consideration should be given to the reliability and safety aspects of the alternate cycles. The reliability of some cycle components could be so high that only 1 instead of 3 components would be required for the system.

The most attractive cycles, based on weight, appear to be the stoichiometric reactor cycle and the recirculation cycle. Another potentially attractive cycle appears to be the heat sink cycle using beryllium provided the heat sink is integrated with the vehicle structure.

APPENDIX C

DEAP COMPUTER PROGRAM

PURPOSE

This computer program is intended to provide a basic tool for the solution of second-order partial differential equations. Parabolic, hyperbolic, and elliptic problems in one, two, or three spatial dimensions can all be solved through use of the Differential Equation Analyzer Program (DEAP). The general hyperbolic differential equation solved by the program can be represented as:

$$\nabla \cdot (K \nabla \phi) + \vec{W} \cdot \nabla \phi + s\phi + q = \lambda \frac{\partial^2 \phi}{\partial t^2} + \rho c \frac{\partial \phi}{\partial t} \quad (1)$$

Normally, several of the coefficients in Eq. 1 will be zero, resulting in the specialization of the equation to a parabolic equation ($\lambda = 0$) or to an elliptic equation ($\lambda = 0$ and $\rho c = 0$). This equation is useful for solution of physical problems relating to mechanical, thermal, mass diffusion, acoustic, magnetic, and electrical physical systems. The DEAP computer program has the capability of solving distributed network problems representing any of these physical systems.

The DEAP computer program solves problems related to the behavior of a continuous physical system through the analogy of a lumped parameter (or nodal) representation that is solved by difference methods. The difference solution method used is a three-time-level method which is a modification of the DuFort Frankel Method that is stable for any computational time increment and is

well suited for non-linear problems (where the coefficients of Eq. 1 are functions of the dependent variable).

PROGRAM DESCRIPTION

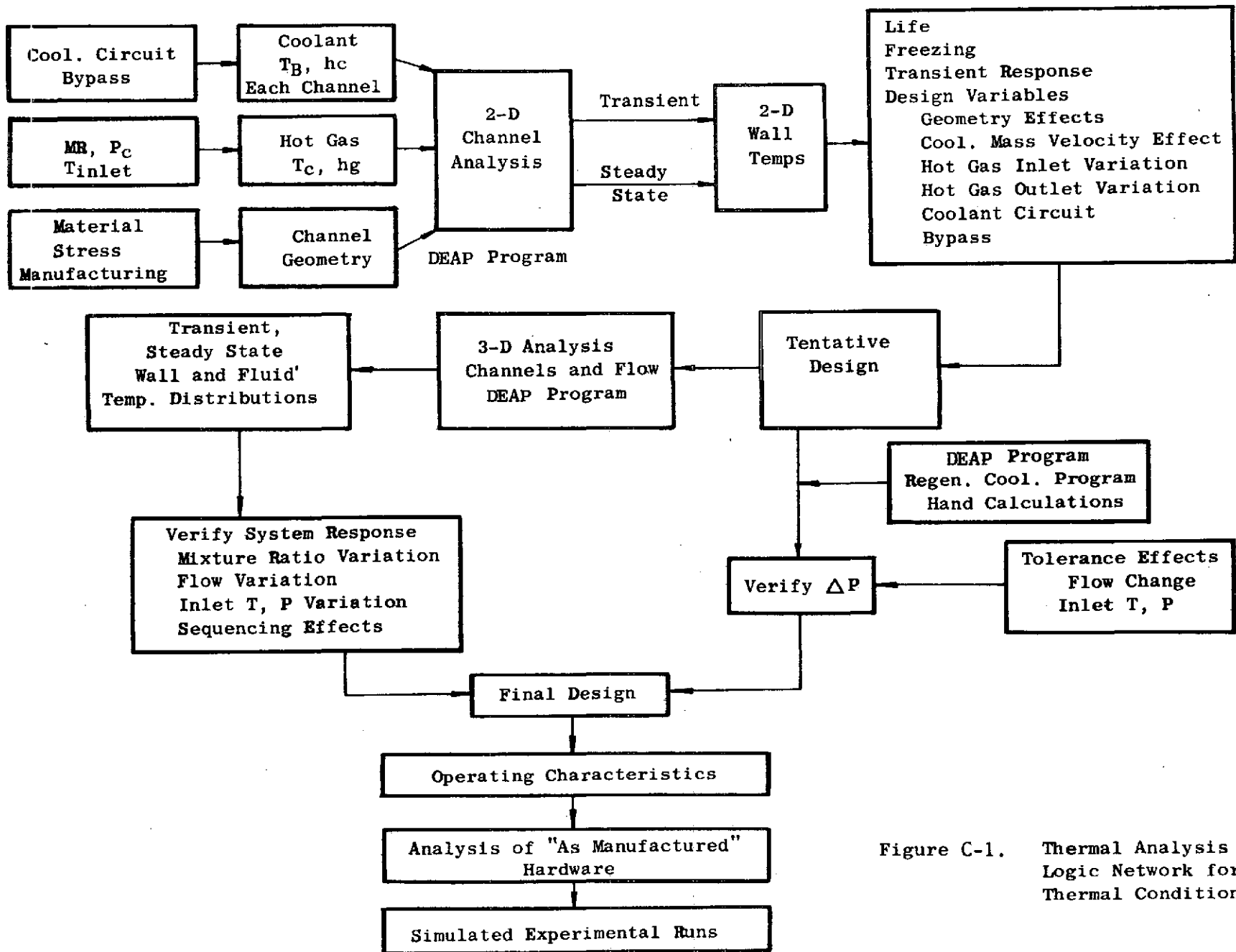
The DEAP computer program described in this manual is a descendant of the Lockheed Thermal Analyzer Program through the TAP computer program which was obtained from AI. The TAP computer program logic was revised and the program capabilities enlarged at Rocketdyne to produce the DEAP computer program. This program has retained the capability to solve any existing TAP problem with only minor changes to the data deck.

The DEAP computer program can solve problems with up to 999 discrete nodes and 2999 connectors allowing for source terms that can either be constant or variable with the dependent variable value at each node. This manual is divided into two major sections. The first section is ENGINEERING ANALYSIS, where the mathematical model is defined and the difference equations used by the computer program to represent this model are stated. The accuracy and limitations of the solution methods are discussed and a discussion of the stability of the equations is presented. The derivation of several special-purpose boundary-condition treatments is also given, followed by a discussion of program logic. The second section gives USAGE INFORMATION and defines the data input requirements first in general terms and then in detail where each of the 11 input sections is described in terms of its requirements and limitations. The program output is described and a sample problem discussed to illustrate the program features.

With relationship to evaluating thermal conditioners, the DEAP program is currently being employed to determine two-dimensional temperature profiles around the coolant channels. For a given gas temperature, gas-side heat transfer coefficient, coolant bulk temperatures (usually different in adjacent passages) and coolant side film coefficients, as well as channel geometry and thermal conductivity (as a function of temperature), the program determines wall temperature profiles, either steady-state or as a function of time (Fig. C-1).

The program has the capability to utilize the geometry directly to determine thermal resistances and capacitances; in this case, specific instructions are included as part of the input to tell the computer how to determine these variables. The program also has the capability of correcting heat transfer coefficients for all temperature. The output is principally the temperature distribution through the wall. This temperature distribution is used directly in the design in numerous ways. It is used to determine if the life criteria will be met, the average heat flux, the distribution of the heat input between adjacent channels, whether the wall surface temperature is too cold and what the best way is to get around this potential problem, whether the coolant mass velocity can be reduced (thereby saving pressure drop), the effect of geometry tolerances, the effect of coolant bypass, selection of coolant circuit, and other variables associated with the design of the conditioner.

In addition, a more sophisticated geometry is being programmed for the DEAP program which would simulate a full baffle. This is a useful tool for analyzing a given design, as it would be capable of analyzing flow transients and would



C-4

Figure C-1. Thermal Analysis Logic Network for Thermal Conditions

be used to insure that the thermal transient requirement would be satisfied. It is also a handy tool for analyzing the effect of flow or mixture ratio changes. The program is even capable of integrating the rest of the APS system to obtain data on the integrated system. This program is a very versatile tool; it does, however, require a fair amount of time to set up the initial geometry of the problem. Once this is done, it is a simple matter to change lengths, heat transfer coefficients, initial conditions, etc.

APPENDIX D
HEAT TRANSFER

The appendix covers the methods used to determine the heat input requirements, the hot gas flow requirements, the gas side heat transfer, and the hot gas passage geometry. Discussion of some of the design limitations are also included. In addition, the relationship of the conditioned propellant passage geometry parameters are covered, with the appropriate design limitations. Also, the method used to obtain the hot gas and conditioned propellant temperature and pressure profiles are discussed. Finally, the two thermal networks used to determine the two-dimensional baffle temperature profiles and the overall baffle heat transfer are shown.

Hydrogen Baffle--Preliminary Design. The first step in determining the hot gas and coolant passage geometry, assuming that the hydrogen flowrate and heat input requirements have been determined, as well as the hot gas mixture ratio, inlet and outlet temperatures is to analyze two dimensional cross sections of the conditioner to determine conditions which will meet the life requirement and which will avoid ice formation on the wall while minimizing weight and pressure drop. The hot gas heat transfer coefficients were based on the Bartz simplified pipe flow equation:

$$N_{NU} = 0.025 N_{RE}^{.8} N_{PR}^{.4 \sigma}$$

where

$$\sigma = \left[.5 \frac{T_{WG}}{T_{AW}} \left(1 + \frac{\gamma-1}{2} M^2 \right) + .5 \right]^{-.68} \left[1 + \frac{\gamma-1}{2} M^2 \right]^{-.12}$$

The hydrogen heat transfer coefficients were based on a Rocketdyne-modified form of the Dipprey-Sabersky equation:

$$C_H = \frac{h(T_W/T_B)^{.55}}{G C_p} = \frac{C_{f/2}}{.92 + (C_{f/2})^{.5} [g(\epsilon^*) - 8.48]}$$

where

$$g(\epsilon^*) = 4.7 (\epsilon^*)^{.2} \quad (\epsilon^* > 7)$$

$$g(\epsilon^*) = 4.5 + .57 (\epsilon^*)^{.75} \quad (\epsilon^* \leq 7)$$

$$\epsilon^* = (\epsilon/D) N_{RE} (C_{f/2})^{.5}$$

Both of the above correlations gave good agreement with experimental data obtained from the single baffle hydrogen conditioner recently tested.

The analysis was based on a Haynes 188 baffle with a stainless steel closeout. The hot gas wall thickness of 0.015 inch was assumed reasonable to manufacture while permitting reasonable channel geometries. Based on the fail-safe requirements, the channel width (coolant channel) was limited to no greater than 5.3 times the gas wall thickness, taking into account the high temperature capability of Haynes 188. Since the thermal conductivity of Haynes 188 is a strong function of temperature, the temperature variation is included in the analysis.

PREPARED BY: JGG	Rocketdyne Division Rockwell International	PAGE NO. _____ OF _____
CHECKED BY:		REPORT NO. _____
DATE:	H ₂ CONDITIONER : Σ Q	MODEL NO. _____

HEAT INPUT REQUIREMENTS:

PUMP DISCHARGE P, PSIA	1100	1600	2100
W _{H₂} , LB/SEC =	5.95	4.5	3.0

A) MAX Q: T_{IN} = 40R
 T_{OUT} = 250R

ΔH, BTU/LB =	779	759	743
ΔQ, BTU/SEC =	4640	3410	2229

B) MIN Q: T_{IN} = 70R
 T_{OUT} = 200R

ΔH, BTU/LB =	503	485	470
ΔQ, BTU/SEC =	3000	2180	1410
ΔQ AVERAGE, B/SEC =	3820	2795	1820

DUE TO THE LARGE RANGE OF POSSIBLE HEAT INPUT REQUIREMENTS REPRESENTED BY THE SPECIFIED RANGE OF H₂ FLOWRATES, INLET AND OUTLET TEMPERATURES (OVER 2/1 DUE TO FLOW VARIATIONS ALONE), A MEAN VALUE OF 2800 BTU/SEC WAS SELECTED FOR SIZING THE CONDITIONER. THIS REPRESENTS A NOMINAL FLOW OF 4.5 LB/SEC @ 1600 PSIA, A NOMINAL T_{IN} = 55R, & T_{OUT} = 225R.

ABOVE BASED ON NBS H₂ PROPERTIES

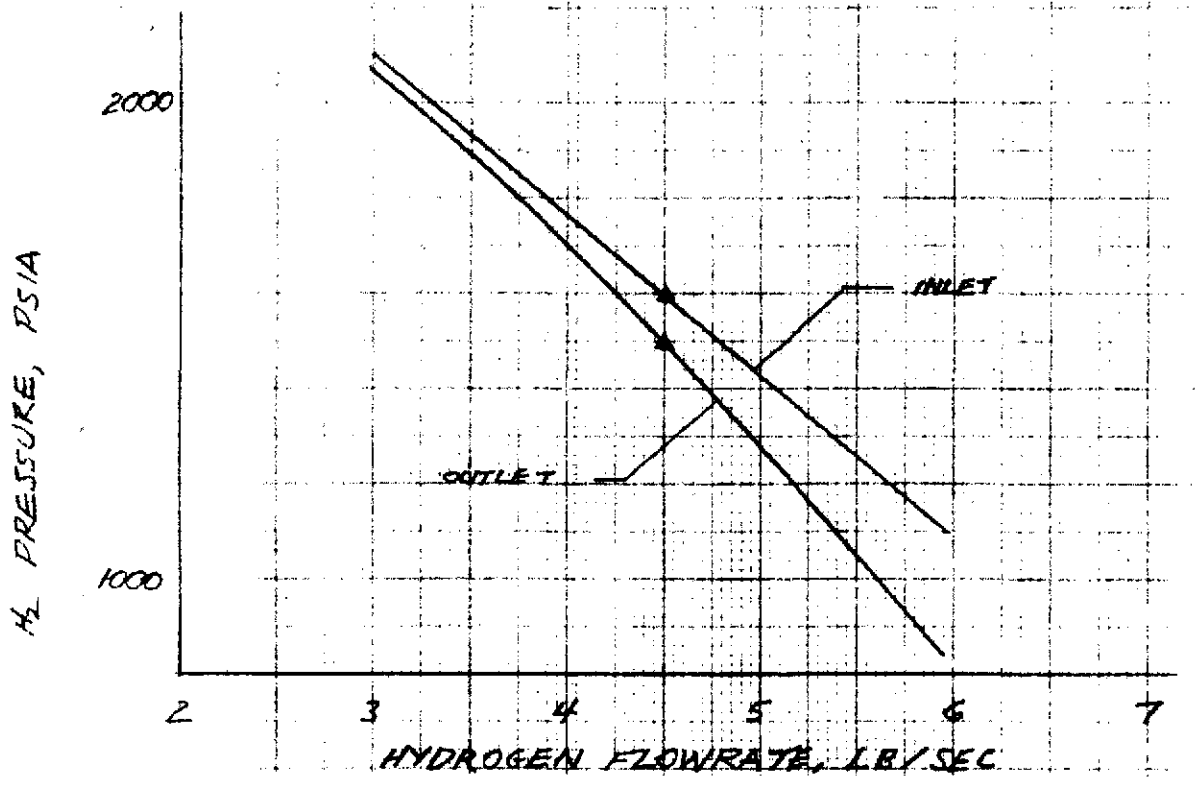
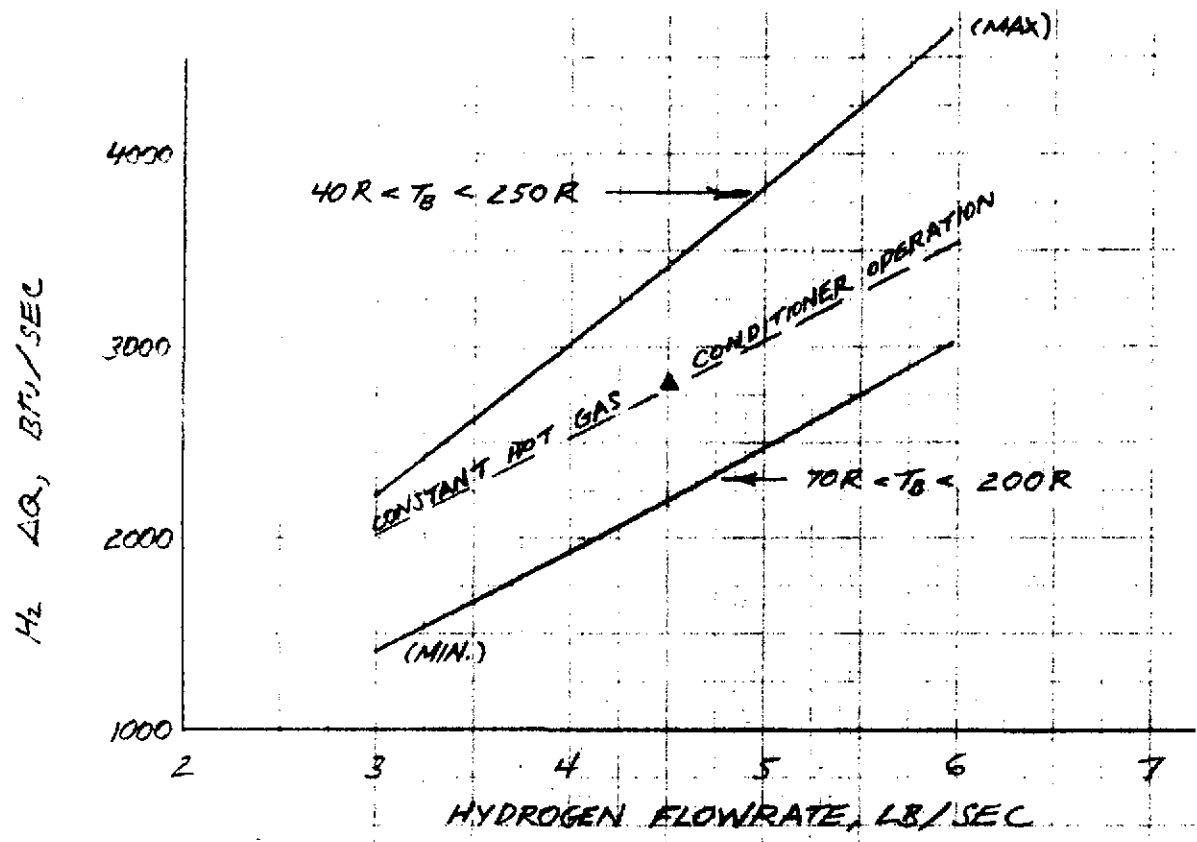


Figure D-5. Hydrogen Conditioner Heat Input

PREPARED BY:	Rocketdyne Division Rockwell International	PAGE NO.	OF
CHECKED BY:		REPORT NO.	
DATE:	H ₂ CONDITIONER: W _{HOT GAS}	MODEL NO.	

DESIGN $\Delta Q = 2800 \text{ BTU/SEC}$

$T(\text{H}_2 \text{ INJECTION}) = 275\text{R}$
 $T(\text{O}_2 \text{ INJECTION}) = 375\text{R}$
 $MR = 1$

(P.16, JULY MONTHLY)
 $T_c (100\% \text{ c}^*) = 1580\text{F}$

FOR A SELECTED HOT GAS $T_{\text{OUT}} = 750\text{R}$,

$H_{\text{IN}} = 520 \text{ B/LB}$
 $H_{\text{OUT}} = 2880 \text{ B/LB}$
 $\Delta H = 2360 \text{ B/LB}$

} FIG. 5, P.19, JULY MONTHLY

$\dot{W}_{\text{H.G.}} = \Delta Q / \Delta H = 2800 / 2360 = 1.19 \text{ LB/SEC}$

$\therefore \text{NOMINAL } \dot{W}_{\text{HG}} / \dot{W}_{\text{H}_2} = 1.19 / 4.5 = .265$

$\Sigma W_{\text{H}_2} (5000 \text{ LBS, MR} = 3.5) = 5000 / (1+3.5) = 1110 \text{ LBS}$

$\therefore \Sigma (W_{\text{HG}})_{\text{H}_2 \text{ CONDITIONER}} = 1110 \text{ LBS} \times .265 = 295 \text{ LBS}$
 (SEE P.22, JULY MONTHLY)

PREPARED BY:	Rocketdyne Division Rockwell International	PAGE NO. _____ OF _____
CHECKED BY:		REPORT NO. _____
DATE:		H ₂ CONDITIONER: (Q/A) HOT GAS

AT ANY POINT ALONG THE CONDITIONER, X,

$$(Q/A)_x = (h_g)_x [(T_{GAS})_x - (T_{WG})_x] = \text{LOCAL HEAT FLUX}$$

WHERE THE WALL TEMP., T_{WG} , IS DETERMINED FROM A STEADY STATE 2-DIMENSIONAL ANALYSIS

T_{GAS} - THE LOCAL HOT GAS TEMPERATURE, IS A FUNCTION OF MIXTURE RATIO, HOT GAS FLOWRATE, COMBUSTION TEMPERATURE, AND THE AMOUNT OF HEAT LOST TO POINT X.

h_g - THE HOT GAS HEAT TRANSFER COEFFICIENT, IS BASED ON THE SIMPLIFIED BARTZ TURBULENT PIPE FLOW CORRELATION:

$$Nu = .025 Re^{.8} Pr^{.4} \sigma$$

$$\text{OR } h_g = .025 \mu^{-.2} C_p G^{.8} \sigma / (d_H^{.2} Pr^{.6})$$

$$\text{WHERE } \sigma = \left[0.5 \frac{T_{WG}}{T_{GAS}} \left(1 + \frac{C_p}{2} M^2 \right) + .5 \right]^{-.68} \left[1 + \frac{C_p}{2} M^2 \right]^{-.12}$$

(T IN DEG. R)

$$G = \text{MASS VELOCITY} = \dot{W} / A_x$$

$$A_x = (\text{PASSAGE HT. } H)(\text{PASSAGE WIDTH } S)(\text{NO. PASSAGES } N)$$

μ, C_p, Pr - BASED ON HOT GAS PROPERTIES VS MR, T

$$d_H - \text{HYDRAULIC DIA.} = 4A_x / \text{WETTED PERIMETER} = 2S$$

THE BARTZ CORRELATION - WHILE FOR PIPE FLOW, IS APPROPRIATE ALSO FOR LARGE L/D PASSAGES TYPICAL OF THE CONDITIONER. THIS IS USED OVER MOST OF THE CONDITIONER. IT UNDER-ESTIMATES Q/A IF CONDENSATION OCCURS. IT ALSO DOES NOT PROPERLY REPRESENT THE STAGNATION VALUE AT THE BAFFLE NOSE. STAGNATION HEAT FLUXES SHOULD BE LESS (D-7) THAN MAX. BAFFLE Q/A DUE TO LOW UPSTREAM MASS VELOCITIES.

PREPARED BY:	Rocketdyne Division Rockwell International	PAGE NO.	OF
CHECKED BY:		REPORT NO.	
DATE:	CONDITIONER HOT GAS GEOMETRY	MODEL NO.	

GEOMETRY CONSISTS OF PASSAGE LENGTH, WIDTH, HEIGHT, AND TAPER.

PASSAGE HEIGHT:

THERE IS NO HEAT TRANSFER REQUIREMENT SPECIFICALLY GOVERNING HEIGHT. THIS MAY BE CHOSEN ON THE BASIS OF OTHER DESIGN, STRESS, OR WEIGHT CONSIDERATIONS. THE ONLY REQUIREMENT IS THAT

$$\text{SURFACE AREA } A_s = 2NHL$$

$$\text{CROSS-SECTION AREA } A_x = \dot{W}/G = NH\delta$$

WHERE

- W = HOT GAS FLOW/RATE
- G = HOT GAS MASS VELOCITY
- N = NO. HOT GAS PASSAGES
- H = PASSAGE HEIGHT
- δ = PASSAGE WIDTH (NO GUIDE RAILS)

ASSUMES: EACH SIDE PLATE IS EQUIVALENT TO 1/2 BAFFLE

NO HEAT INPUT TOP OR BOTTOM

PASSAGE LENGTH

FROM ABOVE TWO EQUATIONS

$$L/\delta = A_s/2A_x$$

WHERE δ AND A_x EVALUATED AT SAME POINT

PREPARED BY:	Rocketdyne Division Rockwell International	PAGE NO. _____ OF _____
CHECKED BY:		REPORT NO. _____
DATE:	CONDITIONER HOT GAS GEOMETRY	MODEL NO. _____

PASSAGE WIDTH

HOT GAS PASSAGE WIDTH SELECTION REQUIRES CARE, AS IT AFFECTS CONDITIONER LENGTH (WEIGHT); COOLANT PASSAGE HEIGHT (WEIGHT, BAFFLE BEND RADIUS). THE SMALLER THE GAP, THE MORE COMPACT AND LIGHTER THE CONDITIONER. MINIMUM PASSAGE WIDTH IS BASED ON MANUFACTURING ABILITY AND TOLERANCE REQUIREMENTS. FOR OPTIMUM RESULTS, A TIGHT TOLERANCE AT THE BACK HALF OF THE CONDITIONER IS HIGHLY DESIRABLE. TOO LARGE A WIDTH RESULTS IN REDUCED HEAT TRANSFER; TOO SMALL A VALUE RESULTS IN EXCESSIVE CHAMBER PRESSURE REQUIREMENTS (LIMITED BY 375 PSIA \pm 10% REGULATORS). IN ADDITION, SMALL GAPS MAY BE MORE PRONE TO ICING, THOUGH MORE DATA REQ'D TO SET MINIMUM GAP TO MEET THIS POSSIBILITY.

CONSIDERING ABOVE ITEMS, A MINIMUM GAP (WIDTH) OF ABOUT .050 IN. HAS BEEN SOMEWHAT ARBITRARILY SELECTED. THIS MAY BE DECREASED IN A LATER, ADVANCED DESIGN. IT IS NOTED THE IRGD H₂ BAFFLE OPERATED SATISFACTORILY WITH APPROX. .033 IN. MIN. GAP.

PASSAGE TAPER

THE PASSAGE WIDTH AT THE FORWARD END OF THE BAFFLE IS TAPERED IN ORDER TO RESTRICT MAXIMUM Q/A - LIMITED BY LIFE CONSIDERATIONS TO ABOUT 4.2 BTU/IN²-SEC. AT MR=1, THIS HAS RELATIVELY MINOR EFFECT ON SURFACE AREA REQUIREMENTS.

PREPARED BY:	Rocketdyne Division Rockwell International	PAGE NO.	OF
CHECKED BY:		REPORT NO.	
DATE:	CONDITIONER HOT GAS GEOMETRY	MODEL NO.	

LIMITING HOT GAS MASS VELOCITY - G

MAXIMUM VALUE OF G IS CONSIDERED TO BE SONIC CONDITIONS (M=1). THIS LIMITATION CAN OCCUR AT EITHER THE UPSTREAM OR DOWNSTREAM END OF THE CONDITIONER, DEPENDING ON MIXTURE RATIO & EXIT TEMPERATURE.

FOR PERFECT GAS:

$$a = \sqrt{\gamma R T}$$

$$R = \bar{R} / M$$

$$T = T_0 / (1 + \frac{\gamma-1}{2}) \quad (\text{MACH NO.} = 1)$$

$$P = P_0 / R T$$

$$G_{\text{MAX}} = P a$$

$$P_0 = P (1 + \frac{\gamma-1}{2})^{\frac{\gamma}{\gamma-1}} \quad (M=1)$$

WHERE

a = ACOUSTIC VELOCITY

γ = SHIFTING SPECIFIC HEAT RATIO = f(MR)

T = STATIC TEMPERATURE

g = GRAVITATIONAL CONSTANT (386 L/S² = 32.2 F/S²)

R = GAS CONSTANT

\bar{R} = UNIVERSAL GAS CONSTANT

M = MOLECULAR WEIGHT = f(MIXTURE RATIO)

P = STATIC PRESSURE

P_0 = TOTAL PRESSURE

PRESSURE DROPS ARE SUCH THAT UPSTREAM P_0

$$(P_0)_{\text{U/S}} \approx 2 (P_0)_{\text{D/S}}$$

TYPICAL RESULTS ARE SHOWN IN FOLLOWING FIGURE.

RESULTS INDICATE MAX. EXIT MASS VELOCITY @ 240 PSIA UPSTREAM & EXIT $T = 750R$ RESULTS IN

$$G_{\text{MAX}} \sim .88 \text{ LB/IN}^2\text{-SEC}$$

PREPARED BY:	Rocketdyne Division Rockwell International	PAGE NO. _____	OF _____
CHECKED BY:		REPORT NO. _____	
DATE:	CONDITIONER HOT GAS GEOMETRY	MODEL NO. _____	

SURFACE AREA REQUIREMENTS - A_s

TO OBTAIN SURFACE AREA, THE FOLLOWING EQ.N. IS SOLVED:

$$Q = \int_{x=0}^L dQ = \int_{x=0}^L (Q/A) dA_s$$

$$\text{OR } A_s = \int_{x=0}^L \frac{dQ}{Q/A} = \sum_{0 < x < L} \frac{\Delta Q}{Q/A}$$

THIS CAN BE APPROXIMATED IN FINITE DIFFERENCE FORM, NOTING THAT

$$\Delta Q = W_{HG} C_{PAV} (T_{HG_1} - T_{HG_2}) = W_{HG} \Delta H_{T_1 \rightarrow T_2}$$

$$Q/A = h_{gAV} (T_{HG} - T_{WG})_{AV}$$

THE WALL SURFACE TEMPERATURES ARE BASED ON STEADY STATE, TWO-DIMENSIONAL ANALYSES AT A PARTICULAR GAS TEMPERATURE AND HEAT TRANSFER COEFFICIENT (WITH APPROPRIATE VALUES FOR h and T FOR THE CONDITIONED PROPELLANT, AND APPROPRIATE CHANNEL GEOMETRY AND THERMAL CONDUCTIVITY).

CONSEQUENTLY BETWEEN ANY TWO GIVEN HOT GAS TEMPERATURES, THE AVERAGE C_p (OR ENTHALPY CHANGE DIRECTLY) WILL GIVE ΔQ , AND THE 2-D ANALYSIS GIVES AN AVERAGE Q/A ; THIS YIELDS A SURFACE AREA REQ'D BETWEEN THE 2 TEMPERATURES. THE TOTAL SURFACE AREA IS THEN THE SUM OF THE INCREMENTAL VALUES. THIS ALSO GIVES THE RELATIVE HEAT FLUX AND HOT GAS TEMPERATURE PROFILES ($T, Q/A$ vs x/L).

PREPARED BY:	Rocketdyne Division Rockwell International	PAGE NO.	OF
CHECKED BY:		REPORT NO.	
DATE:	CONDITIONED H ₂ TEMP. PROFILE	MODEL NO.	

THE CONDITIONED H₂ TEMPERATURE PROFILE IS DETERMINED AT THE SAME TIME AS THE HOT GAS TEMPERATURE PROFILE:

$$\Delta Q = (\dot{W} \Delta H)_{H_2} = (\dot{W} \Delta H)_{HOT GAS}$$

FOR A SELECTED H₂ BYPASS (40%), H₂ INLET AND EXIT LOCATIONS, H₂ AND HOT GAS FLOWRATES AND INLET CONDITIONS, THE HYDROGEN TEMP. PROFILE IS READILY DETERMINED USING THE ABOVE EQUATION.

FOR A FIRST GUESS, THE HEAT INPUT WAS ASSUMED TO SPLIT EQUALLY BETWEEN UPPASS AND DOWNPASS CHANNELS. THIS DOES NOT RESULT IN AN ERROR IN SURFACE AREA AS HEAT FLUX IS QUITE INSENSITIVE TO H₂ TEMP. IN ACTUAL PRACTICE, EVEN THOUGH THE HEATED WALL TEMP. PROFILE IS NOT VERY SENSITIVE TO UPPASS OR DOWNPASS CHANNEL LOCATION, A LARGER FRACTION OF HEAT GOES TO COLDER (UPPASS) CHANNEL, DUE TO HEAT TRANSFER FROM WARMER DOWNPASS CHANNEL TO UPPASS CHANNEL. AS A RESULT, THE ACTUAL TEMP. DISTRIBUTION IS OBTAINED THRU AN ITERATIVE PROCEDURE. THE BAFFLE ANALYSIS PROGRAM DESCRIBED LATER SOLVES THIS DISTRIBUTION DIRECTLY, THEREBY DISPENSING WITH ITERATION PROCEDURE.

PREPARED BY:	Rocketdyne Division Rockwell International	PAGE NO.	OF
CHECKED BY:		REPORT NO.	
DATE:	CONDITIONED H ₂ (O ₂) CHANNEL HEIGHT	MODEL NO.	

CONDITIONED PROPELLANT CHANNEL HEIGHT :

$$A_x = \dot{W}_{(H_2)} / G_{(H_2)} = N_c a h$$

WHERE $N_c = N_B N_H$

AND $N_H = \frac{H - \lambda}{l + a}$

- WHERE
- A_x = TOTAL CROSS-SECTION AREA
 - $\dot{W}_{(H_2)}$ = CONDITIONED PROPELLANT FLOWRATE
 - $G_{(H_2)}$ = " " MASS VELOCITY
 - a = CHANNEL WIDTH
 - h = CHANNEL HEIGHT
 - N_c = TOTAL NO. CHANNELS (EACH DIRECTION)
 - N_B = Σ NO. BAFFLES = NO. BAFFLES + 1 [SIDE PLATES]
 - N_H = NO. CHANNELS / BAFFLE, ONE DIRECTION
 - l = LAND WIDTH
 - H = BAFFLE HEIGHT
 - λ = DIFFERENCE BETWEEN EDGE DISTANCE AND $1/2$ LAND (EACH EDGE)

$$\therefore W_{H_2} / G_{H_2} = (N_B H - N_B \lambda) \left(\frac{a}{l+a} \right) h$$

$$\text{OR } h = \left(\frac{W_{H_2}}{G_{H_2}} \right) \left(1 + \frac{l}{a} \right) / (N_B H - N_B \lambda)$$

FROM HOT GAS GEOMETRY :

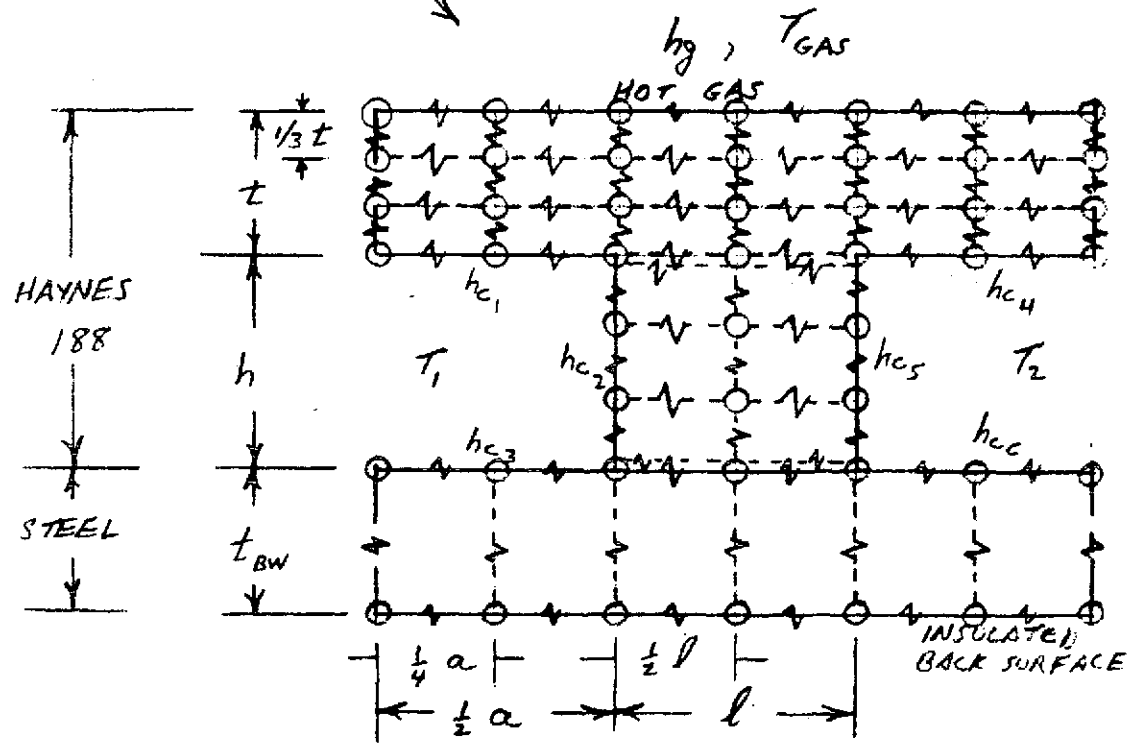
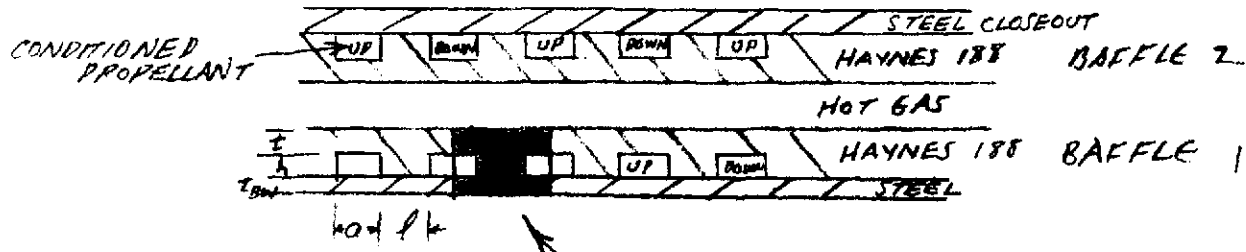
$$A_{xHG} = W_{HG} / G_{HG} = N_B H \delta \quad (\text{NO BLOCKAGE ASSUMED})$$

δ = HOT GAS PASSAGE WIDTH @ G_{HG}

$$\therefore h = \left(\frac{W_{H_2}}{G_{H_2}} \right) \left(\frac{G_{HG}}{W_{HG}} \right) \left(1 + \frac{l}{a} \right) \delta \quad \text{IF } \lambda = 0$$

ASSUMPTION OF $\lambda = 0$ GOOD SINCE $H \sim 5''$, $2\lambda = .12'' - .04'' = .08''$
 $\therefore \lambda / H = .08 / 5 = .016$ - NEGLECTIBLE FOR ANALYSIS

PREPARED BY:	Rocketdyne Division Rockwell International	PAGE NO.	OF
CHECKED BY:		REPORT NO.	
DATE:	2-D TEMPERATURE PROFILES	MODEL NO.	



PROGRAM : DEAD (IBM 360) [OUTPUT = TEMPERATURES]
 NETWORK : AS SHOWN ABOVE
 INPUT :

- GEOMETRY :
- a - CHANNEL WIDTH
 - l - LAND WIDTH
 - t - GAS WALL THICKNESS
 - h - CHANNEL HEIGHT
 - t_{BW} - BACK WALL (CLOSEOUT) THICKNESS
- MAT'L : TABLES - THERMAL CONDUCTIVITY VS TEMP.
- BOUNDARY :
- HOT GAS h_g , TEMPERATURE
 - UPPASS $H_2(O_2)$ $T_1, h_{c1}, h_{c2}, h_{c3}$
 - DOWNPASS $H_2(O_2)$ $T_2, h_{c4}, h_{c5}, h_{cc}$

D-14

DIFFERENT h_c INPUTS ACCOUNT FOR DIFFERENT CURVATURE AND ROUGHNESS VALUES ON EACH CHANNEL SURFACE. INPUT h_c AT $T_{BULK} = T_{WALL}$. PERMITS $h_c = F(T_B/T_W)^n$, $n = \text{INPUT}$

PREPARED BY:	Rocketdyne Division Rockwell International	PAGE NO. _____ OF _____
CHECKED BY:		REPORT NO. _____
DATE:	CONDITIONED H ₂ PRESSURE PROFILE	MODEL NO. _____

- TO OBTAIN THE H₂ PRESSURE PROFILE, REQUIRES
- 1) CHANNEL GEOMETRY (LENGTH, HYDRAULIC DIA)
 - 2) MASS VELOCITY
 - 3) ROUGHNESS, REYNOLDS NO. $\Rightarrow f$ = FRICTION FACTOR
 - 4) TEMPERATURE PROFILE

BECAUSE OF LOW MACH NO., TOTAL TEMP \sim STATIC TEMP.
 \therefore TOTAL TEMPS. USED THROUGHOUT.

$$\text{HYDRAULIC DIAMETER } d_H = \frac{4A}{P} = \frac{4ha}{2(a+h)} = \frac{2a}{\frac{a}{h} + 1}$$

$$d_H = \frac{2 \times .05''}{\frac{.05}{.075} + 1} = .060'' \quad (G_{H_2} = 2.2 \text{ LB/IN}^2\text{-SEC})$$

$$\textcircled{2} G_{H_2} = 1.25 \text{ LB/IN}^2\text{-SEC}, \quad d_H = \frac{2 \times .090''}{\frac{.09}{.075} + 1} = .082''$$

$$\text{FOR } Re = \frac{Gd}{\mu} = \frac{(2.2 \text{ LB/IN}^2\text{-SEC})(.06 \text{ IN})}{3 \times 10^{-6} \text{ LB/IN-SEC}} = 440,000$$

$$\epsilon/d_H = 100 \mu\text{IN} / .060'' = .00167$$

$$\therefore f = .022$$

$$\therefore \Delta P = \sum \left(K \frac{G_{H_2}^2}{2gP_{H_2}} \right)$$

WHERE $K = f L / d_H$ = FRICTION LOSS

$\textcircled{1}$ INLET, $K = .5$ HEAD LOSS

$\textcircled{2}$ EXIT, $K \sim 1$ HEAD LOSS

P_{H_2} FROM NBS PROPERTY TABLES = $f(P, T)$

DESIGN ΔP BASED ON

$$T_{IN} = 55 \text{ R}$$

$$P_{IN} = 1600 \text{ PSIA}$$

$$P \text{ IS STATIC PRESSURE} = P_0 - \frac{G^2}{2gP}$$

PREPARED BY:	Rocketdyne Division Rockwell International	PAGE NO. _____ OF _____
CHECKED BY:		REPORT NO. _____
DATE:	HOT GAS PRESSURE PROFILE	MODEL NO. _____

HOT GAS PRESSURE PROFILE BASED ON
 1) INLET CONDITIONS & FLOWRATE
 2) MASS VELOCITY PROFILE
 3) TEMPERATURE PROFILE

BECAUSE OF HIGH HOT GAS MACH NO ≤ 1 , IT IS NECESSARY TO DETERMINE STATIC TEMPERATURE AND PRESSURE ITERATIVELY AT EACH POINT:

$$d_H = 2 \times \text{HOT GAS GAP} :$$

WITH NO GAS GUIDE RAILS, $.046" < \text{GAS WIDTH} < .092"$

$$\text{GAS MASS VELOCITY} \quad .88 > G_{HG} > .44 \text{ LB/IN}^2\text{-SEC}$$

$$\text{HYDRAULIC DIA} = .092 < d_H < .184"$$

$$\text{FRICTION FACTOR} \sim .020$$

$$\Delta P = K G^2 / 2g\rho$$

$$K = \begin{matrix} fL/d & \text{FRICTION LOSS} \\ = .5 & \text{INLET LOSS} \\ = 1.0 & \text{OUTLET LOSS} \end{matrix}$$

SONIC EXIT:

$$P_E = G_E / \alpha_E = \frac{\text{EXIT MASS VELOCITY}}{\text{EXIT SONIC VELOCITY}}$$

$$\alpha_E = \sqrt{\gamma_E (R/M) T_E g}$$

$$T_E = T_{0E} / (1 + \frac{\gamma-1}{2} M^2) = 750R / (1 + \frac{\gamma-1}{2}) \quad [\text{SONIC}]$$

$$\text{EXIT STATIC PRESSURE} = P_E = P_E (R/M) T_E$$

$$\text{EXIT TOTAL PRESSURE} = P_{0E} = P_E (1 + \frac{\gamma-1}{2})^{\frac{\gamma}{\gamma-1}} \quad [\text{SONIC}]$$

IT IS NOTED HERE THAT IT IS THE EXIT CONDITION WHICH DETERMINES INJECTOR-END PRESSURE. THIS IS SENSITIVE TO FLOWRATE, TEMPERATURE, MIXTURE RATIO, AND HOT GAS EXIT X-SECTION AREA.

PREPARED BY:

Rocketdyne Division
Rockwell International

PAGE NO. OF

CHECKED BY:

REPORT NO.

DATE:

HOT GAS PRESSURE DROP

MODEL NO.

THE TOTAL PRESSURE AT EACH POINT WAS DETERMINED BY:

$$\text{TOTAL } P_{0/5} = P_{0/5} + \left(f \frac{L}{dH}\right) \frac{G^2}{2gP_{0/5}}$$

$$\text{STATIC } P_{0/5} = (\text{TOTAL } P_{0/5}) - \frac{G^2}{2gP_{0/5}}$$

$$\text{WHERE } P_{0/5} = \left[P_{0/5} \left(\frac{R}{M} \right) T_{0/5} \right]_{\text{STATIC}}$$

$$V = G/P$$

$$T_s = T_{\text{TOTAL}} - \frac{V^2}{2gJc_p}$$

$$\text{MACH NO.} = V/a$$

$$a = \sqrt{\gamma \left(\frac{R}{M} \right) T_{\text{STATIC}} g}$$

WHERE

V = LOCAL GAS VELOCITY

a = SONIC VELOCITY

M = MACH NO.

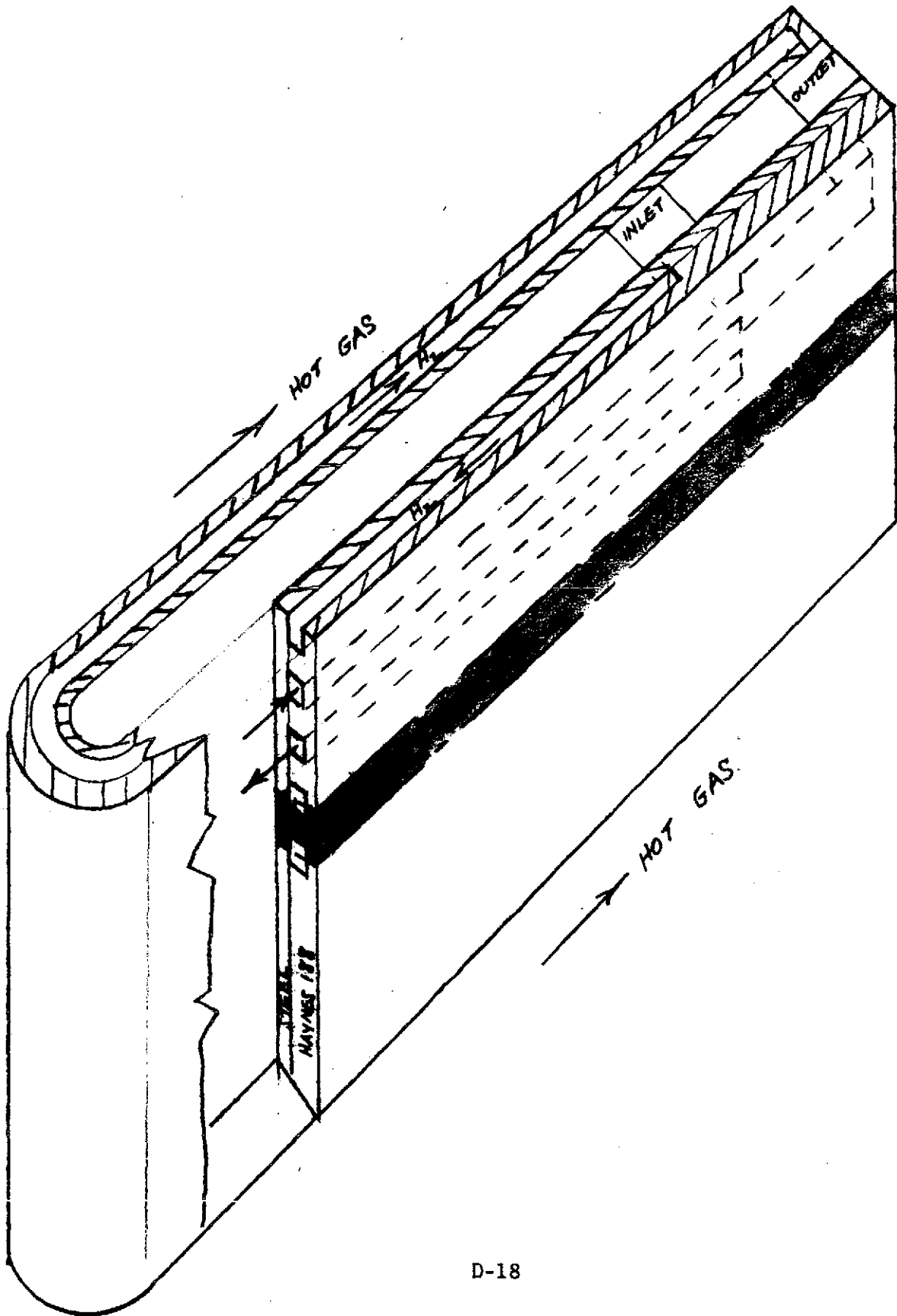
M = MOLECULAR WEIGHT

 γ = SPECIFIC HEAT RATIOc_p = SPECIFIC HEAT @ CONSTANT PRESSUREg = GRAVITATIONAL CONSTANT (386 in/sec²)

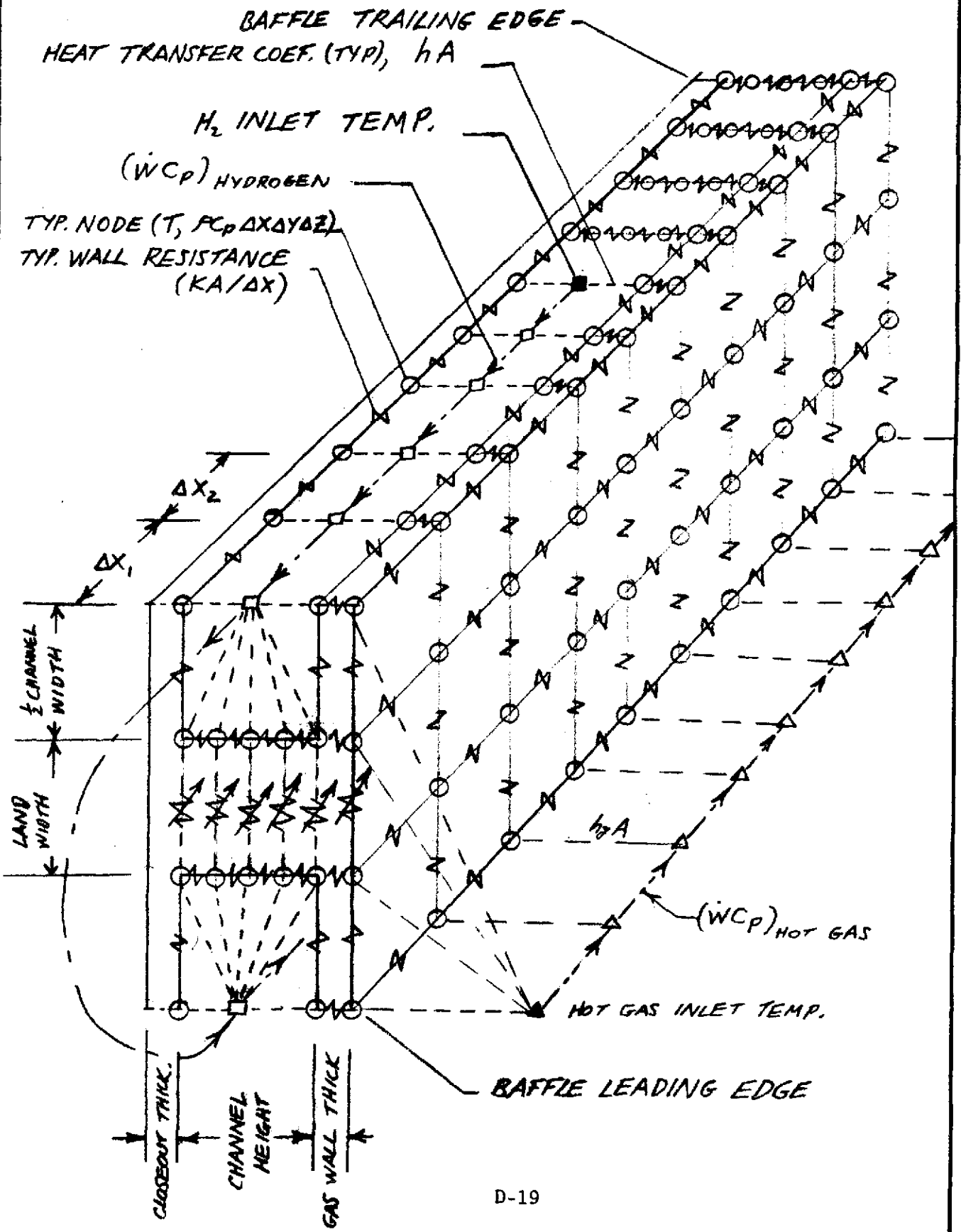
J = ENERGY CONVERSION = 778 FT-LB/BTU

IT IS READILY SEEN THE ABOVE REQUIRES AN ITERATIVE PROCEDURE TO SOLVE OVER EACH INTERVAL.

PREPARED BY:	Rocketdyne Division Rockwell International	PAGE NO. OF
CHECKED BY:		REPORT NO.
DATE:	BAFFLE GEOMETRY	MODEL NO.



PREPARED BY:	Rocketdyne Division Rockwell International	PAGE NO.	OF
CHECKED BY:		REPORT NO.	
DATE:	BAFFLE COMPUTER MODEL	MODEL NO.	



PREPARED BY:	Rocketdyne Division Rockwell International	PAGE NO.	OF
CHECKED BY:		REPORT NO.	
DATE:	BAFFLE COMPUTER MODEL	MODEL NO.	DEAP

INPUT

GEOMETRY

ΔX BETWEEN NODES	(9)
CHANNEL WIDTH	(10)
LAND WIDTH	(10)
GAS WALL THICK.	(10)
CHANNEL HEIGHT	(10)
1-2 PASS LOCATION	(10)

HOT GAS

INLET TEMPERATURE	(1)
h_g - HEAT TRANSFER COEF.	(10)
FLOW CAPACITY $\dot{W}C_p$ / CHANNEL	(1)
h_g MULTIPLIER	(1)

CONDITIONED PROPELLANT

INLET TEMPERATURE	(1)
h_{c1} - HEAT TRANSFER COEF., UP PASS	(10)
h_{c2} - HEAT TRANSFER COEF., DOWN PASS	(10)
FLOW CAPACITY $\dot{W}C_p$ / CHANNEL	(1)
h_c MULTIPLIER	(1)

PROPERTIES

WALL THERMAL CONDUCTIVITY VS TEMPERATURE (TABLES)

INITIAL CONDITIONS

INITIAL WALL TEMP. DISTRIBUTION

NOTE: ALL LOCATION PARAMETERS (GEOMETRY, h_g , h_{c1} , h_{c2})
ARE INPUT IN ORDER FROM LEADING EDGE TO TRAILING EDGE.

METHOD FOR DETERMINING HOT GAS FLOW AREA

$$A_x = W/G^* = \frac{W}{P_o} \left[\frac{\gamma g}{RT_o} \left(\frac{2}{\gamma+1} \right)^{\frac{\gamma+1}{\gamma-1}} \right]^{-0.5}$$

WHERE THE PRESSURE & TEMPERATURE ARE EVALUATED AT THE SAME POINT

- 1) UPSTREAM ANALYSIS: USE COMBUSTION TEMPERATURE & U/S PRESSURE
- 2) DOWNSTREAM ANALYSIS: USE EXIT TEMPERATURE & EXIT TOTAL PRESSURE

TO DETERMINE EXIT TOTAL PRESSURE:

FRICITION LOSS:

$$\Delta P = P_{01} - P_{02} = f \frac{L}{D} \frac{G^2}{2g \rho_{AV}}$$

SONIC EXIT:

$$G^* = P_{02} \left[\frac{\gamma g}{RT_{02}} \left(\frac{2}{\gamma+1} \right)^{\frac{\gamma+1}{\gamma-1}} \right]^{.5}$$

$$\therefore P_{01}/P_{02} = \left[1 + \alpha \left(T_{01}/T_{02} + 1 \right) \frac{\gamma}{2} \left(\frac{2}{\gamma+1} \right)^{\frac{\gamma+1}{\gamma-1}} \right]^{.5}$$

WHERE α IS DETERMINED FROM THE THEORETICAL PRESSURE PROFILE